Characterising the structure-function relationships of apoptotic cell-derived extracellular vesicles in modulation of inflammation

Lois Rose Grant

Doctor of Philosophy

Aston University

March 2022

Characterising the structure-function relationships of apoptotic cell-derived extracellular vesicles in modulation of inflammation

Lois Rose Grant

Doctor of Philosophy

2022

Thesis Summary

Apoptosis and apoptotic cell clearance by phagocytes are essential processes for maintaining tissue homeostasis and resolution of inflammation. Dysfunction in these processes can cause chronic inflammation and autoimmunity. Extracellular vesicles (EVs) mediate intercellular communication and regulate many physiological processes, however, apoptotic cell-derived EVs (ACdEVs) produced by dying immune cells are poorly understood, despite high constitutive levels of immune cell death. This study aimed to address this lack of understanding, in particular the ACdEV proteome, and the role of ACdEV-associated proteins in stimulating macrophage chemoattraction, binding/uptake, and phenotypic changes.

Apoptotic cells (UV-induced) released a heterogeneous population of ACdEVs (~50-1000 nm diameter). The THP-1 monocytic cell line was utilised to establish an in vitro model for interactions between macrophages and ACdEVs: chemotaxis, binding/uptake, and phenotype modulation. Using flow cytometry to assess macrophage phenotype, cell surface markers surprisingly suggested a pro-inflammatory response to ACdEVs, and this was supported by analysis of cytokine release. Proteomic analyses revealed the diversity of ACdEV proteomes, and gene ontology identified numerous ACdEV-associated proteins with relevant functions, including calreticulin and various adhesion molecules.

Comparing the proteomes of ACdEVs produced during early and late apoptosis showed differences in protein abundance/enrichment. Proteins enriched in early ACdEVs may help to ensure timely clearance of apoptotic cells. This study found that EV function can be differentially affected by the isolation method used. Size exclusion chromatography (SEC) resulted in ACdEVs losing their chemoattractive function, whereas ultracentrifugation (UC) did not. This suggests that surface-associated factors mediate some, but not all ACdEV functions. Functional studies suggest that calreticulin plays a role in recruitment of macrophages, in addition to its previously established role mediating phagocytosis.

Data presented here suggest that ACdEVs are complex signalling entities with important roles in apoptotic cell clearance and regulation of inflammation, and much remains to be elucidated regarding mechanisms and molecular players.

Key words: apoptosis, efferocytosis, macrophage, inflammation, extracellular vesicle

Acknowledgements

Firstly, I must express my gratitude to my brilliant supervisors: Professor Andrew Devitt, for giving me the opportunity to undertake this PhD, and guiding and supporting me throughout with immense enthusiasm; and Dr Ivana Milic, for the time she invested in my training and her guidance and kindness throughout. They make a great team and are both inspirational. I would also like to thank Dr Ewan Ross for his help and advice.

Thanks also go to the Master's students I supervised during my PhD, Annaïg Rozo and Jennifer Bevan, for their assistance with the lab work for this project. Thanks also go to Dr James Gavin (Jimmy) for all his help in the lab during the final crunch. I am especially grateful for all the other friendly faces I got to see in the lab every day: Amber, Andrea, Kiran, Nora and Parbata, who made my 3 years at Aston so enjoyable. Amber is a best friend for life, and I am really glad we met.

I have to give a shout-out to my best friends Hannah, Catriona and Lauren. They have cheered me on in all aspects of my life and always been there during the good times and bad. They are amazing and inspirational.

I am eternally grateful for my wonderful parents and my sister who always believe in me and help me to believe in myself. The support of my family throughout my life has helped me achieve so much.

Most of all I am forever thankful for Harry, who has loved and supported me in all my endeavours unconditionally for over a decade already. I am so grateful that he has moved around the country many times in those years to be by my side through all the highs and lows. I wouldn't be where I am now without him.

Contents

List of Abbreviations

ABC	ATP-binding cassette
ACAMP	Apoptotic cell-associated molecular pattern
ACdEV	Apoptotic cell-derived extracellular vesicle
Apaf-1	Apoptotic protease activating factor 1
BSA	Bovine serum albumin
Cryo-EM	Cryo-electron microscopy
CXCL	C-X3-C motif chemokine ligand
CXCR	C-X-C motif chemokine receptor
ER	Endoplasmic reticulum
DISC	Death inducing signalling complex
DLS	Dynamic light scattering
EV	Extracellular vesicle
FasL	Fas ligand
FBS	Foetal bovine serum
FC	Fold change
FITC	Fluorescein isothiocyanate
FSC	Forward scatter
GM-CSF	Granulocyte macrophage colony-stimulating factor
ICAM	Intercellular adhesion molecule
IFN-γ	Interferon gamma
IL	Interleukin
LIPA	Lysosomal acid lipase
LPC	Lysophosphatidylcholine
LPS	Lipopolysaccharide
LRP	Low density lipoprotein receptor-related protein
LXR	Liver X receptor
M-CSF	Macrophage colony-stimulating factor
MerTK	Tyrosine kinase Mer
MFG-E8	Milk fat globule-EGF factor-8
MHC	Major histocompatibility complex
MSC	Mesenchymal stem cell
NTA	Nanoparticle tracking analysis
PE	Phycoerythrin

PECAM	Platelet-endothelial cell adhesion molecule
PI	Propidium iodide
PMA	Phorbol 12-myristate 13-acetate
PPAR	Peroxisome proliferator-activated receptor
PS	Phosphatidylserine
PSR	Phosphatidylserine receptor
S1P	Sphingosine-1-phosphate
SEC	Size exclusion chromatography
SEM	Scanning electron microscopy
SSC	Side scatter
sfRPMI	Serum-free RPMI
SIRPα	Signal regulatory protein alpha
SLE	Systemic lupus erythematosus
SphK1	Sphingosine kinase 1
TEM	Transmission electron microscopy
TFF	Tangential flow filtration
TGF	Transforming growth factor
TRPS	Tuneable resistive pulse sensing
TNF	Tumour necrosis factor
TNFR1	Tumour necrosis factor receptor 1
UC	Ultracentrifugation
VD3	1,25-dihydroxyvitamin D3

List of Figures

List of Tables

1. Introduction

1.1 Apoptosis and clearance of apoptotic cells

1.1.1 Functions of apoptosis – programmed cell death

Kerr et al. first used the term apoptosis in 1972 to describe a "mechanism of controlled cell deletion", involved in cell turnover for homeostasis in healthy adult tissues, elimination of cells during embryonic development, and tumour regression [1]. Apoptosis can also function as a defence mechanism in response to cell damage or infection; DNA damage or metabolic stress may cause a cell to undergo apoptosis, and cytotoxic T cells can destroy pathogen-infected cells by inducing apoptosis [2]. Apoptosis is a tightly regulated, genetically programmed process. Apoptotic cells (ACs) are normally cleared rapidly by phagocytes (professional e.g. macrophages, or non-professional e.g. epithelial cells) [3]; efficient clearance of apoptotic cells prevents cells from progressing to secondary necrosis which involves leakage of intracellular contents and elicits unwanted inflammatory immune responses [4]. Due to its essential role in clearing unwanted cells, dysfunction in apoptosis – too much or too little – plays a role in many diseases including autoimmune disorders, cancer, and neurodegenerative disease.

Apoptosis plays a key role in the resolution of inflammation; immune cells which have served their purpose and are no longer necessary undergo cell death and are cleared by phagocytes [5]. Inflammation is an important physiological response to infection or tissue damage; **Figure 1.1** summarises the processes of inflammation and its resolution. Tissue resident leukocytes involved in innate immunity sense the insult and release chemokine signals to recruit neutrophils and monocytes from the circulation. These cells migrate through the endothelium and into the inflamed tissue. The release of pro-inflammatory mediators stimulates cell activation; monocytes differentiate into macrophages and are polarised to a pro-inflammatory phenotype (classical activation, 'M1'). Resolution of inflammation once the insult has been dealt with involves the depletion of pro-inflammatory signals, inhibition of leukocyte migration and tissue infiltration, and removal of inflammatory immune cells present in the tissue. These inflammatory immune cells undergo apoptosis and are engulfed by macrophages. This process induces a switch in macrophage phenotype from pro- to anti-inflammatory/pro-resolving (alternative activation, 'M2').

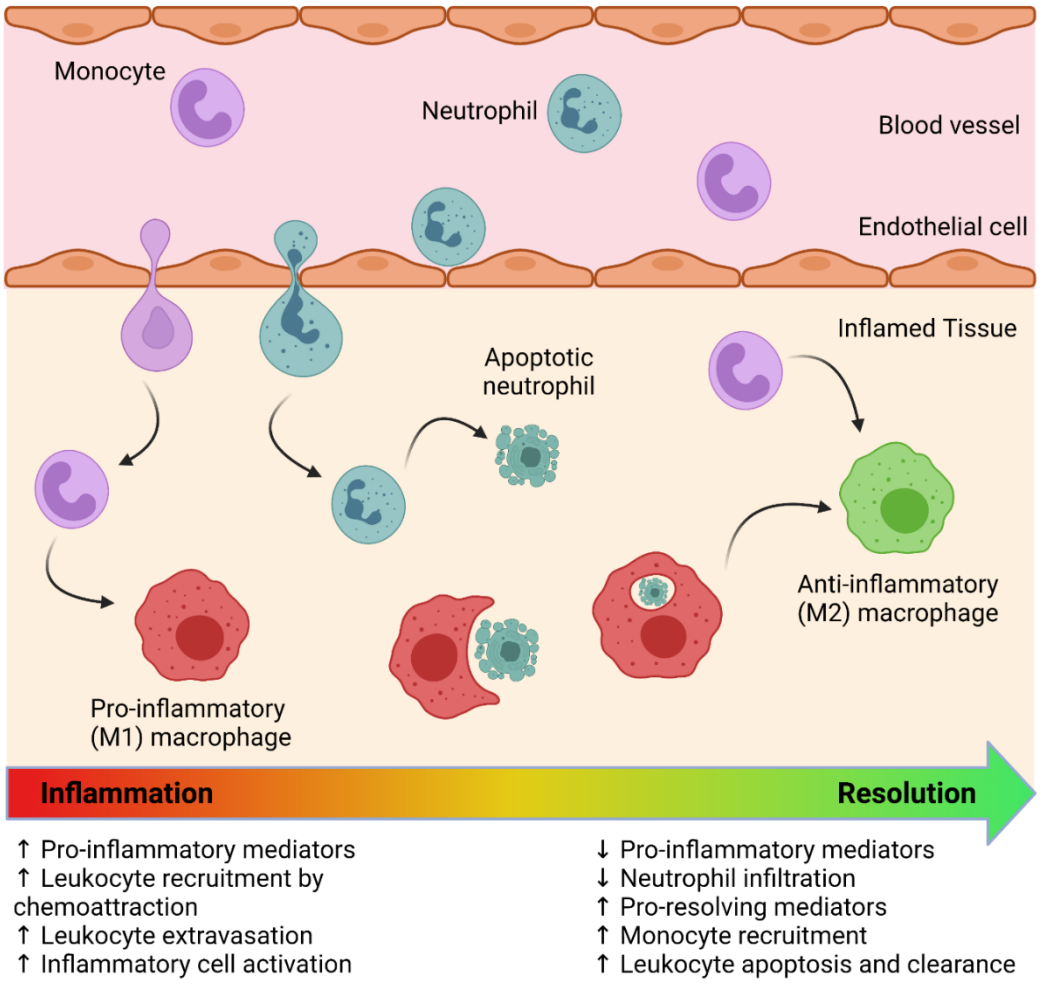

Figure 1.1: Apoptosis and the resolution of inflammation. Inflammation involves the recruitment and activation of immune cells in order to deal with an insult. The resolution of inflammation involves the depletion of pro-inflammatory signals and inhibition of leukocyte migration and tissue infiltration. Apoptosis and clearance of inflammatory cells present at the site that are no longer required is essential for inflammation to be resolved and tissue homeostasis to be restored. The engulfment of apoptotic cells induces a switch in macrophages from pro-inflammatory (classically activated, 'M1') to anti-inflammatory (alternatively activated, M2) which further promotes resolution and tissue repair. (Created with BioRender.com).

1.1.2 Molecular mechanisms of programmed cell death

Apoptosis can be induced by various stimuli including DNA damage, metabolic stress, and cell-to-cell signalling. The main molecular signalling pathways of apoptosis are the intrinsic and extrinsic pathways; the intrinsic pathway involves mitochondrial signalling and the extrinsic pathway involves activation of death receptors on the surface of the cell (**Figure 1.2**). The signals in one pathway can also influence the other [6]. The perforin/granzyme pathway is used by cytotoxic lymphocytes to induce apoptosis in virus-infected cells and tumour cells [7,8]. All apoptosis pathways converge at final execution pathway which is initiated by activation of executioner caspases. Caspases are activated by proteolytic cleavage of their pro-caspase form. Initiator caspases cleave and activate other caspases. Apoptosis involves a caspase cascade which leads to cell shrinkage, pyknosis (condensation of chromatin), DNA fragmentation by caspase-dependent DNase due to caspase-mediated degradation of the inhibitor of caspase-activated DNase (ICAD), extensive plasma membrane blebbing and expression of apoptotic cell-associated molecular patterns for recognition by receptors on phagocytic cells.

The intrinsic pathway of apoptosis is initiated through intracellular signals and involves the mitochondria. These signals may be pro-apoptotic signals or loss of factors which act to inhibit apoptosis such as growth factors, which lead to activation of apoptosis. The intrinsic apoptosis pathway can be induced by cell damage and stress such as DNA damage caused by e.g. radiation, or viral infection, metabolic stress caused by e.g. hypoxia, reactive oxygen species, toxins. In this pathway, various stimuli act on the mitochondria, causing permeabilisation of the outer membrane and release of sequestered pro-apoptotic proteins such as cytochrome c from the intermembrane space into the cytosol [9]. Mitochondrial membrane permeability is controlled by members of the Bcl-2 protein family. Anti-apoptotic members include proteins such as Bcl-2 and Bcl-X, and pro-apoptotic members include proteins such as Bax and Bid. The Bcl-2 proteins are regulated by p53, a tumour suppressor protein. Cytochrome c forms a complex with apoptotic protease activating factor 1 (Apaf-1) and pro-caspase-9, called the apoptosome. This activates caspase-9 which in turn activates executioner caspases. Once committed to apoptosis, the mitochondria also release other proteins including endonucleases which translocate to the nucleus and cause DNA fragmentation and chromatin condensation [10].

Initiation of the extrinsic pathway requires activation of transmembrane receptors known as death receptors, which are members of the tumour necrosis factor (TNF) receptor family. The

cytoplasmic death domain of these receptors transmits the death signal intracellularly. The Fas ligand and Fas receptor (FasL/Fas) and TNF-α/TNFR1 are two well characterised death ligand-receptor pairs. With these examples, the death receptors cluster and bind with their ligands in trimeric form. Adapter proteins in the cytoplasm (FADD/TRADD) are recruited to the oligomerised receptors and facilitate binding of pro-caspase-8; this forms a death-inducing signalling complex (DISC) which activates caspase-8 via autocatalytic cleavage of the pro-caspase [11]. Caspase-8 then activates executioner caspases.

There is crosstalk between intrinsic and extrinsic pathways; for example, cleavage of Bid by caspase-8 leads to its translocation to the mitochondria where it activates Bax, causing pore formation and release of cytochrome c [6]. Ultimately, the intrinsic and extrinsic apoptosis pathways converge on a final execution pathway. Activated executioner caspases, caspase-3, -6 and -7, cleave various substrates which leads to changes in cell structure: cytoskeletal reorganisation results in cell shrinkage; apoptotic bodies and other apoptotic cell-derived extracellular vesicles (ACdEVs) are released [1]; the endonuclease CAD causes DNA fragmentation and stage II chromatin condensation [12]; cells present apoptotic cell-associated molecular patterns on their surface to promote their clearance [13–15].

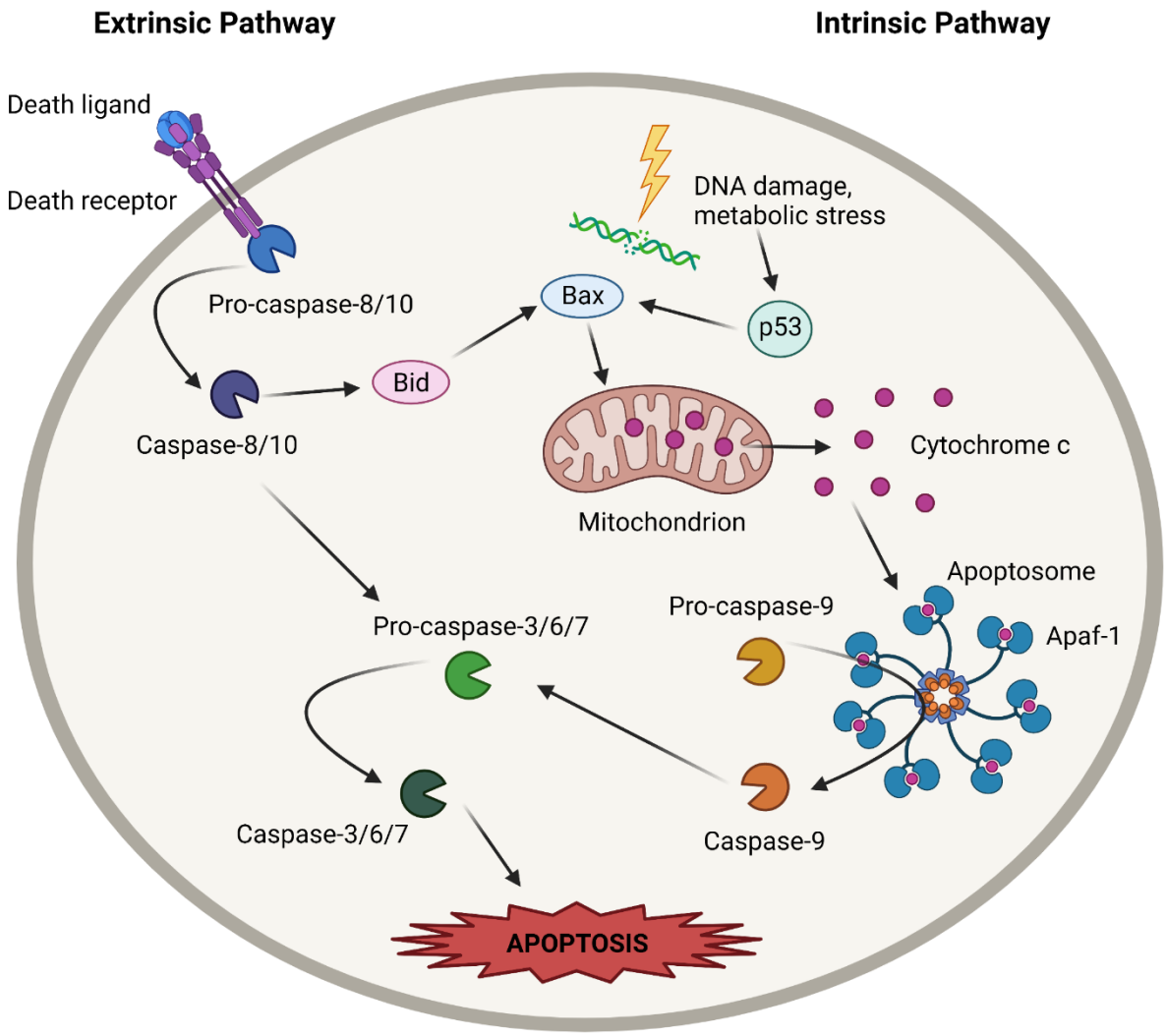

Figure 1.2: Molecular signalling pathways of apoptosis induction. The main pathways of apoptosis, the intrinsic and extrinsic pathways, are summarised. The extrinsic pathway is triggered by activation of death receptors on the cell surface by interaction with their death ligands, whereas the intrinsic pathway is triggered internally by DNA damage or metabolic stress which cause release of pro-apoptotic proteins such as cytochrome c from the mitochondria. Apoptosis is regulated by various proteins and involves caspase cascades where these enzymes proteolytically activate others, resulting in activation of downstream executioner caspases which activate proteins involved in the apoptotic process and disassembly of the cell. (Created with BioRender.com).

1.1.3 Recruitment of phagocytes: apoptotic cell 'find me' signals

Apoptotic cells release molecules which act as 'find me' signals, recruiting phagocytes. Known 'find me' signals include lipids, nucleotides, and proteins. Lysophosphatidylcholine (LPC) was identified as a chemotactic factor secreted by apoptotic cells which attracted human monocytic cell lines and primary macrophages [16]. Release of LPC from apoptotic cells was found to be dependent on activation of caspase-3, and subsequent activation of phospholipase A2. Release of LPC was demonstrated when apoptotic cells were generated using UV-irradiation, and apoptosis-inducing agents staurosporine and mitomycin C. The chemotactic LPC was shown to be soluble and not membrane bleb-associated, as depletion by 0.2 μm-filtration or ultracentrifugation did not diminish the chemoattractive activity of the supernatant [16]. Another soluble lipid 'find me' signal released by apoptotic cells is sphingosine-1-phosphate (S1P) [17]. Apoptosis induced by sphingosine kinase inhibitors or doxorubicin stimulated expression of sphingosine kinase 1 (SphK1) and secretion of S1P in Jurkat T lymphocytes and U937 monocyte-like cells. It was found that S1P was a strong chemoattractant for THP-1, U937 and primary monocytes and primary macrophages [17]. S1P signalling also primes macrophages for phagocytosis by altering gene expression to enhance apoptotic cell clearance [18].

ATP and UTP were found to be released by cells in the early stages of apoptosis, in a caspase-dependent manner in primary mouse thymocytes and human Jurkat T lymphocytes [19]. Release of ATP and UTP was shown to occur during apoptosis induced via UV irradiation and death receptor activation using anti-Fas. ATP and UTP were shown to be chemoattractants as their removal via hydrolysis by apyrase eliminated the chemoattractive effect of apoptotic cell supernatants on monocytes both in vitro and in vivo. This study went further and confirmed that sensing of ATP and UTP released by apoptotic cells occurs through the purinergic P2Y2 receptor on monocytes and macrophages. The chemoattractant(s) were soluble and heat-stable, as ultracentrifugation or boiling of the supernatants did not affect the chemoattractive activity [19]. A subsequent study from this group investigated the mechanism of release of these nucleotides from apoptotic cells, and discovered that controlled release occurs through pannexin 1 channels [20]. Activated caspases (3 & 7) cleave pannexin 1 at a specific site to open the channel.

Apoptotic cells also release chemokines, including CX3CL1 (C-X3-C motif chemokine ligand 1) [21]. CX3CL1 was found to be rapidly released by lymphocytes undergoing apoptosis, and release of CX3CL1 was shown to be mediated by caspases and Bcl-2. CX3CL1-mediated chemoattraction of macrophages was demonstrated with both spontaneously apoptotic and

UV-induced cells. The attraction of macrophages towards apoptotic lymphocytes was also confirmed to be dependent on the CX3CL1 receptor, CX3CR1. Apoptotic cell-derived extracellular vesicles (ACdEVs) can contain apoptotic cell 'find me' signals; the majority of the 60 kDa form of CX3CL1 released during apoptosis was found to be associated with ACdEVs [21]. Furthermore, intercellular adhesion molecule ICAM-3 is lost from the surface of apoptotic leukocytes via release of ACdEVs which strongly promote chemoattraction of macrophages [22]. However, it is not yet known whether ICAM-3 acts as a chemoattractive molecule or as an adhesion molecule which facilitates the action of other molecules. ACdEVs will be discussed further in later sections. Apoptotic cells can also release signals which inhibit the migration of phagocytes, and this can be cell-type specific; for example, lactoferrin released by apoptotic cells inhibits migration of granulocytes but does not inhibit migration of mononuclear phagocytes [23].

1.1.4 Recognition and tethering: 'eat me' and 'don't eat me' signals

Apoptotic cells present apoptotic cell-associated molecular patterns (ACAMPs) on their surface to promote their recognition and engulfment by phagocytes [15]. These ACAMPs are recognised by various receptors; some receptor-ligand pairings have been identified, others have not. One of the most studied 'eat me' signals is the phospholipid phosphatidylserine (PS). Identified as an 'eat me' signal in a study published by Fadok et al. in 1992, PS is externalised by cells undergoing apoptosis, and is specifically recognised by phagocytes [13]. A number of PS receptors have been identified, including phosphatidylserine receptor (PSR), stabilin-2 and Tim4 [24–26]. Another receptor involved in uptake of apoptotic cells is the scavenger receptor SCARF1 [27]. SCARF1-mediated recognition of apoptotic cells occurs via the binding of SCARF1 to the opsonising complement component C1q via phosphatidylserine exposed on apoptotic cells. Annexin 1 (also known as annexin A1), a Ca^{2+}-dependent phospholipid-binding protein, is another molecule presented on the cell surface during apoptosis [28]. Recruitment of annexin 1 from the cytosol and export to the outer leaflet of the cell membrane is mediated by caspases and annexin 1 co-localises with PS on the cell surface [28]. Down-regulation or silencing of annexin 1 on apoptotic cells and/or the phosphatidylserine receptor (PSR) on engulfing (endothelial) cells confirmed that annexin 1 and PSR function in the same engulfment pathway [28].

Calreticulin is a well characterised 'eat me' signal which is externalised by apoptotic cells [14,29–31]. Mainly found in the endoplasmic reticulum (ER), calreticulin is involved in calcium homeostasis in viable cells. During apoptosis, calreticulin is rapidly presented on the cell

surface and promotes phagocytosis with its receptor, low density lipoprotein receptor-related protein (LRP), also known as CD91, on phagocytic cells. Calreticulin/LRP-mediated engulfment of apoptotic cells was shown to involve the process of macropinocytosis [14]. ICAM-3 on the surface of apoptotic leukocytes has also been shown to promote recognition and tethering of macrophages [22,32]. ICAM-3 is only expressed by leukocytes, but apoptosis-induced sub-molecular changes on ICAM-3, for example altered glycosylation patterns, may be occurring on other molecules such that there is functional conservation facilitating apoptotic cell clearance for other cell types.

The fate of a cell interacting with a phagocyte is determined by the balance between 'eat me' signals and 'don't eat me' signals [15]. 'Don't eat me' signals are silenced to facilitate removal of apoptotic cells. A study into calreticulin-mediated engulfment of apoptotic cells determined that the interaction of CD47 (also known as integrin associated protein) with SIRPα (signal regulatory protein α) on phagocytes prevents engulfment of viable cells, and CD47 is altered or lost on apoptotic cells, enabling calreticulin-mediated uptake [29]. In another study, calreticulin was shown to be the dominant pro-apoptotic signal on cells of multiple human cancers which is counterbalanced by high expression of CD47, allowing the cancer cells to prevent phagocytosis [30]. CD31 (also known as PECAM-1 – platelet-endothelial cell adhesion molecule) is another 'don't eat me' signal which promotes cell detachment from phagocytes by homophilic interaction [33]. The function of CD31 was found to be switched in apoptotic cells, where CD31 promotes binding and engulfment [33]. It was later shown that homophilic interaction of CD31 on target cells and phagocytes activates the $\alpha_5\beta_1$ integrin on phagocytes, and fibronectin acts as a selective opsonin which promotes engulfment of apoptotic T cells by forming a bridge with $\alpha_5\beta_1$ integrin [34]. Furthermore, CD31 was found to delay repolarisation of macrophage membranes after contact with apoptotic cells allowing strong binding to facilitate engulfment, by inhibiting a voltage-gated potassium channel (ERG) [35]. Apoptotic cells can also be opsonised by deposition of the complement component C3b; CD46 was found to be rapidly lost from the surface of cells undergoing apoptosis and loss of CD46 resulted in stronger C3b opsonisation of cells exposed to complement [36]. ICAM-1 was recently identified as a macrophage receptor for apoptotic cells [37]. Molecular changes on the apoptotic cell surface and the "phagocytic synapse" between macrophages and apoptotic cells is reviewed in further detail by Barth et al. [38]. Signals released by apoptotic cells can also prime macrophages for efficient phagocytosis of apoptotic cells; S1P, a 'find me' signal secreted by apoptotic cells also activates erythropoeitin signalling in macrophages which promoted phagocytosis and immune tolerance [18]. As with 'find me' signals, ACdEVs can contain 'eat me' signals, and may serve as smaller more easily engulfed fragments of apoptotic cells. A

similar phagocytic synapse may form between macrophages and ACdEVs. **Figure 1.3** summarises the current knowledge of the ‘find me’ and ‘eat me’ signals involved in apoptotic cell clearance. There may be many AC markers and their receptors which remain to be identified.

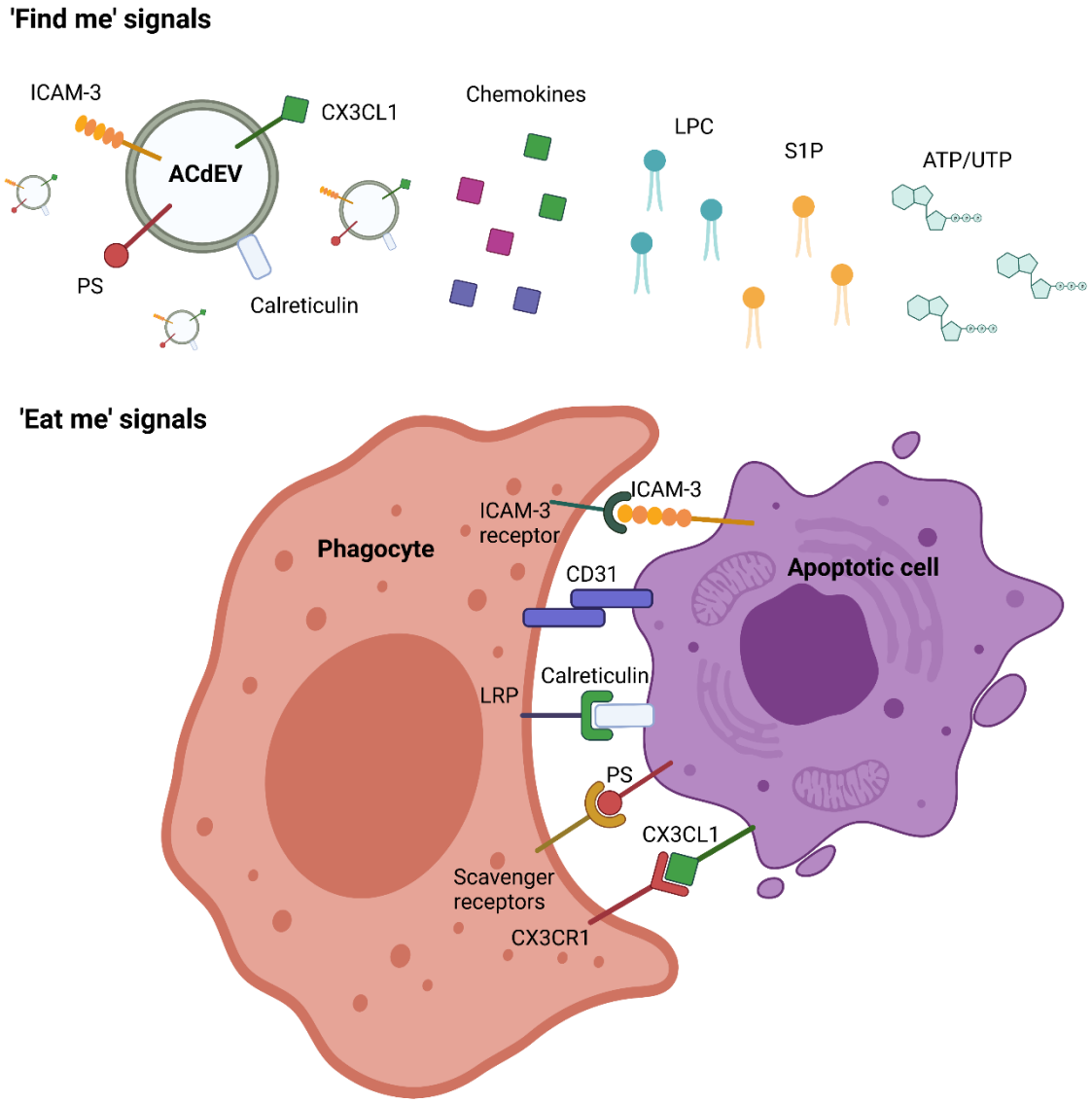

Figure 1.3: Apoptotic cell 'find me' and 'eat me' signals. Apoptotic cells release 'find me' signals to attract phagocytes to sites of cell death, including chemokine proteins such as CX3CL-1, nucleotides (ATP and UTP), and lipids (LPC and S1P). Apoptotic cells are recognised via interactions of apoptotic molecular patterns with various receptors on the surface of phagocytes in the phagocytic synapse. 'Don't eat me' signals are altered, silenced and/or overwhelmed by 'eat me' signals including PS, annexin 1, ICAM-3 and calreticulin, and apoptotic cells are ultimately engulfed by the phagocyte. A similar phagocytic synapse likely forms between macrophages and ACdEVs. (Created with BioRender.com).

1.1.5 Phagocytosis, processing and phagocyte responses

Once AC ‘eat me’ signals are recognised by a phagocytic cell, they are taken up via the process of phagocytosis, also known as ‘efferocytosis’. Henson et al. coined the term ‘efferocytosis’ for uptake of apoptotic cells, from the Latin “effero”, meaning to carry out for burial [39]. The engulfment process involves contractile actin-myosin networks; GTPases and various adaptor proteins facilitate actin polymerisation and remodelling of the actin cytoskeleton [40]. Pseudopod extension forms the phagocytic cup which closes to form a phagosome – a membrane-bound vacuole. Phagosomes fuse with lysosomes to form phagolysosomes which are progressively acidified, and degradative enzymes are activated to degrade the contents of the phagolysosome. Phagocytosis of apoptotic cells induces signalling resulting in various phagocyte responses to promote resolution of inflammation.

Various receptors have been found to play a role in apoptotic cell clearance and associated cell signalling. A-Gonzalez et al. discovered that the nuclear receptor liver X receptor (LXR) in macrophages plays an important role in AC clearance and immune tolerance through transcriptional regulation [41]. Engulfment of ACs activates LXR in macrophages which promotes phagocytosis and suppresses inflammatory pathways; activated LXR promotes expression of the receptor tyrosine kinase Mer (also known as MerTK), a receptor involved in phagocytosis, and suppresses inflammatory gene expression [41]. A study by Mukundan et al. identified peroxisome proliferator-activated receptor-δ (PPAR-δ) as another transcriptional sensor of apoptotic cells which is induced in macrophages when apoptotic cells are phagocytosed and regulates expression of opsonins which facilitate phagocytosis [42]. Engulfment of apoptotic thymocytes by macrophages induced expression of PPAR-δ target genes, encoding the opsonins C1qa, C1qb, milk fat globule-epidermal growth factor-8 (MFG-E8) and thrombospondin-1, and anti-inflammatory mediators MerTK and cytokine transforming growth factor-β1 (TGF-β1). Apoptotic cells enhance their own clearance via activation of PPAR-δ.

Perry et al. found that a chloride sensing pathway and chloride flux are involved in apoptotic cell-induced anti-inflammatory signalling [43]. It was discovered that genes involved in chloride transport are upregulated upon internalisation of apoptotic cells (and not upregulated by soluble factors released or apoptotic cell contact without internalisation); genes in the solute carrier protein SLC12 pathway were found to be co-ordinately regulated, and SLC12A2 transporter-mediated chloride influx was shown to function as a brake on apoptotic cell uptake and controls the anti-inflammatory response to apoptotic cells [43].

Kiss et al. found that apoptotic cells induce a PS-dependent homeostatic response of cholesterol efflux from macrophages to remove excess cholesterol obtained by engulfment of apoptotic cells [44]. This work showed that efflux of cholesterol is achieved via upregulation of expression of the ATP-binding cassette transporter ABCA1, which is regulated by LXR. The PS-induced enhancement of cholesterol efflux was induced by engulfment apoptotic cells specifically, and not necrotic cells which also expose PS. Viaud and Ivanov et al. showed that hydrolysis of ingested cholesterol esters by lysosomal acid lipase (LIPA) in macrophages prevents oxidative stress and inflammation and facilitates efficient clearance of apoptotic cells [45]. Free cholesterol generated by the hydrolysis of cholesterol esters is used to produce anti-inflammatory oxysterols following uptake of apoptotic cells.

Research by Angsana and Chen et al. on macrophage chemokine receptor expression and polarisation identified a role for the chemokine receptor CXCR4 in macrophage inflammation resolution [46]. Specific upregulation of CXCR4 was observed on mouse and human macrophages actively engaged in apoptotic cell uptake (efferocytosis) "$M2_{EFF}$", with no CXCR4 expression detected on M1 macrophages. Furthermore, a CXCR4 antagonist inhibited macrophage migration towards its ligand CXCL12 in a transwell chemotaxis assay, and inhibited emigration of macrophages to draining lymph nodes in vivo; demonstrating another mechanism linking apoptotic cell clearance and resolution of inflammation [46].

1.1.6 Defective clearance of apoptotic cells in disease

Rapid clearance of apoptotic cells is essential for homeostasis, preventing secondary necrosis and leakage of immunogenic intracellular content, and as discussed earlier, apoptotic cell signalling can promote resolution of inflammation and tissue repair. Defects in apoptotic cell clearance is implicated in various diseases including chronic inflammation, autoimmunity and cardiovascular disease [47,48]. Systemic lupus erythematosus (SLE) is an autoimmune disease where autoantibodies against widespread chronic inflammation causes tissue damage in various organs. Research published by Hermann et al. in 1998 established that apoptotic cell clearance is impaired in SLE patients and suggested that this source of autoantigens could cause the autoimmunity [49]. Mice with knockouts affecting uptake of apoptotic cells often develop lupus-like autoimmune disease [18,27,42]. The study by Mukundan et al. on the transcription factor PPAR-β mentioned in the previous section showed that *Ppard*$^{-/-}$ mice develop lupus-like autoimmune disease [42]. S1P, a 'find me' signal released from dying cells, activates EPO signalling in macrophages; this leads to upregulation of PPAR-γ, which regulates macrophage gene expression and enhances apoptotic cell clearance. Mice with

macrophage-specific *Epor* deletion develop age-dependent lupus-like symptoms [18]. A study by Ramirez-Ortiz et al. found that the scavenger receptor SCARF1 is used by macrophages, dendritic cells and endothelial cells for recognition and uptake of apoptotic cells via the complement component C1q. Loss of SCARF1 impaired apoptotic cells clearance and SCARF1-deficient mice exhibit lupus-like disease [27]. Hanayama et al. discovered that Milk MFG-E8 (also known as lactadherin), a secreted glycoprotein, acts as an opsonin for apoptotic cell engulfment by phagocytes [50]. MFG-E8 recognises PS exposed by apoptotic cells and enhances phagocytosis. The group later demonstrated a crucial role for MFG-E8 in the clearance of apoptotic B cells in germinal centres using MFG-E8 deficient macrophages in mice [51]. They found that apoptotic cells bound to *MFG-E8*$^{-/-}$ macrophages but uptake was impaired, and autoimmune disease developed; *MFG-E8*$^{-/-}$ mice spontaneously produced autoantibodies in an age-dependent manner, and could be a good model system for human SLE.

Deficient clearance of apoptotic cells is also implicated in cardiovascular disease, including atherosclerosis and myocardial infarction. Atherosclerosis is the narrowing of the artery lumen caused by the development of fatty plaques on the artery walls. Macrophage dysfunction and defective apoptotic cell clearance lead to increased inflammation and formation of necrotic cores which increase plaque instability and increase the risk of rupture and life-threatening ischaemia. Disruption to calreticulin signalling has been implicated in defective apoptotic cell clearance in atherosclerosis. The apoptotic cell ‘eat me’ signal calreticulin is counterbalanced by integrin-associated protein CD47, a ‘don’t eat me’ signal [14,29,30]. A study by Kojima et al. using mouse models found that antibodies against CD47 ameliorate atherosclerosis by restoring phagocytosis, promoting clearance of diseased vascular tissue [52]. A study by Ye et al. found elevated levels of the long non-coding RNA myocardial infarction associated transcript (MIAT) in the serum of symptomatic atherosclerosis patients and in the macrophages within the necrotic core in a mouse model of advanced atherosclerosis [53]. They determined that MIAT sponges the microRNA miR-149-5p, leading to upregulation of CD47 expression, which inhibits apoptotic cell clearance. Other molecules have been shown to be important in facilitating efficient removal of apoptotic cells and defects associated with atherosclerosis; mutation in the MerTK receptor has been shown to reduce the efficiency of apoptotic cell clearance [54], and complement C1q-mediated apoptotic cell clearance and ameliorates early atherosclerosis in mouse models [55]. Defective apoptotic cell clearance is associated with numerous conditions characterised by uncontrolled inflammation. Galectin-3 secreted by macrophages acts as an opsonin for apoptotic cells and deficiency is associated with chronic inflammatory conditions asthma, and chronic obstructive pulmonary disease [56–58].

1.2 Extracellular vesicles: complex mediators of intercellular communication

Extracellular vesicles are secreted membrane-enclosed structures which incorporate components of their cell of origin and play significant roles in intercellular communication. EVs can contain various molecules on their surface or within their lumen, including lipids, nucleic acids (DNA, RNA, miRNA) and proteins including active enzymes, which can facilitate cell-to-cell signalling. EVs are released by healthy, diseased, and dying cells and are involved in many physiological and pathophysiological processes. Viable cells release exosomes (~30-150 nm) and microvesicles (~100-1000 nm, and apoptotic cells also produce larger extracellular vesicles (>1 μm) called apoptotic bodies. The term 'exosome' was first used by Johnstone et al. in 1987, to describe small membrane vesicles "released during the in vitro culture of sheep reticulocytes which can be harvested by centrifugation at 100,000 x *g* for 90 min"; these exosomes act as a vehicle for maturing reticulocytes to discard plasma membrane components that are lost upon maturation, including the transferrin receptor [59,60]. Exosomes are generated by an endosomal pathway, whereas microvesicles are produced by direct budding of the plasma membrane. Microvesicles were first characterised as vesicles secreted by activated platelets and implicated in the process of coagulation; in 1967, Wolf described 'platelet-dust', which could be isolated by ultracentrifugation, was rich in phospholipid and had coagulant properties [61]. This 'platelet-dust' was later termed microparticles, which are now more commonly referred to as microvesicles.

1.2.1 Biogenesis of exosomes and microvesicles

Biogenesis of exosomes occurs within the endosome system [60,62,63]. Endocytic vesicles fuse with early endosomes and their contents are sorted and targeted for degradation, recycling, or exocytosis. During the maturation of early endosomes into late endosomes, inward budding of the endosomal membrane produces intraluminal vesicles (ILVs) containing cellular contents including proteins, lipids, and nucleic acids. This budding process involves the organisation of the early endosomal membrane into tetraspanin-enriched microdomains [64,65]. The resulting late endosomes containing ILVs are also known as multivesicular bodies (MVBs). MVBs are either targeted to fuse with lysosomes, where their contents are degraded, or with the plasma membrane, resulting in the release of the ILVs outside of the cell; these extracellular vesicles are called exosomes (**Figure 1.4**). The best characterised molecular mechanism of exosome formation is the ESCRT-mediated pathway. This pathway involves ESCRT (Endosomal Sorting Complex Required for Transport) protein complexes ESCRT-0, -

I, -II, and –III. ESCRT-0 clusters ubiquitinated cargo on the endosomal membrane, ESCRT-I and -II are recruited to drive membrane budding and ESCRT-III cleaves off the buds to form vesicles [66]. Various proteins have been shown to be involved in exosome biogenesis [62,63], and ILV formation can be ESCRT-independent [67]. Microvesicles are generated by direct budding of the cell membrane (**Figure 1.4**). This involves redistribution of the phospholipids and changes in the protein composition of the plasma membrane, forming microdomains; for example, Ca^{2+}-activated aminophospholipid translocases alter the composition of the plasma membrane; floppase-mediated translocation of phosphatidylserine to the outer leaflet of the plasma membrane induces budding [62]. Membrane budding occurs via actin-myosin contraction of cytoskeletal structures.

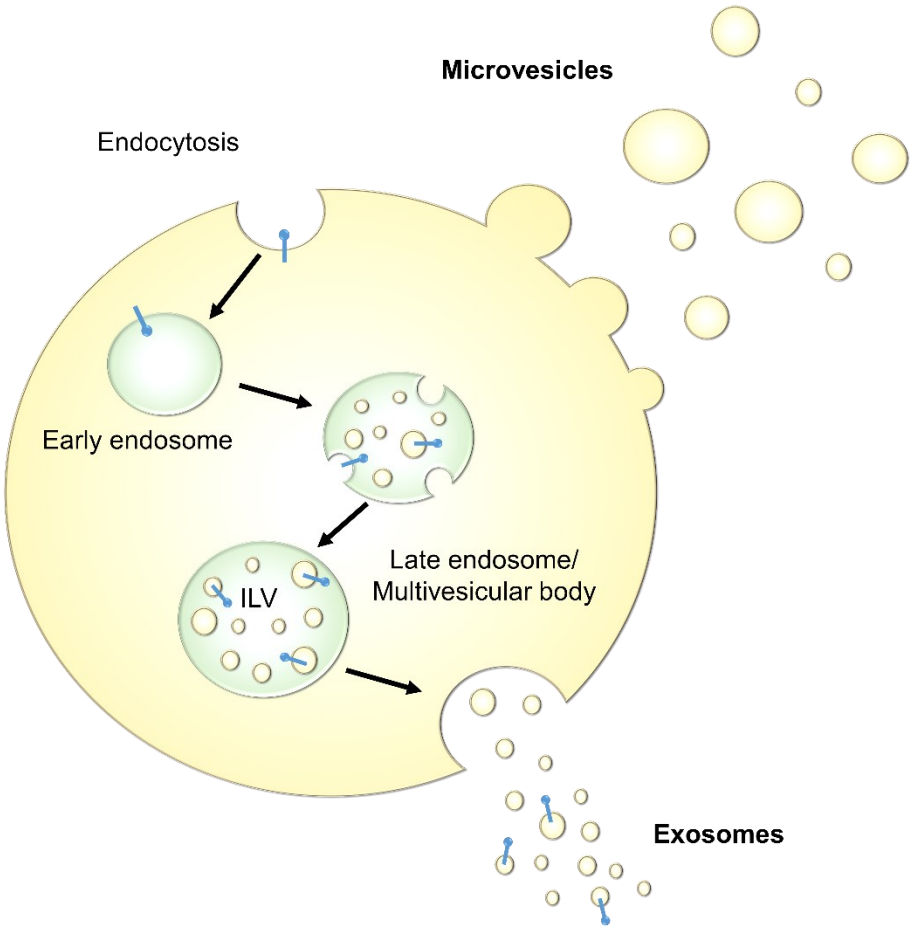

Figure 1.4: Biogenesis of extracellular vesicles. Exosomes (~30-150 nm) are produced within the endosome system; as endosomes mature, inward budding of the membrane creates intraluminal vesicles (ILVs) incorporating cellular contents. These ILVs can be released from the cell via fusion of the multivesicular body with the cell membrane. Microvesicles (~100-1000 nm) are generated via budding of the plasma membrane. EVs contain components from the membrane and cytosol of the cell.

1.2.2 Apoptotic cell disassembly and release of extracellular vesicles

Apoptosis involves disassembly of the cell into smaller fragments, including apoptotic bodies (**Figure 1.5**). When first defining apoptosis in 1972, Kerr et al. stated that “The formation of apoptotic bodies involves marked condensation of both nucleus and cytoplasm, nuclear fragmentation, and separation of protuberances that form on the cell surface to produce many membrane-bounded, compact, but otherwise well-preserved cell remnants of greatly varying size” [1]. Apoptotic bodies are now typically classified as large EVs greater than 1 μm released by cells undergoing apoptosis, as a result of membrane blebbing, and these have been the main focus of ACdEV research so far [68,69]. Membrane blebbing is regulated by kinases; during apoptosis, activation of RHO-associated protein kinase 1 (ROCK1) via cleavage by caspase-3 results in phosphorylation of myosin light chain, causing contraction of actomyosin [68,70]. Apoptotic bodies can also be released via the formation of protrusions called microtubule spikes and apoptopodia [71–73]. Smaller EVs (<1 μm) released by apoptotic cells include both microvesicles and exosomes [74,75].

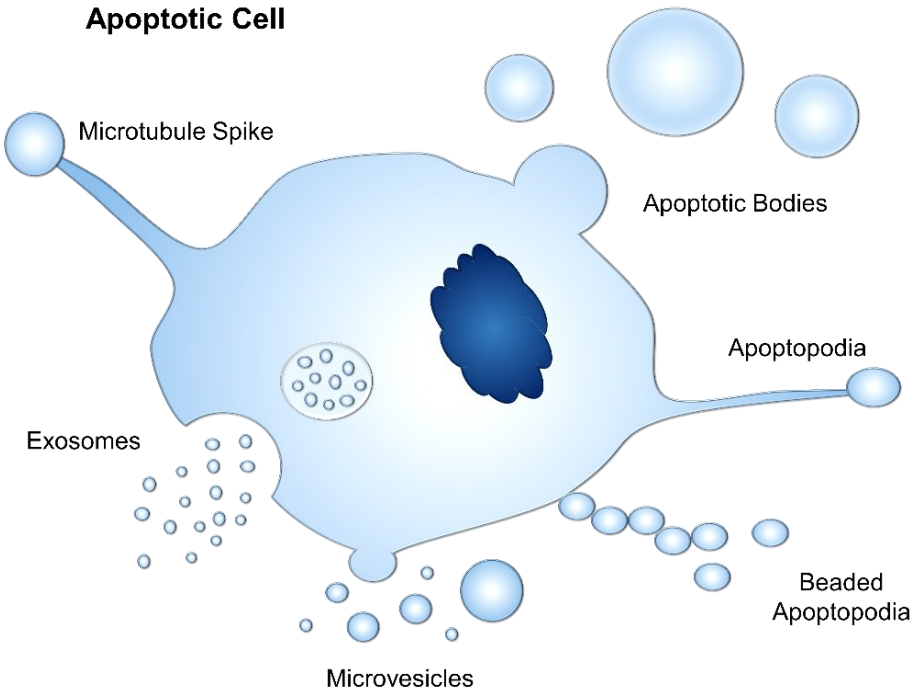

Figure 1.5: Apoptotic cell disassembly and release of extracellular vesicles. During apoptosis, cells disassemble into smaller fragments. Large apoptotic bodies (>1 μm) are formed by the process of membrane blebbing. Other mechanisms of release have been reported: apoptopodia, beaded apoptopodia and microtubule spikes. Apoptotic cells also release small EVs including both microvesicles and exosomes.

1.2.3 Molecular components of extracellular vesicles

Extracellular vesicles incorporate various components of the cell from which they are released. A key question in the EV field is whether EVs are simply a sample of their cell of origin or whether they are preferentially loaded with specific molecules under certain conditions. The lipid bilayer is made up of various phospholipids and EVs can also carry soluble lipid mediators [76–78]. EVs contain lipid rafts, which are subdomains in the membrane where specific lipids and proteins are organised [79,80]. EVs also contain nucleic acids, RNA and DNA [81,82], and evidence of differential sorting of nucleic acids including miRNAs and long non-coding RNAs into EVs has been shown [83–85]. EVs carry numerous proteins, including membrane proteins and cytosolic proteins enclosed in their lumen during their formation. EVs incorporate cell type-specific proteins e.g. receptors as well as general EV-associated proteins that are involved in their biogenesis. Membrane proteins commonly found in abundance in EVs include tetraspanins which are selectively enriched in EVs and have a broad range of functions [64]. EVs also contain major histocompatibility complex (MHC) molecules which are molecules involved in antigen presentation [64,86–88]. EVs can also carry functional enzymes, including proteases such as matrix metalloproteinases (MMPs) and glycosidases such as sialidase [89–91], as well as enzymes involved in synthesis of lipid mediators [92]. EV composition is also affected by the activation state of the cell and the process of apoptosis, as demonstrated in a study by Tucher et al. [93]. The general structure of EVs is depicted in **Figure 1.6**.

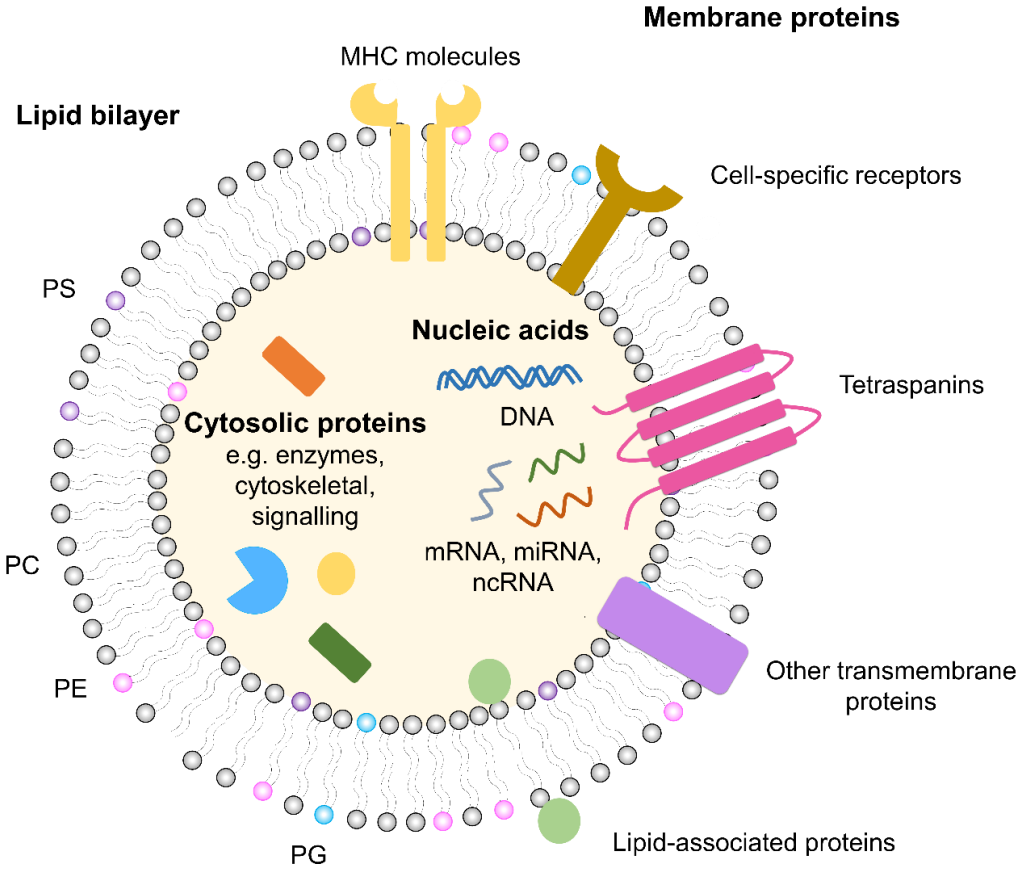

Figure 1.6: Schematic diagram of the molecular composition of extracellular vesicles. EVs incorporate components of their cell of origin, and specific molecules can be differentially sorted into EVs. The lipid bilayer is made up of phospholipids including phosphatidylcholine (PC), phosphatidylethanolamine (PE), phosphatidylglycerol (PG) and phosphatidylserine (PS). The membrane contains various proteins, such as cell-specific receptors and tetraspanins, which can mediate interactions with recipient cells. Within the lumen, there is a range of cytosolic proteins, as well as DNA and RNAs.

1.2.4 Interactions with recipient cells

Interactions between ligands on the EV surface and receptors on recipient cells can transmit signals and induce a cellular response [86,94,95]. Surface interactions also mediate EV internalisation; mechanisms of EV uptake have been reviewed in detail previously by Mulcahy et al. [96]. Ligands on the EV surface include proteins, lipids, and carbohydrates. Cells take up EVs via various endocytic mechanisms, including clathrin-dependent or clathrin-independent, and lipid raft-dependent endocytosis [97]. Cells can also internalise EVs by macropinocytosis, where ruffles in the cell membrane extend and seal to form a macropinosome [98,99]. EVs are also taken up by phagocytosis [100]. EV-cell interactions are summarised in **Figure 1.7**. Once EVs are taken up, their contents may be released to the cytosol. This requires endosomal escape which may involve fusion of the EV membrane with the membrane of the endocytic compartment [96,101]. EVs and their contents may simply be destroyed in lysosomes after internalisation. Alternatively, EV cargo can be delivered directly to the cytosol via fusion of EV membranes with the cell membrane [102]. EVs mediate transfer of RNA and DNA and protein to recipient cells, which can induce cellular responses [81,82,102–104]. There is evidence of EVs being targeted to specific recipient cells, for example Fitzner et al. observed preferential transfer of EVs from oligodendrocytes to a subset of microglia [98]. A study by Bilyy et al. found that macrophages preferentially phagocytose ACdEVs with specific glycosylation patterns over others [105].

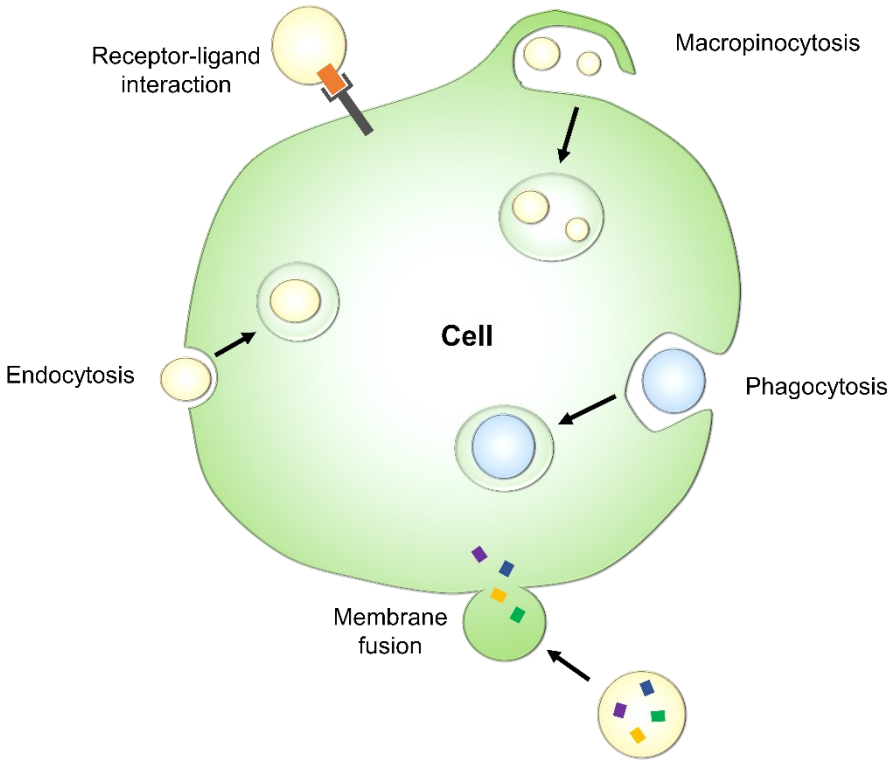

Figure 1.7: Interactions between extracellular vesicles and recipient cells. EVs can transmit signals via interactions between ligands on their surface and receptors on the cell surface. EVs can be internalised via endocytosis, phagocytosis and macropinocytosis, and their contents may subsequently be released inside the cell following endosomal escape, or EV membranes can fuse directly with the cell membrane, releasing their contents directly into the cytosol.

1.2.5 Physiological and pathophysiological functions of extracellular vesicles

EVs play key roles in various physiological processes. EVs are integral, functional components of the extracellular matrix (ECM), for example, carrying MMPs which contribute to ECM remodelling [89,106]. EVs are involved in intercellular communication in the nervous system [90,107,108]. Various studies have investigated the role of EVs as signalling mediators in the immune system. Antigen-presenting cells release antigen-presenting vesicles containing MHC class I and II [86,87]. These vesicles can also carry glycosylphosphatidylinositol-anchored regulators of complement which prevent complement-mediated lysis and support EV survival in the extracellular environment [109]. EVs can also be a source of bioactive lipid mediators which are involved in regulation of inflammation and repair [110]. Human macrophages and dendritic cells release EVs containing enzymes for leukotriene biosynthesis and promote granulocyte migration [92]. EVs from platelets also contain enzymes involved in lipid mediator biosynthesis, lipid mediators and their precursors. ACdEVs have been shown to play a role in the recruitment of phagocytes, which is essential for apoptotic cell clearance and resolution of inflammation [21,22].

EVs can also be significant mediators of signalling in disease, including infection, autoimmune disease, heart disease and cancer. Viral transmission can occur via EVs, as demonstrated with Herpes simplex virus 1 [111]. ACdEVs in plasma from HIV patients inhibit dendritic cell function [112]. ACdEV function is altered in SLE patients, where ACdEV-mediated downregulation of MHC class II expression on the surface of dendritic cells is impaired [113]. EVs can also play a role in the progression of atherosclerosis, for example by promoting cell adhesion to the vasculature and coagulation [114]. EVs from platelets can be pro-inflammatory, and contribute to inflammation in arthritis [115]. EVs can mediate non-targeted effects on bystander cells; for example EVs released by irradiated cells cause non-irradiated cells to exhibit similar responses including DNA damage [116,117]. Tumour-derived EVs contribute to cancer progression, by promoting metastasis and modulating the immune response; tumour ACdEVs support the onco-regenerative niche [118,119]. Functions of ACdEVs in apoptotic cell clearance and the control of inflammation will be discussed in further detail.

1.3 Methods for studying extracellular vesicles

1.3.1 Methods for isolation/enrichment of extracellular vesicles

Many different methods are used by researchers to isolate extracellular vesicles. Evaluation of EV isolation methods and optimisation of protocols are ongoing in the field. The International Society for Extracellular Vesicles (ISEV) published their proposed 'Minimal information for studies of extracellular vesicles' (MISEV) guidelines in 2014 and updated this in 2018 [120,121]. It is important to provide detailed information on the methods used in EV research and to consider the effects or limitations they may have. Standardisation of EV isolation protocols is critical for use of EVs in clinical settings. Choice of isolation method depends on the biological sample from which EVs are to be isolated and the downstream use and analyses to be performed (e.g. the required yield or desired purity). A combination of different isolation techniques may be used in order to increase the purity of EV samples. The isolation method used may affect the composition and functionality of the vesicles, and different isolation methods may enrich different subpopulations of EVs [122]. An important consideration is how physiologically relevant pure EVs are. EVs are unlikely to function in isolation in vivo and as such investigating the effects of isolated EVs is a reductive approach which may produce misleading results.

Ultracentrifugation has been widely used for a long time to isolate EVs; speeds around 100,000 x *g* are used to pellet small EVs, based on the original protocol from Johnstone et al. [60,123]. This ultracentrifugation isolates small EVs including exosomes and microvesicles, although originally thought to isolate only exosomes [124]. Lower centrifugation speeds can be used to pellet larger EVs: around 10,000 x *g* for larger microvesicles and 2000 x *g* for apoptotic bodies. The high speed of ultracentrifugation may cause the generation and co-isolation of protein aggregates and EV aggregation may occur [125,126]. EVs can also be isolated using ultracentrifugation with density gradients, but this method co-isolates high-density lipoproteins [127]. As ultracentrifugation requires expensive specialised equipment, various other approaches have been developed to isolate EVs. Precipitation using polymers is a simple method to collect EVs, however it is unpopular because it also precipitates high levels of contaminants such as lipoproteins and residual precipitation agent can affect functional studies [121]. Size exclusion chromatography (SEC) has become a popular choice for EV isolation, as it is effective at separating EVs from contaminating proteins and lipoproteins [128]. SEC alone will produce dilute samples and therefore ultrafiltration with spin filters is commonly used in addition to SEC when isolating EVs from cell culture medium; EVs isolated in this way have

been used for compositional and function studies [129,130]. Ultrafiltration methods include other techniques such as tangential flow filtration (TFF). Ultrafiltration can be useful for isolating EVs from large volumes and can also be used to exchange media. In 2002, Lamparski et al. published a method for isolation of clinical grade extracellular vesicles which combined TFF with sucrose density ultracentrifugation [131]. Ion exchange chromatography has also been used to isolate EVs from cell culture medium [132].

Various approaches have been utilised to isolate EVs by affinity capture. For example, EV affinity for heparin has been utilised to capture EVs [133]. Ghosh et al. developed synthetic peptides which bind to heat shock proteins which are commonly found on the surface of EVs [134]. Nakai et al. showed that EVs can be captured using the protein Tim4 (T-cell immunoglobulin and mucin domain containing 4); Tim4 is a PS receptor which is expressed by released from Tim4 upon addition of calcium chelators [135]. Immunoaffinity capture with antibodies against EV proteins can also be used, for example with antibodies against MHC II proteins [87]. Immunoaffinity capture is useful for isolating subpopulations of EVs with specific surface proteins. Worldwide surveys were performed by ISEV in 2015 and 2019 to determine which methodologies are being used in EV research, and determined that UC is still the most common isolation technique, but gentler methods, particularly SEC have become more popular in recent years [136].

1.3.2 Methods for characterisation of extracellular vesicles

In the MISEV2018 guidelines, ISEV states that EVs should be characterised to determine their abundance, which can be particle count, protein or lipid content; the presence of EV-associated components should be tested (generic or subtype-specific) as well as the presence of non-vesicular material which may be co-isolated [121]. Basic characterisation of extracellular vesicles typically involves measurement of their size, concentration, and microscopy for visualisation of morphology. There are various techniques for measuring the size distribution and quantifying EVs. Dynamic light scattering (DLS) is a technique which measures fluctuations in the intensity of scattered light due to the Brownian motion of the particles in a sample [137,138]. The accuracy of DLS can be compromised with heterogeneous samples because larger particles scatter more light and can prevent smaller particles from being detected. Nanoparticle tracking analysis (NTA) is commonly used for measurement of EVs, it is able to measure concentration as well as size, and is more useful than DLS for estimating size distribution in polydisperse samples because it measures the hydrodynamic diameter of individual particles by tracking their Brownian motion; however dust,

microorganisms and protein aggregates contaminating the sample are easily detected and will affect the results [139]. Tuneable resistive pulse sensing (TRPS) is an accurate technique for measuring EV size and concentration. TRPS detects single particles as they pass through a nanopore, driven through by applying pressure and voltage, and each particle causes a resistive pulse signal. The amplitude of this blockade signal is proportional to the true physical size of the particle [140,141]. A limitation of TPRS is that different nanopores are required to measure across different size ranges. EV size and concentration can also be estimated using flow cytometry optimised for measurement of nanoparticles. Size measurement is less accurate with flow cytometry which relies on reference beads, due to the heterogeneity of EVs and their refractive index.

Electron microscopy techniques can detect very small EVs which may be missed by the previously mentioned techniques, and allows visualisation of the vesicles, however their morphology can be affected by the sample preparation process [142]. Using scanning electron microscopy (SEM), EVs are observed as spherical structures and sample preparation can affect vesicle shape [142–144]. Using transmission electron microscopy (TEM), EVs appear cup-shaped due to the dehydration during sample preparation causing the vesicles to collapse. Cryo-EM preserves the native morphological state of EVs because the sample is fixed using vitrification, and this allows visualisation of the lipid bilayer and internal structures and accurate size measurement [145–147]. A study by van der Pol et al. comparing transmission electron microscopy, flow cytometry, nanoparticle tracking analysis and resistive pulse sensing found that each method gave a different size distribution and different concentration measurement for the same EV sample.

Various methods have been used for molecular characterisation of EVs. TEM and Cryo-EM can be combined with immunogold labelling of specific EV proteins [81]. Western blotting is commonly used to detect specific proteins in EV samples. EV composition is commonly analysed using proteomics, lipidomics and DNA/RNA profiling. Flow cytometry is an increasingly popular method for EV analysis. This technique is limited with conventional flow cytometers, which are not designed for detection of such small particles. Bead-coupling of EVs can be used to enable analysis of EVs on conventional flow cytometers [87]. The use of violet lasers has improved the detection of EVs, using violet side scatter, and specialised flow cytometers have been developed, for example imaging flow cytometers (e.g. ImageStream) to enable single particle analysis of EVs [148–151]. Nanoparticle-specific machines can enable label-free analysis of EVs [152]. Flow cytometry is a very useful technique which can provide

estimates of size and concentration at the same time as molecular characterisation. Technology for EV characterisation is constantly developing.

1.4 Structure-function relationships of apoptotic cell-derived extracellular vesicles (ACdEVs)

Over 20 years ago, it was proposed by Segundo et al. that 'apoptotic blebs' act as attractants to recruit macrophages to sites of cell death [153]. In this study, many CD molecules including CD11a (integrin alpha L), CD21 (complement receptor 2) and CD54 (ICAM-1) were found to be rapidly lost from the surface of apoptotic germinal centre B cells, partly via secretion of vesicles which were approximately 180 nm in size and stimulated chemotaxis of human monocytes. Since then, a number of functions of ACdEVs as signalling mediators have been discovered. For example, anti-inflammatory signals from ACdEVs have been shown to play a role in the prevention of autoimmune disease; 'apoptotic blebs' from lymphocytes down-regulate MHC II expression on dendritic cells, a process which is impaired in SLE patients [113]. Furthermore, ACdEVs from apoptotic neutrophils suppress the activity of T-helper cells, facilitating the resolution of inflammation [154]. Production of ACdEVs can also create an amplification loop of cell death, promoting apoptosis in macrophages which results in further release of ACdEVs [74]. While ACdEVs have been shown to play a key role in apoptotic cell clearance and control of inflammation, knowledge of the specific molecules mediating their functions is limited [155]. Furthermore, most EV research in the context of apoptosis has focused on the larger apoptotic bodies [73,156,157]. Apoptotic bodies and small ACdEVs are proteomically distinct and can differ in function, as demonstrated in a study on endothelial cell ACdEVs by Dieudé et al. [158]. Proteomic studies performed by Thery et al. (dendritic cells) and Tucher et al. (T lymphocytes) have shown that the compositions of ACdEVs and EVs from viable and activated cells are distinct [93]. ACdEVs contain 'find me' and 'eat me' signals from apoptotic cells and may act as smaller and more readily engulfed fragments of dying cells (**Figure 1.8**). They could potentially also act as vehicles for removal of 'don't eat me' signals from the surface of apoptotic cells to promote cell disposal. Furthermore, these 'don't eat me' signals may also promote vesicle longevity to prolong their signalling.

Interactions between EVs and cells including recognition, uptake and signal transduction are influenced by the EV surface composition. EV-cell interactions may be facilitated by simple physicochemical means such as surface charge, and/or be mediated by specific high-affinity ligand-receptor interactions. These ligands could be proteins, carbohydrates, or lipids. As mentioned previously, it has been shown that macrophages preferentially phagocytose ACdEVs with specific glycosylation patterns over others [105]. How ACdEVs modulate the immune system is currently poorly understood. At present, only the proteins CX3CL1, ICAM-3 and calreticulin have been studied in their ACdEV-associated form in the context of apoptotic

cell clearance. CX3CL1 is a chemokine and an adhesion molecule, expressed by various cell types. Its receptor, CX3CR1, is expressed by mononuclear phagocytes. In a study by Truman et al., migration towards apoptotic B lymphocytes (Mutu-BL cell line) was found to be dependent on the interaction between CX3CL1 and its receptor; CX3CL1 was shown to be rapidly lost from the cell surface when apoptosis was induced, in a 60 kDa cleaved form which was found to be mostly associated with ACdEVs [21]. The adhesion molecule ICAM-3, which is expressed by leukocytes, was found to be released in ACdEVs which potently attract macrophages in vitro [22]. Recently, in a study by Zheng et al. (2021), the apoptotic cell 'eat me' signal calreticulin was shown to mediate macrophage uptake of ACdEVs derived from apoptotic mesenchymal stem cells (MSCs); in a mouse model of type 2 diabetes, uptake of these ACdEVs resulted in reprogramming of liver macrophages towards an anti-inflammatory phenotype, alleviation of macrophage infiltration and restoration of homeostasis in the liver [159].

Many ACdEV-associated molecules have been identified which have known functions in the control of inflammation and apoptotic cell clearance but have not been functionally characterised in their ACdEV-associated forms. PS is well characterised as an important marker for AC recognition by phagocytes, and is also enriched on EV membranes and likely also facilitates recognition of ACdEVs [160]. Annexins, which are calcium-dependent membrane-binding proteins, are commonly present on the surface of EVs [63]. Annexin 1, which co-localises with PS externalised by apoptotic cells, plays a role in the resolution of inflammation, reducing leukocyte infiltration, promoting neutrophil apoptosis and removal by macrophages [161–163]. A study by Leoni et al. found that EVs containing annexin 1 promote epithelial wound repair, and patients with active inflammatory bowel disease had elevated levels of these EVs in their sera compared to healthy individuals [164].

HMGB1 (high mobility group protein 1) functions as a nuclear factor within cells and is also released by immune cells to regulate processes such as chemotaxis and cytokine release [165]. HMGB1 can act as a pro- or anti-inflammatory signal, determined by post-translational modifications of redox sensitive cysteine residues. HMGB1 has been shown to be released in EVs from healthy and apoptotic leukocytes both in vitro and in vivo [93,166–169]. The function of HMGB1 in EV-mediated signalling has however not yet been characterised. A study by Tucher et al. in 2018 comparing the proteomes of small and large subpopulations of EVs released from activated and apoptotic T lymphocytes found that HMGB1 was present exclusively in large EVs from apoptotic cells [93]. This raises the important issue of EV

heterogeneity and the need to understand this, as well as the possibly mechanisms for preferential loading of EVs.

In the recent study by Zheng et al. the proteomes of ACdEVs and their parental MSCs were analysed [159]. A total of 2873 proteins were identified, 481 of which were differentially expressed, and 284 of those were significantly upregulated in ACdEVs. Gene ontology analysis determined that the proteins enriched in ACdEVs are associated with ‘cell growth and death’, ‘cell mobility’, ‘signal transduction’, ‘immune system’ and ‘metabolism’. Furthermore, the authors identified several proteins in MSC ACdEVs with the potential to induce anti-inflammatory polarisation in macrophages, including alpha-crystallin B chain (CRYAB), peroxiredoxin-6 (PRDX6), cAMP-dependent protein kinase type II-alpha regulatory subunit (PRKAR2A), receptor of activated protein C kinase 1 (RACK1) and superoxide dismutase (SOD1).

Although ACdEVs contain pro- and anti-inflammatory mediators, and can play a role in promoting inflammation, apoptosis and AC clearance are typically non-inflammatory processes [75,170–172]. The balance between these mediators in the tissue environment changes over the course of apoptosis, and changes in the composition of ACdEVs released over time may provide key information about the functions of ACdEVs. EVs can also contain active enzymes and their substrates, and synthesise additional signals [92]. Therefore, individual enzymatically active EVs may change over time in composition, function and potentially signalling potency. Functional transporters in the EV membrane may facilitate release of the products into the extracellular space. There are many important questions regarding the structure and functions of ACdEVs which must be addressed. Identification of key ACdEV-associated molecules and their functions will provide valuable insight into how immune responses are modulated and inflammation is controlled, how apoptotic cell clearance is regulated, and the pathophysiology of diseases associated with dysfunction in these systems.

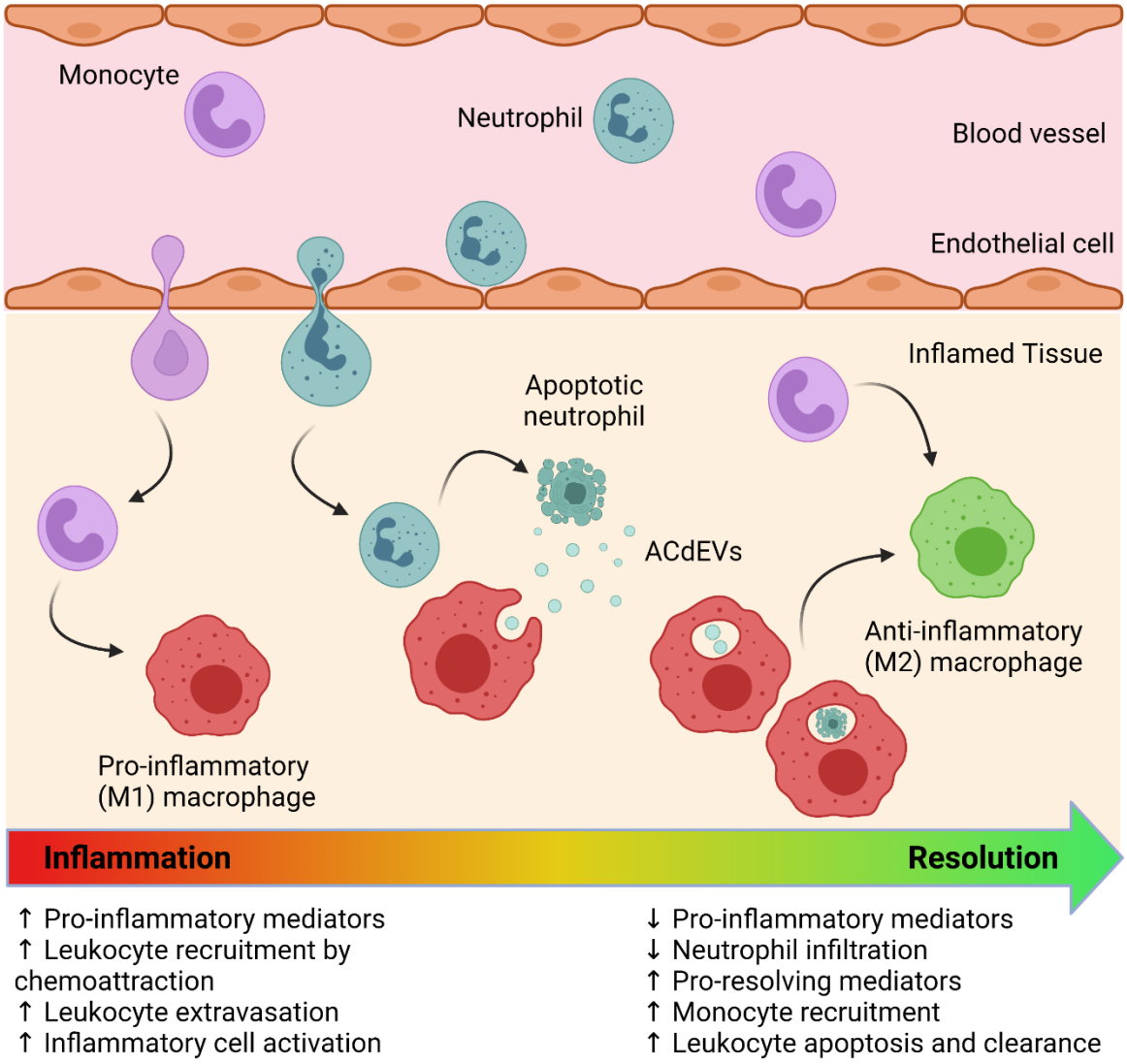

Figure 1.8: Roles of ACdEVs in control of inflammation. Immune cell apoptosis and clearance by phagocytes are essential processes in the resolution of inflammation. Apoptotic cells release ACdEVs which contain 'find me' and 'eat me' signals and promote macrophage chemotaxis towards sites of cell death and macrophages phagocytose ACdEVs and apoptotic cells. The engulfment of apoptotic cells (and likely ACdEVs) by macrophages induces a switch in cell phenotype from pro-inflammatory (classically activated, 'M1') to anti-inflammatory (alternatively activated, M2) which further promotes resolution and tissue repair. (Created with BioRender.com).

1.5 Project aims & objectives

Given the lack of detailed analysis of ACdEV proteomic data, especially of the surface proteome, and the limited knowledge of ACdEV functions, this project had 3 main aims:

1.5.1 Characterise apoptotic cell-derived extracellular vesicle production and their effects on macrophages

This project aimed to characterise the composition and functions of ACdEVs in apoptotic cell clearance and immunomodulation. In order to investigate ACdEVs, cell line models of immune cell apoptosis, ACdEV release and interactions between ACdEVs and macrophages had to be established. This involved measuring the progression of UV-induced apoptosis, characterising ACdEV using basic EV analysis methods, comparing ACdEVs from cells at early and late stages of apoptosis. To characterising ACdEV-macrophage interactions, cell line-derived macrophage models were evaluated and assays to investigate chemotaxis, binding, uptake, and phenotypic responses were developed.

1.5.2 Identify ACdEV-associated proteins that could mediate ACdEV functions

The next aim was to identify key proteins present within apoptotic cell-derived extracellular vesicles that mediate ACdEV function in modulation of the innate immune response and resolution of inflammation. Data from mass spectrometry (MS) analysis of ACdEVs isolated from 4 different human immune cell types were used to create a shortlist of lead molecules for further study. Using gene ontology analysis, the proteomes of ACdEVs released at early and late stages of apoptosis were compared.

1.5.3 Characterise the functions of candidate proteins in interactions between ACdEVs and macrophages

The main aim of this project was to identify ACdEV structure-function relationships, assessing candidate proteins as ligands for macrophage chemoattraction, EV binding, uptake, and other immunomodulatory functions *in vitro*. The roles of the candidate proteins in ACdEV-mediated signalling were investigated by blocking their function using antibodies or other inhibitors. Developing our understanding of the molecular signalling mechanisms facilitating EV function in this context will provide fundamental understanding of the cell death programme and homeostasis in the immune system.

2. Materials and Methods

2.1 Materials

2.1.1 Cell culture

Human monocytic cell line THP-1 (TIB-202) was purchased from ATCC (USA), T lymphocyte cell line Jurkat (CRL-2900) was purchased from LGC Standards (Teddington, UK). Mutu BL cell line was provided by Professor C Gregory (Edinburgh University).

Table 2.1: Cell culture reagents

Reagent	**Manufacturer**
RPMI-1640 cell culture medium (phenol red supplemented and phenol red-free)	Sigma Aldrich
L-glutamine	Sigma Aldrich
Penicillin/Streptomycin	Sigma Aldrich
Dulbecco's phosphate buffered saline (PBS)	Sigma Aldrich
Lipopolysaccharide (LPS) from *E. coli* (O111:B4)	Sigma Aldrich
Cycloheximide	Sigma Aldrich
Foetal calf serum of South American origin	Gibco (Thermo Fisher Scientific)
1α,25-Dihydroxyvitamin D_3 (VD3)	Enzo Life Sciences
Recombinant Human IL-4 Protein	R&D Systems
Phorbol 12-myristate-13-acetate (PMA)	Sigma
Anti-Fas antibody (human, activating, clone CH11)	Merck Millipore

2.1.2 Assay reagents

Table 2.2: Assay reagents

Reagent	Manufacturer
Apoptosis detection kit FITC/APC	eBioscience™ (Thermo Fisher Scientific)
Mouse anti-human CD11b [ICRF44] PE	eBioscience™ (Thermo Fisher Scientific)
Mouse anti-human CD64 [10.1] PE	eBioscience™ (Thermo Fisher Scientific)
Mouse anti-human CD163 [GHI/61] PE	eBioscience™ (Thermo Fisher Scientific)
Mouse anti-human CD206 [19.2] PE	eBioscience™ (Thermo Fisher Scientific)
Mouse anti-human CD54 (ICAM-1) [HA58] PE	eBioscience™ (Thermo Fisher Scientific)
Mouse anti-human CD102 (ICAM-2) [CBR-IC2/2] FITC	eBioscience™ (Thermo Fisher Scientific)
Mouse IgG1kappa isotype control [P3.6.2.8.1] PE	eBioscience™ (Thermo Fisher Scientific)
Rat anti-human CD209 [eB-h209] PE	eBioscience™ (Thermo Fisher Scientific)
Rat IgG2a kappa isotype control [eBR2a] PE	eBioscience™ (Thermo Fisher Scientific)
Mouse anti-human CD86 [BU63] PE	Invitrogen (Thermo Fisher Scientific)
Mouse anti-human CD80 [MEM-233] PE	Invitrogen (Thermo Fisher Scientific)
Mouse anti-human CD40 [HB14] PE	Invitrogen (Thermo Fisher Scientific)
Mouse anti-human CD14 [Tuk4] PE	Invitrogen (Thermo Fisher Scientific)
Mouse anti-human CD16 [3G8] PE	Invitrogen (Thermo Fisher Scientific)
Mouse IgG1 isotype control PE	Invitrogen (Thermo Fisher Scientific)
BODIPY™ FL N-(2-Aminoethyl)) Maleimide	Invitrogen (Thermo Fisher Scientific)
DiR (1,1'-Dioctadecyl-3,3,3',3'-Tetramethylindotricarbocyanine Iodide)	Invitrogen (Thermo Fisher Scientific)
Mouse anti- human calreticulin-PE [FMC 75]	Abcam
Mouse IgG1 isotype control [B11/6] PE	Abcam
Human serum (AB male)	Sigma
PageRuler™ Plus Prestained Protein Ladder	ThermoScientific
Pierce ECL Plus	ThermoScientific
Recombinant HRP Anti-Calreticulin antibody [EPR3924] (ab92516)	Abcam

Recombinant Anti-ICAM3 antibody [EPR3995] (ab108618)	Abcam
Anti-Rabbit IgG (whole molecule)–Peroxidase antibody produced in goat	Sigma
Bio-Rad Protein Assay Kit II (BSA standard)	Bio-Rad
Mini-PROTEAN TGX gel	Bio-Rad
EveryBlot blocking buffer	Bio-Rad
Megamix-Plus Forward Scatter and Side Scatter beads	Biocytex
NanoFCM™ Quality Control Nanospheres	NanoFCM
LEGENDplex™ HU Essential Immune Response Panel (13-plex)	BioLegend

2.1.2.1 Inhibitors

Table 2.3: Inhibitors used in functional assays

Reagent	**Manufacturer**
Calreticulin blocking peptide	MBL International (USA)
Mouse anti-human CD54 (ICAM-1) (HA58), Functional Grade	eBioscience™ (Thermo Fisher Scientific, UK
Mouse anti-human CD102 (ICAM-2) [CBR-IC2/2]	eBioscience™ (Thermo Fisher Scientific, UK)

2.1.3 Equipment

- Cell-IQ Automated Cell Tracking system (CM Technologies, Tampere, Finland)
- Chromato-Vue C-71 light box and UVX radiometer from UV-P Inc. (Upland, CA, USA)
- Amicon® Ultra-15 Centrifugal Filter Unit 30kDa Millipore (Watford, UK)
- qEVoriginal/70 nm columns (Izon Science, Oxford, UK)
- qNano TPRS machine (Izon Science, Oxford, UK)
- Multiskan™ GO Microplate Spectrophotometer from Thermo Scientific (UK)
- Cytoflex s flow cytometer (Beckman Coulter, USA)
- Optima Max-XP ultracentrifuge with TLA-110 rotor (Beckman Coulter, USA)

- Invitrogen™ EVOS™ FL Digital Inverted Microscope (Thermo Fisher Scientific, UK)
- Trans-Blot Turbo Transfer System (Bio-Rad, UK)

2.2 Cell culture

Cell lines were cultured in RPMI-1640 medium supplemented with 10% v/v FBS, 2 mM L-glutamine, 100 U/ml penicillin and 100 µg/ml streptomycin. All cells were cultured at 37°C with 5% CO_2 in a humidified atmosphere. Cells were maintained at a density below 1 x 10^6 cells/ml by passaging every 2-3 days. THP-1 monocyte-derived macrophages were produced by 48-hour incubation of THP-1 monocytes with 100 nM 1,25-dihydroxyvitamin D_3 or 250 nM PMA in complete culture medium.

2.3 Induction of apoptosis

Cells were resuspended in serum-free and phenol red-free RPMI-1640 medium (supplemented with 2 mM L-glutamine, 100 U/ml penicillin and 100 µg/ml streptomycin) at a density of 4 x 10^6 cells/ml. Apoptosis was primarily induced by ultraviolet light (UV) irradiation in a Chromato-Vue C-71 viewing cabinet; UV intensity was measured with a UVP radiometer connected to a UVX-25 detector and cells were irradiated with a dose of 30 mJ/cm^2. For mass spectrometry-based proteomic analysis of ACdEVs from different cell types at early and late stages of apoptosis, apoptosis was induced with cycloheximide (20 µg/ml) and anti-Fas antibody (1/10,000) at 4x10^6 cells/ml. For mass spectrometry-based proteomic investigation of ACdEVs isolated by different methods, apoptosis was induced using UV.

2.4 Isolation of extracellular vesicles

Cell culture supernatant was centrifuged at 300 x *g* for 5 minutes at 4°C to pellet cells. The supernatant was collected and centrifuged at 2000 x *g* for 20 minutes at 4°C to pellet debris and apoptotic bodies. For EV isolation by size exclusion chromatography (SEC), a qEVoriginal/70 nm column was warmed to room temperature and equilibrated with PBS. The 2000 x *g* supernatant was transferred to a 30 kDa molecular weight cut-off Amicon filter tube and concentrated to < 2 ml by centrifugation at 3000 x *g* at 4°C. The concentrated sample was added to the column, followed by PBS once the sample has entered the top-filter. The 3 ml void volume was collected before a 3.5 ml EV fraction was collected. The column was washed with 20 ml PBS for regeneration; qEV columns were re-used up to 5 times as per the manufacturer's instructions. For EV isolation by ultracentrifugation, the 2000 x *g* supernatant

was centrifuged at 100,000 x *g* for 90 minutes at 4°C, the supernatant removed, and the pellet resuspended in serum-free RPMI.

2.5 EV analysis by TRPS

EV size and concentration were measured by tunable resistive pulse sensing (TRPS) with a qNano instrument (Izon Science). Samples were analysed using NP150 pores stretched to 47 mm with 7 mbar pressure applied, and calibration was performed using CPC200 particles. Measurement was stopped after 500 particles were measured.

2.6 Measurement of protein concentration

Protein concentration of EV preparations was measured with a Bradford-based assay using the Bio-Rad Protein Assay Kit II (BSA standard). Serial dilution of BSA from 0.03 to 0.00012 mg/ml was used to produce a standard curve (example shown in **Figure 2.1**). 225 µl of dye was added to 25 µl of standard/sample. After 5 minutes incubation with the dye, the absorbance at 595 nm was measured on a Multiskan™ GO Microplate Spectrophotometer (Thermo Scientific).

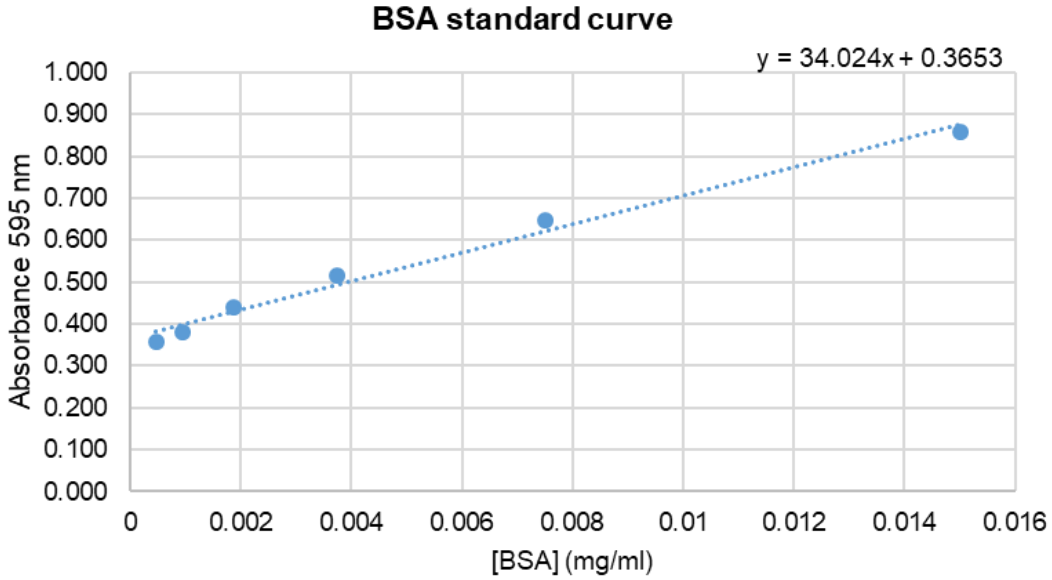

Figure 2.1: Standard curve for measurement of protein concentration

2.7 Flow cytometry

2.7.1 Cells

Flow cytometry was performed on a CytoFLEX S flow cytometer (Beckman Coulter). For staining with antibodies, cells were centrifuged at 300 x *g* for 5 minutes, washed twice with 0.1% (w/v) bovine serum albumin (BSA) in PBS and resuspended in 10% human serum in PBS. Conjugated primary antibodies were added at 1 µl per 10^5 cells (1/100) with cells at a density of 10^6 cells/ml, and incubated on ice in the dark for 30 minutes. Cells were then washed twice and resuspended in 0.1% BSA in PBS before analysis. Protein expression was determined by the percentage of events within the cell gate (gate based on forward and side scatter), with fluorescence greater than that of ~98% of cells stained with the isotype matched control. The mean fluorescence intensity (MFI) of the whole cell population was calculated by subtracting the MFI of the isotype matched control.

2.7.1.1 Apoptosis assay

To measure apoptosis, $2x10^5$ cells were added to 500 µl of annexin V binding buffer (diluted to 1X with deionised water) and 5 µl of annexin V-FITC and 10 µl propidium iodide (PI) were added. Samples were analysed immediately after addition of PI.

2.7.2 Vesicles

Antibodies or dyes were added to the 2000 x *g* supernatants or isolated EV samples, and incubated for at least 30 minutes before analysis on the CytoFLEX S flow cytometer. For annexin V labelling of phosphatidylserine, EV sample was diluted 1/10 in 1X annexin V binding buffer before addition of annexin V-FITC. Megamix-Plus and NanoFCM QC beads were used to adjust the cytometer settings to detect small particles and give a rough approximation of EV size. For analysis, samples were run at a flow rate of 10 µl/min to acquire at least 5 x 10^4 events and violet SSC was used to trigger detection of EVs.

2.8 EV uptake assay

Supernatant was harvested from apoptotic cell culture and BODIPY™ FL N-(2-Aminoethyl)) Maleimide was added and incubated for 30 min in the dark on ice to label EVs. Excess dye was removed and EVs were isolated using SEC. Isolated fluorescent EVs were then incubated with THP-1 monocyte-derived macrophages for up to 4 h. Over the time course, macrophages

were collected and washed by centrifugation (with 0.1% w/v BSA in PBS) to remove unbound EVs before flow cytometry analysis to assess the level of uptake.

2.9 Chemotaxis assays

A transwell vertical migration assay was performed with ACdEVs, whole secretome (2000 x *g* supernatant) or control medium in the lower wells. THP-1 monocyte-derived macrophages were placed in the upper chamber (8.0 µm pore transwell inserts) with 8 x 10^4 cells per well in 300 µl macrophage serum free medium. Migration of cells was monitored using an automated CellIQ Cell Imaging System, with 5 positions per well manually focussed and then automatically imaged every 20 minutes.

2.10 Apoptotic cell clearance assay

THP-1 monocyte-derived macrophages were produced by differentiation with VD3 for 48 h. Macrophages were labelled with DiR (0.5 µg/ml, 1x10^6 cells/ml) and apoptotic cells were labelled with BODIPY™ FL N-(2-Aminoethyl)) Maleimide (5 µM, 4x10^6 cells/ml), incubated for 30 minutes at 37°C before being pelleted and washed twice with serum-free phenol red free RPMI. Macrophages were resuspended at 1x10^6 cells per ml and apoptotic cells resuspended at 1x10^7 cells/ml. Apoptotic cells were incubated with macrophages at a 10:1 ratio. Samples were collected and analysed by flow cytometry, gating macrophages as DiR-positive cells (APC-A750 channel) and measuring acquired fluorescence from apoptotic cells (FITC channel).

2.11 Macrophage polarisation

THP-1 monocyte-derived macrophages (M0) were polarised towards a pro-inflammatory M1 phenotype by treatment with LPS from *E. coli* (100 ng/ml) or an anti-inflammatory M2 phenotype with human recombinant IL-4 (20 ng/ml). Primary monocyte-derived macrophages were polarised towards an M1 phenotype by treatment with LPS (100 ng/ml) and IFN-γ (20 ng/ml), and towards an M2 phenotype with IL-4 (20 ng/ml).

2.12 Cytokine assay

Cell supernatants were collected by removing cells by centrifugation (300 x *g*, 5 minutes) and frozen at -20°C until use. Cytokines were measured by flow cytometry using the LEGENDplex™ HU Essential Immune Response Panel (13-plex) kit following the

manufacturer's instructions. Samples dilution was not necessary for the assay. Cytokines measured by the kit are IL-4, IL-2, CXCL10 (IP-10), IL-1β, TNF-α, CCL2 (MCP-1), IL-17A, IL-6, IL-10, IFN-γ, IL-12p70, CXCL8 (IL-8), TGF-β1. Data were analysed using the LEGENDplex™ Data Analysis Software. Example standard curves generated are shown in **Figure 2.2**.

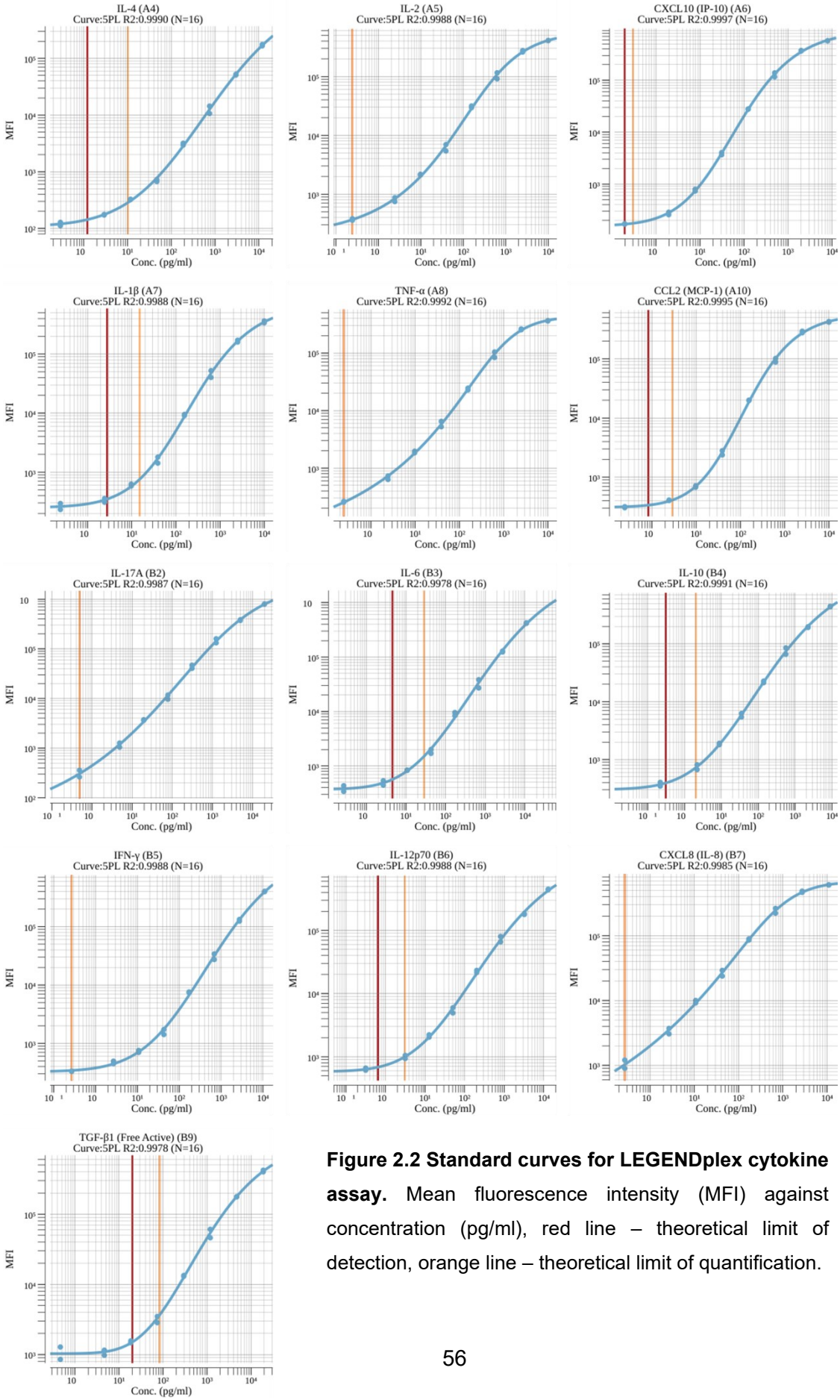

Figure 2.2 Standard curves for LEGENDplex cytokine assay. Mean fluorescence intensity (MFI) against concentration (pg/ml), red line – theoretical limit of detection, orange line – theoretical limit of quantification.

2.13 Mass spectrometry-based proteomics

Mass spectrometry proteomic analysis was performed on ACdEV isolated by size exclusion chromatography and further concentrated using a 0.5 ml 3 kDa Amicon spin column to approximately 200 µl. Protein concentration was measured using a Bradford assay (BioRad, UK) against a BSA calibration curve. Samples (30 µg) were reduced in Laemmli buffer (15 minutes at 65 °C) and loaded on 10% SDS-PAGE for protein separation (100 V constant voltage). Separated proteins were stained with Coomassie G250 blue (0.5% w/v in 40% aqueous methanol and 10% glacial acetic acid) for minimum 4 h. After destaining the gel, each sample lane was divided into five bands across all samples on a gel. Gel sections were excised, diced, and further destained in 50% acetonitrile in 50 mM ammonium bicarbonate. Destained gel pieces were dehydrated with pure acetonitrile and vacuum dried for 30 min in a vacuum concentrator (Eppendorf, UK). Gels were rehydrated on ice with 40 µl of trypsin (Sequencing grade, Promega, UK) in 6 mM ammonium bicarbonate (25:1 protein to trypsin ratio). To each sample tube 200 µl of 6mM ammonium bicarbonate was added to prevent gel dehydration and proteins were digested overnight with shaking (700 x *g*, 37 °C). Extraction of peptides from gel pieces was done sequentially with 30% and 50% of acetonitrile in 50 mM ammonium bicarbonate (15 minutes in an ultrasonic bath), followed by the dehydration in pure acetonitrile. Extracts from a single sample section were combined into one polypropylene tube, vacuum dried and stored at -20 °C prior to analysis.

Samples were reconstituted in 50 µl of 3% aqueous acetonitrile and 0.1% formic acid for liquid chromatography-coupled tandem mass spectrometry (LC-MS/MS) analysis. Peptides (5 µl) were injected onto a trap column (nanoEase M/Z Symmetry C18 Trap Column, 100Å, 5 µm, 180 µm x 20mm, Waters, UK) using a nUPLC system (Acquity M class, Waters, UK) operating in a single pump trapping mode (5 µl/min, 1 min, 1% acetonitrile in aqueous 0.1% formic acid). Peptides were separated on an analytical column (AcclaimTM, PepMapTM C18, 3 µm, 100 Å, 75 µm × 150 mm, ThermoScientific, UK) using 1% of eluent B (acetonitrile in aqueous 0.1% formic acid) at a flow rate of 0.5 µl/min applying the following gradient: 0–45 min 1–45% B, 45-49 min 45–90% B, 49–52 min 90% B, 52–67 min 1% B. Stable electrospray formed at 2200 V using a PicoTipTM emitter (New Objective, Germany) allowed for the sample to be infused into 5600 TripleTof (AB Sciex, UK) and detected while operating in information dependent mode. Thus, the 10 most intense ions from each high-resolution MS survey scan were selected for high sensitivity MS/MS, while acquired peptide ions were temporarily excluded from MS/MS acquisition for 30 s. The mass spectrometer was calibrated prior to acquisition to ensure a high mass accuracy on both MS and tandem mass spectrometry (MS/MS) levels.

Relative protein quantification was performed in a multi fraction setup using Progenesis QI for proteomics software (version 4, Nonlinear Dynamics, UK) allowing only protein-unique peptides to be used for relative quantification. MS/MS data were searched using Mascot Daemon platform (version 2.5) against the curated SwissProt database applying the following search restriction parameters: mass tolerance of 0.1 Da for MS and 0.6 Da for MS/MS spectra, a maximum of 2 trypsin missed-cleavages, Homo sapiens taxonomy, variable modifications of methionine oxidation and cysteine carbamidomethylation.

2.14 Western Blot

To extract protein, cell, or EV (UC) pellets were resuspended in lysis buffer containing 2% CHAPS, 7 M Urea, 2 M Thiourea, and 50 mM TrisHCl (pH 7.5) and agitated for 15 minutes. Lysates were then centrifuged at 14,000 x *g* for 10 minutes at 4°C and the supernatant was collected. Samples (20 µg) were reduced in Laemmli buffer (5 min at 95°C), proteins were resolved on a Mini-PROTEAN TGX gel alongside PageRuler™ Plus Prestained Protein Ladder (ThermoScientific, UK) and then transferred to nitrocellulose membrane. The membrane was probed with primary antibody for 2 hours on an orbital shaker (HRP Anti-calreticulin 1:5000, Anti-ICAM-3 1:2000). For ICAM-3, the membrane was then probed with secondary peroxidase-conjugated antibody. After three washes in TBS-Tween (0.1%), ECL substrate (Pierce, ThermoFisher) was added to the membrane and labelled proteins were detected on a G:BOX XT4 (Syngene, Cambridge, UK). Molecular weight was calculated by relative migration distance using a standard curve based on the protein ladder.

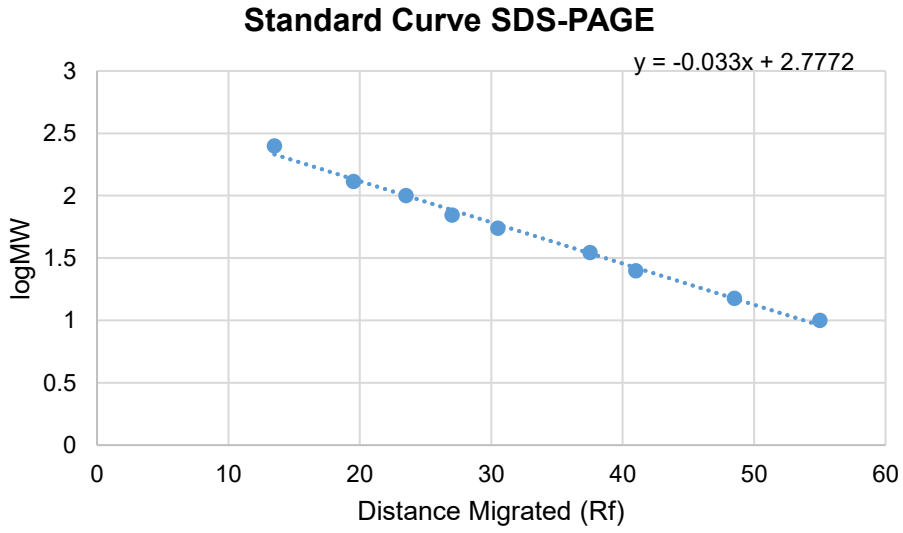

Figure 2.3 SDS-PAGE/Western blot standard curve for molecular weight (MW) estimation

2.15 Data analysis

Data handling was performed using Microsoft Excel. Flow cytometry data was analysed using the CytExpert software version 2.2 or FlowJo version 10.7.1. Images from migration assays were analysed using CellIQ analysis software. The mass spectrometry datasets (generated with Progenesis QI for proteomics, version 4.1) were analysed using functional annotation tool Funrich version 3.1.3. Production of graphs and statistical analysis was performed using GraphPad Prism 7. For statistical analysis, unpaired two-tailed t-tests or one-way ANOVA with Tukey's multiple comparisons test were used. P values less than 0.05 were considered significant: *P<0.05; **P<0.01; ***P<0.001; ****P<0.0001.

3. Results Chapter 1: Cell line model for ACdEV-macrophage interactions & immunomodulatory effects

3.1 Introduction

EVs play important roles as mediators of signalling in the immune system, promoting migration and activation of immune cells, and this has been studied in various contexts [92,110,173–175]. Less is known about the functions of EVs from apoptotic cells and the EV-associated factors that mediate them [155]. ACdEVs stimulate chemotaxis of macrophages to recruit them to sites of cell death, and the proteins CX3CL1 and ICAM-3 have been found to play key roles in this process [21,22]. The apoptotic cell 'eat me' signal calreticulin was recently shown to mediate uptake of ACdEVs by macrophages [159]. The roles of ACdEVs in regulating the immune system and the process of apoptotic cell clearance requires further study. EVs are extremely complex, carrying a vast array of different factors that may transmit important signals to recipient cells. The focus of this work is interactions of ACdEVs with macrophages, which perform the vital process of apoptotic cell clearance in a non-inflammatory manner and are central to the resolution of inflammation [3,172].

Macrophages are professional phagocytes functioning in the innate immune response as well as clearance of apoptotic cells. Macrophages can be stimulated and 'polarised' to a pro- or anti-inflammatory state depending on the stimuli in their environment. Macrophage activation states and phenotypes have been generalised into three main classes: M0, M1 and M2 [176,177]. Unstimulated, or non-polarised, macrophages are commonly referred to as M0. 'Classically activated' macrophages are pro-inflammatory, classified as M1, and macrophages with an anti-inflammatory, pro-resolving phenotype – 'alternatively activated' macrophages – are classified as M2. Subsets within the M2 classes have also been classified based on modes of activation [176]. Experimentally, a pro-inflammatory phenotype is commonly induced in macrophages using bacterial lipopolysaccharide, alone or in combination with the inflammatory cytokine interferon gamma (IFN-γ); anti-inflammatory cytokines including interleukins such as IL-4 (M2a), IL-1 and IL-10 (M2c) are used to polarise macrophages to an M2 phenotype; immune complexes in combination with LPS or IL-1β produce the M2b subtype [178]. In reality the M0/M1/M2 classification system is reductive, as macrophage activation states exist across a spectrum [179].

Polarisation of macrophages is commonly assessed using flow cytometry to measure expression of surface markers, or measurement of cytokine production [178,180].

Transcriptional profiling has also been used to identify genes differentially expressed in macrophages in different activation states [181]. There is discrepancy in the literature on which surface proteins act as markers for the different phenotypes, especially for human macrophages [177,178]. Commonly used markers of an M1 phenotype include CD14 (LPS co-receptor) and co-stimulatory molecules (involved in T cell activation) such as CD40 and CD80. CD86, another co-stimulatory molecule, is often considered an M1 marker but has been found to be a marker of the M2b subtype [182]. CD16 and CD64 are Fcγ receptors which bind to antibodies and are associated with a pro-inflammatory macrophage state. Markers used to identify an anti-inflammatory, pro-resolving M2 phenotype include the scavenger receptors CD163 and CD206 and adhesion molecules such as the integrin CD11b and CD209 (ICAM-3-grabbing non-integrin c type lectin) [177,178,181].

Immortal cell lines are often used in research as they provide a convenient, cost-effective, unlimited supply of pure cell populations and facilitate the production of reproducible results. The human monocytic THP-1 cell line is commonly used to investigate macrophage biology, however macrophages derived from these cells have behaved variably across numerous studies and do not exactly replicate the responses of primary monocyte-derived macrophages. For example, in a study by Tedesco et al. assessing the suitability of phorbol 12-myristate 13-acetate (PMA)-differentiated THP-1 cells as a reliable substitute for primary monocyte-derived macrophages, CD163 was not expressed by THP-1 cells at all, and CD206 was expressed but did not behave as an M2 marker [183]. The authors recommended that THP-1 monocyte-derived macrophages be considered a simplified model of human macrophages, as they did not entirely reproduce the spectrum of activation responses of primary macrophages [183]. In a study by Forrester et al. investigating surface receptor expression in THP-1 monocytes and macrophages, CD163 was expressed but did not behave as an M2 marker [178]. A study by Shiratori et al. compared the polarisation profiles of THP-1 macrophages with primary monocyte-derived macrophages and found that the THP-1 cell line was more suitable for studying pro-inflammatory M1 polarisation than anti-inflammatory M2 polarisation [184]. Although PMA is most commonly used to differentiate THP-1 monocytes, 1,25-dihydroxyvitamin D3 (VD3) can also be used, and there are differences in the state of differentiation; PMA induces a stronger differentiated phenotype in terms of cell adherence and loss of proliferation, and there are differences in gene expression [185,186].

3.2 Aims

The aim of this work was to establish and define a cell line model for macrophage interactions with ACdEVs, with assays to investigate the processes of chemotaxis, binding and uptake, and the effects of ACdEVs on macrophage activation state. This required establishment of a model for apoptosis, using immune cells, and isolation and basic characterisation of ACdEVs. The THP-1 monocytic cell line was utilised and assessed for its suitability for this work, by characterising the pro- and anti-inflammatory responses of THP-1-derived macrophages. The assays developed would enable later characterisation of the structure-function relationships of ACdEV, assessing the functions of ACdEV proteins in mediating macrophage responses.

3.3 Results

3.3.1 Induction of apoptosis & isolation of ACdEVs from immune cell lines

To establish a model for early and late apoptosis, Jurkat T lymphocytes and THP-1 monocytes were subjected to UV irradiation, and progression of cell death was monitored. Apoptosis is evident from cell shrinkage and blebbing observed under the light microscope (**Figure 3.1A**). Apoptosis was measured using annexin V and propidium iodide (PI) labelling of cells before and at 0, 2, 6 and 18 hours post-UV exposure (**Figure 3.1B**). Annexin V binds to phosphatidylserine which is exposed by apoptotic cells; late apoptotic or secondary necrotic cells lose their membrane integrity which means that PI is able to enter the cell. A significant shift into early apoptosis (annexin V positive, PI negative) is observed at 6 hours, and a significant shift into late apoptosis/necrosis (annexin V positive, PI positive) is observed 18 hours post-UV, where almost all cells are no longer viable (**Figure 3.1C**). A similar response is observed with THP-1 monocytes, with early and late apoptosis also at 6 and 18 hours (**Figure 3.2**).

After confirming the time points for early and late apoptosis, ACdEVs were collected from Jurkat T lymphocytes. Results from another member of the research group determined that viable cells failed to release sufficient levels of EVs for valid TPRS measurement in the supernatant, whereas supernatant from apoptotic cells contained many more EVs and required dilution for TPRS measurement, showing that apoptosis boosts EV release. Approximately twice as many ACdEVs were detected 18 h after apoptosis onset compared to 6 h in both THP-1 monocyte and Jurkat T lymphocyte cell lines. Here, cell supernatants were centrifuged to pellet cells, debris and large apoptotic bodies, and concentrated to 2 ml before size exclusion

chromatography to enrich vesicles smaller than 1 μm, separate from soluble protein to be used for EV characterisation and use in functional assays. Analysis of these SEC-isolated samples showed a 2.38-fold increase in EV-associated protein and 2.17-fold increase in the number of particles harvested from the same number of apoptotic cells at 18 hours compared to 6 hours (**Figure 3.3A & B**), consistent with the fold-increase in EVs measured in the 2000 x *g* supernatant. The size distribution of ACdEVs (**Figure 3.3C**) shows over half of the EVs isolated are between 100 and 250 nm in diameter for samples from both time points (6 h: ~58%, 18 h: ~54%), however there were smaller EVs (50-100 nm) in two out of three 18 hour samples, but no EVs smaller than 100 nm in samples collected at 6 hours. There are also fewer of the smallest (100-150 nm) EVs in the 6-hour samples. Microvesicles are ~100-1000 nm in size and exosomes are smaller than 150 nm. The mean and mode particle sizes were not significantly different between 6 and 18 hours.

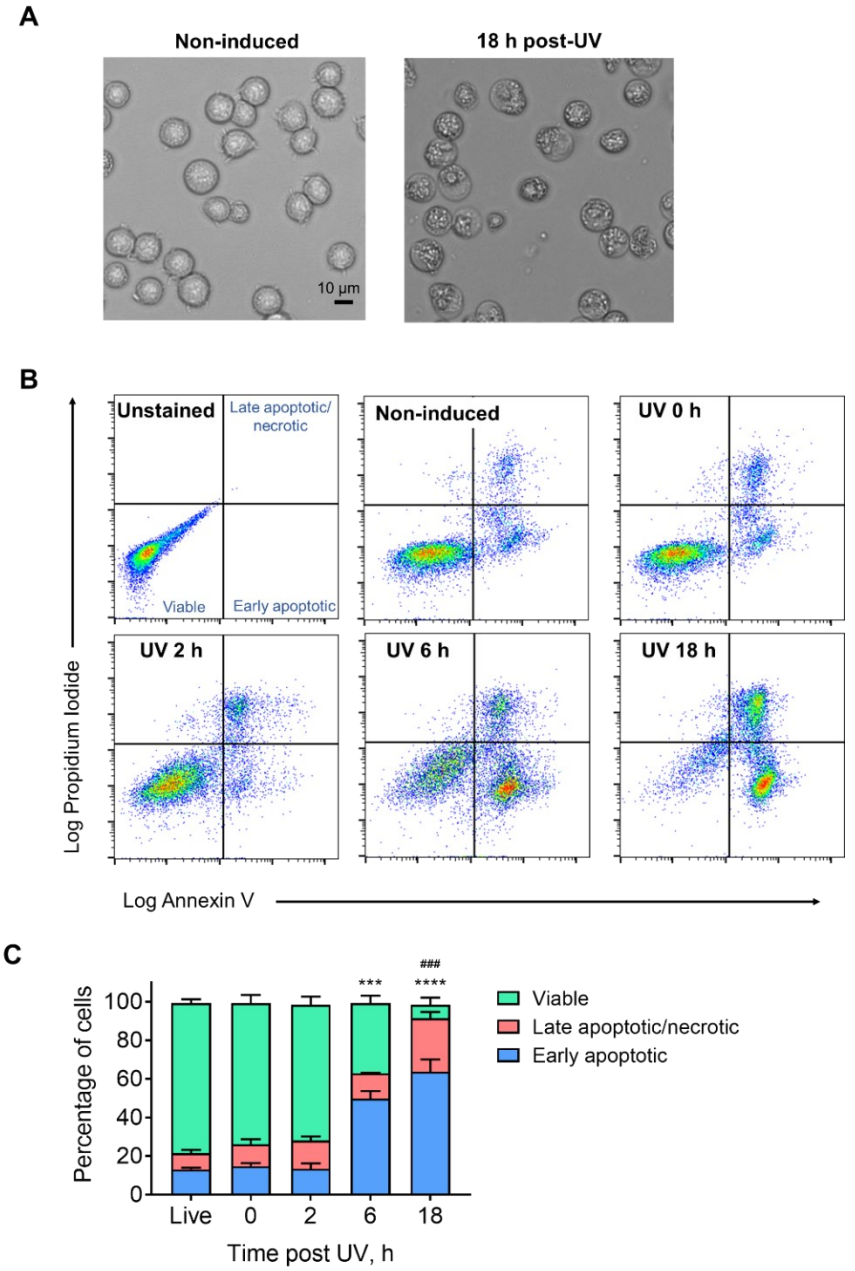

Figure 3.1: UV-induced apoptosis in T lymphocytes. Jurkat T cells were irradiated with a measured dose of UV (30 mJ/cm^2) to induce apoptosis. **(A)** Morphological features of apoptosis – membrane blebbing and cell shrinkage – observed by light microscopy. **(B)** Flow cytometry analysis of phosphatidylserine exposure (Annexin V) and loss of membrane integrity (propidium iodide) was used to determine early and late stages of apoptosis. Early apoptotic cells are positive for annexin V only, and late apoptotic/necrotic cells are also positive for propidium iodide. Representative plots shown. **(C)** Analysis of annexin V/PI (Data presented as mean + SEM, n=3. Results compared to pre-treatment by one way ANOVA and Dunnett's multiple comparisons test; *Early apoptotic cells, ***P<0.001, ****P<0.0001. #Late apoptotic/necrotic cells, ###P<0.001).

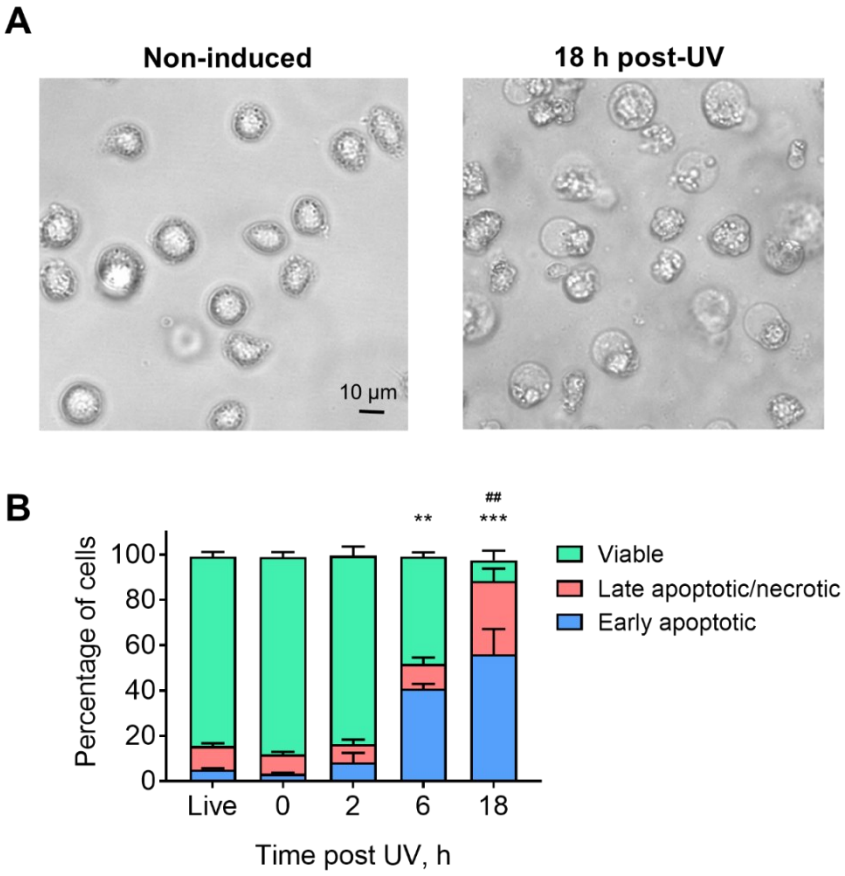

Figure 3.2: UV-induced apoptosis in monocytes THP-1 monocytes were irradiated with a measured dose of UV (30 mJ/cm2) to induce apoptosis. **(A)** Morphological features of apoptosis – membrane blebbing and cell shrinkage – observed by light microscopy. **(B)** Flow cytometry analysis of phosphatidylserine exposure (Annexin V) and loss of membrane integrity (propidium iodide) was used to determine early and late stages of apoptosis. Early apoptotic cells are positive for annexin V only, and late apoptotic/necrotic cells are also positive for propidium iodide. (Data presented as mean + SEM, n=3. Results compared to pre-treatment by one way ANOVA and Dunnett's multiple comparisons test; *Early apoptotic cells, **P<0.01, ***P<0.001. #Late apoptotic/necrotic cells, ###P<0.001).

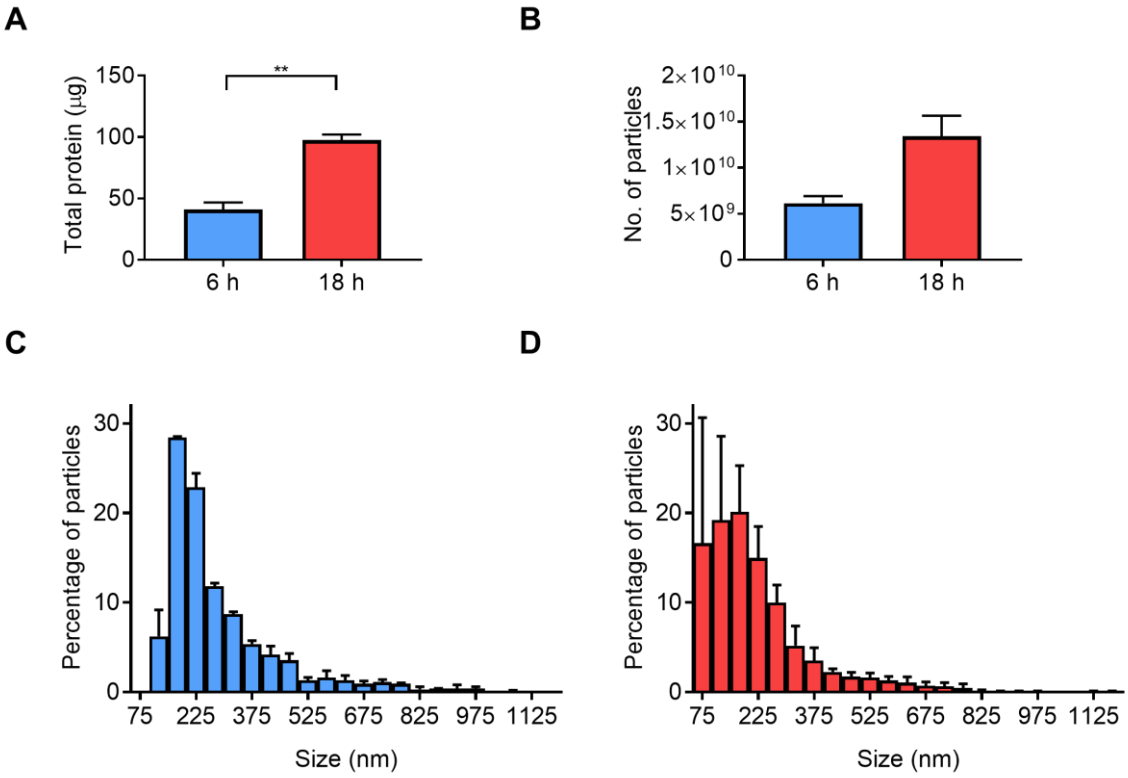

Figure 3.3: Basic analysis of apoptotic cell-derived extracellular vesicles released during early and late apoptosis after isolation by size exclusion chromatography. 1.5 x 10^8 Jurkat cells were irradiated with UV and ACdEVs were isolated using SEC in serum-free RPMI after 6 or 18 hours. **(A)** Protein concentration in ACdEV samples measured using a Bradford-based assay (n=3). **(B)** Particle concentration measured using tuneable resistive pulse sensing (TPRS). **(C)** 6 h ACdEV size distribution measured by TPRS (n=2). **(D)** 18 h ACdEV size distribution measured by TPRS (n=3). (Data presented as mean + SEM, **A & B**: Unpaired two-tailed t-test, **P < 0.01).

3.3.2 Differentiation of THP-1 monocytes to macrophages

In order to characterise the immunomodulatory effects of ACdEVs on macrophages, a cell line model was developed using the THP-1 monocytic cell line. THP-1 monocytes were differentiated to macrophages by treatment with vitamin D3 (VD3) for 48 hours, and differentiation was confirmed by flow cytometry, measuring the levels of surface expression of CD14 and CD11b. Both markers increased significantly after treatment (**Figure 3.4**). CD14 was constitutively expressed on all THP-1 monocytes but significantly upregulated in response to treatment with VD3, with a 31.6-fold increase in expression (mean fluorescence intensity; MFI) on average within the whole population. There was an 8.79-fold increase in overall levels of CD11b within the whole population (MFI), where CD11b was expressed on approximately 63% of THP-1 monocytes before treatment and 96% of cells following treatment with VD3. VD3 treated cells also became slightly more adherent, with many cells sticking to the cell culture plastic.

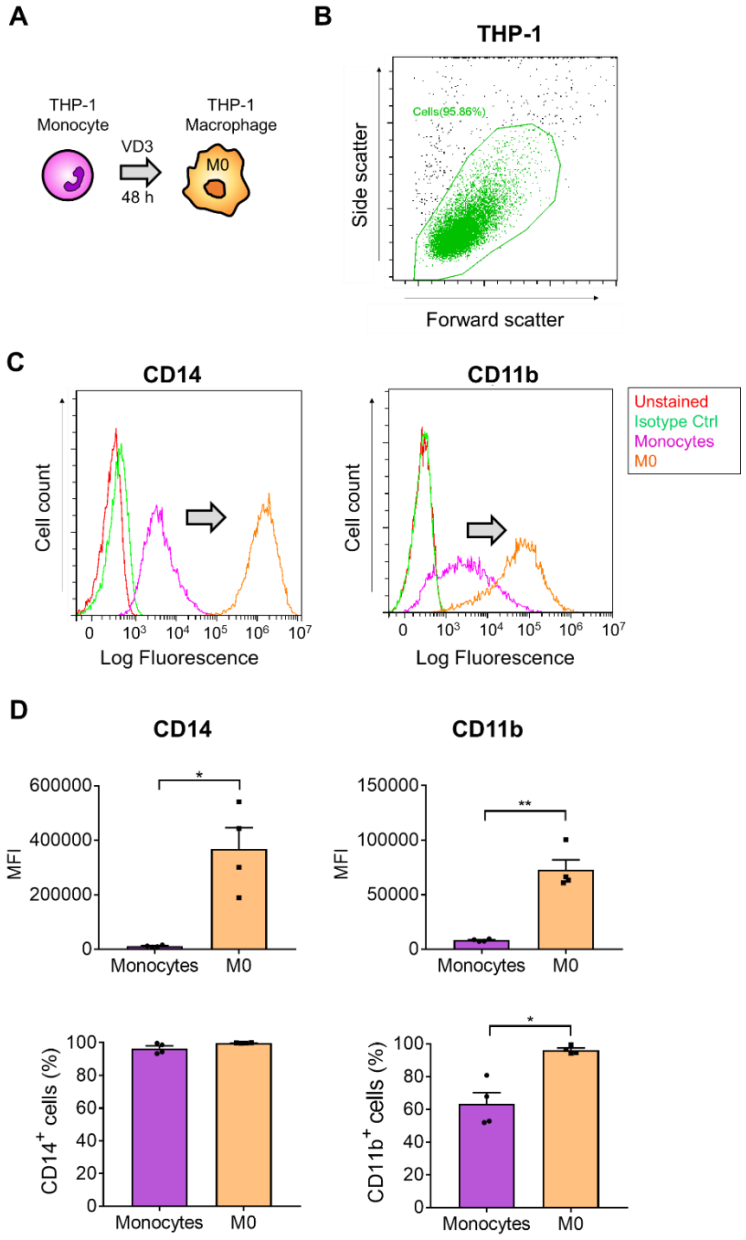

Figure 3.4: THP-1 cell line model of monocyte-derived macrophages: cell surface markers of differentiation. **(A)** THP-1 monocytes were treated with dihydroxyvitamin D3 (VD3; 100 nM) for 48 hours to produce non-polarised macrophages (M0). **(B)** Cells were analysed before and after treatment by flow cytometry. Cells were gated on forward and side scatter. **(C)** Representative histograms showing expression of differentiation markers CD14 and CD11b in monocytes before (purple) and after treatment with VD3 (M0; orange). **(D)** Expression of CD14 and CD11b shown as mean fluorescence intensity (MFI) of the entire cell population (minus isotype control background), and percentage of cells in the population expressing the markers. (Data presented as mean + SEM, n=4, Paired two-tailed t-test, *P<0.05, **P<0.01).

3.3.3 ACdEV-induced macrophage chemotaxis

Apoptotic cells release 'find me' signals to recruit phagocytes in a timely manner [15]. The ability of different apoptotic cell secretomes and their constituent parts (EVs and soluble factors) to promote macrophage recruitment has been previously investigated by this research group, using a vertical transwell migration assay; the early (6 hour) apoptotic secretome was found to be more attractive to macrophages than the late (18 hour) secretome, perhaps supporting the concept that apoptotic cells must direct their rapid clearance to avoid the consequences of secondary necrosis. Both ACdEV and soluble factors in the supernatant from early apoptotic cells (separated by ultracentrifugation, UC) were shown to contribute to macrophage recruitment. Size exclusion chromatography (SEC) has become a popular method for isolation of EVs, effectively enriching EVs with high purity and without applying extreme force. Here, in a vertical migration assay T cell-derived ACdEVs isolated by SEC lost their chemoattractive capacity, whereas ACdEVs isolated by UC attracted macrophages similarly to the whole supernatant which contains both EVs and soluble factors (**Figure 3.5**). These results suggest support the hypothesis that in some cases, a sensitive 'corona' of factors adsorbed to the EV surface, such as proteins, may be responsible for or support EV functions. Care must be taken when studying the function of EVs with reductionist approaches.

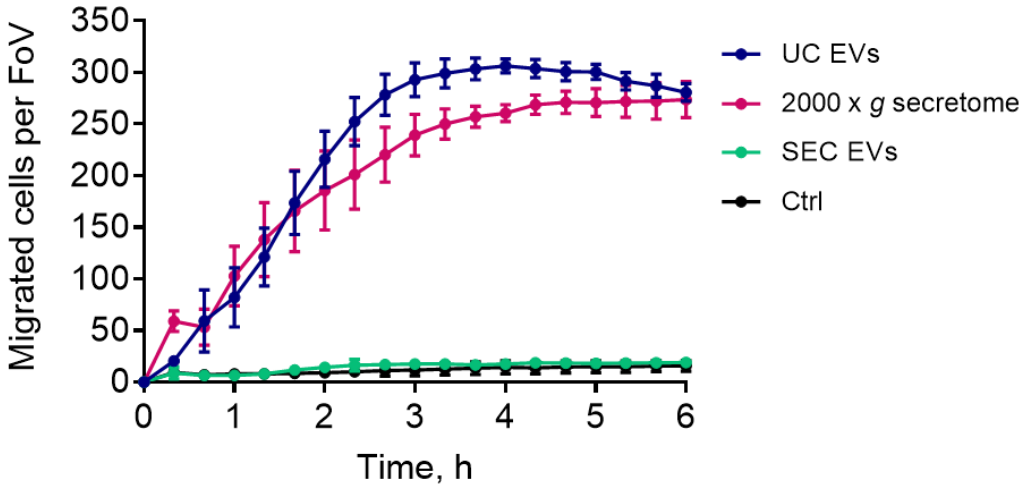

Figure 3.5: Macrophage chemotaxis towards ACdEVs can be affected by EV isolation method. Chemotaxis was assessed using a vertical migration assay. Migration towards T cell (Jurkat) derived secretome (2000 x *g* supernatant), UC-isolated ACdEVs and SEC-isolated ACdEVs harvested at 18 h post-induction of apoptosis, compared to serum-free medium-only control. (Data presented as mean ± SEM, n=3).

3.3.4 Binding and uptake of ACdEVs by macrophages

In order to analyse the binding and uptake of ACdEVs by macrophages, a flow cytometry-based assay was used. EVs were labelled with a thiol-reactive membrane dye (BODIPY FL maleimide), before isolation by SEC, also removing any excess dye. VD3-differentiated THP-1 cells were incubated with EVs for up to 4 hours. Cells were collected at intervals and washed before analysis by flow cytometry. At 30 minutes a large increase in macrophage fluorescence is observed, with approximately half of cells exhibiting fluorescence. After 30 minutes both the percentage of macrophages positive for fluorescence and the overall level of fluorescence in the cell population increases steadily, though at a rate slower than the initial interaction rate (**Figure 3.6A**). Increasing the concentration of the membrane dye from 1 μM to 5 μM meant that the number of apoptotic cells and ACdEVs used could be decreased 5-fold; the histogram shown in **Figure 3.6B** shows that macrophages rapidly associate with ACdEVs as fluorescence is detected in around 60% of cells at the 0 time point where cells were immediately washed after addition of EVs, and increase in fluorescence is shown by further shifts in fluorescence at 10 minutes, 30 minutes and 60 minutes.

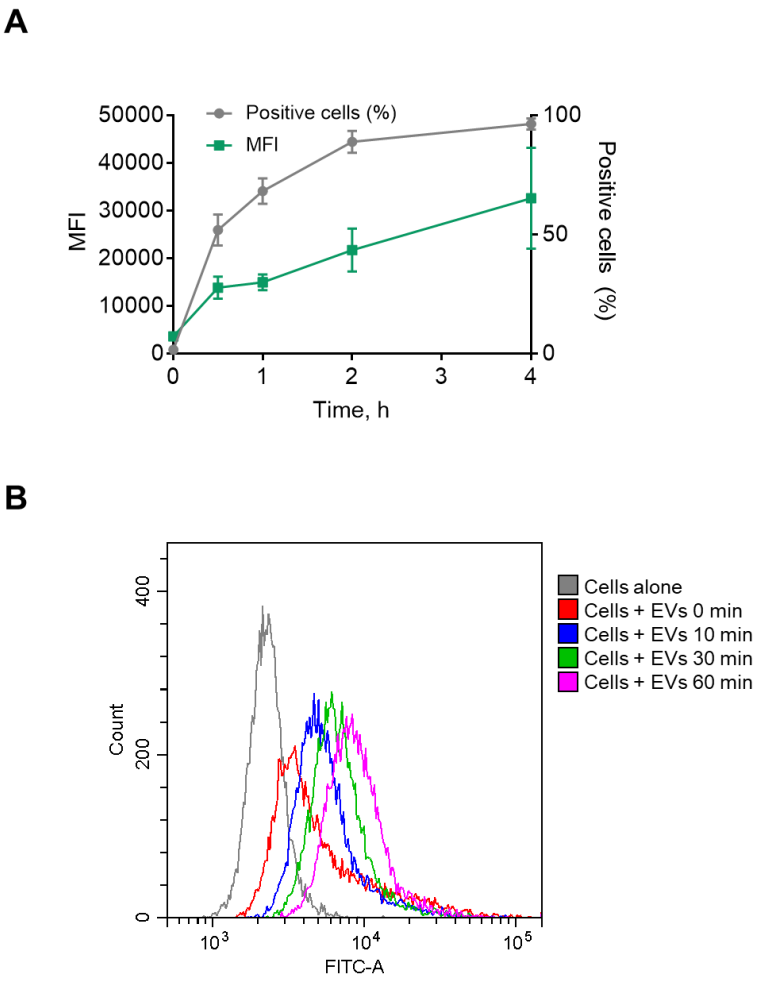

Figure 3.6: Macrophage binding/uptake of ACdEVs. (A) ACdEVs from apoptotic T cells were fluorescently labelled (1 μM BODIPY FL maleimide) and isolated by size exclusion chromatography. The binding and uptake of ACdEVs and macrophages over time was determined by flow cytometry. Data show the mean fluorescence intensity of the whole cell population and the percentage of cells positive for fluorescence, over time. (Data presented as mean ± SEM, n=3). **(B)** ACdEVs from apoptotic T cells were fluorescently labelled with a higher concentration of BODIPY FL maleimide (5 μM), isolated by SEC and interaction (binding/uptake) of ACdEVs by macrophages over time was determined by flow cytometry. Histogram shows acquired fluorescence of macrophages over time.

3.3.5 ACdEV-induced polarisation of THP-1 monocyte-derived macrophages assessed using cell surface phenotypic markers

In order to characterise the polarising effects of ACdEVs on macrophages, the macrophage model was first phenotypically characterised. The protocol for differentiation of monocytes to macrophages (M0, non-polarised) and polarisation to pro-inflammatory ('classical' activation, M1) or anti-inflammatory, pro-resolution ('alternative' activation, M2) is illustrated in **Figure 3.8A**. Differentiation of THP-1 monocytes to macrophages was achieved by treatment with VD3. Lipopolysaccharide (LPS, 100 ng/ml) or interleukin-4 (IL-4, 20 ng/ml) were used to polarise M0 macrophages to M1 or M2, respectively for 24 and 48 hours. Cells treated with LPS became more strongly adherent with more elongated morphology, whereas cells treated with IL-4 remained rounded and were loosely adherent or in suspension (**Figure 3.7**). Expression of macrophage markers was determined by flow cytometry; a panel of cell surface proteins associated with pro- or anti-inflammatory macrophage phenotypes were assessed to determine the best markers. CD14 is constitutively expressed in all conditions (positive cells 100%), but expression is significantly higher with LPS compared to IL-4 at 48 hours (**Figure 3.8B**). Expression of CD40 and CD80 increased after treatment with LPS, but not IL-4; CD40 is constitutively expressed in all conditions but expression increased more than 10-fold based on MFI when cells were treated with LPS, with no difference between 24- and 48-hour incubation times. CD80 levels (MFI) increased significantly with LPS and the percentage of macrophages expressing CD80 increased significantly from 4.5% to 72% on average. For the other pro-inflammatory markers tested, changes in CD64 expression were inconsistent across replicates and CD16 expression was also very variable between replicates and was mostly expressed by a small percentage of cells.

The scavenger receptors CD163 and CD206, considered to be anti-inflammatory, M2 markers, were not detected on THP-1 monocytes or macrophages after any of the treatments (). CD11b expression was highest in macrophages after 48 hours with IL-4, but not significantly different from macrophages treated with LPS for 48 hours (**Figure 3.8B**). Another potential marker of the M2 anti-inflammatory phenotype, CD209 was then investigated. CD209 shows significant upregulation with IL-4 after 48 hours (**Figure 3.8B**). MFI increased only with 48-hour IL-4 treatment. IL-4 the percentage of CD209 positive cells increased to and ~44% at 48 hours.

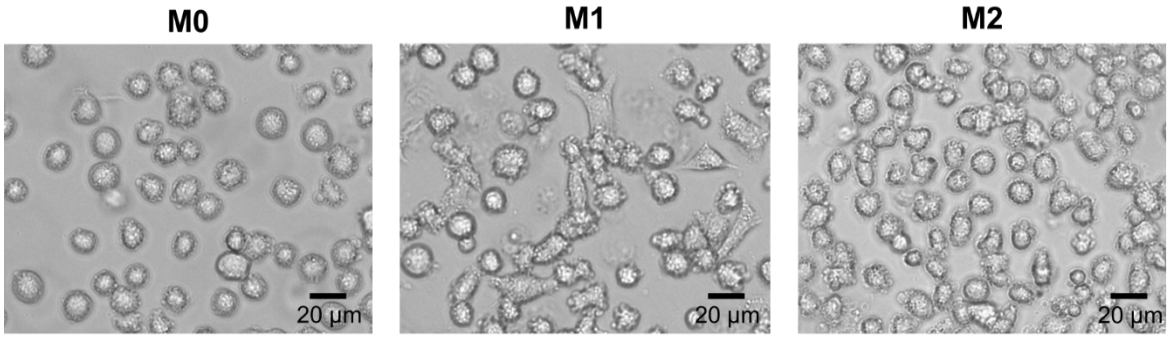

Figure 3.7: Morphology of non-polarised (M0) pro-inflammatory (M1) and anti-inflammatory (M2) THP-1 macrophages. THP-1 monocytes were differentiated to macrophages by treatment with vitamin D3 (M0) then LPS or IL-4 were added to polarise cells towards a pro- (M1) or anti-inflammatory (M2) phenotype, respectively. A change in morphology and increase in adherence is observed in M1, whereas M2 macrophages remain round in shape and mostly in suspension.

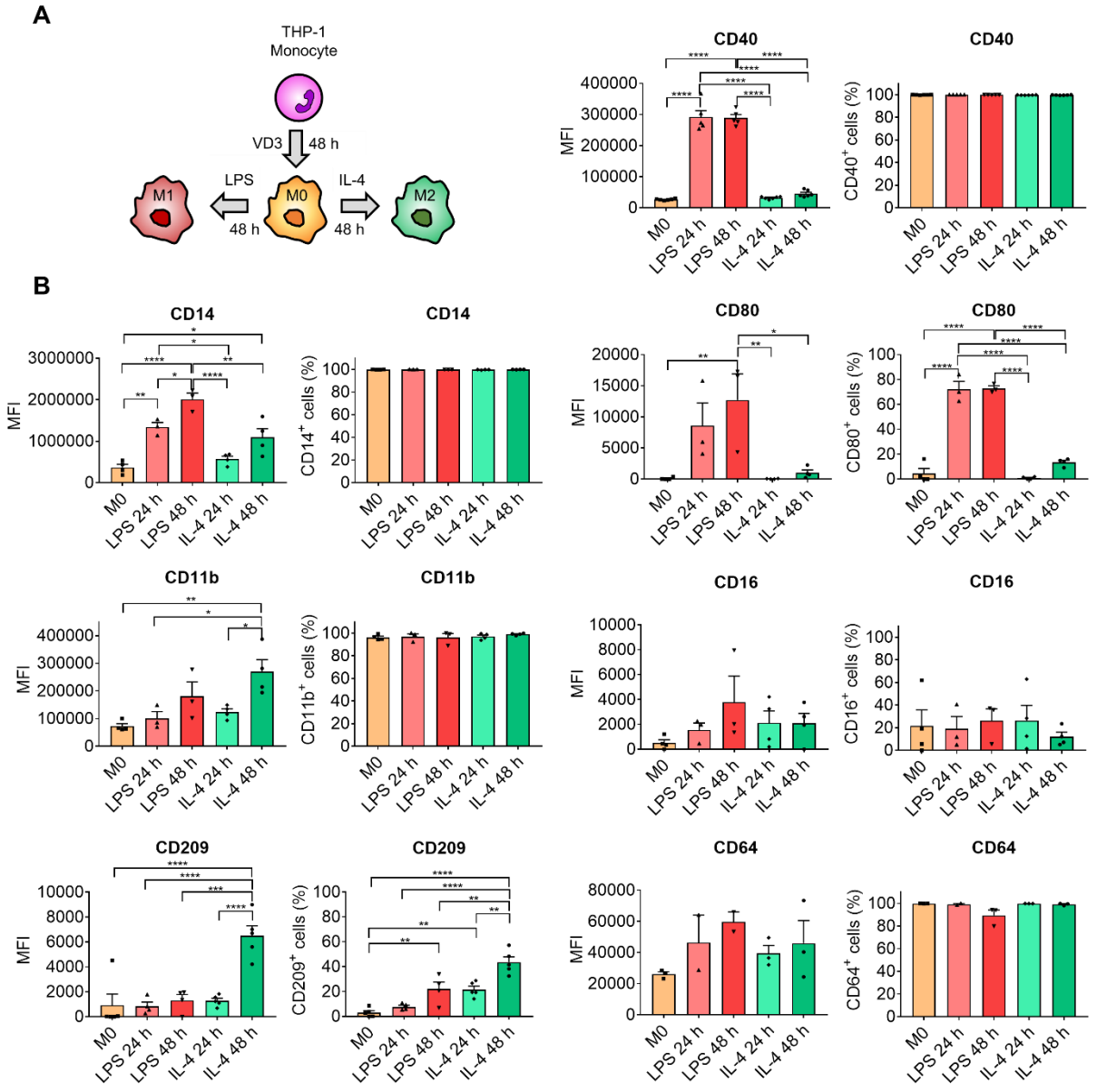

Figure 3.8: Establishing surface markers of polarised macrophage phenotypes. (A) Monocyte-derived macrophages were generated by incubation of THP-1 monocytes with vitamin D3 for 48 hours (5 x 10^5 cells/ml) before addition of a pro- or anti-inflammatory polarising stimulus: LPS at 100 ng/ml or IL-4 at 20 ng/ml, respectively. **(B)** Protein expression was measured for a panel of surface markers by flow cytometry, at 24 and 48 hours. Expression is represented by mean fluorescence intensity (MFI) and percentage of positive cells. Cells did not express CD163 or CD206 under any of the conditions. (Data presented as mean + SEM, n=3; statistical analysis by one-way ANOVA with Tukey's multiple comparisons test; *P<0.05, **P<0.01, ***P<0.001, ****P<0.0001).

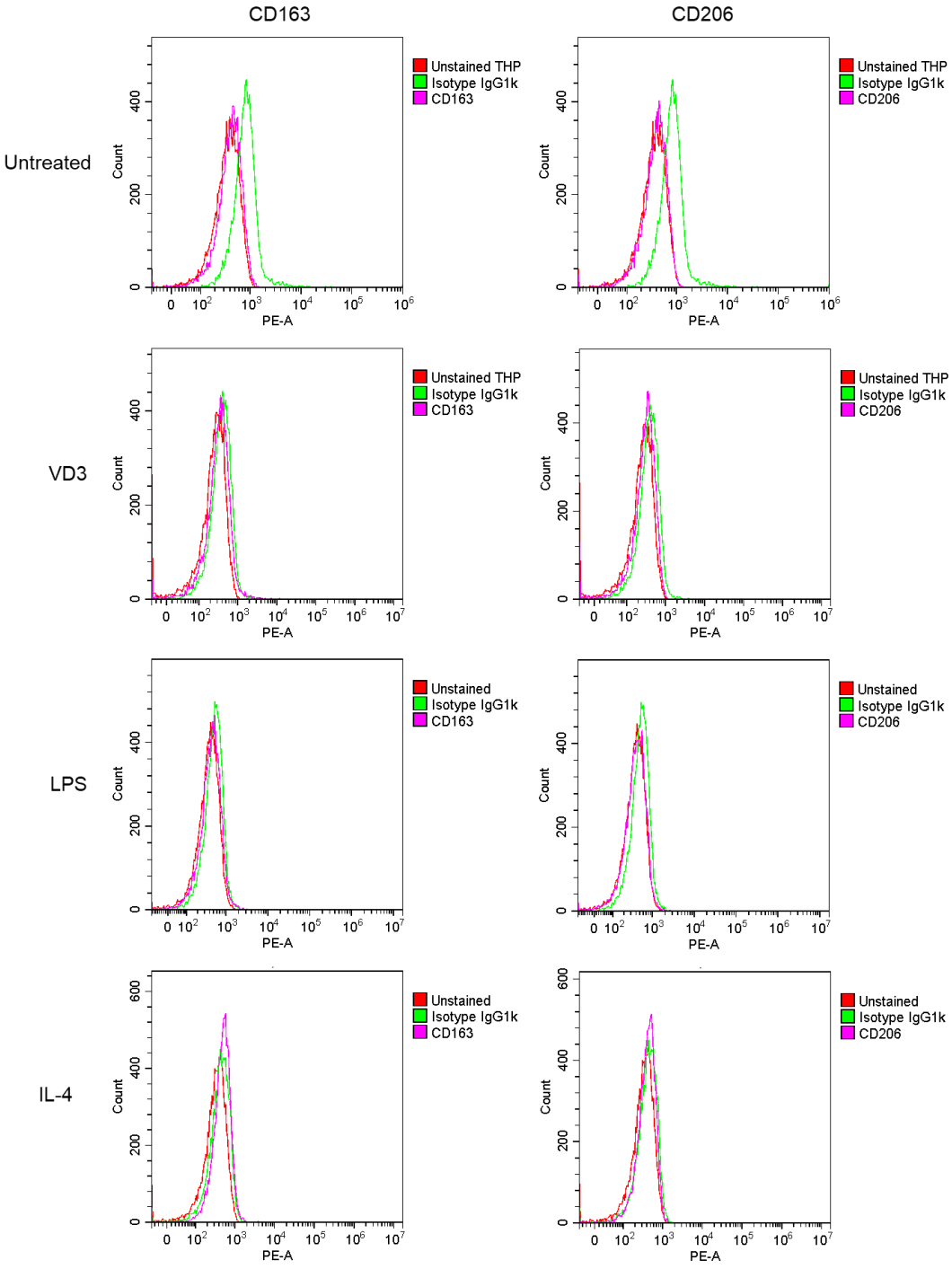

Figure 3.9: THP-1 monocytes and VD3-macrophages do not express CD163 or CD206. Expression of CD163 and CD206 on the surface of THP-1 monocytes, macrophages derived by treatment with VD3, and macrophages polarised with LPS or IL-4 was assessed by flow cytometry. Representative histograms showing unstained (red), antibody isotype control (green) and CD163/CD206-stained cells (pink).

To investigate the ability of ACdEVs to alter macrophage phenotype, non-polarised (M0) macrophages were treated with ACdEVs from early apoptotic and late apoptotic T cells isolated by SEC, and changes in expression of surface markers selected from the previous panel were analysed. Macrophages were also treated with LPS or IL-4 in parallel, as reference pro-inflammatory (M1) and anti-inflammatory (M2) cells, respectively. Surprisingly, both early apoptotic and late apoptotic/necrotic ACdEVs caused non-polarised macrophages to change their surface marker expression similarly to pro-inflammatory M1 macrophages, indicated by a significant increase in expression of CD14, CD40 and CD80, and no change in M2 marker CD209 expression (**Figure 3.10**). There was no significant difference between the measured phenotypic response of macrophages exposed to early apoptotic and late apoptotic/necrotic vesicles, where there were approximately twice as many vesicles in the late apoptotic sample, suggesting a maximal response in upregulation of expression of the protein markers evaluated and possibly highlighting a lower dose of EV may be sufficient to achieve this maximal response. Considering the effect of SEC on ACdEV-mediated macrophage chemoattraction, to investigate whether SEC also affects how ACdEVs polarise macrophages, the same experiment was performed with ACdEVs isolated by UC from early apoptotic Jurkat T cells, and a similar pro-inflammatory effect was observed (**Figure 3.11**). EV samples isolated by UC had slightly higher protein content compared to SEC samples, indicating that SEC separates EVs from soluble protein more effectively (**Figure 3.12**).

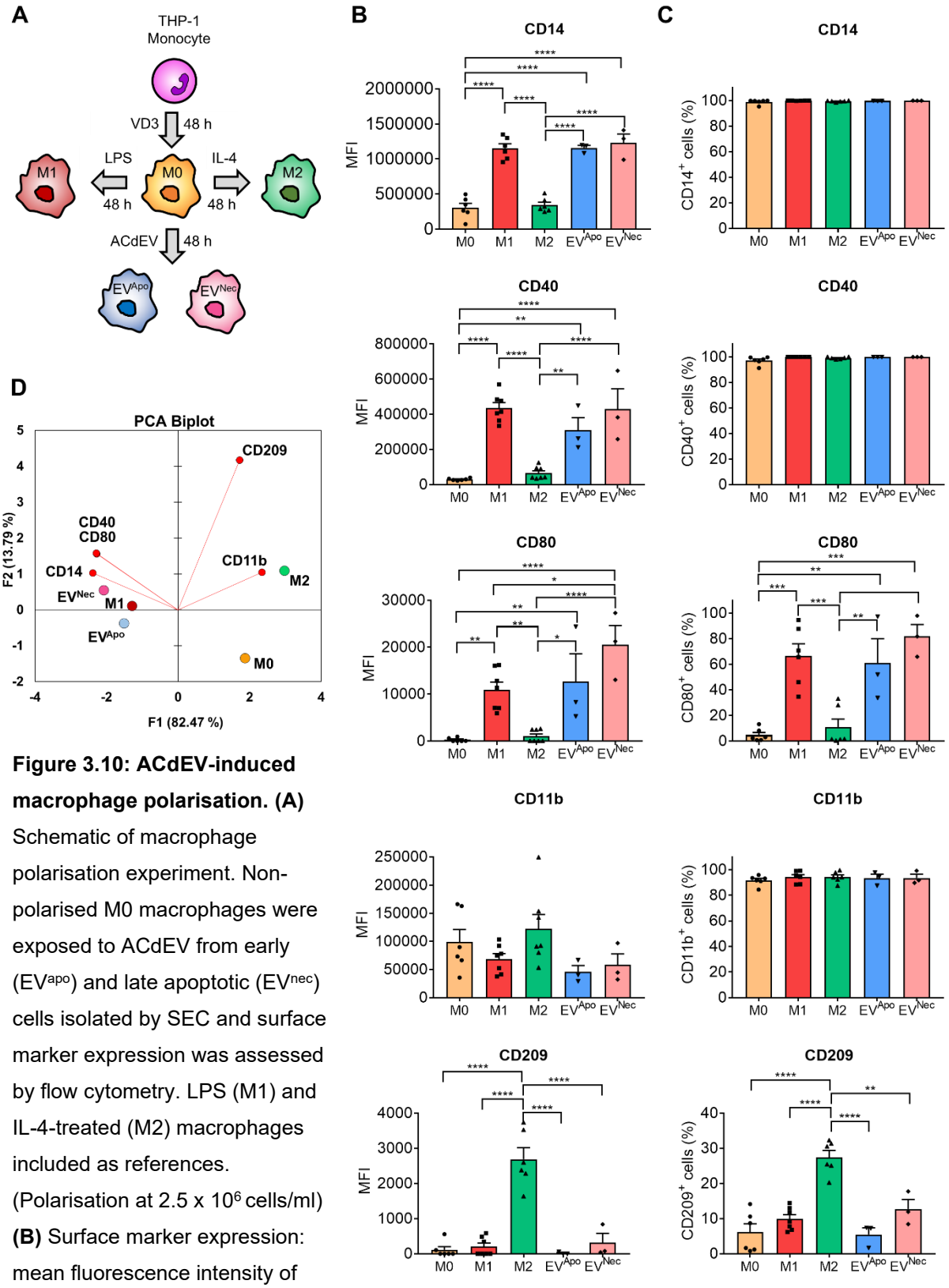

Figure 3.10: ACdEV-induced macrophage polarisation. (A) Schematic of macrophage polarisation experiment. Non-polarised M0 macrophages were exposed to ACdEV from early (EV^{apo}) and late apoptotic (EV^{nec}) cells isolated by SEC and surface marker expression was assessed by flow cytometry. LPS (M1) and IL-4-treated (M2) macrophages included as references. (Polarisation at 2.5 x 10^6 cells/ml) **(B)** Surface marker expression: mean fluorescence intensity of whole cell population **(C)** Percentage of cells expressing marker **(D)** Principal component analysis of phenotype in each of the treatments (average MFI). (Data are shown as mean + S.E.M, n=3-6; statistical analysis by one-way ANOVA with Tukey's multiple comparisons test; *P<0.05, **P<0.01, ***P<0.001, ****P<0.0001).

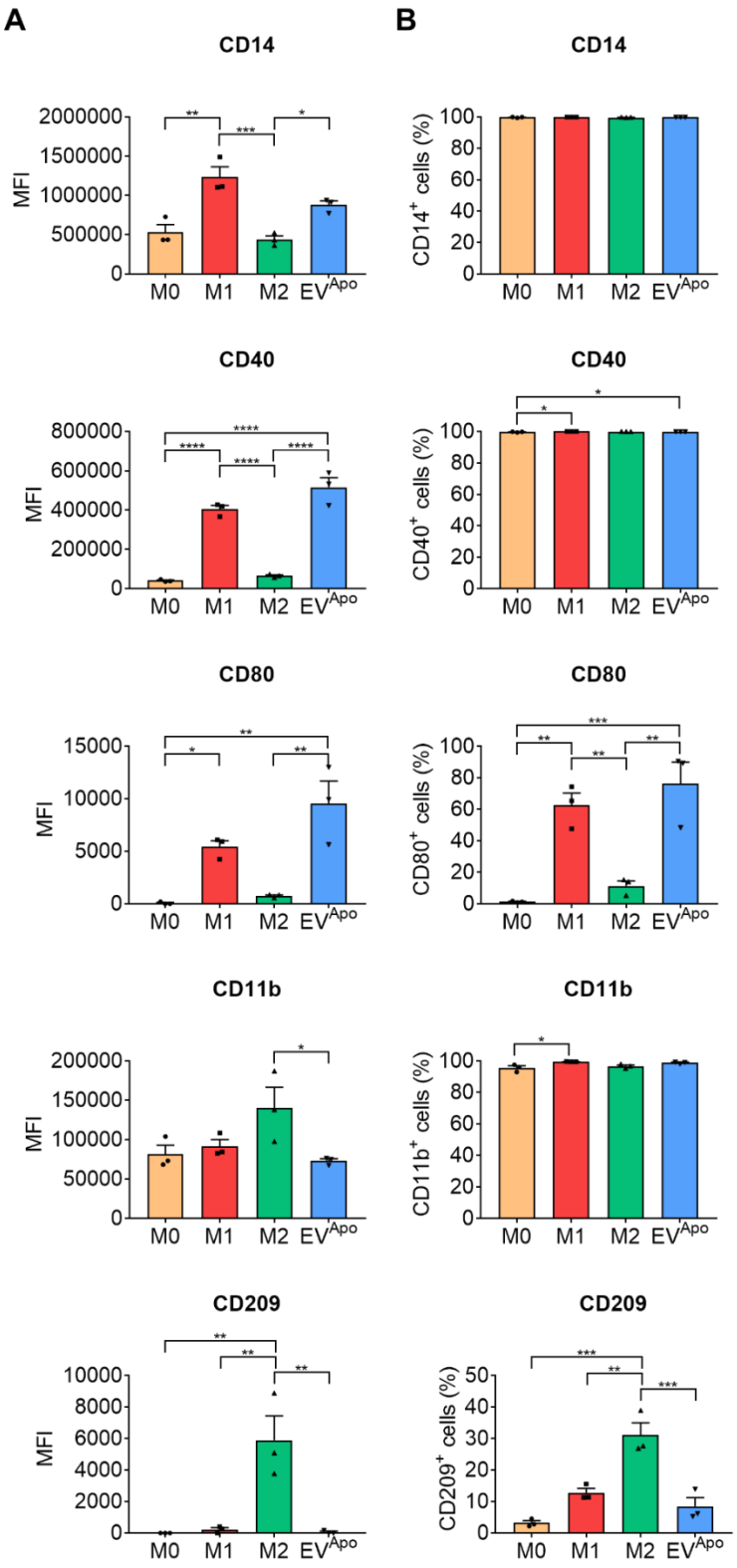

Figure 3.11: ACdEVs isolated by UC induce a similar polarising response in macrophages to those isolated by SEC. Non-polarised M0 macrophages were exposed to ACdEV from early apoptotic cells (EV^{apo}) isolated by UC and surface marker expression was assessed by flow cytometry. LPS (M1) and IL-4-treated (M2) macrophages included as references. **(A)** Surface marker expression: mean fluorescence intensity of whole cell population **(B)** Percentage of cells expressing marker. (Data are shown as mean + S.E.M, n=3; statistical analysis by one-way ANOVA with Tukey's multiple comparisons test; *P<0.05, **P<0.01, ***P<0.001, ****P<0.0001).

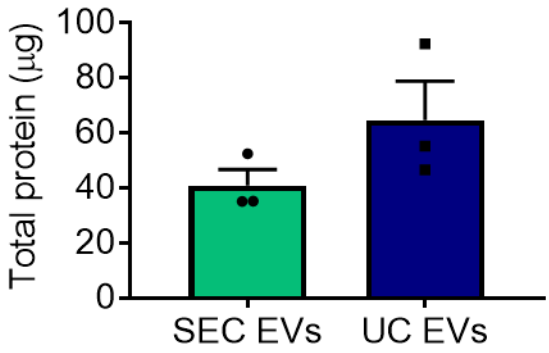

Figure 3.12: Protein content of ACdEV samples isolated by SEC versus UC. ACdEVs collected from 1.5 x 10^8 apoptotic T cells (Jurkat) 6 hours after induction of apoptosis. (Data presented as mean + SEM, n=3; Unpaired two-tailed t-test, not significant).

3.3.6 PMA-differentiated vs VD3-differentiated THP-1 monocyte-derived macrophages as models for macrophage polarisation

PMA is commonly used to differentiate monocytes to macrophages in vitro. PMA and VD3 stimulate differentiation via different signalling pathways [185]. In order to determine whether macrophages produced using PMA behave differently to VD3 macrophages, and assess different *in vitro* models of macrophage phenotype, THP-1 monocytes were treated with VD3 (100 nM), PMA (250 nM) or both (double-stimulated; DS). Whereas VD3-differentiated cells are not fully adherent and adherent cells can be easily detached by gentle scraping or pipetting, PMA treatment produces strongly adherent, elongated cells. PMA-treated and double-stimulated cells required treatment with EDTA (5 mM) before gentle scraping in order to detach with minimal damage to the cells. Observation under light microscope suggests that PMA-treated macrophages fused to form multinucleated giant cells (**Figure 3.13A**). VD3-treated cells maintain some proliferative capability and expand approximately 1.5-fold in 48 hours whereas approximately half the number of PMA-treated cells are recovered (**Figure 3.13B**). Forward and side scatter flow cytometry plots show that PMA-treated cells are larger on average and more heterogeneous in size and granularity, and that cell viability is lower for cells treated with PMA, as a significant population of dead cells is seen outside of the live cell region (**Figure 3.13C**). Cells differentiated using PMA also have higher auto-fluorescence in the PE channel, which means that gating stained samples requires adjustment for the different cell types (**Figure 3.13D**). Changes in the phenotype of THP-1 cells following treatment for differentiation to macrophages were also assessed using flow cytometry to measure cell

surface marker expression (**Figure 3.14**). The batch of THP-1 monocytes used for these experiments did not constitutively express CD14 (approximately 45% of cells were CD14-positive), unlike the batch used in the previous experiments. However, consistent with previous results, VD3 stimulated significant upregulation of CD14 expression, which was also seen for double-stimulated cells. The percentage of CD14-positive cells increased to above 98% and the MFI increased significantly. Cells treated with PMA alone had relatively low levels of CD14 but the percentage of positive cells did increase to 82.5% on average. A similar pattern was observed for CD11b expression. CD16 was expressed on only 2-3% of cells on average under all conditions. As observed previously, expression of CD40 on THP-1 cells is unaffected by VD3 treatment. PMA however significantly upregulated expression of CD40. For double-stimulated cells, VD3 appears to slightly counteract this effect, as the MFI is slightly lower, although not statistically significant. Expression of CD64 was slightly higher after treatment with VD3, whereas treatment with PMA significantly downregulated expression of CD64, reducing the MFI 2.5-fold and reducing the percentage of CD64-positive cells by 30%. Double-stimulated cells behaved similarly to cells treated with PMA alone in terms of CD64 expression. CD80 expression was low for all differentiation conditions, with no significant differences in MFI, but the percentage of positive cells varied for PMA-treated cells, where up to 20.66% of PMA-treated cells were positive for this marker. CD86 expression was significantly upregulated in cells treated with VD3 alone, with a 1.8-fold average increase in MFI and an increase from 10.7% to 20% of cells expressing CD86, compared to untreated monocytes. The effect of VD3 on CD86 expression was counteracted by PMA in the double-stimulated cells, where the percentage of positive cells was unchanged, and MFI was slightly lower for PMA and double-stimulated cells. CD163, CD206 and CD209 were not expressed on monocytes or M0 macrophages treated with VD3 and/or PMA.

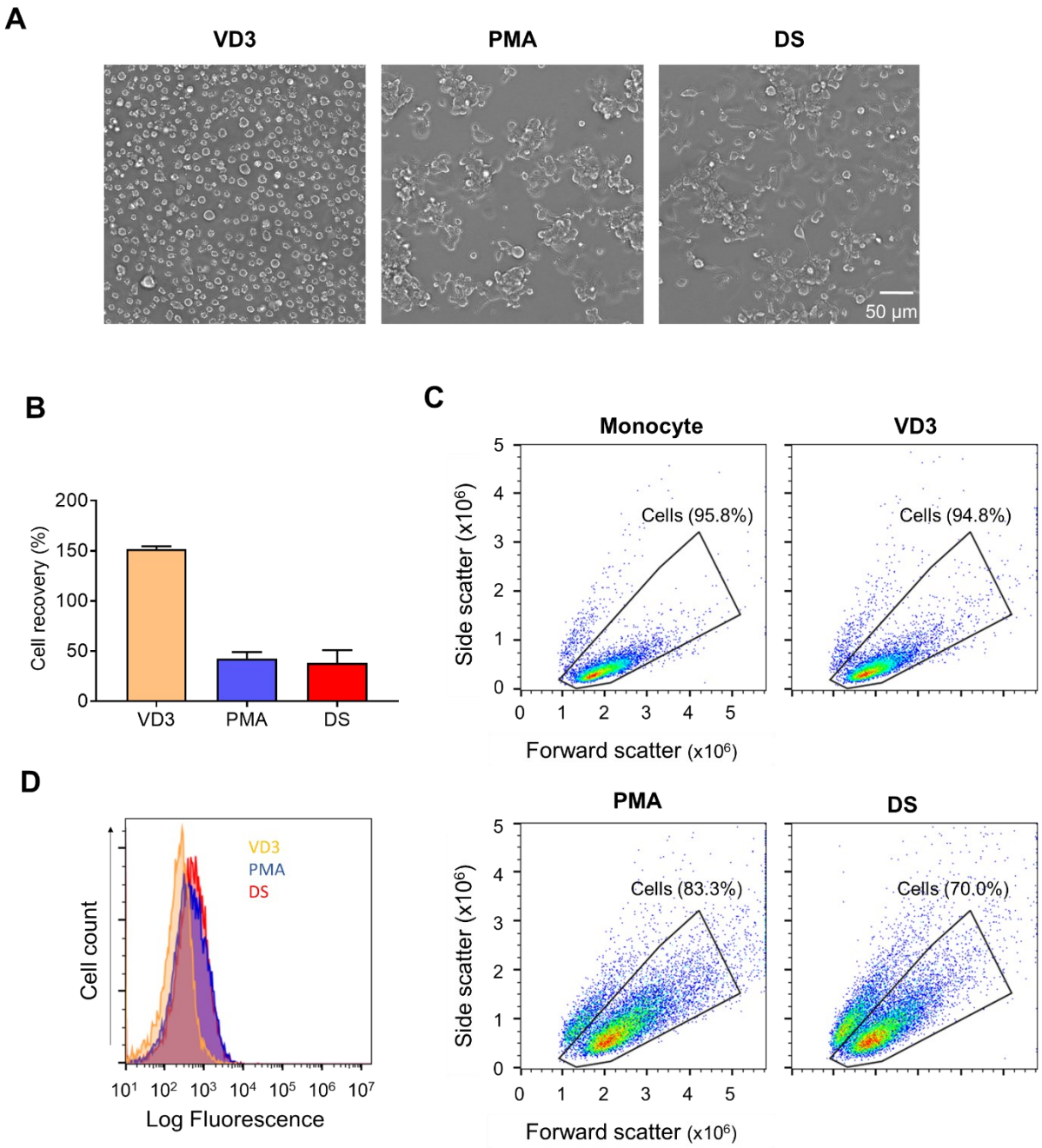

Figure 3.13: Comparison of THP-1 monocyte differentiation to macrophages using VD3 and/or PMA by microscopy and flow cytometry. Cells were treated with 100 nM VD3 and/or 250 nM PMA for 48 hours. **(A)** Morphology of differentiated THP-1 cells viewed under light microscope. **(B)** Recovery of cells after 48-hour differentiation. (Data shown as mean + S.E.M, n=3). **(C)** Forward and side scatter flow cytometry plots showing size (FSC) and granularity (SSC) of THP-1 cells before and after differentiation. Live cells are gated, and percentage of all events shown. **(D)** Auto-fluorescence of THP-1 macrophages in PE channel.

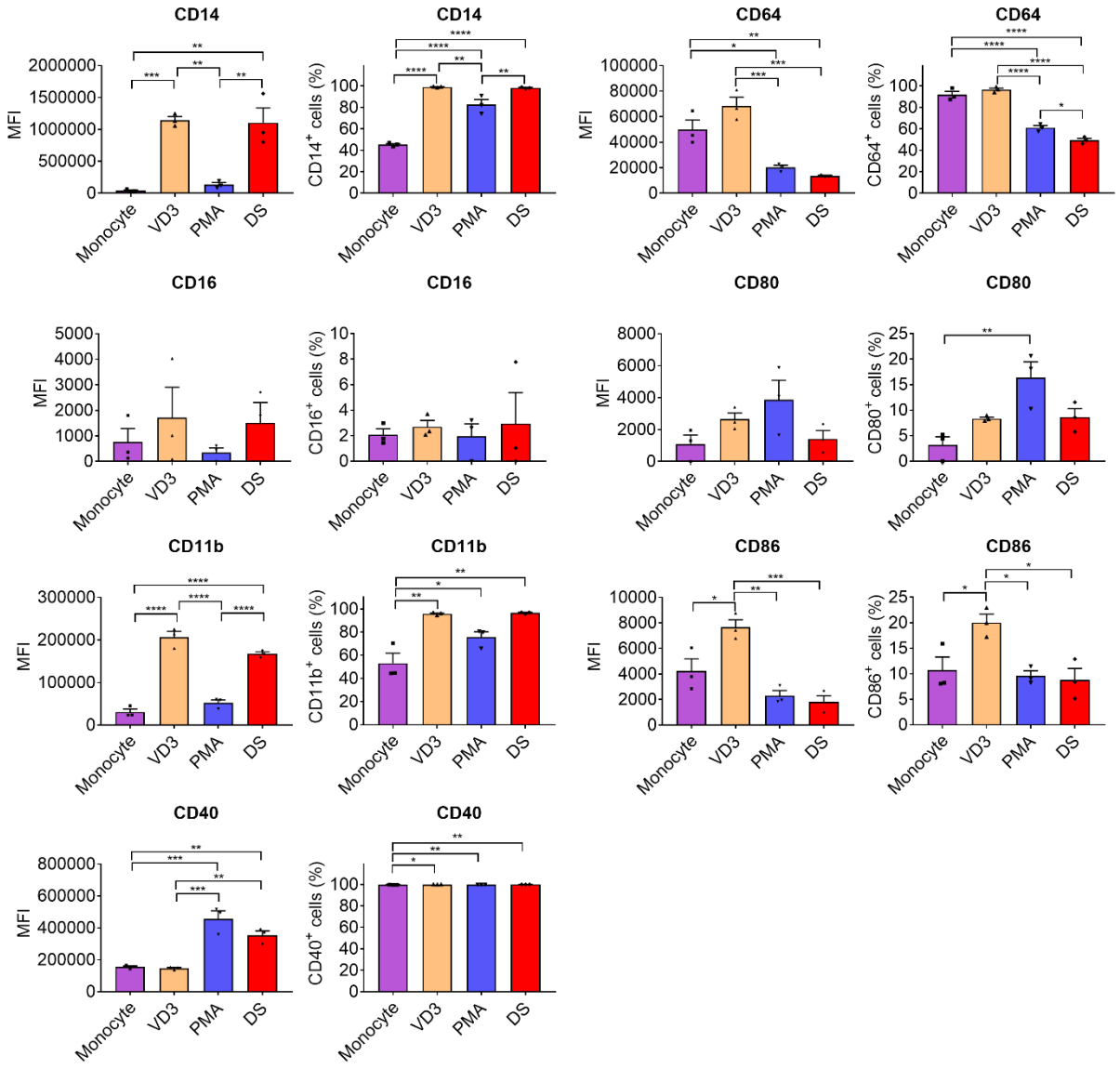

Figure 3.14: Effects of differentiation treatment on THP-1 cell surface protein expression. THP-1 monocytes (1 x 10^6 cells/ml) were treated with 100 nM VD3 and/or 250 nM PMA for 48 hours. Surface marker expression before and after differentiation was analysed by flow cytometry. (Data shown as mean + S.E.M, n=3; statistical analysis by one-way ANOVA with Tukey's multiple comparisons test; *P<0.05, **P<0.01, ***P<0.001, ****P<0.0001). CD163, CD206 and CD209 were not expressed under any of the conditions.

Polarisation of THP-1 macrophages produced by treatment with VD3 and/or PMA to pro- (M1) and anti-inflammatory (M2) phenotypes was also assessed using flow cytometry to measure expression of cell surface markers (**Figure 3.15**). Cells were treated with LPS or IL-4 for 48 hours. Consistent with earlier experiments, for VD3-treated cells, the levels of M1 markers CD14, CD40 and CD80 were significantly higher in LPS-treated cells compared to IL-4 treated. CD11b was significantly upregulated in VD3 macrophages after IL-4 treatment (M2), and CD209 expression was induced only in M2-polarised macrophages.

CD14 expression remained low in PMA treated cells after both polarising treatments and did not distinguish M1 from M2. Interestingly, double-stimulated macrophages downregulated expression of CD14 in response to both LPS and IL-4, with a slightly greater decrease in M2 cells. For VD3 macrophages, CD16 expression was highest in M1, however only 24.72% of cells were positive for CD16. Conversely, CD16 expression in PMA macrophages was significantly higher in M2 compared to M1 and M0 (non-polarised), with the MFI for M1 approximately 6.5-fold higher than M2, and 32.18% were expressing this marker. Double-stimulated macrophages showed a similar trend in CD16 expression to PMA macrophages, although differences in MFI were not statistically significant. CD11b expression was much lower on PMA and double-stimulated macrophages compared to VD3 macrophages. For PMA macrophages, the percentage of cells expressing CD11b was significantly higher in M2 compared to M1 and M0. For double-stimulated cells, CD11b was expressed on almost all cells in all conditions, but MFI was lower in M1 and M2 compared to M0 (not significant).

CD40 is significantly upregulated in M1 for VD3 macrophages. As shown in **Figure 3.13**, PMA treatment alone stimulates an increase in CD40 expression, and the level of CD40 is maintained in M1 and M2. CD64 expression did not differ between M0, M1 and M2 for VD3 macrophages. For PMA and double-stimulated cells, where differentiation treatment had already downregulated CD64 expression, polarisation with LPS or IL-4 further decreased expression of this protein on the cell surface. CD80 behaves as an M1 marker in VD3 macrophages, however for PMA macrophages the percentage of positive cells is significantly higher in M2 compared to M1 and M0, and expression is very low in double-stimulated cells. For VD3 macrophages, CD86 was similarly upregulated in response to LPS and to IL-4 and so did not distinguish M1 from M2. For PMA macrophages, the proportion of cells expressing CD86 was significantly higher in M2 macrophages at 45.66% compared to 18.5% for M1 and 9.62% for M0. CD209 expression was induced in 53.99% of IL-4 treated M2 VD3 macrophages on average and not expressed in M0 or M1 VD3 macrophages. CD209 expression was also induced in M2 PMA macrophages but only in 10.55% of cells. CD209 expression in PMA/VD3

double-stimulated macrophages was induced in only 1 of 3 biological replicates, in 10.4% of cells. The results show that VD3 macrophages behave very differently to PMA in terms of cell surface phenotype, and pro- or anti-inflammatory responses in PMA-differentiated macrophages could not be definitively defined by any of the markers tested.

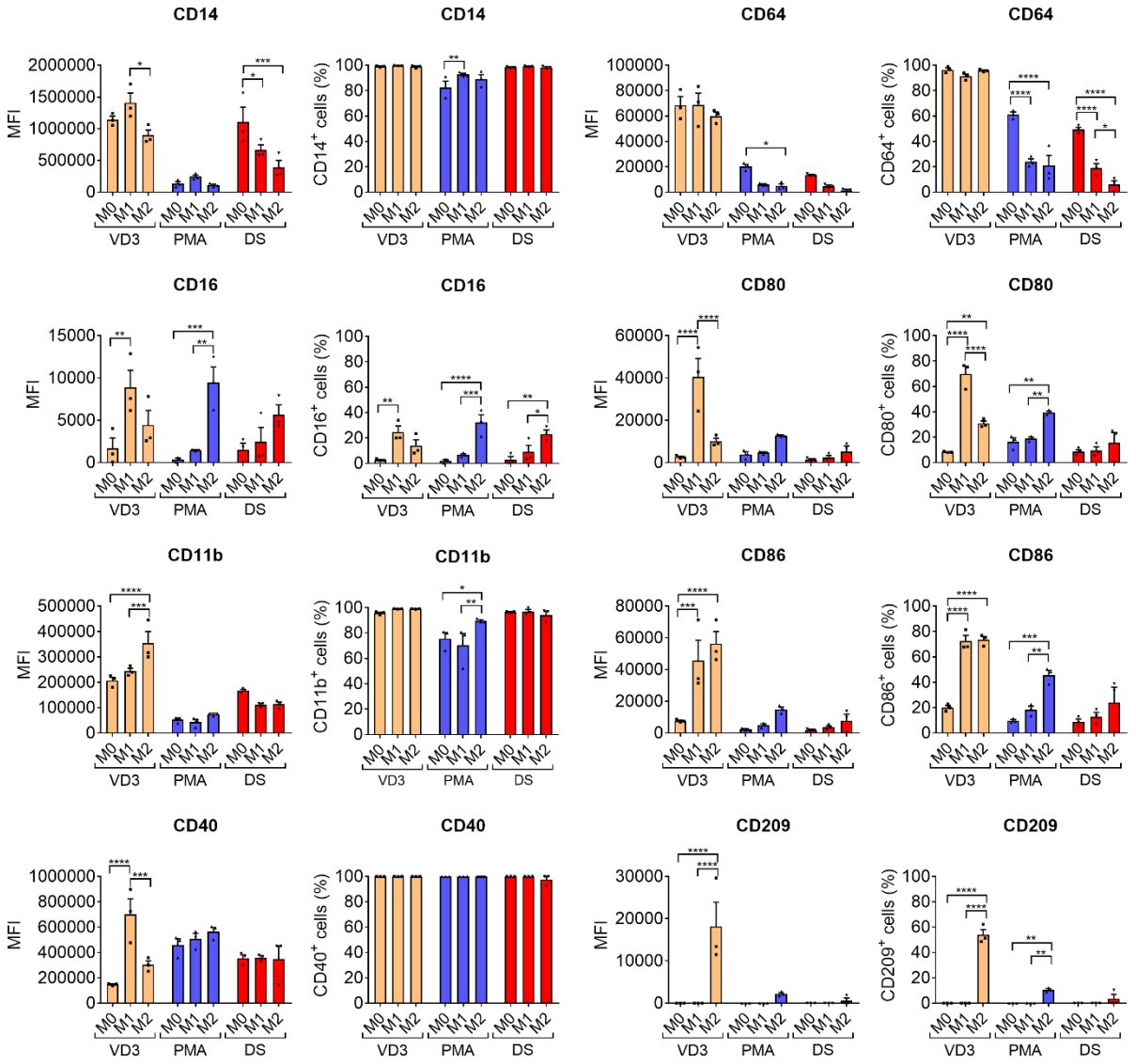

Figure 3.15: Polarisation of THP-1 macrophages differentiated with VD3 and/or PMA. THP-1 monocytes were treated with VD3 and/or PMA for 48 hours (M0) and then polarised to a pro- (M1) or anti-inflammatory (M2) phenotype by 48-hour treatment with LPS or IL-4, respectively. Surface marker expression before and after polarisation was analysed by flow cytometry. (Data shown as mean + S.E.M, n=3; statistical analysis by two-way ANOVA with Tukey's multiple comparisons test within VD3, PMA and DS groups; *P<0.05, **P<0.01, ***P<0.001, ****P<0.0001). CD163 and CD206 were not expressed under any of the conditions.

3.3.7 ACdEV-induced polarisation of THP-1 monocyte-derived macrophages assessed by cytokine release

As macrophage phenotypic responses were similar for ACdEVs from early apoptotic and late apoptotic/necrotic cells in regards to cell surface marker expression, the inflammatory state of the macrophages in response to ACdEVs was assessed by measurement of cytokine release. The concentrations of a panel of pro- and anti-inflammatory cytokines were measured in supernatants harvested from macrophages using a flow cytometry-based assay. As before, THP-1 monocytes were differentiated to macrophages (M0) using VD3 for 48 hours. Then M0 macrophages were polarised to M1 or M2 with LPS or IL-4, respectively, for 48 hours; macrophages (M0) were also treated with ACdEVs from early apoptotic or late apoptotic/necrotic Jurkat T lymphocytes, isolated from cell supernatants by UC or SEC, for 48 hours.

Interleukins

Following differentiation of THP-1 macrophages (M0), no IL-2 was detected in the supernatant. Both LPS (M1) and IL-4 (M2) induced secretion of IL-2 (**Figure 3.16A**), although IL-2 released by macrophages in response to IL-4 was significantly higher compared to LPS. Notably, ACdEVs induce IL-2 secretion from M0 macrophages, though the secretion of IL-2 in response to ACdEVs was not significantly different for ACdEVs from early apoptotic and late apoptotic/necrotic cells. Furthermore, the responses to ACdEVs from early or late apoptotic cells were not significantly different from either M1 or M2, although there was more variation between samples for ACdEVs derived from necrotic cells (ACdEVs isolated by SEC, **Figure 3.16B**). Comparing the cytokine response to ACdEVs isolated by different methods, SEC versus UC, IL-2 secretion in response to ACdEVs from early apoptotic cells was similar (**Figure 3.16C**), and also not significantly different between isolation methods for ACdEVs from late apoptotic/necrotic cells (**Figure 3.16D**).

IL-1β secretion was significantly upregulated in pro-inflammatory (M1) macrophages compared to non-polarised (M0) and anti-inflammatory (M2) macrophages (**Figure 3.17A**). Macrophages exposed to ACdEVs from both early apoptotic and late apoptotic/necrotic cells produced an even greater increase in IL-1β release (**Figure 3.17B**). There was no difference in the effect of ACdEVs from early apoptotic cells using SEC versus UC (**Figure 3.17C**), however the concentration of IL-1β was higher with SEC-isolated ACdEVs compared to UC-isolated from late apoptotic/necrotic cells (**Figure 3.17D**). Secretion of IL-6 was significantly

upregulated in pro-inflammatory (M1) macrophages compared to non-polarised (M0) and anti-inflammatory (M2) macrophages (**Figure 3.18A**). ACdEVs isolated from late apoptotic/necrotic cells produced a similar response to M1, whereas ACdEVs from early apoptotic cells produced significantly higher levels of IL-6 (**Figure 3.18B**). The IL-6 response to ACdEVs was consistent between isolation methods (**Figure 3.18C, D**). IL-10 was not detected in the supernatant of non-polarised macrophages, and the secretion of IL-10 was induced in M1 but not in M2 macrophages **Figure 3.19A**. Release of IL-10 was stimulated by ACdEVs; concentrations were quite variable between replicates, however IL-10 levels were generally slightly higher in response to ACdEVs from early apoptotic versus necrotic cells (**Figure 3.19B**), and higher in response to ACdEVs isolated by UC versus SEC (**Figure 3.19C, D**)

C-X-C motif chemokine ligands

Secretion of C-X-C motif chemokine ligand 8 (CXCL8) was induced in both M1 and M2 macrophages (**Figure 3.20A**), although the concentration was significantly (~200-fold) higher for M1 vs M2. The response to ACdEVs was similar to the M1 response, and similar between ACdEVs from early apoptotic and necrotic cells, and between ACdEVs isolated by SEC and UC. CXCL10, also known as interferon γ-induced protein 10 (IP-10), was present in the supernatant of M0 THP-1 macrophages at a low concentration (~7.0 pg/ml), and polarisation with LPS (M1) induced an approximately 100-fold increase in CXCL10 levels which was significantly higher than the approximately 5-fold increase in response to IL-4 (M2) (**Figure 3.21A**). ACdEVs from both early apoptotic and late apoptotic/necrotic cells stimulated CXCL10 secretion similarly to the pro-inflammatory response to LPS (**Figure 3.21B**). CXCL10 release in response to ACdEVs isolated by SEC was greater compared to ACdEVs isolated by UC from both apoptotic and necrotic cells (**Figure 3.21C, D**).

TNFα

The pro-inflammatory cytokine TNFα was not detected in the supernatant of non-polarised macrophages and secretion of TNFα was induced in both M1 and M2 macrophages, but was significantly higher (approximately 300-fold) in M1 macrophages (**Figure 3.22A**). Secretion of TNFα was even greater when M0 macrophages were exposed to ACdEVs, with a similar response to ACdEVs from both early apoptotic and necrotic cells (**Figure 3.22B**), and ACdEVs isolated by SEC or UC produced similar responses (**Figure 3.22C, D**).

IL-17A, CCL2, IFN-γ, IL-12p70 & TGF-β1

IL-17A was not secreted by non-polarised macrophages but was induced in response to IL-4 (M2), and not induced in cells exposed to LPS (M1; **Figure 3.23A**). Secretion of the chemokine C-C motif ligand 2 (CCL2), also known as monocyte chemoattractant protein 1 (MCP-1), did not distinguish M1 and M2 phenotypes from each other (**Figure 3.23B**). CCL2 secretion in response to ACdEVs was generally higher compared to the M1 and M2 responses, however CCL2 levels varied greatly between replicates. Secretion of the other cytokines examined, IFN-γ, IL-12p70 and free active TGF-β1, also did not distinguish the M1 and M2 phenotypes, and there was no difference between the levels secreted in response to ACdEVs from early apoptotic versus necrotic cells, and no difference between the effects of ACdEVs isolated by (**Figure 3.23C-E**). The cytokine responses are summarised in **Table 3.1**.

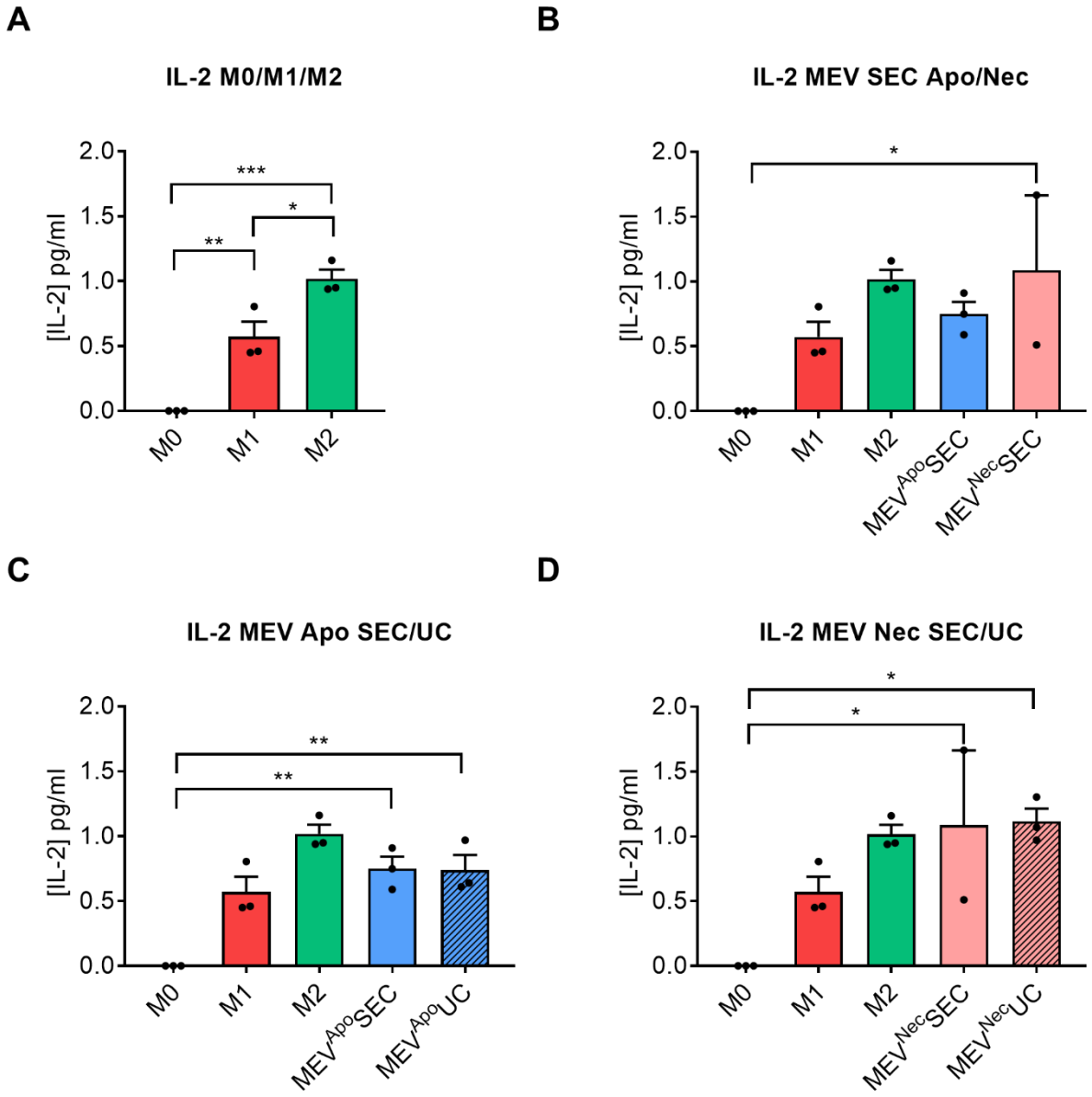

Figure 3.16: IL-2 secretion by polarised THP-1 macrophages. Cytokine concentration was measured in supernatants of THP-1 macrophages using flow cytometry. **(A)** THP-1 monocytes were differentiated to macrophages using VD3 (M0) and then polarised to pro- or anti-inflammatory phenotype with LPS (M1) or IL-4 (M2). **(B)** Non-polarised (M0) macrophages were exposed to ACdEVs from early apoptotic (EV^{Apo}) or late apoptotic/necrotic (EV^{Nec}) Jurkat T lymphocytes isolated by size exclusion chromatography (SEC). **(C)** Comparison of the effect of EV^{Apo} isolated by SEC versus ultracentrifugation (UC). **(D)** Comparison of the effect of EV^{Nec} isolated by SEC versus UC. (Data shown as mean + S.E.M, statistical analysis: one way ANOVA with Tukey's multiple comparisons test **(A)**; one way ANOVA with Sidak's multiple comparisons test **(B-D)** comparing selected groups [MEV groups compared to each other and to M0/M1/M2]; *P<0.05, **P<0.01; ***P<0.001).

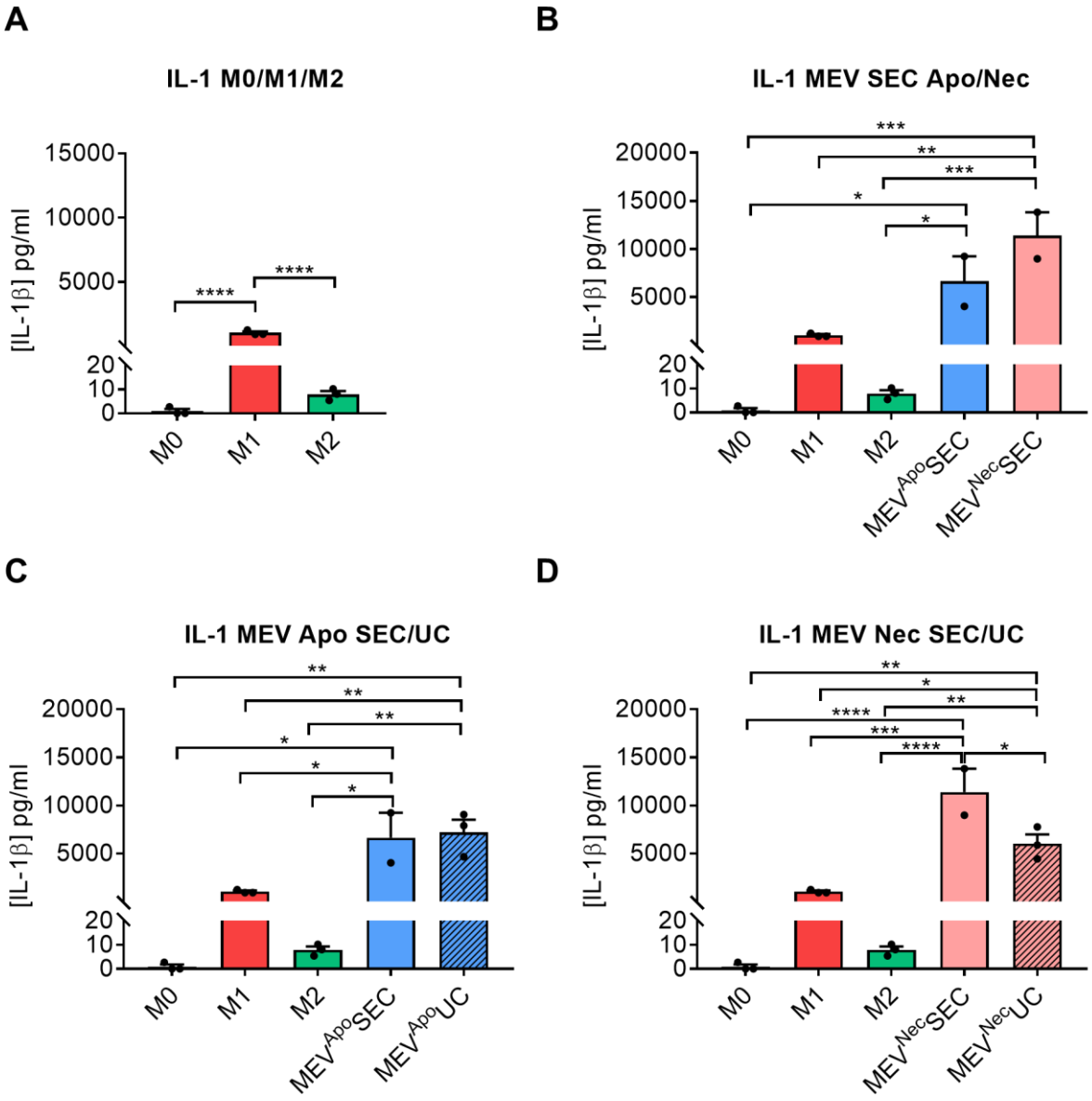

Figure 3.17: IL-1β secretion by polarised THP-1 macrophages. Cytokine concentration was measured in supernatants of THP-1 macrophages using flow cytometry. **(A)** THP-1 monocytes were differentiated to macrophages using VD3 (M0) and then polarised to pro- or anti-inflammatory phenotype with LPS (M1) or IL-4 (M2). **(B)** Non-polarised (M0) macrophages were exposed to ACdEVs from early apoptotic (EV^{Apo}) or late apoptotic/necrotic (EV^{Nec}) Jurkat T lymphocytes isolated by size exclusion chromatography (SEC). **(C)** Comparison of the effect of EV^{Apo} isolated by SEC versus ultracentrifugation (UC). **(D)** Comparison of the effect of EV^{Nec} isolated by SEC versus UC. (Data shown as mean + S.E.M, statistical analysis: one way ANOVA with Tukey's multiple comparisons test **(A)**; one way ANOVA with Sidak's multiple comparisons test **(B-D)** comparing selected groups [MEV groups compared to each other and to M0/M1/M2]; *P<0.05, **P < 0.01; ***P<0.001, ****P<0.0001).

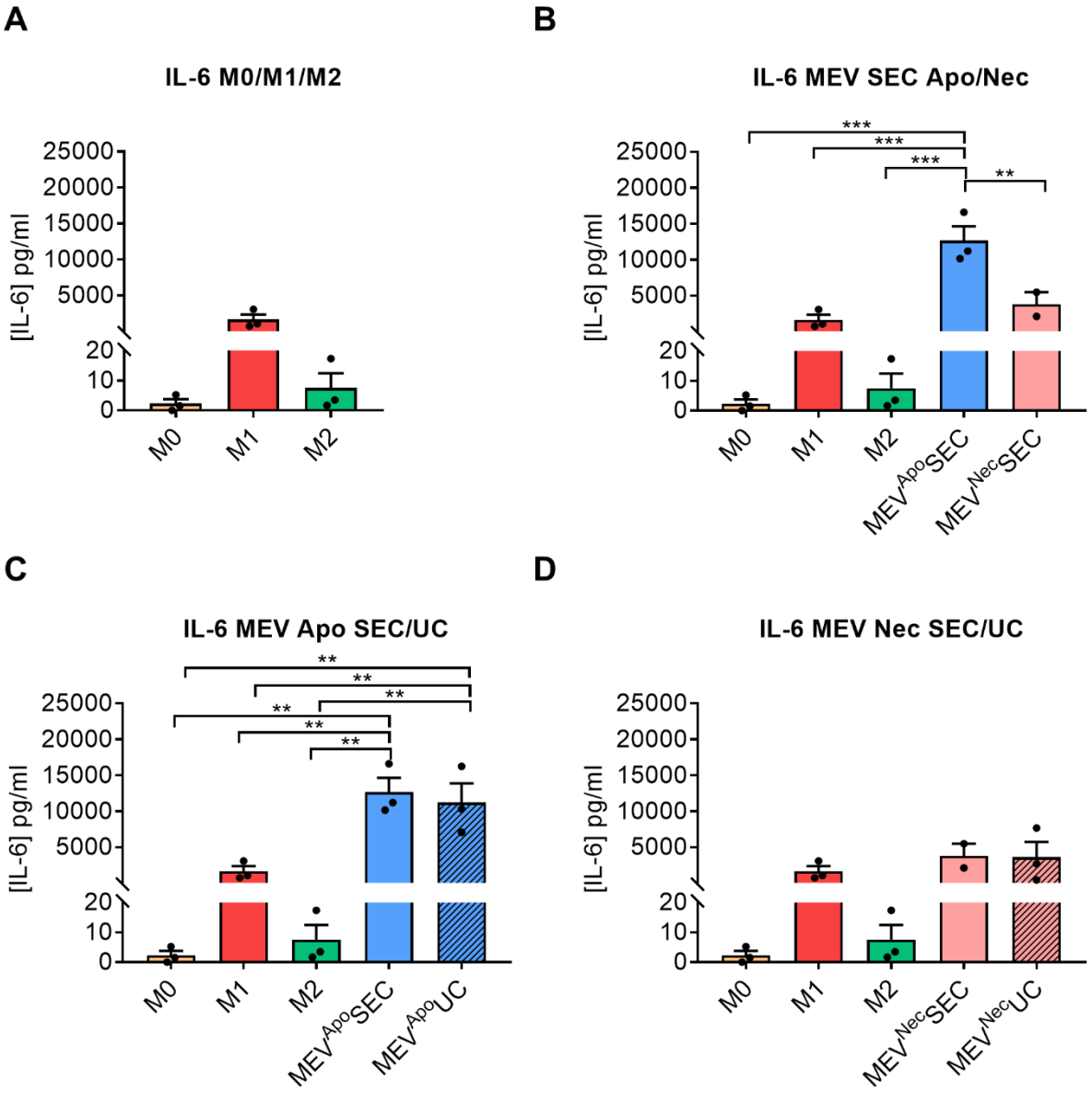

Figure 3.18: IL-6 secretion by polarised THP-1 macrophages. Cytokine concentration was measured in supernatants of THP-1 macrophages using flow cytometry. **(A)** THP-1 monocytes were differentiated to macrophages using VD3 (M0) and then polarised to pro- or anti-inflammatory phenotype with LPS (M1) or IL-4 (M2). **(B)** Non-polarised (M0) macrophages were exposed to ACdEVs from early apoptotic (EV^{Apo}) or late apoptotic/necrotic (EV^{Nec}) Jurkat T lymphocytes isolated by size exclusion chromatography (SEC). **(C)** Comparison of the effect of EV^{Apo} isolated by SEC versus ultracentrifugation (UC). **(D)** Comparison of the effect of EV^{Nec} isolated by SEC versus UC. (Data shown as mean + S.E.M, statistical analysis: one way ANOVA with Tukey's multiple comparisons test **(A)**; one way ANOVA with Sidak's multiple comparisons test **(B-D)** comparing selected groups [MEV groups compared to each other and to M0/M1/M2]; **P<0.01, ***P<0.001).

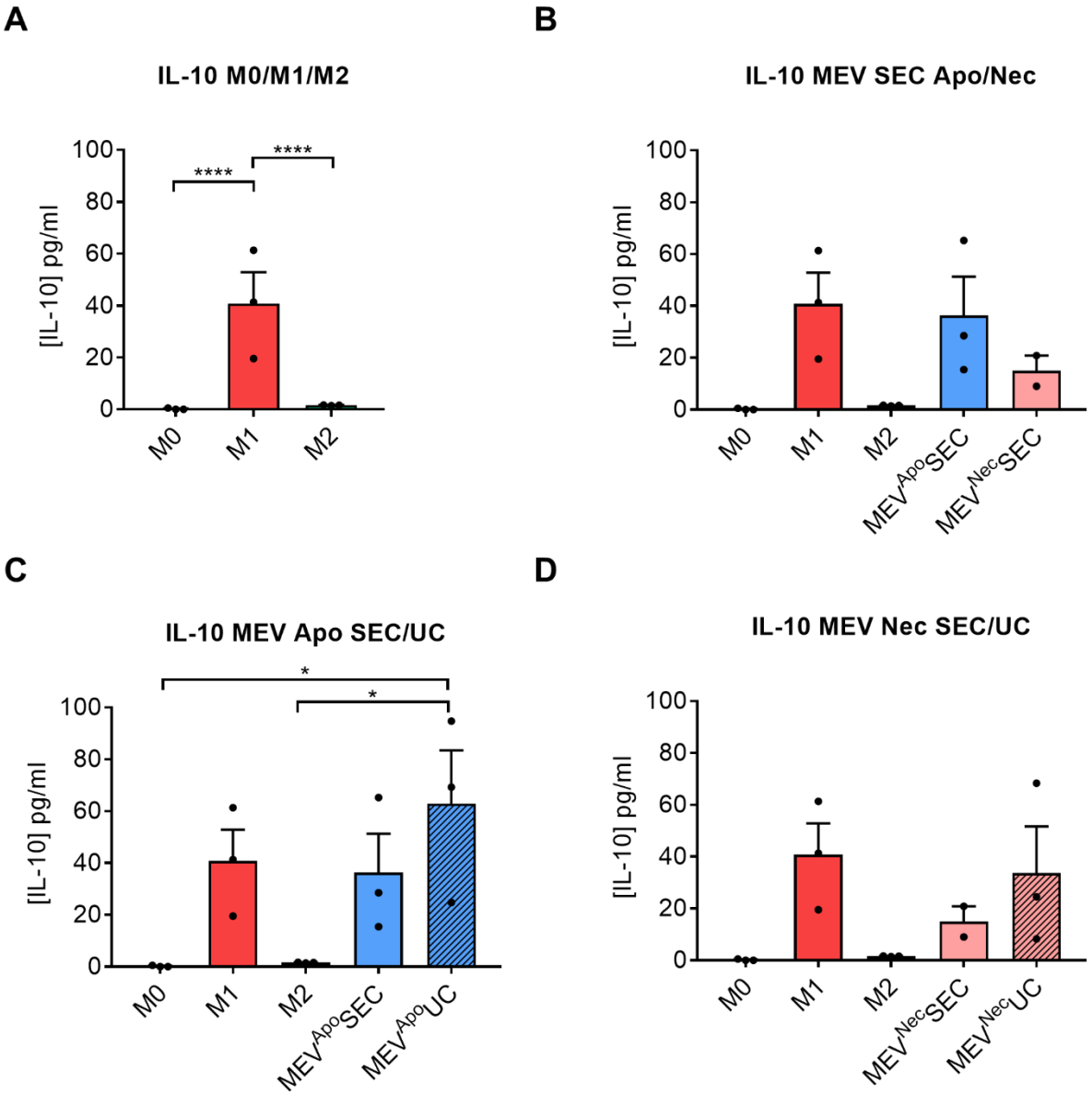

Figure 3.19: IL-10 secretion by polarised THP-1 macrophages. Cytokine concentration was measured in supernatants of THP-1 macrophages using flow cytometry. **(A)** THP-1 monocytes were differentiated to macrophages using VD3 (M0) and then polarised to pro- or anti-inflammatory phenotype with LPS (M1) or IL-4 (M2). **(B)** Non-polarised (M0) macrophages were exposed to ACdEVs from early apoptotic (EV^{Apo}) or late apoptotic/necrotic (EV^{Nec}) Jurkat T lymphocytes isolated by size exclusion chromatography (SEC). **(C)** Comparison of the effect of EV^{Apo} isolated by SEC versus ultracentrifugation (UC). **(D)** Comparison of the effect of EV^{Nec} isolated by SEC versus UC. (Data shown as mean + S.E.M, statistical analysis: one way ANOVA with Tukey's multiple comparisons test (A); one way ANOVA with Sidak's multiple comparisons test **(B-D)** comparing selected groups [MEV groups compared to each other and to M0/M1/M2]; *P<0.05, ****P<0.0001).

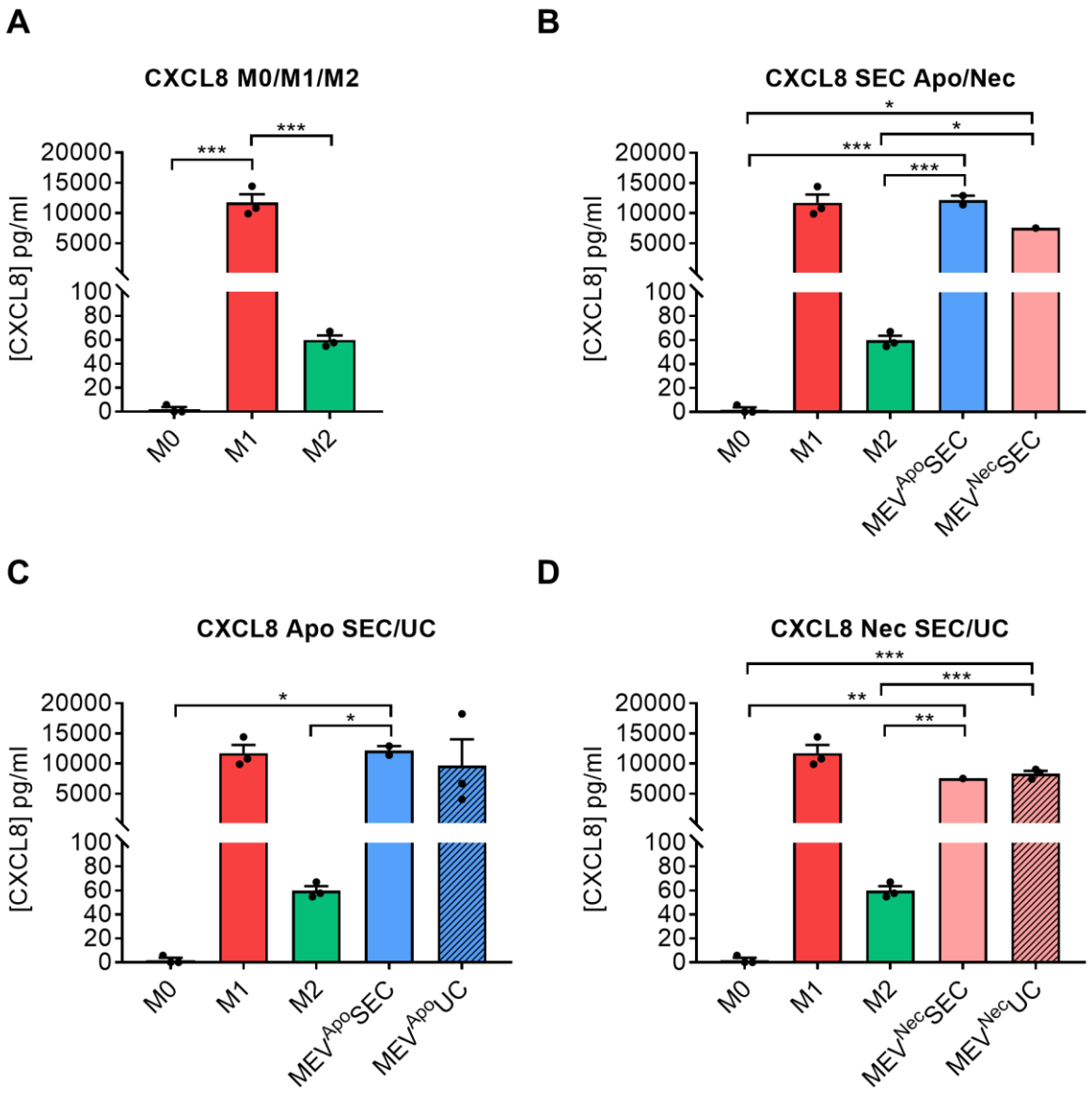

Figure 3.20: CXCL8 secretion by polarised THP-1 macrophages. Cytokine concentration was measured in supernatants of THP-1 macrophages using flow cytometry. **(A)** THP-1 monocytes were differentiated to macrophages using VD3 (M0) and then polarised to pro- or anti-inflammatory phenotype with LPS (M1) or IL-4 (M2). **(B)** Non-polarised (M0) macrophages were exposed to ACdEVs from early apoptotic (EV^{Apo}) or late apoptotic/necrotic (EV^{Nec}) Jurkat T lymphocytes isolated by size exclusion chromatography (SEC). **(C)** Comparison of the effect of EV^{Apo} isolated by SEC versus ultracentrifugation (UC). **(D)** Comparison of the effect of EV^{Nec} isolated by SEC versus UC. (Data shown as mean + S.E.M, statistical analysis: one way ANOVA with Tukey's multiple comparisons test **(A)**; one way ANOVA with Sidak's multiple comparisons test **(B-D)** comparing selected groups [MEV groups compared to each other and to M0/M1/M2]; *P<0.05, **P<0.01, ***P<0.001).

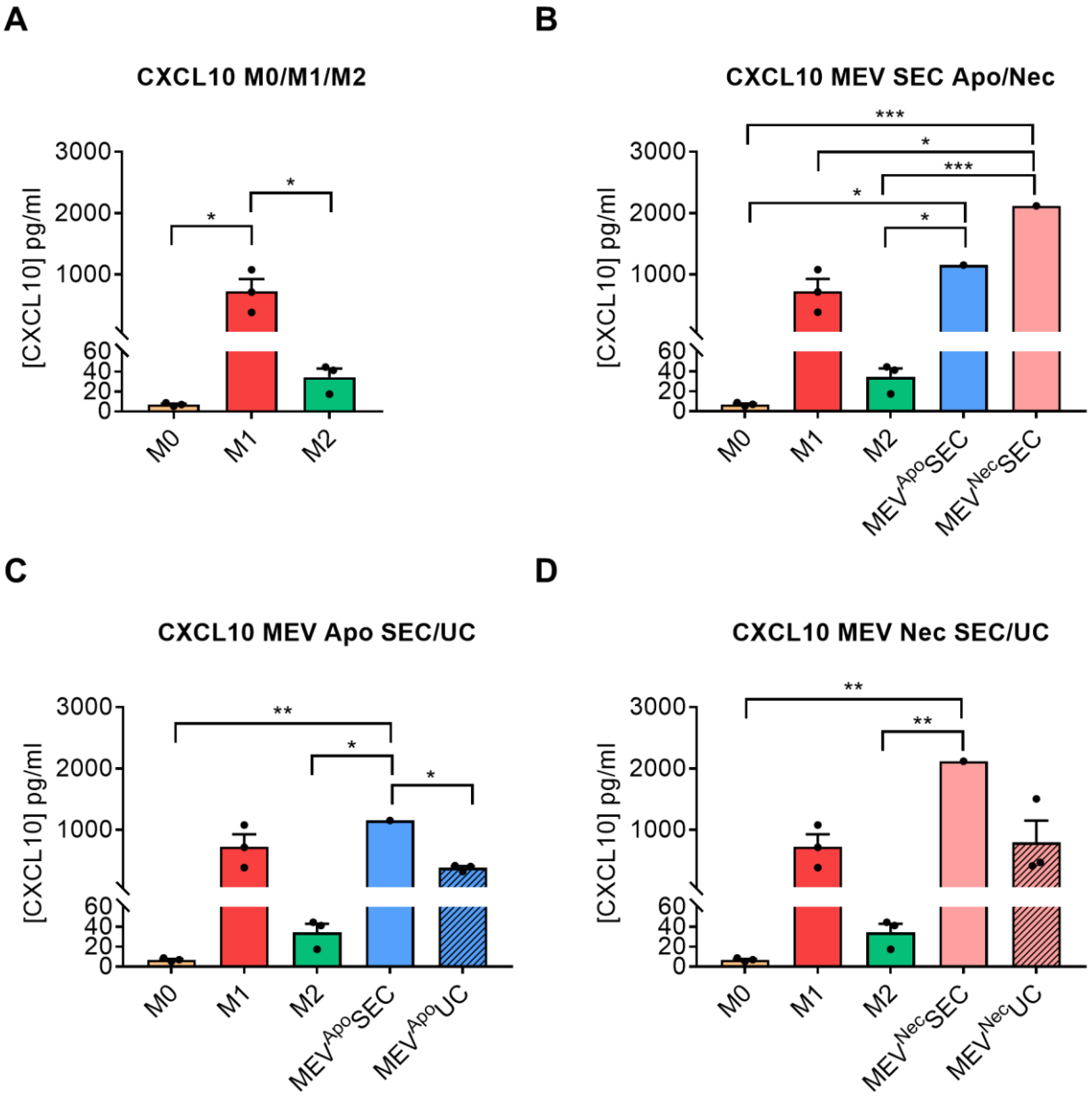

Figure 3.21: CXCL10 secretion by polarised THP-1 macrophages. Cytokine concentration was measured in supernatants of THP-1 macrophages using flow cytometry. **(A)** THP-1 monocytes were differentiated to macrophages using VD3 (M0) and then polarised to pro- or anti-inflammatory phenotype with LPS (M1) or IL-4 (M2). **(B)** Non-polarised (M0) macrophages were exposed to ACdEVs from early apoptotic (EV^{Apo}) or late apoptotic/necrotic (EV^{Nec}) Jurkat T lymphocytes isolated by size exclusion chromatography (SEC). **(C)** Comparison of the effect of EV^{Apo} isolated by SEC versus ultracentrifugation (UC). **(D)** Comparison of the effect of EV^{Nec} isolated by SEC versus UC. (Data shown as mean + S.E.M, statistical analysis: one way ANOVA with Tukey's multiple comparisons test **(A)**; one way ANOVA with Sidak's multiple comparisons test **(B-D)** comparing selected groups [MEV groups compared to each other and to M0/M1/M2]; *P<0.05, **P<0.01; ***P<0.001).

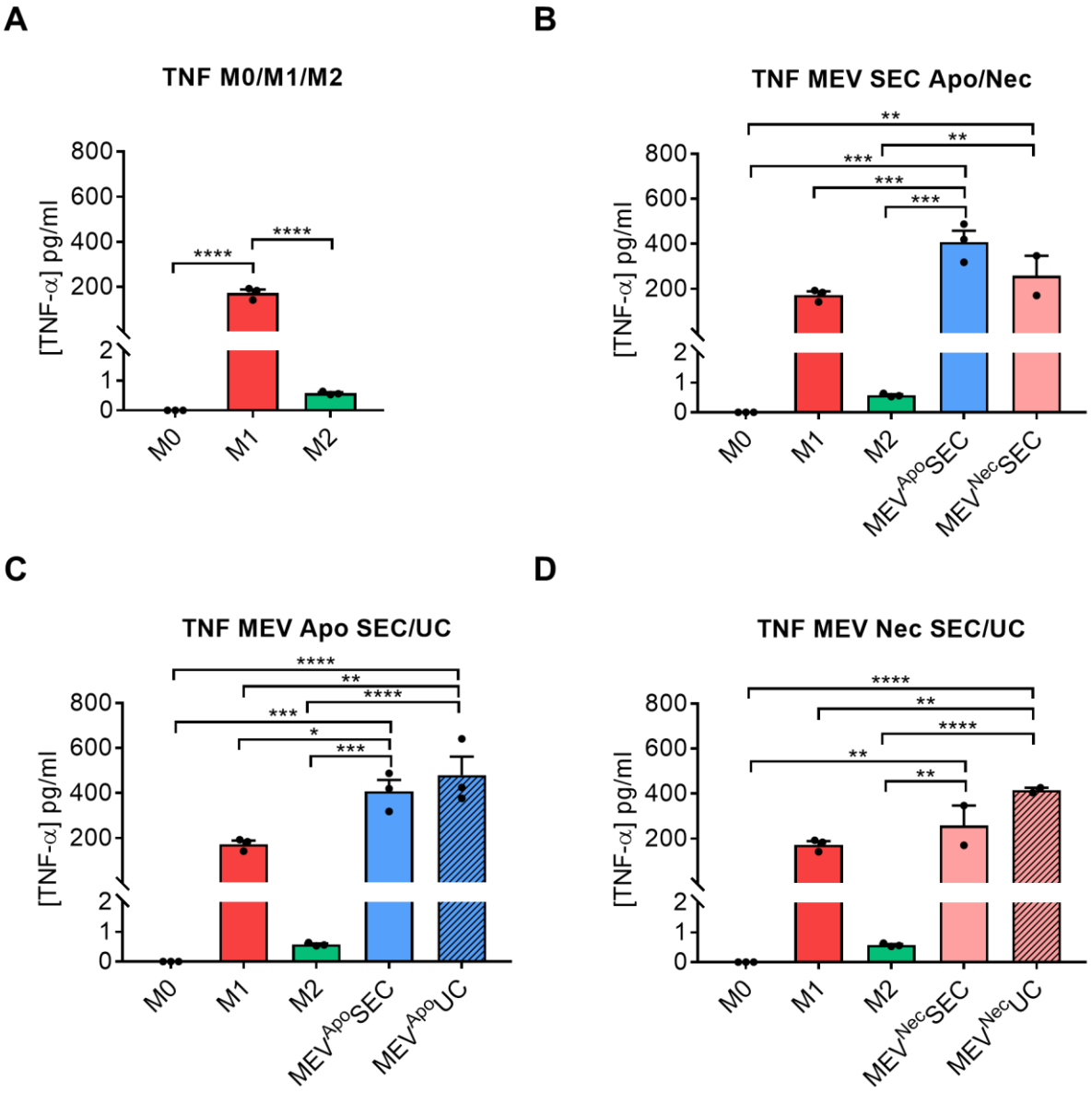

Figure 3.22: TNFα secretion by polarised THP-1 macrophages. Cytokine concentration was measured in supernatants of THP-1 macrophages using flow cytometry. (A) THP-1 monocytes were differentiated to macrophages using VD3 (M0) and then polarised to pro- or anti-inflammatory phenotype with LPS (M1) or IL-4 (M2). **(B)** Non-polarised (M0) macrophages were exposed to ACdEVs from early apoptotic (EV^{Apo}) or late apoptotic/necrotic (EV^{Nec}) Jurkat T lymphocytes isolated by size exclusion chromatography (SEC). **(C)** Comparison of the effect of EV^{Apo} isolated by SEC versus ultracentrifugation (UC). **(D)** Comparison of the effect of EV^{Nec} isolated by SEC versus UC. (Data shown as mean + S.E.M, statistical analysis: one way ANOVA with Tukey's multiple comparisons test **(A)**; one way ANOVA with Sidak's multiple comparisons test **(B-D)** comparing selected groups [MEV groups compared to each other and to M0/M1/M2]; *P<0.05, **P<0.01, ***P<0.001, ****P<0.0001).

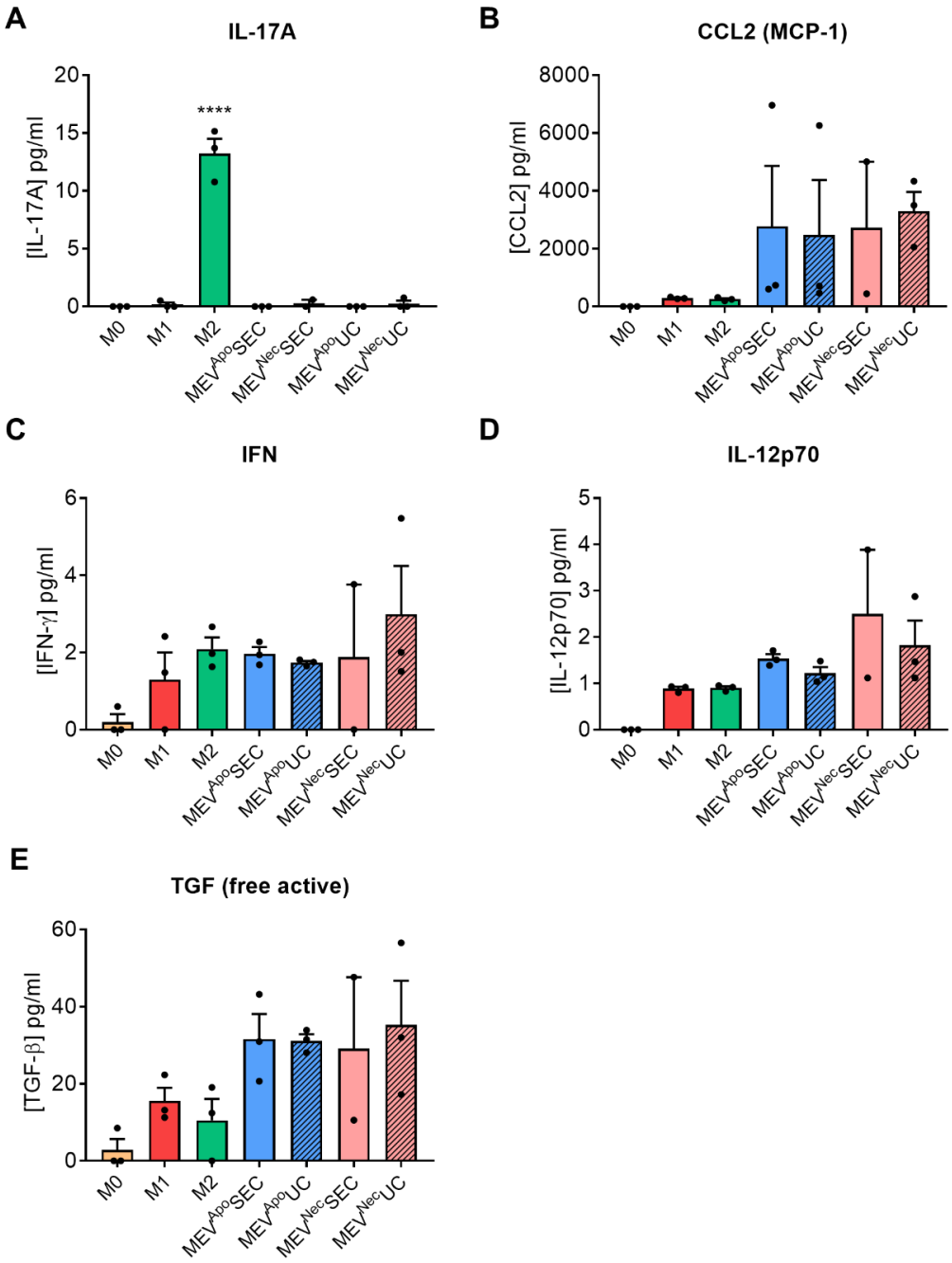

Figure 3.23: Cytokine secretion by polarised THP-1 macrophages. Cytokine concentration was measured in supernatants of THP-1 macrophages using flow cytometry. THP-1 monocytes were differentiated to macrophages using VD3 (M0) and then polarised to pro- or anti-inflammatory phenotype with LPS (M1) or IL-4 (M2) or exposed to ACdEVs from early apoptotic (EV^{Apo}) or late apoptotic/necrotic (EV^{Nec}) Jurkat T lymphocytes isolated by size exclusion chromatography (SEC) or ultracentrifugation (UC). **(A)** IL-17A. **(B)** CCL2. **(C)** IFN-γ. **(D)** IL-12p70. **(E)** Free active TGF-β1. (Data shown as mean + S.E.M, statistical analysis: one way ANOVA with Tukey's multiple comparisons test; ****P<0.0001).

Table 3.1: Summary of cytokine responses of polarised macrophages. Cytokine secretion of non-polarised (M0) macrophages, macrophages polarised with pro-inflammatory (M1), anti-inflammatory (M2) stimuli, or exposed to ACdEVs from early apoptotic (EV^{Apo}) or late apoptotic/necrotic (EV^{Nec}) Jurkat T lymphocytes. "-" low/no secretion; "+" secretion, "++" higher level of secretion. Responses were similar for ACdEVs isolated by SEC or UC.

	M0	M1	M2	MEV^{Apo}	MEV^{Nec}
IL-2	-	+	++	++	++
IL-1β	-	+	-	++	++
IL-6	-	+	-	++	+
IL-10	-	+	-	+	+
CXCL8	-	++	+	++	++
CXCL10	-	++	+	++	++
TNFα	-	+	-	++	++
IL-17A	-	+	-	-	-
CCL2	-	+	+	+	+
IFN-γ	-	+	+	+	+
IL-12p70	-	+	+	+	+
TGF-β1	-	+	+	++	++

3.4 Discussion

3.4.1 Induction of apoptosis & isolation of ACdEVs from immune cell lines

In order to study ACdEVs, firstly, effective methods for inducing apoptosis in cells and collecting ACdEVs were required. Apoptosis can be induced in vitro via a number of different methods. Various molecules can be used to induce cell death, such as activating anti-Fas antibodies or small molecules such as etoposide [187]. UV radiation is also a common method for induction of apoptosis in vitro. As discussed in the introduction, there are intrinsic and extrinsic mechanistic pathways of apoptosis; the extrinsic pathway triggered by activation of death receptors on the cell surface by interaction with their ligands, whereas the intrinsic pathway is triggered internally by DNA damage or metabolic stress which cause release of pro-apoptotic proteins from mitochondria. UV-induced apoptosis is complex, with multiple different molecular pathways of apoptosis being activated. UV induces apoptosis primarily through DNA damage and oxidative stress, but activation of death receptors by their ligands is also involved in UV-mediated induction of apoptosis [188]. Here, UV was used to induce apoptosis in cell lines and cell death was measured using flow cytometry. The progression to apoptosis following a measured dose of UV over an 18-hour time course was similar in the Jurkat T lymphocyte and THP-1 monocyte immune cell lines, with 6 hours and 18 hours deemed to represent early apoptosis and late apoptosis/necrosis, respectively. One of the hypotheses proposed is that ACdEVs released during early and late stages of apoptosis differ in composition and function; therefore this project aims to characterise these populations.

While research on ACdEVs has to date mainly focused on apoptotic bodies which are generally classified as those larger than 1 μm in diameter, this work aims to investigate the smaller vesicles released by apoptotic cells. Therefore, apoptotic bodies were removed from cell supernatant by centrifugation at 2000 x *g* prior to EV isolation. There are numerous EV isolation techniques and choice of method depends on a number of factors including the type of biological fluid and volumes, and the downstream use and analysis of EVs to be performed. While UC is a widely used method for isolation of EVs from biological fluids, various other methods have been developed which are considered to achieve greater purity of EV samples. SEC has become a popular alternative to UC, as a gentler method which effectively removes contaminants such as lipoproteins. The SEC columns used isolate vesicles up to 1 μm in diameter, separate from soluble protein. Using SEC to isolate EVs can be time consuming when working with large volumes of biological fluids as they must first be concentrated to a

volume small enough to load onto the SEC column. Here, SEC was the preferred method to isolate ACdEVs, as a gentle method preserving the native EV state. Characterisation of ACdEVs released by Jurkat T cells using TRPS shows that apoptotic cells release a heterogeneous population of EVs across the size ranges for exosomes and microvesicles, and this is similar to that seen by other researchers [75,93]. The results show that apoptosis boosts EV release and approximately twice the number of ACdEVs are produced in 18 hours (late apoptosis/necrosis) compared to 6 hours (early apoptosis).

3.4.2 Interactions between ACdEVs and macrophages: chemoattraction, binding and uptake

Under normal physiological conditions, apoptotic cells are cleared before they reach late apoptosis/necrosis, and dysfunction in this system is associated with inflammatory pathologies [172]. Previous work from this research group found that the early apoptotic secretome was more effective at promoting macrophage migration than the necrotic secretome, showing that apoptotic cells release specific signals during early apoptosis to promote their removal, whereas uncontrolled release of cell contents from necrotic cells can interfere with this this process. Furthermore, separating the components of the apoptotic secretome using UC showed that both ACdEVs and soluble factors secreted by dying cells can contribute to the chemoattraction of macrophages.

Here, the migration of THP-1-derived macrophages towards ACdEVs isolated by SEC and UC was compared. SEC-isolated ACdEVs appear to lose their chemoattractive capability. The physiological relevance of ‘pure’ isolated EVs is an important issue to consider. EVs would not likely exist and function in this context in vivo and therefore investigating EV function solely in isolation will not provide the full picture and may create artefactual results. Research has shown that macrophage induction of anti-inflammatory and tissue repair genes in macrophages in vivo requires IL-4 or IL-13 together with apoptotic cells [189]. The effects of ACdEVs are likely also affected by other soluble signals in the microenvironment. Given the apparent sensitivity of some EV functions to the isolation technique, we hypothesise that a ‘corona’ surrounding the EV surface likely exists, consisting of protein and perhaps other protein-associated molecules that could play a major role in their signalling. SEC isolation of EVs could potentially remove components of this corona and alter the function of EVs. The protein concentration is slightly higher in UC samples compared to SEC samples which could support this hypothesis, however the difference was not statistically significant. However, this could be due to co-isolation of protein aggregates with UC; SEC is a more stringent method

which produces purer samples compared to UC [128]. Furthermore, our mass spectrometry analysis of SEC-isolated ACdEVs (Results Chapter 2) identified numerous AC-derived surface proteins which are likely to mediate macrophage responses. It could be the case that some of these proteins, such as adhesion molecules, bind to soluble factors in order to exert their effects. The effects of isolation method on EV functions is an important topic for investigation. Although chemoattraction was affected by SEC isolation, these ACdEVs were still able to be taken up by macrophages and change their phenotype. Using fluorescent labelling of EVs and flow cytometry, it was shown that ACdEVs physically interact with macrophages within a short timeframe.

3.4.3 Assessing the THP-1 cell line model of macrophage phenotypes

The THP-1 monocytic cell line is commonly used for in vitro studies of monocytes and macrophages. The use of primary human cells has some issues. Firstly, using primary cells requires a fresh supply of human blood peripheral monocytes for each experiment, as they do not proliferate in vitro. It is therefore difficult to get sufficiently large numbers of cells. Blood leukocyte cones, which are residual products from platelet donation enriched with leukocytes, can be acquired from NHS Blood and Transplant and larger numbers of cells can be harvested compared to normal blood samples. Although primary cells are generally more physiologically relevant, donor variability can be a major issue affecting experimental results. Immortalised cell lines are cost-effective as they can be expanded in vitro and minimises phenotypic variability. However, THP-1 cells are cancerous cells derived from a leukaemia patient and are therefore likely to differ in some aspects of phenotype compared to normal circulating monocytes [190]. Furthermore, differentiating THP-1 monocytes to macrophages in vitro uses different agents to primary cells (PMA/VD3 versus GM-CSF/M-CSF), which may not induce equivalent responses. For this project, cell lines would be used to investigate the structure-function relationships of ACdEVs before results are validated in a primary cell model.

As discussed in the introduction to this chapter, the THP-1 cell line is considered a simplistic model which does not fully replicate the responses of primary monocyte-derived macrophages [183,184]. The results show that THP-1-derived macrophages are attracted to ACdEVs in a vertical migration assay and rapidly take up fluorescently labelled ACdEVs, and the next step was to characterise their pro- and anti-inflammatory polarisation phenotypes and their response to interactions with ACdEVs. Apoptotic cell clearance is considered a non-inflammatory or anti-inflammatory process which promotes resolution and tissue repair. As

such, ACdEVs are likely to facilitate some of the signalling in this process. Uptake of ACdEVs from MSCs has recently been shown to reprogram macrophages, reducing inflammation and restoring liver homeostasis in a mouse model of type 2 diabetes [159]. Macrophage polarisation to a pro- or anti-inflammatory phenotype is commonly determined by measuring expression of marker proteins on the cell surface. THP-1-derived macrophages have behaved variably in different studies of macrophage polarisation, and different polarising stimuli can have distinct effects on expression of surface receptors [178,183,184]. Therefore, for this project, it was necessary to first establish which cell markers would distinguish pro- (M1) and anti-inflammatory (M2) THP-1 macrophages. VD3 was used to differentiate THP-1 monocytes to macrophages, and LPS or IL-4 used to polarise macrophages towards M1 or M2 phenotypes, respectively. Expression of CD14 on THP-1 monocytes varied with different batches of cells, from all of the cells to approximately half expressing CD14; these results differ from work by Thomas et al. which showed no CD14 expression in THP-1 cells until stimulated with VD3 [191]. Despite CD14 expression in THP-1 cells before stimulation, VD3 did stimulate significant upregulation of CD14 expression.

The M1 response was evident in THP-1 macrophages at 24 hours with upregulation of expression of multiple cell surface markers (CD14, CD40 and CD80). M2 polarisation was not as simple to establish. The scavenger receptor CD163 is a widely accepted marker of M2 macrophages, and has been reported to be expressed by THP-1 macrophages in response to IL-4 [192]. However, here, CD163 was undetectable in THP-1 cells under any of the conditions. This lack of CD163 expression has also been reported by Tedesco et al. who used PMA to differentiate THP-1 cells [183]. Furthermore, the scavenger receptor CD206, also considered an M2 marker, was undetectable in THP-1 cells under any of the conditions, which has also been found by another research group [178]. Shiratori et al. found that induction of M1 genes is evident at the mRNA level from 6 hours and at the protein level from 24 hours, and also report limited polarisation capacity of THP-1 macrophages towards M2 phenotypes compared to primary human monocyte-derived macrophages. The adhesion molecule CD209 has previously been shown to act as an M2 marker for THP-1-derived macrophages and primary monocyte-derived macrophages [177,178]. Here, induction of expression of CD209 indicated an M2 response, however its expression was not induced in the whole macrophage population. There may be a more reliable indicator of an M2 phenotype which occurs in the majority of the cell population; a larger panel of cell surface protein markers would need to be analysed.

3.4.4 Effects of ACdEVs on macrophage phenotypes

Based on changes in surface protein marker expression, ACdEVs released by T lymphocytes during both early and late stages of apoptosis appear to polarise THP-1 macrophages towards a pro-inflammatory phenotype. This pro-inflammatory response was unexpected, as previous research shows that apoptotic cells induce anti-inflammatory phenotypes in macrophages [43,180,193]. Work by Fadok et al. over 2 decades ago showed that phagocytosis of apoptotic cells in vitro inhibits pro-inflammatory cytokine production (e.g. IL-1β, IL-8, IL-10, GM-CSF, and TNFα) [193]. Furthermore, recent work by Zheng et al. showed that in vitro phagocytosis of ACdEVs from MSCs induced transcriptional reprogramming in bone marrow-derived macrophages, and restores liver macrophage homeostasis in an in vivo mouse model of type 2 diabetes by inhibiting macrophage infiltration and switching macrophages towards an anti-inflammatory phenotype [159]. Previous unpublished in vivo work from our research group suggested that ACdEVs from Mutu B cells recruit macrophages which are alternatively activated and promote tumour growth [194]. However, there is evidence from other researchers that ACdEVs polarise macrophages to a pro-inflammatory phenotype [75,170]. ACdEVs described as “apoptotic exosome-like vesicles” have been shown to carry danger-associated molecular patterns (DAMPs) which are known inflammatory ligands or pattern-recognition receptors, and induce pro-inflammatory genes in macrophages [75]. The observed upregulation of these surface proteins (CD14, CD40, CD80) may occur in order to increase the capacity of macrophages to phagocytose apoptotic cells, and the macrophages may not actually be pro-inflammatory; for example, CD14 is an important receptor for apoptotic cells [195] and this may extend to other pattern recognition molecules that are involved in apoptotic cell clearance [196,197]. A simple explanation of the effects of ACdEV driving an M1 macrophage phenotype may be that they carry LPS as a result of contamination during the isolation process. This is unlikely given that isolation was performed aseptically and both SEC- and UC-isolated EV show this phenotype change. Based on measurement of cell surface marker expression, the macrophage polarisation by ACdEVs did not appear to be affected by the EV isolation method used, unlike migration where the chemoattractive property is lost using SEC. This suggests that the chemoattractive function and macrophage phenotype-modifying function of ACdEVs are distinct and can be separated.

All of the previous studies of macrophage polarisation discussed here used PMA-differentiated THP-1 cells, which are known to have differences compared to VD3-differentiated cells [185,186]. PMA differentiation of THP-1 monocytes to macrophages produces cells which strongly adhere to the cell culture plastic and are difficult to detach without damaging the cells,

and avoiding enzymatic detachment (e.g. trypsin) which may alter cell surface protein [191,198]. VD3 was therefore the preferred stimulus to produce macrophages from THP-1 monocytes. In light of the seemingly pro-inflammatory, unexpected response of VD3 THP-1 macrophages to ACdEVs, PMA and double stimulated cells treated with both VD3 and PMA were assessed for pro- and anti-inflammatory phenotypes using flow cytometry to measure cell surface protein expression. Cells treated with PMA showed distinct morphological changes compared to VD3-treated cells as has been shown previously by Thomas et al. [191]. Flow cytometry analysis of PMA and double stimulated cells showed lower cell viability compared to VD3 treated cells, possibly due to the strong adherence and sensitivity to detachment. Cell recovery was much lower for PMA and double stimulated cells, as has been found previously [191], meaning approximately twice the number of cells required for experiments must be seeded. Expression of CD14, which is usually highly expressed on macrophages, was much lower in PMA-treated cells compared to VD3 and double stimulated cells, also consistent with previous research [191]. PMA induced an increase in expression of the pro-inflammatory marker CD40. Our research suggests that PMA-differentiated THP-1 cells are inherently M1 in their phenotype, and this is in agreement with the work of Shiratori et al. [184]. Markers which were higher in M1 compared to M2 in VD3 macrophages such as CD80 were actually higher in M2 than M1 for cells treated with PMA. None of the markers tested satisfactorily distinguished M0, M1 and M2 phenotypes in PMA or double stimulated cells. Resting of PMA-treated cells in PMA-free medium prior to use may, however, produce different results; in a number of studies, PMA treated cells are rested for up to 5 days [180,184]. Overall, VD3-differentiated THP-1 macrophages were considered to be most suitable for the assays being used in this project.

In order to further investigate the effects of ACdEVs on macrophage phenotype, the secretion of cytokines by activated macrophages was investigated. The cytokine response to ACdEVs in THP-1-derived macrophages aligned with the apparently pro-inflammatory phenotype assessed by surface protein expression. To further investigate the differences in functional effects of ACdEVs isolated by different methods, cytokine responses were assessed for ACdEVs isolated by UC versus SEC; the results suggested that isolation method did not affect the cytokine responses induced, consistent with the results for flow cytometry-based surface protein phenotyping. EVs are very complex signal transducers and the components mediating different types of ACdEV-mediated communication between AC and macrophages must be identified and characterised.

Whilst the EV-mediated promotion of an inflammatory phenotype was not expected, it is worthwhile to consider the limitations of in vitro assays and, possibly, in vivo cell death may, as a result of a complex microenvironment, enable a more M2 macrophage phenotype to be achieved. For this to be assessed, ACdEVs from Jurkat cells could be injected intraperitoneally in mice to consider the change on macrophage phenotype in an in vivo setting. Future work could also investigate other cell lines (such as U937 and HL-60) for modelling macrophage phenotypes, as these may behave differently. Quantitative PCR could also be used to evaluate macrophage polarisation at the transcriptional level. The effects of ACdEVs on pre-polarised M1 macrophages should be investigated. Work by Kohno et al. demonstrated that exposure of “inflammatory M1-like” THP-1 macrophages (PMA-stimulated then polarised by NK-4) to apoptotic cells resulted in switching to an “anti-inflammatory M2-like” phenotype [180]. Furthermore, cell line models should be compared to primary macrophages to evaluate how physiologically relevant they might be.

Taken together, the data presented here support previous research demonstrating a role for ACdEVs in attracting macrophages and show that and THP-1-derived macrophages are capable of taking on alternative phenotypes which can be modified by exposure to ACdEVs. The ACdEVs appear to be able to promote macrophage phenotype change, unexpectedly, towards a more inflammatory phenotype.

4. Results Chapter 2: Identifying candidates for proteins mediating ACdEV functions

4.1 Introduction

EVs are complex structures carrying a vast array of molecules. Most proteomic studies of EVs to date have not focused on EVs derived from apoptotic cells. The protein composition of ACdEVs may help reveal the molecular routes by which they communicate their presence to the immune system to allow their uptake and elicit immune responses. This could be mediated by relatively simple physicochemical means, such as charge, and/or more specific, high-affinity ligand–receptor interactions, through the recognition of proteins, lipids, or carbohydrates. As discussed in the Introduction, until recently, CX3CL1 and ICAM-3 were the only proteins that have been studied and characterised in their ACdEV-associated form, playing key roles in recruitment of macrophages [21,22]. The apoptotic cell 'eat me' signal calreticulin has recently been shown to mediate uptake of ACdEVs from MSCs which resulted in restoration of liver macrophage homeostasis in a mouse model of type 2 diabetes [159]. In this study, proteomic analysis of ACdEVs from MSCs identified a number of proteins with the potential to induce anti-inflammatory macrophage responses, including alpha-crystallin B chain (CRYAB), peroxiredoxin-6 (PRDX6), cAMP-dependent protein kinase type II-alpha regulatory subunit (PRKAR2A), receptor of activated protein C kinase 1 (RACK1) and superoxide dismutase (SOD1). Many other molecules that are on the surface of, or packaged into, ACdEVs have been identified, which are known to have functions in controlling inflammation and AC clearance, although the ACdEV-associated forms have not been functionally characterised. The balance between inflammatory mediators changes over the course of apoptosis; therefore, changes in the composition of ACdEVs over time should also be investigated.

4.2 Aims

The aim of this work was to analyse the proteomes of ACdEVs from multiple immune cell types and any changes in the protein composition of ACdEVs released during early and late stages of apoptosis, and to identify proteins of interest that could mediate EV function in regulation of the innate immune system, for further study. Apoptotic cells are normally cleared during the early stages of apoptosis in a non-inflammatory/anti-inflammatory manner, and dysfunction in this process results in inflammation. Therefore ACdEVs released during the early, controlled stages of cell death may differ in composition to those released at the late, uncontrolled stages.

4.3 Results

4.3.1 Proteomic analysis of ACdEVs from different immune cell types

A bottom-up proteomics approach with label-free quantification was employed to reveal the protein composition of ACdEVs and analyse changes in the protein composition in ACdEVs released at early and late stages of apoptosis. ACdEVs were isolated from (Jurkat) T cells, (THP-1) monocytes and (Mutu) B cells by size exclusion chromatography (SEC) to allow for the analysis of ACdEV protein composition with minimal contamination with soluble proteins secreted by the cells. There were 1627 different proteins relatively quantified across the three cell lines (T cells: 1086; Monocytes: 1125; B cells: 616 proteins; complete data sets in Appendix). Of these, 596 proteins had not previously been reported within the Vesiclepedia database for any EV studies for T cells, monocytes or B cells (**Figure 4.1**). Approximately one quarter of these (415) proteins were conserved across the three cell lines, and 17 of the conserved proteins had not been previously reported in Vesiclepedia for any of these cell types (RTCB, KHDRBS1, MT-CO2, AIMP1, SNRPB, PRDX4, NUMA1, COPS8, NEK9, NONO, TSNAX, DCTPP1, ZNF500, SETSIP, NUDT21, HMGB2). 346 proteins were unique to ACdEVs from T cells, 402 unique to monocytes and 84 unique to B cells; these included cell-specific receptors (e.g. T cell: CD2, CD3e; Monocyte: CD14, CD64; B cell: CD19, CD20, CD22, CD79). Gene ontology analysis associated 313 of the conserved proteins with the cellular component term ‘Exosomes’ and 92 with ‘Plasma membrane’. Various proteins typically found in EVs were identified, including MHC (HLA) molecules [88], heat shock proteins [134] and Ras-related protein Rab GTPases (involved in membrane trafficking and exosome release [199]). 5 heat shock proteins and 12 Rab proteins were conserved across the three cell types. Other EV proteins identified included annexins, 14-3-3 and cytoskeletal components such as tubulins [200].

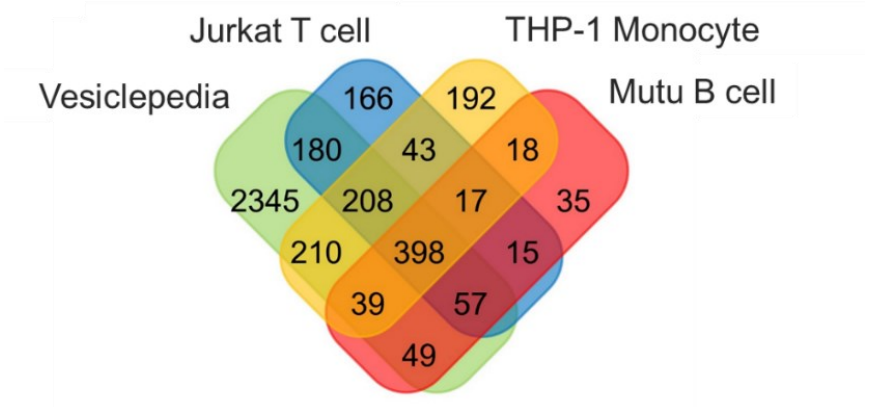

Figure 4.1: Comparison of proteomes of ACdEVs from different immune cell types. Venn diagram comparing proteomes of ACdEVs from Jurkat T cells, THP-1 monocytes and Mutu B cells and proteins reported in the Vesiclepedia database for T cells, monocytes, or B cells. Apoptosis was induced by treatment with anti-Fas and cycloheximide and EVs were isolated by size exclusion chromatography after 6 and 18 hours, before mass spectrometry.

The proteomes were each further analysed using gene ontology. The largest percentage of proteins were associated with the biological processes of 'cell communication', 'signal transduction' or 'transport', which are all relevant to the potential roles of ACdEVs. Proteomes were compared for ACdEVs released at early (6 h) and late (18 h) stages of apoptosis using relative quantification of proteins coupled with gene ontology analysis; this revealed distinct features of these ACdEV populations (**Figure 4.2A**). Proteins associated with cell migration, vesicle mediated transport and regulation of the immune response are enriched in ACdEVs released during early apoptosis compared to ACdEVs from necrotic cells (**Figure 4.2B**) possibly highlighting the importance of these processes and ACdEV in the pro-resolving nature of apoptosis.

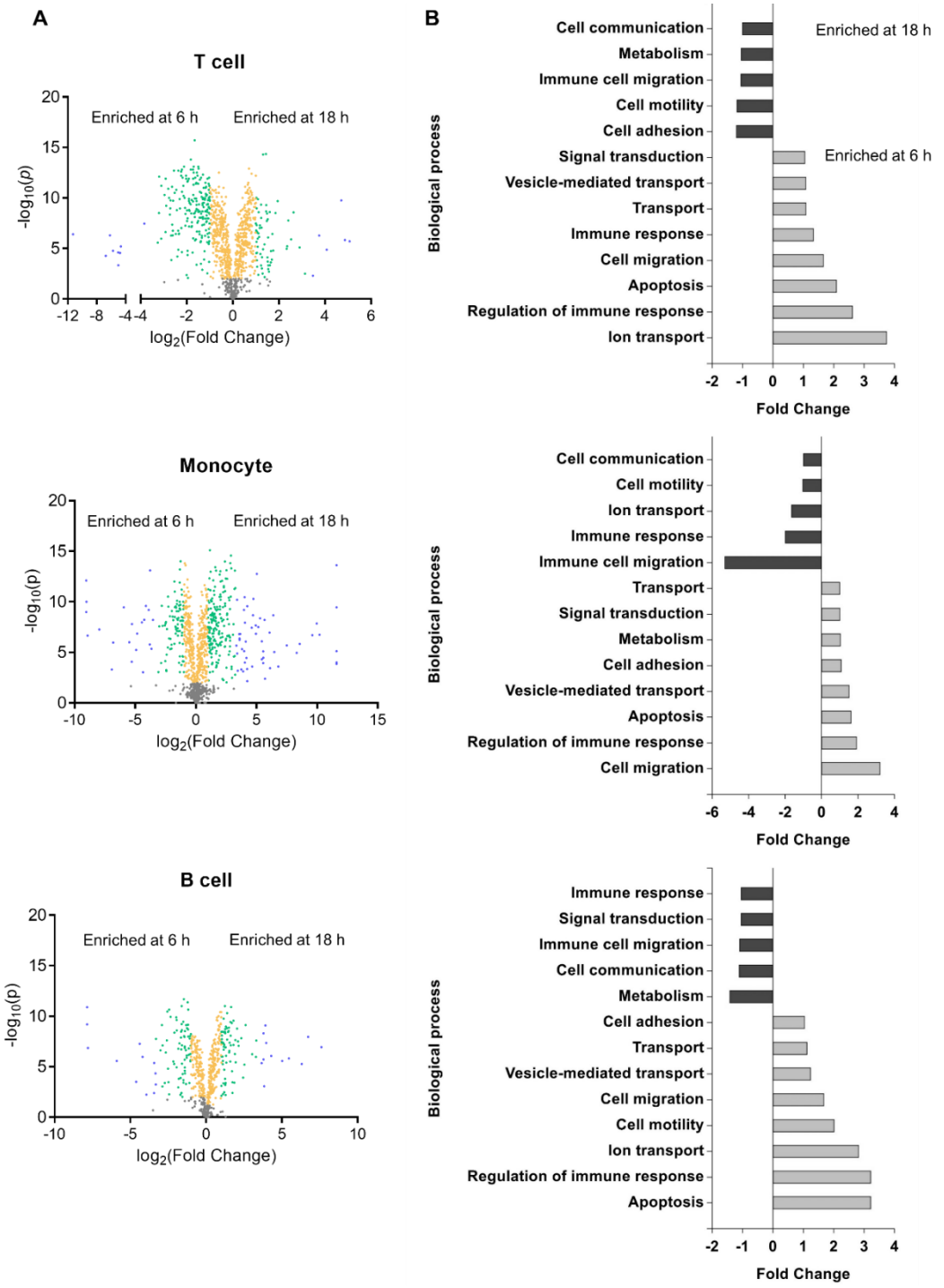

Figure 4.2: Comparison of proteomes of early and late ACdEVs from different cell types. T cell, monocyte and B cell lines were induced to apoptosis and ACdEVs isolated from 2000 x *g* supernatants at 6/18 h post-induction using SEC and protein content analysed by mass spectrometry. **(A)** Enrichment of proteins in ACdEVs at early (6 h) and late (18 h) stages of apoptosis. (Fold change (FC) in abundance: Grey=p>0.01, not significant; Orange=FC<2; Green=2<FC<10; Blue=FC>10). **(B)** Enrichment of biological processes associated with ACdEV proteins at early and late stages of apoptosis.

The ACdEV proteomes from each cell line were then further analysed to identify plasma membrane-associated protein that could be involved in EV-mediated cell recruitment, binding, uptake and regulation of immune responses. The shortlisted proteins and their enrichment in early or late ACdEVs are listed in Table 4.1. Various adhesion molecules were identified including intercellular adhesion molecules (ICAM-1, -2, -3), integrins (alpha-D, -L, -M, -X, -1, -2, -4, -5, -10; beta-1, -2), tetraspanins (e.g. CD81, CD166), and annexins, including annexin A1 which can regulate the immune system to promote resolution of inflammation and tissue repair [162–164,201]. As discussed earlier, ICAM-3 is a characterised ACdEV-associated mediator of apoptotic cell clearance [22]. While ACdEVs from T cells contained ICAM-1, -2 and -3, ACdEVs from monocytes contained only ICAM-1, and from B cells, ACdEVs contained only ICAM-3. Where present, ICAM-1 and ICAM-2 are significantly enriched in ACdEVs at 6 hours compared to 18 hours.

CD31 and CD47, proteins which can act as ‘don’t eat me’ signals on the surface of cells preventing phagocytosis, were found in ACdEVs from all three cell types [29,33,52]. Release of EVs could be an efficient way to rapidly remove these signals from the cell surface to enable apoptotic cell clearance. However, CD31 function can be altered to allow phagocytosis of apoptotic cells and it can also behave as an ‘eat me’ signal [33–35]. Notably, the well-established apoptotic cell ‘eat me’ signal calreticulin [29] was found in ACdEVs from all three cell types and was significantly enriched at 6 hours compared to 18 hours. High mobility group box 1 (HMGB1) was detected in ACdEVs from T and B cells; HMGB1 has previously been shown to be translocated into ACdEVs, and has various signalling functions including regulating immune responses [165,167,202]. HMGB1 can function as an inherent pro-inflammatory danger signal, and when released from necrotic cells, is a potent pro-inflammatory mediator [203]. HMBG1 is enriched in ACdEVs at 18 hours compared to 6 hours (T cells 2-fold, B cells 1.78-fold), suggesting that its release is limited in the early, controlled stages of cell death. Other membrane proteins of interest identified include flotillins which are associated with lipid rafts, protein localisation, endocytosis, and sphingosine signalling [204–207] and syntenin which is a multifunctional adapter protein involved in exosome biogenesis, trafficking of membrane proteins, associated with tetraspanin enriched microdomains and involved in immunomodulation [208,209]. CD147 was present in ACdEVs from all three cell types; CD147 is a transmembrane glycoprotein involved in intercellular recognition, leukocyte migration, regulation of apoptosis and induction of matrix metalloproteinases [210]. Other candidate proteins include CD97, a multifunctional leukocyte adhesion G protein-coupled receptor associated with inflammation, and macrophage migration inhibitory factor (MIF), a multifunctional cytokine involved in regulation of the innate immune system and inflammation

[211–213]. ABC transporters, which can play a role in immunomodulation via the secretion of lipid mediators, were also found in ACdEVs; ABCC1 (also known as MRP1: multidrug resistance protein 1) was present in ACdEVs from all 3 cell types. ABCC1 can export sphingosine-1-phosphate, a known ‘find me’ signal secreted by apoptotic cells [214]. As discussed earlier, analysing the proteomes of ACdEVs from MSCs, Zheng et al. identified a number of proteins that could induce anti-inflammatory polarisation of macrophages; we also found some of those proteins (RACK1, peroxiredoxin-6, and superoxide dismutase) in ACdEVs from all three cell lines.

Table 4.1: Candidates for proteins mediating apoptotic cell-derived extracellular vesicle function in apoptotic cell clearance and the modulation of inflammation. Mass spectrometry was performed to analyse the proteomes of ACdEVs from Jurkat T lymphocytes, Mutu B lymphocytes and THP-1 monocytes; ACdEVs were harvested 6- and 18-hours post-induction of apoptosis to reflect early and late stages of apoptosis, and relative label-free quantification was performed. (Software tool – Progenesis QI for proteomics, version 4.1; n=5. Statistical analysis by ANOVA. ns = not significant; **P<0.01; ***P<0.001; ****P<0.0001; blue= significantly enriched at 6 hours; pink: significantly enriched at 18 hours). The proteomes were analysed using gene ontology functional annotation tools to identify plasma membrane-associated proteins with relevant functions.

	T cell		Monocyte		B cell	
Protein	**Higher at 6 or 18 h**	**Max fold change**	**Higher at 6 or 18 h**	**Max fold change**	**Higher at 6 or 18 h**	**Max fold change**
ICAM-2	6 h	3.14 (****)				
Flotillin-2	6 h	2.06 (****)	18 h	7.08 (****)		
Calreticulin	6 h	2.03 (****)	6 h	1.39 (****)	6 h	5.45 (****)
Flotillin-1	6 h	2.02 (****)			6 h	1.89 (****)
CD81	6 h	1.91 (****)	18 h	1.15 (****)	6 h	1.86 (ns)
ICAM-1	6 h	1.73 (****)	6 h	2.10 (****)		
CD166	6 h	1.45 (***)	18 h	1.83 (****)	18 h	1.46 (****)
ABCC1/MRP1	6 h	1.36 (****)	6 h	3.21 (****)	6 h	1.10 (ns)
Syntenin-1	6 h	1.33 (****)	18 h	1.50 (***)		
CD47	6 h	1.33 (****)	6 h	1.27 (****)	18 h	2.25 (****)
Basigin/CD147	6 h	1.21 (****)	6 h	1.24 (**)	18 h	1.37 (****)
ABCA13	6 h	1.51 (ns)				
Integrin alpha 4	6 h	1.04 (ns)	18 h	1.15 (***)	18 h	1.16 (***)
ICAM-3	6 h	1.00 (ns)			18 h	1.47 (****)
PECAM-1/CD31	18 h	1.02 (ns)	18 h	6.76 (****)	18 h	1.11 (ns)
Integrin beta 1	18 h	1.03 (ns)	18 h	5.51 (****)	18 h	1.11 (ns)
Annexin A1	18 h	1.18 (****)	6 h	1.35 (****)		
MIF	18 h	1.52 (****)	6 h	1.49 (****)		
CD97	18 h	7.46 (****)	6 h	2.24 (****)		
Integrin alpha L			18h	9.32 (****)		
Integrin alpha M			18h	4.05 (****)		
Integrin beta 2			6 h	1.43 (****)		

4.3.2 Release of proteins from apoptotic cells in ACdEVs

Proteomic analysis revealed the diversity of ACdEV proteomes and various proteins that may mediate ACdEV function in immunomodulation. Release of membrane-associated proteins of interest from apoptotic cells in ACdEVs was assessed by flow cytometry analysis of surface expression on cells before and after induction of apoptosis, and on ACdEVs released.

4.3.2.1 Apoptosis-induced changes in cell surface expression of Intercellular Adhesion Molecules (ICAMs)

A study by Torr et al. demonstrated an apoptosis-associated reduction in ICAM-3 due to its release in ACdEVs, which promote recruitment of macrophages [22]. As ICAM-3 is expressed only by human leukocytes, there may be some redundancy in the functions of different ICAMs in the process of apoptotic cell clearance. Furthermore, Torr et al. demonstrated cross-species redundancy as the phagocyte receptor function for human ICAM-3 is present in mice, which naturally do not express ICAM-3 [22]. Other ICAMs have not previously been investigated in ACdEVs. The intercellular adhesion molecule family of proteins has 5 members, ICAM-1 to -5. These adhesion molecules bind to integrins and are important mediators of inflammation and the immune response, involved in signalling as well as cell adhesion. Analysis of ACdEV proteomes found that ICAM-1 (found in ACdEVs from Jurkat T cells and THP-1 monocytes) and ICAM-2 (found in ACdEVs from Jurkat T cells) were both significantly enriched in ACdEVs at 6 hours, early apoptosis. To investigate the release of ICAM-1 and ICAM-2 from cells, cell surface levels of protein were assessed before and after induction of apoptosis in Jurkat T lymphocytes. As shown in Results Chapter 1, progression of apoptosis was assessed using annexin V and propidium iodide staining and flow cytometry. Forward and side scatter plots show two populations, one consisting of larger, less granular cells including both early apoptotic cells and viable cells (“Live cells”), and the other consisting of smaller and more granular cells which are late apoptotic/secondary necrotic (“Dead cells”). 18 hours after induction of apoptosis, the established time point for late apoptosis, the majority of cells have reduced in size and become more granular and are found in the “Dead cells” zone (**Figure 4.3A**). Cell surface levels of ICAM-1 and ICAM-2 were measured by flow cytometry in live untreated and UV-treated apoptotic cells. Almost 100% of healthy, untreated Jurkat cells expressed ICAM-1 on their surface (**Figure 4.3B**). ICAM-1 levels were significantly reduced in late apoptotic cells within the “Dead” zone, shown by significant reduction in MFI and decrease in positive cells to 59.36%. Almost 100% of healthy Jurkat cells also expressed ICAM-2 on their surface (**Figure 4.3C**). ICAM-2 is almost completely lost in late apoptotic cells in the “Dead

cells" zone at 18 hours post-induction of apoptosis, and there is also a significant reduction in ICAM-2 levels in the smaller proportion of cells in the "Live cells" gate, suggesting that loss of ICAM-2 begins in the early stages of apoptosis.

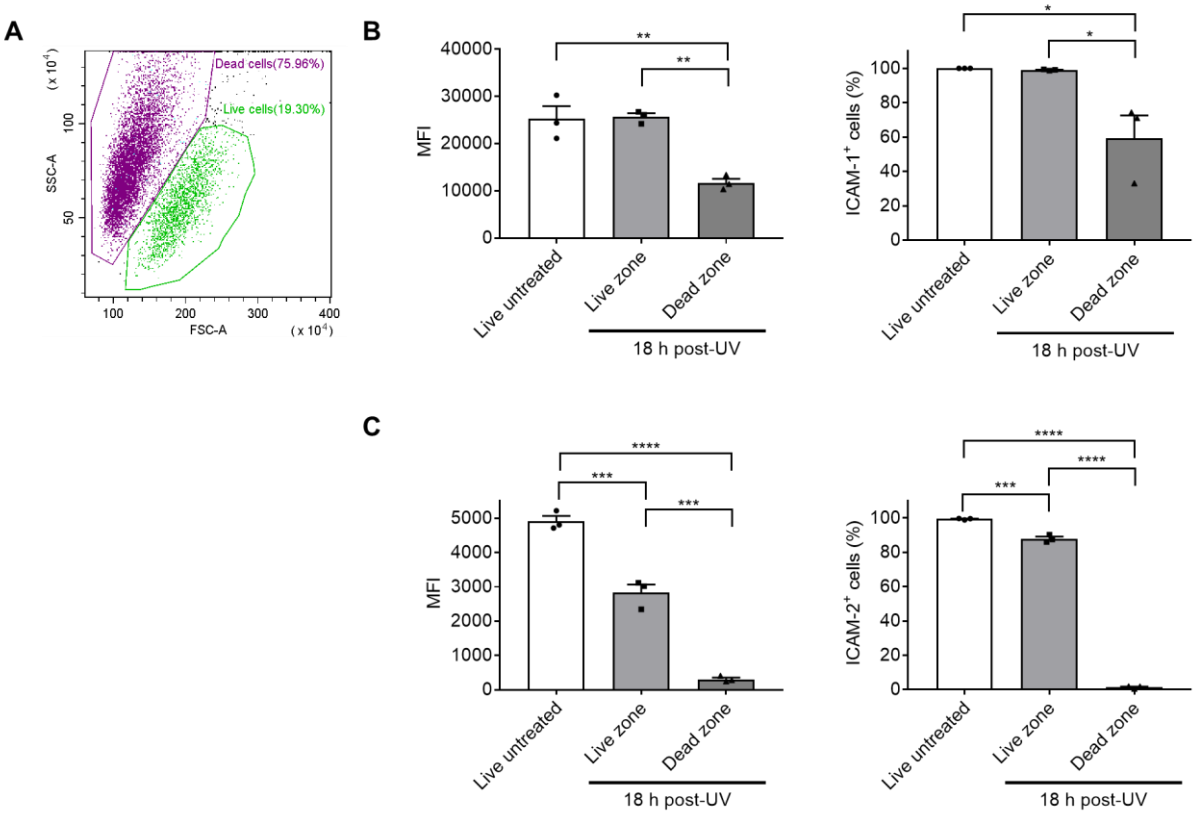

Figure 4.3: Cell surface ICAM-1 and ICAM-2 reduce during apoptosis in T cells. Apoptosis was induced in Jurkat T lymphocytes using UV radiation and cell surface levels ICAM-1 and ICAM-2 were measured by flow cytometry after 18 hours. **(A)** Cell populations gated on size and granularity (forward and side scatter) 18 hours post-UV treatment. **(B)** Cell surface ICAM-1 levels in late apoptotic cells compared to live healthy cells. **(C)** Cell surface ICAM-2 levels in late apoptotic cells compared to live healthy cells. Protein expression shown as mean fluorescence intensity (MFI) and percentage of positive cells. (Data presented as mean + SEM, n=3; statistical analysis by one-way ANOVA with Tukey's multiple comparisons test; *P<0.05, **P<0.01, ***P<0.001, ****P<0.0001).

To determine whether these effects are observed at early apoptosis (6 hours) and whether reduction of surface ICAM expression at 18 hours is not simply due to loss of membrane with cell shrinkage and blebbing, protein expression on the surface of early apoptotic cells 6 hours after induction of apoptosis was measured. The forward and side scatter profiles of viable and early apoptotic cells are similar, as early apoptotic cells remain mostly in the 'live cell' zone (**Figure 4.4A**), therefore in order to distinguish them from viable cells, the cells were stained with annexin V to measure exposure of PS alongside protein measurement. Viable cells in the live cell gate were PS-positive (**Figure 4.4B**), and binding of annexin V was determined to be specific binding as the signal was lost in the absence of calcium. 6 hours after induction of apoptosis, cells in the live zone show two peaks for PS levels, one at the low-level matching viable non-treated cells, and the other matching the higher PS levels of induced cells in the "dead" zone. Cells in the live zone in healthy cells and apoptotic cells (6 h) were then compared in terms of PS exposure and cell surface protein levels for ICAM-1, -2 and -3. Cells with increased PS exposure show decreased levels of all three ICAMs (**Figure 4.5**).

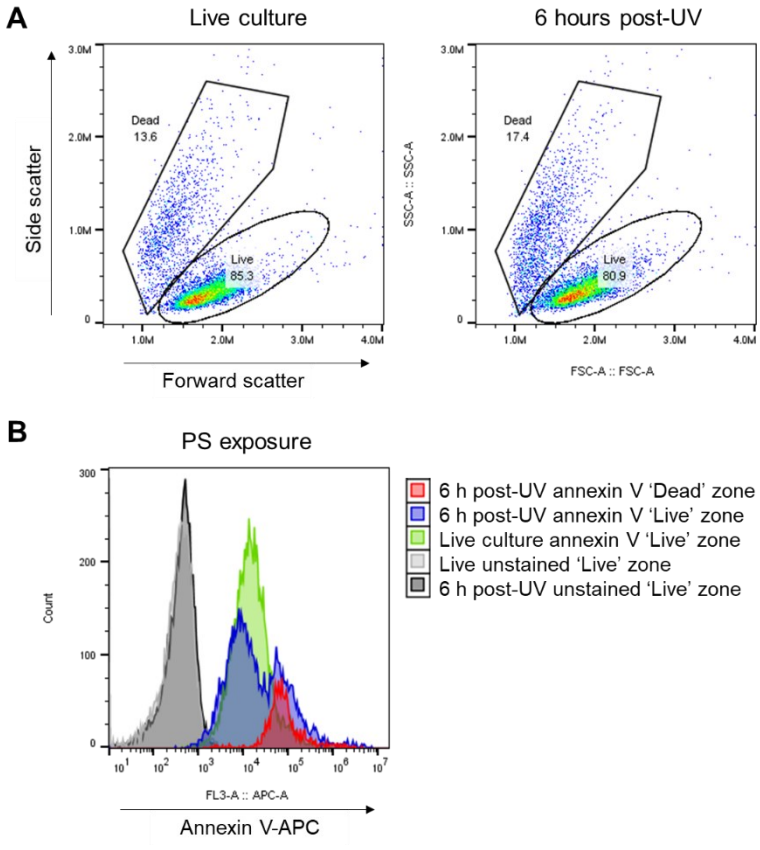

Figure 4.4: Analysis of phosphatidylserine exposure on viable and early apoptotic cells by flow cytometry. (A) Forward and side scatter profiles of Jurkat T cells before (live culture) and 6 hours after induction of apoptosis using UV radiation. At this early apoptosis time point, most cells remain in the 'live' cell zone. **(B)** Measurement of phosphatidylserine exposure on live and apoptotic Jurkat T cells by staining with annexin V.

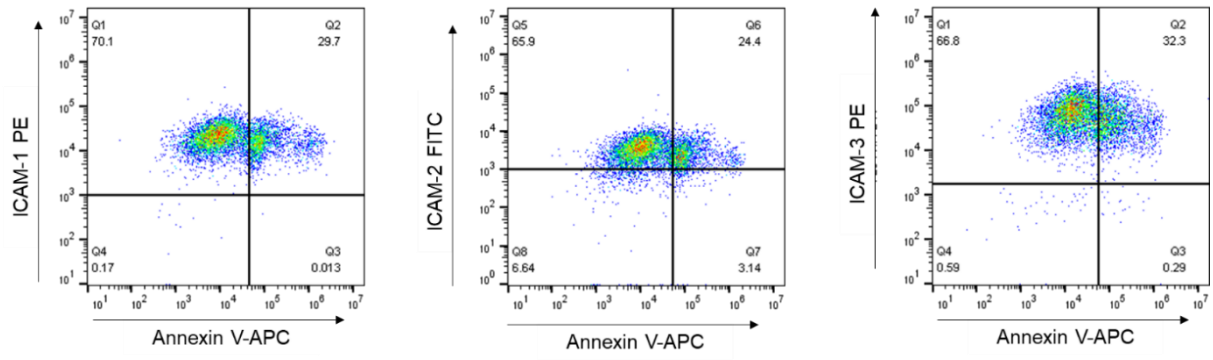

Figure 4.5: Reduction in surface ICAM expression corresponds to PS exposure in early apoptosis. Flow cytometry dot plot showing surface levels of ICAM-1, -2 and -3 versus phosphatidylserine exposure (annexin V) on Jurkat cells 6 hours after UV treatment (early apoptosis). (Cells were gated on the 'live zone' as shown in Figure 4.4A).

4.3.2.2 Apoptosis-induced changes in surface expression of Calreticulin – apoptotic cell 'eat me' signal

Calreticulin is a known 'eat me' signal which is translocated to the cell surface during apoptosis [29–31] and was recently shown to facilitate uptake of EVs released by apoptotic MSCs by macrophages [159]. Calreticulin externalisation following induction of apoptosis was confirmed in Jurkat T lymphocytes by flow cytometry 18 hours after UV exposure. In viable untreated cells, the MFI was relatively low with calreticulin detected on approximately 20% of the cell population. 18 hours after induction of apoptosis, the MFI of cells in the 'dead' zone (~75% of cells) was 154-fold higher compared to live viable cells with calreticulin detected on 77.26% of cells (**Figure 4.6**). Cells in the 'live' zone post-UV had a slightly increased MFI compared to viable cells and 47.65% of those cells exposed calreticulin.

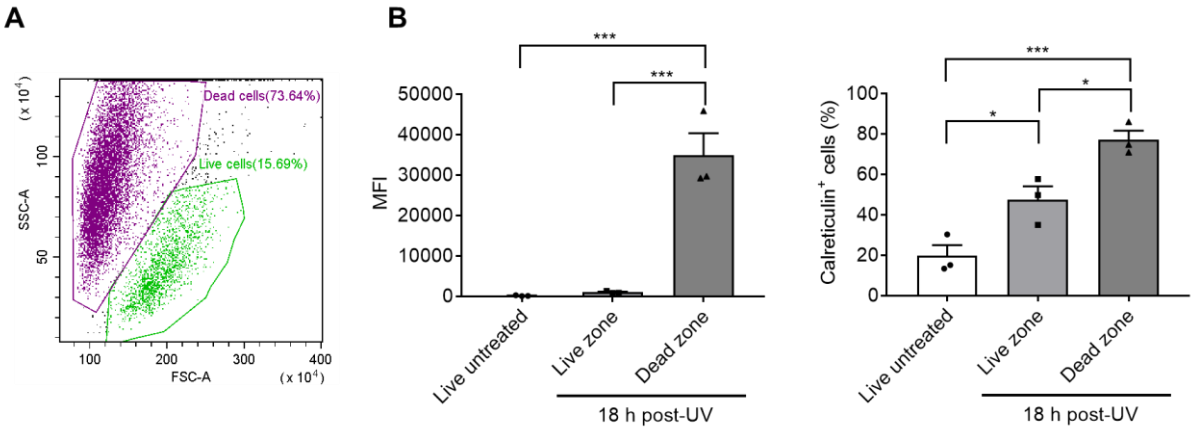

Figure 4.6: Cells undergoing apoptosis externalise calreticulin. (A) Cell populations gated on size and granularity (forward and side scatter) 18 hours post-UV treatment. **(B)** Cell surface expression of calreticulin in late apoptotic cells compared to live healthy cells. Protein expression shown as mean fluorescence intensity (MFI) and percentage of positive cells. (Data presented as mean + SEM, n=3; statistical analysis by one-way ANOVA with Tukey's multiple comparisons test; *P<0.05, ***P<0.001).

4.3.3 Detection of proteins on the surface of ACdEVs by flow cytometry

Proteins on the surface of ACdEVs are likely key mediators of interactions with macrophages. In order to confirm the presence of proteins identified by mass spectrometry on the EV surface, flow cytometry was used. In order to optimise the flow cytometer settings (gain, thresholds) for detection of nano-sized particles, fluorescent beads of known sizes were used; these beads also allow an estimate of EV size (**Figure 4.7A & B**). Violet side scatter (405nm) was used for detection/measurement instead of blue (488 nm) as it has been shown to provide improved resolution for nano-sized particles [148]. Measurement of ACdEVs from Jurkat cells in the 2000 x *g* supernatant showed that the majority of the EVs were less than approximately 200 nm (**Figure 4.7C**). Some background noise was present, particularly in the smaller size regions, as shown in **Figure 4.7D**, where events in a sample of deionised water were recorded for the same duration as the EV sample. In order to distinguish true EVs from background, a fluorescent labelling approach was used. EVs from late apoptotic/necrotic Jurkat and Mutu B cells were labelled with a fluorescent thiol-reactive membrane dye (BODIPY-FL) at 0.5, 1 and 2 μM to determine the optimal concentration for coverage of all vesicles. The results suggest that approximately 70% of the events detected with these settings were vesicles, and 1 μM was sufficient to cover all vesicles in the sample (Figure 4.8).

The flow cytometer settings were further optimised to improve resolution of EVs using a mixture of beads across the size range of 100-900 nm (**Figure 4.9A**). Most ACdEVs from Jurkat cells were smaller than 500 nm, and approximately 80% were smaller than 160 nm (**Figure 4.9B & C**). NanoFCM fluorescent QC beads (250 nm) were then used to adjust the settings for FITC and PE fluorescent channels to provide good separation of fluorescence-positive and fluorescence-negative particles (**Figure 4.10**). There was discrepancy in particle size between the different beads, as the 250 nm NanoFCM QC beads appeared in the region of the 160 nm Megamix beads based on violet side scatter (**Figure 4.10**). Further purification of EV samples by SEC before analysis by flow cytometry reduced background; events detected with violet SSC below 10^4 in 2000 x *g* secretomes (estimated to be <100 nm in size), likely pieces of cellular debris, were no longer present after SEC; EV samples were then gated on violet side scatter to eliminate these particles (**Figure 4.11A**). Pure buffer (PBS) was analysed to further assess the background noise. The event rate was low however many of these events fell within the EV gate, particularly within the region of smaller particles ~100 nm.

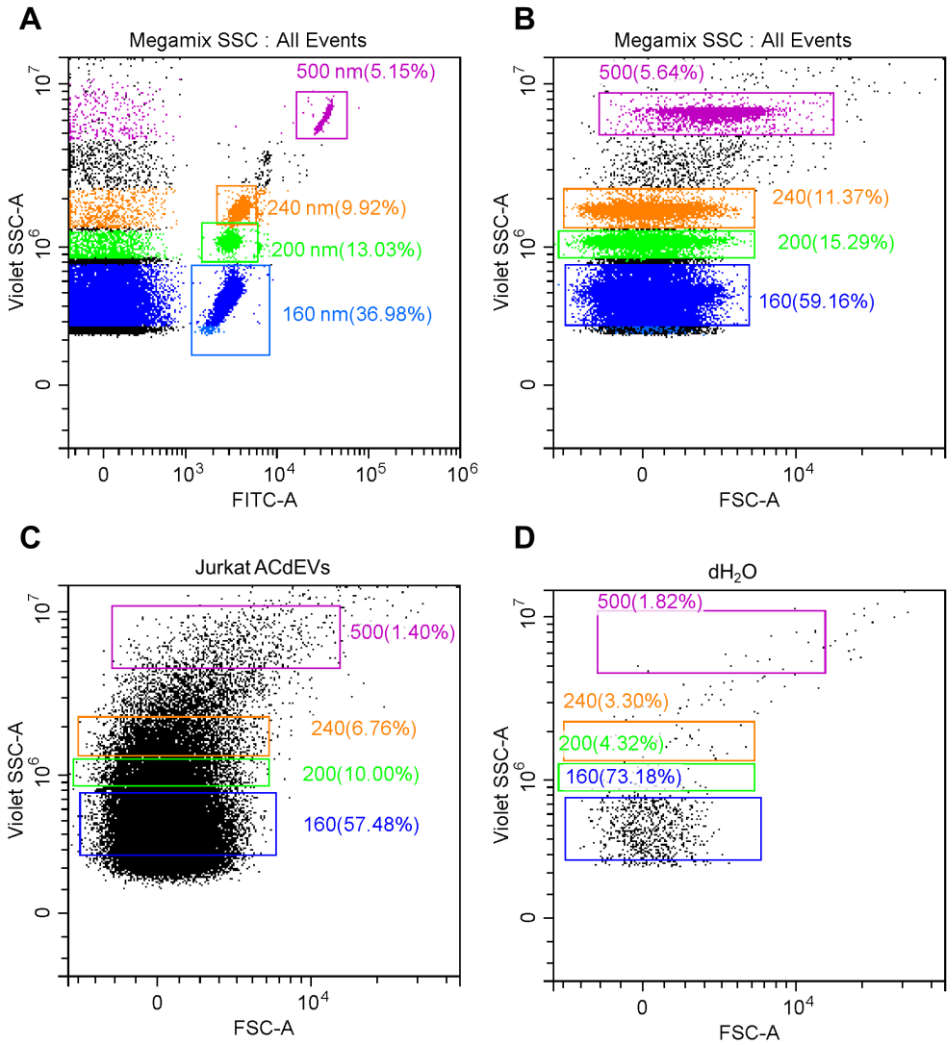

Figure 4.7: Detection of EVs by flow cytometry. (A) MegaMix side scatter beads of given sizes between 160 and 500 nm were used to establish settings for measurement of EVs. Beads are fluorescent in FITC channel, and size differentiated by violet side scatter. **(B)** Beads on forward and violet side scatter plot. **(C)** Apoptosis was induced in Jurkat cells and the 2000 x *g* supernatant was collected after 18 hours and analysed by flow cytometry. **(D)** Background noise observed by measurement of deionised water for the same duration as EV sample.

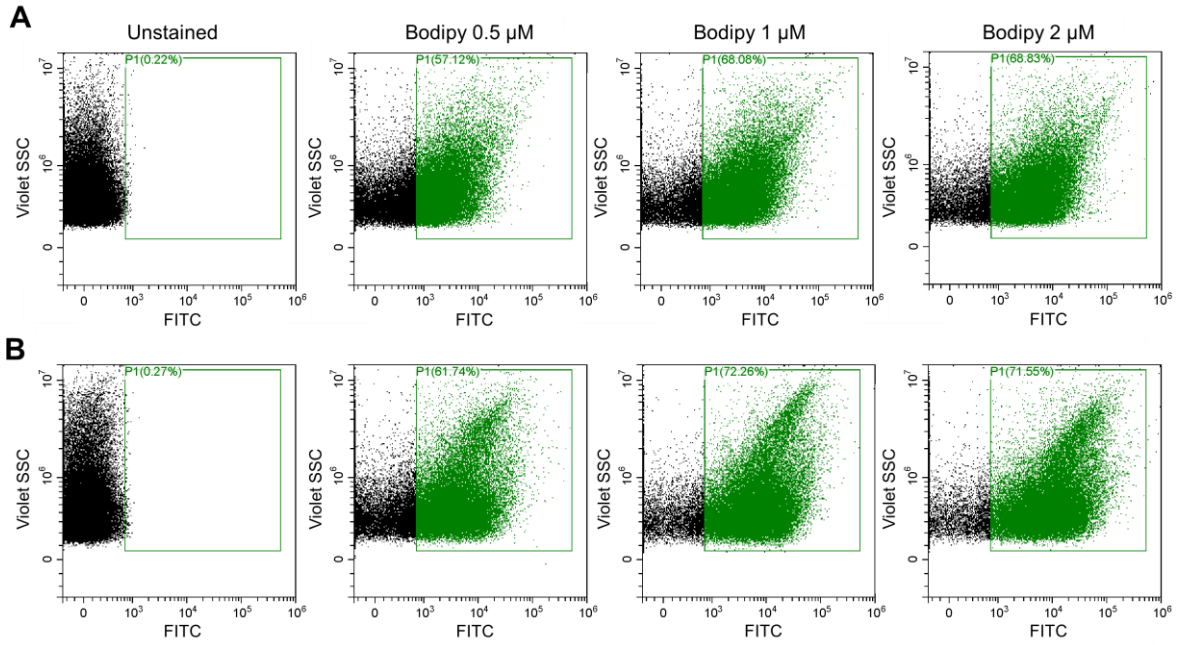

Figure 4.8: Fluorescent labelling of ACdEVs for flow cytometry analysis. ACdEVs from **(A)** Jurkat and **(B)** Mutu B cells, in 2000 x *g* supernatant were labelled with thiol-reactive dye (BODIPY-FL) at different concentrations and measured by flow cytometry.

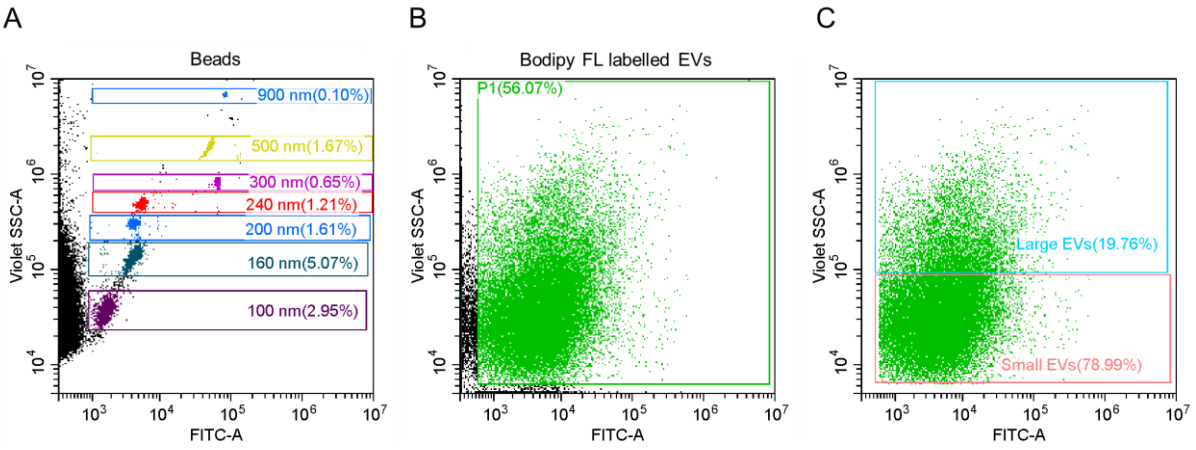

Figure 4.9: Optimising resolution of nano-sized particles and extracellular vesicles between 100 nm and 1 µm. (A) Megamix FSC and SSC fluorescent beads of sizes ranging from 100 nm to 900 nm were used to adjust the flow cytometer settings for detection of EVs. **(B**) ACdEVs from Jurkat T lymphocytes in 2000 x *g* supernatant were labelled with BODIPY-FL maleimide and measured by flow cytometry. **(C)** Estimation of the proportion of small and large EVs in the ACdEV population.

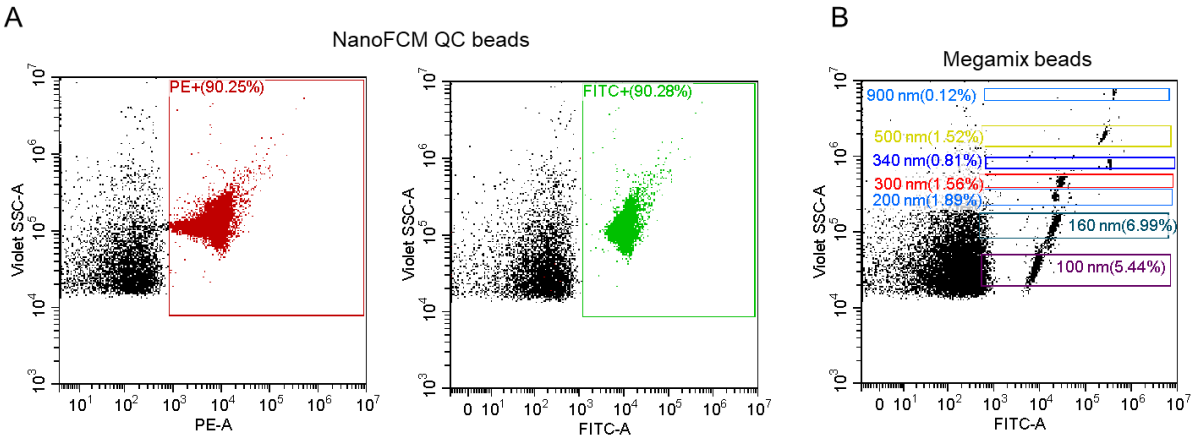

Figure 4.10: Optimising flow cytometer for detection of fluorescent signals from nano-sized particles. (A) 250 nm fluorescent beads were used to optimise the gain to improve the signals in the PE and FITC fluorescence channels. **(B)** Megamix beads ranging in size from 100 to 900 nm measured with the optimised settings.

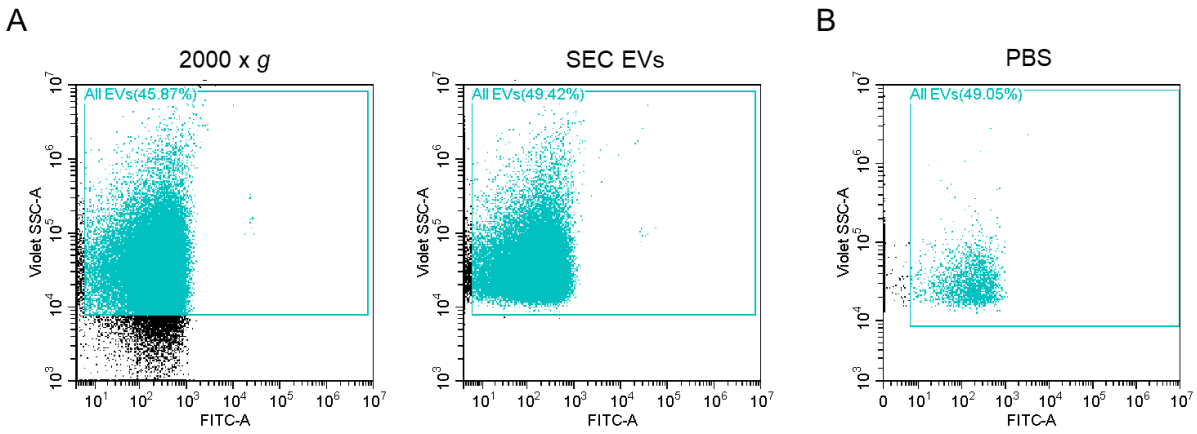

Figure 4.11: Isolation of ACdEVs by SEC reduces background noise. (A) ACdEVs samples were analysed by flow cytometry before (2000 x g supernatant) and after purification by SEC. SEC removes small particles. **(B)** Background events detected during measurement of PBS buffer, recorded for the same duration as the EV samples.

ACdEVs from Jurkat cells were then stained with annexin V-FITC to label phosphatidylserine, an “eat me” signal that is relocated to the surface of apoptotic cells, and commonly found in EVs. Approximately 85% of events in the EV gate were PS-positive, and this population included EVs of all sizes (Figure 4.12). Annexin V-FITC stain alone in buffer (at the same concentration used to label EVs) was also measured and recorded for the same duration; this confirmed that the stain alone did not cause false-positive signals, as the FITC signal from the events detected was below 10^3, as for unstained events. The similarity of the small peaks in the histogram for the annexin-V stain alone in buffer (i.e. no vesicles) and the unstained population of the labelled EV sample suggest that unstained events in the EV sample are non-vesicular.

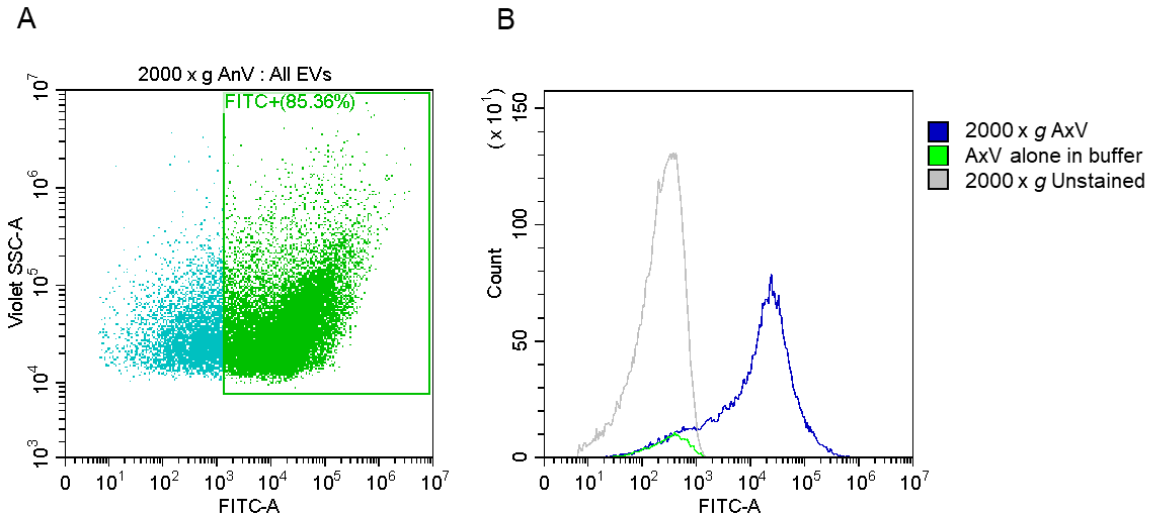

Figure 4.12: Detection of phosphatidylserine on the surface of ACdEVs. 2000 x *g* supernatant from apoptotic Jurkat T lymphocytes was collected 18 hours after induction of apoptosis with UV and ACdEVs were stained with annexin V-FITC (AxV) to label phosphatidylserine on the vesicle surface. **(A)** EVs were gated on size (approximately 100-1000 nm) using violet side scatter (SSC) and then gated on fluorescence in the FITC channel against unstained events (Green=Annexin V-FITC-positive). **(B)** Annexin V-FITC alone (without EVs) was measured to test for false-positive signals.

Next, antibodies were used to detect proteins of interest on the surface of ACdEVs. Antibody staining for calreticulin was performed on ACdEVs from Jurkat T cells 18 hours after induction of apoptosis using UV. Calreticulin was detected on the surface of ACdEVs Figure 4.13. There was a small amount of background signal in the EV region when the antibody alone in buffer was measured. During measurement by flow cytometry, it was also found that the signal in the PE channel shifted depending on the event rate. Undiluted samples (2000 x *g* supernatant), with event rate greater than 10,000 events per second had a much higher signal than samples

diluted to below 10,000 events/second, as shown by the histograms in **Figure 4.14**. This shifting effect was not observed in the FITC channel. Following this finding, all samples were diluted to ensure the event rate was below 10,000 events per second. Calreticulin was detected on the surface of ACdEVs even when SEC was used after staining to purify EVs and remove any excess antibody present (Figure 4.15). Gating positive events using the isotype control, the number of positive events decreased after SEC, however increased again when more antibody was added; the previous measurement of the antibody alone in buffer confirms this restoration of signal cannot be entirely an artefact caused by excess antibody. ACdEVs were also stained using antibodies against ICAM-1, -2 and -3, however these proteins could not be detected above the isotype staining (Figure 4.16).

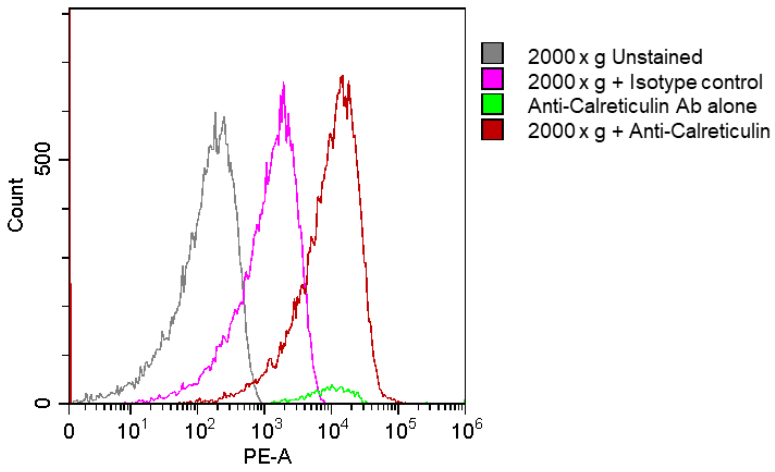

Figure 4.13: Detecting calreticulin on the surface of ACdEVs by flow cytometry. 2000 x *g* supernatant from apoptotic Jurkat T lymphocytes was collected 18 hours after induction of apoptosis with UV and ACdEVs were stained with anti-calreticulin-PE antibody (red) or isotype control (pink). Unstained cells (grey) were also measured and a sample of the antibody alone in buffer was also recorded for the same duration (green).

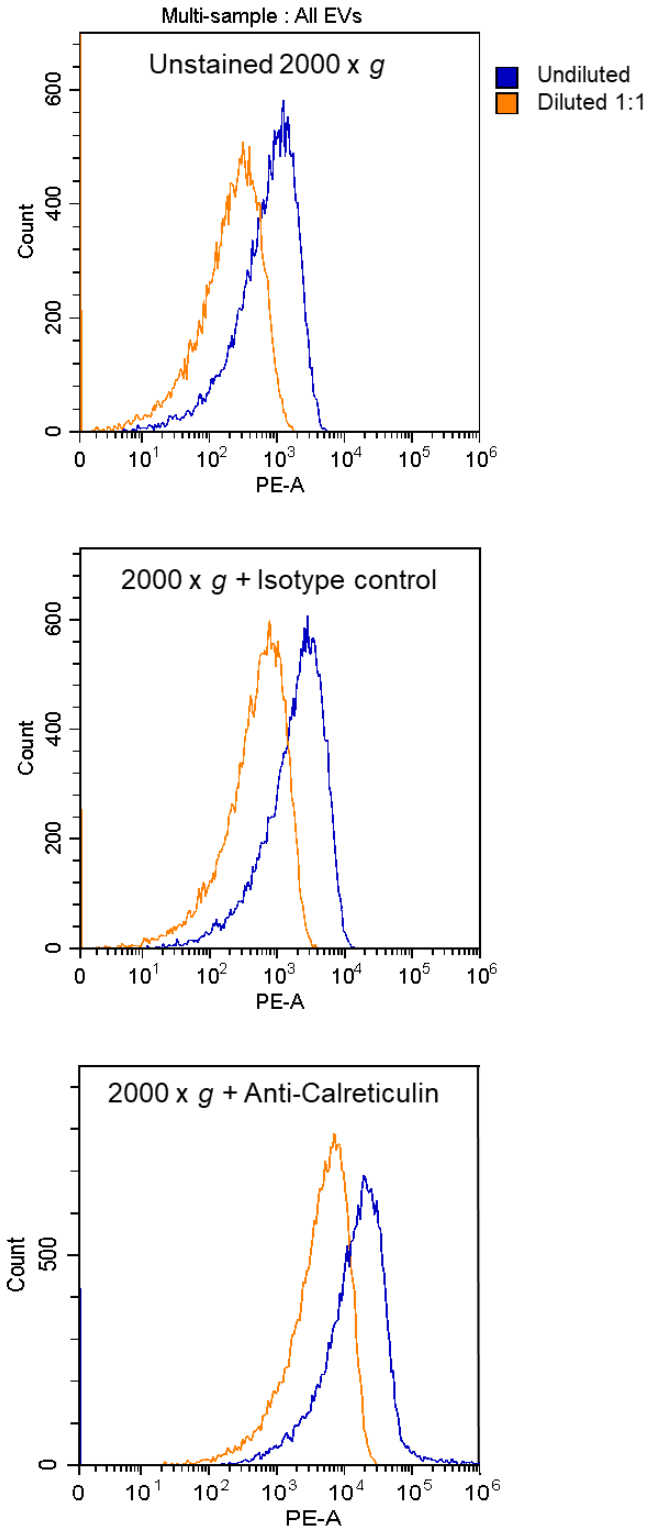

Figure 4.14: Effect of flow rate on fluorescent signal when analysing EVs by flow cytometry. PE signal for undiluted ACdEV samples (event rate >10,000 events/sec, blue) versus samples diluted 1:1 (<10,000 events/second, orange). EV samples were 2000 x *g* supernatant: unstained, isotype control and anti-calreticulin.

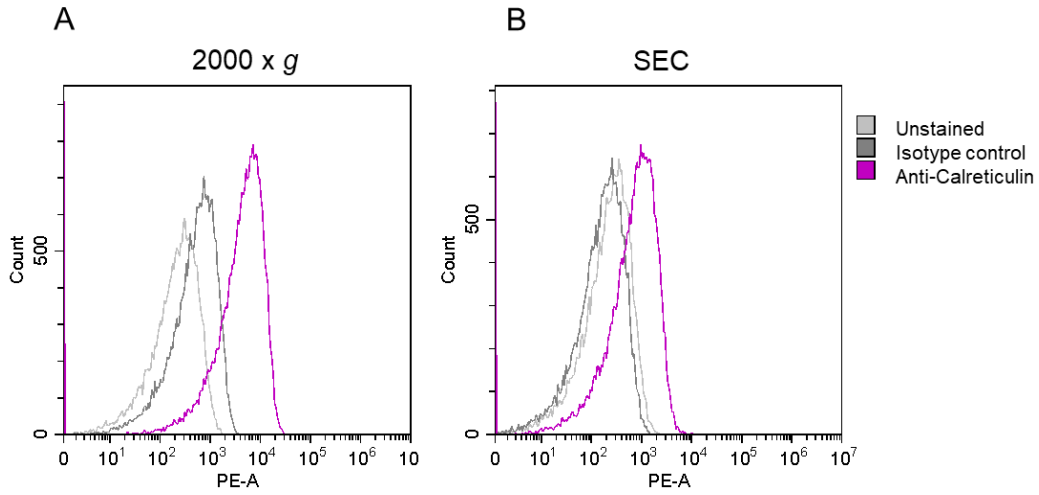

Figure 4.15: Detection of calreticulin on the surface of EVs before and after SEC. 2000 x *g* supernatant from apoptotic Jurkat T lymphocytes was collected 18 hours after induction of apoptosis with UV and ACdEVs were stained with anti-calreticulin-PE antibody (purple) or isotype control (dark grey), and analysed by flow cytometry **(A)** before and **(B)** after SEC. Representative histograms shown (n=3).

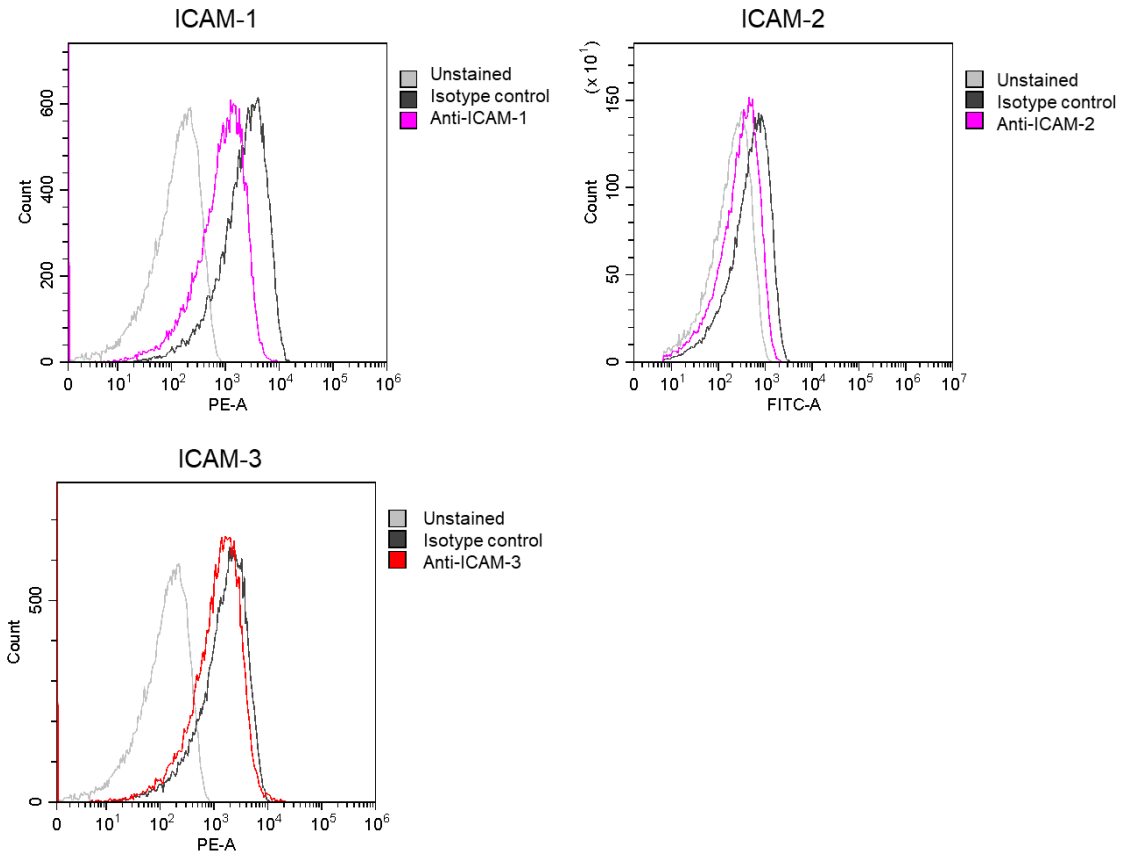

Figure 4.16: ICAM-1, -2 and -3 were not detected on the surface of ACdEVs by flow cytometry. 2000 x *g* supernatant from apoptotic Jurkat T lymphocytes was collected 18 hours after induction of apoptosis with UV and ACdEVs were stained with antibodies to detect ICAM-1, ICAM-2 and ICAM-3 using flow cytometry. Representative histograms shown (n=3).

4.3.4 Determining differences in proteomes of ACdEVs isolated by UC or SEC

To further investigate the hypothesis that isolation techniques may alter the proteomes and therefore functions of EVs, the proteomes of ACdEVs isolated by SEC and UC were compared. Firstly, western blots were used to evaluate the levels of two key apoptotic cell-derived signals, calreticulin and ICAM-3, in healthy versus apoptotic cells, and ACdEVs isolated by UC versus SEC. The concentration of calreticulin was similar between healthy and apoptotic cell lysates. The concentration of calreticulin in ACdEVs was much lower than in cell lysates, with similar faint bands visible for UC- and SEC-isolated samples. The concentration of ICAM-3 appeared to be much lower in ACdEV samples isolated by UC compared to SEC.

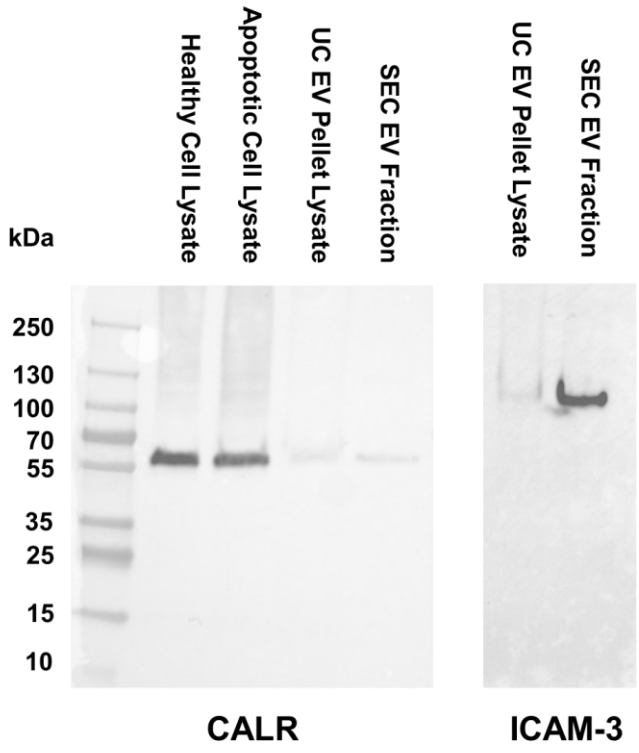

Figure 4.17: Calreticulin and ICAM-3 in ACdEV samples isolated by UC or SEC. Western blots were performed to assess the levels of calreticulin (CALR) and ICAM-3 in ACdEV samples isolated by UC or SEC from apoptotic Jurkat T cells (18 hours post-UV). Equal amounts of protein were loaded in each lane.

To evaluate the effects of isolation method on ACdEV proteomes as a whole, mass spectrometry was used. Apoptosis was induced in Jurkat cells using UV and ACdEVs were collected after 18 hours by UC or SEC, and protein content was analysed by mass spectrometry. A total of 1260 proteins were identified by unique peptides (complete data sets in Appendix), and all but one protein (Leucine-rich repeat-containing protein 47) were found in both SEC and UC isolated ACdEV samples. The abundances of 59% (743) of the proteins identified were not significantly different between the two EV isolation methods. The abundance of calreticulin was not different between isolation methods. ICAM-1, -2, and -3 were all enriched in the SEC sample, with fold changes of 1.7 for ICAM-1 and ICAM-2, and 2.2 for ICAM-3.

Gene ontology analysis revealed that half (374) of the proteins with no significant difference were associated with the cellular component “exosomes”, and 172 with “plasma membrane”. 156 of the proteins were associated with the biological process “signal transduction” and 146 were associated with “protein metabolism”. Of the 517 proteins with significantly different abundances between UC and SEC samples, 196 were significantly enriched with UC, and 321 significantly enriched with SEC (**Figure 4.18**). Most of the proteins enriched with UC were associated with the cellular components “cytoplasm” (144), “nucleus” (124), and “exosomes” (105). Most of the proteins enriched with SEC were associated with the cellular components “exosomes” (195), cytoplasm (190), “lysosome” (147) “plasma membrane” (135), and nucleus (129). The biological processes associated with the proteins enriched by UC or SEC are shown in **Figure 4.19**. Most of the proteins enriched with SEC were associated with “signal transduction”, “cell communication” and “transport” (70, 65 and 56, respectively), whereas a much smaller number of proteins enriched with UC were associated with those biological processes (18, 16 and 10, respectively).

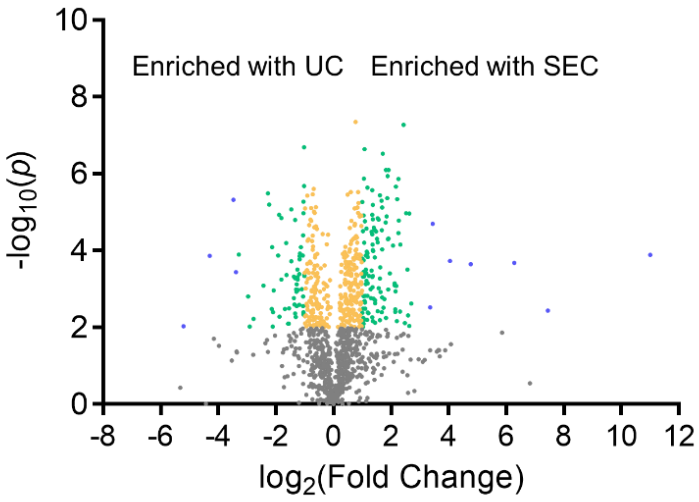

Figure 4.18: Comparison of UC- and SEC-isolated ACdEV proteomes. Enrichment of proteins in ACdEVs from Jurkat T cells isolated by UC or SEC 18 hours after induction of apoptosis using UV. Relative abundance was measured by mass spectrometry. (Fold change (FC) in abundance: Grey=p>0.01, not significant; Orange=FC<2; Green=2<FC<10; Blue=FC>10).

Enriched with UC	
Biological process	**No. of proteins**
Protein metabolism	44
Metabolism	39
Energy pathways	40
Cell growth and/or maintenance	7
Transport	10
Cell communication	16
Signal transduction	18
Regulation of nucleobase, nucleoside, nucleotide and nucleic acid metabolism	51
Regulation of cell cycle	1
Carbohydrate metabolism	1
Immune response	1
Anti-apoptosis	1
Proteolysis and peptidolysis	1
Apoptosis	4
Regulation of immune response	1
Protein folding	3
DNA repair	1
DNA replication	1
RNA localization	1
Transcription	1
Cell recognition	1
Muscle contraction	1

Enriched with SEC	
Biological process	**No. of proteins**
Protein metabolism	47
Metabolism	33
Energy pathways	33
Cell growth and/or maintenance	38
Transport	56
Cell communication	65
Signal transduction	70
Regulation of nucleobase, nucleoside, nucleotide and nucleic acid metabolism	15
Regulation of cell cycle	1
Immune response	14
Endosome transport	1
Apoptosis	4
Regulation of cell growth	1
Cell adhesion	1
Cell proliferation	1
Cell differentiation	2
Cell-cell signaling	1
Chromosome organization and biogenesis	2
Immune cell migration	1

Figure 4.19: Biological processes associated with proteins enriched in ACdEVs when isolated using UC or SEC. The proteomes of ACdEVs from Jurkat T lymphocytes isolated from cell supernatant 18 hours-post UV by UC or SEC were analysed by mass spectrometry and gene ontology analysis used to compare the biological processes associated with proteins enriched with UC or SEC.

4.4 Discussion

4.4.1 Proteomic analysis of ACdEVs from different immune cell types

Apoptotic cells release a variety of 'find me' signals to recruit macrophages, however few of these have been functionally characterised in their ACdEV-associated forms [21,22]. Here, the proteomes of ACdEVs released from T cells, monocytes, and B cells at early and late stages of cell death were analysed. This identified clear differences between ACdEVs released during early and late apoptosis, suggesting that early ACdEV release is a controlled process which serves to facilitate timely clearance of dying cells. The differences in protein enrichment between 6 and 18 hours suggest that major changes to the ACdEVs that are produced dilute out the effects of the composition of the vesicles released during the early stages. There is also the possibility that the composition of the vesicles changes after their release for example with enzyme activity.

Many proteins or protein families were conserved across the different cell types, and various ACdEV-associated proteins identified could potentially facilitate macrophage binding, recognition and uptake of ACdEV and mediate signalling in the context of inflammation, including transmembrane (e.g. ICAMs, integrins) and non-transmembrane proteins (annexins and calreticulin) and other signalling molecules. ACdEV-associated 'eat me' signal calreticulin, enriched in early ACdEVs, could be an important signal released to enable uptake of ACdEVs to promote timely removal of apoptotic cells and resolution or prevention of inflammation [159]. A limitation to the gene ontology approach used here to identify proteins of interest is that it is largely based on past knowledge in the literature, and therefore some proteins that play a role in ACdEV-mediated signalling would likely be overlooked if they had not previously been associated with a relevant biological process.

Notably, ACdEVs also carried signals that, on apoptotic cells, have been considered 'don't eat me' signals. It is possible that ACdEVs are a route by which apoptotic cells remove inhibitory signals to promote their own clearance. For example, loss of CD46 from the surface of apoptotic cells via ACdEVs has been shown to improve the efficiency of removal of apoptotic cells [36]. However, it is also possible that these signals, such as CD31 [33–35], are altered in some way which makes ACdEVs more likely to be taken up by phagocytes so as to exert their effects (e.g. in control of macrophage migration and phenotype). These 'don't eat me' signals may also function to extend the half-life of ACdEVs in circulation and prolong the effects of other signals they present. Interestingly, ABC transporters, which export lipid mediators of inflammation and are involved in resolution of inflammation [44,214], were present in ACdEVs.

Other unpublished work from our group has shown that ACdEVs from monocytes and T cells also carry lipid mediators that promote resolution of inflammation such as resolvins and lipoxins. These findings raise the possibility that lipid mediators are actively released from ACdEVs, and therefore ACdEVs may be continually changing. This possibility also reinforces the argument for the potential weakness of looking at what is only a snapshot of the makeup of EVs. The ability of EVs to change in composition and therefore function could be a key driver of the heterogeneity of EVs that is recognised in the field.

4.4.2 Release of proteins from apoptotic cells in ACdEVs

In 1999, Segundo et al. proposed that 'apoptotic blebs' recruit macrophages to sites of cell death [153]; this study showed, using flow cytometry, that many CD molecules, including ICAM-1 (CD54) are rapidly lost from the surface of apoptotic germinal centre B cells, partly via secretion of vesicles, and these 'blebs' stimulated chemotaxis in human monocytes. Also in 1999, Moffatt et al. demonstrated by western blot that apoptotic cells contain lower levels of ICAM-3 compared to viable cells. Torr et al. later demonstrated that ICAM-3 is shed from the cell surface during apoptosis in ACdEVs [22,32]. Another protein that has been shown to be rapidly lost from the surface off apoptotic B cells via ACdEVs is CX3CL1, in a 60 kDa cleaved form [21].

As ICAM-3 has been shown to play an important role in apoptotic cell clearance [22,32,87], but is only expressed by leukocytes, related mechanisms are likely to occur for other cell types when undergoing apoptosis. Analysis of the proteomes of ACdEVs from different immune cell types found ICAM-1, -2 and -3 in ACdEVs from T cells, whereas ACdEVs from monocytes contained only ICAM-1, and ACdEVs from B cells contained only ICAM-3. All of these cell types express all three of these ICAMs, so the lack of some of these in the ACdEVs is surprising. It may be that these proteins were not present at sufficient levels for detection. It is possible that they may be depleted by caspase-mediated protein degradation. We hypothesise that different ICAMs may function with some redundancy in the context of apoptotic cell signalling. Where present, ICAM-1 and ICAM-2 were significantly enriched in ACdEVs at 6 hours compared to 18 hours, supporting the hypothesis that these molecules are actively released from apoptotic cells during the early stages of apoptosis to promote rapid recruitment of macrophages for their removal.

Flow cytometry was used to measure the levels of ICAM-1, ICAM-2 and calreticulin on the surface of cells before and after induction of apoptosis. This confirmed that ICAM-1 and ICAM-

2 are shed from the surface of cells undergoing apoptosis. The loss of protein in terms of MFI and percentage of positive cells was different for ICAM-1 and ICAM-2 was different, which suggests that this is not simply due to the loss of membrane from apoptotic cells. Furthermore, the increase in surface levels of calreticulin on apoptotic cells shows that controlled changes in surface protein expression during apoptosis.

4.4.3 Analysis of ACdEVs by flow cytometry

Flow cytometry is a useful tool because it allows high-throughput analysis of multiple parameters on single particles. Flow cytometry-based analysis of EVs can provide valuable insight into their composition, and development of new technology has improved this technique [150,151]. Here, flow cytometry was used to investigate the surface proteomes of ACdEVs. ACdEVs had a similar estimated size distribution as that measured by TRPS, shown earlier. Due to their very small size, flow cytometry analysis of EVs, which relies on scattering of light, is much more complex compared to analysis of cells. Here, ACdEVs were detected label-free, and were also stained effectively with a thiol-reactive membrane dye. However, it proved difficult to optimise and eliminate background noise; it is therefore difficult to make any quantitative conclusions from the flow cytometry data. Labelling EVs with a fluorescent dye such as BODIPY is one solution to improve detection of EVs. Calreticulin was detected on the surface of ACdEVs, and although there were some positive events from the antibody in the absence of EVs, these were not sufficient to account for all positive events in the ACdEV samples. The calreticulin staining was reduced after SEC, which could be because SEC removes some calreticulin from the EV surface, or because the affinity of the antibody is low. While key apoptotic signals phosphatidylserine and calreticulin could be detected on the surface of ACdEVs, ICAM-1, -2 and -3 (identified in ACdEVs by mass spectrometry) could not. There are numerous reasons that could explain why these proteins could not be detected; firstly, the amount of protein may simply be too low to detect a signal using this method; using multiple monoclonal antibodies against different epitopes of a protein may amplify the signal. Furthermore, the PE-conjugated isotype controls produced quite a substantial signal on the EVs. There is also the challenge of possible batch-to-batch variation in antibodies and isotype controls and non-specific background (for example caused by precipitates). Bead coupling can be used to analyse EVs by flow cytometry, capturing multiple EVs on each bead and therefore amplifying the signal [87]; this however means that information such as the estimated sizes of EVs and the proportion of EVs expressing a particular molecule cannot be determined. Another explanation could be that steric hindrance due to the presence of binding partners or other membrane-associated molecules may prevent sufficient antibody molecules from binding to a

vesicle to provide a detectable signal. There is also the possibility that the orientation of ICAMs in the membrane is switched and the epitope recognised by the antibody may therefore be on the inside of the vesicle and inaccessible. Significant reorganisation of the membrane occurs during apoptosis, including externalisation of phosphatidylserine and calreticulin [29,160]; there could also be internalisation of molecules occurring or perhaps formation of 'inside-out' vesicles. Further optimisation of the staining of molecules on the surface of ACdEVs and flow cytometer settings to detect them is required.

4.4.4 Determining differences in proteomes of ACdEVs isolated by UC or SEC

Results presented in the previous chapter demonstrate functional differences between ACdEVs isolated by UC and those isolated by SEC. Various molecules are associated with the surface of EVs, which should be considered components of their surface interactome [95]. We hypothesise that a corona of protein and other protein-associated molecules likely exists surrounding the EV surface, and that components of this corona may be removed by stringent isolation methods such as SEC. The initial proteomic analysis of ACdEVs from the three different immune cell types showed that membrane-associated proteins such as calreticulin and annexins are present in samples isolated by SEC, however the levels of these may be reduced by SEC.

In order to determine whether membrane-anchored calreticulin is removed from the surface of ACdEVs during SEC isolation, ACdEVs were isolated by SEC or UC and calreticulin levels assessed by western blot. The results found that calreticulin levels were similar between ACdEVs isolated by UC and SEC, suggesting that SEC did not affect the amount of calreticulin on the EV surface, as previously hypothesised. Western blots were also performed to assess the levels of ICAM-3 in ACdEVs depending on isolation method; ICAM-3 levels appeared much higher in the sample isolated by SEC compared to the sample isolated by UC. The higher concentration of ICAM-3 in SEC sample could be due to SEC removing surface-associated protein resulting in a higher relative abundance of ICAM-3 and other integral membrane proteins as well as luminal proteins. If this was the case, there would be a lower amount of protein per vesicle in SEC samples versus UC samples, and loading the samples with equal amounts of protein for the western blots could mean that more EVs were loaded in the SEC sample versus the UC sample. Future work should assess the differences in protein per vesicle with UC versus SEC, and western blots could be performed with loading controlled by number of particles instead of amount of protein.

Analysis of the whole proteomes of ACdEVs isolated by UC and SEC determined that the majority of proteins are not significantly enriched by one method compared to the other, including calreticulin, which confirms the results of the western blotting. However, there were some differences in the abundance of proteins. For example, the abundances of ICAM-1, -2, and -3 were all significantly higher in the SEC sample, consistent with the western blot for ICAM-3. Again, this could be due to the protein per vesicle being different between SEC-isolated EVs versus UC-isolated. Gene ontology analysis found that more proteins enriched by SEC were associated with signal transduction and cell communication compared to proteins enriched by UC, although it is possible that other molecules that may associate with these proteins in order to exert their effects may be removed by SEC. The potential effects of isolation method on the composition and function of ACdEVs should be explored further, and should be carefully considered in all studies of EV composition and function.

Research by Rai et al. using mass spectrometry to analyse EVs derived from multiple cancer cell lines has shown that there is heterogeneity between the proteomes of small and large EVs, particularly the surface proteomes [215]. While here we have investigated smaller ACdEVs separated from large apoptotic bodies, ranging in size from approximately 100-1000 nm, future work could further separate sub-populations of ACdEVs based on size and compare their proteomes and functions. The surface proteome could be analysed and compared to the whole proteome to investigate which proteins are accessible on the surface of ACdEVs. Rai et al. used a membrane impermeant biotin derivative to capture EV surface proteins for analysis by mass spectrometry [215].

To summarise, the data presented in this chapter support the hypothesis that during apoptosis, cells release proteins in an active, controlled manner in ACdEVs. These ACdEVs contain a vast array of proteins, identified by mass spectrometry, including many potential mediators of ACdEV which include transmembrane (e.g. ICAMs, integrins) and membrane-associated proteins (annexins and calreticulin) as well as other signalling molecules.

5. Results Chapter 3: Characterising the structure-function relationships of ACdEVs

5.1 Introduction

The work presented so far has demonstrated that ACdEVs communicate with macrophages, promoting migration and altering their phenotype, and that ACdEVs released by different immune cell types carry hundreds of different proteins, many of which are signalling molecules associated with regulation of immune responses. While the proteomes of ACdEVs have previously been studied [93,159], the functions of only a few ACdEV-associated proteins have been assessed [21,22,159]. Calreticulin is translocated to the surface of apoptotic cells to act as an 'eat me' signal to macrophages [29,31]. Recently, Zheng et al. found that calreticulin on the surface of ACdEVs derived from apoptotic MSCs also acts as a key 'eat me' signal promoting uptake of ACdEVs by bone marrow-derived macrophages in vitro and by liver macrophages in vivo, in a mouse model of type 2 diabetes [159]. This study also demonstrated that calreticulin-dependent uptake of ACdEVs resulted in reprogramming of macrophages to restore homeostasis. As demonstrated in the previous chapter, dying cells externalise calreticulin during apoptosis, and calreticulin is enriched in ACdEVs released during early apoptosis. This evidence supports the hypothesis that calreticulin is a key signal released by apoptotic cells in ACdEVs. ACdEV-associated ICAM-3 has been shown to promote migration of macrophages towards dying cells [22], whilst also acting as a ligand on apoptotic cells to support their clearance [32]. As discussed previously, we hypothesised that different ICAMs may have redundant functions in apoptotic cell signalling and clearance.

5.2 Aims

The final aim of this project was to characterise ACdEV structure-function relationships, by assessing the roles of proteins of interest as ligands for macrophage chemoattraction, EV binding, uptake and other immunomodulatory functions *in vitro*. The roles of the candidate proteins in ACdEV-mediated signalling were investigated by blocking their function using antibodies or other inhibitors. The THP-1 macrophage model and the assays previously tested were used to investigate the roles of ACdEV-associated calreticulin, ICAM-1, and ICAM-2 as ligands for chemoattraction, uptake and modulation of macrophage phenotypes.

5.3 Functions of ACdEV-associated calreticulin

Firstly, as calreticulin is a known apoptotic 'eat me' signal, calreticulin-mediated uptake of ACdEVs was investigated. A calreticulin blocking peptide which has previously been shown to block calreticulin-mediated phagocytosis [30] was used to block macrophage receptors for calreticulin. ACdEVs were labelled with BODIPY FL maleimide and binding/uptake by THP-1-derived macrophages was assessed by flow cytometry over 4 hours. Calreticulin blocking peptide (4 μg/ml [30]) did not appear to affect binding/uptake of ACdEVs in this assay, regardless of whether the macrophages had been pre-incubated with the blocking peptide for 3 hours before addition of ACdEVs (**Figure 5.1**). Following this, the ability of calreticulin blocking peptide to inhibit binding and uptake of apoptotic cells was assessed. Apoptosis was induced in Jurkat T cells using UV and cells were collected after 18 hours and labelled with BODIPY FL maleimide (**Figure 5.2A**). THP-derived macrophages were labelled with the lipophilic dye DiR and gated on live cells (forward and side scatter) and on fluorescence in the APC-A750 channel, above the background from apoptotic Jurkat cells (**Figure 5.2B**). Apoptotic Jurkat cells were added to macrophages (ratio 10:1) and uptake of apoptotic cells was assessed by flow cytometry over 2 hours. At 10 minutes, the acquired fluorescence was lower for macrophages in the presence of calreticulin blocking peptide, however it was similar with and without blocking peptide at all other time points (**Figure 5.2C**).

Next, the ability of calreticulin to stimulate macrophage chemotaxis was investigated using a vertical transwell migration assay, using THP-1-derived macrophages and the 2000 x *g* secretome of apoptotic Jurkat T cells. The rate of migration was reduced compared to previous results, due to a fault with the machine's temperature control, however addition of calreticulin blocking peptide to macrophages reduced the rate of migration, with the number of migrated cells at 6 hours up to half that of macrophages without inhibitor, although not statistically significant (**Figure 5.3**).

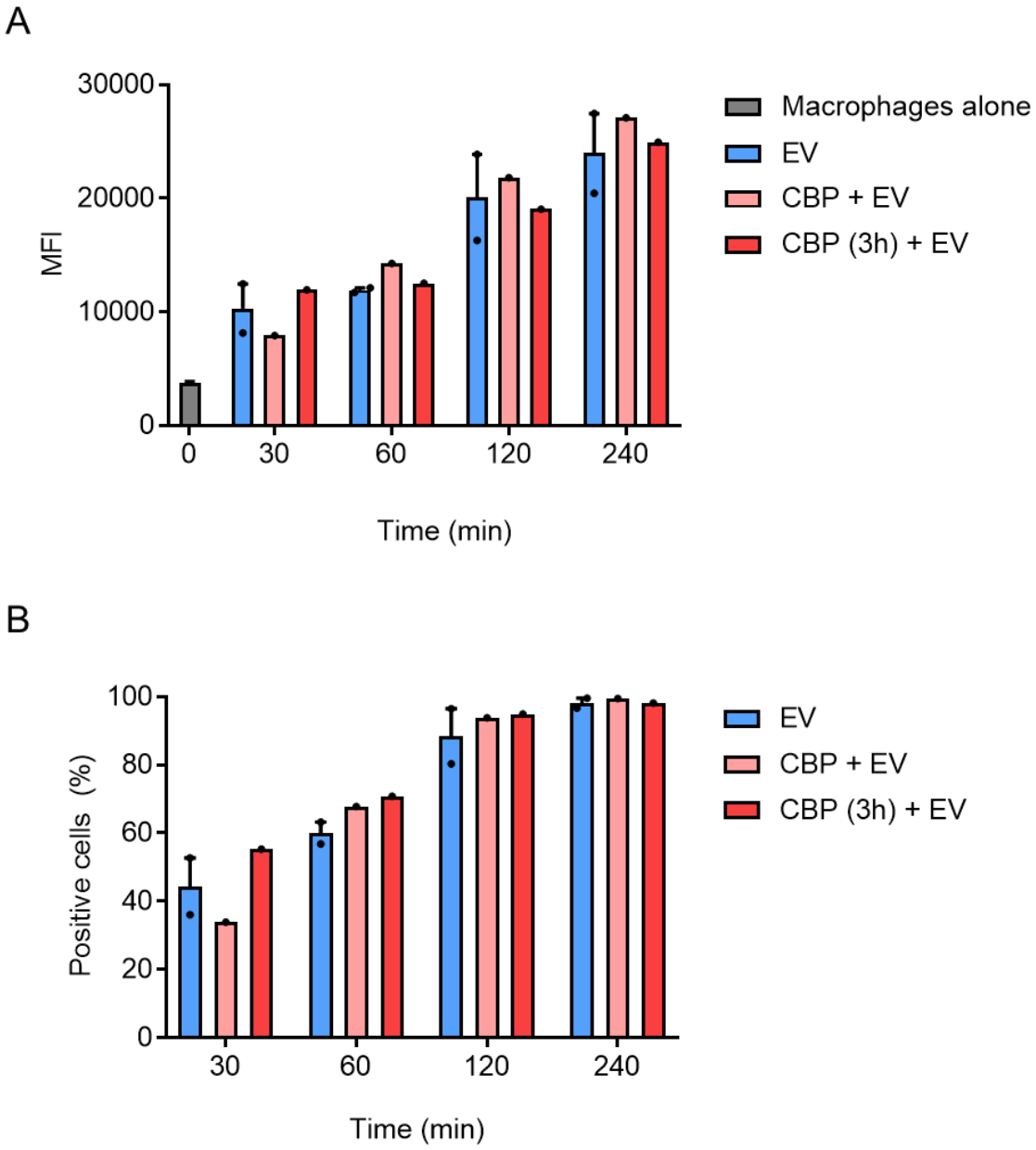

Figure 5.1: Binding and uptake of fluorescent ACdEVs by macrophages in the presence of calreticulin blocking peptide assessed by flow cytometry. THP-1-derived macrophages were exposed to fluorescently labelled ACdEVs (BODIPY FL maleimide labelling) from Jurkat T cells (18 hours post-UV), and acquired fluorescence was measured by flow cytometry. Addition of calreticulin blocking peptide (CBP) to macrophages at the same time as addition of ACdEVs and pre-incubation of blocking peptide with macrophages for 3 hours before addition of ACdEVs was tested. **(A)** Mean fluorescence intensity of entire cell population (MFI). **(B)** Proportion of fluorescence-positive cells. (Data presented as mean + SEM, n=1-2).

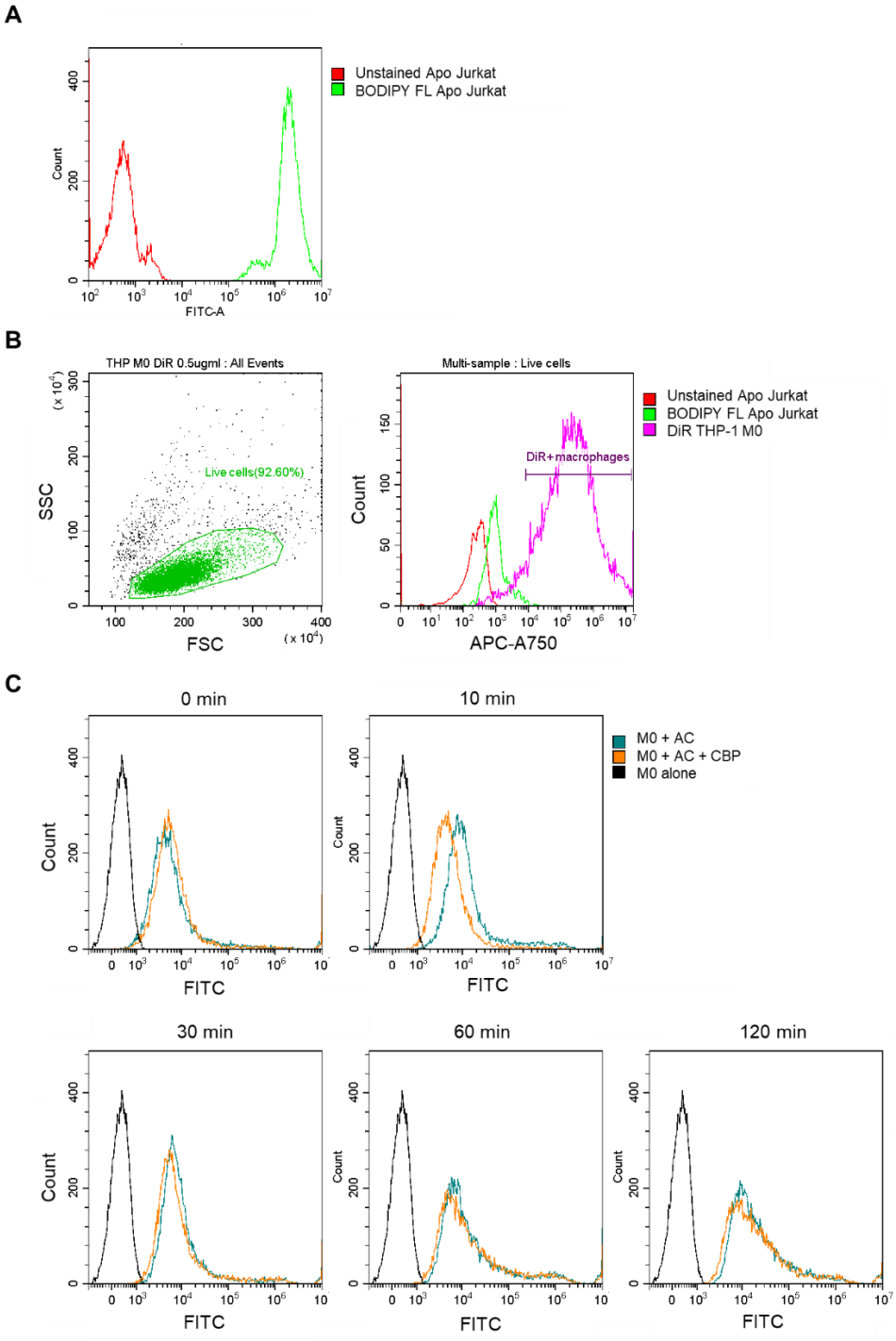

Figure 5.2: Uptake of apoptotic cells by macrophages in the presence of calreticulin blocking peptide assessed by flow cytometry. (A) UV-induced apoptotic Jurkat T cells were labelled with BODIPY-FL. **(B)** THP-derived macrophages were labelled with DiR and gated on live cells (forward and side scatter) and on fluorescence. **(C)** Clearance of apoptotic cells (acquired fluorescence) was assessed over the course of 2 hours (n=1).

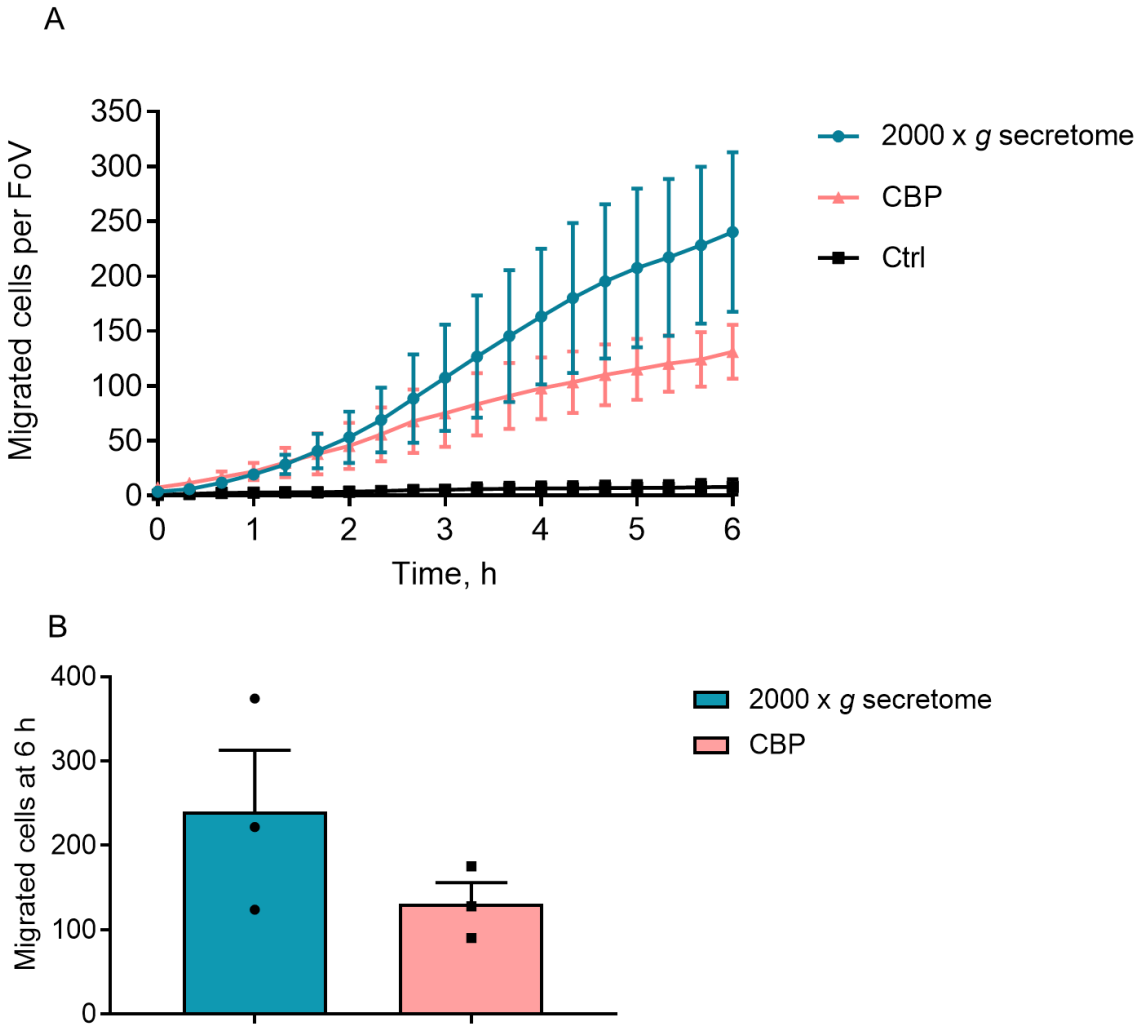

Figure 5.3: Apoptotic cell-derived calreticulin-mediated chemoattraction of macrophages. A transwell migration assay was performed to measure migration of THP-1-derived macrophages with and without calreticulin blocking peptide (CBP) towards the 2000 x *g* supernatant containing ACdEVs from apoptotic (18 h) Jurkat T cells. Serum-free RPMI was used as a medium-only control. **(A)** Macrophage migration over 6 hours. **(B)** Number of cells migrated at 6 hours. (Data presented as mean ± SEM, n=3).

5.4 Functions of ACdEV-associated ICAMs

As discussed earlier, ACdEV-associated ICAM-3 has already been shown to play a role in apoptotic cell clearance by recruiting macrophages [22]. As ICAM-3 is expressed only by leukocytes, we hypothesised that other ICAMs may play the same role for other cell types. To investigate this, vertical migration assays were performed using antibodies to block ICAM-1 [216] and ICAM-2 [217]. ACdEVs from apoptotic Jurkat T cells were isolated 18 hours after induction of apoptosis by UC and migration of THP-1-derived macrophages towards ACdEVs was assessed using the vertical transwell migration assay. The attraction of macrophages by ACdEVs is delayed at first compared to that seen with the secretome, but at around 3 hours the number of migrated cells is the same. The antibodies against ICAM-1 and ICAM-2 did not affect migration (**Figure 5.4**).

Next, the role of ICAM-1 and ICAM-2 in binding and uptake of ACdEVs by macrophages was assessed. ACdEVs were labelled with BODIPY FL maleimide and binding/uptake by THP-1-derived macrophages was assessed by flow cytometry up to 1 hour, at which point almost all macrophages were positive for ACdEV-associated fluorescence. The fluorescence intensity varied substantially between replicates but the antibody did not affect uptake of ACdEVs, for ICAM-1 (**Figure 5.5**) or ICAM-2 (**Figure 5.6**).

A

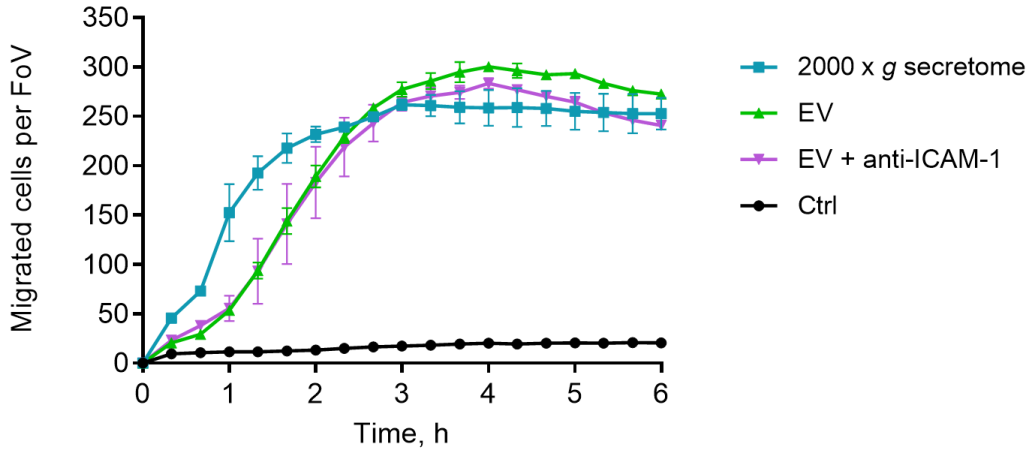

B

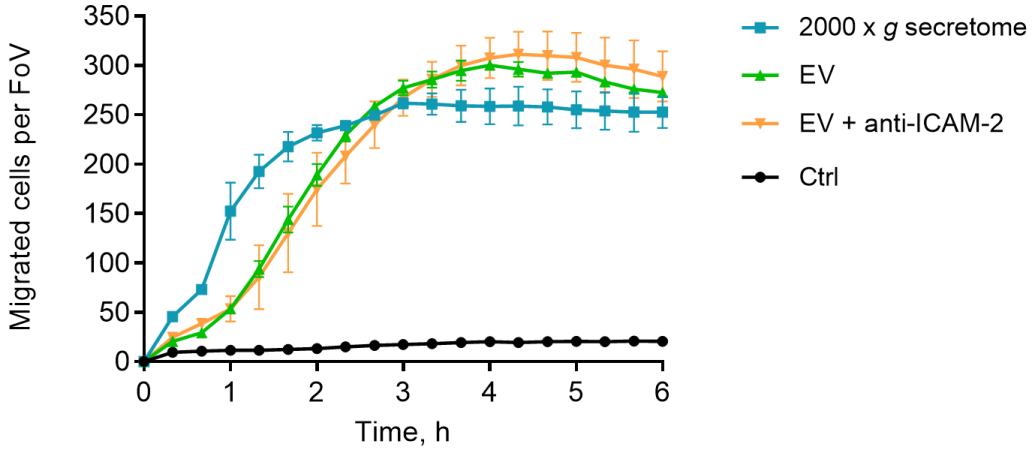

Figure 5.4: ICAM-mediated macrophage chemotaxis towards ACdEVs. A transwell migration assay was performed to measure migration of THP-1-derived macrophages towards ACdEVs (isolated by UC) from apoptotic Jurkat T cells (18 hours post-UV) with and without antibody against **(A)** ICAM-1 and **(B)** ICAM-2. Serum-free RPMI was used as a medium-only control. (Data presented as mean ± SEM, n=3).

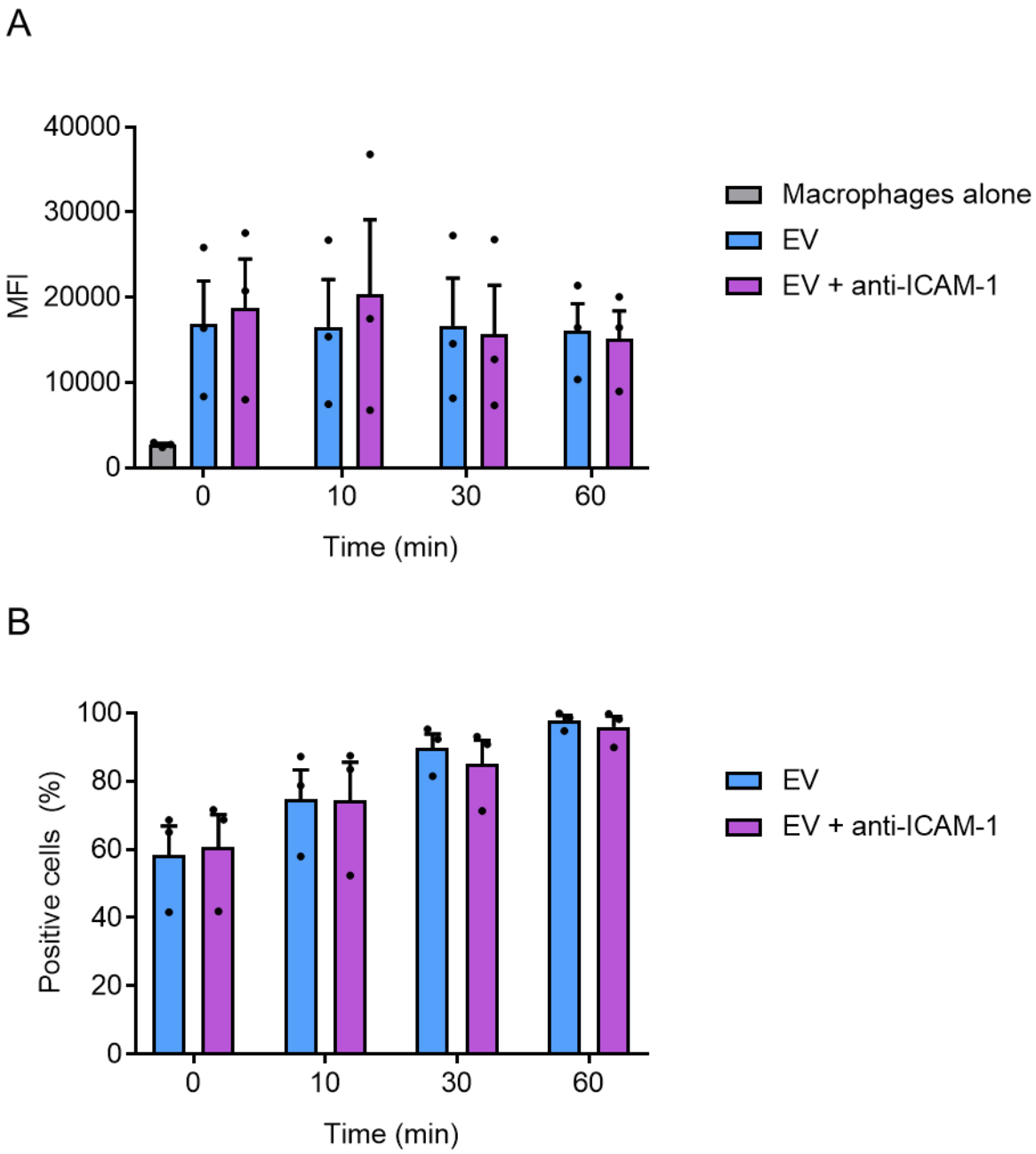

Figure 5.5: Binding and uptake of ACdEVs by macrophages in the presence of anti-ICAM-1 antibody. THP-1-derived macrophages were exposed to fluorescently labelled ACdEVs (BODIPY FL maleimide labelling) from apoptotic Jurkat T cells (18 hours post-UV), with and without anti-ICAM-1 antibody, and acquired fluorescence was measured by flow cytometry over 1 hour. **(A)** Mean fluorescence intensity of entire cell population (MFI). **(B)** Proportion of fluorescence-positive cells. (Data presented as mean + SEM, n=3).

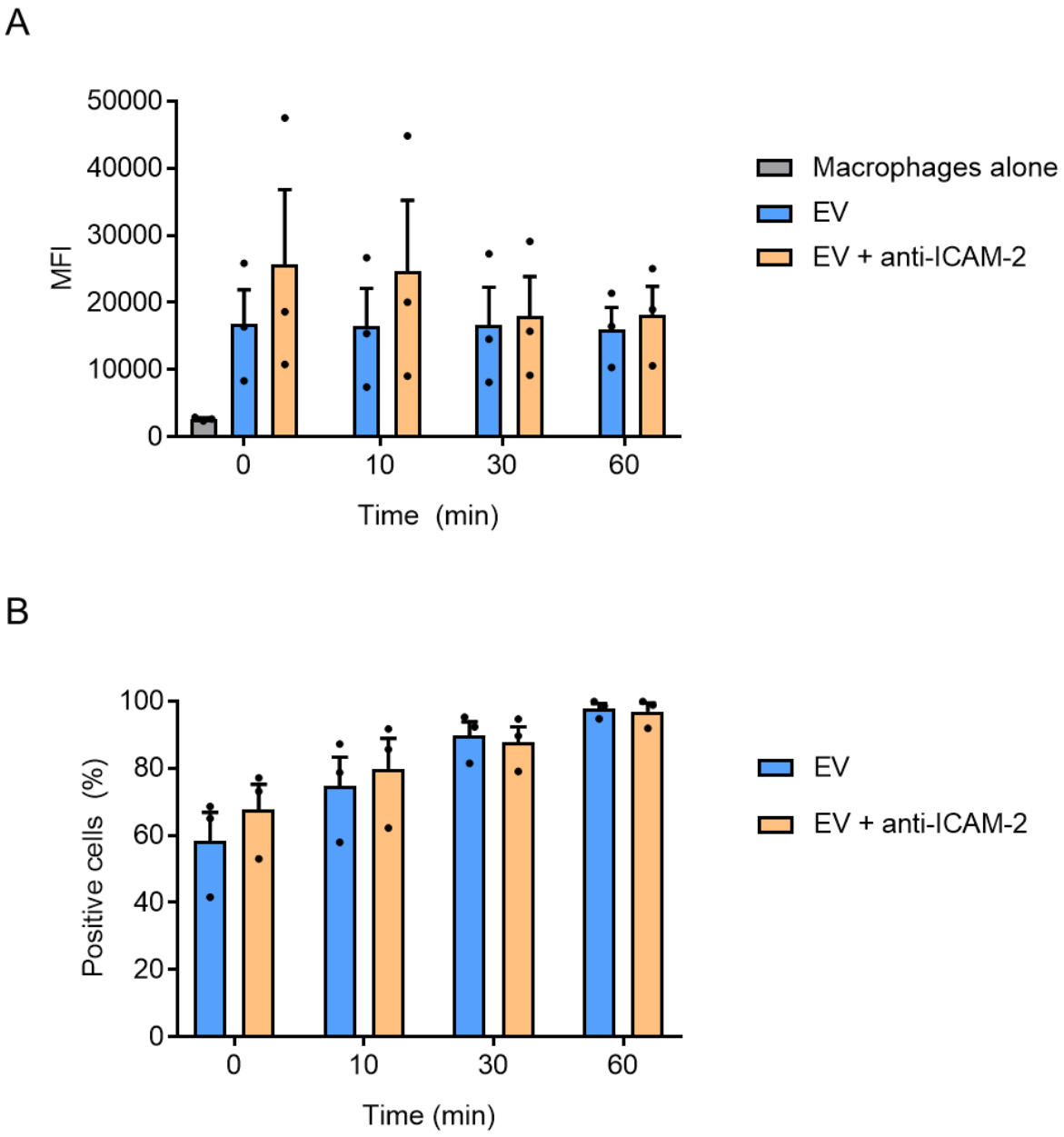

Figure 5.6: Binding and uptake of ACdEVs by macrophages in the presence of anti-ICAM-2 antibody. THP-1-derived macrophages were exposed to fluorescently labelled ACdEVs (BODIPY FL maleimide labelling) from Jurkat T cells (18 hours post-UV), with and without anti-ICAM-2 antibody, and acquired fluorescence was measured by flow cytometry over 1 hour. **(A)** Mean fluorescence intensity of entire cell population (MFI). **(B)** Proportion of fluorescence-positive cells. (Data presented as mean + SEM, n=3).

5.5 Discussion

The aim of this project was to characterise structure-function relationships of ACdEVs in the context of modulation of inflammation. Proteomic analysis of ACdEVs identified a multitude of proteins that could mediate signalling in this context. Due to the COVID-19 pandemic, a substantial amount of time for laboratory-based experimentation was lost. This meant that investigation of the functions of proteins of interest was limited. The first molecule chosen for investigation was calreticulin, which is known to be a key 'eat me' signal exposed by apoptotic cells, and has recently been shown to mediate uptake of ACdEVs by macrophages [29,159]. Zheng et al. used a neutralising antibody against calreticulin and downregulation of calreticulin using RNA interference, and demonstrated reduced uptake of ACdEVs with fluorescence microscopy and flow cytometry. The effect of blocking calreticulin on binding and uptake of ACdEVs could not be demonstrated here using calreticulin blocking peptide and measurement by flow cytometry. This could be due to the concentration of blocking peptide being insufficient or lower affinity of the blocking peptide for receptors on macrophage versus the ACdEV-associated calreticulin. The ability of the blocking peptide to block calreticulin signalling was also tested for uptake of apoptotic cells. A reduction in phagocytosis of apoptotic cells was observed with calreticulin blocking peptide at 10 minutes, but by 30 minutes this difference disappeared; it is possible that with more time the macrophages can use other mechanisms of recognition to compensate. These experiments must be repeated in order to make any robust conclusions.

However, migration of macrophage towards ACdEVs was inhibited by calreticulin blocking peptide, suggesting a role for ACdEV-associated calreticulin in recruitment of macrophages as well as facilitating phagocytosis of apoptotic cells and ACdEVs, but this is perhaps not an important molecule for binding to the surface of macrophages. Soluble recombinant calreticulin has been shown previously to promote macrophage migration [31]. Future work could also use antibodies against calreticulin or knockdown or overexpression of calreticulin to investigate its functions.

While ACdEV-associated ICAM-3 has been previously studied and shown to play a role in recruitment of macrophages [22,194], ICAM-3 is only expressed by leukocytes and therefore other molecules must serve the same purpose to facilitate clearance of other cell types during apoptosis. This redundancy is highlighted by mouse macrophage recognition of ICAM-3 on human apoptotic cells – mice are naturally deficient for ICAM-3 but mouse macrophages can recognise ICAM-3 [22]. It was hypothesised that ICAM-1, ICAM-2 and ICAM-3, which are

structurally similar and all bind to the integrin LFA-1 [218], may have redundant roles in apoptotic cell clearance. To test the hypothesis of redundancy between different ICAMs, antibodies were used to block to ICAM-1 and ICAM-2 and test whether this affected ACdEV functions. While no effect was observed with either antibody, redundancy in their function could explain this observation. Future work could test this using antibodies against multiple ICAMs in combination. The delay observed in migration towards isolated EVs versus the whole 2000 x *g* secretome could be due to the removal of important soluble factors that are released by apoptotic cells.

Other work planned that could not be performed due to the COVID-19 pandemic included expanding the study by investigating the roles of other proteins in mediating ACdEV functions. Other proteins of interest included other adhesion molecules such as CD molecules (e.g. CD31, CD97, and CD166) and integrins, as well as annexins, and ABC transporters that may export lipid mediators from within ACdEVs to the extracellular environment. It was also planned to use additional techniques to assess chemotaxis, uptake, and macrophage polarisation. Assessment of migration could also be performed using a horizontal migration assay instead of a vertical migration assay. Horizontal assays provide a true gradient (rather than a step gradient) and further information on cell motility, as cell trajectories can be tracked, and distance travelled, and velocity can be measured. For investigation of binding and uptake of ACdEVs, use of fluorescence microscopy was planned as an alternative or to complement the flow cytometry-based approach. Microscopy can be used to assess binding of ACdEVs to macrophages and subsequent phagocytosis separately. Different temperatures could also be used to investigate binding (4°C or 20°C for assessment of binding only and 37°C for binding and internalisation) [22].

In this study, a THP-1 cell line model of macrophage polarisation was established and the effects of ACdEVs on macrophage phenotype was assessed. In addition to characterising the functions of proteins of interest in chemoattraction, recognition and uptake of ACdEVs, the roles of these proteins in ACdEV signalling and the phenotypic responses of macrophages should be investigated in future. As well as using inhibitor molecules to investigate protein function, genetically modified cell lines were also considered. This approach was taken by Torr et al. (2012) where cells expressing low levels of ICAM-3 were shown to attract macrophages to a lesser extent [22]. In addition, a knock-in approach was taken by Moffatt et al. (1999) where HEK cells over-expressing ICAM-3 were shown to be recognised to a greater degree when apoptotic [32]. Future work could assess if ACEVs from those cells, carrying ICAM-3 (or other overexpressed adhesion molecules) reveal a greater attractive capacity for macrophages

than EVs from the non-transfected cell line. Effects of inhibition, knockdown or overexpression on macrophage polarisation could be assessed by surface marker expression, cytokine release and possibly also transcriptional analysis by quantitative PCR.

Previous work by our laboratory found that the early apoptotic secretome is more chemoattractive than the late apoptotic secretome [219]. The proteomics presented here show differences in the proteomes of early versus late ACdEVs in terms of the abundances of many different proteins. These results support the hypothesis that dying cells, undergoing the tightly regulated process of apoptosis, actively release signals including ACdEVs containing important factors to ensure macrophages are rapidly recruited to clear them. Future work should further explore the differences between ACdEVs released during different stages of apoptosis. As well as comparing the established early and late time points (6 and 18 hours), the changes in ACdEVs released over time could be investigated, perhaps hourly, to provide a more detailed picture of the progression of apoptotic cell signalling.

Cell lines are useful tools for exploring cell biology, and the THP-1 monocytic cell line has been used extensively as a model for macrophage function [178,180,185]. THP-1 monocytic cell line can however be problematic, and their physiological relevance has been questioned [183]. It was also planned to use primary cells to validate results observed with cell lines in a more biologically relevant model. Cell lines may not exactly replicate primary cells as they have genetic mutations which immortalise them; many cell lines are derived from cancer cells which of course behave aberrantly compared to normal healthy cells. Furthermore, cell lines can also undergo genetic drift over multiple passages resulting in differences in phenotype which can mean that results are inconsistent and not replicable. The use of primary monocyte-derived macrophages and ACdEVs from primary cells is essential in order to be able to make reliable conclusions.

6. Discussion and conclusions

Apoptosis is a well-studied, fundamental biological process, involving cell membrane blebbing and disassembly of cells into smaller fragments [1,2]. EVs are complex mediators of intercellular communication, and the field of EV research has expanded rapidly in the last few decades, with the role of EVs in immune signalling being one area of particular interest [220]. ACdEVs have more recently become an area of interest, and there remains much to elucidate about their structure/composition and functions. It is known that apoptotic cells actively recruit macrophages, via secretion of soluble factors, including lipids (e.g. S1P, LPC), nucleotides (ATP and UTP), [15–17], and via ACdEV-associated proteins [21,22]. Over twenty years ago, it was demonstrated that various proteins are lost from the surface of apoptotic cells in membrane blebs which promote chemotaxis of monocytes [153]. More recently, research has characterised some of the functions of ACdEV-associated ICAM-3, CX3CL1, and, since the commencement of this research project, calreticulin [21,22,159,194].

The role of ACdEVs in apoptotic cell clearance and resolution of inflammation has been recognised in recent years [155,157,221], although research so far has mainly focussed on the large apoptotic bodies that are produced. Previous research has shown that apoptotic bodies (>1 μm) and smaller ACdEVs are proteomically distinct [158]. The work presented here demonstrates that aside from large apoptotic bodies, apoptotic cells also release a heterogeneous population of other ACdEVs across the size range of exosomes and microvesicles, with complex proteomes. Many proteins or protein families were conserved across different immune cell types: T lymphocytes, B lymphocytes and monocytes. Proteins associated with relevant biological processes by gene ontology were identified, including transmembrane (e.g. ICAMs, integrins, flotillins) and non-transmembrane proteins (annexins and calreticulin). The structure of ACdEVs and proteins of interest are summarised in **Figure 6.1.** Proteomic analysis of ACdEVs released during early apoptosis and late apoptosis/necrosis showed significantly different protein enrichment depending on the stage of cell death. Calreticulin, ICAM-1 and ICAM-2 were significantly enriched in early ACdEVs compared to late ACdEVs, while levels of ICAM-3 were similar in both populations. These results suggest that specific signalling molecules are actively released from apoptotic cells during the early stages of apoptosis to promote rapid recruitment of macrophages for their removal.

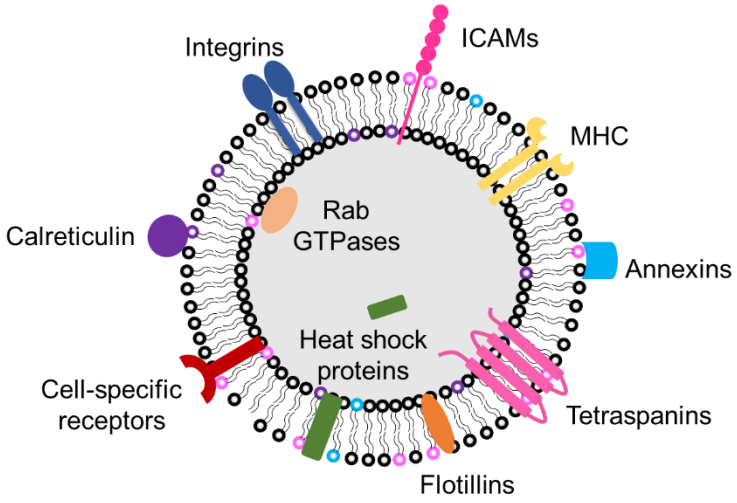

Protein	Relevant Functions
ICAMs	Integrin binding, cell adhesion
Integrins	Cell adhesion
ALCAM/CD166	Cell adhesion, migration
CD81	Integrin binding, cell adhesion
Calreticulin	Apoptotic cell 'eat me' signal
Annexins	Calcium-dependent phospholipid binding, endocytosis, scaffolding proteins, cell adhesion
Basigin/CD147	Intercellular recognition, leukocyte migration, regulation of apoptosis, induction of matrix metalloproteinases
Flotillins	Scaffold proteins, endocytosis adhesion, signalling
PECAM-1/CD31	Cell adhesion, migration, apoptotic cell 'don't eat me' signal/'eat me' signal
CD47	Integrin binding, cell adhesion, apoptotic cell 'don't eat me' signal, inhibition of immune responses

Figure 6.1: Structure of ACdEVs and proteins that may mediate their functions. ACdEVs were analysed by mass spectrometry and proteomes analysed using gene ontology to identify proteins with functions in relevant biological processes.

The data presented demonstrate that ACdEVs play a role in recruitment of macrophages and that ACdEVs associate with macrophages and exert immunomodulatory effects. The results show that the EV proteome can be altered by the isolation method used. We hypothesise that the effect on the chemoattractive property of ACdEVs observed is due to the removal of components of a corona, including surface-associated proteins and other molecules. The EV protein corona has recently become a topic of interest in the EV field. A recently published study by Tóth et al. investigated the formation of a protein corona on the surface of EVs in blood plasma [222], and differences were observed in the proteins in the corona depending on the isolation method used. It is important to consider the potential impact of the isolation method on the composition and functionality of EVs in all research in the EV field. There are numerous widely accepted techniques used for isolation of EVs and no method is considered to be the best option for all characterisation of EV structure and functions [121]. A key issue raised is the physiological relevance of EVs in isolation. EVs stripped of their naturally occurring protein (or other molecular species) corona are likely to behave differently, as molecules located in the EV membrane that are usually masked by the corona may become exposed, and signals from components of the corona are removed. Furthermore, the real microenvironment in which ACdEVs exist is likely much more complex that which is created in vitro. This could explain why ACdEVs unexpectedly induced a pro-inflammatory phenotype in macrophages within the simplified in vitro experiments reported here. Alternatively, ACdEVs may induce a pro-inflammatory phenotype in macrophages to activate macrophages to stimulate apoptotic cell clearance which may, in response to the apoptotic cell corpse itself, be driven towards an anti-inflammatory/pro-resolution ‘M2’ phenotype. CD14, which is upregulated in response to ACdEVs, is a receptor for apoptotic cells [191,195] but is also considered pro-inflammatory as it is an LPS-receptor, a pattern-recognition receptor, working with TLR-4 to stimulate pro-inflammatory signalling. Macrophages exposed to ACdEVs showed upregulated expression of multiple pro-inflammatory cell markers on their surface and secreted pro-inflammatory cytokines. In vivo, ACdEV clearance in isolation may not be likely to occur as it is likely followed by cell corpse clearance that may be the dominant anti-inflammatory event.

Investigation of the functions of proteins of interest was limited as the research was interrupted due to the COVID-19 pandemic. The results presented here suggest a role for calreticulin in recruitment of macrophages to sites of cell death, as well as facilitating phagocytosis [159]. It was hypothesised that there may be some level of redundancy in the functions of different adhesion molecules (e.g. ICAMs) in the context of apoptotic signalling, and this idea should be explored further. The functions of ACdEVs and ACdEV-associated molecules involved in

interaction with macrophages are summarised in **Figure 6.2**, including the results of this research and knowledge from other studies.

While the EVs produced by apoptotic cells change over time from early to late apoptosis, it is also important to consider the possibility that once released, EVs themselves are capable of changing over time. Previous studies have shown that EVs contain active enzymes, including those for lipid mediator leukotriene biosynthesis [92]. Data presented here shows that ACdEVs from monocytes and T cells contain ABC transporters, and other work by our group has shown that ACdEVs also carry lipid mediators of inflammation, which can be exported by ABC transporters. It is therefore possible that ACdEVs produce and release important signals after they have been released by apoptotic cells, and may prolong apoptotic cell signalling.

Another important consideration is the possible alteration of proteins and their functions during apoptosis. Oxidative stress-related protein modifications during apoptosis may be important signals for apoptotic cell clearance. For example, apoptosis has been shown to alter the function of CD31 to facilitate apoptotic cell clearance [33]. Glycosylation patterns have been shown to influence uptake of ACdEVs by macrophages [105]. The potential roles of other molecules that ACdEVs carry including lipids and nucleic acids should also be considered. For example, the composition of phospholipids may fundamentally change the capacity of an EV to modulate immune responses. DHA and EPA, components of membrane phospholipids, are substrates for key enzymes that generate the strongly pro-resolving lipid mediators (e.g. resolvins) [76].

The work presented here has progressed the characterisation of ACdEV structure and function. Future work could utilise the assays used here to investigate the functions of other proteins of interest from the complex ACdEV proteome. Different approaches could also be used to evaluate functions of ACdEVs, for example horizontal migration assays, fluorescence microscopy to assess binding and uptake, and alternative methods to assess macrophage polarisation such as profiling of the macrophage transcriptome. While the functional studies performed here used ACdEVs from Jurkat T cells, ACdEVs from THP-1 monocytes and Mutu B cells, which were also proteomically characterised, could be investigated in future, as well as other cell types. There is currently limited knowledge of the receptors used by recipient cells to interact with EVs. Furthermore, there is the possibility that there are different mechanisms for interactions and uptake of small versus large EVs. Alternatives to the THP-1 cell line should be explored, and findings should be confirmed using primary cell lines, and in vivo experimentation. Given that ACdEVs exert cross species effects [22], it would also be possible

to assess the potential of the human ACdEVs studied here in an in vivo model of inflammation. Apoptosis and apoptotic cell clearance are universal processes and there are likely conserved factors that are central to ACdEV-mediated signalling. While providing insight into the functions of ACdEVs and the molecules that may facilitate their signalling, this work has also highlighted numerous avenues for future exploration.

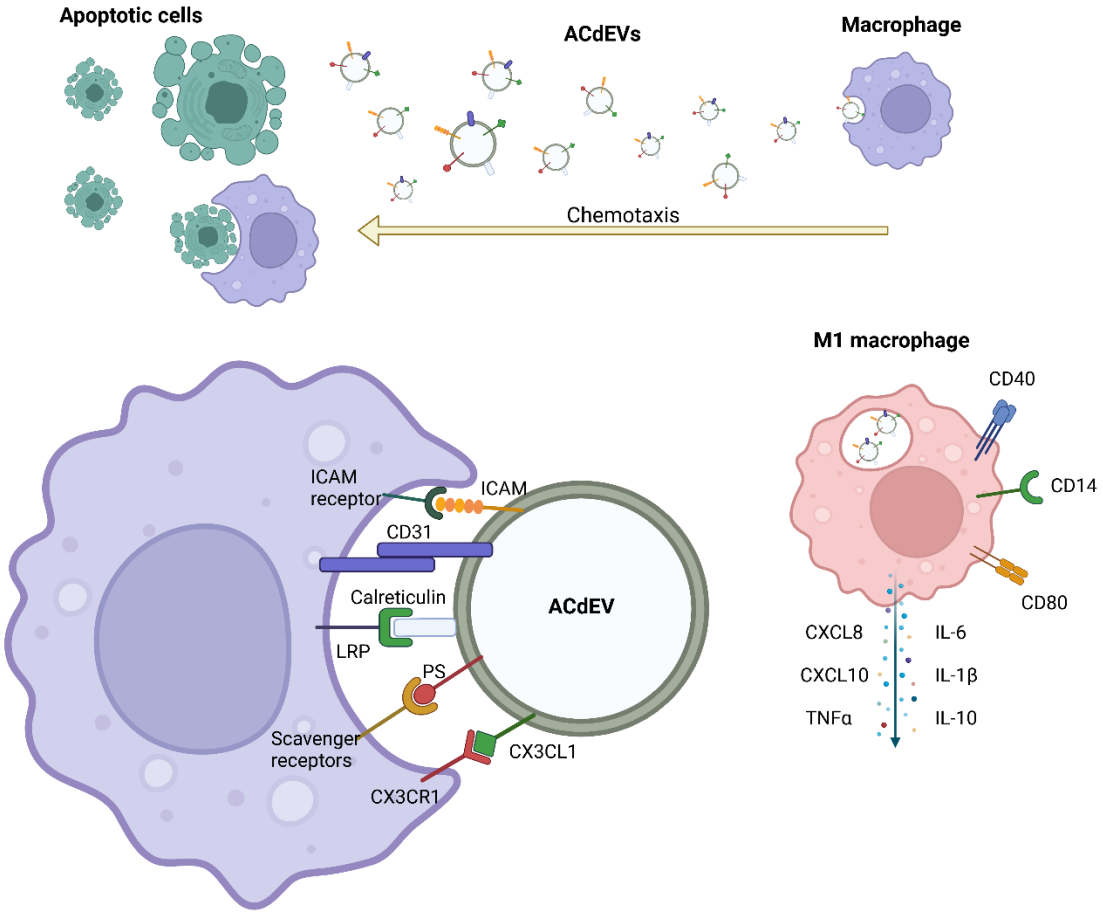

Figure 6.2: Functions of ACdEVs in apoptotic cell clearance and modulation of inflammation. Cells undergoing apoptosis release ACdEVs containing hundreds of different proteins. Phosphatidylserine (PS) is a phospholipid that is externalised by ACdEVs for recognition by phagocytes, and that is found in ACdEVs. ACdEVs carry chemoattractants such as ICAM-3 and CX3CL1, and contribute to recruitment of macrophages to sites of cell death. ACdEVs also contain CD31, a molecule which is usually a signal that prevents phagocytosis of cells, but undergoes functional changes during apoptosis. Macrophages exposed to ACdEVs are polarised to an M1 phenotype, with upregulated surface expression of pro-inflammatory cell markers including the receptors CD14, CD40 and CD80, and secrete pro-inflammatory cytokines including interleukins, C-X-C motif chemokine ligands and TNFα. (Created with BioRender.com).

7. References

1. Kerr JFR, Wyllie AH, Currie AR. Apoptosis: A Basic Biological Phenomenon with Wideranging Implications in Tissue Kinetics. *Br. J. Cancer* 1972; **26**:239–257. doi:10.1038/bjc.1972.33

2. Elmore S. Apoptosis: a review of programmed cell death. *Toxicol. Pathol.* 2007; **35**:495–516. doi:10.1080/01926230701320337

3. Arandjelovic S, Ravichandran KS. Phagocytosis of apoptotic cells in homeostasis. *Nat. Immunol.* 2015; **16**:907–917. doi:10.1038/ni.3253

4. Sachet M, Liang YY, Oehler R. The immune response to secondary necrotic cells. *Apoptosis* 2017; **22**:1189–1204. doi:10.1007/s10495-017-1413-z

5. Ortega-Gómez A, Perretti M, Soehnlein O. Resolution of inflammation: an integrated view. *EMBO Mol. Med.* 2013; **5**:661–74. doi:10.1002/emmm.201202382

6. Li H, Zhu H, Xu CJ, Yuan J. Cleavage of BID by caspase 8 mediates the mitochondrial damage in the Fas pathway of apoptosis. *Cell* 1998; **94**:491–501. doi:10.1016/S0092-8674(00)81590-1

7. Pinkoski MJ, Waterhouse NJ, Heibein JA, Wolf BB, Kuwana T, Goldstein JC, Newmeyer DD, Bleackley RC, Green DR. Granzyme B-mediated Apoptosis Proceeds Predominantly through a Bcl-2-inhibitable Mitochondrial Pathway. *J. Biol. Chem.* 2001; **276**:12060–12067. doi:10.1074/jbc.M009038200

8. Froelich CJ, Metkar SS, Raja SM. Granzyme B-mediated apoptosis - The elephant and the blind men? *Cell Death Differ.* 2004; **11**:369–371. doi:10.1038/sj.cdd.4401381

9. Saelens X, Festjens N, Vande Walle L, Van Gurp M, Van Loo G, Vandenabeele P. Toxic proteins released from mitochondria in cell death. *Oncogene* 2004; **23**:2861–2874. doi:10.1038/sj.onc.1207523

10. Li LY, Luo X, Wang X. Endonuclease G is an apoptotic DNase when released from mitochondria. *Nature* 2001; **412**:95–99. doi:10.1038/35083620

11. Kischkel FC, Hellbardt S, Behrmann I, Germer M, Pawlita M, Krammer PH, Peter ME.

Cytotoxicity-dependent APO-1 (Fas/CD95)-associated proteins form a death-inducing signaling complex (DISC) with the receptor. *EMBO J.* 1995; **14**:5579–5588. doi:10.1002/j.1460-2075.1995.tb00245.x

12. Enari M, Sakahira H, Yokoyama H, Okawa K, Iwamatsu A, Nagata S. A caspase-activated DNase that degrades DNA during apoptosis, and its inhibitor ICAD. *Nature* 1998; **391**:43–50. doi:10.1038/34112

13. Fadok VA, Voelker DR, Campbell PA, Cohen JJ, Bratton DL, Henson PM. Exposure of phosphatidylserine on the surface of apoptotic lymphocytes triggers specific recognition and removal by macrophages. *J. Immunol.* 1992; **148**:2207–16.

14. Ogden CA, deCathelineau A, Hoffmann PR, Bratton D, Ghebrehiwet B, Fadok VA, Henson PM. C1q and mannose binding lectin engagement of cell surface calreticulin and CD91 initiates macropinocytosis and uptake of apoptotic cells. *J. Exp. Med.* 2001; **194**:781–95. doi:10.1084/JEM.194.6.781

15. Grimsley C, Ravichandran KS. Cues for apoptotic cell engulfment: eat-me, don't eat-me and come-get-me signals. *Trends Cell Biol.* 2003; **13**:648–656. doi:10.1016/J.TCB.2003.10.004

16. Lauber K, Bohn E, Kröber SM, Xiao Y, Blumenthal SG, Lindemann RK, Marini P, Wiedig C, Zobywalski A, Baksh S, Xu Y, Autenrieth IB, Schulze-Osthoff K, Belka C, Stuhler G, Wesselborg S. Apoptotic Cells Induce Migration of Phagocytes via Caspase-3-Mediated Release of a Lipid Attraction Signal. *Cell* 2003; **113**:717–730. doi:10.1016/S0092-8674(03)00422-7

17. Gude DR, Alvarez SE, Paugh SW, Mitra P, Yu J, Griffiths R, Barbour SE, Milstien S, Spiegel S. Apoptosis induces expression of sphingosine kinase 1 to release sphingosine-1-phosphate as a "come-and-get-me" signal. *FASEB J.* 2008; **22**:2629–38. doi:10.1096/fj.08-107169

18. Luo B, Gan W, Liu Z, Shen Z, Wang J, Shi R, Liu Y, Liu Y, Jiang M, Zhang Z, Wu Y. Erythropoeitin Signaling in Macrophages Promotes Dying Cell Clearance and Immune Tolerance. *Immunity* 2016; **44**:287–302. doi:10.1016/j.immuni.2016.01.002

19. Elliott MR, Chekeni FB, Trampont PC, Lazarowski ER, Kadl A, Walk SF, Park D, Woodson RI, Ostankovich M, Sharma P, Lysiak JJ, Harden TK, Leitinger N, Ravichandran

KS. Nucleotides released by apoptotic cells act as a find-me signal to promote phagocytic clearance. *Nature* 2009; **461**:282–286. doi:10.1038/nature08296

20. Chekeni FB, Elliott MR, Sandilos JK, Walk SF, Kinchen JM, Lazarowski ER, Armstrong AJ, Penuela S, Laird DW, Salvesen GS, Isakson BE, Bayliss DA, Ravichandran KS. Pannexin 1 channels mediate 'find-me' signal release and membrane permeability during apoptosis. *Nature* 2010; **467**:863–867. doi:10.1038/nature09413

21. Truman LA, Ford CA, Pasikowska M, Pound JD, Wilkinson SJ, Dumitriu IE, Melville L, Melrose LA, Ogden CA, Nibbs R, Graham G, Combadiere C, Gregory CD. CX3CL1/fractalkine is released from apoptotic lymphocytes to stimulate macrophage chemotaxis. *Blood* 2008; **112**:5026–36. doi:10.1182/blood-2008-06-162404

22. Torr EE, Gardner DH, Thomas L, Goodall DM, Bielemeier A, Willetts R, Griffiths HR, Marshall LJ, Devitt A. Apoptotic cell-derived ICAM-3 promotes both macrophage chemoattraction to and tethering of apoptotic cells. *Cell Death Differ.* 2012; **19**:671–679. doi:10.1038/cdd.2011.167

23. Bournazou I, Pound JD, Duffin R, Bournazos S, Melville LA, Brown SB, Rossi AG, Gregory CD. Apoptotic human cells inhibit migration of granulocytes via release of lactoferrin. *J. Clin. Invest.* 2009; **119**:20–32. doi:10.1172/JCI36226

24. Fadok VA, Bratton DL, Rose DM, Pearson A, Ezekewitz RAB, Henson PM. A receptor for phosphatidylserine-specific clearance of apoptotic cells. *Nature* 2000; **405**:85–90. doi:10.1038/35011084

25. Park SY, Jung MY, Kim HJ, Lee SJ, Kim SY, Lee BH, Kwon TH, Park RW, Kim IS. Rapid cell corpse clearance by stabilin-2, a membrane phosphatidylserine receptor. *Cell Death Differ.* 2008; **15**:192–201. doi:10.1038/sj.cdd.4402242

26. Miyanishi M, Tada K, Koike M, Uchiyama Y, Kitamura T, Nagata S. Identification of Tim4 as a phosphatidylserine receptor. *Nature* 2007; **450**:435–439. doi:10.1038/nature06307

27. Ramirez-Ortiz ZG, Pendergraft WF, Prasad A, Byrne MH, Iram T, Blanchette CJ, Luster AD, Hacohen N, Khoury J El, Means TK. The scavenger receptor SCARF1 mediates the clearance of apoptotic cells and prevents autoimmunity. *Nat. Immunol.* 2013; **14**:917–926. doi:10.1038/ni.2670

28. Arur S, Uche UE, Rezaul K, Fong M, Scranton V, Cowan AE, Mohler W, Han DK. Annexin I Is an Endogenous Ligand that Mediates Apoptotic Cell Engulfment. *Dev. Cell* 2003; **4**:587–598. doi:10.1016/S1534-5807(03)00090-X

29. Gardai SJ, McPhillips KA, Frasch SC, Janssen WJ, Starefeldt A, Murphy-Ullrich JE, Bratton DL, Oldenborg P-A, Michalak M, Henson PM. Cell-Surface Calreticulin Initiates Clearance of Viable or Apoptotic Cells through trans-Activation of LRP on the Phagocyte. *Cell* 2005; **123**:321–334. doi:10.1016/J.CELL.2005.08.032

30. Chao MP, Jaiswal S, Weissman-Tsukamoto R, Alizadeh AA, Gentles AJ, Volkmer J, Weiskopf K, Willingham SB, Raveh T, Park CY, Majeti R, Weissman IL. Calreticulin is the dominant pro-phagocytic signal on multiple human cancers and is counterbalanced by CD47. *Sci. Transl. Med.* 2010; **2**:63ra94. doi:10.1126/scitranslmed.3001375

31. Osman R, Tacnet-Delorme P, Kleman J-P, Millet A, Frachet P. Calreticulin Release at an Early Stage of Death Modulates the Clearance by Macrophages of Apoptotic Cells. *Front. Immunol.* 2017; **8**:1034. doi:10.3389/fimmu.2017.01034

32. Moffatt OD, Devitt A, Bell ED, Simmons DL, Gregory CD. Macrophage recognition of ICAM-3 on apoptotic leukocytes. *J. Immunol.* 1999; **162**:6800–10.

33. Brown S, Heinisch I, Ross E, Shaw K, Buckley CD, Savill J. Apoptosis disables CD31-mediated cell detachment from phagocytes promoting binding and engulfment. *Nature* 2002; **418**:200–203. doi:10.1038/nature00811

34. Vernon-Wilson EF. CD31 promotes 1 integrin-dependent engulfment of apoptotic Jurkat T lymphocytes opsonized for phagocytosis by fibronectin. *J. Leukoc. Biol.* 2006; **79**:1260–1267. doi:10.1189/jlb.1005571

35. Vernon-Wilson EF, Auradé F, Tian L, Rowe ICM, Shipston MJ, Savill J, Brown SB. CD31 delays phagocyte membrane repolarization to promote efficient binding of apoptotic cells. *J. Leukoc. Biol.* 2007; **82**:1278–1288. doi:10.1189/jlb.0507283

36. Elward K, Griffiths M, Mizuno M, Harris CL, Neal JW, Morgan BP, Gasque P. CD46 plays a key role in tailoring innate immune recognition of apoptotic and necrotic cells. *J. Biol. Chem.* 2005; **280**:36342–36354. doi:10.1074/jbc.M506579200

37. Wiesolek HL, Bui TM, Lee JJ, Dalal P, Finkielsztein A, Batra A, Thorp EB, Sumagin R.

Intercellular Adhesion Molecule 1 Functions as an Efferocytosis Receptor in Inflammatory Macrophages. *Am. J. Pathol.* 2020; **190**:874–885. doi:10.1016/j.ajpath.2019.12.006

38. Barth ND, Marwick JA, Vendrell M, Rossi AG, Dransfield I. The “Phagocytic synapse” and clearance of apoptotic cells. *Front. Immunol.* 2017; **8**:1708. doi:10.3389/fimmu.2017.01708

39. Gardai SJ, Bratton DL, Ogden CA, Henson PM. Recognition ligands on apoptotic cells: a perspective. *J. Leukoc. Biol.* 2006; **79**:896–903. doi:10.1189/jlb.1005550

40. Flannagan RS, Jaumouillé V, Grinstein S. The Cell Biology of Phagocytosis. *Annu. Rev. Pathol. Mech. Dis.* 2012; **7**:61–98. doi:10.1146/annurev-pathol-011811-132445

41. A-Gonzalez N, Bensinger SJ, Hong C, Beceiro S, Bradley MN, Zelcer N, Deniz J, Ramirez C, Díaz M, Gallardo G, Ruiz de Galarreta C, Salazar J, Lopez F, Edwards P, Parks J, Andujar M, Tontonoz P, Castrillo A. Apoptotic Cells Promote Their Own Clearance and Immune Tolerance through Activation of the Nuclear Receptor LXR. *Immunity* 2009; **31**:245–258. doi:10.1016/j.immuni.2009.06.018

42. Mukundan L, Odegaard JI, Morel CR, Heredia JE, Mwangi JW, Ricardo-Gonzalez RR, Goh YPS, Eagle AR, Dunn SE, Awakuni JUH, Nguyen KD, Steinman L, Michie SA, Chawla A. PPAR-Δ senses and orchestrates clearance of apoptotic cells to promote tolerance. *Nat. Med.* 2009; **15**:1266–1272. doi:10.1038/nm.2048

43. Perry JSA, Morioka S, Medina CB, Iker Etchegaray J, Barron B, Raymond MH, Lucas CD, Onengut-Gumuscu S, Delpire E, Ravichandran KS. Interpreting an apoptotic corpse as anti-inflammatory involves a chloride sensing pathway. *Nat. Cell Biol.* 2019; **21**:1532–1543. doi:10.1038/s41556-019-0431-1

44. Kiss RS, Elliott MR, Ma Z, Marcel YL, Ravichandran KS. Apoptotic Cells Induce a Phosphatidylserine-Dependent Homeostatic Response from Phagocytes. *Curr. Biol.* 2006; **16**:2252–2258. doi:10.1016/j.cub.2006.09.043

45. Viaud M, Ivanov S, Vujic N, Duta-Mare M, Aira LE, Barouillet T, Garcia E, Orange F, Dugail I, Hainault I, Stehlik C, Marchetti S, Boyer L, Guinamard R, Foufelle F, Bochem A, Hovingh KG, Thorp EB, *et al.* Lysosomal cholesterol hydrolysis couples efferocytosis to anti-inflammatory oxysterol production. *Circ. Res.* 2018; **122**:1369–1384. doi:10.1161/CIRCRESAHA.117.312333

46. Angsana J, Chen J, Liu L, Haller CA, Chaikof EL. Efferocytosis as a regulator of macrophage chemokine receptor expression and polarization. *Eur. J. Immunol.* 2016; **46**:1592–1599. doi:10.1002/eji.201546262

47. Szondy Z, Garabuczi É, Joós G, Tsay GJ, Sarang Z. Impaired clearance of apoptotic cells in chronic inflammatory diseases: Therapeutic implications. *Front. Immunol.* 2014; **5**:354. doi:10.3389/fimmu.2014.00354

48. Kawano M, Nagata S. Efferocytosis and autoimmune disease. *Int. Immunol.* 2018; **30**:551–558. doi:10.1093/intimm/dxy055

49. Herrmann M, Voll RE, Zoller OM, Hagenhofer M, Ponner BB, Kalden JR. Impaired phagocytosis of apoptotic cell material by monocyte-derived macrophages from patients with systemic lupus erythematosus. *Arthritis Rheum.* 1998; **41**:1241–1250. doi:10.1002/1529-0131(199807)41:7<1241::AID-ART15>3.0.CO;2-H

50. Hanayama R, Tanaka M, Miwa K, Shinohara A, Iwamatsu A, Nagata S. Identification of a factor that links apoptotic cells to phagocytes. *Nature* 2002; **417**:182–187. doi:10.1038/417182a

51. Hanayama R, Tanaka M, Miyasaka K, Aozasa K, Koike M, Uchiyama Y, Nagata S. Autoimmune disease and impaired uptake of apoptotic cells in MFG-E8-deficient mice. *Science (80-.).* 2004; **304**:1147–1150. doi:10.1126/science.1094359

52. Kojima Y, Volkmer JP, McKenna K, Civelek M, Lusis AJ, Miller CL, Direnzo D, Nanda V, Ye J, Connolly AJ, Schadt EE, Quertermous T, Betancur P, Maegdefessel L, Matic LP, Hedin U, Weissman IL, Leeper NJ. CD47-blocking antibodies restore phagocytosis and prevent atherosclerosis. *Nature* 2016; **536**:86–90. doi:10.1038/nature18935

53. Ye Z, Yang S, Xia Y, Hu R, Chen S, Li B, Chen S, Luo X, Mao L, Li Y, Jin H, Qin C, Hu B. LncRNA MIAT sponges miR-149-5p to inhibit efferocytosis in advanced atherosclerosis through CD47 upregulation. *Cell Death Dis.* 2019; **10**:138. doi:10.1038/s41419-019-1409-4

54. Thorp E, Cui D, Schrijvers DM, Kuriakose G, Tabas I. Mertk receptor mutation reduces efferocytosis efficiency and promotes apoptotic cell accumulation and plaque necrosis in atherosclerotic lesions of Apoe-/- mice. *Arterioscler. Thromb. Vasc. Biol.* 2008; **28**:1421–1428. doi:10.1161/ATVBAHA.108.167197

55. Bhatia VK, Yun S, Leung V, Grimsditch DC, Benson GM, Botto MB, Boyle JJ, Haskard DO. Complement C1q reduces early atherosclerosis in low-density lipoprotein receptor-deficient mice. *Am. J. Pathol.* 2007; **170**:416–426. doi:10.2353/ajpath.2007.060406

56. Karlsson A, Christenson K, Matlak M, Bjïrstad Å, Brown KL, Telemo E, Salomonsson E, Leffler H, Bylund J. Galectin-3 functions as an opsonin and enhances the macrophage clearance of apoptotic neutrophils. *Glycobiology* 2009; **19**:16–20. doi:10.1093/glycob/cwn104

57. Mukaro VR, Bylund J, Hodge G, Holmes M, Jersmann H, Reynolds PN, Hodge S. Lectins Offer New Perspectives in the Development of Macrophage-Targeted Therapies for COPD/Emphysema. *PLoS One* 2013; **8**:e56147. doi:10.1371/journal.pone.0056147

58. Erriah M, Pabreja K, Fricker M, Baines KJ, Donnelly LE, Bylund J, Karlsson A, Simpson JL. Galectin-3 enhances monocyte-derived macrophage efferocytosis of apoptotic granulocytes in asthma. *Respir. Res.* 2019; **20**:1. doi:10.1186/s12931-018-0967-9

59. Pan BT, Teng K, Wu C, Adam M, Johnstone RM. Electron microscopic evidence for externalization of the transferrin receptor in vesicular form in sheep reticulocytes. *J. Cell Biol.* 1985; **101**:942–948. doi:10.1083/jcb.101.3.942

60. Johnstone RM, Adam M, Hammond JR, Orr L, Turbide C. Vesicle formation during reticulocyte maturation. Association of plasma membrane activities with released vesicles (exosomes). *J. Biol. Chem.* 1987; **262**:9412–9420.

61. Wolf P. The Nature and Significance of Platelet Products in Human Plasma. *Br. J. Haematol.* 1967; **13**:269–288. doi:10.1111/j.1365-2141.1967.tb08741.x

62. Akers JC, Gonda D, Kim R, Carter BS, Chen CC. Biogenesis of extracellular vesicles (EV): exosomes, microvesicles, retrovirus-like vesicles, and apoptotic bodies. *J. Neurooncol.* 2013; **113**:1–11. doi:10.1007/s11060-013-1084-8

63. Colombo M, Raposo G, Théry C. Biogenesis, Secretion, and Intercellular Interactions of Exosomes and Other Extracellular Vesicles. *Annu. Rev. Cell Dev. Biol.* 2014; **30**:255–289. doi:10.1146/annurev-cellbio-101512-122326

64. Escola JM, Kleijmeer MJ, Stoorvogel W, Griffith JM, Yoshie O, Geuze HJ. Selective enrichment of tetraspan proteins on the internal vesicles of multivesicular endosomes and on exosomes secreted by human B-lymphocytes. *J. Biol. Chem.* 1998; **273**:20121–20127.

doi:10.1074/jbc.273.32.20121

65. Piper RC, Katzmann DJ. Biogenesis and Function of Multivesicular Bodies. *Annu. Rev. Cell Dev. Biol.* 2007; **23**:519–547. doi:10.1146/annurev.cellbio.23.090506.123319

66. Wollert T, Hurley JH. Molecular mechanism of multivesicular body biogenesis by ESCRT complexes. *Nature* 2010; **464**:864–869. doi:10.1038/nature08849

67. Trajkovic K, Hsu C, Chiantia S, Rajendran L, Wenzel D, Wieland F, Schwille P, Brügger B, Simons M. Ceramide triggers budding of exosome vesicles into multivesicular endosomes. *Science (80-.).* 2008; **319**:1244–1247. doi:10.1126/science.1153124

68. Atkin-Smith GK, Poon IKH. Disassembly of the Dying: Mechanisms and Functions. *Trends Cell Biol.* 2017; **27**:151–162. doi:10.1016/j.tcb.2016.08.011

69. Tixeira R, Poon IKH. Disassembly of dying cells in diverse organisms. *Cell. Mol. Life Sci.* 2019; **76**:245–257. doi:10.1007/s00018-018-2932-7

70. Coleman ML, Sahai EA, Yeo M, Bosch M, Dewar A, Olson MF. Membrane blebbing during apoptosis results from caspase-mediated activation of ROCK I. *Nat. Cell Biol. 2001 34* 2001; **3**:339–345. doi:10.1038/35070009

71. Mills JC, Stone NL, Erhardt J, Pittman RN. Apoptotic membrane blebbing is regulated by myosin light chain phosphorylation. *J. Cell Biol.* 1998; **140**:627–636. doi:10.1083/jcb.140.3.627

72. Moss DK, Betin VM, Malesinski SD, Lane JD. A novel role for microtubules in apoptotic chromatin dynamics and cellular fragmentation. *J. Cell Sci.* 2006; **119**:2362–2374. doi:10.1242/jcs.02959

73. Atkin-Smith GK, Tixeira R, Paone S, Mathivanan S, Collins C, Liem M, Goodall KJ, Ravichandran KS, Hulett MD, Poon IKH. A novel mechanism of generating extracellular vesicles during apoptosis via a beads-on-a-string membrane structure. *Nat. Commun.* 2015; **6**:7439. doi:10.1038/ncomms8439

74. Distler JHW, Huber LC, Hueber AJ, Reich CF, Gay S, Distler O, Pisetsky DS. The release of microparticles by apoptotic cells and their effects on macrophages. *Apoptosis* 2005; **10**:731–741. doi:10.1007/s10495-005-2941-5

75. Park SJ, Kim JM, Kim J, Hur J, Park S, Kim K, Shin H-J, Chwae Y-J. Molecular mechanisms of biogenesis of apoptotic exosome-like vesicles and their roles as damage-associated molecular patterns. *Proc. Natl. Acad. Sci. U. S. A.* 2018; **115**:E11721–E11730. doi:10.1073/pnas.1811432115

76. Dalli J, Serhan CN. Specific lipid mediator signatures of human phagocytes: Microparticles stimulate macrophage efferocytosis and pro-resolving mediators. *Blood* 2012; **120**:e60. doi:10.1182/blood-2012-04-423525

77. Valkonen S, Holopainen M, Colas RA, Impola U, Dalli J, Käkelä R, Siljander PR-M, Laitinen S. Lipid mediators in platelet concentrate and extracellular vesicles: Molecular mechanisms from membrane glycerophospholipids to bioactive molecules. *Biochim. Biophys. Acta - Mol. Cell Biol. Lipids* 2019; **1864**:1168–1182. doi:10.1016/J.BBALIP.2019.03.011

78. Devitt A, Griffiths HR, Milic I. Communicating with the dead: lipids, lipid mediators and extracellular vesicles. *Biochem. Soc. Trans.* 2018; **46**:631–639. doi:10.1042/BST20160477

79. Salzer U, Hinterdorfer P, Hunger U, Borken C, Prohaska R. Ca++-dependent vesicle release from erythrocytes involves stomatin-specific lipid rafts, synexin (annexin VII), and sorcin. *Blood* 2002; **99**:2569–2577. doi:10.1182/BLOOD.V99.7.2569

80. Gassart A de, Géminard C, Février B, Raposo G, Vidal M. Lipid raft-associated protein sorting in exosomes. *Blood* 2003; **102**:4336–4344. doi:10.1182/BLOOD-2003-03-0871

81. Valadi H, Ekström K, Bossios A, Sjöstrand M, Lee JJ, Lötvall JO. Exosome-mediated transfer of mRNAs and microRNAs is a novel mechanism of genetic exchange between cells. *Nat. Cell Biol.* 2007; **9**:654–659. doi:10.1038/ncb1596

82. Thakur BK, Zhang H, Becker A, Matei I, Huang Y, Costa-Silva B, Zheng Y, Hoshino A, Brazier H, Xiang J, Williams C, Rodriguez-Barrueco R, Silva JM, Zhang W, Hearn S, Elemento O, Paknejad N, Manova-Todorova K, *et al.* Double-stranded DNA in exosomes: A novel biomarker in cancer detection. *Cell Res.* 2014; **24**:766–769. doi:10.1038/cr.2014.44

83. Squadrito ML, Baer C, Burdet F, Maderna C, Gilfillan GD, Lyle R, Ibberson M, De Palma M. Endogenous RNAs Modulate MicroRNA Sorting to Exosomes and Transfer to Acceptor Cells. *Cell Rep.* 2014; **8**:1432–1446. doi:10.1016/J.CELREP.2014.07.035

84. Cha DJ, Franklin JL, Dou Y, Liu Q, Higginbotham JN, Demory Beckler M, Weaver AM,

Vickers K, Prasad N, Levy S, Zhang B, Coffey RJ, Patton JG. KRAS-dependent sorting of miRNA to exosomes. *Elife* 2015; **4**:e07197. doi:10.7554/eLife.07197

85. Hinger SA, Cha DJ, Franklin JL, Weaver AM, Coffey RJ, Patton Correspondence JG. Diverse Long RNAs Are Differentially Sorted into Extracellular Vesicles Secreted by Colorectal Cancer Cells. *Cell Rep.* 2018; **25**:715–725. doi:10.1016/j.celrep.2018.09.054

86. Raposo G, Nijman HW, Stoorvogel W, Liejendekker R, Harding C V, Melief CJ, Geuze HJ. B lymphocytes secrete antigen-presenting vesicles. *J. Exp. Med.* 1996; **183**:1161–72.

87. Clayton A, Court J, Navabi H, Adams M, Mason MD, Hobot JA, Newman GR, Jasani B. Analysis of antigen presenting cell derived exosomes, based on immuno-magnetic isolation and flow cytometry. *J. Immunol. Methods* 2001; **247**:163–174. doi:10.1016/S0022-1759(00)00321-5

88. Synowsky SA, Shirran SL, Cooke FGM, Antoniou AN, Botting CH, Powis SJ. The major histocompatibility complex class I immunopeptidome of extracellular vesicles. *J. Biol. Chem.* 2017; **292**:17084–17092. doi:10.1074/jbc.M117.805895

89. Hakulinen J, Sankkila L, Sugiyama N, Lehti K, Keski-Oja J. Secretion of active membrane type 1 matrix metalloproteinase (MMP-14) into extracellular space in microvesicular exosomes. *J. Cell. Biochem.* 2008; **105**:1211–1218. doi:10.1002/jcb.21923

90. Sumida M, Hane M, Yabe U, Shimoda Y, Pearce OMT, Kiso M, Miyagi T, Sawada M, Varki A, Kitajima K, Sato C. Rapid Trimming of Cell Surface Polysialic Acid (PolySia) by Exovesicular Sialidase Triggers Release of Preexisting Surface Neurotrophin. *J. Biol. Chem.* 2015; **290**:13202–14. doi:10.1074/jbc.M115.638759

91. Sanderson RD, Bandari SK, Vlodavsky I. Proteases and glycosidases on the surface of exosomes: Newly discovered mechanisms for extracellular remodeling. *Matrix Biol.* 2017; **75**–**76**:160–169. doi:10.1016/J.MATBIO.2017.10.007

92. Esser J, Gehrmann U, D'Alexandri FL, Hidalgo-Estévez AM, Wheelock CE, Scheynius A, Gabrielsson S, Rådmark O. Exosomes from human macrophages and dendritic cells contain enzymes for leukotriene biosynthesis and promote granulocyte migration. *J. Allergy Clin. Immunol.* 2010; **126**:1032-1040.e4. doi:10.1016/J.JACI.2010.06.039

93. Tucher C, Bode K, Schiller P, Claßen L, Birr C, Souto-Carneiro MM, Blank N, Lorenz H-

M, Schiller M. Extracellular Vesicle Subtypes Released From Activated or Apoptotic T-Lymphocytes Carry a Specific and Stimulus-Dependent Protein Cargo. *Front. Immunol.* 2018; **9**:534. doi:10.3389/fimmu.2018.00534

94. Martínez-Lorenzo MJ, Anel A, Gamen S, Monleón I, Lasierra P, Larrad L, Piñeiro A, Alava MA, Naval J. Activated Human T Cells Release Bioactive Fas Ligand and APO2 Ligand in Microvesicles. *J. Immunol.* 1999; **163**.

95. Buzás EI, Tóth EÁ, Sódar BW, Szabó-Taylor KÉ. Molecular interactions at the surface of extracellular vesicles. *Semin. Immunopathol.* 2018; **40**:453–464. doi:10.1007/s00281-018-0682-0

96. Mulcahy LA, Pink RC, Carter DRF. Routes and mechanisms of extracellular vesicle uptake. *J. Extracell. Vesicles* 2014; **3**:24641. doi:10.3402/jev.v3.24641

97. Svensson KJ, Christianson HC, Wittrup A, Bourseau-Guilmain E, Lindqvist E, Svensson LM, Mörgelin M, Belting M. Exosome uptake depends on ERK1/2-heat shock protein 27 signaling and lipid Raft-mediated endocytosis negatively regulated by caveolin-1. *J. Biol. Chem.* 2013; **288**:17713–24. doi:10.1074/jbc.M112.445403

98. Fitzner D, Schnaars M, van Rossum D, Krishnamoorthy G, Dibaj P, Bakhti M, Regen T, Hanisch U-K, Simons M. Selective transfer of exosomes from oligodendrocytes to microglia by macropinocytosis. *J. Cell Sci.* 2011; **124**:447–58. doi:10.1242/jcs.074088

99. Kerr MC, Teasdale RD. Defining macropinocytosis. *Traffic* 2009; **10**:364–371. doi:10.1111/j.1600-0854.2009.00878.x

100. Feng D, Zhao W-L, Ye Y-Y, Bai X-C, Liu R-Q, Chang L-F, Zhou Q, Sui S-F. Cellular Internalization of Exosomes Occurs Through Phagocytosis. *Traffic* 2010; **11**:675–687. doi:10.1111/j.1600-0854.2010.01041.x

101. Mathieu M, Martin-Jaular L, Lavieu G, Théry C. Specificities of secretion and uptake of exosomes and other extracellular vesicles for cell-to-cell communication. *Nat. Cell Biol.* 2019; **21**:9–17. doi:10.1038/s41556-018-0250-9

102. Montecalvo A, Larregina AT, Shufesky WJ, Stolz DB, Sullivan MLG, Karlsson JM, Baty CJ, Gibson GA, Erdos G, Wang Z, Milosevic J, Tkacheva OA, Divito SJ, Jordan R, Lyons-Weiler J, Watkins SC, Morelli AE. Mechanism of transfer of functional microRNAs between

mouse dendritic cells via exosomes. *Blood* 2012; **119**:756–766. doi:10.1182/BLOOD-2011-02-338004

103. Sheldon H, Heikamp E, Turley H, Dragovic R, Thomas P, Oon CE, Leek R, Edelmann M, Kessler B, Sainson RCA, Sargent I, Li JL, Harris AL. New mechanism for Notch signaling to endothelium at a distance by delta-like 4 incorporation into exosomes. *Blood* 2010; **116**:2385–2394. doi:10.1182/blood-2009-08-239228

104. Skog J, Würdinger T, van Rijn S, Meijer DH, Gainche L, Curry WT, Carter BS, Krichevsky AM, Breakefield XO. Glioblastoma microvesicles transport RNA and proteins that promote tumour growth and provide diagnostic biomarkers. *Nat. Cell Biol.* 2008; **10**:1470–1476. doi:10.1038/ncb1800

105. Bilyy RO, Shkandina T, Tomin A, Muñoz LE, Franz S, Antonyuk V, Kit YY, Zirngibl M, Fürnrohr BG, Janko C, Lauber K, Schiller M, Schett G, Stoika RS, Herrmann M. Macrophages discriminate glycosylation patterns of apoptotic cell-derived microparticles. *J. Biol. Chem.* 2012; **287**:496–503. doi:10.1074/jbc.M111.273144

106. Rilla K, Mustonen A-M, Arasu UT, Härkönen K, Matilainen J, Nieminen P. Extracellular vesicles are integral and functional components of the extracellular matrix. *Matrix Biol.* 2017; **75**–**76**:201–219. doi:10.1016/J.MATBIO.2017.10.003

107. Frühbeis C, Fröhlich D, Kuo WP, Amphornrat J, Thilemann S, Saab AS, Kirchhoff F, Möbius W, Goebbels S, Nave KA, Schneider A, Simons M, Klugmann M, Trotter J, Krämer-Albers EM. Neurotransmitter-Triggered Transfer of Exosomes Mediates Oligodendrocyte-Neuron Communication. *PLoS Biol.* 2013; **11**:1001604. doi:10.1371/journal.pbio.1001604

108. Basso M, Bonetto V. Extracellular vesicles and a novel form of communication in the brain. *Front. Neurosci.* 2016; **10**:127. doi:10.3389/fnins.2016.00127

109. Clayton A, Harris CL, Court J, Mason MD, Morgan BP. Antigen-presenting cell exosomes are protected from complement-mediated lysis by expression of CD55 and CD59. *Eur. J. Immunol.* 2003; **33**:522–531. doi:10.1002/immu.200310028

110. Sagini K, Costanzi E, Emiliani C, Buratta S, Urbanelli L, Sagini K, Costanzi E, Emiliani C, Buratta S, Urbanelli L. Extracellular Vesicles as Conveyors of Membrane-Derived Bioactive Lipids in Immune System. *Int. J. Mol. Sci.* 2018; **19**:1227. doi:10.3390/ijms19041227

111. Bello-Morales R, Praena B, de la Nuez C, Rejas MT, Guerra M, Galán-Ganga M, Izquierdo M, Calvo V, Krummenacher C, López-Guerrero JA. Role of Microvesicles in the Spread of Herpes Simplex Virus 1 in Oligodendrocytic Cells. *J. Virol.* 2018; **92**:e00088-18. doi:10.1128/JVI.00088-18

112. Frleta D, Ochoa CE, Kramer HB, Khan SA, Stacey AR, Borrow P, Kessler BM, Haynes BF, Bhardwaj N. HIV-1 infection-induced apoptotic microparticles inhibit human DCs via CD44. *J. Clin. Invest.* 2012; **122**:4685–97. doi:10.1172/JCI64439

113. Fehr E-M, Spoerl S, Heyder P, Herrmann M, Bekeredjian-Ding I, Blank N, Lorenz H-M, Schiller M. Apoptotic-cell-derived membrane vesicles induce an alternative maturation of human dendritic cells which is disturbed in SLE. *J. Autoimmun.* 2013; **40**:86–95. doi:10.1016/J.JAUT.2012.08.003

114. Paone S, Baxter AA, Hulett MD, Poon IKH. Endothelial cell apoptosis and the role of endothelial cell-derived extracellular vesicles in the progression of atherosclerosis. *Cell. Mol. Life Sci.* 2018:1–14. doi:10.1007/s00018-018-2983-9

115. Boilard E, Nigrovic PA, Larabee K, Watts GFM, Coblyn JS, Weinblatt ME, Massarotti EM, Remold-O'Donnell E, Farndale RW, Ware J, Lee DM. Platelets amplify inflammation in arthritis via collagen-dependent microparticle production. *Science (80-.).* 2010; **327**:580–583. doi:10.1126/science.1181928

116. Al-Mayah A, Bright S, Chapman K, Irons S, Luo P, Carter D, Goodwin E, Kadhim M. The non-targeted effects of radiation are perpetuated by exosomes. *Mutat. Res. Mol. Mech. Mutagen.* 2015; **772**:38–45. doi:10.1016/j.mrfmmm.2014.12.007

117. Al-Mayah AHJ, Irons SL, Pink RC, Carter DRF, Kadhim MA, Kadhim M. Possible role of exosomes containing RNA in mediating nontargeted effect of ionizing radiation. *Radiat. Res.* 2012; **177**:539–45. doi:10.1667/RR2868.1

118. Gregory CD, Dransfield I. Apoptotic Tumor Cell-Derived Extracellular Vesicles as Important Regulators of the Onco-Regenerative Niche. *Front. Immunol.* 2018; **9**:1111. doi:10.3389/fimmu.2018.01111

119. Muhsin-Sharafaldine M-R, McLellan AD. Tumor-Derived Apoptotic Vesicles: With Death They Do Part. *Front. Immunol.* 2018; **9**:957. doi:10.3389/fimmu.2018.00957

120. Lötvall J, Hill AF, Hochberg F, Buzás EI, Vizio D Di, Gardiner C, Gho YS, Kurochkin I V., Mathivanan S, Quesenberry P, Sahoo S, Tahara H, Wauben MH, Witwer KW, Théry C. Minimal experimental requirements for definition of extracellular vesicles and their functions: A position statement from the International Society for Extracellular Vesicles. *J. Extracell. Vesicles* 2014; **3**:26913. doi:10.3402/jev.v3.26913

121. Théry C, Witwer KW, Aikawa E, Alcaraz MJ, Anderson JD, Andriantsitohaina R, Antoniou A, Arab T, Archer F, Atkin-Smith GK, Ayre DC, Bach J-M, Bachurski D, Baharvand H, Balaj L, Baldacchino S, Bauer NN, Baxter AA, *et al.* Minimal information for studies of extracellular vesicles 2018 (MISEV2018): a position statement of the International Society for Extracellular Vesicles and update of the MISEV2014 guidelines. *J. Extracell. Vesicles* 2018; **7**:1535750. doi:10.1080/20013078.2018.1535750

122. Royo F, Zuñiga-Garcia P, Sanchez-Mosquera P, Egia A, Perez A, Loizaga A, Arceo R, Lacasa I, Rabade A, Arrieta E, Bilbao R, Unda M, Carracedo A, Falcon-Perez JM. Different EV enrichment methods suitable for clinical settings yield different subpopulations of urinary extracellular vesicles from human samples. *J. Extracell. Vesicles* 2016; **5**:29497. doi:10.3402/jev.v5.29497

123. Théry C, Amigorena S, Raposo G, Clayton A. Isolation and Characterization of Exosomes from Cell Culture Supernatants and Biological Fluids. *Curr. Protoc. Cell Biol.* 2006; **30**:3.22.1-3.22.29. doi:10.1002/0471143030.cb0322s30

124. Bobrie A, Colombo M, Krumeich S, Raposo G, Théry C. Diverse subpopulations of vesicles secreted by different intracellular mechanisms are present in exosome preparations obtained by differential ultracentrifugation. *J. Extracell. Vesicles* 2012; **1**:18397. doi:10.3402/jev.v1i0.18397

125. György B, Módos K, Pállinger É, Pálóczi K, Pásztói M, Misják P, Deli MA, Sipos Á, Szalai A, Voszka I, Polgár A, Tóth K, Csete M, Nagy G, Gay S, Falus A, Kittel Á, Buzás EI. Detection and isolation of cell-derived microparticles are compromised by protein complexes resulting from shared biophysical parameters. *Blood* 2011; **117**:39–48. doi:10.1182/blood-2010-09-307595

126. Linares R, Tan S, Gounou C, Arraud N, Brisson AR. High-speed centrifugation induces aggregation of extracellular vesicles. *J. Extracell. Vesicles* 2015; **4**:29509. doi:10.3402/jev.v4.29509

127. Yuana Y, Levels J, Grootemaat A, Sturk A, Nieuwland R. Co-isolation of extracellular vesicles and high-density lipoproteins using density gradient ultracentrifugation. *J. Extracell. Vesicles* 2014; **3**:23262. doi:10.3402/jev.v3.23262

128. Böing AN, van der Pol E, Grootemaat AE, Coumans FAW, Sturk A, Nieuwland R. Single-step isolation of extracellular vesicles by size-exclusion chromatography. *J. Extracell. Vesicles* 2014; **3**:23430. doi:10.3402/jev.v3.23430

129. Benedikter BJ, Bouwman FG, Vajen T, Heinzmann ACA, Grauls G, Mariman EC, Wouters EFM, Savelkoul PH, Lopez-Iglesias C, Koenen RR, Rohde GGU, Stassen FRM. Ultrafiltration combined with size exclusion chromatography efficiently isolates extracellular vesicles from cell culture media for compositional and functional studies. *Sci. Rep.* 2017; **7**:1–13. doi:10.1038/s41598-017-15717-7

130. Nordin JZ, Lee Y, Vader P, Mäger I, Johansson HJ, Heusermann W, Wiklander OPB, Hällbrink M, Seow Y, Bultema JJ, Gilthorpe J, Davies T, Fairchild PJ, Gabrielsson S, Meisner-Kober NC, Lehtiö J, Smith CIE, Wood MJA, *et al.* Ultrafiltration with size-exclusion liquid chromatography for high yield isolation of extracellular vesicles preserving intact biophysical and functional properties. *Nanomedicine Nanotechnology, Biol. Med.* 2015; **11**:879–883. doi:10.1016/j.nano.2015.01.003

131. Lamparski HG, Metha-Damani A, Yao JY, Patel S, Hsu DH, Ruegg C, Le Pecq JB. Production and characterization of clinical grade exosomes derived from dendritic cells. *J. Immunol. Methods* 2002; **270**:211–226. doi:10.1016/S0022-1759(02)00330-7

132. Heath N, Grant L, De Oliveira TM, Rowlinson R, Osteikoetxea X, Dekker N, Overman R. Rapid isolation and enrichment of extracellular vesicle preparations using anion exchange chromatography. *Sci. Rep.* 2018; **8**:5730. doi:10.1038/s41598-018-24163-y

133. Balaj L, Atai NA, Chen W, Mu D, Tannous BA, Breakefield XO, Skog J, Maguire CA. Heparin affinity purification of extracellular vesicles. *Sci. Rep.* 2015; **5**:10266. doi:10.1038/srep10266

134. Ghosh A, Davey M, Chute IC, Griffiths SG, Lewis S, Chacko S, Barnett D, Crapoulet N, Fournier S, Joy A, Caissie MC, Ferguson AD, Daigle M, Meli MV, Lewis SM, Ouellette RJ. Rapid Isolation of Extracellular Vesicles from Cell Culture and Biological Fluids Using a Synthetic Peptide with Specific Affinity for Heat Shock Proteins. Fan G-C, ed. *PLoS One*

2014; **9**:e110443. doi:10.1371/journal.pone.0110443

135. Nakai W, Yoshida T, Diez D, Miyatake Y, Nishibu T, Imawaka N, Naruse K, Sadamura Y, Hanayama R. A novel affinity-based method for the isolation of highly purified extracellular vesicles. *Sci. Rep.* 2016; **6**:33935. doi:10.1038/srep33935

136. Royo F, Théry C, Falcón-Pérez JM, Nieuwland R, Witwer KW. Methods for Separation and Characterization of Extracellular Vesicles: Results of a Worldwide Survey Performed by the ISEV Rigor and Standardization Subcommittee. *Cells* 2020; **9**. doi:10.3390/cells9091955

137. Lawrie AS, Albanyan A, Cardigan RA, Mackie IJ, Harrison P. Microparticle sizing by dynamic light scattering in fresh-frozen plasma. *Vox Sang.* 2009; **96**:206–212. doi:10.1111/j.1423-0410.2008.01151.x

138. Palmieri V, Lucchetti D, Gatto I, Maiorana A, Marcantoni M, Maulucci G, Papi M, Pola R, De Spirito M, Sgambato A. Dynamic light scattering for the characterization and counting of extracellular vesicles: a powerful noninvasive tool. *J. Nanoparticle Res.* 2014; **16**:1–8. doi:10.1007/s11051-014-2583-z

139. Filipe V, Hawe A, Jiskoot W. Critical evaluation of nanoparticle tracking analysis (NTA) by NanoSight for the measurement of nanoparticles and protein aggregates. *Pharm. Res.* 2010; **27**:796–810. doi:10.1007/s11095-010-0073-2

140. Vogel R, Willmott G, Kozak D, Roberts GS, Anderson W, Groenewegen L, Glossop B, Barnett A, Turner A, Trau M. Quantitative sizing of nano/microparticles with a tunable elastomeric pore sensor. *Anal. Chem.* 2011; **83**:3499–3506. doi:10.1021/ac200195n

141. Coumans FAW, van der Pol E, Böing AN, Hajji N, Sturk G, van Leeuwen TG, Nieuwland R. Reproducible extracellular vesicle size and concentration determination with tunable resistive pulse sensing. *J. Extracell. Vesicles* 2014; **3**:25922. doi:10.3402/jev.v3.25922

142. Chuo ST-Y, Chien JC-Y, Lai CP-K. Imaging extracellular vesicles: current and emerging methods. *J. Biomed. Sci.* 2018; **25**:91. doi:10.1186/s12929-018-0494-5

143. Kondratov KA, Petrova TA, Mikhailovskii VY, Ivanova AN, Kostareva AA, Fedorov A V. A study of extracellular vesicles isolated from blood plasma conducted by low-voltage scanning electron microscopy. *Cell tissue biol.* 2017; **11**:181–190. doi:10.1134/S1990519X17030051

144. Pitanga T, de Aragão França L, Rocha VC, Meirelles T, Matos Borges V, Gonçalves M, Pontes-de-Carvalho L, Noronha-Dutra A, dos-Santos WL. Neutrophil-derived microparticles induce myeloperoxidase-mediated damage of vascular endothelial cells. *BMC Cell Biol.* 2014; **15**:21. doi:10.1186/1471-2121-15-21

145. Poliakov A, Spilman M, Dokland T, Amling CL, Mobley JA. Structural heterogeneity and protein composition of exosome-like vesicles (prostasomes) in human semen. *Prostate* 2009; **69**:159–167. doi:10.1002/pros.20860

146. Tatischeff I, Larquet E, Falcón-Pérez JM, Turpin PY, Kruglik SG. Fast characterisation of cell-derived extracellular vesicles by nanoparticles tracking analysis, cryo-electron microscopy, and Raman tweezers microspectroscopy. *J. Extracell. Vesicles* 2012; **1**:19179. doi:10.3402/jev.v1i0.19179

147. Emelyanov A, Shtam T, Kamyshinsky R, Garaeva L, Verlov N, Miliukhina I, Kudrevatykh A, Gavrilov G, Zabrodskaya Y, Pchelina S, Konevega A. Cryo-electron microscopy of extracellular vesicles from cerebrospinal fluid. *PLoS One* 2020; **15**:e0227949. doi:10.1371/journal.pone.0227949

148. McVey MJ, Spring CM, Kuebler WM. Improved resolution in extracellular vesicle populations using 405 instead of 488 nm side scatter. *J. Extracell. Vesicles* 2018; **7**:1454776. doi:10.1080/20013078.2018.1454776

149. Erdbrügger U, Rudy CK, E. Etter M, Dryden KA, Yeager M, Klibanov AL, Lannigan J. Imaging flow cytometry elucidates limitations of microparticle analysis by conventional flow cytometry. *Cytom. Part A* 2014; **85**:756–770. doi:10.1002/cyto.a.22494

150. Botha J, Pugsley HR, Handberg A. Conventional, high-resolution and imaging flow cytometry: Benchmarking performance in characterisation of extracellular vesicles. *Biomedicines* 2021; **9**:124. doi:10.3390/biomedicines9020124

151. Salmond N, Khanna K, Owen GR, Williams KC. Nanoscale flow cytometry for immunophenotyping and quantitating extracellular vesicles in blood plasma. *Nanoscale* 2021; **13**:2012–2025. doi:10.1039/d0nr05525e

152. Tian Y, Ma L, Gong M, Su G, Zhu S, Zhang W, Wang S, Li Z, Chen C, Li L, Wu L, Yan X. Protein Profiling and Sizing of Extracellular Vesicles from Colorectal Cancer Patients via Flow Cytometry. *ACS Nano* 2018; **12**:671–680. doi:10.1021/acsnano.7b07782

153. Segundo C, Medina F, Rodríguez C, Martínez-Palencia R, Leyva-Cobián F, Brieva JA. Surface Molecule Loss and Bleb Formation by Human Germinal Center B Cells Undergoing Apoptosis: Role of Apoptotic Blebs in Monocyte Chemotaxis. *Blood* 1999; **94**:1012–1020.

154. Shen G, Krienke S, Schiller P, Nießen A, Neu S, Eckstein V, Schiller M, Lorenz H-M, Tykocinski L-O. Microvesicles released by apoptotic human neutrophils suppress proliferation and IL-2/IL-2 receptor expression of resting T helper cells. *Eur. J. Immunol.* 2017; **47**:900–910. doi:10.1002/eji.201546203

155. Grant LR, Milic I, Devitt A. Apoptotic cell-derived extracellular vesicles: structure-function relationships. *Biochem. Soc. Trans.* 2019; **47**:509–516. doi:10.1042/BST20180080

156. Baxter AA, Phan TK, Hanssen E, Liem M, Hulett MD, Mathivanan S, Poon IKH. Analysis of extracellular vesicles generated from monocytes under conditions of lytic cell death. *Sci. Rep.* 2019; **9**:7538. doi:10.1038/s41598-019-44021-9

157. Poon IKH, Parkes MAF, Jiang L, Atkin-Smith GK, Tixeira R, Gregory CD, Ozkocak DC, Rutter SF, Caruso S, Santavanond JP, Paone S, Shi B, Hodge AL, Hulett MD, Chow JDY, Phan TK, Baxter AA. Moving beyond size and phosphatidylserine exposure: evidence for a diversity of apoptotic cell-derived extracellular vesicles in vitro. *J. Extracell. Vesicles* 2019; **8**:1608786. doi:10.1080/20013078.2019.1608786

158. Dieudé M, Bell C, Turgeon J, Beillevaire D, Pomerleau L, Yang B, Hamelin K, Qi S, Pallet N, Béland C, Dhahri W, Cailhier JF, Rousseau M, Duchez AC, Lévesque T, Lau A, Rondeau C, Gingras D, *et al.* The 20S proteasome core, active within apoptotic exosome-like vesicles, induces autoantibody production and accelerates rejection. *Sci. Transl. Med.* 2015; **7**:318ra200. doi:10.1126/scitranslmed.aac9816

159. Zheng C, Sui B, Zhang X, Hu J, Chen J, Liu J, Wu D, Ye Q, Xiang L, Qiu X, Liu S, Deng Z, Zhou J, Liu S, Shi S, Jin Y. Apoptotic vesicles restore liver macrophage homeostasis to counteract type 2 diabetes. *J. Extracell. Vesicles* 2021; **10**:e12109. doi:10.1002/jev2.12109

160. Fadok VA, de Cathelineau A A de, Daleke DL, Henson PM, Bratton DL. Loss of phospholipid asymmetry and surface exposure of phosphatidylserine is required for phagocytosis of apoptotic cells by macrophages and fibroblasts. *J. Biol. Chem.* 2001; **276**:1071–7. doi:10.1074/jbc.M003649200

161. Dalli J, Norling L V, Renshaw D, Cooper D, Leung K-Y, Perretti M. Annexin 1 mediates

the rapid anti-inflammatory effects of neutrophil-derived microparticles. *Blood* 2008; **112**:2512–9. doi:10.1182/blood-2008-02-140533

162. Sugimoto MA, Vago JP, Teixeira MM, Sousa LP. Annexin A1 and the Resolution of Inflammation: Modulation of Neutrophil Recruitment, Apoptosis, and Clearance. *J. Immunol. Res.* 2016; **2016**:8239258. doi:10.1155/2016/8239258

163. Zhao C, Zhang B, Jiang J, Wang Y, Wu Y. Up-regulation of ANXA1 suppresses polymorphonuclear neutrophil infiltration and myeloperoxidase activity by activating STAT3 signaling pathway in rat models of myocardial ischemia-reperfusion injury. *Cell. Signal.* 2019; **62**:109325. doi:10.1016/J.CELLSIG.2019.05.010

164. Leoni G, Neumann P-A, Kamaly N, Quiros M, Nishio H, Jones HR, Sumagin R, Hilgarth RS, Alam A, Fredman G, Argyris I, Rijcken E, Kusters D, Reutelingsperger C, Perretti M, Parkos CA, Farokhzad OC, Neish AS, *et al.* Annexin A1–containing extracellular vesicles and polymeric nanoparticles promote epithelial wound repair. *J. Clin. Invest.* 2015; **125**:1215–1227. doi:10.1172/JCI76693

165. Yang H, Antoine DJ, Andersson U, Tracey KJ. The many faces of HMGB1: molecular structure-functional activity in inflammation, apoptosis, and chemotaxis. *J. Leukoc. Biol.* 2013; **93**:865–873. doi:10.1189/jlb.1212662

166. Chen Y, Li G, Liu Y, Werth VP, Williams KJ, Liu M-L. Translocation of Endogenous Danger Signal HMGB1 From Nucleus to Membrane Microvesicles in Macrophages. *J. Cell. Physiol.* 2016; **231**:2319–2326. doi:10.1002/jcp.25352

167. Schiller M, Heyder P, Ziegler S, Niessen A, Claßen L, Lauffer A, Lorenz H-M. During apoptosis HMGB1 is translocated into apoptotic cell-derived membraneous vesicles. *Autoimmunity* 2013; **46**:342–346. doi:10.3109/08916934.2012.750302

168. Spencer DM, Mobarrez F, Wallén H, Pisetsky DS. The Expression of HMGB1 on Microparticles from Jurkat and HL-60 Cells Undergoing Apoptosis *in vitro*. *Scand. J. Immunol.* 2014; **80**:101–110. doi:10.1111/sji.12191

169. Pisetsky DS. The expression of HMGB1 on microparticles released during cell activation and cell death in vitro and in vivo. *Mol. Med.* 2014; **20**:158–63. doi:10.2119/molmed.2014.00014

170. Niessen A, Heyder P, Krienke S, Blank N, Tykocinski L-O, Lorenz H-M, Schiller M. Apoptotic-cell-derived membrane microparticles and IFN-α induce an inflammatory immune response. *J. Cell Sci.* 2015; **128**:2443–53. doi:10.1242/jcs.162735

171. Schiller M, Parcina M, Heyder P, Foermer S, Ostrop J, Leo A, Heeg K, Herrmann M, Lorenz H-M, Bekeredjian-Ding I. Induction of type I IFN is a physiological immune reaction to apoptotic cell-derived membrane microparticles. *J. Immunol.* 2012; **189**:1747–56. doi:10.4049/jimmunol.1100631

172. Doran AC, Yurdagul A, Tabas I. Efferocytosis in health and disease. *Nat. Rev. Immunol.* 2019; **20**:254–267. doi:10.1038/s41577-019-0240-6

173. Robbins PD, Morelli AE. Regulation of immune responses by extracellular vesicles. *Nat. Rev. Immunol.* 2014; **14**. doi:10.1038/nri3622

174. Buzas EI, György B, Nagy G, Falus A, Gay S. Emerging role of extracellular vesicles in inflammatory diseases. *Nat. Rev. Rheumatol.* 2014; **10**:356–364. doi:10.1038/nrrheum.2014.19

175. Yarana C, Thompson H, Chaiswing L, Butterfield DA, Weiss H, Bondada S, Alhakeem S, Sukati S, St. Clair DK. Extracellular vesicle-mediated macrophage activation: An insight into the mechanism of thioredoxin-mediated immune activation. *Redox Biol.* 2019; **26**:101237. doi:10.1016/J.REDOX.2019.101237

176. Martinez FO, Sica A, Mantovani A, Locati M. Macrophage activation and polarization. *Front. Biosci.* 2008; **13**:453–461. doi:10.2741/2692

177. Tarique AA, Logan J, Thomas E, Holt PG, Sly PD, Fantino E. Phenotypic, Functional, and Plasticity Features of Classical and Alternatively Activated Human Macrophages. *Am. J. Respir. Cell Mol. Biol.* 2015; **53**:676–688. doi:10.1165/rcmb.2015-0012OC

178. Forrester MA, Wassall HJ, Hall LS, Cao H, Wilson HM, Barker RN, Vickers MA. Similarities and differences in surface receptor expression by THP-1 monocytes and differentiated macrophages polarized using seven different conditioning regimens. *Cell. Immunol.* 2018; **332**:58–76. doi:10.1016/J.CELLIMM.2018.07.008

179. Martinez FO, Gordon S. The M1 and M2 paradigm of macrophage activation: Time for reassessment. *F1000Prime Rep.* 2014; **6**. doi:10.12703/P6-13

180. Kohno K, Koya-Miyata S, Harashima A, Tsukuda T, Katakami M, Ariyasu T, Ushio S, Iwaki K. Inflammatory M1-like macrophages polarized by NK-4 undergo enhanced phenotypic switching to an anti-inflammatory M2-like phenotype upon co-culture with apoptotic cells. *J. Inflamm. (United Kingdom)* 2021; **18**. doi:10.1186/s12950-020-00267-z

181. Martinez FO, Gordon S, Locati M, Mantovani A. Transcriptional Profiling of the Human Monocyte-to-Macrophage Differentiation and Polarization: New Molecules and Patterns of Gene Expression. *J. Immunol.* 2006; **177**:7303–7311. doi:10.4049/jimmunol.177.10.7303

182. Wang L, Zhang S, Wu H, Rong X, Guo J. M2b macrophage polarization and its roles in diseases. *J. Leukoc. Biol.* 2019; **106**:345–358. doi:10.1002/JLB.3RU1018-378RR

183. Tedesco S, De Majo F, Kim J, Trenti A, Trevisi L, Fadini GP, Bolego C, Zandstra PW, Cignarella A, Vitiello L. Convenience versus biological significance: Are PMA-differentiated THP-1 cells a reliable substitute for blood-derived macrophages when studying in vitro polarization? *Front. Pharmacol.* 2018; **9**:71. doi:10.3389/fphar.2018.00071

184. Shiratori H, Feinweber C, Luckhardt S, Linke B, Resch E, Geisslinger G, Weigert A, Parnham MJ. THP-1 and human peripheral blood mononuclear cell-derived macrophages differ in their capacity to polarize in vitro. *Mol. Immunol.* 2017; **88**:58–68. doi:10.1016/j.molimm.2017.05.027

185. Schwende H, Fitzke E, Ambs P, Dieter P. Differences in the state of differentiation of THP-1 cells induced by phorbol ester and 1,25-dihydroxyvitamin D $_3$. *J. Leukoc. Biol.* 1996; **59**:555–561. doi:10.1002/jlb.59.4.555

186. Daigneault M, Preston JA, Marriott HM, Whyte MKB, Dockrell DH. The Identification of Markers of Macrophage Differentiation in PMA-Stimulated THP-1 Cells and Monocyte-Derived Macrophages. *PLoS One* 2010; **5**. doi:10.1371/JOURNAL.PONE.0008668

187. Fujino M, Xiao-Kang LI, Kitazawa Y, Guo LEI, Kawasaki M, Funeshima N, Amano T, Suzuki S. Distinct pathways of apoptosis triggered by FTY720, etoposide, and anti-Fas antibody in human T-lymphoma cell line (Jurkat cells). *J. Pharmacol. Exp. Ther.* 2002; **300**:939–945. doi:10.1124/jpet.300.3.939

188. Kulms D, Schwarz T. Molecular mechanisms of UV-induced apoptosis. *Photodermatol Photoimmunol Photomed* 2000; **16**:195–201. doi:10.1034/j.1600-0781.2000.160501.x

189. Bosurgi L, Cao YG, Cabeza-Cabrerizo M, Tucci A, Hughes LD, Kong Y, Weinstein JS, Licona-Limon P, Schmid ET, Pelorosso F, Gagliani N, Craft JE, Flavell RA, Ghosh S, Rothlin C V. Macrophage function in tissue repair and remodeling requires IL-4 or IL-13 with apoptotic cells. *Science (80-.).* 2017; **356**:1072–1076. doi:10.1126/science.aai8132

190. Tsuchiya S, Yamabe M, Yamaguchi Y, Kobayashi Y, Konno T, Tada K. Establishment and characterization of a human acute monocytic leukemia cell line (THP-1). *Int. J. Cancer* 1980; **26**:171–176. doi:10.1002/IJC.2910260208

191. Thomas L, Bielemeier A, Lambert PA, Darveau RP, Marshall LJ, Devitt A. The N-Terminus of CD14 Acts to Bind Apoptotic Cells and Confers Rapid-Tethering Capabilities on Non-Myeloid Cells. Wang X, ed. *PLoS One* 2013; **8**:e70691. doi:10.1371/journal.pone.0070691

192. Soldano S, Pizzorni C, Paolino S, Trombetta AC, Montagna P, Brizzolara R, Ruaro B, Sulli A, Cutolo M. Alternatively Activated (M2) Macrophage Phenotype Is Inducible by Endothelin-1 in Cultured Human Macrophages. *PLoS One* 2016; **11**:e0166433. doi:10.1371/JOURNAL.PONE.0166433

193. Fadok VA, Bratton DL, Konowal A, Freed PW, Westcott JY, Henson PM. Macrophages that have ingested apoptotic cells in vitro inhibit proinflammatory cytokine production through autocrine/paracrine mechanisms involving TGF-β, PGE2, and PAF. *J. Clin. Invest.* 1998; **101**:890–898. doi:10.1172/JCI1112

194. Alghareeb K. Characterising the Role of ICAM-3 and Apoptotic Cell-derived Extracellular Vesicles in the Clearance of Apoptotic Cells. (Unpublished doctoral thesis). 2017.

195. Devitt A, Moffatt OD, Raykundalia C, Capra JD, Simmons DL, Gregory CD. Human CD14 mediates recognition and phagocytosis of apoptotic cells. *Nature* 1998; **392**:505–509. doi:10.1038/33169

196. Platt N, Da Silva RP, Gordon S. Class A scavenger receptors and the phagocytosis of apoptotic cells. *Immunol. Lett.* 1999; **65**:15–19. doi:10.1016/S0165-2478(98)00118-7

197. Savill J, Dransfield I, Gregory C, Haslett C. A blast from the past: clearance of apoptotic cells regulates immune responses. *Nat. Rev. Immunol.* 2002; **2**:965–975. doi:10.1038/NRI957

198. Nowak-Terpiłowska A, Śledziński P, Zeyland J. Impact of cell harvesting methods on detection of cell surface proteins and apoptotic markers. *Brazilian J. Med. Biol. Res.* 2021; **54**:1–7. doi:10.1590/1414-431X202010197

199. Stenmark H. Rab GTPases as coordinators of vesicle traffic. *Nat. Rev. Mol. Cell Biol.* 2009; **10**:513–525. doi:10.1038/nrm2728

200. Théry C, Zitvogel L, Amigorena S. Exosomes: Composition, biogenesis and function. *Nat. Rev. Immunol.* 2002; **2**:569–579. doi:10.1038/nri855

201. Weyd H, Abeler-Dörner L, Linke B, Mahr A, Jahndel V, Pfrang S, Schnölzer M, Falk CS, Krammer PH. Annexin A1 on the Surface of Early Apoptotic Cells Suppresses CD8+ T Cell Immunity. Castro MG, ed. *PLoS One* 2013; **8**:e62449. doi:10.1371/journal.pone.0062449

202. Bell CW, Jiang W, Reich CF, Pisetsky DS. The extracellular release of HMGB1 during apoptotic cell death. *Am. J. Physiol. - Cell Physiol.* 2006; **291**:1318–1325. doi:10.1152/ajpcell.00616.2005

203. Scaffidi P, Misteli T, Bianchi ME. Release of chromatin protein HMGB1 by necrotic cells triggers inflammation. *Nature* 2002; **418**:191–195. doi:10.1038/nature00858

204. Giri B, Dixit VD, Ghosh MC, Collins GD, Khan IU, Madara K, Weeraratna AT, Taub DD. CXCL12-induced partitioning of flotillin-1 with lipid rafts plays a role in CXCR4 function. *Eur. J. Immunol.* 2007; **37**:2104–2116. doi:10.1002/eji.200636680

205. Bodin S, Planchon D, Morris ER, Comunale F, Gauthier-Rouviére C. Flotillins in intercellular adhesion - From cellular physiology to human diseases. *J. Cell Sci.* 2014; **127**:5139–5147. doi:10.1242/jcs.159764

206. Fork C, Hitzel J, Nichols BJ, Tikkanen R, Brandes RP. Flotillin-1 facilitates toll-like receptor 3 signaling in human endothelial cells. *Basic Res. Cardiol.* 2014; **109**:439. doi:10.1007/s00395-014-0439-4

207. Riento K, Zhang Q, Clark J, Begum F, Stephens E, Wakelam MJ, Nichols BJ. Flotillin proteins recruit sphingosine to membranes and maintain cellular sphingosine-1-phosphate levels. *PLoS One* 2018; **13**:e0197401. doi:10.1371/journal.pone.0197401

208. Philley J V., Kannan A, Dasgupta S. MDA-9/Syntenin Control. *J. Cell. Physiol.* 2016;

231:545–550. doi:10.1002/JCP.25136

209. Imjeti NS, Menck K, Egea-Jimenez AL, Lecointre C, Lembo F, Bouguenina H, Badache A, Ghossoub R, David G, Roche S, Zimmermann P. Syntenin mediates SRC function in exosomal cell-to-cell communication. *Proc. Natl. Acad. Sci. U.S.A.* 2017; **114**:12495–12500. doi:10.1073/pnas.1713433114

210. Iacono KT, Brown AL, Greene MI, Saouaf SJ. CD147 Immunoglobulin Superfamily Receptor Function and Role in Pathology. *Exp. Mol. Pathol.* 2007; **83**:283. doi:10.1016/J.YEXMP.2007.08.014

211. Gray JX, Haino M, Roth MJ, Maguire JE, Jensen PN, Yarme A, Stetler-Stevenson MA, Siebenlist U, Kelly K. CD97 is a processed, seven-transmembrane, heterodimeric receptor associated with inflammation. *J. Immunol.* 1996; **157**:5438–5447.

212. Calandra T, Roger T. Macrophage migration inhibitory factor: a regulator of innate immunity. *Nat. Rev. Immunol. 2003 310* 2003; **3**:791–800. doi:10.1038/nri1200

213. Kasama T, Ohtsuka K, Sato M, Takahashi R, Wakabayashi K, Kobayashi K. Macrophage Migration Inhibitory Factor: A Multifunctional Cytokine in Rheumatic Diseases. *Arthritis* 2010; **2010**:1–10. doi:10.1155/2010/106202

214. Mitra P, Oskeritzian CA, Payne SG, Beaven MA, Milstien S, Spiegel S. Role of ABCC1 in export of sphingosine-1-phosphate from mast cells. *Proc. Natl. Acad. Sci. U.S.A.* 2006; **103**:16394–16399. doi:10.1073/pnas.0603734103

215. Rai A, Fang H, Claridge B, Simpson RJ, Greening DW. Proteomic dissection of large extracellular vesicle surfaceome unravels interactive surface platform. *J. Extracell. Vesicles* 2021; **10**:e12164. doi:10.1002/JEV2.12164

216. Schierloh P, Yokobori N, Alemán M, Landoni V, Geffner L, Musella RM, Castagnino J, Baldini M, Abbate E, De La Barrera SS, Sasiain MC. Mycobacterium tuberculosis-Induced Gamma Interferon Production by Natural Killer Cells Requires Cross Talk with Antigen-Presenting Cells Involving Toll-Like Receptors 2 and 4 and the Mannose Receptor in Tuberculous Pleurisy. *Infect. Immun.* 2007; **75**:5325. doi:10.1128/IAI.00381-07

217. Diacovo TG, DeFougerolles AR, Bainton DF, Springer TA. A functional integrin ligand on the surface of platelets: intercellular adhesion molecule-2. *J. Clin. Invest.* 1994; **94**:1243.

doi:10.1172/JCI117442

218. Butini L, De Fougerolles AR, Vaccarezza M, Graziosi C, Cohen DI, Montroni M, Springer TA, Pantaleo G, Fauci AS. Intercellular adhesion molecules (ICAM)-1 ICAM-2 and ICAM-3 function as counter-receptors for lymphocyte function-associated molecule 1 in human immunodeficiency virus-mediated syncytia formation. *Eur. J. Immunol.* 1994; **24**:2191–2195. doi:10.1002/eji.1830240939

219. Cameron A. Attracted to Death: Apoptotic Cell-derived Extracellular Vesicles towards a basic characterisation (Unpublished doctoral thesis). 2018.

220. Robbins PD, Morelli AE. Regulation of immune responses by extracellular vesicles. *Nat. Rev. Immunol.* 2014; **14**:195–208. doi:10.1038/nri3622

221. Caruso S, Poon IKH. Apoptotic Cell-Derived Extracellular Vesicles: More Than Just Debris. *Front. Immunol.* 2018; **9**:1486. doi:10.3389/fimmu.2018.01486

222. Tóth E, Turiák L, Visnovitz T, Cserép C, Mázló A, Sódar BW, Försönits AI, Petővári G, Sebestyén A, Komlósi Z, Drahos L, Kittel Á, Nagy G, Bácsi A, Dénes Á, Gho YS, Szabó-Taylor K, Buzás EI. Formation of a protein corona on the surface of extracellular vesicles in blood plasma. *J. Extracell. Vesicles* 2021; **10**:e12140. doi:10.1002/JEV2.12140

Appendix. Supplementary Proteomics Data

Table 1: T cell early (6 h) versus late (18 h) ACdEV proteomes

Accession	Description	Peptide count	Unique peptides	Confidence score	Anova (p)	Highest mean condition	Max fold change
NUCL_HUMAN	Nucleolin	23	23	2235.72	2.22E-16	6h	3.16
TPP2_HUMAN	Tripeptidyl-peptidase 2	29	29	1995.22	4.55E-15	18h	2.70
NUMA1_HUMAN	Nuclear mitotic apparatus protein 1	51	48	4411.67	5.00E-15	18h	2.49
ATPA_HUMAN	ATP synthase subunit alpha, mitochondrial	16	14	1282.25	1.73E-14	6h	3.54
FUS_HUMAN	RNA-binding protein FUS	6	5	625.71	7.14E-14	6h	4.35
RL12_HUMAN	60S ribosomal protein L12	3	3	223.99	7.54E-14	6h	3.25
RL10A_HUMAN	60S ribosomal protein L10a	7	7	323.16	8.10E-14	6h	2.82
MDHM_HUMAN	Malate dehydrogenase, mitochondrial	9	9	753.24	1.13E-13	6h	2.81
TCPB_HUMAN	T-complex protein 1 subunit beta	23	22	3109.42	1.30E-13	18h	1.62
PTBP1_HUMAN	Polypyrimidine tract-binding protein 1	11	10	1163.46	1.46E-13	6h	3.32
PARP1_HUMAN	Poly [ADP-ribose] polymerase 1	11	10	683.18	1.57E-13	6h	4.65
H4_HUMAN	Histone H4	12	11	1174.12	1.65E-13	6h	3.55
HNRPM_HUMAN	Heterogeneous nuclear ribonucleoprotein M	9	8	491.56	1.92E-13	6h	5.15
VDAC1_HUMAN	Voltage-dependent anion-selective channel protein 1	5	4	325.68	2.15E-13	6h	5.88
VDAC2_HUMAN	Voltage-dependent anion-selective channel protein 2	5	5	348.28	2.30E-13	6h	4.73
ILF3_HUMAN	Interleukin enhancer-binding factor 3	12	12	925.84	3.03E-13	6h	3.25
LCK_HUMAN	Tyrosine-protein kinase Lck	15	13	1371.87	3.18E-13	6h	1.52
HNRPR_HUMAN	Heterogeneous nuclear ribonucleoprotein R	8	4	579.24	3.47E-13	6h	2.95
TPR_HUMAN	Nucleoprotein TPR	23	23	1847.79	3.56E-13	18h	1.76
C1QBP_HUMAN	Complement component 1 Q subcomponent-binding protein, mitochondrial	3	3	220.32	4.85E-13	6h	2.46
HMGA1_HUMAN	High mobility group protein HMG-I/HMG-Y	1	1	44.08	5.65E-13	6h	4.72
CLH1_HUMAN	Clathrin heavy chain 1	69	56	6986.78	6.33E-13	18h	1.99
PRDX3_HUMAN	Thioredoxin-dependent peroxide reductase, mitochondrial	3	3	172.12	6.37E-13	6h	2.89
THOC4_HUMAN	THO complex subunit 4	3	3	145.61	6.99E-13	6h	4.08
H1X_HUMAN	Histone H1x	3	1	119.89	8.60E-13	6h	9.20
ADT2_HUMAN	ADP/ATP translocase 2	6	2	335.56	9.10E-13	6h	3.11
ATPO_HUMAN	ATP synthase subunit O, mitochondrial	5	5	450.74	9.25E-13	6h	2.61
SF3B2_HUMAN	Splicing factor 3B subunit 2	2	2	126.95	9.89E-13	6h	4.55
RLA0_HUMAN	60S acidic ribosomal protein P0	9	5	875.9	1.01E-12	6h	2.04
RL27_HUMAN	60S ribosomal protein L27	5	5	375.46	1.16E-12	6h	3.30
PHB2_HUMAN	Prohibitin-2	8	8	603.09	1.21E-12	6h	3.74
ILF2_HUMAN	Interleukin enhancer-binding factor 2	11	11	852.57	1.26E-12	6h	2.15
RL22_HUMAN	60S ribosomal protein L22	5	3	284.37	1.35E-12	6h	3.77
COX2_HUMAN	Cytochrome c oxidase subunit 2	2	2	125.6	1.38E-12	6h	7.53
STML2_HUMAN	Stomatin-like protein 2, mitochondrial	2	2	120.05	1.38E-12	6h	4.05
CH60_HUMAN	60 kDa heat shock protein, mitochondrial	25	25	2387.59	1.43E-12	6h	2.70
ROA2_HUMAN	Heterogeneous nuclear ribonucleoproteins A2/B1	8	5	720.3	1.82E-12	6h	3.86
TOM22_HUMAN	Mitochondrial import receptor subunit TOM22 homolog	2	2	97.6	2.26E-12	6h	3.92
YBOX1_HUMAN	Nuclease-sensitive element-binding protein 1	8	4	753.95	2.95E-12	6h	2.99

T cell early (6 h) versus late (18 h) ACdEV proteomes

Accession	Description	Peptide count	Unique peptides	Confidence score	Anova (p)	Highest mean condition	Max fold change
TCPQ_HUMAN	T-complex protein 1 subunit theta	25	25	2155.58	3.06E-12	18h	1.59
HNRPQ_HUMAN	Heterogeneous nuclear ribonucleoprotein Q	7	3	522.35	3.09E-12	6h	2.28
SMC2_HUMAN	Structural maintenance of chromosomes protein 2	9	8	509.34	3.86E-12	6h	2.07
RTRAF_HUMAN	RNA transcription, translation and transport factor protein	7	7	573.91	3.95E-12	6h	3.04
RS9_HUMAN	40S ribosomal protein S9	8	8	396.88	4.24E-12	6h	2.84
SSRP1_HUMAN	FACT complex subunit SSRP1	7	7	393.7	5.45E-12	6h	3.28
EF1G_HUMAN	Elongation factor 1-gamma	12	12	970.09	5.48E-12	18h	1.56
KHDR3_HUMAN	KH domain-containing, RNA-binding, signal transduction-associated protein 3	1	1	61.45	6.20E-12	6h	8.62
ATP5H_HUMAN	ATP synthase subunit d, mitochondrial	3	3	139.4	6.36E-12	6h	4.43
CALR_HUMAN	Calreticulin	9	9	816.81	6.55E-12	6h	2.03
ACLY_HUMAN	ATP-citrate synthase	23	23	1805.55	7.64E-12	18h	1.45
SMD2_HUMAN	Small nuclear ribonucleoprotein Sm D2	5	5	299.72	7.78E-12	6h	2.24
MCM7_HUMAN	DNA replication licensing factor MCM7	14	14	989.98	7.86E-12	6h	1.52
SIT1_HUMAN	Signaling threshold-regulating transmembrane adapter 1	1	1	57.25	8.59E-12	6h	6.21
MCM5_HUMAN	DNA replication licensing factor MCM5	10	10	746.06	9.07E-12	6h	1.33
RLA2_HUMAN	60S acidic ribosomal protein P2	10	8	957.06	9.26E-12	6h	2.27
BIP_HUMAN	Endoplasmic reticulum chaperone BiP	21	18	1577.89	9.27E-12	6h	2.41
UBA1_HUMAN	Ubiquitin-like modifier-activating enzyme 1	22	21	2136.49	9.92E-12	18h	1.65
ATPB_HUMAN	ATP synthase subunit beta, mitochondrial	21	21	1952.64	1.11E-11	6h	1.98
SFXN1_HUMAN	Sideroflexin-1	2	2	90.89	1.28E-11	6h	6.98
RS4X_HUMAN	40S ribosomal protein S4, X isoform	11	5	762.59	1.51E-11	6h	1.67
SRSF1_HUMAN	Serine/arginine-rich splicing factor 1	6	6	352.42	1.55E-11	6h	2.07
RS3A_HUMAN	40S ribosomal protein S3a	5	5	329.85	1.62E-11	6h	1.85
TCPD_HUMAN	T-complex protein 1 subunit delta	18	17	1851.48	1.67E-11	18h	1.57
RBP56_HUMAN	TATA-binding protein-associated factor 2N	2	1	157.83	1.72E-11	6h	5.48
PROF1_HUMAN	Profilin-1	8	8	621.05	1.94E-11	6h	1.76
FAS_HUMAN	Fatty acid synthase	31	30	2234.51	1.98E-11	18h	1.70
RS2_HUMAN	40S ribosomal protein S2	8	8	459.63	2.49E-11	6h	1.97
TPM4_HUMAN	Tropomyosin alpha-4 chain	10	3	782.07	2.49E-11	18h	1.70
UCRIL_HUMAN	Putative cytochrome b-c1 complex subunit Rieske-like protein 1	1	1	68.7	2.56E-11	6h	4.61
RL5_HUMAN	60S ribosomal protein L5	11	11	686.59	2.68E-11	6h	2.69
TCPG_HUMAN	T-complex protein 1 subunit gamma	20	19	1717.88	2.80E-11	18h	1.54
DOCK2_HUMAN	Dedicator of cytokinesis protein 2	9	9	448.13	2.86E-11	6h	1.65
RU17_HUMAN	U1 small nuclear ribonucleoprotein 70 kDa	2	2	84.67	2.88E-11	6h	5.77
GNAI2_HUMAN	Guanine nucleotide-binding protein G(i) subunit alpha-2	8	6	773.74	2.91E-11	6h	1.53
SNAA_HUMAN	Alpha-soluble NSF attachment protein	6	3	413.22	3.01E-11	6h	1.53
PDIA1_HUMAN	Protein disulfide-isomerase	5	5	300.73	3.09E-11	6h	2.59
PRP19_HUMAN	Pre-mRNA-processing factor 19	8	8	634.31	3.12E-11	18h	1.47
ENPL_HUMAN	Endoplasmin	12	9	812.57	3.21E-11	6h	2.00
RAN_HUMAN	GTP-binding nuclear protein Ran	6	6	468.88	3.22E-11	18h	1.77
EIF3A_HUMAN	Eukaryotic translation initiation factor 3 subunit A	16	16	1289.83	3.35E-11	18h	1.53
RL9_HUMAN	60S ribosomal protein L9	8	8	482.38	3.59E-11	6h	2.26
TCPA_HUMAN	T-complex protein 1 subunit alpha	23	23	2486.11	3.83E-11	18h	1.62
GRP75_HUMAN	Stress-70 protein, mitochondrial	11	10	844.48	4.43E-11	6h	1.92

T cell early (6 h) versus late (18 h) ACdEV proteomes

Accession	Description	Peptide count	Unique peptides	Confidence score	Anova (p)	Highest mean condition	Max fold change
GANAB_HUMAN	Neutral alpha-glucosidase AB	7	7	370.13	4.50E-11	6h	2.18
H2AY_HUMAN	Core histone macro-H2A.1	3	1	167.56	4.58E-11	6h	7.83
CAND1_HUMAN	Cullin-associated NEDD8-dissociated protein 1	18	16	1266.19	5.05E-11	18h	1.77
RBM8A_HUMAN	RNA-binding protein 8A	1	1	72.24	5.30E-11	6h	3.28
EFTU_HUMAN	Elongation factor Tu, mitochondrial	4	4	249.82	5.81E-11	6h	2.23
COX5B_HUMAN	Cytochrome c oxidase subunit 5B, mitochondrial	1	1	38.27	6.01E-11	6h	4.41
PSA3_HUMAN	Proteasome subunit alpha type-3	7	7	559.12	7.36E-11	18h	1.68
RS16_HUMAN	40S ribosomal protein S16	9	9	543.52	7.76E-11	6h	1.40
ACTB_HUMAN	Actin, cytoplasmic 1	36	12	4419.79	8.19E-11	6h	1.23
CHMP6_HUMAN	Charged multivesicular body protein 6	2	2	64.75	8.28E-11	6h	1.86
RS3_HUMAN	40S ribosomal protein S3	14	14	955.22	8.47E-11	6h	1.61
HNRPU_HUMAN	Heterogeneous nuclear ribonucleoprotein U	3	3	203.54	8.55E-11	6h	2.00
TMEDA_HUMAN	Transmembrane emp24 domain-containing protein 10	3	3	171.06	8.63E-11	6h	2.56
ARF6_HUMAN	ADP-ribosylation factor 6	2	2	96.18	8.94E-11	6h	2.43
TSR1_HUMAN	Pre-rRNA-processing protein TSR1 homolog	3	3	217.92	9.31E-11	6h	6.81
EEA1_HUMAN	Early endosome antigen 1	9	8	527.66	9.39E-11	18h	2.03
PUR6_HUMAN	Multifunctional protein ADE2	10	10	836.32	9.66E-11	18h	1.33
CDC73_HUMAN	Parafibromin	1	1	122.38	9.98E-11	6h	4.28
IMDH2_HUMAN	Inosine-5'-monophosphate dehydrogenase 2	6	6	430.46	1.00E-10	6h	2.06
DHYS_HUMAN	Deoxyhypusine synthase	2	2	110.4	1.01E-10	18h	1.83
PSA1_HUMAN	Proteasome subunit alpha type-1	10	10	634.42	1.07E-10	18h	1.62
IDHP_HUMAN	Isocitrate dehydrogenase [NADP], mitochondrial	3	3	185.85	1.07E-10	6h	2.31
ICAM2_HUMAN	Intercellular adhesion molecule 2	2	2	226.15	1.13E-10	6h	3.14
LPPRC_HUMAN	Leucine-rich PPR motif-containing protein, mitochondrial	6	4	337.9	1.14E-10	6h	3.01
CISY_HUMAN	Citrate synthase, mitochondrial	1	1	55.67	1.19E-10	18h	1.98
HNRDL_HUMAN	Heterogeneous nuclear ribonucleoprotein D-like	2	1	86.21	1.23E-10	6h	3.75
MPCP_HUMAN	Phosphate carrier protein, mitochondrial	4	4	259.68	1.28E-10	6h	4.96
RL6_HUMAN	60S ribosomal protein L6	10	10	987.73	1.28E-10	6h	2.48
BABA2_HUMAN	BRISC and BRCA1-A complex member 2	2	2	125.08	1.33E-10	18h	2.13
ROA3_HUMAN	Heterogeneous nuclear ribonucleoprotein A3	4	2	293.72	1.51E-10	6h	2.01
HCD2_HUMAN	3-hydroxyacyl-CoA dehydrogenase type-2	5	5	486.72	1.52E-10	6h	2.33
MATR3_HUMAN	Matrin-3	1	1	188.86	1.54E-10	6h	3.46
PSMG2_HUMAN	Proteasome assembly chaperone 2	1	1	59.7	1.64E-10	18h	1.85
TCPE_HUMAN	T-complex protein 1 subunit epsilon	22	20	2198.54	1.64E-10	18h	1.69
TCPH_HUMAN	T-complex protein 1 subunit eta	23	22	2095.37	1.67E-10	18h	1.80
MARE1_HUMAN	Microtubule-associated protein RP/EB family member 1	2	2	99.97	1.70E-10	6h	2.11
RNH2B_HUMAN	Ribonuclease H2 subunit B	2	2	74.12	1.78E-10	18h	26.09
ATPG_HUMAN	ATP synthase subunit gamma, mitochondrial	2	2	117.71	1.79E-10	6h	6.50
FA49B_HUMAN	Protein FAM49B	7	5	537.48	1.81E-10	6h	1.75
RS15A_HUMAN	40S ribosomal protein S15a	5	5	216.43	1.86E-10	6h	1.81
LETM1_HUMAN	Mitochondrial proton/calcium exchanger protein	1	1	38.11	1.90E-10	6h	6.03
ML12A_HUMAN	Myosin regulatory light chain 12A	8	3	606.42	1.92E-10	6h	2.00
PHB_HUMAN	Prohibitin	6	5	438.46	1.94E-10	6h	3.75
DX39B_HUMAN	Spliceosome RNA helicase DDX39B	3	1	136.74	1.95E-10	18h	1.65

T cell early (6 h) versus late (18 h) ACdEV proteomes

Accession	Description	Peptide count	Unique peptides	Confidence score	Anova (p)	Highest mean condition	Max fold change
NAA15_HUMAN	N-alpha-acetyltransferase 15, NatA auxiliary subunit	2	2	146.29	2.04E-10	18h	3.85
FKBP3_HUMAN	Peptidyl-prolyl cis-trans isomerase FKBP3	3	3	131.79	2.05E-10	6h	2.98
TCPZ_HUMAN	T-complex protein 1 subunit zeta	23	19	2093.58	2.23E-10	18h	1.58
IDH3B_HUMAN	Isocitrate dehydrogenase [NAD] subunit beta, mitochondrial	2	2	151.1	2.23E-10	6h	3.31
MRP1_HUMAN	Multidrug resistance-associated protein 1	5	5	299.73	2.27E-10	6h	1.36
PSB4_HUMAN	Proteasome subunit beta type-4	4	4	364.04	2.45E-10	18h	1.62
RL7_HUMAN	60S ribosomal protein L7	10	10	503.08	2.73E-10	6h	1.57
MCM6_HUMAN	DNA replication licensing factor MCM6	2	2	161.86	2.80E-10	18h	1.72
EWS_HUMAN	RNA-binding protein EWS	2	2	128.67	2.96E-10	6h	1.74
TECR_HUMAN	Very-long-chain enoyl-CoA reductase	1	1	46.72	3.02E-10	6h	3.69
SAHH_HUMAN	Adenosylhomocysteinase	10	9	516.27	3.02E-10	18h	1.61
PA2G4_HUMAN	Proliferation-associated protein 2G4	6	6	320.67	3.05E-10	6h	2.40
ABCE1_HUMAN	ATP-binding cassette sub-family E member 1	4	4	205.05	3.19E-10	18h	1.99
SRSF2_HUMAN	Serine/arginine-rich splicing factor 2	2	1	186.43	3.34E-10	6h	2.49
PDIA3_HUMAN	Protein disulfide-isomerase A3	10	10	535.77	3.36E-10	6h	1.72
TLN1_HUMAN	Talin-1	32	31	2981.01	3.37E-10	18h	1.57
IF4A3_HUMAN	Eukaryotic initiation factor 4A-III	6	5	428.5	3.55E-10	6h	1.27
EF2_HUMAN	Elongation factor 2	27	27	2612.13	3.69E-10	18h	1.73
XRCC6_HUMAN	X-ray repair cross-complementing protein 6	16	16	1313.61	3.76E-10	18h	1.58
XPO1_HUMAN	Exportin-1	9	9	576.52	3.78E-10	18h	1.95
VAMP5_HUMAN	Vesicle-associated membrane protein 5	1	1	58.16	3.87E-10	6h	2.12
MPRI_HUMAN	Cation-independent mannose-6-phosphate receptor	20	20	1523.72	4.04E-10	18h	1.55
ELAV1_HUMAN	ELAV-like protein 1	4	4	268.57	4.04E-10	6h	2.11
RISC_HUMAN	Retinoid-inducible serine carboxypeptidase	1	1	50.79	4.26E-10	6h	3.56
RS6_HUMAN	40S ribosomal protein S6	5	3	413.12	4.27E-10	6h	1.58
AIMP1_HUMAN	Aminoacyl tRNA synthase complex-interacting multifunctional protein 1	5	5	287.42	4.34E-10	6h	2.10
HNRPC_HUMAN	Heterogeneous nuclear ribonucleoproteins C1/C2	4	2	216.18	4.41E-10	6h	2.77
XRCC5_HUMAN	X-ray repair cross-complementing protein 5	13	13	994.3	4.53E-10	18h	2.33
RSMB_HUMAN	Small nuclear ribonucleoprotein-associated proteins B and B'	4	3	210.44	4.58E-10	6h	2.18
RL36_HUMAN	60S ribosomal protein L36	1	1	68.44	4.76E-10	6h	2.98
EF1A1_HUMAN	Elongation factor 1-alpha 1	13	6	1256.55	4.78E-10	6h	1.31
MPRD_HUMAN	Cation-dependent mannose-6-phosphate receptor	1	1	174.57	5.03E-10	18h	2.73
FKBP4_HUMAN	Peptidyl-prolyl cis-trans isomerase FKBP4	7	7	448.59	5.04E-10	18h	1.43
GNAI3_HUMAN	Guanine nucleotide-binding protein G(k) subunit alpha	5	3	387.5	5.11E-10	6h	1.91
RS26_HUMAN	40S ribosomal protein S26	2	1	155.41	5.14E-10	6h	2.49
DDX6_HUMAN	Probable ATP-dependent RNA helicase DDX6	4	4	285.44	5.18E-10	6h	1.91
GAPR1_HUMAN	Golgi-associated plant pathogenesis-related protein 1	3	3	229.98	5.22E-10	6h	1.66
PYR1_HUMAN	CAD protein	26	23	1690.2	5.31E-10	6h	1.51
TMOD3_HUMAN	Tropomodulin-3	2	2	141.15	5.65E-10	6h	1.64
MRT4_HUMAN	mRNA turnover protein 4 homolog	3	3	219.81	5.93E-10	6h	7.43
HNRL1_HUMAN	Heterogeneous nuclear ribonucleoprotein U-like protein 1	2	2	145.25	6.52E-10	6h	1.85
NUDT5_HUMAN	ADP-sugar pyrophosphatase	2	2	94.93	6.62E-10	6h	1.48
GLYM_HUMAN	Serine hydroxymethyltransferase, mitochondrial	6	5	406.09	6.65E-10	6h	1.55
CPNE1_HUMAN	Copine-1	1	1	84.35	6.93E-10	6h	1.76

T cell early (6 h) versus late (18 h) ACdEV proteomes

Accession	Description	Peptide count	Unique peptides	Confidence score	Anova (p)	Highest mean condition	Max fold change
HNRPK_HUMAN	Heterogeneous nuclear ribonucleoprotein K	9	9	836.37	7.58E-10	6h	2.06
UBP14_HUMAN	Ubiquitin carboxyl-terminal hydrolase 14	3	3	158.79	7.68E-10	18h	1.96
SRRT_HUMAN	Serrate RNA effector molecule homolog	1	1	97.14	7.98E-10	18h	1.89
CD81_HUMAN	CD81 antigen	1	1	153.59	8.03E-10	6h	1.91
RL3_HUMAN	60S ribosomal protein L3	4	3	214.25	8.19E-10	6h	2.42
PSA6_HUMAN	Proteasome subunit alpha type-6	7	7	618.55	8.28E-10	18h	1.41
SRSF7_HUMAN	Serine/arginine-rich splicing factor 7	3	3	195.37	8.65E-10	6h	2.07
ECHA_HUMAN	Trifunctional enzyme subunit alpha, mitochondrial	3	3	196.31	9.75E-10	6h	4.21
FLNB_HUMAN	Filamin-B	49	49	3812.28	9.78E-10	18h	1.43
FA5_HUMAN	Coagulation factor V	5	4	267.56	1.02E-09	6h	1.41
THOC2_HUMAN	THO complex subunit 2	4	4	262.73	1.07E-09	18h	2.04
VDAC3_HUMAN	Voltage-dependent anion-selective channel protein 3	3	2	220.13	1.07E-09	6h	6.57
RFC5_HUMAN	Replication factor C subunit 5	3	3	166.47	1.10E-09	6h	2.00
ROA0_HUMAN	Heterogeneous nuclear ribonucleoprotein A0	3	2	214.04	1.11E-09	6h	4.91
TERA_HUMAN	Transitional endoplasmic reticulum ATPase	20	18	1889.17	1.23E-09	18h	1.61
TRA2A_HUMAN	Transformer-2 protein homolog alpha	2	2	126.93	1.27E-09	6h	2.98
RS13_HUMAN	40S ribosomal protein S13	6	6	448.84	1.29E-09	6h	1.41
KINH_HUMAN	Kinesin-1 heavy chain	8	6	475.41	1.31E-09	18h	1.35
ARC1B_HUMAN	Actin-related protein 2/3 complex subunit 1B	3	2	178.53	1.37E-09	18h	1.66
RALA_HUMAN	Ras-related protein Ral-A	5	1	271.4	1.42E-09	6h	1.65
BTAF1_HUMAN	TATA-binding protein-associated factor 172	1	1	37.16	1.45E-09	6h	2.16
U2AF1_HUMAN	Splicing factor U2AF 35 kDa subunit	1	1	86.61	1.47E-09	6h	1.88
DHX9_HUMAN	ATP-dependent RNA helicase A	19	19	1287.22	1.49E-09	6h	1.37
ATPK_HUMAN	ATP synthase subunit f, mitochondrial	2	2	137.54	1.54E-09	6h	3.74
NHRF1_HUMAN	Na(+)/H(+) exchange regulatory cofactor NHE-RF1	2	2	134.69	1.55E-09	6h	1.85
NF1_HUMAN	Neurofibromin	1	1	39.25	1.59E-09	6h	2.86
RALYL_HUMAN	RNA-binding Raly-like protein	1	1	50.83	1.62E-09	6h	5.39
PSMD6_HUMAN	26S proteasome non-ATPase regulatory subunit 6	8	8	672.32	1.67E-09	18h	1.30
IF2B1_HUMAN	Insulin-like growth factor 2 mRNA-binding protein 1	1	1	59.9	1.68E-09	6h	3.96
DDAH2_HUMAN	N(G),N(G)-dimethylarginine dimethylaminohydrolase 2	3	3	198.32	1.76E-09	6h	1.50
PDIA6_HUMAN	Protein disulfide-isomerase A6	6	6	395.12	1.80E-09	6h	2.15
PSA5_HUMAN	Proteasome subunit alpha type-5	5	4	432.39	1.83E-09	18h	1.45
RS23_HUMAN	40S ribosomal protein S23	1	1	50.16	1.85E-09	6h	2.21
CSN7B_HUMAN	COP9 signalosome complex subunit 7b	2	2	195.21	1.88E-09	18h	1.83
P5CR1_HUMAN	Pyrroline-5-carboxylate reductase 1, mitochondrial	1	1	88.65	1.90E-09	6h	3.68
PUR1_HUMAN	Amidophosphoribosyltransferase	2	2	116.25	1.91E-09	18h	1.81
ERP29_HUMAN	Endoplasmic reticulum resident protein 29	2	2	103.99	1.99E-09	6h	3.05
ROCK2_HUMAN	Rho-associated protein kinase 2	2	1	102.08	1.99E-09	18h	1.50
DDB1_HUMAN	DNA damage-binding protein 1	8	8	509.75	1.99E-09	18h	1.58
SYIC_HUMAN	Isoleucine--tRNA ligase, cytoplasmic	18	18	975.09	2.01E-09	18h	1.26
DDX21_HUMAN	Nucleolar RNA helicase 2	4	3	182.46	2.03E-09	6h	1.69
A16A1_HUMAN	Aldehyde dehydrogenase family 16 member A1	2	2	134.07	2.09E-09	18h	2.72
TAGL2_HUMAN	Transgelin-2	5	5	453.08	2.09E-09	6h	1.46
NOG1_HUMAN	Nucleolar GTP-binding protein 1	1	1	35.52	2.11E-09	6h	2.49

T cell early (6 h) versus late (18 h) ACdEV proteomes

Accession	Description	Peptide count	Unique peptides	Confidence score	Anova (p)	Highest mean condition	Max fold change
RU2A_HUMAN	U2 small nuclear ribonucleoprotein A'	6	6	468.24	2.13E-09	6h	2.31
RFC1_HUMAN	Replication factor C subunit 1	1	1	86.85	2.21E-09	6h	2.70
NB5R3_HUMAN	NADH-cytochrome b5 reductase 3	1	1	68.09	2.35E-09	6h	2.82
RL18_HUMAN	60S ribosomal protein L18	6	5	451.85	2.43E-09	6h	2.17
ARI1A_HUMAN	AT-rich interactive domain-containing protein 1A	1	1	118.37	2.47E-09	18h	3.04
RAB8B_HUMAN	Ras-related protein Rab-8B	7	3	548.55	2.49E-09	6h	1.47
EIF3I_HUMAN	Eukaryotic translation initiation factor 3 subunit I	3	3	146.18	2.56E-09	18h	1.78
PSB5_HUMAN	Proteasome subunit beta type-5	6	6	534.15	2.58E-09	18h	1.53
CLCA_HUMAN	Clathrin light chain A	2	1	78.52	2.61E-09	18h	2.18
PLEC_HUMAN	Plectin	2	1	93.87	2.65E-09	18h	6.19
HYOU1_HUMAN	Hypoxia up-regulated protein 1	6	6	449.52	2.68E-09	6h	1.78
U5S1_HUMAN	116 kDa U5 small nuclear ribonucleoprotein component	14	14	951.56	2.81E-09	6h	1.68
PUR2_HUMAN	Trifunctional purine biosynthetic protein adenosine-3	1	1	99.31	2.81E-09	6h	1.34
PPIA_HUMAN	Peptidyl-prolyl cis-trans isomerase A	7	6	570.68	2.98E-09	6h	1.34
ZAP70_HUMAN	Tyrosine-protein kinase ZAP-70	1	1	54.33	3.10E-09	6h	3.14
NHP2_HUMAN	H/ACA ribonucleoprotein complex subunit 2	1	1	44.3	3.11E-09	6h	2.04
DNM1L_HUMAN	Dynamin-1-like protein	1	1	175.43	3.14E-09	18h	3.61
GSHR_HUMAN	Glutathione reductase, mitochondrial	6	4	332.73	3.16E-09	18h	1.64
LAR1B_HUMAN	La-related protein 1B	1	1	146.21	3.20E-09	6h	9.25
KPYM_HUMAN	Pyruvate kinase PKM	29	27	2869.82	3.23E-09	18h	1.17
GLU2B_HUMAN	Glucosidase 2 subunit beta	3	3	170.16	3.30E-09	6h	1.95
FA98B_HUMAN	Protein FAM98B	2	2	75.55	3.33E-09	6h	3.50
RTCB_HUMAN	tRNA-splicing ligase RtcB homolog	10	10	575.83	3.35E-09	6h	1.39
RPN1_HUMAN	Dolichyl-diphosphooligosaccharide--protein glycosyltransferase subunit 1	2	2	130.68	3.50E-09	6h	3.21
RFA3_HUMAN	Replication protein A 14 kDa subunit	1	1	58.28	3.54E-09	18h	2.80
APEX1_HUMAN	DNA-(apurinic or apyrimidinic site) lyase	2	2	247.04	3.61E-09	6h	2.59
CUTA_HUMAN	Protein CutA	1	1	78.26	3.72E-09	6h	2.01
TOP1_HUMAN	DNA topoisomerase 1	2	2	97.88	3.83E-09	6h	4.15
PEBP1_HUMAN	Phosphatidylethanolamine-binding protein 1	1	1	126.08	3.95E-09	6h	1.95
SEPT9_HUMAN	Septin-9	7	6	496.18	4.17E-09	18h	1.23
NCBP1_HUMAN	Nuclear cap-binding protein subunit 1	2	2	193.21	4.17E-09	18h	1.46
LA_HUMAN	Lupus La protein	3	3	180.41	4.33E-09	6h	1.80
RM44_HUMAN	39S ribosomal protein L44, mitochondrial	1	1	58.54	4.36E-09	6h	6.66
SPTB2_HUMAN	Spectrin beta chain, non-erythrocytic 1	87	72	8082.27	4.47E-09	18h	1.19
THOC7_HUMAN	THO complex subunit 7 homolog	1	1	36.71	4.48E-09	18h	1.63
MYH10_HUMAN	Myosin-10	59	44	5308.91	4.69E-09	6h	1.24
MIF_HUMAN	Macrophage migration inhibitory factor	1	1	62.49	4.79E-09	18h	1.52
RAB7A_HUMAN	Ras-related protein Rab-7a	7	7	454.24	4.92E-09	6h	1.53
ARK72_HUMAN	Aflatoxin B1 aldehyde reductase member 2	2	2	110.67	5.08E-09	18h	1.54
ALBU_HUMAN	Serum albumin	1	1	202.05	5.34E-09	6h	2.20
RBMX_HUMAN	RNA-binding motif protein, X chromosome	3	1	232.34	5.35E-09	6h	1.61
SRP14_HUMAN	Signal recognition particle 14 kDa protein	1	1	115.07	5.37E-09	6h	1.78
EIF3E_HUMAN	Eukaryotic translation initiation factor 3 subunit E	9	9	606.39	5.93E-09	18h	1.40
PNPH_HUMAN	Purine nucleoside phosphorylase	8	8	613.56	6.25E-09	6h	1.39

T cell early (6 h) versus late (18 h) ACdEV proteomes

Accession	Description	Peptide count	Unique peptides	Confidence score	Anova (p)	Highest mean condition	Max fold change
OST48_HUMAN	Dolichyl-diphosphooligosaccharide--protein glycosyltransferase 48 kDa subunit	1	1	57.84	6.34E-09	6h	1.80
RAC1_HUMAN	Ras-related C3 botulinum toxin substrate 1	4	3	219.17	6.78E-09	6h	1.83
ERF1_HUMAN	Eukaryotic peptide chain release factor subunit 1	3	3	218.37	6.82E-09	6h	1.73
MOB1A_HUMAN	MOB kinase activator 1A	1	1	42.81	7.57E-09	6h	1.80
PR40A_HUMAN	Pre-mRNA-processing factor 40 homolog A	1	1	47.44	7.69E-09	6h	2.47
DSRAD_HUMAN	Double-stranded RNA-specific adenosine deaminase	1	1	38.21	7.77E-09	6h	3.13
PRKDC_HUMAN	DNA-dependent protein kinase catalytic subunit	34	31	2359.74	7.79E-09	6h	1.26
PA1B3_HUMAN	Platelet-activating factor acetylhydrolase IB subunit gamma	2	2	150.17	7.80E-09	18h	1.41
MPZL1_HUMAN	Myelin protein zero-like protein 1	1	1	40.7	8.02E-09	6h	1.41
MPP6_HUMAN	MAGUK p55 subfamily member 6	1	1	40.76	8.53E-09	6h	2.52
AP2A2_HUMAN	AP-2 complex subunit alpha-2	3	2	207.68	8.56E-09	18h	1.58
CATD_HUMAN	Cathepsin D	2	2	108.14	8.69E-09	6h	2.64
DLDH_HUMAN	Dihydrolipoyl dehydrogenase, mitochondrial	2	2	79.77	8.74E-09	6h	2.72
HAT1_HUMAN	Histone acetyltransferase type B catalytic subunit	1	1	102.76	8.78E-09	18h	1.96
SNR40_HUMAN	U5 small nuclear ribonucleoprotein 40 kDa protein	3	2	152.81	8.84E-09	6h	1.77
MCM2_HUMAN	DNA replication licensing factor MCM2	11	9	623.63	9.04E-09	18h	1.55
PUR9_HUMAN	Bifunctional purine biosynthesis protein PURH	12	12	784.63	9.18E-09	18h	1.48
P5CR3_HUMAN	Pyrroline-5-carboxylate reductase 3	2	2	139.73	9.27E-09	18h	2.34
NPM_HUMAN	Nucleophosmin	4	4	621.33	9.35E-09	18h	1.86
CSN1_HUMAN	COP9 signalosome complex subunit 1	2	2	97.91	9.43E-09	18h	1.68
LAT1_HUMAN	Large neutral amino acids transporter small subunit 1	6	5	477.67	9.72E-09	6h	1.35
GDIR2_HUMAN	Rho GDP-dissociation inhibitor 2	4	3	271.3	1.00E-08	6h	1.44
AT5F1_HUMAN	ATP synthase F(0) complex subunit B1, mitochondrial	3	3	141.23	1.01E-08	6h	3.91
EF1D_HUMAN	Elongation factor 1-delta	7	7	548.74	1.04E-08	18h	1.29
LDHA_HUMAN	L-lactate dehydrogenase A chain	14	12	1332.42	1.04E-08	6h	1.28
PLRG1_HUMAN	Pleiotropic regulator 1	7	7	486.19	1.05E-08	6h	1.39
PSB2_HUMAN	Proteasome subunit beta type-2	5	5	397.42	1.05E-08	18h	1.51
ABL2_HUMAN	Abelson tyrosine-protein kinase 2	1	1	37.74	1.05E-08	6h	2.14
ELMO1_HUMAN	Engulfment and cell motility protein 1	7	6	592.91	1.06E-08	6h	1.71
COR1C_HUMAN	Coronin-1C	5	5	269.91	1.06E-08	6h	1.47
COX5A_HUMAN	Cytochrome c oxidase subunit 5A, mitochondrial	1	1	63.05	1.07E-08	6h	2.08
LTOR1_HUMAN	Ragulator complex protein LAMTOR1	1	1	53.34	1.13E-08	6h	2.30
KCAB2_HUMAN	Voltage-gated potassium channel subunit beta-2	6	4	324.45	1.13E-08	6h	1.60
ECH1_HUMAN	Delta(3,5)-Delta(2,4)-dienoyl-CoA isomerase, mitochondrial	4	4	355.59	1.14E-08	6h	2.46
XPO2_HUMAN	Exportin-2	13	13	707.72	1.14E-08	18h	1.57
HDAC2_HUMAN	Histone deacetylase 2	4	1	261.59	1.16E-08	18h	1.88
GNAS1_HUMAN	Guanine nucleotide-binding protein G(s) subunit alpha isoforms XLas	7	6	581.64	1.16E-08	6h	1.50
RL26L_HUMAN	60S ribosomal protein L26-like 1	1	1	47.77	1.17E-08	18h	1.57
MYO1G_HUMAN	Unconventional myosin-Ig	17	17	1269.08	1.19E-08	6h	1.27
TBB4A_HUMAN	Tubulin beta-4A chain	23	4	2437.19	1.22E-08	18h	1.55
TPD52_HUMAN	Tumor protein D52	2	2	92.14	1.23E-08	6h	1.44
MAEA_HUMAN	Macrophage erythroblast attacher	1	1	110.04	1.30E-08	18h	2.86
NASP_HUMAN	Nuclear autoantigenic sperm protein	3	3	132.62	1.32E-08	18h	1.95
PSB1_HUMAN	Proteasome subunit beta type-1	9	9	1060.51	1.38E-08	18h	1.48

T cell early (6 h) versus late (18 h) ACdEV proteomes

Accession	Description	Peptide count	Unique peptides	Confidence score	Anova (p)	Highest mean condition	Max fold change
NP1L1_HUMAN	Nucleosome assembly protein 1-like 1	7	5	411.29	1.44E-08	6h	1.63
RNPS1_HUMAN	RNA-binding protein with serine-rich domain 1	1	1	33.73	1.46E-08	6h	1.63
RAC2_HUMAN	Ras-related C3 botulinum toxin substrate 2	3	2	135.18	1.52E-08	6h	1.94
RL11_HUMAN	60S ribosomal protein L11	2	2	204.85	1.54E-08	6h	1.94
HTSF1_HUMAN	HIV Tat-specific factor 1	1	1	62.8	1.57E-08	18h	1.70
CYBP_HUMAN	Calcyclin-binding protein	4	4	296.71	1.59E-08	6h	1.35
RL4_HUMAN	60S ribosomal protein L4	2	2	118.74	1.67E-08	6h	1.34
ACTN1_HUMAN	Alpha-actinin-1	16	6	1008.91	1.67E-08	18h	1.53
IPO11_HUMAN	Importin-11	1	1	33.31	1.68E-08	18h	5.30
HSP7C_HUMAN	Heat shock cognate 71 kDa protein	30	20	3708.12	1.77E-08	18h	1.46
RL7A_HUMAN	60S ribosomal protein L7a	4	3	415.25	1.80E-08	6h	1.36
RPN2_HUMAN	Dolichyl-diphosphooligosaccharide--protein glycosyltransferase subunit 2	2	1	98.81	1.87E-08	6h	3.97
COPG2_HUMAN	Coatomer subunit gamma-2	1	1	56.5	1.87E-08	18h	2.78
MACF1_HUMAN	Microtubule-actin cross-linking factor 1, isoforms 1/2/3/5	1	1	71.98	1.89E-08	6h	2.84
RL15_HUMAN	60S ribosomal protein L15	5	5	308.38	1.97E-08	6h	1.37
STK25_HUMAN	Serine/threonine-protein kinase 25	1	1	66.58	2.01E-08	6h	2.19
BLMH_HUMAN	Bleomycin hydrolase	2	2	170.16	2.04E-08	18h	1.43
EIF3B_HUMAN	Eukaryotic translation initiation factor 3 subunit B	7	7	397.72	2.04E-08	18h	1.33
SND1_HUMAN	Staphylococcal nuclease domain-containing protein 1	6	6	293.42	2.07E-08	6h	1.46
PSMG1_HUMAN	Proteasome assembly chaperone 1	2	2	141.85	2.08E-08	18h	1.40
TBB5_HUMAN	Tubulin beta chain	29	7	3427.53	2.16E-08	6h	1.28
RANG_HUMAN	Ran-specific GTPase-activating protein	1	1	37.57	2.36E-08	6h	1.77
COPA_HUMAN	Coatomer subunit alpha	8	8	448.39	2.47E-08	6h	1.27
RL23_HUMAN	60S ribosomal protein L23	1	1	77.59	2.48E-08	6h	2.22
SNUT2_HUMAN	U4/U6.U5 tri-snRNP-associated protein 2	2	2	115.26	2.51E-08	6h	1.49
VPS35_HUMAN	Vacuolar protein sorting-associated protein 35	10	10	745.96	2.51E-08	18h	1.32
SURF4_HUMAN	Surfeit locus protein 4	2	2	153.76	2.58E-08	6h	3.41
KTN1_HUMAN	Kinectin	4	4	216.89	2.60E-08	18h	1.47
ICAM1_HUMAN	Intercellular adhesion molecule 1	3	3	167.01	2.70E-08	6h	1.73
ANXA3_HUMAN	Annexin A3	1	1	88.15	2.80E-08	6h	1.39
U2AF2_HUMAN	Splicing factor U2AF 65 kDa subunit	2	2	157.5	2.87E-08	6h	2.91
RHOG_HUMAN	Rho-related GTP-binding protein RhoG	4	4	245.7	2.90E-08	6h	1.33
SMD3_HUMAN	Small nuclear ribonucleoprotein Sm D3	1	1	75.9	2.98E-08	6h	1.65
PSA4_HUMAN	Proteasome subunit alpha type-4	6	5	416.53	3.07E-08	18h	1.27
ZEP3_HUMAN	Transcription factor HIVEP3	1	1	32.69	3.08E-08	6h	1.89
PSB6_HUMAN	Proteasome subunit beta type-6	2	2	114.76	3.14E-08	18h	1.37
ESTD_HUMAN	S-formylglutathione hydrolase	4	3	246.12	3.16E-08	18h	1.50
HMGB1_HUMAN	High mobility group protein B1	2	1	73.8	3.32E-08	18h	2.00
FLOT1_HUMAN	Flotillin-1	2	1	85.61	3.42E-08	6h	2.02
STRBP_HUMAN	Spermatid perinuclear RNA-binding protein	1	1	57.45	3.49E-08	6h	14.36
TADBP_HUMAN	TAR DNA-binding protein 43	1	1	71.94	3.53E-08	6h	1.84
HCDH_HUMAN	Hydroxyacyl-coenzyme A dehydrogenase, mitochondrial	3	3	220.02	3.66E-08	6h	1.67
IF2A_HUMAN	Eukaryotic translation initiation factor 2 subunit 1	6	6	451.59	3.93E-08	6h	1.45
CPSF6_HUMAN	Cleavage and polyadenylation specificity factor subunit 6	1	1	41.81	4.05E-08	6h	1.88

T cell early (6 h) versus late (18 h) ACdEV proteomes

Accession	Description	Peptide count	Unique peptides	Confidence score	Anova (p)	Highest mean condition	Max fold change
CAP1_HUMAN	Adenylyl cyclase-associated protein 1	8	8	832.17	4.06E-08	18h	1.56
PPIB_HUMAN	Peptidyl-prolyl cis-trans isomerase B	3	3	184.85	4.13E-08	6h	2.37
RS17_HUMAN	40S ribosomal protein S17	5	5	416.11	4.16E-08	6h	1.45
SYRC_HUMAN	Arginine--tRNA ligase, cytoplasmic	3	3	193.17	4.21E-08	18h	1.46
PUM3_HUMAN	Pumilio homolog 3	1	1	51.83	4.32E-08	6h	6.20
TKT_HUMAN	Transketolase	9	9	745.86	4.34E-08	18h	1.68
PTCA_HUMAN	Protein tyrosine phosphatase receptor type C-associated protein	3	3	153.35	4.36E-08	6h	1.33
CAPR1_HUMAN	Caprin-1	1	1	75.77	4.40E-08	6h	1.89
PTPRC_HUMAN	Receptor-type tyrosine-protein phosphatase C	22	21	2027.87	4.48E-08	6h	1.15
IGSF8_HUMAN	Immunoglobulin superfamily member 8	4	4	293.56	4.59E-08	6h	1.38
STXB3_HUMAN	Syntaxin-binding protein 3	4	4	293.89	4.76E-08	6h	1.55
VP13A_HUMAN	Vacuolar protein sorting-associated protein 13A	1	1	34.77	4.78E-08	18h	1.74
SF3B3_HUMAN	Splicing factor 3B subunit 3	21	20	1707.48	4.86E-08	18h	1.25
SC24C_HUMAN	Protein transport protein Sec24C	2	2	197.65	4.93E-08	18h	2.04
ACTN4_HUMAN	Alpha-actinin-4	26	14	1818.71	5.01E-08	18h	1.35
MGN_HUMAN	Protein mago nashi homolog	4	4	226.87	5.02E-08	6h	2.52
PNMA2_HUMAN	Paraneoplastic antigen Ma2	1	1	40.11	5.10E-08	18h	2.27
PRP4B_HUMAN	Serine/threonine-protein kinase PRP4 homolog	1	1	83.14	5.49E-08	6h	4.16
ATX10_HUMAN	Ataxin-10	2	2	128.42	5.58E-08	18h	1.33
SEPT7_HUMAN	Septin-7	7	6	391.77	5.61E-08	18h	1.21
XPO7_HUMAN	Exportin-7	7	7	436.36	5.65E-08	18h	1.57
ARPC5_HUMAN	Actin-related protein 2/3 complex subunit 5	3	3	193.6	5.77E-08	6h	1.64
CKAP5_HUMAN	Cytoskeleton-associated protein 5	3	3	145.2	5.91E-08	6h	3.42
PYRG1_HUMAN	CTP synthase 1	6	6	446.13	5.93E-08	18h	1.77
ANX11_HUMAN	Annexin A11	9	9	517.46	6.08E-08	6h	1.21
THOC5_HUMAN	THO complex subunit 5 homolog	4	4	192.63	6.11E-08	18h	1.65
ADHX_HUMAN	Alcohol dehydrogenase class-3	3	3	218.52	6.12E-08	18h	1.31
ARPC4_HUMAN	Actin-related protein 2/3 complex subunit 4	4	4	202.94	6.50E-08	6h	1.43
ACON_HUMAN	Aconitate hydratase, mitochondrial	1	1	45.07	6.71E-08	6h	3.73
CSN4_HUMAN	COP9 signalosome complex subunit 4	4	4	333.76	7.00E-08	18h	1.65
PRP8_HUMAN	Pre-mRNA-processing-splicing factor 8	14	14	946.52	7.06E-08	6h	1.31
RS15_HUMAN	40S ribosomal protein S15	3	3	353.63	7.08E-08	6h	1.35
AP2M1_HUMAN	AP-2 complex subunit mu	2	2	104.57	7.32E-08	6h	1.31
ATP6_HUMAN	ATP synthase subunit a	1	1	48.82	7.64E-08	6h	3.48
RN213_HUMAN	E3 ubiquitin-protein ligase RNF213	2	2	133.08	8.60E-08	6h	1.98
LMNB1_HUMAN	Lamin-B1	8	7	349.37	8.68E-08	18h	2.37
PRS8_HUMAN	26S proteasome regulatory subunit 8	2	2	184.7	8.99E-08	18h	1.47
G6PD_HUMAN	Glucose-6-phosphate 1-dehydrogenase	1	1	56.69	9.40E-08	18h	2.24
ZB6CL_HUMAN	ZBED6 C-terminal-like protein	1	1	33.93	9.48E-08	6h	4.71
SMC4_HUMAN	Structural maintenance of chromosomes protein 4	6	5	324.75	9.76E-08	6h	1.61
E41L2_HUMAN	Band 4.1-like protein 2	5	5	292.07	1.00E-07	6h	1.40
ACTZ_HUMAN	Alpha-centractin	7	3	600.53	1.03E-07	18h	1.58
HSP74_HUMAN	Heat shock 70 kDa protein 4	9	9	634.58	1.06E-07	18h	1.34
PDCD6_HUMAN	Programmed cell death protein 6	2	2	119.62	1.12E-07	6h	1.48
RBBP4_HUMAN	Histone-binding protein RBBP4	4	3	228.58	1.14E-07	18h	1.43

T cell early (6 h) versus late (18 h) ACdEV proteomes

Accession	Description	Peptide count	Unique peptides	Confidence score	Anova (p)	Highest mean condition	Max fold change
ODP2_HUMAN	Dihydrolipoyllysine-residue acetyltransferase component of pyruvate dehydrogenase complex, mitochondrial	1	1	86.07	1.15E-07	6h	2.05
GDIR1_HUMAN	Rho GDP-dissociation inhibitor 1	2	2	133.3	1.17E-07	6h	1.48
C1TC_HUMAN	C-1-tetrahydrofolate synthase, cytoplasmic	23	23	1689.1	1.20E-07	6h	1.25
CSK22_HUMAN	Casein kinase II subunit alpha'	1	1	38.08	1.20E-07	18h	1.50
BASI_HUMAN	Basigin	8	8	776.66	1.21E-07	6h	1.21
IF4E_HUMAN	Eukaryotic translation initiation factor 4E	1	1	53.48	1.23E-07	18h	1.35
RAB14_HUMAN	Ras-related protein Rab-14	2	1	98.4	1.24E-07	6h	1.41
ANXA6_HUMAN	Annexin A6	35	35	3674.1	1.29E-07	18h	1.29
HVCN1_HUMAN	Voltage-gated hydrogen channel 1	1	1	63.25	1.30E-07	18h	1.53
RUXF_HUMAN	Small nuclear ribonucleoprotein F	1	1	65.72	1.30E-07	6h	1.74
RL13A_HUMAN	60S ribosomal protein L13a	5	3	212.22	1.32E-07	18h	1.33
RIR1_HUMAN	Ribonucleoside-diphosphate reductase large subunit	3	3	122.46	1.34E-07	6h	1.60
PSDE_HUMAN	26S proteasome non-ATPase regulatory subunit 14	5	5	409.38	1.34E-07	18h	1.23
MCM4_HUMAN	DNA replication licensing factor MCM4	10	10	732.72	1.34E-07	6h	1.22
RSSA_HUMAN	40S ribosomal protein SA	6	6	479.07	1.38E-07	18h	1.18
CD47_HUMAN	Leukocyte surface antigen CD47	4	4	193.73	1.44E-07	6h	1.33
PSA2_HUMAN	Proteasome subunit alpha type-2	4	4	475.72	1.51E-07	18h	1.67
ADA10_HUMAN	Disintegrin and metalloproteinase domain-containing protein 10	2	2	83.16	1.51E-07	6h	1.79
SYAC_HUMAN	Alanine--tRNA ligase, cytoplasmic	5	5	424.29	1.53E-07	18h	1.42
LYPA2_HUMAN	Acyl-protein thioesterase 2	2	2	102.3	1.59E-07	18h	1.64
CATC_HUMAN	Dipeptidyl peptidase 1	1	1	34.88	1.59E-07	6h	1.66
SYLM_HUMAN	Probable leucine--tRNA ligase, mitochondrial	1	1	33.22	1.60E-07	6h	2.25
TPPC3_HUMAN	Trafficking protein particle complex subunit 3	1	1	41.89	1.61E-07	6h	1.76
VPS29_HUMAN	Vacuolar protein sorting-associated protein 29	1	1	69.38	1.65E-07	18h	2.01
STX4_HUMAN	Syntaxin-4	4	4	262.52	1.70E-07	6h	1.56
PPIL1_HUMAN	Peptidyl-prolyl cis-trans isomerase-like 1	1	1	38.06	1.71E-07	6h	1.43
RT26_HUMAN	28S ribosomal protein S26, mitochondrial	1	1	45.49	1.74E-07	6h	5.18
RBM25_HUMAN	RNA-binding protein 25	1	1	56.47	1.74E-07	6h	6.06
SPC24_HUMAN	Kinetochore protein Spc24	1	1	45.35	1.77E-07	6h	5.13
4F2_HUMAN	4F2 cell-surface antigen heavy chain	18	18	1697.79	1.84E-07	6h	1.18
CNOT7_HUMAN	CCR4-NOT transcription complex subunit 7	2	2	180.75	2.06E-07	6h	1.78
HNRH1_HUMAN	Heterogeneous nuclear ribonucleoprotein H	5	2	522.72	2.09E-07	6h	2.75
LRC59_HUMAN	Leucine-rich repeat-containing protein 59	1	1	57.11	2.11E-07	6h	2.95
SP16H_HUMAN	FACT complex subunit SPT16	3	3	143.51	2.13E-07	6h	1.79
ROAA_HUMAN	Heterogeneous nuclear ribonucleoprotein A/B	2	2	90.62	2.21E-07	6h	1.43
RUXE_HUMAN	Small nuclear ribonucleoprotein E	2	2	109.09	2.24E-07	6h	1.54
CNOT9_HUMAN	CCR4-NOT transcription complex subunit 9	1	1	46.87	2.24E-07	6h	1.74
SETLP_HUMAN	Protein SETSIP	4	1	317.04	2.32E-07	18h	2.08
TSN_HUMAN	Translin	4	4	264.42	2.33E-07	18h	1.76
STAU1_HUMAN	Double-stranded RNA-binding protein Staufen homolog 1	1	1	77.66	2.39E-07	6h	7.57
CAZA1_HUMAN	F-actin-capping protein subunit alpha-1	5	4	367.52	2.44E-07	6h	1.16
RASN_HUMAN	GTPase NRas	4	1	273.15	2.47E-07	6h	1.67
GID8_HUMAN	Glucose-induced degradation protein 8 homolog	1	1	59.85	2.60E-07	18h	2.08
OR8H2_HUMAN	Olfactory receptor 8H2	1	1	43.6	2.61E-07	6h	1.46

T cell early (6 h) versus late (18 h) ACdEV proteomes

Accession	Description	Peptide count	Unique peptides	Confidence score	Anova (p)	Highest mean condition	Max fold change
APT_HUMAN	Adenine phosphoribosyltransferase	4	4	191.35	2.62E-07	6h	1.44
EXOS6_HUMAN	Exosome complex component MTR3	2	2	111.07	2.69E-07	18h	1.97
RLA1_HUMAN	60S acidic ribosomal protein P1	3	1	364.23	2.71E-07	6h	1.45
AT1B3_HUMAN	Sodium/potassium-transporting ATPase subunit beta-3	6	6	409.47	2.75E-07	6h	1.22
VATA_HUMAN	V-type proton ATPase catalytic subunit A	10	9	707.99	2.84E-07	18h	1.42
KIF23_HUMAN	Kinesin-like protein KIF23	2	1	88.34	2.86E-07	6h	2.03
2AAA_HUMAN	Serine/threonine-protein phosphatase 2A 65 kDa regulatory subunit A alpha isoform	7	5	639.14	2.88E-07	18h	1.16
TOP2B_HUMAN	DNA topoisomerase 2-beta	3	2	137.19	2.94E-07	6h	1.60
XPOT_HUMAN	Exportin-T	4	4	350.78	3.01E-07	18h	1.49
IMA1_HUMAN	Importin subunit alpha-1	2	2	141.8	3.11E-07	18h	1.39
GTR1_HUMAN	Solute carrier family 2, facilitated glucose transporter member 1	7	6	551.01	3.12E-07	6h	1.19
NP1L4_HUMAN	Nucleosome assembly protein 1-like 4	4	2	310.99	3.12E-07	18h	1.26
ZN500_HUMAN	Zinc finger protein 500	1	1	35.1	3.14E-07	18h	1.36
RAB5C_HUMAN	Ras-related protein Rab-5C	7	5	613.22	3.15E-07	6h	1.31
RUXGL_HUMAN	Putative small nuclear ribonucleoprotein G-like protein 15	1	1	47.53	3.17E-07	18h	1.73
AN32A_HUMAN	Acidic leucine-rich nuclear phosphoprotein 32 family member A	3	2	211.02	3.27E-07	18h	2.16
RAP1B_HUMAN	Ras-related protein Rap-1b	9	1	700.94	3.30E-07	6h	5.03
ZCCHL_HUMAN	Zinc finger CCCH-type antiviral protein 1-like	1	1	71.91	3.33E-07	18h	1.50
KAP2_HUMAN	cAMP-dependent protein kinase type II-alpha regulatory subunit	3	3	297.38	3.37E-07	6h	1.46
MOV10_HUMAN	Putative helicase MOV-10	2	2	90.77	3.37E-07	6h	1.92
ACADM_HUMAN	Medium-chain specific acyl-CoA dehydrogenase, mitochondrial	1	1	109.62	3.54E-07	6h	2.14
NAT10_HUMAN	RNA cytidine acetyltransferase	1	1	69.42	3.60E-07	6h	5.57
K2013_HUMAN	Uncharacterized protein KIAA2013	1	1	72.76	3.63E-07	18h	3.28
SERPH_HUMAN	Serpin H1	1	1	63.26	3.70E-07	6h	5.07
PEF1_HUMAN	Peflin	3	3	252.87	3.88E-07	6h	1.58
CDK5_HUMAN	Cyclin-dependent-like kinase 5	1	1	34.03	3.92E-07	6h	2.73
PCBP2_HUMAN	Poly(rC)-binding protein 2	3	2	141.19	3.95E-07	6h	1.46
SNG2_HUMAN	Synaptogyrin-2	1	1	34.09	3.99E-07	6h	1.27
CH10_HUMAN	10 kDa heat shock protein, mitochondrial	2	2	143.81	3.99E-07	6h	1.70
KPRA_HUMAN	Phosphoribosyl pyrophosphate synthase-associated protein 1	2	1	130.13	4.00E-07	6h	2487.23
AAAT_HUMAN	Neutral amino acid transporter B(0)	9	7	657.8	4.23E-07	6h	1.33
SPTN1_HUMAN	Spectrin alpha chain, non-erythrocytic 1	113	105	10608.95	4.31E-07	18h	1.08
IMB1_HUMAN	Importin subunit beta-1	13	12	1044.58	4.53E-07	18h	1.19
CAZA2_HUMAN	F-actin-capping protein subunit alpha-2	2	1	166.09	4.72E-07	6h	1.61
H2A2A_HUMAN	Histone H2A type 2-A	8	3	795.08	4.85E-07	6h	72.12
AP2S1_HUMAN	AP-2 complex subunit sigma	1	1	34.31	4.98E-07	6h	1.82
KPCA_HUMAN	Protein kinase C alpha type	5	3	339.6	5.05E-07	6h	1.17
URP2_HUMAN	Fermitin family homolog 3	2	2	105.56	5.05E-07	6h	1.48
CHD4_HUMAN	Chromodomain-helicase-DNA-binding protein 4	1	1	43.12	5.06E-07	6h	6.09
EIF3K_HUMAN	Eukaryotic translation initiation factor 3 subunit K	2	2	106.04	5.17E-07	6h	1.30
RL21_HUMAN	60S ribosomal protein L21	2	2	78.71	5.24E-07	6h	1.51
SNP23_HUMAN	Synaptosomal-associated protein 23	2	2	120.93	5.25E-07	6h	2.31
NDUA7_HUMAN	NADH dehydrogenase [ubiquinone] 1 alpha subcomplex subunit 7	1	1	59.88	5.29E-07	6h	6.41
SCAM2_HUMAN	Secretory carrier-associated membrane protein 2	1	1	96.44	5.30E-07	18h	1.40

T cell early (6 h) versus late (18 h) ACdEV proteomes

Accession	Description	Peptide count	Unique peptides	Confidence score	Anova (p)	Highest mean condition	Max fold change
HDAC1_HUMAN	Histone deacetylase 1	4	1	212.2	5.36E-07	18h	1.47
UBE4A_HUMAN	Ubiquitin conjugation factor E4 A	1	1	36.07	5.38E-07	18h	13.43
EZRI_HUMAN	Ezrin	11	4	687.6	5.41E-07	6h	1.33
RL29_HUMAN	60S ribosomal protein L29	1	1	126.19	5.44E-07	18h	1.41
VAMP7_HUMAN	Vesicle-associated membrane protein 7	1	1	33.16	5.44E-07	6h	2.53
CYB5B_HUMAN	Cytochrome b5 type B	1	1	92.6	5.51E-07	6h	2.32
GDIB_HUMAN	Rab GDP dissociation inhibitor beta	13	8	935.2	5.67E-07	6h	1.21
NUBP2_HUMAN	Cytosolic Fe-S cluster assembly factor NUBP2	1	1	55.4	5.79E-07	6h	1.73
RL10_HUMAN	60S ribosomal protein L10	6	4	471.88	5.80E-07	6h	1.46
STRAP_HUMAN	Serine-threonine kinase receptor-associated protein	3	3	144.52	5.87E-07	18h	1.16
SEPT2_HUMAN	Septin-2	7	7	530.48	6.05E-07	18h	1.23
THIL_HUMAN	Acetyl-CoA acetyltransferase, mitochondrial	1	1	88.11	6.41E-07	6h	1.64
CD3E_HUMAN	T-cell surface glycoprotein CD3 epsilon chain	1	1	31.74	6.41E-07	6h	1.82
IQGA1_HUMAN	Ras GTPase-activating-like protein IQGAP1	25	23	1849.87	6.44E-07	6h	1.16
PSMD7_HUMAN	26S proteasome non-ATPase regulatory subunit 7	7	7	563.5	6.49E-07	18h	1.12
BAG2_HUMAN	BAG family molecular chaperone regulator 2	6	6	402.62	6.64E-07	18h	1.35
PLIN3_HUMAN	Perilipin-3	1	1	71.18	6.81E-07	18h	1.46
MTA2_HUMAN	Metastasis-associated protein MTA2	5	3	267.75	7.02E-07	18h	1.35
PSD12_HUMAN	26S proteasome non-ATPase regulatory subunit 12	4	4	245.49	7.21E-07	18h	1.48
EIFCL_HUMAN	Eukaryotic translation initiation factor 3 subunit C-like protein	7	7	542.02	7.31E-07	18h	1.28
HS105_HUMAN	Heat shock protein 105 kDa	1	1	42.07	7.33E-07	18h	2.21
WDR12_HUMAN	Ribosome biogenesis protein WDR12	1	1	47.64	7.49E-07	18h	1.80
HNRPF_HUMAN	Heterogeneous nuclear ribonucleoprotein F	3	1	258.2	7.53E-07	6h	2.08
VATB2_HUMAN	V-type proton ATPase subunit B, brain isoform	2	1	105.26	7.57E-07	18h	1.40
TNPO1_HUMAN	Transportin-1	1	1	43.47	7.77E-07	18h	1.39
XYLB_HUMAN	Xylulose kinase	1	1	49.67	7.94E-07	18h	1.49
SMC3_HUMAN	Structural maintenance of chromosomes protein 3	4	4	222.42	7.99E-07	18h	1.25
RS18_HUMAN	40S ribosomal protein S18	5	5	282.51	8.10E-07	18h	1.14
MYG1_HUMAN	UPF0160 protein MYG1, mitochondrial	2	2	83.25	8.25E-07	18h	2.89
CALM1_HUMAN	Calmodulin-1	2	2	117.9	8.44E-07	6h	1.33
VAT1_HUMAN	Synaptic vesicle membrane protein VAT-1 homolog	9	8	802.73	8.52E-07	18h	1.20
ALMS1_HUMAN	Alstrom syndrome protein 1	1	1	31.74	8.71E-07	6h	1.24
MDN1_HUMAN	Midasin	1	1	51.17	8.87E-07	6h	2.54
DNJA2_HUMAN	DnaJ homolog subfamily A member 2	1	1	61.29	9.31E-07	6h	1.38
SYYC_HUMAN	Tyrosine--tRNA ligase, cytoplasmic	1	1	64.21	9.56E-07	6h	1.82
CPNS1_HUMAN	Calpain small subunit 1	2	2	146.79	9.72E-07	18h	1.80
P5CS_HUMAN	Delta-1-pyrroline-5-carboxylate synthase	2	2	123.21	9.99E-07	6h	3.30
PSB3_HUMAN	Proteasome subunit beta type-3	5	5	444.6	1.00E-06	18h	1.17
PRDX4_HUMAN	Peroxiredoxin-4	2	1	187.81	1.01E-06	6h	1.82
SDCB1_HUMAN	Syntenin-1	2	2	251.92	1.04E-06	6h	1.33
SF01_HUMAN	Splicing factor 1	1	1	48.65	1.05E-06	6h	8.67
UBA6_HUMAN	Ubiquitin-like modifier-activating enzyme 6	1	1	48.17	1.07E-06	18h	2.10
TM109_HUMAN	Transmembrane protein 109	1	1	70.23	1.16E-06	6h	1.75
ASPM_HUMAN	Abnormal spindle-like microcephaly-associated protein	1	1	37.42	1.22E-06	18h	5.77

T cell early (6 h) versus late (18 h) ACdEV proteomes

Accession	Description	Peptide count	Unique peptides	Confidence score	Anova (p)	Highest mean condition	Max fold change
HMGB2_HUMAN	High mobility group protein B2	3	2	134.48	1.23E-06	6h	3.05
RL8_HUMAN	60S ribosomal protein L8	4	4	367.56	1.26E-06	6h	1.18
ALDOA_HUMAN	Fructose-bisphosphate aldolase A	12	12	1214.33	1.36E-06	18h	1.09
COPE_HUMAN	Coatomer subunit epsilon	3	3	265.14	1.38E-06	6h	1.38
U520_HUMAN	U5 small nuclear ribonucleoprotein 200 kDa helicase	9	9	690.03	1.39E-06	18h	1.32
ANXA1_HUMAN	Annexin A1	6	6	383.78	1.41E-06	18h	1.18
EPN4_HUMAN	Clathrin interactor 1	1	1	42.98	1.46E-06	18h	29.12
GARS_HUMAN	Glycine--tRNA ligase	9	9	765.83	1.48E-06	18h	1.13
CCD47_HUMAN	Coiled-coil domain-containing protein 47	1	1	36.28	1.54E-06	6h	3.12
RS24_HUMAN	40S ribosomal protein S24	1	1	52.1	1.63E-06	6h	1.76
MEP50_HUMAN	Methylosome protein 50	2	2	89	1.68E-06	18h	1.47
FMNL1_HUMAN	Formin-like protein 1	5	5	365.69	1.74E-06	6h	1.21
SEPT6_HUMAN	Septin-6	5	4	304.46	1.80E-06	18h	1.29
SCPDL_HUMAN	Saccharopine dehydrogenase-like oxidoreductase	1	1	40.2	1.88E-06	6h	2.03
IF4G2_HUMAN	Eukaryotic translation initiation factor 4 gamma 2	1	1	45.24	1.91E-06	6h	2.62
IDH3A_HUMAN	Isocitrate dehydrogenase [NAD] subunit alpha, mitochondrial	1	1	169.07	1.91E-06	6h	2.03
ANM5_HUMAN	Protein arginine N-methyltransferase 5	8	7	401.64	1.92E-06	18h	1.50
PSMD3_HUMAN	26S proteasome non-ATPase regulatory subunit 3	8	7	637.58	1.95E-06	18h	1.17
CSN2_HUMAN	COP9 signalosome complex subunit 2	4	4	231.75	1.97E-06	18h	1.34
HLAH_HUMAN	Putative HLA class I histocompatibility antigen, alpha chain H	4	1	341.37	1.99E-06	18h	33.57
EIF3L_HUMAN	Eukaryotic translation initiation factor 3 subunit L	10	10	582.11	2.03E-06	18h	1.41
EIF3F_HUMAN	Eukaryotic translation initiation factor 3 subunit F	9	9	832.77	2.17E-06	18h	1.42
HS90A_HUMAN	Heat shock protein HSP 90-alpha	47	18	4644.31	2.17E-06	18h	1.54
TFIP8_HUMAN	Tumor necrosis factor alpha-induced protein 8	1	1	191.42	2.17E-06	18h	2.04
LRC57_HUMAN	Leucine-rich repeat-containing protein 57	1	1	33.71	2.29E-06	6h	1.60
CARL2_HUMAN	Capping protein, Arp2/3 and myosin-I linker protein 2	1	1	86.3	2.32E-06	6h	2.64
ACTA_HUMAN	Actin, aortic smooth muscle	21	1	2039.97	2.33E-06	6h	1.33
RCC2_HUMAN	Protein RCC2	7	7	464.31	2.34E-06	6h	1.19
EIF3M_HUMAN	Eukaryotic translation initiation factor 3 subunit M	4	4	431.94	2.35E-06	18h	1.22
GLOD4_HUMAN	Glyoxalase domain-containing protein 4	1	1	105.28	2.36E-06	6h	1.69
RL30_HUMAN	60S ribosomal protein L30	2	2	65.56	2.37E-06	6h	2.17
S4A7_HUMAN	Sodium bicarbonate cotransporter 3	4	3	225.78	2.42E-06	6h	1.22
BAG6_HUMAN	Large proline-rich protein BAG6	1	1	69.02	2.50E-06	18h	1.53
ANM1_HUMAN	Protein arginine N-methyltransferase 1	2	2	79.53	2.52E-06	18h	1.42
GNAQ_HUMAN	Guanine nucleotide-binding protein G(q) subunit alpha	7	6	547.78	2.55E-06	6h	1.22
SNG1_HUMAN	Synaptogyrin-1	1	1	33.52	2.56E-06	6h	1.74
AQR_HUMAN	Intron-binding protein aquarius	1	1	55.95	2.57E-06	6h	1.60
TCEA1_HUMAN	Transcription elongation factor A protein 1	2	2	166.71	2.62E-06	6h	1.52
FBRL_HUMAN	rRNA 2'-O-methyltransferase fibrillarin	1	1	73.79	2.71E-06	6h	9.55
2ABA_HUMAN	Serine/threonine-protein phosphatase 2A 55 kDa regulatory subunit B alpha isoform	3	3	265.23	2.71E-06	18h	1.64
IPYR_HUMAN	Inorganic pyrophosphatase	4	3	362.71	2.79E-06	6h	1.22
MLEC_HUMAN	Malectin	1	1	37.18	2.82E-06	6h	2.08
MFGM_HUMAN	Lactadherin	2	2	117.28	2.86E-06	6h	1.71
AHSA1_HUMAN	Activator of 90 kDa heat shock protein ATPase homolog 1	1	1	87.28	2.87E-06	18h	1.47

T cell early (6 h) versus late (18 h) ACdEV proteomes

Accession	Description	Peptide count	Unique peptides	Confidence score	Anova (p)	Highest mean condition	Max fold change
SPAT5_HUMAN	Spermatogenesis-associated protein 5	1	1	95.73	2.91E-06	6h	1.84
RTN4_HUMAN	Reticulon-4	1	1	78.09	2.93E-06	18h	1.34
RENT1_HUMAN	Regulator of nonsense transcripts 1	3	3	269.22	3.01E-06	6h	1.54
VATH_HUMAN	V-type proton ATPase subunit H	3	3	168.32	3.25E-06	18h	1.53
UBP7_HUMAN	Ubiquitin carboxyl-terminal hydrolase 7	3	3	235.95	3.33E-06	18h	1.58
AP1B1_HUMAN	AP-1 complex subunit beta-1	3	1	298.42	3.38E-06	18h	1.44
DCTN4_HUMAN	Dynactin subunit 4	1	1	40.8	3.47E-06	18h	1.66
LYPA1_HUMAN	Acyl-protein thioesterase 1	1	1	39.71	3.53E-06	18h	1.31
RAB2A_HUMAN	Ras-related protein Rab-2A	1	1	60.02	3.58E-06	6h	1.57
FLOT2_HUMAN	Flotillin-2	1	1	51.03	3.62E-06	6h	2.06
UBE2N_HUMAN	Ubiquitin-conjugating enzyme E2 N	1	1	79.01	3.64E-06	6h	1.81
TALDO_HUMAN	Transaldolase	3	3	149.4	3.78E-06	18h	1.34
GSLG1_HUMAN	Golgi apparatus protein 1	1	1	83.2	3.94E-06	18h	2.59
GDE_HUMAN	Glycogen debranching enzyme	1	1	92.27	4.21E-06	18h	1.62
IPO9_HUMAN	Importin-9	1	1	198.33	4.41E-06	18h	1.58
NOP58_HUMAN	Nucleolar protein 58	2	2	270.07	4.41E-06	18h	1.47
PGK1_HUMAN	Phosphoglycerate kinase 1	18	12	1328.66	4.42E-06	18h	1.13
TFR1_HUMAN	Transferrin receptor protein 1	18	18	1065.58	4.49E-06	6h	1.13
SYSC_HUMAN	Serine--tRNA ligase, cytoplasmic	8	8	574.82	4.52E-06	18h	1.20
STMN1_HUMAN	Stathmin	2	1	72.52	4.54E-06	6h	1.25
SYQ_HUMAN	Glutamine--tRNA ligase	3	2	164.22	4.62E-06	18h	1.45
IPO5_HUMAN	Importin-5	9	7	533.32	4.76E-06	18h	1.20
G3P_HUMAN	Glyceraldehyde-3-phosphate dehydrogenase	25	24	2487.01	4.84E-06	18h	1.19
DPP3_HUMAN	Dipeptidyl peptidase 3	1	1	104.89	5.02E-06	18h	1.50
NMT1_HUMAN	Glycylpeptide N-tetradecanoyltransferase 1	2	2	136.82	5.06E-06	18h	1.39
S38A2_HUMAN	Sodium-coupled neutral amino acid transporter 2	1	1	121.71	5.31E-06	6h	1.39
KPRB_HUMAN	Phosphoribosyl pyrophosphate synthase-associated protein 2	4	3	403.38	5.54E-06	18h	1.50
TIF1B_HUMAN	Transcription intermediary factor 1-beta	4	4	182.53	5.84E-06	18h	1.26
GSTP1_HUMAN	Glutathione S-transferase P	9	9	1042.77	5.90E-06	6h	1.14
COPB_HUMAN	Coatomer subunit beta	3	3	286.62	5.95E-06	18h	1.77
PSA7_HUMAN	Proteasome subunit alpha type-7	8	5	509.93	5.99E-06	18h	1.16
PML_HUMAN	Protein PML	1	1	54.54	6.01E-06	18h	5.11
SPEE_HUMAN	Spermidine synthase	4	4	233.39	6.14E-06	18h	1.22
RL1D1_HUMAN	Ribosomal L1 domain-containing protein 1	1	1	44.79	6.14E-06	6h	1.63
RL13_HUMAN	60S ribosomal protein L13	1	1	42.47	6.15E-06	6h	1.61
H2AV_HUMAN	Histone H2A.V	2	1	182.37	6.19E-06	6h	25.00
MTOR_HUMAN	Serine/threonine-protein kinase mTOR	1	1	34.75	6.25E-06	18h	1.95
RL27A_HUMAN	60S ribosomal protein L27a	1	1	83.77	6.54E-06	6h	1.38
KCY_HUMAN	UMP-CMP kinase O	1	1	52.99	6.64E-06	18h	2.11
DDX47_HUMAN	Probable ATP-dependent RNA helicase DDX47	1	1	45.51	6.80E-06	6h	1.80
RL24_HUMAN	60S ribosomal protein L24	1	1	35.67	7.44E-06	6h	1.19
CD97_HUMAN	CD97 antigen	1	1	69.52	7.67E-06	18h	7.46
CUL2_HUMAN	Cullin-2	1	1	65.37	7.85E-06	18h	1.57
PUR4_HUMAN	Phosphoribosylformylglycinamidine synthase	6	6	372.52	8.30E-06	18h	1.30
PLP2_HUMAN	Proteolipid protein 2	1	1	54.26	9.02E-06	18h	1.66

T cell early (6 h) versus late (18 h) ACdEV proteomes

Accession	Description	Peptide count	Unique peptides	Confidence score	Anova (p)	Highest mean condition	Max fold change
PRDX1_HUMAN	Peroxiredoxin-1	13	10	1170.16	9.23E-06	6h	1.17
GRHPR_HUMAN	Glyoxylate reductase/hydroxypyruvate reductase	1	1	48.62	9.50E-06	18h	1.26
RPP30_HUMAN	Ribonuclease P protein subunit p30	1	1	125.28	9.56E-06	6h	1.46
CSN7A_HUMAN	COP9 signalosome complex subunit 7a	1	1	167.25	9.75E-06	18h	1.74
SYCC_HUMAN	Cysteine--tRNA ligase, cytoplasmic	1	1	31.19	1.02E-05	18h	1.34
RFA1_HUMAN	Replication protein A 70 kDa DNA-binding subunit	1	1	61.51	1.02E-05	18h	1.33
AT1A3_HUMAN	Sodium/potassium-transporting ATPase subunit alpha-3	10	1	1314.46	1.06E-05	6h	1.31
SAE2_HUMAN	SUMO-activating enzyme subunit 2	1	1	48.12	1.07E-05	18h	5.05
ACOX1_HUMAN	Peroxisomal acyl-coenzyme A oxidase 1	1	1	86.73	1.10E-05	6h	1.66
PLSL_HUMAN	Plastin-2	33	27	2728.89	1.15E-05	6h	1.17
HDDC2_HUMAN	HD domain-containing protein 2	1	1	49	1.18E-05	18h	2.48
TTL12_HUMAN	Tubulin--tyrosine ligase-like protein 12	1	1	36.75	1.20E-05	18h	1.41
RAD50_HUMAN	DNA repair protein RAD50	2	2	100.19	1.21E-05	6h	1.37
RAB8A_HUMAN	Ras-related protein Rab-8A	5	1	324.41	1.25E-05	6h	1.26
H2B1B_HUMAN	Histone H2B type 1-B	12	1	1114.3	1.29E-05	6h	1.65
P66A_HUMAN	Transcriptional repressor p66-alpha	1	1	56.9	1.30E-05	6h	1.32
HBA_HUMAN	Hemoglobin subunit alpha	2	2	107.17	1.31E-05	6h	1.35
CSN6_HUMAN	COP9 signalosome complex subunit 6	1	1	90.5	1.31E-05	6h	5.14
CD2_HUMAN	T-cell surface antigen CD2	1	1	32.7	1.32E-05	18h	16.85
RS27L_HUMAN	40S ribosomal protein S27-like	1	1	47.4	1.33E-05	6h	1.10
PRS7_HUMAN	26S proteasome regulatory subunit 7	7	7	422	1.35E-05	6h	1.13
VATE1_HUMAN	V-type proton ATPase subunit E 1	3	3	297.4	1.44E-05	6h	1.39
ASNS_HUMAN	Asparagine synthetase [glutamine-hydrolyzing]	2	2	110.63	1.49E-05	18h	1.30
CDC42_HUMAN	Cell division control protein 42 homolog	1	1	153.82	1.51E-05	6h	1.21
WDR1_HUMAN	WD repeat-containing protein 1	2	2	126.39	1.52E-05	6h	1.16
PCBP1_HUMAN	Poly(rC)-binding protein 1	2	2	171.46	1.55E-05	6h	1.21
1A03_HUMAN	HLA class I histocompatibility antigen, A-3 alpha chain	8	2	654.4	1.60E-05	18h	1.38
RS8_HUMAN	40S ribosomal protein S8	5	5	418.67	1.60E-05	6h	1.24
ARP3B_HUMAN	Actin-related protein 3B	2	1	145.02	1.61E-05	18h	3.36
DREB_HUMAN	Drebrin	2	2	67	1.62E-05	6h	1.60
COPZ1_HUMAN	Coatomer subunit zeta-1	1	1	51.58	1.66E-05	6h	53.17
GBB1_HUMAN	Guanine nucleotide-binding protein G(I)/G(S)/G(T) subunit beta-1	3	2	284.35	1.71E-05	6h	1.25
ACTC_HUMAN	Actin, alpha cardiac muscle 1	23	1	2284.25	1.72E-05	6h	3.89
RS20_HUMAN	40S ribosomal protein S20 O	2	2	274.95	1.73E-05	6h	1.20
HAUS1_HUMAN	HAUS augmin-like complex subunit 1	1	1	63.39	1.76E-05	6h	1.47
TSNAX_HUMAN	Translin-associated protein X	3	3	296.22	1.79E-05	18h	1.14
DEOC_HUMAN	Deoxyribose-phosphate aldolase	2	2	148.99	1.79E-05	18h	1.84
LEUK_HUMAN	Leukosialin	1	1	56.63	1.80E-05	6h	1.23
M4K1_HUMAN	Mitogen-activated protein kinase kinase kinase kinase 1	1	1	47.84	1.80E-05	6h	1.66
THIO_HUMAN	Thioredoxin	1	1	34.75	1.81E-05	18h	3.14
LDHB_HUMAN	L-lactate dehydrogenase B chain	14	13	1190.49	1.82E-05	6h	1.10
DDX3X_HUMAN	ATP-dependent RNA helicase DDX3X	2	1	131.83	1.89E-05	6h	1.36
PARK7_HUMAN	Protein/nucleic acid deglycase DJ-1	2	2	127.84	1.89E-05	6h	2.35
AATM_HUMAN	Aspartate aminotransferase, mitochondrial	1	1	75.23	1.89E-05	6h	1.53

T cell early (6 h) versus late (18 h) ACdEV proteomes

Accession	Description	Peptide count	Unique peptides	Confidence score	Anova (p)	Highest mean condition	Max fold change
GALT2_HUMAN	Polypeptide N-acetylgalactosaminyltransferase 2	1	1	46.71	1.91E-05	18h	1.71
PRS6B_HUMAN	26S proteasome regulatory subunit 6B	6	6	538.87	1.93E-05	18h	1.25
STIP1_HUMAN	Stress-induced-phosphoprotein 1	13	13	676.25	2.07E-05	18h	1.13
RS5_HUMAN	40S ribosomal protein S5	4	3	301.16	2.07E-05	6h	1.35
WDR5_HUMAN	WD repeat-containing protein 5	3	3	166.83	2.20E-05	6h	1.17
AP180_HUMAN	Clathrin coat assembly protein AP180	1	1	34.93	2.21E-05	6h	1.29
TPM3_HUMAN	Tropomyosin alpha-3 chain	11	3	909	2.24E-05	6h	1.15
MMS19_HUMAN	MMS19 nucleotide excision repair protein homolog	1	1	75.9	2.24E-05	6h	1.39
CSK21_HUMAN	Casein kinase II subunit alpha	2	1	131.95	2.27E-05	18h	1.27
H2A1B_HUMAN	Histone H2A type 1-B/E	7	1	726.79	2.30E-05	6h	4.63
ARF1_HUMAN	ADP-ribosylation factor 1	5	3	414.21	2.42E-05	6h	1.30
SFPQ_HUMAN	Splicing factor, proline- and glutamine-rich	7	6	480.94	2.43E-05	6h	1.10
TNPO3_HUMAN	Transportin-3	1	1	119.61	2.47E-05	18h	1.50
EIF3H_HUMAN	Eukaryotic translation initiation factor 3 subunit H	3	3	171.45	2.47E-05	18h	1.21
PUR8_HUMAN	Adenylosuccinate lyase	4	4	286.76	2.53E-05	18h	1.18
VATL_HUMAN	V-type proton ATPase 16 kDa proteolipid subunit	1	1	75	2.54E-05	6h	32.39
MIC60_HUMAN	MICOS complex subunit MIC60	1	1	93.35	2.55E-05	6h	3.35
PCNA_HUMAN	Proliferating cell nuclear antigen	3	3	293.13	2.56E-05	6h	1.17
NXN_HUMAN	Nucleoredoxin	4	4	217.69	2.56E-05	18h	1.13
AN32B_HUMAN	Acidic leucine-rich nuclear phosphoprotein 32 family member B	3	2	160.11	2.71E-05	18h	2.07
SC23A_HUMAN	Protein transport protein Sec23A	3	1	287.57	2.76E-05	18h	1.75
DCTP1_HUMAN	dCTP pyrophosphatase 1	2	2	118.78	2.77E-05	6h	27.20
DUT_HUMAN	Deoxyuridine 5'-triphosphate nucleotidohydrolase, mitochondrial	1	1	49.55	2.78E-05	18h	1.36
TELO2_HUMAN	Telomere length regulation protein TEL2 homolog	1	1	84.13	2.79E-05	6h	1.80
THTM_HUMAN	3-mercaptopyruvate sulfurtransferase	1	1	97.54	2.79E-05	18h	1.25
SPRE_HUMAN	Sepiapterin reductase	1	1	127.99	2.83E-05	18h	2.02
6PGD_HUMAN	6-phosphogluconate dehydrogenase, decarboxylating	10	9	686.63	2.91E-05	18h	1.09
PIMT_HUMAN	Protein-L-isoaspartate(D-aspartate) O-methyltransferase	1	1	70.21	2.91E-05	6h	1.25
SERC_HUMAN	Phosphoserine aminotransferase	6	6	337.3	2.96E-05	6h	1.13
TBB4B_HUMAN	Tubulin beta-4B chain	25	1	3040.99	3.19E-05	18h	1.16
EF1B_HUMAN	Elongation factor 1-beta	4	4	338.74	3.26E-05	18h	1.11
AIMP2_HUMAN	Aminoacyl tRNA synthase complex-interacting multifunctional protein 2	3	3	192.08	3.27E-05	6h	1.13
HPRT_HUMAN	Hypoxanthine-guanine phosphoribosyltransferase	5	4	309.3	3.31E-05	6h	1.14
CYFP2_HUMAN	Cytoplasmic FMR1-interacting protein 2	4	2	292.45	3.33E-05	18h	1.45
PSB7_HUMAN	Proteasome subunit beta type-7	1	1	78.48	3.34E-05	18h	1.28
SODC_HUMAN	Superoxide dismutase [Cu-Zn]	1	1	36.49	3.48E-05	18h	2.29
GFPT1_HUMAN	Glutamine--fructose-6-phosphate aminotransferase [isomerizing] 1	4	3	281.42	3.54E-05	18h	1.83
ARF4_HUMAN	ADP-ribosylation factor 4 O	4	2	295.41	3.63E-05	18h	1.27
GUAA_HUMAN	GMP synthase [glutamine-hydrolyzing]	1	1	60.18	4.06E-05	18h	1.39
ACOC_HUMAN	Cytoplasmic aconitate hydratase	3	3	236.44	4.15E-05	18h	1.50
1433T_HUMAN	14-3-3 protein theta	7	5	542.96	4.19E-05	18h	1.11
MOES_HUMAN	Moesin	31	24	2998.4	4.32E-05	6h	1.24
SYEP_HUMAN	Bifunctional glutamate/proline--tRNA ligase	1	1	106.13	4.32E-05	6h	1.24
S43A3_HUMAN	Solute carrier family 43 member 3	2	2	90.33	4.39E-05	6h	1.28

T cell early (6 h) versus late (18 h) ACdEV proteomes

Accession	Description	Peptide count	Unique peptides	Confidence score	Anova (p)	Highest mean condition	Max fold change
RS7_HUMAN	40S ribosomal protein S7	1	1	55.68	4.40E-05	6h	3.91
CLIC1_HUMAN	Chloride intracellular channel protein 1	3	3	272.72	4.48E-05	6h	1.15
MYO7B_HUMAN	Unconventional myosin-VIIb	1	1	75.99	4.68E-05	6h	1.66
STOM_HUMAN	Erythrocyte band 7 integral membrane protein	1	1	136.75	4.85E-05	6h	1.28
GRB2_HUMAN	Growth factor receptor-bound protein 2	1	1	38.73	4.93E-05	6h	1.60
THUM1_HUMAN	THUMP domain-containing protein 1	1	1	41.54	5.03E-05	6h	1.30
DIP2B_HUMAN	Disco-interacting protein 2 homolog B	7	6	472.39	5.08E-05	6h	1.14
DEN2D_HUMAN	DENN domain-containing protein 2D	1	1	94.35	5.23E-05	18h	1.24
DCTN3_HUMAN	Dynactin subunit 3	1	1	36.67	5.35E-05	6h	107.29
TPIS_HUMAN	Triosephosphate isomerase	7	7	467.54	5.58E-05	6h	1.12
DDX17_HUMAN	Probable ATP-dependent RNA helicase DDX17	8	5	486.5	5.84E-05	6h	1.16
FRIL_HUMAN	Ferritin light chain	1	1	80.22	5.92E-05	18h	1.37
RINI_HUMAN	Ribonuclease inhibitor	1	1	60.46	6.05E-05	18h	1.32
H11_HUMAN	Histone H1.1	1	1	69.26	6.08E-05	18h	1.35
EVL_HUMAN	Ena/VASP-like protein	1	1	48.88	6.14E-05	6h	5.32
ROA1_HUMAN	Heterogeneous nuclear ribonucleoprotein A1	9	2	952.95	6.62E-05	6h	1.62
RAB1B_HUMAN	Ras-related protein Rab-1B	7	1	447.34	6.69E-05	18h	1.96
FANCI_HUMAN	Fanconi anemia group I protein	2	1	109.98	7.20E-05	6h	1.47
MTA1_HUMAN	Metastasis-associated protein MTA1	2	1	124.9	7.30E-05	18h	2.40
REEP6_HUMAN	Receptor expression-enhancing protein 6	1	1	64.99	7.40E-05	18h	2.83
SF3A1_HUMAN	Splicing factor 3A subunit 1	4	4	158.72	7.47E-05	6h	1.41
AT1A1_HUMAN	Sodium/potassium-transporting ATPase subunit alpha-1	19	10	2003.87	7.72E-05	6h	1.16
KAD2_HUMAN	Adenylate kinase 2, mitochondrial	2	2	118.28	7.95E-05	6h	1.49
1433G_HUMAN	14-3-3 protein gamma	8	5	795.41	8.02E-05	18h	1.24
PSPC1_HUMAN	Paraspeckle component 1	1	1	42.14	8.05E-05	6h	1.20
VIME_HUMAN	Vimentin	14	11	1120.63	8.44E-05	6h	1.12
GCN1_HUMAN	eIF-2-alpha kinase activator GCN1	8	8	534.25	8.51E-05	6h	1.28
CCAR2_HUMAN	Cell cycle and apoptosis regulator protein 2	4	4	305.54	8.86E-05	6h	1.09
RL17_HUMAN	60S ribosomal protein L17	3	3	103.93	8.95E-05	6h	1.17
MCA3_HUMAN	Eukaryotic translation elongation factor 1 epsilon-1	5	5	415.09	9.33E-05	18h	1.25
PCNP_HUMAN	PEST proteolytic signal-containing nuclear protein	1	1	37.31	9.80E-05	6h	1.50
PPM1G_HUMAN	Protein phosphatase 1G	1	1	35.35	0.00010732	6h	1.30
THOC6_HUMAN	THO complex subunit 6 homolog	6	5	495.69	0.00011118	18h	1.22
PFKAP_HUMAN	ATP-dependent 6-phosphofructokinase, platelet type	8	6	467.03	0.00011151	6h	1.06
PSD13_HUMAN	26S proteasome non-ATPase regulatory subunit 13	8	8	485.87	0.00011283	18h	1.10
CAPZB_HUMAN	F-actin-capping protein subunit beta	6	6	555.21	0.00012192	18h	1.10
INP4A_HUMAN	Type I inositol 3,4-bisphosphate 4-phosphatase	1	1	72.04	0.00012374	18h	1.26
CMS1_HUMAN	Protein CMSS1	1	1	45.48	0.00012482	6h	2.38
UB2L3_HUMAN	Ubiquitin-conjugating enzyme E2 L3	1	1	83.39	0.00012958	18h	3.23
ERBIN_HUMAN	Erbin	2	2	159.17	0.0001303	6h	1.30
ALDOC_HUMAN	Fructose-bisphosphate aldolase C	3	3	272.59	0.00013137	18h	1.16
PP1G_HUMAN	Serine/threonine-protein phosphatase PP1-gamma catalytic subunit	6	1	435.99	0.00013181	18h	1.18
SF3A2_HUMAN	Splicing factor 3A subunit 2	2	2	83.55	0.00013605	6h	1.17

T cell early (6 h) versus late (18 h) ACdEV proteomes

Accession	Description	Peptide count	Unique peptides	Confidence score	Anova (p)	Highest mean condition	Max fold change
RSU1_HUMAN	Ras suppressor protein 1	1	1	31.41	0.000137 02	6h	1.38
PSN1_HUMAN	Presenilin-1	1	1	38.77	0.000141 72	6h	6.35
MYH9_HUMAN	Myosin-9	92	78	9633.61	0.000149 56	6h	1.05
NUP85_HUMAN	Nuclear pore complex protein Nup85	1	1	45.78	0.000149 79	18h	2.05
AP1G1_HUMAN	AP-1 complex subunit gamma-1	2	2	210.14	0.000157 21	18h	1.97
RAB21_HUMAN	Ras-related protein Rab-21	1	1	34.18	0.000157 93	18h	1.85
PP1B_HUMAN	Serine/threonine-protein phosphatase PP1-beta catalytic subunit	6	1	482.57	0.000161 83	18h	1.22
GNA13_HUMAN	Guanine nucleotide-binding protein subunit alpha-13	2	1	142.87	0.000163 41	6h	1.28
GNPI1_HUMAN	Glucosamine-6-phosphate isomerase 1	1	1	38.71	0.000166 14	6h	1.26
EIF3D_HUMAN	Eukaryotic translation initiation factor 3 subunit D	2	2	155.93	0.000167 27	18h	1.14
RL19_HUMAN	60S ribosomal protein L19	1	1	149.32	0.000176 35	18h	1.23
PANX1_HUMAN	Pannexin-1	1	1	58.66	0.000176 36	6h	1.42
RACK1_HUMAN	Receptor of activated protein C kinase 1	10	10	760.12	0.000177 38	18h	1.11
RB_HUMAN	Retinoblastoma-associated protein	1	1	38.26	0.000181 29	6h	1.45
CHSP1_HUMAN	Calcium-regulated heat-stable protein 1	1	1	66.04	0.000185 78	6h	1.73
SRPK1_HUMAN	SRSF protein kinase 1	1	1	34.77	0.000185 84	18h	1.27
ESYT1_HUMAN	Extended synaptotagmin-1	3	3	253.41	0.000188 33	6h	1.13
PSMD2_HUMAN	26S proteasome non-ATPase regulatory subunit 2	20	19	1794.52	0.000192 48	18h	1.19
FLNA_HUMAN	Filamin-A	5	4	322.29	0.000193 02	6h	1.10
TRBC1_HUMAN	T-cell receptor beta-1 chain C region	2	2	85.49	0.000194 13	6h	1.18
TBB2A_HUMAN	Tubulin beta-2A chain	21	1	2512.72	0.000195 05	6h	1.43
WDR61_HUMAN	WD repeat-containing protein 61	1	1	169.34	0.000196 52	18h	2.86
SEP11_HUMAN	Septin-11 O	4	1	203.97	0.000198 49	18h	1.79
HYES_HUMAN	Bifunctional epoxide hydrolase 2	2	2	268.07	0.000204 64	18h	1.83
PI4KA_HUMAN	Phosphatidylinositol 4-kinase alpha	3	2	132.98	0.000207 06	6h	2.04
OLA1_HUMAN	Obg-like ATPase 1	2	2	183.39	0.000210 6	18h	1.37
SRS10_HUMAN	Serine/arginine-rich splicing factor 10	1	1	57.25	0.000212 97	6h	1.62
SRSF6_HUMAN	Serine/arginine-rich splicing factor 6	2	1	106.66	0.000214 86	6h	1.42
COR1A_HUMAN	Coronin-1A	11	10	777.41	0.000216 47	18h	1.08
VINC_HUMAN	Vinculin	1	1	136.54	0.000225 92	18h	1.33
NACAM_HUMAN	Nascent polypeptide-associated complex subunit alpha, muscle-specific form	2	2	136.04	0.000227 35	6h	1.24
STAT3_HUMAN	Signal transducer and activator of transcription 3	1	1	31.28	0.000233 82	18h	3.13
1433Z_HUMAN	14-3-3 protein zeta/delta	8	5	887.42	0.000243 17	6h	1.08
IF5_HUMAN	Eukaryotic translation initiation factor 5	1	1	97.61	0.000248 31	6h	1.22
RAP2B_HUMAN	Ras-related protein Rap-2b	2	1	163.42	0.000260 45	6h	1.34
PFKAL_HUMAN	ATP-dependent 6-phosphofructokinase, liver type	3	1	189.16	0.000262 78	6h	1.12
NUDC_HUMAN	Nuclear migration protein nudC	2	2	112.07	0.000276 11	18h	1.34
PDS5B_HUMAN	Sister chromatid cohesion protein PDS5 homolog B	1	1	44.51	0.000277 8	18h	1.47
GLO2_HUMAN	Hydroxyacylglutathione hydrolase, mitochondrial	1	1	49.36	0.000302 63	6h	1.23
LCAP_HUMAN	Leucyl-cystinyl aminopeptidase	4	4	280.97	0.000315 67	18h	1.22

T cell early (6 h) versus late (18 h) ACdEV proteomes

Accession	Description	Peptide count	Unique peptides	Confidence score	Anova (p)	Highest mean condition	Max fold change
ANXA5_HUMAN	Annexin A5	10	9	848.32	0.000319 06	6h	1.12
FXR1_HUMAN	Fragile X mental retardation syndrome-related protein 1	1	1	39.15	0.000320 71	6h	2.61
NICA_HUMAN	Nicastrin	5	4	268.56	0.000325 14	6h	1.12
DYHC1_HUMAN	Cytoplasmic dynein 1 heavy chain 1	32	29	2121.89	0.000327 5	18h	1.07
COPG1_HUMAN	Coatomer subunit gamma-1	2	1	142.91	0.000339 56	18h	1.13
MCTS1_HUMAN	Malignant T-cell-amplified sequence 1	3	3	273.02	0.000344 17	18h	1.35
SF3B1_HUMAN	Splicing factor 3B subunit 1	15	15	1026.86	0.000356 28	18h	1.20
MYL6_HUMAN	Myosin light polypeptide 6	7	3	698.22	0.000372 82	6h	1.23
MCM3_HUMAN	DNA replication licensing factor MCM3	12	12	985.27	0.000374 65	6h	1.06
PP2AA_HUMAN	Serine/threonine-protein phosphatase 2A catalytic subunit alpha isoform	3	3	236.68	0.000375 99	6h	1.15
CD166_HUMAN	CD166 antigen	1	1	31.76	0.000377 5	6h	1.45
IF4A2_HUMAN	Eukaryotic initiation factor 4A-II	5	1	447.03	0.000382 79	18h	1.20
DRG1_HUMAN	Developmentally-regulated GTP-binding protein 1	1	1	59.89	0.000387 36	6h	1.35
ARP2_HUMAN	Actin-related protein 2	2	2	162.77	0.000397 19	18h	1.16
SNTB1_HUMAN	Beta-1-syntrophin	1	1	37.97	0.000408 1	6h	2.99
CSN8_HUMAN	COP9 signalosome complex subunit 8	2	2	131.43	0.000408 66	18h	1.34
GLYC_HUMAN	Serine hydroxymethyltransferase, cytosolic	1	1	69.09	0.000409 69	18h	1.13
GMFG_HUMAN	Glia maturation factor gamma	1	1	129.94	0.000432 45	6h	1.23
TSN7_HUMAN	Tetraspanin-7	2	2	127.1	0.000438 79	18h	1.11
CSK2B_HUMAN	Casein kinase II subunit beta	1	1	39.6	0.000457 37	6h	31.79
ELP3_HUMAN	Elongator complex protein 3	1	1	49.99	0.000457 57	18h	1.23
DDX23_HUMAN	Probable ATP-dependent RNA helicase DDX23	1	1	47.12	0.000460 09	18h	3.06
MOT1_HUMAN	Monocarboxylate transporter 1	6	6	386.05	0.000469 21	18h	1.08
EFHD1_HUMAN	EF-hand domain-containing protein D1	2	2	85.29	0.000471 84	6h	1.24
RLA0L_HUMAN	60S acidic ribosomal protein P0-like	4	2	274.03	0.000472 84	18h	1.17
KDM1A_HUMAN	Lysine-specific histone demethylase 1A	1	1	193.34	0.000473 16	18h	2.90
PP1R7_HUMAN	Protein phosphatase 1 regulatory subunit 7	1	1	78.7	0.000473 66	18h	1.26
CD82_HUMAN	CD82 antigen	1	1	116.58	0.000476 68	6h	1.66
ECM29_HUMAN	Proteasome-associated protein ECM29 homolog	2	2	136.93	0.000481 93	18h	2.33
TRRAP_HUMAN	Transformation/transcription domain-associated protein	1	1	50.81	0.000495 59	6h	1.10
PRDX6_HUMAN	Peroxiredoxin-6	3	3	203.48	0.000520 51	6h	1.17
TE2IP_HUMAN	Telomeric repeat-binding factor 2-interacting protein 1	1	1	57.35	0.000520 56	18h	1.71
DPYL2_HUMAN	Dihydropyrimidinase-related protein 2	6	5	355.55	0.000520 93	18h	1.17
CPNE3_HUMAN	Copine-3	1	1	73.12	0.000522 63	6h	1.17
ITK_HUMAN	Tyrosine-protein kinase ITK/TSK	1	1	103.33	0.000528 34	6h	1.16
TPM1_HUMAN	Tropomyosin alpha-1 chain	8	1	579.28	0.000550 7	18h	1.20
KAP0_HUMAN	cAMP-dependent protein kinase type I-alpha regulatory subunit	1	1	39.54	0.000567 84	6h	1.44
DKC1_HUMAN	H/ACA ribonucleoprotein complex subunit 4	2	2	136.58	0.000580 42	6h	1.24
PFD3_HUMAN	Prefoldin subunit 3	1	1	41.63	0.000597 04	18h	1.64
USO1_HUMAN	General vesicular transport factor p115	2	2	82.25	0.000647 27	18h	2.07

T cell early (6 h) versus late (18 h) ACdEV proteomes

Accession	Description	Peptide count	Unique peptides	Confidence score	Anova (p)	Highest mean condition	Max fold change
DCTN1_HUMAN	Dynactin subunit 1	4	4	381.44	0.000647 79	18h	1.24
IF5A1_HUMAN	Eukaryotic translation initiation factor 5A-1	3	1	201.87	0.000655 2	18h	1.30
NCKPL_HUMAN	Nck-associated protein 1-like	4	4	333.37	0.000722 88	18h	1.32
DIAP1_HUMAN	Protein diaphanous homolog 1	1	1	33.67	0.000730 62	18h	1.79
TXNL1_HUMAN	Thioredoxin-like protein 1	2	2	103	0.000742 56	6h	1.14
CPSF5_HUMAN	Cleavage and polyadenylation specificity factor subunit 5	2	2	171.71	0.000755	18h	1.49
XPO5_HUMAN	Exportin-5	2	2	195.99	0.000776 21	18h	1.19
RCC1_HUMAN	Regulator of chromosome condensation	1	1	58	0.000783 7	6h	1.19
HEXB_HUMAN	Beta-hexosaminidase subunit beta	1	1	58.71	0.000843 56	6h	1.13
PDC10_HUMAN	Programmed cell death protein 10	1	1	86.96	0.000847 82	6h	1.09
IMA3_HUMAN	Importin subunit alpha-3	1	1	139.65	0.000872 81	18h	1.38
CTR1_HUMAN	High affinity cationic amino acid transporter 1	2	1	137.73	0.000887 65	6h	1.26
PSB8_HUMAN	Proteasome subunit beta type-8	2	2	114.68	0.000893 48	18h	1.13
CPSF2_HUMAN	Cleavage and polyadenylation specificity factor subunit 2	1	1	86.25	0.000944 77	18h	2.39
SYK_HUMAN	Lysine--tRNA ligase	4	4	196.23	0.000975 63	18h	1.12
JAM3_HUMAN	Junctional adhesion molecule C	3	3	184.86	0.000993 77	6h	1.09
HS90B_HUMAN	Heat shock protein HSP 90-beta	51	14	5255.6	0.000994 7	18h	1.20
EHD1_HUMAN	EH domain-containing protein 1	4	3	282.67	0.001068 98	6h	1.12
AR6P1_HUMAN	ADP-ribosylation factor-like protein 6-interacting protein 1	1	1	66.25	0.001097 64	18h	2.91
BACH_HUMAN	Cytosolic acyl coenzyme A thioester hydrolase	6	6	381.54	0.001106 29	6h	1.12
THIC_HUMAN	Acetyl-CoA acetyltransferase, cytosolic	1	1	103.05	0.001192 75	18h	1.18
PP1A_HUMAN	Serine/threonine-protein phosphatase PP1-alpha catalytic subunit	6	2	447.69	0.001241 49	18h	1.09
PRS4_HUMAN	26S proteasome regulatory subunit 4	1	1	80.06	0.001248 44	6h	1.38
IF2G_HUMAN	Eukaryotic translation initiation factor 2 subunit 3	5	1	314.82	0.001281 25	6h	2.51
CGL_HUMAN	Cystathionine gamma-lyase	1	1	89.87	0.001310 9	18h	1.30
CN37_HUMAN	2',3'-cyclic-nucleotide 3'-phosphodiesterase	4	4	205.15	0.001322 54	6h	1.20
VPS52_HUMAN	Vacuolar protein sorting-associated protein 52 homolog	1	1	36.13	0.001338 41	6h	1.40
PAPS1_HUMAN	Bifunctional 3'-phosphoadenosine 5'-phosphosulfate synthase 1	1	1	132.02	0.001625 38	18h	1.95
ICLN_HUMAN	Methylosome subunit pICln	1	1	85.44	0.001638 72	18h	1.44
ELP1_HUMAN	Elongator complex protein 1	2	2	119.02	0.001658 36	18h	1.29
SORT_HUMAN	Sortilin	1	1	68.41	0.001679 48	18h	1.36
HDHD5_HUMAN	Haloacid dehalogenase-like hydrolase domain-containing 5	1	1	88.07	0.001728 64	6h	1.20
FKB15_HUMAN	FK506-binding protein 15	1	1	58.74	0.001740 48	6h	1.18
MDC1_HUMAN	Mediator of DNA damage checkpoint protein 1	1	1	68.11	0.001742 84	6h	1.51
FKB1A_HUMAN	Peptidyl-prolyl cis-trans isomerase FKBP1A	1	1	63.15	0.001927 78	18h	1.15
EXOC7_HUMAN	Exocyst complex component 7	1	1	37.94	0.001959 98	18h	2.97
PPID_HUMAN	Peptidyl-prolyl cis-trans isomerase D	2	1	95.25	0.001967 16	18h	1.18
VTNC_HUMAN	Vitronectin	1	1	78.27	0.002010 22	6h	1.17
TARB1_HUMAN	Probable methyltransferase TARBP1	2	2	114.93	0.002098 34	6h	1.79
S29A1_HUMAN	Equilibrative nucleoside transporter 1	4	4	281.62	0.002132 07	6h	1.12

T cell early (6 h) versus late (18 h) ACdEV proteomes

Accession	Description	Peptide count	Unique peptides	Confidence score	Anova (p)	Highest mean condition	Max fold change
RL36A_HUMAN	60S ribosomal protein L36a	1	1	74.18	0.002181 34	18h	1.29
BUB3_HUMAN	Mitotic checkpoint protein BUB3	4	4	180.67	0.002390 5	6h	1.12
IF4A1_HUMAN	Eukaryotic initiation factor 4A-I	14	10	1095.81	0.002436 29	18h	1.06
CDK2_HUMAN	Cyclin-dependent kinase 2	2	1	78.77	0.002478 59	6h	1.36
PLPHP_HUMAN	Pyridoxal phosphate homeostasis protein	3	3	170.71	0.002589 23	6h	1.25
SPA5L_HUMAN	Spermatogenesis-associated protein 5-like protein 1	2	1	90.86	0.002775 76	6h	1.21
PCH2_HUMAN	Pachytene checkpoint protein 2 homolog	1	1	43.5	0.002864 44	6h	2.15
EIF1A_HUMAN	Probable RNA-binding protein EIF1AD	1	1	61.85	0.003007 85	18h	2.45
DCXR_HUMAN	L-xylulose reductase	1	1	57.21	0.003018 53	18h	1.89
POGZ_HUMAN	Pogo transposable element with ZNF domain	1	1	34.06	0.003134 9	18h	8.75
NEK9_HUMAN	Serine/threonine-protein kinase Nek9	1	1	51.52	0.003204 97	18h	1.13
COPB2_HUMAN	Coatomer subunit beta'	5	5	297.59	0.003226 52	18h	1.13
1433B_HUMAN	14-3-3 protein beta/alpha	4	2	318.72	0.003380 85	18h	1.17
HPCL1_HUMAN	Hippocalcin-like protein 1	1	1	46.49	0.003499 43	18h	1.17
GOGA3_HUMAN	Golgin subfamily A member 3	1	1	36.4	0.003623 51	18h	1.16
COPD_HUMAN	Coatomer subunit delta	1	1	58.56	0.003699 76	6h	1.17
RPIA_HUMAN	Ribose-5-phosphate isomerase	1	1	133.57	0.003716 02	6h	1.10
APC1_HUMAN	Anaphase-promoting complex subunit 1	1	1	31.69	0.003864 08	18h	1.19
MYO1B_HUMAN	Unconventional myosin-Ib	7	3	434.61	0.004010 92	6h	1.18
RNH2A_HUMAN	Ribonuclease H2 subunit A	1	1	42.89	0.004035 04	18h	2.16
ARPC3_HUMAN	Actin-related protein 2/3 complex subunit 3	4	4	243.87	0.004037 76	18h	1.05
RB11A_HUMAN	Ras-related protein Rab-11A	5	1	393.11	0.004264 7	6h	4.02
CDK1_HUMAN	Cyclin-dependent kinase 1	3	3	120.92	0.004354 66	6h	1.16
DYH9_HUMAN	Dynein heavy chain 9, axonemal	1	1	34.26	0.004425 62	18h	1.29
SMD1_HUMAN	Small nuclear ribonucleoprotein Sm D1	2	2	292.4	0.004566 79	18h	1.19
RAC3_HUMAN	Ras-related C3 botulinum toxin substrate 3	3	1	141.47	0.004588 06	18h	1.15
HS2ST_HUMAN	Heparan sulfate 2-O-sulfotransferase 1	1	1	56.04	0.004613 99	18h	1.69
PLSI_HUMAN	Plastin-1	2	1	114.68	0.004712 76	6h	1.35
PSD11_HUMAN	26S proteasome non-ATPase regulatory subunit 11	6	5	333.62	0.004732 94	18h	1.06
PRAF2_HUMAN	PRA1 family protein 2	1	1	84.51	0.004790 69	6h	1.14
AP2A1_HUMAN	AP-2 complex subunit alpha-1	2	1	97.52	0.004826 26	6h	1.42
TRXR1_HUMAN	Thioredoxin reductase 1, cytoplasmic	2	2	108.66	0.004861 77	18h	1.17
CUL1_HUMAN	Cullin-1	1	1	57.97	0.004971 77	18h	11.14
PFD2_HUMAN	Prefoldin subunit 2	3	3	216.76	0.005049 69	6h	1.10
SYLC_HUMAN	Leucine--tRNA ligase, cytoplasmic	4	4	261.75	0.005318 56	18h	1.03
SYNC_HUMAN	Asparagine--tRNA ligase, cytoplasmic	2	2	115.06	0.005464 51	6h	1.11
CYFP1_HUMAN	Cytoplasmic FMR1-interacting protein 1	3	2	240.47	0.005679 16	18h	1.07
PPP6_HUMAN	Serine/threonine-protein phosphatase 6 catalytic subunit	3	3	154.9	0.005733 46	6h	1.13
SYWC_HUMAN	Tryptophan--tRNA ligase, cytoplasmic	3	3	221.28	0.006003 37	6h	1.10
CG050_HUMAN	Uncharacterized protein C7orf50	1	1	33.01	0.006198 23	6h	1.95

T cell early (6 h) versus late (18 h) ACdEV proteomes

Accession	Description	Peptide count	Unique peptides	Confidence score	Anova (p)	Highest mean condition	Max fold change
PRS10_HUMAN	26S proteasome regulatory subunit 10B	5	5	359.97	0.0064014	6h	1.07
PPCE_HUMAN	Prolyl endopeptidase	1	1	71.18	0.00645612	6h	1.22
RS25_HUMAN	40S ribosomal protein S25	2	2	124.29	0.00655528	6h	1.07
SYFB_HUMAN	Phenylalanine--tRNA ligase beta subunit	4	3	152.51	0.00666011	6h	1.27
ARL1_HUMAN	ADP-ribosylation factor-like protein 1	1	1	92.5	0.00674634	18h	2.59
NPTN_HUMAN	Neuroplastin	1	1	108.31	0.0071656	6h	1.11
RHOA_HUMAN	Transforming protein RhoA	3	2	161.36	0.00734911	6h	1.08
CBX1_HUMAN	Chromobox protein homolog 1	1	1	73.88	0.00761919	6h	1.05
VN1R5_HUMAN	Vomeronasal type-1 receptor 5	1	1	32.13	0.00770993	6h	1.12
MD2L1_HUMAN	Mitotic spindle assembly checkpoint protein MAD2A	1	1	72.47	0.00804533	6h	3.86
IF4G1_HUMAN	Eukaryotic translation initiation factor 4 gamma 1	1	1	61.04	0.00816672	6h	1.39
CNTRL_HUMAN	Centriolin	1	1	32.02	0.00831303	18h	1.30
NONO_HUMAN	Non-POU domain-containing octamer-binding protein	3	3	276.44	0.00833423	18h	1.21
PDCD5_HUMAN	Programmed cell death protein 5	2	2	138.23	0.00841727	6h	1.09
AP3D1_HUMAN	AP-3 complex subunit delta-1	1	1	33.62	0.00868221	6h	1.21
NHLC1_HUMAN	E3 ubiquitin-protein ligase NHLRC1	1	1	38.95	0.00875985	6h	1.82
TYSY_HUMAN	Thymidylate synthase	1	1	53.89	0.00896941	18h	1.10
RD23A_HUMAN	UV excision repair protein RAD23 homolog A	1	1	50.35	0.00924965	18h	1.22
DDX1_HUMAN	ATP-dependent RNA helicase DDX1	1	1	137.2	0.00958692	6h	1.28
FNTA_HUMAN	Protein farnesyltransferase/geranylgeranyltransferase type-1 subunit alpha	1	1	147.79	0.01016874	18h	1.20
TCTP_HUMAN	Translationally-controlled tumor protein	1	1	37.69	0.0102389	6h	1.36
TBCD_HUMAN	Tubulin-specific chaperone D	4	3	410.16	0.01036145	18h	1.53
ARP3_HUMAN	Actin-related protein 3	5	3	352.42	0.01039201	18h	1.09
P4R3A_HUMAN	Serine/threonine-protein phosphatase 4 regulatory subunit 3A	1	1	37.56	0.01056923	6h	1.18
SERA_HUMAN	D-3-phosphoglycerate dehydrogenase	8	7	596.01	0.01076373	18h	1.02
LGUL_HUMAN	Lactoylglutathione lyase	1	1	35.14	0.01077988	18h	1.46
LAMP2_HUMAN	Lysosome-associated membrane glycoprotein 2	1	1	55.97	0.01106291	6h	1.07
BID_HUMAN	BH3-interacting domain death agonist	1	1	178.64	0.01158362	18h	2.78
HNRPD_HUMAN	Heterogeneous nuclear ribonucleoprotein D0	3	2	218.37	0.01204153	6h	1.05
SET_HUMAN	Protein SET	5	1	370.43	0.01270254	6h	5.22
ZZEF1_HUMAN	Zinc finger ZZ-type and EF-hand domain-containing protein 1	1	1	69.06	0.0135085	18h	1.28
DHX15_HUMAN	Pre-mRNA-splicing factor ATP-dependent RNA helicase DHX15	9	8	510.59	0.01356543	6h	1.09
WDR82_HUMAN	WD repeat-containing protein 82	2	1	141.88	0.01366544	18h	1.08
LIN7A_HUMAN	Protein lin-7 homolog A	1	1	91.5	0.01491981	18h	1.71
GBB4_HUMAN	Guanine nucleotide-binding protein subunit beta-4	3	1	209.88	0.01493619	6h	1.10
RAB10_HUMAN	Ras-related protein Rab-10	4	2	237.59	0.01536505	18h	1.17
ANO6_HUMAN	Anoctamin-6	2	2	100.83	0.01554412	18h	1.06
PRPS1_HUMAN	Ribose-phosphate pyrophosphokinase 1	6	3	599.15	0.01595942	18h	1.06
SYTC_HUMAN	Threonine--tRNA ligase, cytoplasmic	9	7	537.04	0.0167293	6h	1.04

T cell early (6 h) versus late (18 h) ACdEV proteomes

Accession	Description	Peptide count	Unique peptides	Confidence score	Anova (p)	Highest mean condition	Max fold change
SAP18_HUMAN	Histone deacetylase complex subunit SAP18	1	1	112.95	0.016935 36	18h	1.55
EXOS7_HUMAN	Exosome complex component RRP42	1	1	62.17	0.018203 78	18h	1.09
ETFA_HUMAN	Electron transfer flavoprotein subunit alpha, mitochondrial	1	1	48.46	0.018634 27	18h	1.12
ACAP1_HUMAN	Arf-GAP with coiled-coil, ANK repeat and PH domain-containing protein 1	1	1	57.27	0.018681 42	18h	3.05
PDXK_HUMAN	Pyridoxal kinase	1	1	37.8	0.019196 51	6h	1.23
LAGE3_HUMAN	EKC/KEOPS complex subunit LAGE3	1	1	51.85	0.019486 56	18h	1.10
NOP56_HUMAN	Nucleolar protein 56	1	1	51.1	0.020698 56	18h	1.64
WASC4_HUMAN	WASH complex subunit 4	1	1	53.64	0.020816 07	6h	1.25
VAV_HUMAN	Proto-oncogene vav	1	1	34.28	0.021283 15	6h	7.85
SPTC1_HUMAN	Serine palmitoyltransferase 1	1	1	64.27	0.022120 86	6h	1.21
RL14_HUMAN	60S ribosomal protein L14	1	1	61.43	0.022311 87	6h	1.33
FPPS_HUMAN	Farnesyl pyrophosphate synthase	1	1	53.69	0.022335 45	18h	1.30
SYPL1_HUMAN	Synaptophysin-like protein 1	1	1	50.18	0.024881 76	6h	1.09
SMC1A_HUMAN	Structural maintenance of chromosomes protein 1A	4	4	276.25	0.024941 37	18h	1.10
SRC_HUMAN	Proto-oncogene tyrosine-protein kinase Src	2	1	120.64	0.026138 97	18h	1.08
BZW2_HUMAN	Basic leucine zipper and W2 domain-containing protein 2	2	2	230.63	0.027537 07	18h	1.11
CDC37_HUMAN	Hsp90 co-chaperone Cdc37	3	3	254.85	0.027816 96	18h	1.09
ACL6A_HUMAN	Actin-like protein 6A	2	2	119.16	0.028488 4	6h	1.04
ACPH_HUMAN	Acylamino-acid-releasing enzyme	1	1	77.05	0.028496 75	18h	1.07
SDHA_HUMAN	Succinate dehydrogenase [ubiquinone] flavoprotein subunit, mitochondrial	1	1	111.23	0.029103 65	6h	1.15
DBLOH_HUMAN	Diablo homolog, mitochondrial	1	1	56.77	0.029549 11	18h	2.25
PSME1_HUMAN	Proteasome activator complex subunit 1	2	2	98.11	0.029973 92	6h	1.12
HNRPL_HUMAN	Heterogeneous nuclear ribonucleoprotein L	5	5	274.11	0.030269 56	6h	1.11
PDC6I_HUMAN	Programmed cell death 6-interacting protein	10	10	671.55	0.030498 37	6h	1.03
GNAO_HUMAN	Guanine nucleotide-binding protein G(o) subunit alpha	2	1	179.62	0.030652 78	6h	1.35
SRSF3_HUMAN	Serine/arginine-rich splicing factor 3	1	1	41.13	0.032914 85	6h	1.05
GSTO1_HUMAN	Glutathione S-transferase omega-1	2	2	105.46	0.033763 17	6h	1.05
CBPD_HUMAN	Carboxypeptidase D	1	1	31.53	0.034427 28	6h	2.50
SYMC_HUMAN	Methionine--tRNA ligase, cytoplasmic	7	6	466.8	0.035769 92	6h	1.05
ISOC1_HUMAN	Isochorismatase domain-containing protein 1	1	1	160.33	0.037804 63	6h	1.18
SATT_HUMAN	Neutral amino acid transporter A	3	2	231.61	0.037984 26	6h	1.07
ENOG_HUMAN	Gamma-enolase	5	3	515.56	0.039827 05	18h	1.05
SHPK_HUMAN	Sedoheptulokinase	1	1	44.39	0.042227 95	18h	1.43
GLCNE_HUMAN	Bifunctional UDP-N-acetylglucosamine 2-epimerase/N-acetylmannosamine kinase	1	1	41.29	0.043000 37	18h	1.43
UBR4_HUMAN	E3 ubiquitin-protein ligase UBR4	9	9	731.98	0.043560 41	6h	1.12
RRBP1_HUMAN	Ribosome-binding protein 1	2	2	89.64	0.045131 89	18h	2.90
RO60_HUMAN	60 kDa SS-A/Ro ribonucleoprotein	2	2	158.62	0.046794 28	18h	1.05
1433F_HUMAN	14-3-3 protein eta	4	2	314.08	0.047079 52	18h	1.09
PFD4_HUMAN	Prefoldin subunit 4	1	1	72.05	0.048490 61	6h	1.24
TBG1_HUMAN	Tubulin gamma-1 chain	2	2	163.55	0.048781 47	18h	1.12

T cell early (6 h) versus late (18 h) ACdEV proteomes

Accession	Description	Peptide count	Unique peptides	Confidence score	Anova (p)	Highest mean condition	Max fold change
ITB1_HUMAN	Integrin beta-1	7	6	608.72	0.056416 39	18h	1.03
PRDX5_HUMAN	Peroxiredoxin-5, mitochondrial	3	3	130.92	0.058705 53	18h	1.07
ITA4_HUMAN	Integrin alpha-4	6	6	372.96	0.060750 5	6h	1.04
PSME3_HUMAN	Proteasome activator complex subunit 3	2	2	182.6	0.061007 97	18h	1.05
H15_HUMAN	Histone H1.5	1	1	63.64	0.061207 91	18h	1.38
BTF3_HUMAN	Transcription factor BTF3	1	1	67.26	0.062237 58	6h	1.23
NOLC1_HUMAN	Nucleolar and coiled-body phosphoprotein 1	2	2	82.25	0.064741 78	18h	1.14
RFC2_HUMAN	Replication factor C subunit 2	1	1	195.55	0.065403 45	6h	1.14
GNA1_HUMAN	Glucosamine 6-phosphate N-acetyltransferase	1	1	51.7	0.066776 63	18h	1.25
ELP5_HUMAN	Elongator complex protein 5	1	1	58.5	0.068096 84	18h	1.26
ABCAD_HUMAN	ATP-binding cassette sub-family A member 13	1	1	39.37	0.068487 24	6h	1.51
CELF1_HUMAN	CUGBP Elav-like family member 1	1	1	46.24	0.070057 61	6h	1.15
PGM1_HUMAN	Phosphoglucomutase-1	1	1	87.67	0.076931 4	6h	1.15
GSTM1_HUMAN	Glutathione S-transferase Mu 1	1	1	38.42	0.077313 48	18h	1.09
UBC9_HUMAN	SUMO-conjugating enzyme UBC9	1	1	37.05	0.083515 03	6h	1.08
PI42A_HUMAN	Phosphatidylinositol 5-phosphate 4-kinase type-2 alpha	2	1	97.37	0.090477 25	6h	1.22
DNJB1_HUMAN	DnaJ homolog subfamily B member 1	1	1	32.62	0.095292 29	6h	1.05
CAPG_HUMAN	Macrophage-capping protein	1	1	64.13	0.095668 67	6h	1.04
PLCG1_HUMAN	1-phosphatidylinositol 4,5-bisphosphate phosphodiesterase gamma-1	1	1	57.27	0.097761 35	18h	1.09
ARL8A_HUMAN	ADP-ribosylation factor-like protein 8A	1	1	33.85	0.107938 04	6h	1.04
M4K4_HUMAN	Mitogen-activated protein kinase kinase kinase kinase 4	2	1	103.96	0.110273 19	6h	1.20
MRP_HUMAN	MARCKS-related protein	1	1	114.27	0.120995 09	18h	1.30
STX11_HUMAN	Syntaxin-11	1	1	33.15	0.128054 73	6h	1.17
AT2B4_HUMAN	Plasma membrane calcium-transporting ATPase 4	9	3	642.04	0.131126 66	6h	1.04
PPM1F_HUMAN	Protein phosphatase 1F	1	1	64.85	0.139207 15	18h	1.07
DNJA1_HUMAN	DnaJ homolog subfamily A member 1	2	2	200.84	0.142938 43	18h	1.05
SYVC_HUMAN	Valine--tRNA ligase	3	3	234.68	0.143924 61	18h	1.08
GSTM3_HUMAN	Glutathione S-transferase Mu 3	1	1	169.47	0.144258 73	18h	1.17
KHDR1_HUMAN	KH domain-containing, RNA-binding, signal transduction-associated protein 1	1	1	40.13	0.148446 44	6h	1.25
PABP1_HUMAN	Polyadenylate-binding protein 1	6	1	359.86	0.154957 41	18h	1.03
DCTN2_HUMAN	Dynactin subunit 2	6	5	389.23	0.159567 08	18h	1.02
SORCN_HUMAN	Sorcin	1	1	34.8	0.161979 9	6h	1.10
MOT4_HUMAN	Monocarboxylate transporter 4	1	1	65.97	0.162497 75	18h	1.65
RFC3_HUMAN	Replication factor C subunit 3	1	1	42.53	0.172838 74	18h	1.51
ENOA_HUMAN	Alpha-enolase	26	21	2698.68	0.186973 08	6h	1.01
PRDX2_HUMAN	Peroxiredoxin-2	6	5	622.09	0.201266 54	18h	1.02
CIP2A_HUMAN	Protein CIP2A	1	1	34.76	0.201816 68	18h	1.15
CTL1_HUMAN	Choline transporter-like protein 1	1	1	40.21	0.206143 48	18h	1.05
RS12_HUMAN	40S ribosomal protein S12	2	2	152.4	0.210895 86	6h	1.18
COG7_HUMAN	Conserved oligomeric Golgi complex subunit 7	1	1	63.47	0.211627 23	18h	1.18

T cell early (6 h) versus late (18 h) ACdEV proteomes

Accession	Description	Peptide count	Unique peptides	Confidence score	Anova (p)	Highest mean condition	Max fold change
PSMD1_HUMAN	26S proteasome non-ATPase regulatory subunit 1	11	11	758.14	0.21267401	6h	1.02
COF1_HUMAN	Cofilin-1	6	3	414.77	0.21322225	6h	1.05
ADA_HUMAN	Adenosine deaminase	6	6	335.91	0.2215659	18h	1.03
RUVB1_HUMAN	RuvB-like 1	9	9	574.68	0.22395724	18h	1.02
PSA_HUMAN	Puromycin-sensitive aminopeptidase	1	1	52.91	0.22630949	6h	1.13
MY18A_HUMAN	Unconventional myosin-XVIIIa	3	3	188.87	0.22776379	18h	1.02
NTPCR_HUMAN	Cancer-related nucleoside-triphosphatase	1	1	44.94	0.23441143	18h	1.15
IPO4_HUMAN	Importin-4	6	6	621.48	0.23846281	18h	1.02
PSME2_HUMAN	Proteasome activator complex subunit 2	2	2	172.95	0.23886608	18h	1.06
ALDR_HUMAN	Aldose reductase	1	1	80.65	0.25363626	18h	1.02
ESYT2_HUMAN	Extended synaptotagmin-2	2	1	109.83	0.26925857	6h	2.37
ASF1B_HUMAN	Histone chaperone ASF1B	1	1	35.55	0.26977866	18h	1.07
RS27A_HUMAN	Ubiquitin-40S ribosomal protein S27a	5	5	334.38	0.27545194	6h	1.01
DOCK7_HUMAN	Dedicator of cytokinesis protein 7	1	1	61.2	0.28634803	18h	1.14
IF6_HUMAN	Eukaryotic translation initiation factor 6	2	2	89.52	0.28828421	18h	1.02
RUVB2_HUMAN	RuvB-like 2	7	7	530.95	0.30907725	6h	1.01
SYDC_HUMAN	Aspartate--tRNA ligase, cytoplasmic	10	10	728.31	0.31244621	6h	1.01
MDHC_HUMAN	Malate dehydrogenase, cytoplasmic	3	3	150.02	0.33473335	6h	1.02
RTN3_HUMAN	Reticulon-3	1	1	47.58	0.33748032	6h	1.03
FUBP1_HUMAN	Far upstream element-binding protein 1	1	1	52.83	0.34308306	6h	1.04
UN45A_HUMAN	Protein unc-45 homolog A	1	1	51.26	0.34913786	6h	1.24
HDHD2_HUMAN	Haloacid dehalogenase-like hydrolase domain-containing protein 2	1	1	80.03	0.35312226	18h	1.03
PGAM1_HUMAN	Phosphoglycerate mutase 1	9	5	710.01	0.35535221	18h	1.02
VAMP1_HUMAN	Vesicle-associated membrane protein 1	1	1	51.57	0.35811766	6h	1.06
NDKA_HUMAN	Nucleoside diphosphate kinase A	5	2	322.51	0.39625996	18h	1.09
TIGAR_HUMAN	Fructose-2,6-bisphosphatase TIGAR	1	1	40.22	0.39776231	6h	1.06
CXCR4_HUMAN	C-X-C chemokine receptor type 4	2	2	167.54	0.41585496	18h	1.05
CA050_HUMAN	Uncharacterized protein C1orf50	1	1	65.56	0.44838892	18h	1.06
PSMD8_HUMAN	26S proteasome non-ATPase regulatory subunit 8	5	5	218.72	0.472995	18h	1.01
ARPC2_HUMAN	Actin-related protein 2/3 complex subunit 2	6	5	374.89	0.48955604	6h	1.02
PA1B2_HUMAN	Platelet-activating factor acetylhydrolase IB subunit beta	2	2	127.14	0.50192007	18h	1.02
RPAB3_HUMAN	DNA-directed RNA polymerases I, II, and III subunit RPABC3	1	1	41.06	0.50416781	6h	1.04
MPPA_HUMAN	Mitochondrial-processing peptidase subunit alpha	1	1	230.59	0.52284466	18h	1.11
XPP1_HUMAN	Xaa-Pro aminopeptidase 1	1	1	43.63	0.52833972	18h	1.04
TF3C4_HUMAN	General transcription factor 3C polypeptide 4	1	1	49.28	0.53134727	6h	1.04
PECA1_HUMAN	Platelet endothelial cell adhesion molecule	1	1	73.26	0.55184943	18h	1.02
ANXA2_HUMAN	Annexin A2	8	3	575.01	0.58174797	6h	1.01
MAP1S_HUMAN	Microtubule-associated protein 1S	1	1	48.35	0.58198366	18h	1.06
PFD5_HUMAN	Prefoldin subunit 5	1	1	131.76	0.60711901	6h	1.03
RAP2C_HUMAN	Ras-related protein Rap-2c	2	1	212.78	0.61389742	6h	1.03

T cell early (6 h) versus late (18 h) ACdEV proteomes

Accession	Description	Peptide count	Unique peptides	Confidence score	Anova (p)	Highest mean condition	Max fold change
SYFA_HUMAN	Phenylalanine--tRNA ligase alpha subunit	3	3	170.98	0.646343 07	6h	1.01
2A5E_HUMAN	Serine/threonine-protein phosphatase 2A 56 kDa regulatory subunit epsilon isoform	1	1	82.27	0.664890 69	18h	1.01
PDIA4_HUMAN	Protein disulfide-isomerase A4	2	2	111.55	0.668490 32	6h	1.99
HUWE1_HUMAN	E3 ubiquitin-protein ligase HUWE1	6	6	336.95	0.673783 98	18h	1.01
PRS6A_HUMAN	26S proteasome regulatory subunit 6A	3	3	337.09	0.697152 71	18h	1.01
RS10_HUMAN	40S ribosomal protein S10	1	1	55.76	0.697344 17	6h	1.09
1433E_HUMAN	14-3-3 protein epsilon	9	7	864.79	0.706017 98	6h	1.01
DPY30_HUMAN	Protein dpy-30 homolog	1	1	33.06	0.709476 54	18h	1.05
CNDP2_HUMAN	Cytosolic non-specific dipeptidase	2	2	78.51	0.711799 67	18h	1.01
CHMP5_HUMAN	Charged multivesicular body protein 5	1	1	137.72	0.712460 02	18h	1.02
LC7L3_HUMAN	Luc7-like protein 3	1	1	62.91	0.769958 98	18h	1.02
PSMD5_HUMAN	26S proteasome non-ATPase regulatory subunit 5	3	2	245.26	0.805027 06	18h	1.01
PURA2_HUMAN	Adenylosuccinate synthetase isozyme 2	1	1	68.71	0.806141 06	18h	1.01
CNO11_HUMAN	CCR4-NOT transcription complex subunit 11	1	1	77.89	0.817052 34	18h	1.02
DOC10_HUMAN	Dedicator of cytokinesis protein 10	1	1	78.22	0.871000 4	6h	1.01
AAKG1_HUMAN	5'-AMP-activated protein kinase subunit gamma-1	1	1	113.74	0.875188 79	6h	1.02
DDX5_HUMAN	Probable ATP-dependent RNA helicase DDX5	5	2	326.99	0.882448 39	6h	1.00
DHSO_HUMAN	Sorbitol dehydrogenase	2	2	130.42	0.882510 78	6h	1.00
AP2B1_HUMAN	AP-2 complex subunit beta	5	3	454.8	0.906414 62	18h	1.00
LAMP1_HUMAN	Lysosome-associated membrane glycoprotein 1	1	1	110.65	0.950087 91	6h	1.01
ICAM3_HUMAN	Intercellular adhesion molecule 3	3	3	177.69	0.974687 83	6h	1.00
SMRC1_HUMAN	SWI/SNF complex subunit SMARCC1	1	1	43.56	0.980080 81	18h	1.02

Table 2: Monocyte early (6 h) versus late (18 h) ACdEV proteomes

Accession	Description	Peptide count	Unique peptides	Confidence score	Anova (p)	Highest mean condition	Max fold change
TPPC5_HUMAN	Trafficking protein particle complex subunit 5	1	1	39.1	0	18h	Infinity
URP2_HUMAN	Fermitin family homolog 3	14	13	945.38	7.77E-16	18h	2.24
AMPN_HUMAN	Aminopeptidase N	39	37	3569.92	2.66E-15	18h	7.43
MOES_HUMAN	Moesin	33	24	3554.62	9.66E-15	6h	2.39
TLN1_HUMAN	Talin-1	40	35	3376.68	1.03E-14	18h	5.27
FAS_HUMAN	Fatty acid synthase	44	42	3681.5	1.49E-14	18h	7.19
PLSL_HUMAN	Plastin-2	32	26	2984.16	1.53E-14	6h	1.88
SAP18_HUMAN	Histone deacetylase complex subunit SAP18	1	1	52.75	2.33E-14	18h	3109.19
ANXA4_HUMAN	Annexin A4	20	16	1793.95	2.80E-14	6h	1.79
ACLY_HUMAN	ATP-citrate synthase	17	14	1362.15	3.83E-14	18h	3.05
CLH1_HUMAN	Clathrin heavy chain 1	45	33	4030.95	4.88E-14	18h	7.61
BIP_HUMAN	Endoplasmic reticulum chaperone BiP	24	21	2243.26	6.07E-14	6h	2.49
PTPRC_HUMAN	Receptor-type tyrosine-protein phosphatase C	20	19	1581.81	7.52E-14	18h	5.74
CKAP5_HUMAN	Cytoskeleton-associated protein 5	1	1	57.32	7.68E-14	6h	13.60
ITAL_HUMAN	Integrin alpha-L	17	17	1559.38	8.09E-14	18h	9.32
CATG_HUMAN	Cathepsin G	4	4	335.66	8.23E-14	18h	3.19
LAMP2_HUMAN	Lysosome-associated membrane glycoprotein 2	2	2	93.01	9.60E-14	18h	4.06
DOC10_HUMAN	Dedicator of cytokinesis protein 10	2	2	99.21	1.04E-13	18h	2.33
CAND1_HUMAN	Cullin-associated NEDD8-dissociated protein 1	8	8	553.42	1.72E-13	18h	32.42
RALB_HUMAN	Ras-related protein Ral-B	6	2	310.65	2.03E-13	18h	3.91
STX4_HUMAN	Syntaxin-4	4	4	362.4	4.78E-13	18h	2.17
ITB1_HUMAN	Integrin beta-1	7	7	424.06	4.98E-13	18h	5.51
ANO6_HUMAN	Anoctamin-6	8	7	494.07	5.22E-13	18h	5.95
AAAT_HUMAN	Neutral amino acid transporter B(0)	11	11	811.15	5.80E-13	6h	1.61
RD23B_HUMAN	UV excision repair protein RAD23 homolog B	1	1	63.81	7.19E-13	6h	Infinity
STMN1_HUMAN	Stathmin	5	3	262.52	7.46E-13	18h	2.71
HBA_HUMAN	Hemoglobin subunit alpha	2	2	110.32	8.54E-13	18h	4.45
CATZ_HUMAN	Cathepsin Z	2	2	93.19	9.84E-13	18h	4.08
FLVC1_HUMAN	Feline leukemia virus subgroup C receptor-related protein 1	1	1	104.27	1.07E-12	6h	3.40
PROF1_HUMAN	Profilin-1	6	5	396.53	1.14E-12	6h	2.50
CATA_HUMAN	Catalase	14	14	1439.83	2.06E-12	6h	1.94
CD276_HUMAN	CD276 antigen	1	1	91.77	2.26E-12	18h	1.64
DDB1_HUMAN	DNA damage-binding protein 1	9	8	558.09	2.74E-12	18h	4.98
TPP2_HUMAN	Tripeptidyl-peptidase 2	15	15	1040.82	3.27E-12	18h	2.99
SPTN1_HUMAN	Spectrin alpha chain, non-erythrocytic 1	13	11	804.89	3.76E-12	18h	4.97
KPYM_HUMAN	Pyruvate kinase PKM	24	23	2523.67	4.31E-12	6h	1.63
NICA_HUMAN	Nicastrin	6	5	384.43	4.40E-12	18h	9.59
MYH9_HUMAN	Myosin-9	65	54	6349.84	4.88E-12	18h	1.76
MARE1_HUMAN	Microtubule-associated protein RP/EB family member 1	1	1	84.63	5.24E-12	18h	9.14
TECR_HUMAN	Very-long-chain enoyl-CoA reductase	2	2	87.25	5.81E-12	18h	2.05
AP1G1_HUMAN	AP-1 complex subunit gamma-1	5	4	311.19	6.18E-12	6h	2.26

Monocyte early (6 h) versus late (18 h) ACdEV proteomes

Accession	Description	Peptide count	Unique peptides	Confidence score	Anova (p)	Highest mean condition	Max fold change
ARPC3_HUMAN	Actin-related protein 2/3 complex subunit 3	8	8	448.9	6.61E-12	18h	1.79
RHOG_HUMAN	Rho-related GTP-binding protein RhoG	6	6	607.76	7.33E-12	18h	2.29
RLA0_HUMAN	60S acidic ribosomal protein P0	7	3	396.14	8.19E-12	18h	2.81
MVP_HUMAN	Major vault protein	16	14	1057.57	8.90E-12	18h	5.31
DPYL2_HUMAN	Dihydropyrimidinase-related protein 2	8	6	595.17	9.49E-12	6h	3.34
E41L2_HUMAN	Band 4.1-like protein 2	4	4	280.01	9.49E-12	6h	1.98
PUR9_HUMAN	Bifunctional purine biosynthesis protein PURH	7	6	460.68	9.81E-12	6h	1.52
STOM_HUMAN	Erythrocyte band 7 integral membrane protein	10	9	749.34	1.01E-11	18h	1.39
DNJC5_HUMAN	DnaJ homolog subfamily C member 5	1	1	198.71	1.09E-11	18h	4.77
GDIR2_HUMAN	Rho GDP-dissociation inhibitor 2	9	9	708.55	1.65E-11	18h	1.90
CD97_HUMAN	CD97 antigen	8	7	745.44	1.84E-11	6h	2.24
ITAM_HUMAN	Integrin alpha-M	11	10	906.74	1.86E-11	18h	4.05
HSP7C_HUMAN	Heat shock cognate 71 kDa protein	35	23	4051.86	2.03E-11	6h	1.73
UBA1_HUMAN	Ubiquitin-like modifier-activating enzyme 1	19	19	1727.03	2.06E-11	18h	2.88
HSPB1_HUMAN	Heat shock protein beta-1	4	4	413.7	2.07E-11	18h	1.82
GDIR1_HUMAN	Rho GDP-dissociation inhibitor 1	3	3	295.12	2.08E-11	18h	1.45
HS90B_HUMAN	Heat shock protein HSP 90-beta	37	11	3869.35	2.42E-11	6h	1.76
ACTN4_HUMAN	Alpha-actinin-4	35	24	3065.55	2.45E-11	6h	1.72
CH60_HUMAN	60 kDa heat shock protein, mitochondrial	22	22	1703.71	2.49E-11	6h	1.91
HS90A_HUMAN	Heat shock protein HSP 90-alpha	34	15	3333.69	2.75E-11	6h	1.74
SH3L1_HUMAN	SH3 domain-binding glutamic acid-rich-like protein	1	1	72.92	3.01E-11	6h	4.93
ANXA1_HUMAN	Annexin A1	17	16	1452.09	3.01E-11	6h	1.35
PAK2_HUMAN	Serine/threonine-protein kinase PAK 2	2	1	110.43	3.06E-11	18h	4.13
PTPRJ_HUMAN	Receptor-type tyrosine-protein phosphatase eta	9	8	522.22	3.09E-11	18h	7.40
TPD54_HUMAN	Tumor protein D54	5	5	388.34	3.27E-11	18h	1.90
PSN1_HUMAN	Presenilin-1	3	1	160.13	3.28E-11	18h	3.87
ROA2_HUMAN	Heterogeneous nuclear ribonucleoproteins A2/B1	5	3	349.68	3.45E-11	18h	1.85
SDF2L_HUMAN	Stromal cell-derived factor 2-like protein 1	1	1	31.76	3.54E-11	18h	16.27
STX11_HUMAN	Syntaxin-11	2	1	142.49	3.96E-11	18h	6.57
ANXA6_HUMAN	Annexin A6	44	42	4054.16	4.00E-11	6h	1.44
ACTN1_HUMAN	Alpha-actinin-1	30	20	2738.43	4.41E-11	6h	1.58
GPC1_HUMAN	Glypican-1	1	1	33.87	4.62E-11	18h	2.53
DIAP1_HUMAN	Protein diaphanous homolog 1	6	6	396.17	5.15E-11	18h	26.71
DHX9_HUMAN	ATP-dependent RNA helicase A	8	6	584.27	6.15E-11	18h	4.09
LIN7A_HUMAN	Protein lin-7 homolog A	1	1	91.88	6.16E-11	18h	10.51
VATE1_HUMAN	V-type proton ATPase subunit E 1	2	2	211.4	6.83E-11	18h	1.92
ELNE_HUMAN	Neutrophil elastase	1	1	72.3	6.84E-11	18h	2.34
PECA1_HUMAN	Platelet endothelial cell adhesion molecule	10	10	1067.09	7.01E-11	18h	6.76
K22E_HUMAN	Keratin, type II cytoskeletal 2 epidermal	9	4	448.98	7.27E-11	6h	2.92
MLEC_HUMAN	Malectin	1	1	111.69	7.42E-11	18h	2.03
AT1A1_HUMAN	Sodium/potassium-transporting ATPase subunit alpha-1	30	15	3374.88	7.95E-11	6h	1.75
MCM3_HUMAN	DNA replication licensing factor MCM3	2	2	96.48	8.42E-11	18h	2.49
PPT1_HUMAN	Palmitoyl-protein thioesterase 1	2	2	248.18	9.07E-11	18h	2.43

Monocyte early (6 h) versus late (18 h) ACdEV proteomes

Accession	Description	Peptide count	Unique peptides	Confidence score	Anova (p)	Highest mean condition	Max fold change
HCLS1_HUMAN	Hematopoietic lineage cell-specific protein	1	1	105.78	9.40E-11	6h	519.43
PSMD2_HUMAN	26S proteasome non-ATPase regulatory subunit 2	18	17	1426.23	9.68E-11	6h	2.06
MARCS_HUMAN	Myristoylated alanine-rich C-kinase substrate	5	5	369.44	9.69E-11	6h	2.50
K2C1_HUMAN	Keratin, type II cytoskeletal 1	10	7	736.36	9.89E-11	6h	1.74
4F2_HUMAN	4F2 cell-surface antigen heavy chain	9	9	774.67	1.18E-10	18h	2.16
RL34_HUMAN	60S ribosomal protein L34	1	1	39.98	1.30E-10	6h	1.91
MYOF_HUMAN	Myoferlin	1	1	64.15	1.43E-10	18h	5.32
RS14_HUMAN	40S ribosomal protein S14	1	1	93.49	1.62E-10	6h	2.95
XPO1_HUMAN	Exportin-1	11	11	721.2	1.64E-10	18h	2.79
SMD3_HUMAN	Small nuclear ribonucleoprotein Sm D3	1	1	76.09	1.96E-10	6h	2.42
STXB3_HUMAN	Syntaxin-binding protein 3	8	8	604.12	2.29E-10	6h	2.61
HNRH1_HUMAN	Heterogeneous nuclear ribonucleoprotein H	4	1	268.83	2.33E-10	18h	1.87
EHD1_HUMAN	EH domain-containing protein 1	8	4	495.18	2.49E-10	6h	7.01
ENPL_HUMAN	Endoplasmin	24	20	1896.54	2.50E-10	6h	2.03
RADI_HUMAN	Radixin	10	1	767.4	2.56E-10	6h	17.44
GAPT_HUMAN	Protein GAPT	1	1	54.56	2.59E-10	18h	5.31
CALX_HUMAN	Calnexin	11	11	921.87	2.62E-10	6h	1.71
FCG2A_HUMAN	Low affinity immunoglobulin gamma Fc region receptor II-a	2	1	98.04	2.67E-10	18h	18.97
TCPG_HUMAN	T-complex protein 1 subunit gamma	14	14	1168.11	2.69E-10	6h	1.44
TPM3_HUMAN	Tropomyosin alpha-3 chain	9	6	479.78	2.71E-10	18h	1.33
TRBM_HUMAN	Thrombomodulin	1	1	199.3	2.74E-10	6h	3.16
APEX1_HUMAN	DNA-(apurinic or apyrimidinic site) lyase	2	2	95.92	2.80E-10	6h	1.78
ATP5H_HUMAN	ATP synthase subunit d, mitochondrial	2	2	87.24	2.89E-10	18h	3.96
DC1I2_HUMAN	Cytoplasmic dynein 1 intermediate chain 2	1	1	36.3	3.05E-10	6h	4.82
PDCD6_HUMAN	Programmed cell death protein 6	4	4	242.54	3.11E-10	18h	3.33
CBPM_HUMAN	Carboxypeptidase M	10	10	938.07	3.13E-10	6h	1.60
SYIC_HUMAN	Isoleucine--tRNA ligase, cytoplasmic	5	5	267.36	3.20E-10	18h	2.93
TXNL1_HUMAN	Thioredoxin-like protein 1	2	2	88.2	3.25E-10	18h	1.86
PSMD3_HUMAN	26S proteasome non-ATPase regulatory subunit 3	8	8	452.09	3.31E-10	6h	1.95
RAB8B_HUMAN	Ras-related protein Rab-8B	7	2	446.45	3.32E-10	18h	4.68
AP2B1_HUMAN	AP-2 complex subunit beta	9	4	581.24	3.35E-10	6h	3.32
SRG2B_HUMAN	SLIT-ROBO Rho GTPase-activating protein 2B	3	1	190.79	3.47E-10	6h	61.05
TM41A_HUMAN	Transmembrane protein 41A	1	1	63.92	3.49E-10	18h	Infinity
RPN1_HUMAN	Dolichyl-diphosphooligosaccharide--protein glycosyltransferase subunit 1	7	7	465.01	3.58E-10	6h	1.97
ELMO1_HUMAN	Engulfment and cell motility protein 1	2	2	204.91	3.76E-10	6h	3.10
PRDX3_HUMAN	Thioredoxin-dependent peroxide reductase, mitochondrial	2	2	88.07	4.30E-10	18h	1.89
TERA_HUMAN	Transitional endoplasmic reticulum ATPase	19	17	1797.33	4.35E-10	6h	1.87
EZRI_HUMAN	Ezrin	18	11	1408.37	4.38E-10	6h	2.54
K1C9_HUMAN	Keratin, type I cytoskeletal 9	8	7	570.08	4.61E-10	6h	1.73
HEXB_HUMAN	Beta-hexosaminidase subunit beta	4	4	226.3	4.63E-10	18h	2.35
COPA_HUMAN	Coatomer subunit alpha	8	6	442.51	4.90E-10	18h	2.05
NRDC_HUMAN	Nardilysin	5	4	234.87	5.13E-10	18h	3.06
LAMP1_HUMAN	Lysosome-associated membrane glycoprotein 1	2	2	203.91	5.17E-10	18h	7.04

Monocyte early (6 h) versus late (18 h) ACdEV proteomes

Accession	Description	Peptide count	Unique peptides	Confidence score	Anova (p)	Highest mean condition	Max fold change
IMB1_HUMAN	Importin subunit beta-1	12	12	1081.58	5.36E-10	6h	2.05
TCTP_HUMAN	Translationally-controlled tumor protein	4	3	208.71	5.46E-10	18h	3.97
HYOU1_HUMAN	Hypoxia up-regulated protein 1	6	6	559.06	5.60E-10	18h	3.54
CATD_HUMAN	Cathepsin D	3	3	138.2	5.68E-10	18h	1.72
MAP2_HUMAN	Methionine aminopeptidase 2	1	1	85.99	5.91E-10	6h	2.43
CHMP6_HUMAN	Charged multivesicular body protein 6	2	2	79.74	6.07E-10	18h	2.04
P85A_HUMAN	Phosphatidylinositol 3-kinase regulatory subunit alpha	1	1	45.54	6.39E-10	6h	14.75
HDDC2_HUMAN	HD domain-containing protein 2	1	1	47.1	6.53E-10	18h	15.55
GBB1_HUMAN	Guanine nucleotide-binding protein G(I)/G(S)/G(T) subunit beta-1	4	3	377.62	7.01E-10	18h	3.25
IF4E_HUMAN	Eukaryotic translation initiation factor 4E	2	2	96.59	7.13E-10	18h	1.41
SNTB1_HUMAN	Beta-1-syntrophin	2	2	135.74	8.15E-10	6h	3.96
HCK_HUMAN	Tyrosine-protein kinase HCK	6	4	434.28	8.51E-10	6h	2.71
UBE2N_HUMAN	Ubiquitin-conjugating enzyme E2 N	2	2	145.91	8.52E-10	6h	3.00
RAB7A_HUMAN	Ras-related protein Rab-7a	12	11	817.01	8.79E-10	18h	1.74
AIMP1_HUMAN	Aminoacyl tRNA synthase complex-interacting multifunctional protein 1	3	3	227.46	9.05E-10	18h	1.85
SYMC_HUMAN	Methionine--tRNA ligase, cytoplasmic	1	1	41.37	1.02E-09	6h	Infinity
TPM4_HUMAN	Tropomyosin alpha-4 chain	6	2	329.33	1.03E-09	18h	1.82
PLXB2_HUMAN	Plexin-B2	9	7	474.37	1.24E-09	18h	2.58
ANXA2_HUMAN	Annexin A2	18	4	1422.02	1.26E-09	18h	1.45
COPB2_HUMAN	Coatomer subunit beta'	8	8	480.86	1.27E-09	6h	1.75
PSDE_HUMAN	26S proteasome non-ATPase regulatory subunit 14	4	4	291.33	1.34E-09	18h	1.50
TCPQ_HUMAN	T-complex protein 1 subunit theta	18	18	1202.23	1.42E-09	6h	1.30
LFA3_HUMAN	Lymphocyte function-associated antigen 3	1	1	73.13	1.44E-09	6h	1.54
ITAX_HUMAN	Integrin alpha-X	7	5	397.15	1.45E-09	18h	5.96
ARF1_HUMAN	ADP-ribosylation factor 1	12	7	839.85	1.45E-09	18h	1.85
PGES2_HUMAN	Prostaglandin E synthase 2	1	1	43.24	1.46E-09	18h	1.80
PRTN3_HUMAN	Myeloblastin	2	2	122.81	1.49E-09	18h	2.92
RAC2_HUMAN	Ras-related C3 botulinum toxin substrate 2	4	3	221.91	1.58E-09	18h	2.52
AT2B4_HUMAN	Plasma membrane calcium-transporting ATPase 4	12	5	879.58	1.60E-09	18h	3.95
HSP74_HUMAN	Heat shock 70 kDa protein 4	4	4	258.32	1.66E-09	18h	2.88
PPCS_HUMAN	Phosphopantothenate--cysteine ligase	3	3	150.95	1.70E-09	6h	1.72
UBA7_HUMAN	Ubiquitin-like modifier-activating enzyme 7	1	1	49.79	1.74E-09	18h	2.72
RL23A_HUMAN	60S ribosomal protein L23a	3	3	193.85	1.80E-09	6h	1.94
LMNB2_HUMAN	Lamin-B2	4	3	244.66	1.90E-09	6h	1.49
MOGS_HUMAN	Mannosyl-oligosaccharide glucosidase	1	1	46.74	1.94E-09	18h	1.64
ARL1_HUMAN	ADP-ribosylation factor-like protein 1	3	3	196.89	1.95E-09	18h	5.91
SYLC_HUMAN	Leucine--tRNA ligase, cytoplasmic	1	1	90.78	2.03E-09	18h	2.29
GGT2_HUMAN	Inactive glutathione hydrolase 2	5	1	520.26	2.07E-09	6h	1.81
PLCG2_HUMAN	1-phosphatidylinositol 4,5-bisphosphate phosphodiesterase gamma-2	1	1	45.47	2.08E-09	18h	26.31
NUMA1_HUMAN	Nuclear mitotic apparatus protein 1	1	1	85.22	2.11E-09	18h	83.22
EF1D_HUMAN	Elongation factor 1-delta	9	8	751.95	2.17E-09	18h	1.20
SNX3_HUMAN	Sorting nexin-3	2	2	107.75	2.18E-09	18h	2.71
APT_HUMAN	Adenine phosphoribosyltransferase	5	4	287.29	2.41E-09	18h	2.47

Monocyte early (6 h) versus late (18 h) ACdEV proteomes

Accession	Description	Peptide count	Unique peptides	Confidence score	Anova (p)	Highest mean condition	Max fold change
CD109_HUMAN	CD109 antigen	2	1	148.01	2.62E-09	6h	4.40
ATPO_HUMAN	ATP synthase subunit O, mitochondrial	3	3	175.47	2.69E-09	18h	1.63
RAB14_HUMAN	Ras-related protein Rab-14	7	6	557.03	2.69E-09	18h	1.48
TKT_HUMAN	Transketolase	9	8	755.89	2.76E-09	6h	1.40
SCRB1_HUMAN	Scavenger receptor class B member 1	2	2	140.26	2.88E-09	6h	3.75
RL7_HUMAN	60S ribosomal protein L7	14	13	696.52	2.90E-09	6h	1.59
IPO9_HUMAN	Importin-9	4	4	441.37	3.02E-09	18h	3.03
FA49B_HUMAN	Protein FAM49B	8	6	732.22	3.04E-09	18h	1.52
MX1_HUMAN	Interferon-induced GTP-binding protein Mx1	4	3	364.01	3.10E-09	6h	3.36
K1C10_HUMAN	Keratin, type I cytoskeletal 10	13	9	991.36	3.12E-09	6h	2.22
PDC6I_HUMAN	Programmed cell death 6-interacting protein	20	20	1430.21	3.24E-09	6h	1.40
SNP23_HUMAN	Synaptosomal-associated protein 23	6	6	440.65	3.51E-09	18h	2.77
ALBU_HUMAN	Serum albumin	16	16	1234.57	3.60E-09	18h	2.02
DPP9_HUMAN	Dipeptidyl peptidase 9	1	1	67.93	3.68E-09	6h	2.06
PGM2_HUMAN	Phosphoglucomutase-2	3	2	232.21	3.69E-09	6h	1.37
RL17_HUMAN	60S ribosomal protein L17	1	1	36.1	3.71E-09	6h	1.92
RB22A_HUMAN	Ras-related protein Rab-22A	2	1	88.45	3.72E-09	18h	3.12
AMPB_HUMAN	Aminopeptidase B	8	8	553.44	3.82E-09	6h	1.54
TPPC3_HUMAN	Trafficking protein particle complex subunit 3	4	4	255.08	3.82E-09	18h	1.59
ITB2_HUMAN	Integrin beta-2	15	14	1382.63	3.84E-09	6h	1.43
ERP29_HUMAN	Endoplasmic reticulum resident protein 29	3	3	181.4	3.88E-09	18h	1.36
CPIN1_HUMAN	Anamorsin	1	1	56.31	3.90E-09	18h	4.22
RPN2_HUMAN	Dolichyl-diphosphooligosaccharide--protein glycosyltransferase subunit 2	7	5	664.96	4.01E-09	6h	2.69
LAT1_HUMAN	Large neutral amino acids transporter small subunit 1	3	3	325.91	4.16E-09	18h	39.17
RAB23_HUMAN	Ras-related protein Rab-23	2	2	75.55	4.22E-09	18h	3.12
USO1_HUMAN	General vesicular transport factor p115	3	1	151.28	4.47E-09	18h	4.24
ARPC2_HUMAN	Actin-related protein 2/3 complex subunit 2	13	13	1012.93	4.53E-09	18h	1.28
SCAM2_HUMAN	Secretory carrier-associated membrane protein 2	2	2	228.12	4.69E-09	18h	1.87
EFHD2_HUMAN	EF-hand domain-containing protein D2	5	3	294.7	4.75E-09	18h	1.43
PLS1_HUMAN	Phospholipid scramblase 1	1	1	105.18	4.82E-09	6h	2.93
ROA0_HUMAN	Heterogeneous nuclear ribonucleoprotein A0	2	1	144.05	5.02E-09	18h	2.40
PRAF3_HUMAN	PRA1 family protein 3	2	2	105.38	5.08E-09	18h	2.70
LCAP_HUMAN	Leucyl-cystinyl aminopeptidase	3	3	190.66	5.27E-09	18h	6.07
CDV3_HUMAN	Protein CDV3 homolog	1	1	93.38	5.96E-09	18h	4.82
ACON_HUMAN	Aconitate hydratase, mitochondrial	1	1	59.93	6.01E-09	6h	19.14
H2AY_HUMAN	Core histone macro-H2A.1	2	1	97.07	6.07E-09	18h	50.43
RL19_HUMAN	60S ribosomal protein L19	1	1	171.48	6.12E-09	6h	2.83
PPIB_HUMAN	Peptidyl-prolyl cis-trans isomerase B	10	10	581.15	6.14E-09	18h	1.44
XRCC6_HUMAN	X-ray repair cross-complementing protein 6	11	10	877.2	6.17E-09	6h	1.54
CPSF6_HUMAN	Cleavage and polyadenylation specificity factor subunit 6	1	1	43	6.23E-09	6h	11.60
GT251_HUMAN	Procollagen galactosyltransferase 1	1	1	59.26	6.51E-09	6h	3.64
SODM_HUMAN	Superoxide dismutase [Mn], mitochondrial	4	4	306.52	6.59E-09	18h	2.78
NOP53_HUMAN	Ribosome biogenesis protein NOP53	1	1	31.4	7.29E-09	6h	2.20

Monocyte early (6 h) versus late (18 h) ACdEV proteomes

Accession	Description	Peptide count	Unique peptides	Confidence score	Anova (p)	Highest mean condition	Max fold change
ADA10_HUMAN	Disintegrin and metalloproteinase domain-containing protein 10	1	1	39.5	7.36E-09	6h	2.41
KHDR1_HUMAN	KH domain-containing, RNA-binding, signal transduction-associated protein 1	1	1	51.28	7.55E-09	6h	2.09
F220P_HUMAN	Putative protein FAM220BP	1	1	32.28	7.62E-09	18h	2.51
GANAB_HUMAN	Neutral alpha-glucosidase AB	11	9	544.78	7.63E-09	18h	2.97
SF3B3_HUMAN	Splicing factor 3B subunit 3	8	7	528.93	8.21E-09	18h	4.47
NSF_HUMAN	Vesicle-fusing ATPase	2	2	95.05	8.22E-09	18h	3.11
CPNE1_HUMAN	Copine-1	8	7	659.26	8.39E-09	6h	1.45
SATT_HUMAN	Neutral amino acid transporter A	5	5	420.44	8.77E-09	6h	1.69
1433B_HUMAN	14-3-3 protein beta/alpha	6	4	341.31	9.64E-09	6h	1.59
LMNB1_HUMAN	Lamin-B1	6	5	367.82	9.78E-09	6h	1.57
RAB2A_HUMAN	Ras-related protein Rab-2A	8	4	667.16	9.89E-09	18h	1.38
AMPD3_HUMAN	AMP deaminase 3	1	1	51.7	1.00E-08	6h	5.53
GLCM_HUMAN	Glucosylceramidase	1	1	34.29	1.04E-08	6h	21.87
EF2_HUMAN	Elongation factor 2	23	23	2040.77	1.04E-08	6h	1.38
HBB_HUMAN	Hemoglobin subunit beta	1	1	53.14	1.08E-08	18h	3.64
RB27A_HUMAN	Ras-related protein Rab-27A	4	2	214.68	1.10E-08	18h	2.47
PSME3_HUMAN	Proteasome activator complex subunit 3	2	2	80.19	1.10E-08	6h	1.41
PSB8_HUMAN	Proteasome subunit beta type-8	4	4	394.21	1.11E-08	18h	2.10
CBR1_HUMAN	Carbonyl reductase [NADPH] 1	1	1	58.82	1.13E-08	18h	1.49
STAT1_HUMAN	Signal transducer and activator of transcription 1-alpha/beta	6	5	446.73	1.14E-08	6h	1.79
SMC3_HUMAN	Structural maintenance of chromosomes protein 3	1	1	78.33	1.15E-08	18h	16.54
CPSF5_HUMAN	Cleavage and polyadenylation specificity factor subunit 5	1	1	39.51	1.20E-08	6h	1.85
P3H1_HUMAN	Prolyl 3-hydroxylase 1	1	1	36.3	1.31E-08	6h	5.66
CTL1_HUMAN	Choline transporter-like protein 1	11	11	1110.89	1.34E-08	6h	1.49
H4_HUMAN	Histone H4	6	6	438.95	1.35E-08	18h	1.21
CLIC1_HUMAN	Chloride intracellular channel protein 1	6	5	445.07	1.36E-08	18h	1.18
CQ062_HUMAN	Uncharacterized protein C17orf62	1	1	34.36	1.39E-08	18h	1001.68
RASN_HUMAN	GTPase NRas	6	1	352.85	1.44E-08	18h	3.25
PYGL_HUMAN	Glycogen phosphorylase, liver form	13	11	914.41	1.47E-08	6h	1.41
CC50A_HUMAN	Cell cycle control protein 50A	1	1	70.21	1.49E-08	6h	1.75
DHX15_HUMAN	Pre-mRNA-splicing factor ATP-dependent RNA helicase DHX15	2	1	138.31	1.54E-08	6h	1.58
NIBL1_HUMAN	Niban-like protein 1	1	1	46.9	1.55E-08	6h	38.49
AT5F1_HUMAN	ATP synthase F(0) complex subunit B1, mitochondrial	3	3	114.06	1.60E-08	18h	8.57
RS13_HUMAN	40S ribosomal protein S13	5	5	373.12	1.61E-08	6h	1.21
GGACT_HUMAN	Gamma-glutamylaminecyclotransferase	1	1	43.82	1.61E-08	18h	6.62
RL13_HUMAN	60S ribosomal protein L13	7	7	425.52	1.65E-08	6h	1.24
ABRX2_HUMAN	BRISC complex subunit Abraxas 2	1	1	40.96	1.69E-08	6h	2.82
STXB2_HUMAN	Syntaxin-binding protein 2	3	3	207.47	1.73E-08	6h	2.24
PCNA_HUMAN	Proliferating cell nuclear antigen	2	2	142.58	1.83E-08	6h	1.42
SUMO2_HUMAN	Small ubiquitin-related modifier 2	1	1	76.48	1.90E-08	6h	1.71
RL22_HUMAN	60S ribosomal protein L22	3	3	287.01	1.91E-08	6h	1.68
PRDX4_HUMAN	Peroxiredoxin-4	6	4	310.5	2.03E-08	18h	1.56
LEG9B_HUMAN	Galectin-9B	1	1	95.38	2.05E-08	18h	3.25

Monocyte early (6 h) versus late (18 h) ACdEV proteomes

Accession	Description	Peptide count	Unique peptides	Confidence score	Anova (p)	Highest mean condition	Max fold change
RRAS_HUMAN	Ras-related protein R-Ras	2	1	123.29	2.08E-08	18h	30.70
EIF2A_HUMAN	Eukaryotic translation initiation factor 2A	1	1	38.34	2.12E-08	6h	5.84
MDHM_HUMAN	Malate dehydrogenase, mitochondrial	7	7	490.31	2.31E-08	18h	1.25
KPCD_HUMAN	Protein kinase C delta type	4	4	197.38	2.34E-08	18h	1.71
SAE1_HUMAN	SUMO-activating enzyme subunit 1	1	1	35.28	2.38E-08	6h	6.68
ARF6_HUMAN	ADP-ribosylation factor 6	4	4	329.42	2.40E-08	18h	5.03
RASH_HUMAN	GTPase HRas	5	1	294.45	2.46E-08	18h	3.55
RS6_HUMAN	40S ribosomal protein S6	3	3	215.62	2.52E-08	6h	1.40
RL28_HUMAN	60S ribosomal protein L28	1	1	62.51	2.63E-08	6h	8.08
RS19_HUMAN	40S ribosomal protein S19	3	2	137.04	2.68E-08	6h	2.14
AP2A1_HUMAN	AP-2 complex subunit alpha-1	8	5	602.96	2.74E-08	6h	1.50
MRP1_HUMAN	Multidrug resistance-associated protein 1	1	1	82.3	2.85E-08	6h	3.21
PDIA4_HUMAN	Protein disulfide-isomerase A4	6	6	382.84	2.97E-08	6h	1.96
PP1G_HUMAN	Serine/threonine-protein phosphatase PP1-gamma catalytic subunit	2	1	125.07	2.99E-08	18h	2.02
TIPRL_HUMAN	TIP41-like protein	1	1	53.38	3.02E-08	6h	1.85
SSRA_HUMAN	Translocon-associated protein subunit alpha	1	1	59.76	3.03E-08	18h	1.78
CIB1_HUMAN	Calcium and integrin-binding protein 1	5	4	322.8	3.06E-08	18h	35.55
MRCKA_HUMAN	Serine/threonine-protein kinase MRCK alpha	1	1	35.9	3.23E-08	18h	2.24
FA50A_HUMAN	Protein FAM50A	1	1	47.7	3.23E-08	6h	3.16
PTN6_HUMAN	Tyrosine-protein phosphatase non-receptor type 6	4	4	257.84	3.23E-08	6h	2.15
CATS_HUMAN	Cathepsin S	3	3	189.06	3.31E-08	18h	2.01
RS25_HUMAN	40S ribosomal protein S25	3	3	209.01	3.39E-08	6h	1.42
RTN3_HUMAN	Reticulon-3	2	2	117.89	3.45E-08	18h	1.59
RL14_HUMAN	60S ribosomal protein L14	1	1	84.75	3.62E-08	18h	2.30
ZNT1_HUMAN	Zinc transporter 1	1	1	63.33	3.68E-08	18h	24.30
PPIH_HUMAN	Peptidyl-prolyl cis-trans isomerase H	5	5	293.07	3.86E-08	18h	1.73
IPO5_HUMAN	Importin-5	4	3	253.05	3.94E-08	18h	3.01
RSMB_HUMAN	Small nuclear ribonucleoprotein-associated proteins B and B'	1	1	55	4.15E-08	18h	1.46
RIR1_HUMAN	Ribonucleoside-diphosphate reductase large subunit	1	1	56.05	4.29E-08	6h	2.81
EEA1_HUMAN	Early endosome antigen 1	3	2	141.72	4.38E-08	18h	2.09
RAP1A_HUMAN	Ras-related protein Rap-1A	10	3	836.21	4.42E-08	18h	2.40
SYNC_HUMAN	Asparagine--tRNA ligase, cytoplasmic	4	4	205.94	4.62E-08	18h	1.39
HNRPD_HUMAN	Heterogeneous nuclear ribonucleoprotein D0	2	2	138.64	4.79E-08	6h	1.87
GUAA_HUMAN	GMP synthase [glutamine-hydrolyzing]	1	1	90.56	4.89E-08	6h	5.23
HDGF_HUMAN	Hepatoma-derived growth factor	1	1	48.53	4.91E-08	6h	1.68
ECHA_HUMAN	Trifunctional enzyme subunit alpha, mitochondrial	3	3	308.31	5.08E-08	6h	3.12
KTHY_HUMAN	Thymidylate kinase	3	3	140.45	5.08E-08	18h	2.75
TKFC_HUMAN	Triokinase/FMN cyclase	1	1	50.02	5.38E-08	6h	249.71
OSTF1_HUMAN	Osteoclast-stimulating factor 1	4	4	196.03	5.53E-08	18h	1.87
CATC_HUMAN	Dipeptidyl peptidase 1	1	1	46.79	5.54E-08	18h	1.94
EM55_HUMAN	55 kDa erythrocyte membrane protein	2	2	101.53	5.54E-08	6h	1.65
KCY_HUMAN	UMP-CMP kinase	2	2	94.56	5.56E-08	18h	3.26
SPCS2_HUMAN	Signal peptidase complex subunit 2	1	1	45.5	5.97E-08	18h	1.67

Monocyte early (6 h) versus late (18 h) ACdEV proteomes

Accession	Description	Peptide count	Unique peptides	Confidence score	Anova (p)	Highest mean condition	Max fold change
CD44_HUMAN	CD44 antigen	7	7	603.56	6.01E-08	6h	1.22
PRP8_HUMAN	Pre-mRNA-processing-splicing factor 8	2	2	102.53	6.08E-08	18h	2.78
TMEDA_HUMAN	Transmembrane emp24 domain-containing protein 10	4	4	250.16	6.52E-08	18h	1.97
DIRA2_HUMAN	GTP-binding protein Di-Ras2	1	1	39.29	6.58E-08	18h	2.19
AP1B1_HUMAN	AP-1 complex subunit beta-1	9	3	628.08	6.65E-08	6h	1.37
RAB18_HUMAN	Ras-related protein Rab-18	1	1	54.79	6.67E-08	18h	1.37
XRCC5_HUMAN	X-ray repair cross-complementing protein 5	5	5	511.3	6.95E-08	6h	1.51
HPRT_HUMAN	Hypoxanthine-guanine phosphoribosyltransferase	5	5	324.01	7.28E-08	18h	1.28
MGN_HUMAN	Protein mago nashi homolog	1	1	67.81	7.46E-08	6h	2.48
FCGR1_HUMAN	High affinity immunoglobulin gamma Fc receptor I	2	1	156.07	7.60E-08	6h	2.96
CY24A_HUMAN	Cytochrome b-245 light chain	2	2	90	7.72E-08	18h	2.80
RAB10_HUMAN	Ras-related protein Rab-10	10	7	722.43	7.75E-08	18h	3.78
ACSL4_HUMAN	Long-chain-fatty-acid--CoA ligase 4	1	1	64.17	7.76E-08	6h	2.71
STIP1_HUMAN	Stress-induced-phosphoprotein 1	10	9	573.07	8.01E-08	6h	1.43
NPM_HUMAN	Nucleophosmin	3	3	293.99	8.61E-08	6h	1.92
NUCL_HUMAN	Nucleolin	12	12	773.66	9.31E-08	6h	1.43
CPZIP_HUMAN	CapZ-interacting protein	1	1	63.46	9.42E-08	6h	1.93
SYVC_HUMAN	Valine--tRNA ligase	4	4	362.36	1.10E-07	18h	2.20
CHP1_HUMAN	Calcineurin B homologous protein 1	2	1	125.06	1.10E-07	18h	2.04
SRP14_HUMAN	Signal recognition particle 14 kDa protein	1	1	110.79	1.12E-07	18h	67.38
GPX1_HUMAN	Glutathione peroxidase 1	5	5	277.67	1.15E-07	18h	1.62
MTM1_HUMAN	Myotubularin	2	2	210.46	1.15E-07	6h	2.20
ARPC5_HUMAN	Actin-related protein 2/3 complex subunit 5	6	4	433.75	1.19E-07	18h	1.94
RAP2B_HUMAN	Ras-related protein Rap-2b	7	3	469.51	1.20E-07	18h	3.74
DPP3_HUMAN	Dipeptidyl peptidase 3	3	3	206.04	1.23E-07	6h	1.48
RS11_HUMAN	40S ribosomal protein S11	3	3	165.4	1.28E-07	6h	1.51
RALA_HUMAN	Ras-related protein Ral-A	6	2	332.78	1.32E-07	18h	2.74
RRAS2_HUMAN	Ras-related protein R-Ras2	2	2	104.22	1.32E-07	18h	4.46
MMP9_HUMAN	Matrix metalloproteinase-9	4	2	237.72	1.37E-07	6h	28.67
LTOR1_HUMAN	Ragulator complex protein LAMTOR1	1	1	65.37	1.37E-07	18h	2.56
GRP75_HUMAN	Stress-70 protein, mitochondrial	3	2	229.71	1.42E-07	6h	3.15
RL6_HUMAN	60S ribosomal protein L6	9	9	813.45	1.42E-07	18h	1.15
NR4A3_HUMAN	Nuclear receptor subfamily 4 group A member 3	1	1	32.27	1.43E-07	18h	30.81
H31T_HUMAN	Histone H3.1t	3	1	174.27	1.43E-07	18h	1.41
DCK_HUMAN	Deoxycytidine kinase	2	1	90.54	1.44E-07	6h	1.54
SODC_HUMAN	Superoxide dismutase [Cu-Zn]	4	3	159.38	1.45E-07	6h	1.28
NACAM_HUMAN	Nascent polypeptide-associated complex subunit alpha, muscle-specific form	2	2	133.3	1.46E-07	6h	1.27
RL26L_HUMAN	60S ribosomal protein L26-like 1	3	3	118	1.48E-07	18h	1.35
CD63_HUMAN	CD63 antigen	3	2	189.47	1.51E-07	6h	1.37
KINH_HUMAN	Kinesin-1 heavy chain	3	2	172.44	1.52E-07	18h	12.68
MPRI_HUMAN	Cation-independent mannose-6-phosphate receptor	1	1	34.99	1.53E-07	18h	11.91
CYBP_HUMAN	Calcyclin-binding protein	4	4	180.59	1.54E-07	18h	1.57
UBC9_HUMAN	SUMO-conjugating enzyme UBC9	1	1	37.19	1.54E-07	6h	1.41

Monocyte early (6 h) versus late (18 h) ACdEV proteomes

Accession	Description	Peptide count	Unique peptides	Confidence score	Anova (p)	Highest mean condition	Max fold change
UFC1_HUMAN	Ubiquitin-fold modifier-conjugating enzyme 1	1	1	80.24	1.57E-07	6h	1.53
SNAG_HUMAN	Gamma-soluble NSF attachment protein	2	2	81.7	1.57E-07	18h	1.79
FRIL_HUMAN	Ferritin light chain	2	2	133.07	1.64E-07	18h	3.77
RL32_HUMAN	60S ribosomal protein L32	1	1	71.38	1.65E-07	6h	1.89
CAPZB_HUMAN	F-actin-capping protein subunit beta	5	5	491.25	1.76E-07	18h	1.23
UBR4_HUMAN	E3 ubiquitin-protein ligase UBR4	2	2	155.38	1.81E-07	18h	8.38
TMCO1_HUMAN	Calcium load-activated calcium channel	1	1	59.69	1.82E-07	18h	1179.85
PSMD8_HUMAN	26S proteasome non-ATPase regulatory subunit 8	2	2	87.6	1.87E-07	18h	1.33
TPR_HUMAN	Nucleoprotein TPR	3	3	267.9	1.87E-07	18h	1.65
IF4B_HUMAN	Eukaryotic translation initiation factor 4B	1	1	57.2	1.95E-07	18h	777.68
GPSM3_HUMAN	G-protein-signaling modulator 3	2	2	184.1	2.04E-07	18h	6.61
DDX1_HUMAN	ATP-dependent RNA helicase DDX1	1	1	48.07	2.08E-07	6h	2.23
STT3A_HUMAN	Dolichyl-diphosphooligosaccharide--protein glycosyltransferase subunit STT3A	3	2	113.09	2.13E-07	6h	1.94
RAB9A_HUMAN	Ras-related protein Rab-9A	1	1	34.26	2.16E-07	18h	1.66
1433T_HUMAN	14-3-3 protein theta	6	4	512.36	2.19E-07	18h	1.26
ELAV1_HUMAN	ELAV-like protein 1	2	1	147.96	2.22E-07	18h	1.47
RMXL1_HUMAN	RNA binding motif protein, X-linked-like-1	1	1	81.22	2.23E-07	6h	2.78
BIN2_HUMAN	Bridging integrator 2	1	1	61.19	2.26E-07	6h	486.04
HVCN1_HUMAN	Voltage-gated hydrogen channel 1	2	2	134.51	2.26E-07	18h	1.33
GRB2_HUMAN	Growth factor receptor-bound protein 2	3	2	127.48	2.33E-07	6h	1.39
KITH_HUMAN	Thymidine kinase, cytosolic	1	1	49.91	2.33E-07	18h	6.05
SYRC_HUMAN	Arginine--tRNA ligase, cytoplasmic	7	7	397.19	2.35E-07	6h	1.13
RL13A_HUMAN	60S ribosomal protein L13a	5	2	236.15	2.37E-07	18h	1.59
ERC2_HUMAN	ERC protein 2	1	1	35.31	2.52E-07	18h	6.77
BLVRB_HUMAN	Flavin reductase (NADPH)	1	1	73.35	2.53E-07	18h	2.00
GSTM3_HUMAN	Glutathione S-transferase Mu 3	4	3	192.02	2.71E-07	18h	2.68
IGL1_HUMAN	Immunoglobulin lambda-1 light chain	1	1	52.71	2.72E-07	6h	1.76
PIPNB_HUMAN	Phosphatidylinositol transfer protein beta isoform	2	2	98.29	2.91E-07	18h	1.76
CDC42_HUMAN	Cell division control protein 42 homolog	5	5	319.43	3.04E-07	18h	4.61
G3P_HUMAN	Glyceraldehyde-3-phosphate dehydrogenase	18	17	1502.25	3.16E-07	18h	1.21
PSMD1_HUMAN	26S proteasome non-ATPase regulatory subunit 1	5	4	243.48	3.18E-07	18h	2.15
CHIP_HUMAN	E3 ubiquitin-protein ligase CHIP	1	1	48.77	3.32E-07	18h	1.53
RAP2C_HUMAN	Ras-related protein Rap-2c	4	1	324.85	3.34E-07	18h	7.00
F234A_HUMAN	Protein FAM234A	1	1	32.18	3.40E-07	18h	2.12
1433F_HUMAN	14-3-3 protein eta	4	2	197.64	3.56E-07	18h	1.21
RL27A_HUMAN	60S ribosomal protein L27a	2	2	144.47	3.60E-07	6h	1.42
VINC_HUMAN	Vinculin	4	4	372.61	3.60E-07	18h	4.10
ITA5_HUMAN	Integrin alpha-5	6	6	287.29	3.68E-07	18h	1.63
DTD1_HUMAN	D-aminoacyl-tRNA deacylase 1	1	1	79.91	3.83E-07	6h	1.60
SNAA_HUMAN	Alpha-soluble NSF attachment protein	6	5	422.09	3.84E-07	18h	1.30
NAC1_HUMAN	Sodium/calcium exchanger 1	1	1	32.4	3.88E-07	18h	2.05
PCNP_HUMAN	PEST proteolytic signal-containing nuclear protein	1	1	62.21	3.96E-07	18h	1.48
PSA_HUMAN	Puromycin-sensitive aminopeptidase	9	5	522.89	4.12E-07	6h	1.51

Monocyte early (6 h) versus late (18 h) ACdEV proteomes

Accession	Description	Peptide count	Unique peptides	Confidence score	Anova (p)	Highest mean condition	Max fold change
IF_HUMAN	Gastric intrinsic factor	1	1	36.8	4.18E-07	18h	12.19
PLOD3_HUMAN	Procollagen-lysine,2-oxoglutarate 5-dioxygenase 3	1	1	32.01	4.31E-07	6h	4.66
TXD12_HUMAN	Thioredoxin domain-containing protein 12	1	1	41.18	4.33E-07	18h	5.65
STX6_HUMAN	Syntaxin-6	1	1	34.92	4.35E-07	18h	2.34
SYTC_HUMAN	Threonine--tRNA ligase, cytoplasmic	7	6	404.2	4.44E-07	6h	1.25
TOIP1_HUMAN	Torsin-1A-interacting protein 1	1	1	52.06	4.44E-07	18h	2.25
A16A1_HUMAN	Aldehyde dehydrogenase family 16 member A1	1	1	69.81	4.53E-07	6h	4.26
RS15A_HUMAN	40S ribosomal protein S15a	3	3	125.18	4.75E-07	6h	1.64
CAN2_HUMAN	Calpain-2 catalytic subunit	4	4	319.09	4.87E-07	6h	1.97
DUS3_HUMAN	Dual specificity protein phosphatase 3	2	2	108.54	4.94E-07	6h	1.39
RL5_HUMAN	60S ribosomal protein L5	7	7	580.3	5.05E-07	18h	1.21
RLA1_HUMAN	60S acidic ribosomal protein P1	2	1	182.37	5.09E-07	18h	2.88
CD81_HUMAN	CD81 antigen	2	2	132.56	5.13E-07	18h	1.15
COPZ1_HUMAN	Coatomer subunit zeta-1	3	3	170.48	5.35E-07	18h	2.25
TFIP8_HUMAN	Tumor necrosis factor alpha-induced protein 8	1	1	104.31	5.63E-07	18h	12.21
VPS35_HUMAN	Vacuolar protein sorting-associated protein 35	7	7	519.02	5.69E-07	6h	1.24
HS71A_HUMAN	Heat shock 70 kDa protein 1A	13	6	1144.6	6.11E-07	6h	1.34
2AAA_HUMAN	Serine/threonine-protein phosphatase 2A 65 kDa regulatory subunit A alpha isoform	8	7	750.51	6.12E-07	6h	1.35
IF4G2_HUMAN	Eukaryotic translation initiation factor 4 gamma 2	1	1	35.24	6.50E-07	18h	5.52
PP1R7_HUMAN	Protein phosphatase 1 regulatory subunit 7	1	1	42	6.58E-07	6h	1.47
TCPA_HUMAN	T-complex protein 1 subunit alpha	18	18	1565.96	6.83E-07	6h	1.28
CYFP1_HUMAN	Cytoplasmic FMR1-interacting protein 1	1	1	61.87	6.91E-07	18h	2.75
FLOT2_HUMAN	Flotillin-2	2	2	134.43	6.95E-07	18h	7.08
FCERG_HUMAN	High affinity immunoglobulin epsilon receptor subunit gamma	2	2	206.4	7.37E-07	18h	1.65
RS12_HUMAN	40S ribosomal protein S12	1	1	56	7.40E-07	6h	1.34
PPP6_HUMAN	Serine/threonine-protein phosphatase 6 catalytic subunit	1	1	54.47	7.70E-07	18h	1.49
RS20_HUMAN	40S ribosomal protein S20	2	2	197.1	7.75E-07	6h	1.58
RHEB_HUMAN	GTP-binding protein Rheb	4	4	242.73	7.80E-07	18h	3.08
GNAL_HUMAN	Guanine nucleotide-binding protein G(olf) subunit alpha	1	1	77.62	7.84E-07	18h	2.10
SF3B1_HUMAN	Splicing factor 3B subunit 1	4	3	240.48	7.88E-07	18h	2.26
PABP4_HUMAN	Polyadenylate-binding protein 4	4	3	237.7	7.92E-07	6h	1.91
RL12_HUMAN	60S ribosomal protein L12	3	3	234.45	7.94E-07	18h	1.45
ABHD8_HUMAN	Protein ABHD8	1	1	34.16	7.99E-07	18h	43.20
TSN14_HUMAN	Tetraspanin-14	1	1	50.46	8.31E-07	18h	1.65
ARL8B_HUMAN	ADP-ribosylation factor-like protein 8B	2	1	174.75	8.50E-07	18h	17.39
PSME1_HUMAN	Proteasome activator complex subunit 1	9	9	547.92	8.53E-07	6h	1.18
NPTN_HUMAN	Neuroplastin	3	3	216.57	8.87E-07	6h	1.76
RISC_HUMAN	Retinoid-inducible serine carboxypeptidase	2	2	147.2	9.06E-07	18h	4.40
GLU2B_HUMAN	Glucosidase 2 subunit beta	4	4	286.8	9.08E-07	6h	1.42
NNRE_HUMAN	NAD(P)H-hydrate epimerase	1	1	64.35	9.16E-07	18h	1.68
WDR1_HUMAN	WD repeat-containing protein 1	6	6	381.85	9.80E-07	6h	1.28
CSF2R_HUMAN	Granulocyte-macrophage colony-stimulating factor receptor subunit alpha	1	1	53.1	1.00E-06	6h	45.05
TMX1_HUMAN	Thioredoxin-related transmembrane protein 1	1	1	69.06	1.02E-06	18h	1.36

Monocyte early (6 h) versus late (18 h) ACdEV proteomes

Accession	Description	Peptide count	Unique peptides	Confidence score	Anova (p)	Highest mean condition	Max fold change
ASCC2_HUMAN	Activating signal cointegrator 1 complex subunit 2	1	1	73.33	1.08E-06	6h	112.12
LMAN2_HUMAN	Vesicular integral-membrane protein VIP36	3	3	141.42	1.11E-06	18h	1.35
MAOX_HUMAN	NADP-dependent malic enzyme	2	2	103.5	1.14E-06	6h	2.54
TMED9_HUMAN	Transmembrane emp24 domain-containing protein 9	2	2	92.61	1.14E-06	6h	1.61
GGT1_HUMAN	Glutathione hydrolase 1 proenzyme	2	1	180.72	1.16E-06	18h	4.03
HTAI2_HUMAN	Oxidoreductase HTATIP2	1	1	42.29	1.20E-06	18h	1.63
PDXK_HUMAN	Pyridoxal kinase	2	2	119.06	1.23E-06	18h	1.75
ST14_HUMAN	Suppressor of tumorigenicity 14 protein	3	3	206.71	1.30E-06	6h	1.47
IMDH2_HUMAN	Inosine-5'-monophosphate dehydrogenase 2	1	1	46.74	1.31E-06	18h	2.36
SDHA_HUMAN	Succinate dehydrogenase [ubiquinone] flavoprotein subunit, mitochondrial	1	1	77.16	1.33E-06	6h	1.79
PCBP2_HUMAN	Poly(rC)-binding protein 2	1	1	36.44	1.33E-06	18h	2.55
IN35_HUMAN	Interferon-induced 35 kDa protein	1	1	56.47	1.35E-06	18h	1.40
RS10_HUMAN	40S ribosomal protein S10	1	1	57.37	1.36E-06	18h	3.21
EST1_HUMAN	Liver carboxylesterase 1	4	1	302.35	1.37E-06	6h	3.41
LRC57_HUMAN	Leucine-rich repeat-containing protein 57	3	2	110.01	1.43E-06	18h	1.91
ICAM1_HUMAN	Intercellular adhesion molecule 1	1	1	54.04	1.46E-06	6h	2.10
LSM1_HUMAN	U6 snRNA-associated Sm-like protein LSm1	1	1	44.67	1.46E-06	18h	378.13
RS16_HUMAN	40S ribosomal protein S16	5	4	280.56	1.51E-06	6h	1.42
AT1B3_HUMAN	Sodium/potassium-transporting ATPase subunit beta-3	6	6	612.21	1.52E-06	18h	1.60
RANG_HUMAN	Ran-specific GTPase-activating protein	2	2	139.02	1.52E-06	18h	1.38
NINJ1_HUMAN	Ninjurin-1	2	2	147.08	1.53E-06	18h	3.91
LEUK_HUMAN	Leukosialin	3	3	167.89	1.59E-06	18h	2.26
RS5_HUMAN	40S ribosomal protein S5	2	1	93.55	1.60E-06	6h	1.23
PSA2_HUMAN	Proteasome subunit alpha type-2	6	6	358.92	1.60E-06	18h	2.20
CAZA2_HUMAN	F-actin-capping protein subunit alpha-2	2	1	197.32	1.63E-06	18h	2.48
TNAP2_HUMAN	Tumor necrosis factor alpha-induced protein 2	1	1	58.34	1.63E-06	6h	13.85
1433Z_HUMAN	14-3-3 protein zeta/delta	11	8	932.44	1.65E-06	18h	1.13
LYAG_HUMAN	Lysosomal alpha-glucosidase	1	1	77.95	1.67E-06	18h	1.50
TLR2_HUMAN	Toll-like receptor 2	1	1	64.47	1.72E-06	6h	4.01
RS3_HUMAN	40S ribosomal protein S3	10	10	667.11	1.75E-06	18h	1.10
TMM33_HUMAN	Transmembrane protein 33	3	2	164.53	1.76E-06	18h	2.32
CNN2_HUMAN	Calponin-2	1	1	118.69	1.82E-06	18h	1.41
DYHC1_HUMAN	Cytoplasmic dynein 1 heavy chain 1	6	6	362.82	1.84E-06	18h	3.47
PSB4_HUMAN	Proteasome subunit beta type-4	6	6	627.81	1.88E-06	18h	1.39
RU2A_HUMAN	U2 small nuclear ribonucleoprotein A'	2	2	104.2	1.91E-06	18h	4.14
RAB5C_HUMAN	Ras-related protein Rab-5C	8	5	783.28	1.92E-06	18h	1.81
PCBP1_HUMAN	Poly(rC)-binding protein 1	1	1	66.8	1.98E-06	18h	2.20
UBP7_HUMAN	Ubiquitin carboxyl-terminal hydrolase 7	1	1	35.36	2.00E-06	18h	180.46
CKAP4_HUMAN	Cytoskeleton-associated protein 4	6	6	457.52	2.02E-06	6h	1.74
EIF1A_HUMAN	Probable RNA-binding protein EIF1AD	1	1	74.82	2.04E-06	18h	2.21
IPO7_HUMAN	Importin-7	3	3	169.7	2.09E-06	18h	10.16
SSRG_HUMAN	Translocon-associated protein subunit gamma	1	1	65.3	2.23E-06	18h	3.59
ALDR_HUMAN	Aldose reductase	5	4	262.53	2.34E-06	6h	1.37

Monocyte early (6 h) versus late (18 h) ACdEV proteomes

Accession	Description	Peptide count	Unique peptides	Confidence score	Anova (p)	Highest mean condition	Max fold change
LDHA_HUMAN	L-lactate dehydrogenase A chain	14	13	1242.06	2.46E-06	18h	1.07
RLA0L_HUMAN	60S acidic ribosomal protein P0-like	4	1	261.54	2.56E-06	18h	7.00
EIF3L_HUMAN	Eukaryotic translation initiation factor 3 subunit L	5	5	267.15	2.56E-06	6h	1.15
KAD1_HUMAN	Adenylate kinase isoenzyme 1	1	1	162.77	2.61E-06	18h	5.33
DEOC_HUMAN	Deoxyribose-phosphate aldolase	1	1	74.27	2.65E-06	18h	1.43
RS18_HUMAN	40S ribosomal protein S18	5	5	280.92	2.76E-06	6h	1.32
PP2AA_HUMAN	Serine/threonine-protein phosphatase 2A catalytic subunit alpha isoform	1	1	79.08	2.78E-06	18h	1.54
RHOA_HUMAN	Transforming protein RhoA	5	3	417.74	2.80E-06	18h	5.21
RAB1B_HUMAN	Ras-related protein Rab-1B	10	1	873.1	2.97E-06	18h	1.29
NDUBB_HUMAN	NADH dehydrogenase [ubiquinone] 1 beta subcomplex subunit 11, mitochondrial	1	1	38.54	3.02E-06	6h	1.38
CAP7_HUMAN	Azurocidin	1	1	78.12	3.06E-06	18h	2.60
IPYR2_HUMAN	Inorganic pyrophosphatase 2, mitochondrial	2	1	99.3	3.11E-06	18h	1.48
PABP3_HUMAN	Polyadenylate-binding protein 3	2	1	159.44	3.23E-06	6h	4.99
RAB13_HUMAN	Ras-related protein Rab-13	5	3	300.98	3.31E-06	18h	2.96
LYPA1_HUMAN	Acyl-protein thioesterase 1	3	3	180.75	3.48E-06	6h	1.26
ECH1_HUMAN	Delta(3,5)-Delta(2,4)-dienoyl-CoA isomerase, mitochondrial	6	5	305.02	3.56E-06	18h	1.12
SPTB2_HUMAN	Spectrin beta chain, non-erythrocytic 1	8	5	539.49	3.63E-06	18h	1.96
YKT6_HUMAN	Synaptobrevin homolog YKT6	1	1	46.61	3.66E-06	18h	2.20
PSME2_HUMAN	Proteasome activator complex subunit 2	10	10	687.01	4.10E-06	6h	1.13
ESYT1_HUMAN	Extended synaptotagmin-1	5	5	508.63	4.26E-06	18h	1.25
DNM1L_HUMAN	Dynamin-1-like protein	1	1	42.92	4.28E-06	6h	4.03
TAGL2_HUMAN	Transgelin-2	13	12	1052.98	4.31E-06	18h	1.41
PSA1_HUMAN	Proteasome subunit alpha type-1	9	9	540.76	4.38E-06	18h	1.17
SC23B_HUMAN	Protein transport protein Sec23B	2	1	75.98	4.51E-06	6h	12.65
PI4KA_HUMAN	Phosphatidylinositol 4-kinase alpha	1	1	59.34	4.53E-06	18h	2.55
SAMH1_HUMAN	Deoxynucleoside triphosphate triphosphohydrolase SAMHD1	1	1	33.01	4.66E-06	6h	4.32
CA050_HUMAN	Uncharacterized protein C1orf50	1	1	72.52	4.71E-06	18h	13.92
ADT2_HUMAN	ADP/ATP translocase 2	6	2	329.32	4.78E-06	18h	1.31
UB2V1_HUMAN	Ubiquitin-conjugating enzyme E2 variant 1	4	1	231.39	5.02E-06	6h	1.32
GARS_HUMAN	Glycine--tRNA ligase	8	8	638.81	5.10E-06	6h	1.71
ELOB_HUMAN	Elongin-B	1	1	37.85	5.24E-06	6h	1.28
MYADM_HUMAN	Myeloid-associated differentiation marker	4	4	229.76	5.50E-06	18h	1.68
MA2B1_HUMAN	Lysosomal alpha-mannosidase	1	1	51.91	5.74E-06	6h	30.40
PSA3_HUMAN	Proteasome subunit alpha type-3	7	7	454.27	5.77E-06	18h	1.18
MCTS1_HUMAN	Malignant T-cell-amplified sequence 1	1	1	67.89	5.91E-06	18h	2.33
CAN1_HUMAN	Calpain-1 catalytic subunit	7	5	324.41	6.15E-06	6h	1.17
GGCT_HUMAN	Gamma-glutamylcyclotransferase	1	1	68.58	6.17E-06	6h	1.40
GTR5_HUMAN	Solute carrier family 2, facilitated glucose transporter member 5	3	3	140.91	6.26E-06	6h	1.51
PLIN3_HUMAN	Perilipin-3	3	3	236.31	6.54E-06	18h	1.73
PSB9_HUMAN	Proteasome subunit beta type-9	3	3	168.51	6.65E-06	18h	1.18
CAZA1_HUMAN	F-actin-capping protein subunit alpha-1	6	5	531.24	7.07E-06	18h	1.16
VAMP7_HUMAN	Vesicle-associated membrane protein 7	1	1	40.84	7.17E-06	18h	3.26
TPIS_HUMAN	Triosephosphate isomerase	9	8	893.17	7.54E-06	18h	1.11

Monocyte early (6 h) versus late (18 h) ACdEV proteomes

Accession	Description	Peptide count	Unique peptides	Confidence score	Anova (p)	Highest mean condition	Max fold change
HNRPQ_HUMAN	Heterogeneous nuclear ribonucleoprotein Q	6	3	457.93	7.56E-06	6h	1.27
PFD3_HUMAN	Prefoldin subunit 3	4	3	177.27	7.58E-06	18h	15.82
CHMP5_HUMAN	Charged multivesicular body protein 5	1	1	35.16	7.60E-06	18h	Infinity
XPO4_HUMAN	Exportin-4	1	1	64.98	7.66E-06	18h	6.88
CBX1_HUMAN	Chromobox protein homolog 1	1	1	72.88	7.67E-06	18h	46.86
NEK9_HUMAN	Serine/threonine-protein kinase Nek9	1	1	63.16	7.74E-06	18h	1.81
CD47_HUMAN	Leukocyte surface antigen CD47	3	3	148.67	7.75E-06	6h	1.27
VATA_HUMAN	V-type proton ATPase catalytic subunit A	10	9	731.07	8.54E-06	6h	1.76
RB11B_HUMAN	Ras-related protein Rab-11B	10	2	667.96	8.59E-06	18h	2.19
SYQ_HUMAN	Glutamine--tRNA ligase	3	2	137.34	8.83E-06	6h	1.51
INSR_HUMAN	Insulin receptor	1	1	31.69	9.10E-06	18h	88.29
RAN_HUMAN	GTP-binding nuclear protein Ran	6	6	387.76	9.71E-06	6h	1.20
RBM15_HUMAN	Putative RNA-binding protein 15	1	1	42.37	1.00E-05	18h	1.55
TCPZ_HUMAN	T-complex protein 1 subunit zeta	13	9	951.19	1.01E-05	6h	1.23
ARPC4_HUMAN	Actin-related protein 2/3 complex subunit 4	7	7	363.57	1.05E-05	18h	1.24
PRKDC_HUMAN	DNA-dependent protein kinase catalytic subunit	4	2	181.29	1.09E-05	18h	2.27
CPNS1_HUMAN	Calpain small subunit 1	6	4	371.38	1.09E-05	18h	1.41
KCMF1_HUMAN	E3 ubiquitin-protein ligase KCMF1	1	1	50.31	1.11E-05	18h	319.04
VPS29_HUMAN	Vacuolar protein sorting-associated protein 29	2	2	118.86	1.17E-05	18h	1.18
IFM1_HUMAN	Interferon-induced transmembrane protein 1	1	1	143.99	1.25E-05	6h	1.24
OXLA_HUMAN	L-amino-acid oxidase	2	2	133.87	1.27E-05	18h	10.67
PRDX5_HUMAN	Peroxiredoxin-5, mitochondrial	1	1	34.19	1.29E-05	18h	3.18
RAB4A_HUMAN	Ras-related protein Rab-4A	2	1	127.81	1.30E-05	6h	1.21
KAD2_HUMAN	Adenylate kinase 2, mitochondrial	7	7	501.41	1.32E-05	6h	1.15
RL36_HUMAN	60S ribosomal protein L36	1	1	56.73	1.34E-05	6h	1.42
PRS6B_HUMAN	26S proteasome regulatory subunit 6B	4	4	327.08	1.35E-05	18h	2.45
PSB2_HUMAN	Proteasome subunit beta type-2	7	7	466.41	1.47E-05	18h	1.23
BRI3B_HUMAN	BRI3-binding protein	1	1	90.02	1.47E-05	18h	1.37
RAB6A_HUMAN	Ras-related protein Rab-6A	2	1	103.9	1.48E-05	6h	1.34
PSMG2_HUMAN	Proteasome assembly chaperone 2	1	1	53.26	1.49E-05	18h	1.20
LEG8_HUMAN	Galectin-8	1	1	54.86	1.59E-05	18h	1.92
CD166_HUMAN	CD166 antigen	3	3	133.05	1.65E-05	18h	1.83
RNT2_HUMAN	Ribonuclease T2	3	3	179.78	1.65E-05	18h	1.66
ZYX_HUMAN	Zyxin	1	1	40.93	1.67E-05	6h	5.33
G3BP1_HUMAN	Ras GTPase-activating protein-binding protein 1	1	1	46.39	1.68E-05	18h	6.59
GSTP1_HUMAN	Glutathione S-transferase P	12	12	1042.44	1.78E-05	18h	1.91
PSB3_HUMAN	Proteasome subunit beta type-3	6	5	350.75	1.88E-05	18h	1.61
SC24C_HUMAN	Protein transport protein Sec24C	1	1	47.27	1.94E-05	6h	1.46
PSA5_HUMAN	Proteasome subunit alpha type-5	6	5	386.19	1.94E-05	18h	1.09
COPG1_HUMAN	Coatomer subunit gamma-1	5	4	349.55	2.03E-05	6h	1.28
ANXA5_HUMAN	Annexin A5	18	16	1177.77	2.04E-05	6h	1.26
RAB31_HUMAN	Ras-related protein Rab-31	4	2	278.86	2.10E-05	18h	3.92
ARF4_HUMAN	ADP-ribosylation factor 4	9	4	626.71	2.13E-05	6h	1.21

Monocyte early (6 h) versus late (18 h) ACdEV proteomes

Accession	Description	Peptide count	Unique peptides	Confidence score	Anova (p)	Highest mean condition	Max fold change
PSA6_HUMAN	Proteasome subunit alpha type-6	6	6	526.64	2.21E-05	18h	1.14
SAMN1_HUMAN	SAM domain-containing protein SAMSN-1	1	1	67.14	2.28E-05	18h	9.20
RS4X_HUMAN	40S ribosomal protein S4, X isoform	9	4	487.14	2.41E-05	18h	1.29
AN32B_HUMAN	Acidic leucine-rich nuclear phosphoprotein 32 family member B	2	1	109.1	2.42E-05	6h	1.45
ATG7_HUMAN	Ubiquitin-like modifier-activating enzyme ATG7	1	1	151.11	2.42E-05	6h	2.15
MESD_HUMAN	LRP chaperone MESD	1	1	34.62	2.47E-05	18h	1.63
PGM1_HUMAN	Phosphoglucomutase-1	2	2	90.93	2.53E-05	6h	2.48
ARC1B_HUMAN	Actin-related protein 2/3 complex subunit 1B	8	8	643.78	2.55E-05	18h	1.16
H2A1A_HUMAN	Histone H2A type 1-A	2	1	100.64	2.56E-05	18h	8.80
TTYH3_HUMAN	Protein tweety homolog 3	1	1	188.86	2.66E-05	6h	2.08
GMFB_HUMAN	Glia maturation factor beta	2	1	134.29	2.66E-05	6h	1.84
COF1_HUMAN	Cofilin-1	4	3	420.05	2.99E-05	18h	2.44
GPX4_HUMAN	Phospholipid hydroperoxide glutathione peroxidase	1	1	52.5	3.14E-05	18h	1.20
EF1G_HUMAN	Elongation factor 1-gamma	12	11	811.76	3.30E-05	6h	1.13
LAIR1_HUMAN	Leukocyte-associated immunoglobulin-like receptor 1	1	1	100.56	3.32E-05	18h	47.09
LGUL_HUMAN	Lactoylglutathione lyase	9	8	474.33	3.45E-05	18h	1.23
SYEP_HUMAN	Bifunctional glutamate/proline--tRNA ligase	7	7	353.99	3.52E-05	6h	1.37
RGS19_HUMAN	Regulator of G-protein signaling 19	1	1	46.67	3.54E-05	18h	18.00
SC11A_HUMAN	Signal peptidase complex catalytic subunit SEC11A	2	1	79.38	3.75E-05	18h	1.40
VDAC1_HUMAN	Voltage-dependent anion-selective channel protein 1	5	3	364.03	3.79E-05	18h	1.17
ATRAP_HUMAN	Type-1 angiotensin II receptor-associated protein	1	1	45.92	3.83E-05	6h	1.74
RS3A_HUMAN	40S ribosomal protein S3a	7	7	323.98	3.92E-05	6h	1.17
SCAM3_HUMAN	Secretory carrier-associated membrane protein 3	2	1	169.49	3.97E-05	18h	1.27
LMNA_HUMAN	Prelamin-A/C	17	16	1225.74	4.12E-05	6h	1.18
PEBP1_HUMAN	Phosphatidylethanolamine-binding protein 1	3	3	354.33	4.24E-05	6h	1.16
VATL_HUMAN	V-type proton ATPase 16 kDa proteolipid subunit	1	1	110.33	4.76E-05	18h	43.27
PSA4_HUMAN	Proteasome subunit alpha type-4	6	6	495.22	4.96E-05	18h	1.09
CKLF6_HUMAN	CKLF-like MARVEL transmembrane domain-containing protein 6	3	3	131.6	5.01E-05	18h	1.41
RSU1_HUMAN	Ras suppressor protein 1	2	2	112.08	5.13E-05	18h	1.44
AP3D1_HUMAN	AP-3 complex subunit delta-1	2	2	79.61	5.26E-05	6h	1.34
PA1B3_HUMAN	Platelet-activating factor acetylhydrolase IB subunit gamma	1	1	61.49	5.45E-05	18h	3.69
MYL6_HUMAN	Myosin light polypeptide 6	7	4	422.41	6.24E-05	18h	1.31
CALR_HUMAN	Calreticulin	11	11	1214.23	6.61E-05	6h	1.39
SNUT1_HUMAN	U4/U6.U5 tri-snRNP-associated protein 1	1	1	31.48	7.17E-05	6h	5.73
2A5D_HUMAN	Serine/threonine-protein phosphatase 2A 56 kDa regulatory subunit delta isoform	1	1	38.99	7.46E-05	6h	2.11
VDAC2_HUMAN	Voltage-dependent anion-selective channel protein 2	2	2	126.79	7.76E-05	18h	1.25
VATD_HUMAN	V-type proton ATPase subunit D	1	1	105.21	7.77E-05	18h	1.33
NUCKS_HUMAN	Nuclear ubiquitous casein and cyclin-dependent kinase substrate 1	1	1	39.75	7.84E-05	6h	2.01
RAB1A_HUMAN	Ras-related protein Rab-1A	6	1	595.52	8.37E-05	18h	1.82
TM206_HUMAN	Transmembrane protein 206	1	1	47.82	8.53E-05	6h	38.90
KCAB2_HUMAN	Voltage-gated potassium channel subunit beta-2	2	2	110.23	8.60E-05	18h	1.47
CREG1_HUMAN	Protein CREG1	1	1	42.72	9.27E-05	18h	3.25
RL15_HUMAN	60S ribosomal protein L15	6	6	360.74	9.38E-05	6h	1.17

Monocyte early (6 h) versus late (18 h) ACdEV proteomes

Accession	Description	Peptide count	Unique peptides	Confidence score	Anova (p)	Highest mean condition	Max fold change
SORCN_HUMAN	Sorcin	2	2	93.68	9.56E-05	6h	1.29
RS7_HUMAN	40S ribosomal protein S7	5	5	333.01	0.0001	18h	1.91
RAB7B_HUMAN	Ras-related protein Rab-7b	1	1	77.8	0.0001	18h	16.39
BID_HUMAN	BH3-interacting domain death agonist	1	1	149.18	0.00011	18h	2.57
EIFCL_HUMAN	Eukaryotic translation initiation factor 3 subunit C-like protein	2	2	92.85	0.00011	6h	2.61
SAR1A_HUMAN	GTP-binding protein SAR1a	1	1	31.25	0.00011	18h	3.56
DDX3Y_HUMAN	ATP-dependent RNA helicase DDX3Y	1	1	63.93	0.00011	6h	7.28
ECM29_HUMAN	Proteasome adapter and scaffold protein ECM29	2	2	92.75	0.00011	18h	46.66
GTR9_HUMAN	Solute carrier family 2, facilitated glucose transporter member 9	1	1	48.09	0.00011	6h	1.76
AK1A1_HUMAN	Alcohol dehydrogenase [NADP(+)]	1	1	51.25	0.00012	6h	1.11
RL24_HUMAN	60S ribosomal protein L24	3	3	160.47	0.00012	18h	1.18
TCPE_HUMAN	T-complex protein 1 subunit epsilon	14	13	1184.37	0.00012	6h	1.50
SYSC_HUMAN	Serine--tRNA ligase, cytoplasmic	1	1	35.99	0.00012	18h	1.28
ICLN_HUMAN	Methylosome subunit pICln	1	1	104.84	0.00013	18h	1.44
RM12_HUMAN	39S ribosomal protein L12, mitochondrial	1	1	42.88	0.00014	18h	Infinity
U520_HUMAN	U5 small nuclear ribonucleoprotein 200 kDa helicase	1	1	55.92	0.00014	18h	2.51
HIKES_HUMAN	Protein Hikeshi	1	1	89.94	0.00015	6h	1.20
PGP_HUMAN	Glycerol-3-phosphate phosphatase	2	2	85.91	0.00016	6h	1.15
CDK1_HUMAN	Cyclin-dependent kinase 1	2	2	88.25	0.00016	18h	1.39
COPD_HUMAN	Coatomer subunit delta	3	3	146.38	0.00017	6h	1.18
TPC1_HUMAN	Two pore calcium channel protein 1	1	1	38.42	0.00018	6h	2.27
EHD4_HUMAN	EH domain-containing protein 4	4	2	291.65	0.00018	6h	1.87
RMD1_HUMAN	Regulator of microtubule dynamics protein 1	1	1	66.78	0.00018	18h	1.22
OR8H2_HUMAN	Olfactory receptor 8H2	1	1	43.68	0.00018	18h	1.32
FLNB_HUMAN	Filamin-B	1	1	60.17	0.00019	18h	3.28
ATPG_HUMAN	ATP synthase subunit gamma, mitochondrial	3	3	193.37	0.0002	18h	1.07
PSB1_HUMAN	Proteasome subunit beta type-1	11	11	676.38	0.00021	18h	1.34
SPCS3_HUMAN	Signal peptidase complex subunit 3	1	1	71.91	0.00022	18h	1.63
EFR3A_HUMAN	Protein EFR3 homolog A	3	2	309.37	0.00022	6h	1.88
IPYR_HUMAN	Inorganic pyrophosphatase	3	2	233.43	0.00023	18h	1.18
IST1_HUMAN	IST1 homolog	2	2	102.57	0.00023	6h	1.29
PHB2_HUMAN	Prohibitin-2	1	1	48.85	0.00023	18h	1.59
ODO2_HUMAN	Dihydrolipoyllysine-residue succinyltransferase component of 2-oxoglutarate dehydrogenase complex, mitochondrial	1	1	50.1	0.00024	18h	1.35
AP3B1_HUMAN	AP-3 complex subunit beta-1	1	1	49.2	0.00024	18h	1.47
UCRIL_HUMAN	Putative cytochrome b-c1 complex subunit Rieske-like protein 1	1	1	59.13	0.00024	18h	2.02
MALD1_HUMAN	MARVEL domain-containing protein 1	1	1	45.54	0.00024	18h	24.98
CALM1_HUMAN	Calmodulin-1	3	3	231.48	0.00024	18h	1.81
TMED2_HUMAN	Transmembrane emp24 domain-containing protein 2	1	1	79.78	0.00024	18h	111.05
ERD22_HUMAN	ER lumen protein-retaining receptor 2	1	1	96.99	0.00025	18h	7.76
FA5_HUMAN	Coagulation factor V	2	2	111.13	0.00025	18h	1.36
CLCA_HUMAN	Clathrin light chain A	1	1	39.99	0.00025	18h	1.17
DECR_HUMAN	2,4-dienoyl-CoA reductase, mitochondrial	1	1	42.39	0.00025	18h	1.37

Monocyte early (6 h) versus late (18 h) ACdEV proteomes

Accession	Description	Peptide count	Unique peptides	Confidence score	Anova (p)	Highest mean condition	Max fold change
REEP6_HUMAN	Receptor expression-enhancing protein 6	1	1	70.75	0.00026	18h	3.24
RS24_HUMAN	40S ribosomal protein S24	1	1	34.67	0.00027	18h	1.58
GSTO1_HUMAN	Glutathione S-transferase omega-1	1	1	61.5	0.00027	18h	1.13
RAB21_HUMAN	Ras-related protein Rab-21	4	3	320.04	0.00028	18h	1.91
RL18A_HUMAN	60S ribosomal protein L18a	2	2	75.44	0.00029	18h	1.28
IF5A1_HUMAN	Eukaryotic translation initiation factor 5A-1	3	1	192.98	0.00029	18h	3.18
ATP6_HUMAN	ATP synthase subunit a	1	1	57.13	0.0003	18h	1.65
ACTB_HUMAN	Actin, cytoplasmic 1	35	10	4552.7	0.00031	18h	1.23
VIME_HUMAN	Vimentin	1	1	73.85	0.00032	18h	5.74
TRI25_HUMAN	E3 ubiquitin/ISG15 ligase TRIM25	3	3	139.63	0.00032	6h	1.24
MDHC_HUMAN	Malate dehydrogenase, cytoplasmic	8	8	707.77	0.00033	6h	1.09
DUT_HUMAN	Deoxyuridine 5'-triphosphate nucleotidohydrolase, mitochondrial	3	3	315.71	0.00035	18h	1.20
TMED5_HUMAN	Transmembrane emp24 domain-containing protein 5	1	1	46.29	0.00036	18h	69.25
ITA4_HUMAN	Integrin alpha-4	6	6	339.27	0.0004	18h	1.15
ACTA_HUMAN	Actin, aortic smooth muscle	24	1	2169.23	0.0004	18h	1.23
TCPD_HUMAN	T-complex protein 1 subunit delta	10	10	911.18	0.00042	6h	1.11
GCN1_HUMAN	eIF-2-alpha kinase activator GCN1	1	1	53.49	0.00043	18h	7.76
RAB32_HUMAN	Ras-related protein Rab-32	2	1	92.94	0.00044	18h	18.80
RS17_HUMAN	40S ribosomal protein S17	3	3	137.85	0.00045	18h	1.61
SH3K1_HUMAN	SH3 domain-containing kinase-binding protein 1	1	1	60.39	0.00047	18h	13.33
GNAI2_HUMAN	Guanine nucleotide-binding protein G(i) subunit alpha-2	9	6	1121.71	0.00049	18h	1.52
PLPHP_HUMAN	Pyridoxal phosphate homeostasis protein	3	3	185.1	0.00051	18h	1.33
SC23A_HUMAN	Protein transport protein Sec23A	2	1	75.26	0.00051	6h	121.20
DERL1_HUMAN	Derlin-1	1	1	34.18	0.00053	18h	1.64
SDCB1_HUMAN	Syntenin-1	4	3	413.54	0.00055	18h	1.50
MIF_HUMAN	Macrophage migration inhibitory factor	1	1	68.85	0.00055	6h	1.49
CUL1_HUMAN	Cullin-1	1	1	62.2	0.00056	6h	5.42
TFR1_HUMAN	Transferrin receptor protein 1	12	10	827.74	0.00056	18h	1.16
TBB5_HUMAN	Tubulin beta chain	18	4	1488.52	0.00058	18h	1.66
MCM4_HUMAN	DNA replication licensing factor MCM4	2	2	96.99	0.00063	6h	1.29
CSN8_HUMAN	COP9 signalosome complex subunit 8	1	1	84.99	0.00065	18h	10.96
CALL3_HUMAN	Calmodulin-like protein 3	1	1	32.05	0.00066	18h	1.75
MOB1A_HUMAN	MOB kinase activator 1A	2	2	87.81	0.00068	18h	1.25
SWP70_HUMAN	Switch-associated protein 70	1	1	56.02	0.0007	6h	5.37
TBB4B_HUMAN	Tubulin beta-4B chain	18	1	1589.73	0.00075	18h	1.86
H2AV_HUMAN	Histone H2A.V	2	1	168.69	0.00075	18h	14.88
APLP2_HUMAN	Amyloid-like protein 2	1	1	78.31	0.00075	6h	1.64
NDKA_HUMAN	Nucleoside diphosphate kinase A	7	3	432.22	0.00077	18h	1.09
SKP1_HUMAN	S-phase kinase-associated protein 1	2	2	97.29	0.00079	18h	2.64
SNG2_HUMAN	Synaptogyrin-2	2	2	99.82	0.00081	18h	1.15
PFKAL_HUMAN	ATP-dependent 6-phosphofructokinase, liver type	6	5	401.12	0.00082	18h	1.08
MPCP_HUMAN	Phosphate carrier protein, mitochondrial	4	4	191.76	0.00084	18h	1.07
CD36_HUMAN	Platelet glycoprotein 4	1	1	71.71	0.00086	6h	2.48

Monocyte early (6 h) versus late (18 h) ACdEV proteomes

Accession	Description	Peptide count	Unique peptides	Confidence score	Anova (p)	Highest mean condition	Max fold change
ACOC_HUMAN	Cytoplasmic aconitate hydratase	1	1	43.62	0.00087	6h	2.00
QSOX1_HUMAN	Sulfhydryl oxidase 1	1	1	31.99	0.00088	6h	8.48
CY24B_HUMAN	Cytochrome b-245 heavy chain	2	2	108.82	0.0009	18h	1.21
GYS1_HUMAN	Glycogen [starch] synthase, muscle	1	1	52.16	0.0009	6h	1.72
SRP72_HUMAN	Signal recognition particle subunit SRP72	1	1	46.26	0.00091	6h	20.50
NUD16_HUMAN	U8 snoRNA-decapping enzyme	1	1	39.4	0.00091	18h	2.24
UBC12_HUMAN	NEDD8-conjugating enzyme Ubc12	3	3	134.54	0.00099	6h	1.17
PRPS1_HUMAN	Ribose-phosphate pyrophosphokinase 1	2	1	110.78	0.00101	18h	1.47
RS2_HUMAN	40S ribosomal protein S2	6	6	360.21	0.00102	18h	1.08
S10AB_HUMAN	Protein S100-A11	1	1	135.93	0.00106	18h	1.81
SYPL1_HUMAN	Synaptophysin-like protein 1	1	1	56.75	0.00115	18h	1.13
SFT2A_HUMAN	Vesicle transport protein SFT2A	1	1	73.34	0.0012	18h	1.76
TM164_HUMAN	Transmembrane protein 164	1	1	46.01	0.00121	18h	1.12
RAC1_HUMAN	Ras-related C3 botulinum toxin substrate 1	5	2	256.73	0.00123	6h	1.09
UBP14_HUMAN	Ubiquitin carboxyl-terminal hydrolase 14	1	1	36.7	0.00134	18h	1.06
RAB5B_HUMAN	Ras-related protein Rab-5B	3	1	179.31	0.00138	18h	1.80
NB5R3_HUMAN	NADH-cytochrome b5 reductase 3	2	2	115.34	0.00147	6h	1.11
MCM2_HUMAN	DNA replication licensing factor MCM2	4	3	199.57	0.00153	6h	1.48
RB11A_HUMAN	Ras-related protein Rab-11A	9	1	656.7	0.00162	18h	9.43
RL29_HUMAN	60S ribosomal protein L29	2	2	150.04	0.00164	6h	1.13
COX2_HUMAN	Cytochrome c oxidase subunit 2	3	3	169.02	0.00173	18h	1.31
LASP1_HUMAN	LIM and SH3 domain protein 1	2	2	107.8	0.00177	18h	1.35
PARK7_HUMAN	Protein/nucleic acid deglycase DJ-1	16	14	1306.94	0.00179	6h	1.16
PRDX1_HUMAN	Peroxiredoxin-1	14	10	880.93	0.0018	18h	1.06
COTL1_HUMAN	Coactosin-like protein	1	1	37.35	0.00187	6h	1.21
EMP3_HUMAN	Epithelial membrane protein 3	1	1	40.75	0.00189	18h	1.36
MTCH2_HUMAN	Mitochondrial carrier homolog 2	1	1	33.47	0.00197	6h	1.12
TNPO1_HUMAN	Transportin-1	1	1	31.3	0.00198	6h	1.76
PRDX6_HUMAN	Peroxiredoxin-6	9	9	592.78	0.00199	18h	1.10
LIRA2_HUMAN	Leukocyte immunoglobulin-like receptor subfamily A member 2	1	1	59.29	0.00205	6h	1.56
PNPH_HUMAN	Purine nucleoside phosphorylase	10	9	571.43	0.0021	18h	1.06
IDI1_HUMAN	Isopentenyl-diphosphate Delta-isomerase 1	1	1	38.34	0.00219	18h	1.44
DCPS_HUMAN	m7GpppX diphosphatase	1	1	36.17	0.00232	6h	1.60
FUBP2_HUMAN	Far upstream element-binding protein 2	2	2	108.69	0.00235	6h	1.84
ARK72_HUMAN	Aflatoxin B1 aldehyde reductase member 2	2	2	141.13	0.00236	6h	1.05
EF1B_HUMAN	Elongation factor 1-beta	4	3	253.13	0.00236	18h	1.10
RL35_HUMAN	60S ribosomal protein L35	2	2	102.89	0.00241	6h	1.10
UGGG1_HUMAN	UDP-glucose:glycoprotein glucosyltransferase 1	1	1	67.29	0.00274	18h	1.49
DNSL1_HUMAN	Deoxyribonuclease-1-like 1	1	1	48.07	0.00274	18h	1.10
SSA27_HUMAN	Sjoegren syndrome/scleroderma autoantigen 1	1	1	33.58	0.00279	18h	1.61
BASI_HUMAN	Basigin	8	8	811.09	0.00279	6h	1.24
SC22B_HUMAN	Vesicle-trafficking protein SEC22b	2	2	120.78	0.00291	18h	1.78
AP2A2_HUMAN	AP-2 complex subunit alpha-2	6	3	471.11	0.00312	6h	1.62

Monocyte early (6 h) versus late (18 h) ACdEV proteomes

Accession	Description	Peptide count	Unique peptides	Confidence score	Anova (p)	Highest mean condition	Max fold change
DCXR_HUMAN	L-xylulose reductase	1	1	73.21	0.00327	18h	7.92
EF1A1_HUMAN	Elongation factor 1-alpha 1	11	5	936.07	0.00342	18h	1.54
MYO1F_HUMAN	Unconventional myosin-If	3	2	357.64	0.00343	6h	1.53
SND1_HUMAN	Staphylococcal nuclease domain-containing protein 1	3	2	125.57	0.00344	6h	1.07
HMGB2_HUMAN	High mobility group protein B2	3	2	148.36	0.00357	18h	1.13
S10A9_HUMAN	Protein S100-A9	4	4	315.6	0.00361	18h	1.51
ARBK1_HUMAN	Beta-adrenergic receptor kinase 1	1	1	35.83	0.00362	6h	1.35
CAH2_HUMAN	Carbonic anhydrase 2	12	12	926.98	0.00404	6h	1.03
CAPR1_HUMAN	Caprin-1	2	2	111.97	0.00407	6h	1.50
TP4A1_HUMAN	Protein tyrosine phosphatase type IVA 1	3	1	184.97	0.00413	18h	51.99
IQGA1_HUMAN	Ras GTPase-activating-like protein IQGAP1	33	31	2481.62	0.00415	6h	1.05
SSRD_HUMAN	Translocon-associated protein subunit delta	2	2	148.52	0.00419	18h	4.58
RACK1_HUMAN	Receptor of activated protein C kinase 1	6	6	331.27	0.0044	18h	1.04
CTR1_HUMAN	High affinity cationic amino acid transporter 1	1	1	66.53	0.00497	18h	1.24
GELS_HUMAN	Gelsolin	14	14	1357.35	0.00511	6h	1.25
RHOC_HUMAN	Rho-related GTP-binding protein RhoC	4	2	339.69	0.00554	18h	4.82
PYRG1_HUMAN	CTP synthase 1	10	8	831.62	0.00556	6h	1.06
AHNK_HUMAN	Neuroblast differentiation-associated protein AHNAK	1	1	55.03	0.0057	18h	1.97
PSMD4_HUMAN	26S proteasome non-ATPase regulatory subunit 4	1	1	49.06	0.00587	18h	1.79
ITPA_HUMAN	Inosine triphosphate pyrophosphatase	1	1	37.71	0.00594	18h	2.09
LKHA4_HUMAN	Leukotriene A-4 hydrolase	4	4	162.84	0.00599	18h	1.06
CD70_HUMAN	CD70 antigen	2	2	148.35	0.00602	6h	1.15
ACPH_HUMAN	Acylamino-acid-releasing enzyme	3	3	229.18	0.00612	6h	1.12
RS8_HUMAN	40S ribosomal protein S8	6	6	525.26	0.00639	6h	1.07
RL10A_HUMAN	60S ribosomal protein L10a	3	3	127.98	0.00684	6h	1.05
DNPH1_HUMAN	2'-deoxynucleoside 5'-phosphate N-hydrolase 1	2	2	154.95	0.00706	18h	18.87
PLP2_HUMAN	Proteolipid protein 2	1	1	66.86	0.00723	6h	1.08
HUWE1_HUMAN	E3 ubiquitin-protein ligase HUWE1	1	1	45.8	0.00731	18h	1.70
VDAC3_HUMAN	Voltage-dependent anion-selective channel protein 3	3	2	249.78	0.00768	18h	1.07
CSK22_HUMAN	Casein kinase II subunit alpha'	1	1	62.6	0.00777	6h	1.09
GTR1_HUMAN	Solute carrier family 2, facilitated glucose transporter member 1	6	5	459.15	0.00809	6h	1.17
EIF3K_HUMAN	Eukaryotic translation initiation factor 3 subunit K	2	2	162.71	0.00817	6h	1.13
SYAC_HUMAN	Alanine--tRNA ligase, cytoplasmic	9	8	716.2	0.00827	18h	1.11
IF1AX_HUMAN	Eukaryotic translation initiation factor 1A, X-chromosomal	1	1	34.34	0.00892	18h	5.77
EIF2D_HUMAN	Eukaryotic translation initiation factor 2D	1	1	53.39	0.0095	18h	1.43
RS15_HUMAN	40S ribosomal protein S15	4	4	350.37	0.00974	18h	1.11
RL27_HUMAN	60S ribosomal protein L27	4	4	234.79	0.00976	18h	1.04
CPPED_HUMAN	Serine/threonine-protein phosphatase CPPED1	2	2	103.78	0.01063	18h	1.08
DHB12_HUMAN	Very-long-chain 3-oxoacyl-CoA reductase	2	2	133.02	0.01215	6h	1.08
HNRPK_HUMAN	Heterogeneous nuclear ribonucleoprotein K	9	9	653.17	0.01221	18h	1.15
ASC_HUMAN	Apoptosis-associated speck-like protein containing a CARD	8	8	588.39	0.01281	18h	1.12
RL10_HUMAN	60S ribosomal protein L10	3	1	144.01	0.01301	6h	1.21
MFS10_HUMAN	Major facilitator superfamily domain-containing protein 10	1	1	84.2	0.01303	18h	1.31

Monocyte early (6 h) versus late (18 h) ACdEV proteomes

Accession	Description	Peptide count	Unique peptides	Confidence score	Anova (p)	Highest mean condition	Max fold change
EMAL4_HUMAN	Echinoderm microtubule-associated protein-like 4	1	1	33.12	0.01345	18h	1.08
ERBIN_HUMAN	Erbin	2	2	101.21	0.01376	6h	2.05
VAMP8_HUMAN	Vesicle-associated membrane protein 8	2	2	117.63	0.01396	18h	1.05
ADHX_HUMAN	Alcohol dehydrogenase class-3	2	2	116.73	0.01437	6h	1.08
PRDX2_HUMAN	Peroxiredoxin-2	6	5	460.06	0.01463	18h	1.08
COPB_HUMAN	Coatomer subunit beta	2	1	137.53	0.01474	6h	1.22
U5S1_HUMAN	116 kDa U5 small nuclear ribonucleoprotein component	2	2	102.48	0.01475	6h	1.09
CDC37_HUMAN	Hsp90 co-chaperone Cdc37	3	3	326.29	0.01503	6h	1.35
TRPV2_HUMAN	Transient receptor potential cation channel subfamily V member 2	1	1	78.9	0.01508	6h	1.09
RL9_HUMAN	60S ribosomal protein L9	4	4	310.37	0.01539	18h	1.22
IMPA1_HUMAN	Inositol monophosphatase 1	1	1	58.94	0.01604	6h	1.06
RUVB1_HUMAN	RuvB-like 1	8	8	659.22	0.01643	18h	1.06
AR6P1_HUMAN	ADP-ribosylation factor-like protein 6-interacting protein 1	2	2	184.86	0.01669	18h	1.85
EMB_HUMAN	Embigin	1	1	86.81	0.01827	6h	9.79
GMFG_HUMAN	Glia maturation factor gamma	4	3	213.73	0.01881	18h	1.11
VP13D_HUMAN	Vacuolar protein sorting-associated protein 13D	2	2	67.26	0.01919	6h	1.13
EIF3M_HUMAN	Eukaryotic translation initiation factor 3 subunit M	2	2	166.18	0.02025	18h	1.24
OPA1_HUMAN	Dynamin-like 120 kDa protein, mitochondrial	1	1	69.36	0.02095	6h	3.23
VATB2_HUMAN	V-type proton ATPase subunit B, brain isoform	4	3	255.5	0.02118	18h	1.47
MD2L1_HUMAN	Mitotic spindle assembly checkpoint protein MAD2A	1	1	66.48	0.02151	18h	2.75
AHSA1_HUMAN	Activator of 90 kDa heat shock protein ATPase homolog 1	1	1	44.41	0.02168	6h	40.90
TALDO_HUMAN	Transaldolase	11	10	668.59	0.02196	6h	1.30
ATPB_HUMAN	ATP synthase subunit beta, mitochondrial	13	13	1088.63	0.02288	18h	1.07
CCAR2_HUMAN	Cell cycle and apoptosis regulator protein 2	1	1	59.32	0.02296	18h	1.24
RS9_HUMAN	40S ribosomal protein S9	11	11	490.7	0.02346	18h	1.03
SURF4_HUMAN	Surfeit locus protein 4	3	3	250.2	0.02381	18h	1.08
SAR1B_HUMAN	GTP-binding protein SAR1b	1	1	50.71	0.02437	18h	1.14
LEG1_HUMAN	Galectin-1	2	2	161.45	0.02473	6h	1.06
RAB5A_HUMAN	Ras-related protein Rab-5A	5	2	348.51	0.02475	18h	1.18
LIMS1_HUMAN	LIM and senescent cell antigen-like-containing domain protein 1	1	1	73.9	0.02503	18h	1.08
PVR_HUMAN	Poliovirus receptor	1	1	73.13	0.02556	6h	1.31
ROA3_HUMAN	Heterogeneous nuclear ribonucleoprotein A3	2	2	134.84	0.02598	18h	1.40
ANM5_HUMAN	Protein arginine N-methyltransferase 5	4	4	208.95	0.02623	6h	1.09
XRP2_HUMAN	Protein XRP2	4	4	191.74	0.02625	18h	1.13
OST48_HUMAN	Dolichyl-diphosphooligosaccharide--protein glycosyltransferase 48 kDa subunit	4	4	215.31	0.02654	18h	1.14
PSMD6_HUMAN	26S proteasome non-ATPase regulatory subunit 6	6	6	391.77	0.027	18h	1.23
ECHD1_HUMAN	Ethylmalonyl-CoA decarboxylase	1	1	60.65	0.02775	6h	1.10
ALDOC_HUMAN	Fructose-bisphosphate aldolase C	3	3	428.31	0.0283	6h	1.13
FBXL7_HUMAN	F-box/LRR-repeat protein 7	1	1	35.54	0.02922	6h	1.64
THIL_HUMAN	Acetyl-CoA acetyltransferase, mitochondrial	2	2	144.55	0.02936	6h	1.95
1433G_HUMAN	14-3-3 protein gamma	6	3	575.56	0.02953	6h	1.05
PSD12_HUMAN	26S proteasome non-ATPase regulatory subunit 12	5	5	250.52	0.02973	18h	1.58
RN123_HUMAN	E3 ubiquitin-protein ligase RNF123	1	1	35.04	0.03018	6h	1.14

Monocyte early (6 h) versus late (18 h) ACdEV proteomes

Accession	Description	Peptide count	Unique peptides	Confidence score	Anova (p)	Highest mean condition	Max fold change
2ABA_HUMAN	Serine/threonine-protein phosphatase 2A 55 kDa regulatory subunit B alpha isoform	2	2	160.33	0.03074	18h	1.13
PLEK_HUMAN	Pleckstrin	3	3	132.89	0.03185	18h	1.83
IF2A_HUMAN	Eukaryotic translation initiation factor 2 subunit 1	4	4	258.79	0.03235	18h	1.06
STK24_HUMAN	Serine/threonine-protein kinase 24	1	1	45.83	0.03256	18h	2.78
KT3K_HUMAN	Ketosamine-3-kinase	1	1	33.5	0.03262	6h	1.03
LDHB_HUMAN	L-lactate dehydrogenase B chain	13	13	958.13	0.03428	6h	1.03
RS27A_HUMAN	Ubiquitin-40S ribosomal protein S27a	4	4	294.2	0.03494	18h	1.10
H2A2A_HUMAN	Histone H2A type 2-A	5	2	459.04	0.03541	18h	3.57
PSD13_HUMAN	26S proteasome non-ATPase regulatory subunit 13	6	6	370.16	0.03621	18h	1.19
CD14_HUMAN	Monocyte differentiation antigen CD14	2	2	206.63	0.03695	18h	1.74
SYWC_HUMAN	Tryptophan--tRNA ligase, cytoplasmic	5	5	297.37	0.03783	18h	1.09
NASP_HUMAN	Nuclear autoantigenic sperm protein	1	1	36.15	0.03821	6h	1.42
AP2M1_HUMAN	AP-2 complex subunit mu	1	1	44.65	0.03834	18h	1.47
6PGL_HUMAN	6-phosphogluconolactonase	5	5	303.32	0.03849	6h	1.02
BLMH_HUMAN	Bleomycin hydrolase	2	2	155.39	0.03877	18h	1.16
AGRL2_HUMAN	Adhesion G protein-coupled receptor L2	2	1	122.98	0.03921	18h	8.80
ILF3_HUMAN	Interleukin enhancer-binding factor 3	2	2	128.84	0.0401	6h	2.02
TIMP3_HUMAN	Metalloproteinase inhibitor 3	1	1	50.3	0.04132	18h	1.07
PDIA6_HUMAN	Protein disulfide-isomerase A6	10	10	1127.9	0.04194	18h	1.20
IDH3A_HUMAN	Isocitrate dehydrogenase [NAD] subunit alpha, mitochondrial	1	1	35.21	0.04208	18h	1.72
C1TC_HUMAN	C-1-tetrahydrofolate synthase, cytoplasmic	5	5	276.71	0.04272	18h	1.24
CAB39_HUMAN	Calcium-binding protein 39	4	2	180.97	0.04371	18h	1.57
RTCA_HUMAN	RNA 3'-terminal phosphate cyclase	1	1	50.8	0.04446	18h	2.23
GRHPR_HUMAN	Glyoxylate reductase/hydroxypyruvate reductase	1	1	59.19	0.04506	6h	1.09
GNAQ_HUMAN	Guanine nucleotide-binding protein G(q) subunit alpha	6	4	458.49	0.04527	18h	1.49
AIMP2_HUMAN	Aminoacyl tRNA synthase complex-interacting multifunctional protein 2	1	1	44.79	0.04544	18h	2.83
OSBP1_HUMAN	Oxysterol-binding protein 1	1	1	47.13	0.04584	6h	1.11
NHRF1_HUMAN	Na(+)/H(+) exchange regulatory cofactor NHE-RF1	1	1	53.75	0.04703	18h	2.74
ITA10_HUMAN	Integrin alpha-10	1	1	39.05	0.04712	18h	1.10
CH3L1_HUMAN	Chitinase-3-like protein 1	4	4	251.6	0.04727	18h	1.46
PSMD7_HUMAN	26S proteasome non-ATPase regulatory subunit 7	7	7	365.85	0.04749	18h	1.20
FACE1_HUMAN	CAAX prenyl protease 1 homolog	7	7	421.65	0.04814	18h	1.35
IF4A1_HUMAN	Eukaryotic initiation factor 4A-I	9	4	771.74	0.04855	18h	1.76
FAAA_HUMAN	Fumarylacetoacetase	3	3	124.83	0.04927	6h	1.23
SPEE_HUMAN	Spermidine synthase	5	5	270.8	0.04988	18h	1.04
AT1B1_HUMAN	Sodium/potassium-transporting ATPase subunit beta-1	1	1	38.67	0.05004	18h	1.33
ASNA_HUMAN	ATPase ASNA1	1	1	50.39	0.05009	18h	1.61
GNAS1_HUMAN	Guanine nucleotide-binding protein G(s) subunit alpha isoforms Xlas	7	6	536.89	0.05037	18h	1.41
CLIC4_HUMAN	Chloride intracellular channel protein 4	2	1	131.3	0.05109	18h	1.16
RU17_HUMAN	U1 small nuclear ribonucleoprotein 70 kDa	1	1	42.26	0.05261	6h	3.71
S29A1_HUMAN	Equilibrative nucleoside transporter 1	3	3	214.65	0.053	6h	1.17
UB2L3_HUMAN	Ubiquitin-conjugating enzyme E2 L3	2	1	199.21	0.05331	18h	2.72
PDIA1_HUMAN	Protein disulfide-isomerase	27	27	2083	0.05419	6h	1.14

Monocyte early (6 h) versus late (18 h) ACdEV proteomes

Accession	Description	Peptide count	Unique peptides	Confidence score	Anova (p)	Highest mean condition	Max fold change
ATX10_HUMAN	Ataxin-10	1	1	53.24	0.05618	18h	2.08
GNAI3_HUMAN	Guanine nucleotide-binding protein G(k) subunit alpha	9	6	881.8	0.05618	18h	1.27
AP180_HUMAN	Clathrin coat assembly protein AP180	1	1	84.5	0.0563	18h	1.64
SETLP_HUMAN	Protein SETSIP	1	1	63.73	0.05651	6h	2.10
PGK1_HUMAN	Phosphoglycerate kinase 1	21	14	1798.09	0.05841	6h	1.15
IF5_HUMAN	Eukaryotic translation initiation factor 5	1	1	33.78	0.05937	18h	1.30
STAT3_HUMAN	Signal transducer and activator of transcription 3	2	2	176.73	0.05982	6h	4.53
PGAM1_HUMAN	Phosphoglycerate mutase 1	5	2	496.43	0.06109	18h	1.03
6PGD_HUMAN	6-phosphogluconate dehydrogenase, decarboxylating	11	11	813.77	0.06123	6h	1.13
ATAD1_HUMAN	ATPase family AAA domain-containing protein 1	1	1	39.52	0.0613	18h	1.41
ZN500_HUMAN	Zinc finger protein 500	1	1	34.49	0.06148	18h	1.15
TSNAX_HUMAN	Translin-associated protein X	1	1	81.41	0.06162	18h	1.25
RLA2_HUMAN	60S acidic ribosomal protein P2	2	1	120.39	0.06177	6h	1.26
GDIB_HUMAN	Rab GDP dissociation inhibitor beta	18	11	1226.87	0.06184	18h	1.12
CLC11_HUMAN	C-type lectin domain family 11 member A	5	4	368.97	0.06216	18h	1.96
HNRPC_HUMAN	Heterogeneous nuclear ribonucleoproteins C1/C2	1	1	32.52	0.06361	18h	1.22
CD99_HUMAN	CD99 antigen	2	2	164.55	0.06432	18h	1.11
TPSN_HUMAN	Tapasin	1	1	36.62	0.06637	18h	1.27
P2RY8_HUMAN	P2Y purinoceptor 8	1	1	59.22	0.06776	18h	1.06
PAIRB_HUMAN	Plasminogen activator inhibitor 1 RNA-binding protein	1	1	31.89	0.06894	18h	2.35
PRS6A_HUMAN	26S proteasome regulatory subunit 6A	2	2	103.73	0.06904	18h	1.60
VTNC_HUMAN	Vitronectin	1	1	67.8	0.06905	18h	1.70
LYN_HUMAN	Tyrosine-protein kinase Lyn	7	4	525.72	0.06949	18h	1.83
SIAS_HUMAN	Sialic acid synthase	1	1	65.97	0.06974	6h	1.25
PSB6_HUMAN	Proteasome subunit beta type-6	3	3	172.06	0.07051	18h	1.06
PCP_HUMAN	Lysosomal Pro-X carboxypeptidase	1	1	35.97	0.07228	6h	1.32
GLOD4_HUMAN	Glyoxalase domain-containing protein 4	1	1	105.33	0.07257	18h	1.05
S19A1_HUMAN	Folate transporter 1	1	1	70.72	0.07354	18h	1.32
NONO_HUMAN	Non-POU domain-containing octamer-binding protein	2	2	148.38	0.07357	18h	1.09
AP1M1_HUMAN	AP-1 complex subunit mu-1	1	1	62.36	0.07377	18h	1.28
MOT1_HUMAN	Monocarboxylate transporter 1	5	5	297.07	0.07547	18h	1.25
FSCN1_HUMAN	Fascin	6	6	286.45	0.07572	18h	1.29
CN37_HUMAN	2',3'-cyclic-nucleotide 3'-phosphodiesterase	4	3	220.1	0.0761	18h	1.70
BIEA_HUMAN	Biliverdin reductase A	1	1	41.32	0.07675	18h	1.33
RHG01_HUMAN	Rho GTPase-activating protein 1	1	1	42.09	0.07678	6h	1.30
VATC1_HUMAN	V-type proton ATPase subunit C 1	2	1	78.04	0.07842	18h	1.24
FUMH_HUMAN	Fumarate hydratase, mitochondrial	1	1	38.61	0.08046	18h	2.84
YBOX1_HUMAN	Nuclease-sensitive element-binding protein 1	1	1	109.95	0.08283	6h	1.15
ILF2_HUMAN	Interleukin enhancer-binding factor 2	6	6	403.72	0.08286	6h	1.60
SPRE_HUMAN	Sepiapterin reductase	1	1	40.11	0.08375	18h	1.19
TPP1_HUMAN	Tripeptidyl-peptidase 1	3	3	297.77	0.08458	18h	1.85
DDX6_HUMAN	Probable ATP-dependent RNA helicase DDX6	1	1	43.37	0.08688	18h	1.12
RINI_HUMAN	Ribonuclease inhibitor	4	4	360.82	0.08696	6h	1.10

Monocyte early (6 h) versus late (18 h) ACdEV proteomes

Accession	Description	Peptide count	Unique peptides	Confidence score	Anova (p)	Highest mean condition	Max fold change
PPIA_HUMAN	Peptidyl-prolyl cis-trans isomerase A	12	11	795.48	0.08757	18h	1.11
HMGA1_HUMAN	High mobility group protein HMG-I/HMG-Y	1	1	32.03	0.08788	18h	1.14
1A02_HUMAN	HLA class I histocompatibility antigen, A-2 alpha chain	12	3	1380.92	0.08806	18h	1.23
FPPS_HUMAN	Farnesyl pyrophosphate synthase	3	3	177.61	0.08809	6h	1.08
ANX11_HUMAN	Annexin A11	5	4	242	0.08826	18h	1.19
TMOD3_HUMAN	Tropomodulin-3	2	2	143.19	0.0921	18h	1.11
SAE2_HUMAN	SUMO-activating enzyme subunit 2	3	3	160.01	0.09225	6h	1.06
ARP3_HUMAN	Actin-related protein 3	12	9	793	0.09262	18h	1.11
SERC_HUMAN	Phosphoserine aminotransferase	5	5	301.57	0.09333	6h	1.26
ANM1_HUMAN	Protein arginine N-methyltransferase 1	5	5	260.15	0.09387	6h	1.33
WDR61_HUMAN	WD repeat-containing protein 61	1	1	35.02	0.09422	18h	2.64
FCL_HUMAN	GDP-L-fucose synthase	1	1	52.9	0.09442	18h	1.15
PSB10_HUMAN	Proteasome subunit beta type-10	1	1	69.64	0.09687	18h	1.21
BROX_HUMAN	BRO1 domain-containing protein BROX	4	4	378.63	0.09867	6h	1.13
PCYOX_HUMAN	Prenylcysteine oxidase 1	1	1	65.66	0.09889	18h	1.17
ARP2_HUMAN	Actin-related protein 2	10	10	1108.06	0.10104	18h	1.07
NADC_HUMAN	Nicotinate-nucleotide pyrophosphorylase [carboxylating]	1	1	46.64	0.10104	6h	1.07
RPE_HUMAN	Ribulose-phosphate 3-epimerase	2	2	78.19	0.10135	6h	1.19
ERLN2_HUMAN	Erlin-2	4	2	269.53	0.10153	18h	1.16
ILEU_HUMAN	Leukocyte elastase inhibitor	2	2	158.38	0.10206	6h	1.10
DYN2_HUMAN	Dynamin-2	1	1	37.99	0.1023	6h	1.44
TBB2A_HUMAN	Tubulin beta-2A chain	14	1	1234.42	0.10336	18h	1.05
GNA13_HUMAN	Guanine nucleotide-binding protein subunit alpha-13	3	2	216.34	0.10356	18h	1.47
ERP44_HUMAN	Endoplasmic reticulum resident protein 44	1	1	52.2	0.10587	18h	1.13
CD82_HUMAN	CD82 antigen	3	3	228.28	0.10702	18h	1.09
COR1B_HUMAN	Coronin-1B	1	1	42.81	0.10724	6h	1.06
GFPT1_HUMAN	Glutamine--fructose-6-phosphate aminotransferase [isomerizing] 1	1	1	85.52	0.10847	6h	1.58
G6PD_HUMAN	Glucose-6-phosphate 1-dehydrogenase	7	7	362.6	0.10941	18h	1.11
UB2V2_HUMAN	Ubiquitin-conjugating enzyme E2 variant 2	4	1	254.97	0.10964	6h	1.05
FCGRN_HUMAN	IgG receptor FcRn large subunit p51	1	1	36.12	0.10988	18h	1.30
TTL12_HUMAN	Tubulin--tyrosine ligase-like protein 12	1	1	44.34	0.11116	6h	1.04
TBA1A_HUMAN	Tubulin alpha-1A chain	11	1	1230.24	0.11167	6h	1.07
FUS_HUMAN	RNA-binding protein FUS	1	1	86.11	0.11346	6h	1.07
SAHH_HUMAN	Adenosylhomocysteinase	10	8	604.15	0.11521	6h	1.08
2A5G_HUMAN	Serine/threonine-protein phosphatase 2A 56 kDa regulatory subunit gamma isoform	1	1	32.67	0.11534	18h	1.24
NP1L1_HUMAN	Nucleosome assembly protein 1-like 1	5	4	282.39	0.11546	18h	1.06
IF4E2_HUMAN	Eukaryotic translation initiation factor 4E type 2	1	1	34.2	0.11803	18h	1.05
CHM2A_HUMAN	Charged multivesicular body protein 2a	1	1	59.27	0.12033	18h	1.03
JAM1_HUMAN	Junctional adhesion molecule A	3	3	212.2	0.12416	18h	1.22
H2B1A_HUMAN	Histone H2B type 1-A	2	1	108.65	0.12436	6h	1.69
DCTP1_HUMAN	dCTP pyrophosphatase 1	1	1	37.86	0.12692	18h	2.14
API5_HUMAN	Apoptosis inhibitor 5	1	1	83.87	0.12814	6h	2.41
BST1_HUMAN	ADP-ribosyl cyclase/cyclic ADP-ribose hydrolase 2	5	5	244.92	0.13	18h	1.10

Monocyte early (6 h) versus late (18 h) ACdEV proteomes

Accession	Description	Peptide count	Unique peptides	Confidence score	Anova (p)	Highest mean condition	Max fold change
ZDHC5_HUMAN	Palmitoyltransferase ZDHHC5	1	1	36.78	0.13111	18h	1.85
HBS1L_HUMAN	HBS1-like protein	1	1	31.92	0.13155	18h	1.13
CPSF7_HUMAN	Cleavage and polyadenylation specificity factor subunit 7	2	2	86.83	0.13326	6h	1.07
SIRB1_HUMAN	Signal-regulatory protein beta-1	1	1	71.22	0.13381	6h	1.28
EIF3B_HUMAN	Eukaryotic translation initiation factor 3 subunit B	1	1	42.01	0.13499	18h	1.19
IDHP_HUMAN	Isocitrate dehydrogenase [NADP], mitochondrial	3	2	169.48	0.13636	18h	1.37
PARP1_HUMAN	Poly [ADP-ribose] polymerase 1	10	10	623.52	0.14477	18h	1.07
NUDC_HUMAN	Nuclear migration protein nudC	1	1	71.48	0.14669	6h	1.48
PUR8_HUMAN	Adenylosuccinate lyase	4	4	206.76	0.148	6h	1.23
PRP19_HUMAN	Pre-mRNA-processing factor 19	1	1	47.09	0.15023	6h	1.16
SF3A1_HUMAN	Splicing factor 3A subunit 1	1	1	43.39	0.15035	6h	1.72
TYPH_HUMAN	Thymidine phosphorylase	9	8	700.58	0.15043	6h	1.18
UCHL3_HUMAN	Ubiquitin carboxyl-terminal hydrolase isozyme L3	1	1	82	0.15171	6h	1.03
PFD5_HUMAN	Prefoldin subunit 5	2	2	103.86	0.15652	18h	1.12
PDIA3_HUMAN	Protein disulfide-isomerase A3	16	16	1242.99	0.15812	18h	1.20
DCUP_HUMAN	Uroporphyrinogen decarboxylase	2	2	68.67	0.15984	6h	1.29
SYHC_HUMAN	Histidine--tRNA ligase, cytoplasmic	2	1	104.79	0.16074	6h	1.09
PE2R4_HUMAN	Prostaglandin E2 receptor EP4 subtype	1	1	102.52	0.16181	6h	1.42
CAH11_HUMAN	Carbonic anhydrase-related protein 11	1	1	31.3	0.16203	18h	1.03
NP1L4_HUMAN	Nucleosome assembly protein 1-like 4	4	3	286.85	0.16671	6h	1.15
EIF3E_HUMAN	Eukaryotic translation initiation factor 3 subunit E	4	4	208.03	0.16878	6h	1.06
DHSO_HUMAN	Sorbitol dehydrogenase	1	1	63.15	0.1729	6h	1.41
CNDP2_HUMAN	Cytosolic non-specific dipeptidase	2	2	126.09	0.17298	6h	1.06
LA_HUMAN	Lupus La protein	2	1	129.44	0.17329	6h	1.60
RL8_HUMAN	60S ribosomal protein L8	3	3	250.39	0.17474	18h	1.03
SYFB_HUMAN	Phenylalanine--tRNA ligase beta subunit	3	3	131.48	0.17837	6h	1.03
RTN4_HUMAN	Reticulon-4	3	3	166.28	0.17886	6h	1.06
DKC1_HUMAN	H/ACA ribonucleoprotein complex subunit 4	2	2	104.11	0.18588	6h	1.15
PP2BA_HUMAN	Serine/threonine-protein phosphatase 2B catalytic subunit alpha isoform	4	1	217.4	0.18921	18h	1.08
CD38_HUMAN	ADP-ribosyl cyclase/cyclic ADP-ribose hydrolase 1	4	4	432.3	0.19132	18h	1.15
ARP3B_HUMAN	Actin-related protein 3B	2	1	161.78	0.19144	18h	1.17
RSSA_HUMAN	40S ribosomal protein SA	5	5	440.38	0.19437	6h	1.10
RCC2_HUMAN	Protein RCC2	3	3	151.19	0.20455	6h	1.14
SNX6_HUMAN	Sorting nexin-6	1	1	39.18	0.20624	18h	1.56
ENOA_HUMAN	Alpha-enolase	29	23	3025.11	0.2092	6h	1.08
BZW2_HUMAN	Basic leucine zipper and W2 domain-containing protein 2	3	2	124.54	0.21185	18h	1.20
KPCA_HUMAN	Protein kinase C alpha type	1	1	58.41	0.21347	6h	1.24
CSN4_HUMAN	COP9 signalosome complex subunit 4	3	3	169.04	0.21805	6h	1.15
APMAP_HUMAN	Adipocyte plasma membrane-associated protein	1	1	42.22	0.22067	18h	1.07
EIF3A_HUMAN	Eukaryotic translation initiation factor 3 subunit A	4	4	290.39	0.22536	6h	1.05
FCGRB_HUMAN	High affinity immunoglobulin gamma Fc receptor IB	1	1	74.08	0.23484	18h	1.03
LZIC_HUMAN	Protein LZIC	2	2	81.59	0.24179	18h	1.16
RBBP4_HUMAN	Histone-binding protein RBBP4	3	3	166.18	0.24231	6h	1.09

Monocyte early (6 h) versus late (18 h) ACdEV proteomes

Accession	Description	Peptide count	Unique peptides	Confidence score	Anova (p)	Highest mean condition	Max fold change
DX39B_HUMAN	Spliceosome RNA helicase DDX39B	4	1	248.18	0.24551	6h	1.13
THIC_HUMAN	Acetyl-CoA acetyltransferase, cytosolic	4	4	187.06	0.24846	6h	1.33
MMP14_HUMAN	Matrix metalloproteinase-14	1	1	36.45	0.25105	6h	1.08
MOT4_HUMAN	Monocarboxylate transporter 4	7	7	462.67	0.25461	6h	1.17
AMPL_HUMAN	Cytosol aminopeptidase	18	18	1045.04	0.25473	18h	1.08
UGPA_HUMAN	UTP--glucose-1-phosphate uridylyltransferase	6	6	332.54	0.25474	6h	1.10
S10A8_HUMAN	Protein S100-A8	3	3	219.4	0.2568	18h	1.44
STML2_HUMAN	Stomatin-like protein 2, mitochondrial	1	1	47.66	0.26387	6h	1.60
GMPPA_HUMAN	Mannose-1-phosphate guanyltransferase alpha	1	1	84.29	0.26633	6h	1.62
S38A1_HUMAN	Sodium-coupled neutral amino acid transporter 1	2	2	113.78	0.27122	18h	1.02
SERA_HUMAN	D-3-phosphoglycerate dehydrogenase	7	5	548.8	0.27374	18h	1.13
HCDH_HUMAN	Hydroxyacyl-coenzyme A dehydrogenase, mitochondrial	3	3	143.06	0.27606	18h	1.06
IF4A3_HUMAN	Eukaryotic initiation factor 4A-III	2	1	232.59	0.28027	18h	1.04
VN1R5_HUMAN	Vomeronasal type-1 receptor 5	1	1	31.88	0.28304	6h	1.15
S10A4_HUMAN	Protein S100-A4	1	1	42.75	0.29469	6h	1.02
EIF3H_HUMAN	Eukaryotic translation initiation factor 3 subunit H	1	1	39.19	0.2956	6h	1.17
FNTA_HUMAN	Protein farnesyltransferase/geranylgeranyltransferase type-1 subunit alpha	1	1	46.44	0.29683	18h	1.85
RL18_HUMAN	60S ribosomal protein L18	4	4	323.08	0.29922	18h	1.02
SEP11_HUMAN	Septin-11	5	2	249.9	0.31241	18h	1.26
PSA7_HUMAN	Proteasome subunit alpha type-7	6	4	356.84	0.31295	6h	1.02
PHB_HUMAN	Prohibitin	2	2	81.35	0.31664	18h	1.03
GNS_HUMAN	N-acetylglucosamine-6-sulfatase	1	1	51.72	0.3168	18h	1.04
KYNU_HUMAN	Kynureninase	8	8	683.64	0.32105	18h	1.04
DPP2_HUMAN	Dipeptidyl peptidase 2	3	3	190.6	0.32142	18h	1.11
NAA50_HUMAN	N-alpha-acetyltransferase 50	1	1	43.74	0.32256	6h	1.03
GMIP_HUMAN	GEM-interacting protein	1	1	49.62	0.32377	6h	1.33
PPM1F_HUMAN	Protein phosphatase 1F	1	1	59.07	0.32972	18h	1.95
CPNE2_HUMAN	Copine-2	1	1	40	0.33585	6h	1.09
COR1A_HUMAN	Coronin-1A	8	8	633.9	0.33638	18h	1.08
HEM3_HUMAN	Porphobilinogen deaminase	1	1	68.34	0.33985	6h	1.32
S61A1_HUMAN	Protein transport protein Sec61 subunit alpha isoform 1	2	1	113.08	0.3421	6h	1.13
RUVB2_HUMAN	RuvB-like 2	7	7	535.54	0.35049	18h	1.06
CAP1_HUMAN	Adenylyl cyclase-associated protein 1	36	34	3827.38	0.35632	6h	1.06
PURA2_HUMAN	Adenylosuccinate synthetase isozyme 2	3	3	167.39	0.35707	6h	1.06
HNRPR_HUMAN	Heterogeneous nuclear ribonucleoprotein R	4	1	268.09	0.36537	6h	1.10
VKORL_HUMAN	Vitamin K epoxide reductase complex subunit 1-like protein 1	1	1	57.67	0.36817	18h	1.14
RL11_HUMAN	60S ribosomal protein L11	2	2	203.52	0.37371	6h	1.05
NAGAB_HUMAN	Alpha-N-acetylgalactosaminidase	1	1	105.14	0.37414	18h	1.36
GLGB_HUMAN	1,4-alpha-glucan-branching enzyme	1	1	74.43	0.37455	18h	1.04
ESYT2_HUMAN	Extended synaptotagmin-2	1	1	33.06	0.37512	18h	1.08
GAPR1_HUMAN	Golgi-associated plant pathogenesis-related protein 1	2	2	163.33	0.38085	18h	1.02
SFPQ_HUMAN	Splicing factor, proline- and glutamine-rich	3	3	230.72	0.38281	18h	1.01

Monocyte early (6 h) versus late (18 h) ACdEV proteomes

Accession	Description	Peptide count	Unique peptides	Confidence score	Anova (p)	Highest mean condition	Max fold change
ERLN1_HUMAN	Erlin-1	3	1	183.49	0.38477	18h	1.28
IF2GL_HUMAN	Putative eukaryotic translation initiation factor 2 subunit 3-like protein	2	2	105.11	0.38884	6h	1.04
SRC_HUMAN	Proto-oncogene tyrosine-protein kinase Src	2	1	87.79	0.39386	18h	2.05
DDX17_HUMAN	Probable ATP-dependent RNA helicase DDX17	3	2	184.67	0.39397	6h	1.12
MRP_HUMAN	MARCKS-related protein	1	1	123.07	0.39426	6h	1.09
TCPH_HUMAN	T-complex protein 1 subunit eta	15	14	1249.66	0.40208	6h	1.02
IF4G1_HUMAN	Eukaryotic translation initiation factor 4 gamma 1	1	1	42.45	0.40999	6h	1.14
PUR6_HUMAN	Multifunctional protein ADE2	7	7	425.26	0.41372	6h	1.04
RS23_HUMAN	40S ribosomal protein S23	2	2	108.39	0.42185	6h	1.03
SERPH_HUMAN	Serpin H1	1	1	103.65	0.43828	6h	1.08
CSN5_HUMAN	COP9 signalosome complex subunit 5	1	1	54.21	0.43989	6h	1.04
TFG_HUMAN	Protein TFG	2	1	101.77	0.44144	18h	1.06
TRXR1_HUMAN	Thioredoxin reductase 1, cytoplasmic	1	1	64.64	0.44703	6h	1.09
DX39A_HUMAN	ATP-dependent RNA helicase DDX39A	3	1	196.59	0.45817	18h	1.43
H2B1B_HUMAN	Histone H2B type 1-B	6	1	585.35	0.4607	6h	1.06
CISY_HUMAN	Citrate synthase, mitochondrial	2	2	115.72	0.46152	6h	1.04
SEPT2_HUMAN	Septin-2	2	2	173.47	0.46678	18h	1.03
SF3A3_HUMAN	Splicing factor 3A subunit 3	1	1	72.07	0.47902	6h	1.01
TXTP_HUMAN	Tricarboxylate transport protein, mitochondrial	2	2	104.53	0.48029	18h	1.02
UCHL5_HUMAN	Ubiquitin carboxyl-terminal hydrolase isozyme L5	2	2	103.19	0.48065	6h	1.08
RTCB_HUMAN	tRNA-splicing ligase RtcB homolog	1	1	64.18	0.49426	18h	1.17
MEF2D_HUMAN	Myocyte-specific enhancer factor 2D	1	1	68.35	0.49543	6h	1.01
RL4_HUMAN	60S ribosomal protein L4	2	2	111.32	0.5028	6h	1.03
XPO2_HUMAN	Exportin-2	9	9	496.7	0.50785	6h	1.02
SC24A_HUMAN	Protein transport protein Sec24A	1	1	32.22	0.51145	18h	1.10
NEUL_HUMAN	Neurolysin, mitochondrial	1	1	83.34	0.52085	6h	1.03
S43A3_HUMAN	Solute carrier family 43 member 3	3	3	264.82	0.52553	6h	1.04
HS105_HUMAN	Heat shock protein 105 kDa	1	1	38.18	0.53168	18h	1.16
SNRPA_HUMAN	U1 small nuclear ribonucleoprotein A	1	1	43.73	0.53713	6h	1.04
1433E_HUMAN	14-3-3 protein epsilon	11	9	770.14	0.53892	6h	1.01
CHM4B_HUMAN	Charged multivesicular body protein 4b	1	1	62.8	0.54719	18h	1.03
NIBAN_HUMAN	Protein Niban	1	1	103.48	0.55512	6h	1.02
BAG2_HUMAN	BAG family molecular chaperone regulator 2	2	2	122.03	0.55931	6h	1.02
SPB6_HUMAN	Serpin B6	1	1	56.57	0.56376	18h	1.13
ATPA_HUMAN	ATP synthase subunit alpha, mitochondrial	12	11	863.72	0.56546	6h	1.02
ALDOA_HUMAN	Fructose-bisphosphate aldolase A	15	15	1822.25	0.56688	18h	1.01
PA2G4_HUMAN	Proliferation-associated protein 2G4	3	2	145.82	0.57092	6h	1.06
POTEF_HUMAN	POTE ankyrin domain family member F	6	1	985.46	0.58402	18h	1.09
ESTD_HUMAN	S-formylglutathione hydrolase	3	3	163.39	0.58647	18h	1.01
EIF3I_HUMAN	Eukaryotic translation initiation factor 3 subunit I	2	1	118.47	0.59504	6h	1.02
VAT1_HUMAN	Synaptic vesicle membrane protein VAT-1 homolog	6	6	669.43	0.59934	6h	1.03
THOP1_HUMAN	Thimet oligopeptidase	2	2	76.28	0.60204	6h	1.03
TCPB_HUMAN	T-complex protein 1 subunit beta	16	15	1168.89	0.60292	6h	1.03

Monocyte early (6 h) versus late (18 h) ACdEV proteomes

Accession	Description	Peptide count	Unique peptides	Confidence score	Anova (p)	Highest mean condition	Max fold change
PPCE_HUMAN	Prolyl endopeptidase	2	2	185.32	0.60797	18h	1.01
CYBR1_HUMAN	Cytochrome b reductase 1	2	2	103.25	0.60855	6h	1.04
ALDH2_HUMAN	Aldehyde dehydrogenase, mitochondrial	1	1	72.3	0.61559	18h	1.01
RO60_HUMAN	60 kDa SS-A/Ro ribonucleoprotein	2	2	140.03	0.62319	6h	1.08
GFAP_HUMAN	Glial fibrillary acidic protein	1	1	39.52	0.62467	18h	1.03
SYK_HUMAN	Lysine--tRNA ligase	3	3	136.29	0.63017	6h	1.03
KAP2_HUMAN	cAMP-dependent protein kinase type II-alpha regulatory subunit	4	3	295.03	0.63218	6h	1.04
PDZD8_HUMAN	PDZ domain-containing protein 8	1	1	31.3	0.65431	18h	1.01
PTBP1_HUMAN	Polypyrimidine tract-binding protein 1	4	3	192.67	0.65717	6h	1.04
KCC2D_HUMAN	Calcium/calmodulin-dependent protein kinase type II subunit delta	1	1	99.45	0.6652	18h	1.02
MCEM1_HUMAN	Mast cell-expressed membrane protein 1	2	2	95.7	0.68157	18h	1.01
EIF3F_HUMAN	Eukaryotic translation initiation factor 3 subunit F	4	4	338.45	0.68749	18h	1.03
UN45A_HUMAN	Protein unc-45 homolog A	1	1	34.04	0.69605	6h	1.02
RS26_HUMAN	40S ribosomal protein S26	2	1	112.84	0.70341	18h	1.03
SYDC_HUMAN	Aspartate--tRNA ligase, cytoplasmic	4	4	247.05	0.71228	18h	1.02
P2RY2_HUMAN	P2Y purinoceptor 2	1	1	89.62	0.7166	18h	1.08
RL7A_HUMAN	60S ribosomal protein L7a	5	4	349.36	0.71909	6h	1.00
PRS4_HUMAN	26S proteasome regulatory subunit 4	1	1	140.48	0.72078	6h	1.03
ERF1_HUMAN	Eukaryotic peptide chain release factor subunit 1	3	3	197.21	0.72079	18h	1.04
VASP_HUMAN	Vasodilator-stimulated phosphoprotein	7	7	475.95	0.72767	6h	1.03
GSHR_HUMAN	Glutathione reductase, mitochondrial	3	2	212	0.73025	6h	1.03
LACB2_HUMAN	Endoribonuclease LACTB2	1	1	47.58	0.73142	18h	1.01
OLA1_HUMAN	Obg-like ATPase 1	5	5	411.66	0.73947	6h	1.01
NAGK_HUMAN	N-acetyl-D-glucosamine kinase	1	1	34.87	0.75021	6h	1.01
PFD2_HUMAN	Prefoldin subunit 2	2	2	177.92	0.75219	6h	1.02
PSD11_HUMAN	26S proteasome non-ATPase regulatory subunit 11	4	4	249.87	0.7531	18h	1.02
DRA_HUMAN	HLA class II histocompatibility antigen, DR alpha chain	2	1	74.04	0.76946	6h	1.01
DHB4_HUMAN	Peroxisomal multifunctional enzyme type 2	1	1	71.74	0.77829	18h	1.02
DYH8_HUMAN	Dynein heavy chain 8, axonemal	1	1	33.78	0.7896	6h	1.01
SEPT7_HUMAN	Septin-7	2	1	72.11	0.79024	6h	1.03
CSN1_HUMAN	COP9 signalosome complex subunit 1	1	1	45.43	0.80193	6h	1.02
HGH1_HUMAN	Protein HGH1 homolog	1	1	31.83	0.80345	18h	1.13
OTUB1_HUMAN	Ubiquitin thioesterase OTUB1	1	1	50.73	0.81788	18h	1.00
DNJA1_HUMAN	DnaJ homolog subfamily A member 1	1	1	43.68	0.8987	18h	1.70
SNX1_HUMAN	Sorting nexin-1	1	1	36.54	0.90533	6h	1.00
PRS10_HUMAN	26S proteasome regulatory subunit 10B	1	1	36.22	0.9106	18h	1.08
PNCB_HUMAN	Nicotinate phosphoribosyltransferase	7	6	531.88	0.9142	6h	1.00
GNPI1_HUMAN	Glucosamine-6-phosphate isomerase 1	2	1	115.56	0.91757	6h	1.01
SCPDL_HUMAN	Saccharopine dehydrogenase-like oxidoreductase	1	1	69.96	0.92258	18h	1.60
IMA3_HUMAN	Importin subunit alpha-3	1	1	129.22	0.92422	6h	1.03
IDHC_HUMAN	Isocitrate dehydrogenase [NADP] cytoplasmic	5	4	419.89	0.94607	6h	1.00
ARGL1_HUMAN	Arginine and glutamate-rich protein 1	1	1	32.49	0.94918	18h	1.26
IF4A2_HUMAN	Eukaryotic initiation factor 4A-II	6	1	552.06	0.95012	6h	1.00

Monocyte early (6 h) versus late (18 h) ACdEV proteomes

Accession	Description	Peptide count	Unique peptides	Confidence score	Anova (p)	Highest mean condition	Max fold change
LCP2_HUMAN	Lymphocyte cytosolic protein 2	1	1	45.6	0.95014	18h	1.78
AL9A1_HUMAN	4-trimethylaminobutyraldehyde dehydrogenase	4	4	186.7	0.95768	6h	1.00
ROA1_HUMAN	Heterogeneous nuclear ribonucleoprotein A1	5	1	317.1	0.96058	6h	3.14
UBE2K_HUMAN	Ubiquitin-conjugating enzyme E2 K	2	2	109.89	0.9621	18h	1.02
NUCB2_HUMAN	Nucleobindin-2	1	1	54.96	0.97095	18h	1.18
KCRB_HUMAN	Creatine kinase B-type	1	1	56.32	0.98327	18h	1.18
G6PI_HUMAN	Glucose-6-phosphate isomerase	13	13	903.95	0.98533	18h	1.01
XPO7_HUMAN	Exportin-7	1	1	35.39	0.98731	18h	1.00
CAPG_HUMAN	Macrophage-capping protein	8	7	835.05	0.98961	18h	1.00
BYST_HUMAN	Bystin	1	1	37.94	0.99002	18h	1.08
NDRG1_HUMAN	Protein NDRG1	2	2	119.47	0.99868	18h	1.02

Table 3: B cell early (6 h) versus late (18 h) ACdEV proteomes

Accession	Description	Peptide count	Unique peptides	Confidence score	Anova (p)	Highest mean condition	Max fold change
PDIA3_HUMAN	Protein disulfide-isomerase A3	13	12	784.56	2.03E-12	6h	2.77
ATPA_HUMAN	ATP synthase subunit alpha, mitochondrial	12	9	826.45	4.26E-12	6h	2.33
CH60_HUMAN	60 kDa heat shock protein, mitochondrial	19	19	1705.06	9.77E-12	6h	3.08
RAB1B_HUMAN	Ras-related protein Rab-1B	8	1	522.46	1.02E-11	18h	2.36
PSME1_HUMAN	Proteasome activator complex subunit 1	7	7	442.75	1.17E-11	18h	3.14
PR40A_HUMAN	Pre-mRNA-processing factor 40 homolog A	1	1	47.01	1.30E-11	6h	Infinity
ROA2_HUMAN	Heterogeneous nuclear ribonucleoproteins A2/B1	4	4	254.27	2.16E-11	6h	2.27
CALR_HUMAN	Calreticulin OS=Homo sapiens	5	5	472.17	2.20E-11	6h	5.45
RLA0_HUMAN	60S acidic ribosomal protein P0	10	3	862.52	3.46E-11	6h	5.89
6PGD_HUMAN	6-phosphogluconate dehydrogenase, decarboxylating	6	6	403.87	3.94E-11	18h	1.99
KPYM_HUMAN	Pyruvate kinase PKM	22	20	1880.3	4.12E-11	18h	1.90
ENOA_HUMAN	Alpha-enolase	28	23	2670.65	5.51E-11	18h	2.60
1433T_HUMAN	14-3-3 protein theta	3	2	342.16	9.98E-11	18h	1.77
MDHM_HUMAN	Malate dehydrogenase, mitochondrial	8	8	747.29	1.13E-10	6h	5.08
ATPB_HUMAN	ATP synthase subunit beta, mitochondrial	18	18	1635.67	1.29E-10	6h	3.92
RAB5C_HUMAN	Ras-related protein Rab-5C	3	2	232.6	1.29E-10	18h	1.99
RAB7A_HUMAN	Ras-related protein Rab-7a	8	8	613.22	1.36E-10	18h	1.64
LKHA4_HUMAN	Leukotriene A-4 hydrolase	5	5	272.47	1.77E-10	18h	2.24
COR1A_HUMAN	Coronin-1A	8	8	707.06	2.35E-10	18h	1.64
RD23B_HUMAN	UV excision repair protein RAD23 homolog B	1	1	77.71	2.36E-10	6h	3.87
AMPL_HUMAN	Cytosol aminopeptidase	12	12	887.41	2.65E-10	18h	1.69
TKT_HUMAN	Transketolase	14	13	1165.49	2.77E-10	18h	3.48
HNRPQ_HUMAN	Heterogeneous nuclear ribonucleoprotein Q	4	3	362.5	3.54E-10	6h	2.85
TPIS_HUMAN	Triosephosphate isomerase	10	9	1128.25	3.67E-10	18h	3.05
LGUL_HUMAN	Lactoylglutathione lyase	3	3	162.6	4.67E-10	18h	3.22
RL13_HUMAN	60S ribosomal protein L13	4	4	262.57	5.42E-10	18h	1.94
GDIB_HUMAN	Rab GDP dissociation inhibitor beta	19	10	1475.92	5.89E-10	18h	1.93
PDIA1_HUMAN	Protein disulfide-isomerase	2	2	156.02	6.05E-10	6h	3.07
SEPT2_HUMAN	Septin-2	3	3	156.55	6.12E-10	18h	1.96
SYK_HUMAN	Lysine--tRNA ligase	1	1	41	6.34E-10	6h	Infinity
SYDC_HUMAN	Aspartate--tRNA ligase, cytoplasmic	5	5	265.35	6.82E-10	6h	2.30
VTNC_HUMAN	Vitronectin	1	1	190.44	7.42E-10	6h	2.50
RGS12_HUMAN	Regulator of G-protein signaling 12	1	1	33.7	7.45E-10	18h	6.09
MPRD_HUMAN	Cation-dependent mannose-6-phosphate receptor	1	1	62.65	7.59E-10	6h	7.55
PGM1_HUMAN	Phosphoglucomutase-1	1	1	56.14	8.15E-10	18h	14.99
RB11A_HUMAN	Ras-related protein Rab-11A	5	4	363.29	8.28E-10	18h	1.79
RS15_HUMAN	40S ribosomal protein S15	3	3	265.92	1.05E-09	18h	2.48
FKBP4_HUMAN	Peptidyl-prolyl cis-trans isomerase FKBP4	4	4	287.56	1.13E-09	18h	1.84
PGAM1_HUMAN	Phosphoglycerate mutase 1	9	5	597.39	1.34E-09	18h	2.85

NUDC_HUMAN	Nuclear migration protein nudC	1	1	64.33	1.47E-09	18h	2.61
RS26_HUMAN	40S ribosomal protein S26	2	1	165.2	1.49E-09	6h	2.39
CPIN1_HUMAN	Anamorsin	1	1	46.1	1.67E-09	18h	4.10
BAP31_HUMAN	B-cell receptor-associated protein 31	1	1	36.57	1.86E-09	18h	1.74
ARF1_HUMAN	ADP-ribosylation factor 1	6	3	435.44	1.89E-09	18h	2.39
RL3_HUMAN	60S ribosomal protein L3	6	5	349.09	2.05E-09	6h	2.30
PIBF1_HUMAN	Progesterone-induced-blocking factor 1	1	1	35.96	2.17E-09	18h	1.74
PNPH_HUMAN	Purine nucleoside phosphorylase	6	6	443.59	2.23E-09	18h	1.81
SYPL1_HUMAN	Synaptophysin-like protein 1	2	2	111.65	2.40E-09	6h	3.06
GSHB_HUMAN	Glutathione synthetase	1	1	42.1	2.53E-09	6h	3.83
1433Z_HUMAN	14-3-3 protein zeta/delta	8	6	650.22	2.57E-09	18h	1.74
STMN1_HUMAN	Stathmin	3	2	286.9	2.88E-09	18h	2.78
ADT2_HUMAN	ADP/ATP translocase 2	7	2	353.37	2.98E-09	6h	2.62
ARHG4_HUMAN	Rho guanine nucleotide exchange factor 4	1	1	52.71	3.39E-09	6h	3.15
UCHL3_HUMAN	Ubiquitin carboxyl-terminal hydrolase isozyme L3	1	1	41.47	3.40E-09	18h	2.15
UGPA_HUMAN	UTP--glucose-1-phosphate uridylyltransferase	5	5	311.9	3.47E-09	18h	2.00
DUT_HUMAN	Deoxyuridine 5'-triphosphate nucleotidohydrolase, mitochondrial	2	2	165.79	3.49E-09	18h	2.36
NDKA_HUMAN	Nucleoside diphosphate kinase A	7	4	481.36	3.66E-09	18h	2.74
RL23A_HUMAN	60S ribosomal protein L23a	2	2	133.97	4.06E-09	18h	2.33
UCRIL_HUMAN	Putative cytochrome b-c1 complex subunit Rieske-like protein 1	1	1	91.67	4.18E-09	6h	4.29
GDIR1_HUMAN	Rho GDP-dissociation inhibitor 1	4	4	303.71	4.73E-09	18h	2.40
SEPT7_HUMAN	Septin-7	2	1	90.25	4.89E-09	18h	13.73
G6PI_HUMAN	Glucose-6-phosphate isomerase	9	9	681.29	5.31E-09	18h	1.92
TPD54_HUMAN	Tumor protein D54	3	3	216.6	5.82E-09	6h	2.02
SAHH_HUMAN	Adenosylhomocysteinase	10	9	648.34	6.29E-09	18h	1.58
PGK1_HUMAN	Phosphoglycerate kinase 1	14	8	978.14	8.21E-09	18h	2.06
RL26L_HUMAN	60S ribosomal protein L26-like 1	2	2	107.83	8.27E-09	18h	3.07
TFR1_HUMAN	Transferrin receptor protein 1	19	17	1516.59	8.94E-09	6h	1.85
DREB_HUMAN	Drebrin	1	1	59.58	9.14E-09	6h	2.09
H4_HUMAN	Histone H4	7	7	420.04	9.24E-09	6h	2.74
LMNB1_HUMAN	Lamin-B1	4	4	260.65	9.45E-09	18h	1.82
RL14_HUMAN	60S ribosomal protein L14	2	2	134.34	1.01E-08	6h	1.64
MRT4_HUMAN	mRNA turnover protein 4 homolog	1	1	38.63	1.04E-08	6h	2.26
CDC37_HUMAN	Hsp90 co-chaperone Cdc37	1	1	49.69	1.09E-08	18h	106.49
ATP5H_HUMAN	ATP synthase subunit d, mitochondrial	4	4	258.81	1.16E-08	6h	2.70
RL12_HUMAN	60S ribosomal protein L12	3	3	342.2	1.30E-08	6h	1.71
GANAB_HUMAN	Neutral alpha-glucosidase AB	1	1	83.97	1.30E-08	6h	3.16
HMGB1_HUMAN	High mobility group protein B1	6	4	386.12	1.46E-08	18h	1.78
TSNAX_HUMAN	Translin-associated protein X	1	1	98.94	1.52E-08	18h	5.01
CD63_HUMAN	CD63 antigen	1	1	48.47	1.55E-08	6h	1.94
PRKDC_HUMAN	DNA-dependent protein kinase catalytic subunit	26	20	1535.66	1.60E-08	6h	2.11
AT5F1_HUMAN	ATP synthase F(0) complex subunit B1, mitochondrial	1	1	39.71	1.78E-08	6h	9.89
HSP7C_HUMAN	Heat shock cognate 71 kDa protein	26	17	2441.41	1.83E-08	18h	1.83

SUMO2_HUMAN	Small ubiquitin-related modifier 2	1	1	101.32	1.90E-08	18h	2.05
NACAM_HUMAN	Nascent polypeptide-associated complex subunit alpha, muscle-specific form	4	4	407.39	2.01E-08	18h	1.48
MAP2_HUMAN	Methionine aminopeptidase 2	2	2	139.12	2.02E-08	18h	2.60
H2A1D_HUMAN	Histone H2A type 1-D	3	1	305.24	2.24E-08	6h	1.79
EVL_HUMAN	Ena/VASP-like protein	1	1	57.83	2.29E-08	18h	3.81
RL6_HUMAN	60S ribosomal protein L6	10	10	749.84	2.32E-08	6h	1.91
PRDX3_HUMAN	Thioredoxin-dependent peroxide reductase, mitochondrial	2	2	106.63	2.43E-08	6h	6.05
TCPE_HUMAN	T-complex protein 1 subunit epsilon	10	8	1004.98	2.45E-08	18h	1.43
THIC_HUMAN	Acetyl-CoA acetyltransferase, cytosolic	2	2	121.85	2.52E-08	18h	1.86
FIBB_HUMAN	Fibrinogen beta chain	2	1	149.31	2.54E-08	18h	9.87
RS15A_HUMAN	40S ribosomal protein S15a	5	4	222.26	2.60E-08	6h	1.49
TBB5_HUMAN	Tubulin beta chain	20	4	1526.06	2.67E-08	6h	1.36
FUS_HUMAN	RNA-binding protein FUS	2	2	139.98	2.71E-08	6h	1.86
PLSL_HUMAN	Plastin-2	28	22	2648.81	2.82E-08	18h	1.89
RS2_HUMAN	40S ribosomal protein S2	7	7	429.23	2.92E-08	6h	1.47
RS4X_HUMAN	40S ribosomal protein S4, X isoform	7	3	480.81	3.11E-08	6h	1.95
PSME2_HUMAN	Proteasome activator complex subunit 2	4	4	392.5	3.12E-08	18h	4.28
HMCS1_HUMAN	Hydroxymethylglutaryl-CoA synthase, cytoplasmic	1	1	51.32	3.56E-08	18h	2.02
RCC1_HUMAN	Regulator of chromosome condensation	1	1	86.72	3.66E-08	18h	1.71
R13P3_HUMAN	Putative 60S ribosomal protein L13a protein RPL13AP3	2	2	112.47	3.87E-08	18h	1.48
NP1L4_HUMAN	Nucleosome assembly protein 1-like 4	2	1	184.05	3.95E-08	18h	2.13
BASP1_HUMAN	Brain acid soluble protein 1	6	6	739.38	4.10E-08	18h	1.48
RS9_HUMAN	40S ribosomal protein S9	9	9	418.33	4.23E-08	6h	1.53
EWS_HUMAN	RNA-binding protein EWS	1	1	74.93	4.30E-08	18h	2.93
ARPC2_HUMAN	Actin-related protein 2/3 complex subunit 2	8	8	527.81	4.33E-08	6h	1.93
DX39A_HUMAN	ATP-dependent RNA helicase DDX39A	1	1	70.26	4.49E-08	18h	15.57
STX7_HUMAN	Syntaxin-7	3	3	333.67	4.83E-08	6h	3.39
1433B_HUMAN	14-3-3 protein beta/alpha	6	2	339.77	4.90E-08	18h	2.22
RL29_HUMAN	60S ribosomal protein L29	2	2	202.75	4.90E-08	18h	1.42
XPO2_HUMAN	Exportin-2	8	7	438.11	5.17E-08	18h	1.76
TAGL2_HUMAN	Transgelin-2	8	7	781.97	5.18E-08	18h	2.01
TMEDA_HUMAN	Transmembrane emp24 domain-containing protein 10	1	1	50.69	5.18E-08	6h	1.68
C1QBP_HUMAN	Complement component 1 Q subcomponent-binding protein, mitochondrial	2	2	179.56	5.33E-08	6h	20.87
PHB2_HUMAN	Prohibitin-2	3	3	169.87	5.74E-08	6h	1.92
AIMP1_HUMAN	Aminoacyl tRNA synthase complex-interacting multifunctional protein 1	1	1	79.2	6.00E-08	6h	1.95
GNAS1_HUMAN	Guanine nucleotide-binding protein G(s) subunit alpha isoforms Xlas	6	4	564.24	6.03E-08	18h	1.55
RL18A_HUMAN	60S ribosomal protein L18a	3	3	127.88	6.23E-08	6h	1.69
NAA50_HUMAN	N-alpha-acetyltransferase 50	2	2	120.12	6.31E-08	18h	1.98
RS10_HUMAN	40S ribosomal protein S10	1	1	69.07	6.72E-08	18h	2.29
NCF2_HUMAN	Neutrophil cytosol factor 2	1	1	38.61	6.98E-08	18h	3.49
EF1G_HUMAN	Elongation factor 1-gamma	6	6	399.41	7.36E-08	18h	1.34
LA_HUMAN	Lupus La protein	3	3	185.37	7.40E-08	18h	3.09
RS14_HUMAN	40S ribosomal protein S14	1	1	59.01	7.50E-08	6h	3.03

PDIA6_HUMAN	Protein disulfide-isomerase A6	3	3	184.93	7.69E-08	6h	7.33
PARP1_HUMAN	Poly [ADP-ribose] polymerase 1	15	15	1109.44	8.38E-08	6h	1.48
2B13_HUMAN	HLA class II histocompatibility antigen, DRB1-3 chain	6	1	450.87	8.38E-08	18h	4.43
MSHR_HUMAN	Melanocyte-stimulating hormone receptor	1	1	38.16	8.47E-08	6h	2.04
H3C_HUMAN	Histone H3.3C	2	1	137.09	9.03E-08	6h	1.65
VDAC1_HUMAN	Voltage-dependent anion-selective channel protein 1	8	7	552.54	9.84E-08	6h	2.65
SMC4_HUMAN	Structural maintenance of chromosomes protein 4	1	1	47.94	1.02E-07	6h	1.99
CD47_HUMAN	Leukocyte surface antigen CD47	3	3	166.96	1.04E-07	18h	2.25
RAN_HUMAN	GTP-binding nuclear protein Ran	5	5	318.33	1.05E-07	18h	1.32
IF4A2_HUMAN	Eukaryotic initiation factor 4A-II	5	1	435.16	1.15E-07	18h	194.93
ATPO_HUMAN	ATP synthase subunit O, mitochondrial	1	1	45.58	1.16E-07	6h	1.55
H12_HUMAN	Histone H1.2	7	1	467.74	1.21E-07	18h	2.44
FA5_HUMAN	Coagulation factor V	8	7	463	1.36E-07	6h	1.59
IDH3B_HUMAN	Isocitrate dehydrogenase [NAD] subunit beta, mitochondrial	1	1	37.73	1.39E-07	6h	2.65
VATB2_HUMAN	V-type proton ATPase subunit B, brain isoform	1	1	48.6	1.39E-07	6h	221.06
CLIC1_HUMAN	Chloride intracellular channel protein 1	4	4	390.07	1.56E-07	6h	1.95
CSK21_HUMAN	Casein kinase II subunit alpha	4	4	249.35	1.58E-07	6h	2.22
ADT3_HUMAN	ADP/ATP translocase 3	6	1	301.49	1.60E-07	6h	3.58
RS13_HUMAN	40S ribosomal protein S13	4	4	226.02	1.62E-07	18h	1.55
FIBA_HUMAN	Fibrinogen alpha chain	2	2	80.94	1.72E-07	18h	1.40
PLIN3_HUMAN	Perilipin-3	1	1	45.79	1.74E-07	18h	1.78
RL7A_HUMAN	60S ribosomal protein L7a	4	4	362.89	1.85E-07	6h	1.29
RLA1_HUMAN	60S acidic ribosomal protein P1	2	1	295.94	1.86E-07	6h	1.50
MPCP_HUMAN	Phosphate carrier protein, mitochondrial	4	4	212.3	1.92E-07	6h	3.13
CAP1_HUMAN	Adenylyl cyclase-associated protein 1	6	6	468.93	1.92E-07	18h	1.64
CLH1_HUMAN	Clathrin heavy chain 1	38	28	3107.91	2.01E-07	6h	1.36
NASP_HUMAN	Nuclear autoantigenic sperm protein	2	2	124.65	2.06E-07	18h	2.24
CD20_HUMAN	B-lymphocyte antigen CD20	16	16	1434.73	2.19E-07	6h	1.63
H2AY_HUMAN	Core histone macro-H2A.1	9	6	895.97	2.32E-07	6h	2.52
WDR54_HUMAN	WD repeat-containing protein 54	1	1	34.36	2.37E-07	6h	8.14
PUR9_HUMAN	Bifunctional purine biosynthesis protein PURH	7	7	387.74	2.41E-07	18h	1.72
ELMO1_HUMAN	Engulfment and cell motility protein 1	1	1	82.6	2.45E-07	6h	1.61
TBB4B_HUMAN	Tubulin beta-4B chain	18	1	1365.29	2.54E-07	18h	1.28
PPIA_HUMAN	Peptidyl-prolyl cis-trans isomerase A	7	7	380.69	2.71E-07	18h	2.89
CD19_HUMAN	B-lymphocyte antigen CD19	8	7	737.13	2.74E-07	18h	1.44
EIF3L_HUMAN	Eukaryotic translation initiation factor 3 subunit L	2	2	75.85	2.83E-07	18h	1.35
FLOT1_HUMAN	Flotillin-1	3	3	185.87	3.14E-07	6h	1.89
H31_HUMAN	Histone H3.1	3	1	254.76	3.20E-07	6h	1.56
S29A1_HUMAN	Equilibrative nucleoside transporter 1	6	6	515.73	3.21E-07	18h	1.48
ILF3_HUMAN	Interleukin enhancer-binding factor 3	11	9	651.77	3.31E-07	6h	1.78
HPRT_HUMAN	Hypoxanthine-guanine phosphoribosyltransferase	2	2	156.25	3.77E-07	18h	2.86
ARP3_HUMAN	Actin-related protein 3	8	6	495.26	3.78E-07	6h	1.20
XPO1_HUMAN	Exportin-1	4	4	162.2	3.80E-07	18h	1.65
ACTA_HUMAN	Actin, aortic smooth muscle	17	1	1150.77	3.90E-07	6h	6.33

H2A1B_HUMAN	Histone H2A type 1-B/E	4	1	420.32	3.95E-07	6h	1.61
RHOG_HUMAN	Rho-related GTP-binding protein RhoG	2	2	108.12	3.98E-07	18h	1.35
RL9_HUMAN	60S ribosomal protein L9	3	3	244.3	4.33E-07	6h	1.87
RS3_HUMAN	40S ribosomal protein S3	7	7	473.3	4.82E-07	6h	1.48
STIP1_HUMAN	Stress-induced-phosphoprotein 1	3	3	177.59	4.91E-07	18h	1.73
RALA_HUMAN	Ras-related protein Ral-A	1	1	53.71	5.01E-07	18h	1.37
DPB1_HUMAN	HLA class II histocompatibility antigen, DP beta 1 chain	6	5	371.73	5.29E-07	18h	1.21
COPE_HUMAN	Coatomer subunit epsilon	1	1	104.31	5.50E-07	18h	3.71
CAZA1_HUMAN	F-actin-capping protein subunit alpha-1	5	4	572.68	5.58E-07	6h	2.06
ACTC_HUMAN	Actin, alpha cardiac muscle 1	15	1	976.64	5.76E-07	18h	8.23
RBM25_HUMAN	RNA-binding protein 25	1	1	39.35	6.71E-07	6h	2.21
TCPH_HUMAN	T-complex protein 1 subunit eta	15	15	1226.95	6.76E-07	18h	1.26
RSMB_HUMAN	Small nuclear ribonucleoprotein-associated proteins B and B'	4	4	213.74	6.85E-07	6h	1.36
RCC2_HUMAN	Protein RCC2	3	3	156.73	7.27E-07	18h	1.68
RS7_HUMAN	40S ribosomal protein S7	3	3	175.21	7.32E-07	18h	1.98
KHDR1_HUMAN	KH domain-containing, RNA-binding, signal transduction-associated protein 1	1	1	36.08	7.92E-07	6h	2.44
FIBG_HUMAN	Fibrinogen gamma chain	1	1	46.35	8.14E-07	18h	2.50
CNDP2_HUMAN	Cytosolic non-specific dipeptidase	5	5	319.61	8.20E-07	18h	1.37
GMPPA_HUMAN	Mannose-1-phosphate guanyltransferase alpha	1	1	35.86	8.26E-07	18h	19.51
CAPR1_HUMAN	Caprin-1	2	2	123.57	8.73E-07	6h	1.53
SODC_HUMAN	Superoxide dismutase [Cu-Zn]	1	1	41.96	9.64E-07	18h	2.01
TBB3_HUMAN	Tubulin beta-3 chain	14	1	1161.09	9.90E-07	18h	2.12
COX2_HUMAN	Cytochrome c oxidase subunit 2	1	1	45.29	1.03E-06	6h	1.98
PTBP1_HUMAN	Polypyrimidine tract-binding protein 1	4	3	283.94	1.05E-06	6h	18.20
SET_HUMAN	Protein SET	4	1	219.42	1.07E-06	18h	9.68
RS16_HUMAN	40S ribosomal protein S16	7	7	469.76	1.10E-06	6h	1.36
SNG2_HUMAN	Synaptogyrin-2	2	1	114.17	1.18E-06	6h	1.50
KAD2_HUMAN	Adenylate kinase 2, mitochondrial	5	5	376.72	1.21E-06	18h	1.38
LCAP_HUMAN	Leucyl-cystinyl aminopeptidase	10	8	530.19	1.22E-06	6h	1.49
ROA1_HUMAN	Heterogeneous nuclear ribonucleoprotein A1	3	1	241.86	1.24E-06	6h	1.72
RS3A_HUMAN	40S ribosomal protein S3a	6	6	316.8	1.26E-06	6h	1.27
HS90B_HUMAN	Heat shock protein HSP 90-beta	28	5	2461.18	1.28E-06	18h	1.51
BIP_HUMAN	Endoplasmic reticulum chaperone BiP	18	16	1495.93	1.29E-06	6h	2.44
PPIB_HUMAN	Peptidyl-prolyl cis-trans isomerase B	3	3	243.6	1.42E-06	6h	1.56
PSDE_HUMAN	26S proteasome non-ATPase regulatory subunit 14	5	5	307.69	1.45E-06	6h	1.34
TCPQ_HUMAN	T-complex protein 1 subunit theta	21	21	1570.31	1.47E-06	18h	1.21
OLA1_HUMAN	Obg-like ATPase 1	1	1	76.33	1.48E-06	18h	43.89
GDIR2_HUMAN	Rho GDP-dissociation inhibitor 2	7	7	437.41	1.48E-06	18h	1.70
CDC42_HUMAN	Cell division control protein 42 homolog	3	3	290.31	1.61E-06	18h	1.48
CD38_HUMAN	ADP-ribosyl cyclase/cyclic ADP-ribose hydrolase 1	5	5	381.05	1.61E-06	18h	1.81
CAND1_HUMAN	Cullin-associated NEDD8-dissociated protein 1	8	5	536.17	1.65E-06	18h	1.49
DQA1_HUMAN	HLA class II histocompatibility antigen, DQ alpha 1 chain	1	1	151.67	1.71E-06	6h	1.66
SETLP_HUMAN	Protein SETSIP	3	2	163.86	1.77E-06	18h	1.28

YBOX1_HUMAN	Nuclease-sensitive element-binding protein 1	9	5	937.04	1.86E-06	6h	1.61
PSA3_HUMAN	Proteasome subunit alpha type-3	6	6	371.82	1.87E-06	18h	1.14
IPO5_HUMAN	Importin-5	13	9	866.92	1.88E-06	18h	1.50
EIF3M_HUMAN	Eukaryotic translation initiation factor 3 subunit M	1	1	126.42	1.92E-06	18h	13.70
PSMG2_HUMAN	Proteasome assembly chaperone 2	2	2	92.74	1.93E-06	18h	1.38
RTCB_HUMAN	tRNA-splicing ligase RtcB homolog	1	1	64.39	2.02E-06	6h	2.68
IF4A1_HUMAN	Eukaryotic initiation factor 4A-I	6	2	513.05	2.10E-06	6h	1.87
ARP2_HUMAN	Actin-related protein 2	7	6	494.88	2.14E-06	6h	1.93
UBA1_HUMAN	Ubiquitin-like modifier-activating enzyme 1	11	11	935.2	2.20E-06	18h	1.72
SRSF1_HUMAN	Serine/arginine-rich splicing factor 1	3	3	188.73	2.21E-06	6h	2.03
IF4E_HUMAN	Eukaryotic translation initiation factor 4E	1	1	50.22	2.45E-06	18h	1.47
HDAC1_HUMAN	Histone deacetylase 1	2	2	78.6	2.53E-06	6h	2.04
PUR4_HUMAN	Phosphoribosylformylglycinamidine synthase	3	3	182.9	2.60E-06	18h	2.16
PA1B3_HUMAN	Platelet-activating factor acetylhydrolase IB subunit gamma	1	1	68.33	2.62E-06	18h	32.35
CISY_HUMAN	Citrate synthase, mitochondrial	1	1	48.09	2.70E-06	6h	59.24
CATA_HUMAN	Catalase	1	1	86.02	2.83E-06	6h	2.06
ANX11_HUMAN	Annexin A11	6	6	292.13	2.86E-06	6h	1.53
ARC1B_HUMAN	Actin-related protein 2/3 complex subunit 1B	4	3	247.71	2.88E-06	6h	1.51
NDRG3_HUMAN	Protein NDRG3	1	1	80.33	2.99E-06	18h	1.68
HLAF_HUMAN	HLA class I histocompatibility antigen, alpha chain F	1	1	61.58	2.99E-06	6h	4.47
RS18_HUMAN	40S ribosomal protein S18	2	2	92.06	3.00E-06	18h	3.00
RUVB1_HUMAN	RuvB-like 1	9	9	542.27	3.21E-06	6h	1.29
LDHA_HUMAN	L-lactate dehydrogenase A chain	17	15	1696.23	3.40E-06	18h	1.34
EF1D_HUMAN	Elongation factor 1-delta	5	5	405.61	3.45E-06	6h	1.33
NUCL_HUMAN	Nucleolin	19	19	1770.76	3.54E-06	6h	1.31
DCK_HUMAN	Deoxycytidine kinase	4	3	214.25	3.66E-06	18h	3.87
FPPS_HUMAN	Farnesyl pyrophosphate synthase	2	2	93.03	3.76E-06	18h	1.38
DPP3_HUMAN	Dipeptidyl peptidase 3	1	1	91.04	3.92E-06	18h	2.51
XPP1_HUMAN	Xaa-Pro aminopeptidase 1	4	3	182.12	3.99E-06	18h	1.99
PSMD6_HUMAN	26S proteasome non-ATPase regulatory subunit 6	3	3	135.32	4.18E-06	6h	10.79
HS90A_HUMAN	Heat shock protein HSP 90-alpha	29	11	2366.1	4.22E-06	18h	1.38
TBA4A_HUMAN	Tubulin alpha-4A chain	9	2	618.77	4.29E-06	6h	1.31
XRCC5_HUMAN	X-ray repair cross-complementing protein 5	22	19	1601.59	4.41E-06	6h	1.54
NONO_HUMAN	Non-POU domain-containing octamer-binding protein	1	1	80.18	4.43E-06	18h	12.63
RL18_HUMAN	60S ribosomal protein L18	6	6	570.85	4.68E-06	6h	1.22
EF1B_HUMAN	Elongation factor 1-beta	3	3	280.18	4.68E-06	6h	1.33
PABP1_HUMAN	Polyadenylate-binding protein 1	6	2	398.01	4.90E-06	6h	3.01
MOB1A_HUMAN	MOB kinase activator 1A	2	2	101.85	5.03E-06	18h	1.50
RGF1B_HUMAN	Ras-GEF domain-containing family member 1B	1	1	37.92	5.31E-06	6h	4.33
TTC24_HUMAN	Tetratricopeptide repeat protein 24	1	1	46.74	5.37E-06	6h	1.58
IF2GL_HUMAN	Putative eukaryotic translation initiation factor 2 subunit 3-like protein	1	1	37.06	5.40E-06	18h	79.10
DHX9_HUMAN	ATP-dependent RNA helicase A	9	9	629.47	5.40E-06	6h	1.39
CDV3_HUMAN	Protein CDV3 homolog	1	1	59.41	5.65E-06	18h	2.15

GTR1_HUMAN	Solute carrier family 2, facilitated glucose transporter member 1	5	4	308.43	6.11E-06	18h	1.42
IMDH2_HUMAN	Inosine-5'-monophosphate dehydrogenase 2	3	3	143.62	6.29E-06	18h	5.79
PLCG2_HUMAN	1-phosphatidylinositol 4,5-bisphosphate phosphodiesterase gamma-2	4	4	199.33	6.39E-06	18h	1.56
RL10A_HUMAN	60S ribosomal protein L10a	8	7	582.45	6.49E-06	6h	1.81
LAT1_HUMAN	Large neutral amino acids transporter small subunit 1	5	4	390.81	6.54E-06	18h	1.44
TPD52_HUMAN	Tumor protein D52	4	4	301.63	6.83E-06	6h	1.34
BASI_HUMAN	Basigin	7	7	585.05	7.05E-06	18h	1.15
PUR6_HUMAN	Multifunctional protein ADE2	8	8	530.92	7.22E-06	18h	1.19
RL4_HUMAN	60S ribosomal protein L4	4	4	180.85	7.48E-06	18h	1.52
PTPRC_HUMAN	Receptor-type tyrosine-protein phosphatase C	23	23	1664.05	7.59E-06	18h	1.27
EF2_HUMAN	Elongation factor 2	21	21	1365.4	7.72E-06	18h	1.29
PUR8_HUMAN	Adenylosuccinate lyase	1	1	62.25	8.73E-06	18h	1.44
PSA1_HUMAN	Proteasome subunit alpha type-1	10	10	763.28	8.99E-06	6h	1.29
RL27_HUMAN	60S ribosomal protein L27	3	3	167.5	9.63E-06	6h	1.38
TLN1_HUMAN	Talin-1	10	7	571.82	9.88E-06	18h	1.36
PTCA_HUMAN	Protein tyrosine phosphatase receptor type C-associated protein	2	2	95.65	1.00E-05	6h	1.55
PODXL_HUMAN	Podocalyxin	1	1	63.8	1.03E-05	6h	1.28
RS27L_HUMAN	40S ribosomal protein S27-like	1	1	128.46	1.09E-05	6h	1.82
TALDO_HUMAN	Transaldolase	5	5	272.1	1.10E-05	18h	1.26
HG2A_HUMAN	HLA class II histocompatibility antigen gamma chain	3	3	303.19	1.16E-05	6h	3.86
DNJA2_HUMAN	DnaJ homolog subfamily A member 2	1	1	43.89	1.18E-05	6h	2.64
MTA2_HUMAN	Metastasis-associated protein MTA2	2	1	135.47	1.34E-05	18h	1.43
ANXA4_HUMAN	Annexin A4	3	2	167.49	1.34E-05	6h	1.42
DHE3_HUMAN	Glutamate dehydrogenase 1, mitochondrial	4	1	248.66	1.56E-05	6h	5.74
MOES_HUMAN	Moesin	32	20	2491.51	1.60E-05	18h	1.45
1433E_HUMAN	14-3-3 protein epsilon	8	7	655.26	1.66E-05	18h	1.18
CD166_HUMAN	CD166 antigen	1	1	37.46	1.68E-05	18h	1.46
ACLY_HUMAN	ATP-citrate synthase	16	16	1040.53	1.82E-05	18h	1.33
SFPQ_HUMAN	Splicing factor, proline- and glutamine-rich	5	4	371.23	1.90E-05	18h	1.80
RS25_HUMAN	40S ribosomal protein S25	4	3	247.34	1.97E-05	6h	1.14
NPTN_HUMAN	Neuroplastin	1	1	42.22	2.00E-05	18h	2.29
SPTN1_HUMAN	Spectrin alpha chain, non-erythrocytic 1	2	1	91.32	2.13E-05	6h	1.56
XRP2_HUMAN	Protein XRP2	4	4	171.63	2.14E-05	6h	1.45
IF2A_HUMAN	Eukaryotic translation initiation factor 2 subunit 1	5	5	307.03	2.16E-05	6h	1.21
GTR5_HUMAN	Solute carrier family 2, facilitated glucose transporter member 5	4	4	196.09	2.16E-05	18h	1.43
RL5_HUMAN	60S ribosomal protein L5	8	7	420.6	2.35E-05	6h	1.26
GLGB_HUMAN	1,4-alpha-glucan-branching enzyme	1	1	63.26	2.39E-05	18h	1.79
TNR6_HUMAN	Tumor necrosis factor receptor superfamily member 6	1	1	46.16	2.40E-05	6h	1.38
ENPL_HUMAN	Endoplasmin	4	2	319.05	2.46E-05	6h	2.65
SATT_HUMAN	Neutral amino acid transporter A	4	4	387.31	2.46E-05	18h	1.25
ACTB_HUMAN	Actin, cytoplasmic 1	26	9	2685.52	2.47E-05	6h	1.21
MOT1_HUMAN	Monocarboxylate transporter 1	4	4	205.9	2.53E-05	18h	1.25
XRCC6_HUMAN	X-ray repair cross-complementing protein 6	19	17	1592.03	2.79E-05	6h	1.42

ALDR_HUMAN	Aldose reductase	3	2	164.21	2.83E-05	18h	3.28
P2RY8_HUMAN	P2Y purinoceptor 8	1	1	48.5	2.87E-05	18h	1.75
CD37_HUMAN	Leukocyte antigen CD37	2	2	147.27	2.90E-05	18h	1.34
PSB8_HUMAN	Proteasome subunit beta type-8	2	2	99.14	2.96E-05	18h	1.39
RAB14_HUMAN	Ras-related protein Rab-14	4	3	316.28	3.13E-05	18h	1.66
H15_HUMAN	Histone H1.5	11	10	754.06	3.23E-05	18h	1.14
RL27A_HUMAN	60S ribosomal protein L27a	2	2	129.03	3.66E-05	6h	1.49
ANXA6_HUMAN	Annexin A6	17	17	1036.01	3.70E-05	18h	1.29
HSP74_HUMAN	Heat shock 70 kDa protein 4	7	6	422.1	3.90E-05	18h	1.78
PRDX1_HUMAN	Peroxiredoxin-1	12	7	710.43	4.01E-05	18h	1.20
MYH9_HUMAN	Myosin-9	56	44	4648.19	4.44E-05	6h	1.18
VDAC2_HUMAN	Voltage-dependent anion-selective channel protein 2	1	1	57.77	4.47E-05	6h	2.62
PABP4_HUMAN	Polyadenylate-binding protein 4	2	1	126.29	4.50E-05	6h	10.10
TCPD_HUMAN	T-complex protein 1 subunit delta	12	11	961.5	4.59E-05	18h	1.16
COF1_HUMAN	Cofilin-1	5	3	449.71	4.60E-05	18h	1.63
RL11_HUMAN	60S ribosomal protein L11	2	2	208.57	4.89E-05	6h	1.38
E41L2_HUMAN	Band 4.1-like protein 2	1	1	45.59	5.08E-05	6h	1.33
ZDBF2_HUMAN	DBF4-type zinc finger-containing protein 2	1	1	34.33	5.28E-05	6h	2.93
PP1R7_HUMAN	Protein phosphatase 1 regulatory subunit 7	1	1	49.94	5.36E-05	6h	1.64
EIF3I_HUMAN	Eukaryotic translation initiation factor 3 subunit I	3	2	138.71	5.36E-05	6h	1.72
APEX1_HUMAN	DNA-(apurinic or apyrimidinic site) lyase	2	2	121.18	5.41E-05	18h	1.22
RL15_HUMAN	60S ribosomal protein L15	5	5	295.78	5.49E-05	6h	1.23
SNAA_HUMAN	Alpha-soluble NSF attachment protein	7	4	523.77	5.78E-05	6h	1.97
SCAM2_HUMAN	Secretory carrier-associated membrane protein 2	1	1	42.7	6.06E-05	6h	1.68
RL7_HUMAN	60S ribosomal protein L7	11	11	704.04	6.33E-05	6h	1.10
HNRPC_HUMAN	Heterogeneous nuclear ribonucleoproteins C1/C2	1	1	59.09	6.38E-05	6h	1.78
PA2G4_HUMAN	Proliferation-associated protein 2G4	6	6	404.44	6.48E-05	18h	1.24
ICAM3_HUMAN	Intercellular adhesion molecule 3	1	1	50.78	6.79E-05	18h	1.47
EIF3H_HUMAN	Eukaryotic translation initiation factor 3 subunit H	3	3	146.5	6.82E-05	6h	1.39
SMC2_HUMAN	Structural maintenance of chromosomes protein 2	2	2	87.86	6.85E-05	6h	1.70
RBBP4_HUMAN	Histone-binding protein RBBP4	3	3	177.92	7.05E-05	18h	1.54
DC1I2_HUMAN	Cytoplasmic dynein 1 intermediate chain 2	1	1	92.9	7.12E-05	6h	1.85
AT1B3_HUMAN	Sodium/potassium-transporting ATPase subunit beta-3	6	6	575.71	7.59E-05	6h	1.24
RS12_HUMAN	40S ribosomal protein S12	1	1	38.2	7.97E-05	6h	1.27
CALX_HUMAN	Calnexin	2	2	89.93	8.18E-05	6h	1.44
MCA3_HUMAN	Eukaryotic translation elongation factor 1 epsilon-1	2	2	125.8	8.42E-05	6h	1.40
EHD1_HUMAN	EH domain-containing protein 1	6	4	333.83	9.02E-05	18h	1.20
1433G_HUMAN	14-3-3 protein gamma	7	3	377.95	9.11E-05	18h	1.63
IF6_HUMAN	Eukaryotic translation initiation factor 6	2	2	145.79	9.75E-05	18h	1.28
SRSF3_HUMAN	Serine/arginine-rich splicing factor 3	1	1	41.29	0.000101	6h	1.22
DRA_HUMAN	HLA class II histocompatibility antigen, DR alpha chain	5	4	800.53	0.000103	6h	1.16
ITA4_HUMAN	Integrin alpha-4	2	2	173.82	0.000103	18h	1.16
RS20_HUMAN	40S ribosomal protein S20	2	2	130.31	0.000103	6h	1.18

EZRI_HUMAN	Ezrin	27	15	1941.56	0.000105	18h	1.26
PRDX6_HUMAN	Peroxiredoxin-6	2	2	142.43	0.000114	18h	1.49
RAB2A_HUMAN	Ras-related protein Rab-2A	3	2	320.43	0.000118	18h	5.41
PSD11_HUMAN	26S proteasome non-ATPase regulatory subunit 11	2	2	158.35	0.00013	6h	3.21
ANM1_HUMAN	Protein arginine N-methyltransferase 1	2	2	134.09	0.000134	18h	1.23
RFTN1_HUMAN	Raftlin	3	3	202.51	0.000136	6h	1.62
IF4E2_HUMAN	Eukaryotic translation initiation factor 4E type 2	1	1	53.45	0.000136	18h	1.29
G3P_HUMAN	Glyceraldehyde-3-phosphate dehydrogenase	25	24	2367.12	0.000144	18h	1.27
TEX10_HUMAN	Testis-expressed protein 10	1	1	40.37	0.000148	18h	1.37
PYR1_HUMAN	CAD protein	5	4	275.04	0.000149	6h	1.17
HNRPM_HUMAN	Heterogeneous nuclear ribonucleoprotein M	1	1	50.26	0.000154	6h	3.50
CLIC4_HUMAN	Chloride intracellular channel protein 4	1	1	52.91	0.000159	18h	2.38
F234A_HUMAN	Protein FAM234A	1	1	47.27	0.000169	18h	1.30
HMGA1_HUMAN	High mobility group protein HMG-I/HMG-Y	2	2	160.91	0.00017	6h	1.19
IGHM_HUMAN	Immunoglobulin heavy constant mu	11	5	969.02	0.000194	18h	1.44
DKC1_HUMAN	H/ACA ribonucleoprotein complex subunit DKC1	2	1	136.56	0.000203	6h	2.82
TCPZ_HUMAN	T-complex protein 1 subunit zeta	12	7	835.24	0.000225	18h	1.13
RU17_HUMAN	U1 small nuclear ribonucleoprotein 70 kDa	5	5	230.55	0.000226	6h	1.26
4F2_HUMAN	4F2 cell-surface antigen heavy chain	13	13	1096.06	0.000253	18h	1.15
AAAT_HUMAN	Neutral amino acid transporter B(0)	9	9	868.82	0.000261	18h	1.24
ECE1_HUMAN	Endothelin-converting enzyme 1	3	3	137.56	0.000263	18h	1.23
LPPRC_HUMAN	Leucine-rich PPR motif-containing protein, mitochondrial	2	1	77.29	0.000295	6h	1.39
DHB12_HUMAN	Very-long-chain 3-oxoacyl-CoA reductase	1	1	43.77	0.000306	6h	24.51
HNRPR_HUMAN	Heterogeneous nuclear ribonucleoprotein R	4	2	291.84	0.000338	6h	5.59
BCAT1_HUMAN	Branched-chain-amino-acid aminotransferase, cytosolic	1	1	49.98	0.000349	18h	3.34
PUR1_HUMAN	Amidophosphoribosyltransferase	1	1	71.12	0.00037	6h	2.80
PARK7_HUMAN	Protein/nucleic acid deglycase DJ-1	5	3	460.88	0.000385	18h	3.62
PSA5_HUMAN	Proteasome subunit alpha type-5	4	3	241.07	0.000396	18h	1.13
HCDH_HUMAN	Hydroxyacyl-coenzyme A dehydrogenase, mitochondrial	1	1	37.45	0.000403	6h	2.16
RS24_HUMAN	40S ribosomal protein S24	1	1	55.16	0.000409	18h	2.43
SF3A3_HUMAN	Splicing factor 3A subunit 3	1	1	81.95	0.000409	6h	6.63
RS8_HUMAN	40S ribosomal protein S8	5	4	496.25	0.000422	6h	1.36
PEBP1_HUMAN	Phosphatidylethanolamine-binding protein 1	3	3	228.75	0.000433	18h	2.20
HNRH1_HUMAN	Heterogeneous nuclear ribonucleoprotein H	2	1	153.57	0.000437	18h	1.25
PRDX4_HUMAN	Peroxiredoxin-4	3	1	152.39	0.000445	6h	1.33
PSD13_HUMAN	26S proteasome non-ATPase regulatory subunit 13	1	1	46.91	0.000447	6h	1.54
HNRPU_HUMAN	Heterogeneous nuclear ribonucleoprotein U	2	2	110.13	0.000483	6h	1.45
RS6_HUMAN	40S ribosomal protein S6	4	4	248.5	0.000502	6h	1.23
ALDOC_HUMAN	Fructose-bisphosphate aldolase C	1	1	124.85	0.000514	6h	2.51
MCM5_HUMAN	DNA replication licensing factor MCM5	3	3	162.78	0.000514	6h	1.23
LSP1_HUMAN	Lymphocyte-specific protein 1	4	4	205	0.000516	18h	1.22
PSMD7_HUMAN	26S proteasome non-ATPase regulatory subunit 7	1	1	41.37	0.000533	6h	1.21

SRSF2_HUMAN	Serine/arginine-rich splicing factor 2	1	1	63.96	0.000566	6h	1.23
RAB21_HUMAN	Ras-related protein Rab-21	1	1	75.16	0.00057	18h	1.35
EIF3D_HUMAN	Eukaryotic translation initiation factor 3 subunit D	1	1	39.38	0.000581	6h	10.00
TPP2_HUMAN	Tripeptidyl-peptidase 2	9	8	572.79	0.000626	6h	1.16
SEPT9_HUMAN	Septin-9	2	2	88.74	0.000627	18h	2.40
ACTY_HUMAN	Beta-centractin	1	1	60.51	0.000644	18h	1.18
TOP1_HUMAN	DNA topoisomerase 1	9	7	596.72	0.00067	6h	1.15
PSB2_HUMAN	Proteasome subunit beta type-2	6	6	344.17	0.000748	18h	1.18
AT1A1_HUMAN	Sodium/potassium-transporting ATPase subunit alpha-1	25	14	2585.49	0.000789	18h	1.18
GSTP1_HUMAN	Glutathione S-transferase P	9	9	857.09	0.0008	18h	2.01
CTCFL_HUMAN	Transcriptional repressor CTCFL	1	1	42.35	0.000841	6h	1.35
BLMH_HUMAN	Bleomycin hydrolase	1	1	52.9	0.000841	18h	14.27
PSB7_HUMAN	Proteasome subunit beta type-7	2	2	199.45	0.000863	18h	1.31
GARS_HUMAN	Glycine--tRNA ligase	4	4	247.94	0.000876	18h	1.35
ATPG_HUMAN	ATP synthase subunit gamma, mitochondrial	1	1	88.57	0.000876	6h	7.37
RAC1_HUMAN	Ras-related C3 botulinum toxin substrate 1	4	3	197.4	0.000879	18h	1.29
SORL_HUMAN	Sortilin-related receptor	1	1	43.17	0.000942	6h	1.65
H2A1A_HUMAN	Histone H2A type 1-A	2	1	142.84	0.000963	6h	1.77
RS17_HUMAN	40S ribosomal protein S17	3	3	196.77	0.000974	6h	1.16
UBE2K_HUMAN	Ubiquitin-conjugating enzyme E2 K	1	1	79.38	0.001002	18h	1.59
CTL2_HUMAN	Choline transporter-like protein 2	4	3	197.07	0.001084	18h	1.29
ECH1_HUMAN	Delta(3,5)-Delta(2,4)-dienoyl-CoA isomerase, mitochondrial	1	1	57.77	0.001115	6h	3.57
LDHB_HUMAN	L-lactate dehydrogenase B chain	14	12	1323.88	0.001117	18h	1.16
CPSF5_HUMAN	Cleavage and polyadenylation specificity factor subunit 5	3	3	133.82	0.001131	18h	1.15
NP1L1_HUMAN	Nucleosome assembly protein 1-like 1	4	3	313.68	0.001189	6h	1.34
C1TC_HUMAN	C-1-tetrahydrofolate synthase, cytoplasmic	6	4	336.15	0.001207	18h	1.30
SMC1A_HUMAN	Structural maintenance of chromosomes protein 1A	1	1	33.9	0.001223	18h	1.49
FAS_HUMAN	Fatty acid synthase	21	20	1262.63	0.001291	18h	1.17
RL10_HUMAN	60S ribosomal protein L10	2	1	108.77	0.001308	6h	1.21
SYLC_HUMAN	Leucine--tRNA ligase, cytoplasmic	3	2	154.21	0.001388	6h	1.79
JAM1_HUMAN	Junctional adhesion molecule A	1	1	72.25	0.001402	6h	1.93
PSB1_HUMAN	Proteasome subunit beta type-1	5	5	377.24	0.001425	18h	1.22
RS27A_HUMAN	Ubiquitin-40S ribosomal protein S27a	5	5	356.42	0.001494	6h	1.10
IQGA1_HUMAN	Ras GTPase-activating-like protein IQGAP1	13	11	721.11	0.001504	18h	1.20
FLNB_HUMAN	Filamin-B	3	2	141.12	0.001521	6h	1.24
SYFB_HUMAN	Phenylalanine--tRNA ligase beta subunit	2	1	104.82	0.001525	18h	1.32
ACTN4_HUMAN	Alpha-actinin-4	18	12	1591.76	0.001591	18h	1.22
ZN500_HUMAN	Zinc finger protein 500	1	1	38.65	0.001676	18h	1.44
CD79B_HUMAN	B-cell antigen receptor complex-associated protein beta chain	3	3	168.68	0.00183	18h	1.21
ALBU_HUMAN	Serum albumin	6	6	339.56	0.00184	6h	1.10
OAS2_HUMAN	2'-5'-oligoadenylate synthase 2	1	1	36.38	0.002144	6h	1.12
PUR2_HUMAN	Trifunctional purine biosynthetic protein adenosine-3	1	1	61.63	0.002264	6h	1.24
RAP2A_HUMAN	Ras-related protein Rap-2a	1	1	103.2	0.00234	18h	1.32

SND1_HUMAN	Staphylococcal nuclease domain-containing protein 1	2	1	87.4	0.002443	6h	1.37
RHOA_HUMAN	Transforming protein RhoA	3	1	220.93	0.002452	18h	1.43
CPNE1_HUMAN	Copine-1	3	3	195.29	0.00254	6h	1.18
EIF3F_HUMAN	Eukaryotic translation initiation factor 3 subunit F	7	7	663.95	0.002801	18h	1.22
RL17_HUMAN	60S ribosomal protein L17	2	2	82.28	0.002958	6h	1.14
IMB1_HUMAN	Importin subunit beta-1	7	7	301.29	0.003069	18h	1.22
RAB10_HUMAN	Ras-related protein Rab-10	3	1	219.85	0.003189	18h	1.28
PFD2_HUMAN	Prefoldin subunit 2	2	2	189.76	0.003276	18h	2.30
RL21_HUMAN	60S ribosomal protein L21	2	2	102.02	0.003293	18h	1.09
HNRPD_HUMAN	Heterogeneous nuclear ribonucleoprotein D0	5	4	297.02	0.003457	18h	1.26
PGM2_HUMAN	Phosphoglucomutase-2	1	1	43.22	0.003532	18h	1.21
GON4L_HUMAN	GON-4-like protein	1	1	35.08	0.003542	18h	1.36
DDB1_HUMAN	DNA damage-binding protein 1	5	5	262.59	0.003567	18h	1.15
SRSF7_HUMAN	Serine/arginine-rich splicing factor 7	1	1	53.9	0.003837	6h	3.09
RAB8A_HUMAN	Ras-related protein Rab-8A	5	1	409.31	0.003906	18h	1.34
WDR1_HUMAN	WD repeat-containing protein 1	1	1	51.41	0.004014	18h	3.33
LYN_HUMAN	Tyrosine-protein kinase Lyn	1	1	34.97	0.004064	6h	10.83
CAPZB_HUMAN	F-actin-capping protein subunit beta	5	5	340.54	0.004105	6h	1.09
VATA_HUMAN	V-type proton ATPase catalytic subunit A	2	1	116.9	0.004109	18h	1.19
PRS10_HUMAN	26S proteasome regulatory subunit 10B	1	1	40.89	0.0042	6h	1.32
ITB1_HUMAN	Integrin beta-1	6	5	346.68	0.004489	18h	1.15
U5S1_HUMAN	116 kDa U5 small nuclear ribonucleoprotein component	4	4	220.81	0.004995	6h	1.18
IGKC_HUMAN	Immunoglobulin kappa constant	3	1	448.36	0.005013	18h	1.24
RASN_HUMAN	GTPase Nras	4	1	227.7	0.005097	18h	2.18
RS23_HUMAN	40S ribosomal protein S23	1	1	56.58	0.005369	6h	5.42
GNAI2_HUMAN	Guanine nucleotide-binding protein G(i) subunit alpha-2	10	7	940.93	0.005481	6h	1.19
SNP23_HUMAN	Synaptosomal-associated protein 23	1	1	104.57	0.005647	6h	15.30
RIR1_HUMAN	Ribonucleoside-diphosphate reductase large subunit	1	1	94.6	0.006016	6h	3.24
TCPB_HUMAN	T-complex protein 1 subunit beta	17	16	1314.46	0.00609	18h	1.07
DCTP1_HUMAN	dCTP pyrophosphatase 1	3	2	146.84	0.006108	18h	2.42
AN32B_HUMAN	Acidic leucine-rich nuclear phosphoprotein 32 family member B	2	1	111.93	0.006928	6h	1.37
RL19_HUMAN	60S ribosomal protein L19	1	1	174.33	0.007017	6h	1.61
RS11_HUMAN	40S ribosomal protein S11	2	2	97.32	0.007119	6h	1.30
CD22_HUMAN	B-cell receptor CD22	2	2	120.53	0.007172	6h	1.24
SF3B3_HUMAN	Splicing factor 3B subunit 3	14	14	995.13	0.007257	6h	1.07
PRDX2_HUMAN	Peroxiredoxin-2	2	1	177.36	0.007498	18h	1.14
MYL6_HUMAN	Myosin light polypeptide 6	3	1	164.03	0.007564	6h	1.36
ANM5_HUMAN	Protein arginine N-methyltransferase 5	2	2	79.56	0.00765	18h	2.00
SYVC_HUMAN	Valine--tRNA ligase	2	1	110.36	0.007732	6h	1.13
EIF3E_HUMAN	Eukaryotic translation initiation factor 3 subunit E	10	9	616.67	0.008285	6h	1.06
DDX17_HUMAN	Probable ATP-dependent RNA helicase DDX17	3	1	163.68	0.008418	6h	1.37
ARPC4_HUMAN	Actin-related protein 2/3 complex subunit 4	4	4	221.79	0.008647	6h	1.15
SF3A2_HUMAN	Splicing factor 3A subunit 2	1	1	64.82	0.009397	6h	2.96

CD180_HUMAN	CD180 antigen	1	1	77.6	0.00982	6h	1.84
2B1E_HUMAN	HLA class II histocompatibility antigen, DRB1-14 beta chain	4	1	316.27	0.010348	18h	1.06
CKLF6_HUMAN	CKLF-like MARVEL transmembrane domain-containing protein 6	1	1	80.41	0.010886	6h	1.26
2AAA_HUMAN	Serine/threonine-protein phosphatase 2A 65 kDa regulatory subunit A alpha isoform	2	2	101.91	0.011171	18h	1.19
RLA0L_HUMAN	60S acidic ribosomal protein P0-like	7	1	407.78	0.011463	6h	1.99
TCPA_HUMAN	T-complex protein 1 subunit alpha	14	13	1165.94	0.011607	18h	1.04
CTR3_HUMAN	Cationic amino acid transporter 3	3	3	173.46	0.012295	18h	1.55
SF3B1_HUMAN	Splicing factor 3B subunit 1	10	10	620.18	0.012389	18h	1.12
PRP8_HUMAN	Pre-mRNA-processing-splicing factor 8	5	4	279.88	0.012701	6h	1.13
PSA_HUMAN	Puromycin-sensitive aminopeptidase	3	2	191.23	0.01323	18h	1.95
HSDL1_HUMAN	Inactive hydroxysteroid dehydrogenase-like protein 1	1	1	33	0.01365	6h	1.15
U520_HUMAN	U5 small nuclear ribonucleoprotein 200 kDa helicase	6	6	365.79	0.015145	6h	1.10
RRBP1_HUMAN	Ribosome-binding protein 1	1	1	116.6	0.016094	6h	1.99
ROAA_HUMAN	Heterogeneous nuclear ribonucleoprotein A/B	2	2	85.86	0.017622	6h	1.13
PELP1_HUMAN	Proline-, glutamic acid- and leucine-rich protein 1	2	1	111.46	0.017906	6h	5.88
TBA1A_HUMAN	Tubulin alpha-1A chain	11	4	1134.86	0.019568	6h	1.07
NUMA1_HUMAN	Nuclear mitotic apparatus protein 1	16	15	976.09	0.019908	6h	1.08
AN32A_HUMAN	Acidic leucine-rich nuclear phosphoprotein 32 family member A	2	1	105.71	0.019939	18h	1.11
RL23_HUMAN	60S ribosomal protein L23	1	1	90.68	0.022716	6h	2.20
EIF3K_HUMAN	Eukaryotic translation initiation factor 3 subunit K	1	1	57.32	0.023055	6h	1.35
IPYR_HUMAN	Inorganic pyrophosphatase	3	1	244.99	0.02371	18h	1.12
ST14_HUMAN	Suppressor of tumorigenicity 14 protein	3	3	205.55	0.024174	6h	2.65
AT2B1_HUMAN	Plasma membrane calcium-transporting ATPase 1	6	2	343	0.024705	18h	1.12
ROA3_HUMAN	Heterogeneous nuclear ribonucleoprotein A3	1	1	61.48	0.026334	6h	1.65
TCPG_HUMAN	T-complex protein 1 subunit gamma	12	12	794.82	0.027336	18h	1.08
PSMD1_HUMAN	26S proteasome non-ATPase regulatory subunit 1	4	3	293.89	0.028738	6h	1.69
MCM3_HUMAN	DNA replication licensing factor MCM3	2	2	104.8	0.030619	6h	1.12
IGSF8_HUMAN	Immunoglobulin superfamily member 8	3	3	175.74	0.03229	18h	1.19
LC7L3_HUMAN	Luc7-like protein 3	1	1	61.57	0.033373	6h	1.16
DHX15_HUMAN	Pre-mRNA-splicing factor ATP-dependent RNA helicase DHX15	3	2	183.83	0.033883	6h	1.22
RL22_HUMAN	60S ribosomal protein L22	2	2	172.94	0.037091	6h	1.06
EF1A1_HUMAN	Elongation factor 1-alpha 1	8	3	561.97	0.03931	18h	1.07
MARCS_HUMAN	Myristoylated alanine-rich C-kinase substrate	2	2	127.41	0.040391	18h	1.09
HMGB2_HUMAN	High mobility group protein B2	2	2	122.03	0.042662	18h	1.05
MYL6B_HUMAN	Myosin light chain 6B	1	1	78.54	0.04277	18h	1.07
ML12A_HUMAN	Myosin regulatory light chain 12A	3	2	190.01	0.045407	6h	1.64
RL35_HUMAN	60S ribosomal protein L35	2	2	82.45	0.045711	18h	1.10
PSA4_HUMAN	Proteasome subunit alpha type-4	4	4	227.33	0.046318	6h	1.07
PCNA_HUMAN	Proliferating cell nuclear antigen	2	2	167.18	0.048359	6h	1.23
PDIA4_HUMAN	Protein disulfide-isomerase A4	3	3	220.73	0.048915	6h	1.14
ANXA5_HUMAN	Annexin A5	3	2	153.49	0.050749	6h	1.23
MX1_HUMAN	Interferon-induced GTP-binding protein Mx1	9	7	678.05	0.051415	18h	1.09

TPR_HUMAN	Nucleoprotein TPR	3	3	185.18	0.051419	6h	1.07
S38A5_HUMAN	Sodium-coupled neutral amino acid transporter 5	1	1	53.44	0.054842	18h	1.37
SYEP_HUMAN	Bifunctional glutamate/proline--tRNA ligase	1	1	54.74	0.054881	6h	1.12
DDX21_HUMAN	Nucleolar RNA helicase 2	7	3	308.57	0.055253	6h	1.17
RACK1_HUMAN	Receptor of activated protein C kinase 1	6	6	371.29	0.05772	6h	1.08
NPM_HUMAN	Nucleophosmin	5	5	411.34	0.059624	18h	1.08
CIB1_HUMAN	Calcium and integrin-binding protein 1	1	1	48.54	0.061171	18h	1.12
PSB4_HUMAN	Proteasome subunit beta type-4	6	6	489.24	0.066402	18h	1.05
HNRPK_HUMAN	Heterogeneous nuclear ribonucleoprotein K	3	3	190.95	0.071162	18h	1.18
SYFA_HUMAN	Phenylalanine--tRNA ligase alpha subunit	2	2	88.01	0.07433	18h	1.04
PECA1_HUMAN	Platelet endothelial cell adhesion molecule	1	1	31.2	0.075482	18h	1.11
PSA6_HUMAN	Proteasome subunit alpha type-6	6	6	399.09	0.077607	6h	1.05
CYFP1_HUMAN	Cytoplasmic FMR1-interacting protein 1	4	1	268.54	0.082487	18h	1.07
DDX1_HUMAN	ATP-dependent RNA helicase DDX1	1	1	62.94	0.083738	6h	1.69
ACPH_HUMAN	Acylamino-acid-releasing enzyme	2	2	118.82	0.09044	18h	1.14
ILF2_HUMAN	Interleukin enhancer-binding factor 2	7	7	706.63	0.091544	18h	1.05
CSN4_HUMAN	COP9 signalosome complex subunit 4	3	3	212.18	0.092184	18h	1.06
GBB1_HUMAN	Guanine nucleotide-binding protein G(I)/G(S)/G(T) subunit beta-1	3	2	162.02	0.099967	6h	1.08
GNAI3_HUMAN	Guanine nucleotide-binding protein G(k) subunit alpha	5	2	335.97	0.112766	18h	1.27
PSB6_HUMAN	Proteasome subunit beta type-6	2	2	142.16	0.115688	18h	1.03
CD81_HUMAN	CD81 antigen	1	1	224.67	0.11612	6h	1.86
TALD3_HUMAN	Protein TALPID3	1	1	31.99	0.118487	18h	1.10
CY24B_HUMAN	Cytochrome b-245 heavy chain	1	1	58.13	0.11885	18h	1.17
APT_HUMAN	Adenine phosphoribosyltransferase	1	1	50.72	0.121731	18h	1.12
MCM2_HUMAN	DNA replication licensing factor MCM2	2	1	125.86	0.130893	18h	1.40
HS105_HUMAN	Heat shock protein 105 kDa	4	4	227.37	0.134008	6h	1.05
RL8_HUMAN	60S ribosomal protein L8	2	2	185.96	0.136096	18h	1.03
PROF1_HUMAN	Profilin-1	2	2	101.22	0.145431	18h	1.07
DQB1_HUMAN	HLA class II histocompatibility antigen, DQ beta 1 chain	1	1	69.05	0.148076	18h	1.05
S43A3_HUMAN	Solute carrier family 43 member 3	3	3	151.92	0.149518	18h	1.03
PSB9_HUMAN	Proteasome subunit beta type-9	3	3	201.27	0.152796	18h	1.06
FUBP2_HUMAN	Far upstream element-binding protein 2	1	1	51.49	0.152868	6h	1.12
MARE1_HUMAN	Microtubule-associated protein RP/EB family member 1	2	2	98.08	0.153502	18h	1.12
PDCD6_HUMAN	Programmed cell death protein 6	2	2	106.94	0.155552	6h	1.24
KCC2D_HUMAN	Calcium/calmodulin-dependent protein kinase type II subunit delta	1	1	61.79	0.166347	6h	1.07
H13_HUMAN	Histone H1.3	8	1	499.87	0.168182	6h	1.03
MAT2B_HUMAN	Methionine adenosyltransferase 2 subunit beta	1	1	37.44	0.171156	6h	1.29
PSMD2_HUMAN	26S proteasome non-ATPase regulatory subunit 2	7	6	484.83	0.177711	6h	1.12
ALDOA_HUMAN	Fructose-bisphosphate aldolase A	14	13	1288.24	0.178182	18h	1.06
NEP_HUMAN	Neprilysin	6	6	463.93	0.192053	6h	1.09
NHP2_HUMAN	H/ACA ribonucleoprotein complex subunit 2	1	1	58.43	0.202808	6h	11.39
AT1A3_HUMAN	Sodium/potassium-transporting ATPase subunit alpha-3	15	1	1727.86	0.208959	6h	1.34
SF3A1_HUMAN	Splicing factor 3A subunit 1	5	5	299.06	0.209151	6h	1.07

NDK8_HUMAN	Putative nucleoside diphosphate kinase	3	1	295.45	0.210145	18h	1.09
SCRB1_HUMAN	Scavenger receptor class B member 1	2	2	141.35	0.22346	6h	1.28
WDR5_HUMAN	WD repeat-containing protein 5	1	1	34.3	0.253235	6h	1.23
DYHC1_HUMAN	Cytoplasmic dynein 1 heavy chain 1	1	1	39.96	0.262443	6h	1.15
S1PR2_HUMAN	Sphingosine 1-phosphate receptor 2	1	1	31.39	0.274301	18h	2.12
MRP_HUMAN	MARCKS-related protein	2	2	280.42	0.279226	6h	1.05
2B17_HUMAN	HLA class II histocompatibility antigen, DRB1-7 beta chain	11	3	827.67	0.279783	18h	1.08
PLP2_HUMAN	Proteolipid protein 2	1	1	61.4	0.297708	6h	1.02
F10A1_HUMAN	Hsc70-interacting protein	4	1	261.79	0.303439	18h	1.93
CD79A_HUMAN	B-cell antigen receptor complex-associated protein alpha chain	2	2	134.4	0.317234	18h	1.06
ARPC5_HUMAN	Actin-related protein 2/3 complex subunit 5	1	1	36.76	0.326371	18h	1.25
FKBP5_HUMAN	Peptidyl-prolyl cis-trans isomerase FKBP5	1	1	43.57	0.334191	18h	1.12
PSA7_HUMAN	Proteasome subunit alpha type-7	5	2	449.14	0.345553	6h	1.06
SYRC_HUMAN	Arginine--tRNA ligase, cytoplasmic	2	2	89.22	0.353519	6h	1.12
MLX_HUMAN	Max-like protein X	1	1	31.59	0.358427	6h	1.06
RUVB2_HUMAN	RuvB-like 2	4	4	257.07	0.364401	6h	1.04
PSB3_HUMAN	Proteasome subunit beta type-3	4	4	351	0.366746	18h	1.10
DRB3_HUMAN	HLA class II histocompatibility antigen, DR beta 3 chain	6	1	498.87	0.380332	18h	1.21
RAP1A_HUMAN	Ras-related protein Rap-1A	5	1	413.63	0.385327	18h	1.04
TERA_HUMAN	Transitional endoplasmic reticulum ATPase	19	17	1454.65	0.389039	6h	1.06
ARF6_HUMAN	ADP-ribosylation factor 6	2	2	127.54	0.392883	6h	1.17
MCM6_HUMAN	DNA replication licensing factor MCM6	1	1	42.89	0.394103	6h	1.12
ARPC3_HUMAN	Actin-related protein 2/3 complex subunit 3	5	5	385.58	0.400875	6h	1.02
TPM1_HUMAN	Tropomyosin alpha-1 chain	1	1	58.67	0.404742	18h	1.12
ELAV1_HUMAN	ELAV-like protein 1	1	1	48.22	0.41992	18h	1.28
EIF3B_HUMAN	Eukaryotic translation initiation factor 3 subunit B	6	5	368.32	0.440778	6h	1.02
EEA1_HUMAN	Early endosome antigen 1	6	6	323.35	0.444506	6h	1.02
CYFP2_HUMAN	Cytoplasmic FMR1-interacting protein 2	7	3	381.83	0.461319	18h	1.03
BBOF1_HUMAN	Basal body-orientation factor 1	1	1	34.18	0.488326	18h	1.04
TNPO1_HUMAN	Transportin-1	1	1	33.55	0.538216	6h	1.07
FREM1_HUMAN	FRAS1-related extracellular matrix protein 1	1	1	35.81	0.550417	18h	1.02
GPM6A_HUMAN	Neuronal membrane glycoprotein M6-a	2	2	98.1	0.567271	18h	1.69
UB2L3_HUMAN	Ubiquitin-conjugating enzyme E2 L3	1	1	54.44	0.577576	6h	1.15
PSB5_HUMAN	Proteasome subunit beta type-5	2	2	123.91	0.586279	18h	1.03
MCM4_HUMAN	DNA replication licensing factor MCM4	1	1	75.05	0.593653	18h	1.30
PP2AA_HUMAN	Serine/threonine-protein phosphatase 2A catalytic subunit alpha isoform	1	1	73.3	0.595835	18h	1.66
TFIP8_HUMAN	Tumor necrosis factor alpha-induced protein 8	1	1	88.21	0.62462	6h	1.06
EIFCL_HUMAN	Eukaryotic translation initiation factor 3 subunit C-like protein	1	1	50.28	0.642036	18h	1.23
RAC2_HUMAN	Ras-related C3 botulinum toxin substrate 2	3	2	239.26	0.642588	18h	1.06
PSME3_HUMAN	Proteasome activator complex subunit 3	2	2	66.7	0.644308	18h	1.08
RSSA_HUMAN	40S ribosomal protein SA	3	3	346.31	0.694806	18h	1.01
CTL1_HUMAN	Choline transporter-like protein 1	3	3	164.28	0.711713	18h	1.01

EIF3A_HUMAN	Eukaryotic translation initiation factor 3 subunit A	8	8	568.1	0.714814	6h	1.03
MRP1_HUMAN	Multidrug resistance-associated protein 1	1	1	38.85	0.714894	6h	1.10
STX4_HUMAN	Syntaxin-4	3	3	213.26	0.72049	6h	1.01
S38A1_HUMAN	Sodium-coupled neutral amino acid transporter 1	1	1	32.42	0.779261	18h	1.08
CD86_HUMAN	T-lymphocyte activation antigen CD86	1	1	74.56	0.78398	18h	1.00
NEK9_HUMAN	Serine/threonine-protein kinase Nek9	1	1	41.66	0.80219	18h	1.01
MDHC_HUMAN	Malate dehydrogenase, cytoplasmic	7	6	455.79	0.802371	6h	1.01
ROA0_HUMAN	Heterogeneous nuclear ribonucleoprotein A0	1	1	91.66	0.805812	6h	1.02
SYHC_HUMAN	Histidine--tRNA ligase, cytoplasmic	1	1	34.38	0.877125	18h	2.42
CSN8_HUMAN	COP9 signalosome complex subunit 8	1	1	53.3	0.877452	6h	1.02
SC6A6_HUMAN	Sodium- and chloride-dependent taurine transporter	1	1	44.89	0.887864	18h	1.13
SF3B2_HUMAN	Splicing factor 3B subunit 2	1	1	31.53	0.890438	18h	1.01
RAB1A_HUMAN	Ras-related protein Rab-1A	5	1	362.67	0.909993	18h	1.10
PURA2_HUMAN	Adenylosuccinate synthetase isozyme 2	1	1	33.49	0.928214	18h	1.03
ISG20_HUMAN	Interferon-stimulated gene 20 kDa protein	1	1	69.79	0.93502	18h	1.00
SYIC_HUMAN	Isoleucine--tRNA ligase, cytoplasmic	4	4	202.75	0.935941	6h	1.00
PSA2_HUMAN	Proteasome subunit alpha type-2	4	4	339.97	0.947402	18h	1.01
CTR1_HUMAN	High affinity cationic amino acid transporter 1	2	1	146.66	0.962541	18h	1.04
SEPT6_HUMAN	Septin-6	4	3	190.81	0.987433	18h	1.02
FLVC1_HUMAN	Feline leukemia virus subgroup C receptor-related protein 1	1	1	51.66	0.995235	6h	1.02

Table 4: T cell 18 h ACdEV proteomes when isolated by SEC versus UC

Accession	Description	Peptide count	Unique peptides	Confidence score	Anova (p)	Highest mean condition	Max fold change
LRC47_HUMAN	Leucine-rich repeat-containing protein 47	1	1	64.51	0.373901	UC	Infinity
SMD1_HUMAN	Small nuclear ribonucleoprotein Sm D1	1	1	96.18	0.00013	SEC	2060.53
UB2V1_HUMAN	Ubiquitin-conjugating enzyme E2 variant 1	5	1	287.71	0.003631	SEC	174.70
PLAK_HUMAN	Junction plakoglobin	2	1	101.99	0.282373	SEC	113.52
MPCP_HUMAN	Phosphate carrier protein, mitochondrial	1	1	80.63	0.000209	SEC	77.59
ATNG_HUMAN	Sodium/potassium-transporting ATPase subunit gamma	1	1	85.82	0.013707	SEC	58.24
SH21A_HUMAN	SH2 domain-containing protein 1A	1	1	37.94	0.009285	UC	36.95
SURF4_HUMAN	Surfeit locus protein 4	1	1	63.49	0.000228	SEC	27.40
SHRM3_HUMAN	Protein Shroom3	1	1	37.63	0.963804	UC	21.59
U2AF1_HUMAN	Splicing factor U2AF 35 kDa subunit	1	1	68.64	0.000138	UC	19.69
2A5D_HUMAN	Serine/threonine-protein phosphatase 2A 56 kDa regulatory subunit delta isoform	1	1	41.62	0.01968	UC	17.69
VAMP2_HUMAN	Vesicle-associated membrane protein 2	1	1	84.06	0.027353	SEC	16.94
NINJ1_HUMAN	Ninjurin-1	1	1	91.87	0.000188	SEC	16.57
PSB8_HUMAN	Proteasome subunit beta type-8	1	1	61.01	0.030252	UC	15.68
NAA50_HUMAN	N-alpha-acetyltransferase 50	1	1	37.44	0.038943	SEC	15.03
VANG1_HUMAN	Vang-like protein 1	1	1	41.7	0.039416	SEC	14.79
SVIP_HUMAN	Small VCP/p97-interacting protein	1	1	73.63	0.056465	SEC	12.94
GAS2_HUMAN	Growth arrest-specific protein 2	1	1	62.9	0.039481	SEC	12.76
CRCM1_HUMAN	Calcium release-activated calcium channel protein 1	1	1	54.96	0.038582	SEC	12.54
SCAM1_HUMAN	Secretory carrier-associated membrane protein 1	1	1	66.7	0.042897	SEC	12.09
HNRH1_HUMAN	Heterogeneous nuclear ribonucleoprotein H	4	1	243.74	0.073243	UC	11.50
H3C_HUMAN	Histone H3.3C	1	1	59.61	4.77E-06	UC	11.08
S12A7_HUMAN	Solute carrier family 12 member 7	3	2	180.2	2.03E-05	SEC	10.91
DHE3_HUMAN	Glutamate dehydrogenase 1, mitochondrial	1	1	66.93	0.000365	UC	10.44
TM9S4_HUMAN	Transmembrane 9 superfamily member 4	1	1	51.83	0.037871	SEC	10.42
SH3L1_HUMAN	SH3 domain-binding glutamic acid-rich-like protein	1	1	71.73	0.039559	SEC	10.30
RSMB_HUMAN	Small nuclear ribonucleoprotein-associated proteins B and B'	1	1	60.44	0.042248	UC	10.28
MRP4_HUMAN	ATP-binding cassette sub-family C member 4	1	1	59.98	0.003036	SEC	10.24
GANAB_HUMAN	Neutral alpha-glucosidase AB	2	1	112.1	0.045338	UC	10.23
CASP3_HUMAN	Caspase-3	1	1	50.6	0.000127	UC	9.76
MTPN_HUMAN	Myotrophin	1	1	73.99	0.069729	SEC	9.03
TSN33_HUMAN	Tetraspanin-33	1	1	38.85	0.079079	SEC	8.59
RS21_HUMAN	40S ribosomal protein S21	1	1	101.87	0.001578	UC	7.77
NINJ2_HUMAN	Ninjurin-2	1	1	55.51	0.06788	SEC	7.77
PAPS1_HUMAN	Bifunctional 3'-phosphoadenosine 5'-phosphosulfate synthase 1	1	1	56.5	0.009458	UC	7.48
CPNS1_HUMAN	Calpain small subunit 1	1	1	106.12	0.068384	SEC	6.43
HIKES_HUMAN	Protein Hikeshi	1	1	123.46	0.0091	SEC	6.23
CYRIB_HUMAN	CYFIP-related Rac1 interactor B	12	9	1213.75	1.09E-05	SEC	6.22
NDRG3_HUMAN	Protein NDRG3	1	1	49.97	0.016717	SEC	6.09
RL30_HUMAN	60S ribosomal protein L30	2	1	81.85	0.004877	SEC	6.06

T cell 18 h ACdEV proteomes when isolated by SEC versus UC

Accession	Description	Peptide count	Unique peptides	Confidence score	Anova (p)	Highest mean condition	Max fold change
ADAM9_HUMAN	Disintegrin and metalloproteinase domain-containing protein 9	1	1	48.18	0.509251	SEC	6.04
IFM1_HUMAN	Interferon-induced transmembrane protein 1	2	2	199.15	0.174792	SEC	5.96
AT1B1_HUMAN	Sodium/potassium-transporting ATPase subunit beta-1	1	1	54.3	0.000311	SEC	5.95
TVA82_HUMAN	T cell receptor alpha variable 8-2	2	2	123.09	1.07E-05	SEC	5.77
RL13A_HUMAN	60S ribosomal protein L13a	5	1	208.57	0.007739	SEC	5.61
SEM4D_HUMAN	Semaphorin-4D	1	1	35.48	0.014741	SEC	5.42
AT1A1_HUMAN	Sodium/potassium-transporting ATPase subunit alpha-1	39	18	3347.08	5.34E-08	SEC	5.41
ACTY_HUMAN	Beta-centractin	5	1	305.87	0.000813	UC	5.39
ARPC5_HUMAN	Actin-related protein 2/3 complex subunit 5	3	1	135.17	0.141875	SEC	5.30
GBRAP_HUMAN	Gamma-aminobutyric acid receptor-associated protein	1	1	42.38	0.038249	SEC	5.28
HDAC2_HUMAN	Histone deacetylase 2	4	1	216.65	0.026047	UC	5.15
LRC57_HUMAN	Leucine-rich repeat-containing protein 57	2	2	73.57	0.016415	SEC	5.10
SC5A6_HUMAN	Sodium-dependent multivitamin transporter	1	1	73.57	6.98E-05	SEC	5.02
LAT3_HUMAN	Large neutral amino acids transporter small subunit 3	1	1	61.69	0.003872	SEC	4.99
CDK6_HUMAN	Cyclin-dependent kinase 6	2	1	100.76	0.021173	UC	4.95
S38A1_HUMAN	Sodium-coupled neutral amino acid transporter 1	3	2	145.66	1.67E-05	SEC	4.85
ROA2_HUMAN	Heterogeneous nuclear ribonucleoproteins A2/B1	6	6	404.23	3.25E-06	UC	4.84
MAT2B_HUMAN	Methionine adenosyltransferase 2 subunit beta	2	2	159.42	0.043329	UC	4.82
POMP_HUMAN	Proteasome maturation protein	2	2	151.17	3.52E-05	SEC	4.80
GTR1_HUMAN	Solute carrier family 2, facilitated glucose transporter member 1	6	5	436.89	1.37E-06	SEC	4.78
TRFL_HUMAN	Lactotransferrin	1	1	58.46	6.32E-06	UC	4.70
DTD1_HUMAN	D-aminoacyl-tRNA deacylase 1	1	1	108.81	0.048307	SEC	4.69
NUMA1_HUMAN	Nuclear mitotic apparatus protein 1	24	22	1702.75	4.56E-06	SEC	4.65
DOPD_HUMAN	D-dopachrome decarboxylase	1	1	40.84	0.018651	SEC	4.62
TPPC3_HUMAN	Trafficking protein particle complex subunit 3	1	1	68.09	0.00687	SEC	4.60
RL10A_HUMAN	60S ribosomal protein L10a	3	3	133.42	0.000827	SEC	4.56
ENPP4_HUMAN	Bis(5'-adenosyl)-triphosphatase ENPP4	1	1	50.7	2.18E-06	SEC	4.49
AT11C_HUMAN	Phospholipid-transporting ATPase IG	2	2	96.92	0.001146	SEC	4.48
ASPM_HUMAN	Abnormal spindle-like microcephaly-associated protein	2	2	83.3	0.003917	SEC	4.45
BID_HUMAN	BH3-interacting domain death agonist	2	2	172.56	0.003374	SEC	4.44
2A5E_HUMAN	Serine/threonine-protein phosphatase 2A 56 kDa regulatory subunit epsilon isoform	1	1	62.5	0.049938	SEC	4.41
UBP5_HUMAN	Ubiquitin carboxyl-terminal hydrolase 5	1	1	31.17	0.00331	UC	4.41
COCH_HUMAN	Cochlin	2	2	116.99	8.12E-05	UC	4.39
TPR_HUMAN	Nucleoprotein TPR	5	5	296.67	0.000714	SEC	4.36
IF1AX_HUMAN	Eukaryotic translation initiation factor 1A, X-chromosomal	2	2	91.61	0.000796	SEC	4.36
DLDH_HUMAN	Dihydrolipoyl dehydrogenase, mitochondrial	2	2	137.8	0.009586	UC	4.30
TNPO3_HUMAN	Transportin-3	1	1	109.09	0.004002	UC	4.28
H2A1A_HUMAN	Histone H2A type 1-A	3	2	336.4	0.078412	SEC	4.26
EEA1_HUMAN	Early endosome antigen 1	4	4	222.68	7.37E-05	SEC	4.21
P5CR3_HUMAN	Pyrroline-5-carboxylate reductase 3	1	1	75.05	0.001086	UC	4.21
CSN2_HUMAN	COP9 signalosome complex subunit 2	2	2	93.57	0.016312	UC	4.06
YLAT2_HUMAN	Y+L amino acid transporter 2	2	1	94.07	0.000393	SEC	3.90
TKFC_HUMAN	Triokinase/FMN cyclase	1	1	64.37	0.047963	SEC	3.83

T cell 18 h ACdEV proteomes when isolated by SEC versus UC

Accession	Description	Peptide count	Unique peptides	Confidence score	Anova (p)	Highest mean condition	Max fold change
TRAC_HUMAN	T cell receptor alpha chain constant	3	3	188.65	4.84E-05	SEC	3.78
EXOS4_HUMAN	Exosome complex component RRP41	1	1	67.71	0.000136	UC	3.78
CXCR4_HUMAN	C-X-C chemokine receptor type 4	3	3	357.8	7.95E-07	SEC	3.77
S39AA_HUMAN	Zinc transporter ZIP10	1	1	50.16	0.001036	SEC	3.75
B2MG_HUMAN	Beta-2-microglobulin	3	3	133.51	0.014509	SEC	3.71
AT1A3_HUMAN	Sodium/potassium-transporting ATPase subunit alpha-3	22	2	1899.76	5.04E-05	SEC	3.71
S38A2_HUMAN	Sodium-coupled neutral amino acid transporter 2	6	6	584.59	1.15E-06	SEC	3.69
CH60_HUMAN	60 kDa heat shock protein, mitochondrial	30	27	2733.66	1.18E-05	UC	3.68
XPO5_HUMAN	Exportin-5	3	3	294.47	0.00528	UC	3.66
FABP5_HUMAN	Fatty acid-binding protein 5	1	1	39.89	0.017167	SEC	3.66
AT2B4_HUMAN	Plasma membrane calcium-transporting ATPase 4	20	8	1747.93	4.33E-06	SEC	3.65
LAT1_HUMAN	Large neutral amino acids transporter small subunit 1	9	7	659.83	1.28E-05	SEC	3.60
GMFB_HUMAN	Glia maturation factor beta	1	1	67.68	0.005689	SEC	3.56
H2A1B_HUMAN	Histone H2A type 1-B/E	2	1	272.11	0.056445	SEC	3.56
PA24F_HUMAN	Cytosolic phospholipase A2 zeta	1	1	34.51	0.011589	SEC	3.54
ANO6_HUMAN	Anoctamin-6 OS=Homo sapiens	8	7	438.53	7.98E-07	SEC	3.54
S29A2_HUMAN	Equilibrative nucleoside transporter 2	2	2	107.05	1.86E-05	SEC	3.52
BUB3_HUMAN	Mitotic checkpoint protein BUB3	4	4	231.38	1.42E-05	UC	3.51
HNRH3_HUMAN	Heterogeneous nuclear ribonucleoprotein H3	1	1	74.83	0.000567	UC	3.49
RCC1_HUMAN	Regulator of chromosome condensation	1	1	47.72	0.10098	UC	3.44
SRP14_HUMAN	Signal recognition particle 14 kDa protein	2	2	164.31	0.001822	SEC	3.41
RS28_HUMAN	40S ribosomal protein S28	1	1	47.4	0.115738	SEC	3.38
S35F2_HUMAN	Solute carrier family 35 member F2	1	1	33.67	0.059564	SEC	3.37
CFA44_HUMAN	Cilia- and flagella-associated protein 44	1	1	32.99	0.044704	UC	3.36
IGSF3_HUMAN	Immunoglobulin superfamily member 3	1	1	47.75	0.044834	SEC	3.33
RAB1B_HUMAN	Ras-related protein Rab-1B	11	2	985.23	0.003044	SEC	3.33
SMRC1_HUMAN	SWI/SNF complex subunit SMARCC1	1	1	47.43	0.360003	UC	3.30
4F2_HUMAN	4F2 cell-surface antigen heavy chain	23	21	2491.46	2.99E-07	SEC	3.28
TBB4A_HUMAN	Tubulin beta-4A chain	20	1	1887.48	0.036878	UC	3.28
NPTN_HUMAN	Neuroplastin	4	3	219.01	7.53E-06	SEC	3.24
CD1B_HUMAN	T-cell surface glycoprotein CD1b	1	1	40.39	0.001655	SEC	3.23
SC5A3_HUMAN	Sodium/myo-inositol cotransporter	2	2	84.09	9.29E-05	SEC	3.23
SODC_HUMAN	Superoxide dismutase [Cu-Zn]	1	1	32.97	0.198605	UC	3.22
H1T_HUMAN	Histone H1t	1	1	64.44	0.00334	UC	3.21
CNR2_HUMAN	Cannabinoid receptor 2	1	1	48.77	0.004003	SEC	3.21
RL7_HUMAN	60S ribosomal protein L7	14	11	870.59	2.97E-05	SEC	3.201
ORN_HUMAN	Oligoribonuclease, mitochondrial	1	1	36.03	0.173714	SEC	3.20
MRP1_HUMAN	Multidrug resistance-associated protein 1	22	21	1495.92	5.05E-06	SEC	3.18
RTN4_HUMAN	Reticulon-4	3	3	146.74	0.00119	SEC	3.13
PP12C_HUMAN	Protein phosphatase 1 regulatory subunit 12C	1	1	31.69	6.37E-05	UC	3.11
WDR54_HUMAN	WD repeat-containing protein 54	1	1	39.84	0.000273	SEC	3.10
PYR1_HUMAN	CAD protein	5	5	329.37	0.000435	UC	3.09
HNRDL_HUMAN	Heterogeneous nuclear ribonucleoprotein D-like	2	1	85.7	0.034814	UC	3.06

T cell 18 h ACdEV proteomes when isolated by SEC versus UC

Accession	Description	Peptide count	Unique peptides	Confidence score	Anova (p)	Highest mean condition	Max fold change
KAPCA_HUMAN	cAMP-dependent protein kinase catalytic subunit alpha	2	1	105.27	0.000531	SEC	3.06
AAAT_HUMAN	Neutral amino acid transporter B(0)	13	11	1213.34	3.63E-06	SEC	3.06
GAPR1_HUMAN	Golgi-associated plant pathogenesis-related protein 1	2	2	241.01	0.016599	SEC	3.06
PMM2_HUMAN	Phosphomannomutase 2	1	1	32.95	0.00645	SEC	3.05
TADBP_HUMAN	TAR DNA-binding protein 43	1	1	74.94	0.187558	UC	3.02
DDX3X_HUMAN	ATP-dependent RNA helicase DDX3X	2	1	156.4	0.008053	UC	2.98
ITA5_HUMAN	Integrin alpha-5	2	2	82.27	0.000947	SEC	2.97
AP2M1_HUMAN	AP-2 complex subunit mu	6	5	326.24	1.58E-05	SEC	2.97
TPPC5_HUMAN	Trafficking protein particle complex subunit 5	1	1	31.84	0.092363	SEC	2.94
ELOB_HUMAN	Elongin-B	1	1	35.89	0.015664	SEC	2.93
PITH1_HUMAN	PITH domain-containing protein 1	2	2	82.73	0.008055	UC	2.93
ZN500_HUMAN	Zinc finger protein 500	1	1	41.59	0.003191	UC	2.92
INADL_HUMAN	InaD-like protein	1	1	41.25	0.016312	UC	2.91
HARS1_HUMAN	Histidine--tRNA ligase, cytoplasmic	5	2	341.21	6.09E-05	SEC	2.90
SPSY_HUMAN	Spermine synthase	2	2	143.48	0.003806	SEC	2.90
S38A5_HUMAN	Sodium-coupled neutral amino acid transporter 5	5	3	331.5	1.44E-05	SEC	2.90
TECR_HUMAN	Very-long-chain enoyl-CoA reductase	1	1	60.95	0.017682	SEC	2.88
COTL1_HUMAN	Coactosin-like protein	3	3	190.82	0.054137	SEC	2.86
SL7A1_HUMAN	High affinity cationic amino acid transporter 1	1	1	94.48	5.00E-05	SEC	2.86
FKB1A_HUMAN	Peptidyl-prolyl cis-trans isomerase FKBP1A	1	1	84.37	0.048394	SEC	2.84
TRFE_HUMAN	Serotransferrin	1	1	71.02	0.023194	UC	2.83
GGPPS_HUMAN	Geranylgeranyl pyrophosphate synthase	1	1	35.52	0.052512	SEC	2.82
H4_HUMAN	Histone H4	7	7	604.32	0.051174	SEC	2.82
TVBL3_HUMAN	T cell receptor beta variable 12-3	1	1	194.73	3.18E-05	SEC	2.80
SC31A_HUMAN	Protein transport protein Sec31A	1	1	42.53	0.062943	SEC	2.79
AP3D1_HUMAN	AP-3 complex subunit delta-1	1	1	48.4	0.019845	UC	2.78
FUBP1_HUMAN	Far upstream element-binding protein 1	4	2	257.7	8.48E-06	UC	2.75
MEP50_HUMAN	Methylosome protein 50	2	2	132.12	0.000189	UC	2.75
PANX1_HUMAN	Pannexin-1	2	2	137.28	0.001965	SEC	2.73
PTN6_HUMAN	Tyrosine-protein phosphatase non-receptor type 6	1	1	53.37	0.030472	UC	2.74
F234A_HUMAN	Protein FAM234A	1	1	39.69	0.02341	SEC	2.73
CUTA_HUMAN	Protein CutA OS=Homo sapiens	1	1	70.72	0.007555	SEC	2.72
CD99_HUMAN	CD99 antigen	2	2	122.88	0.002327	SEC	2.72
ATRN_HUMAN	Attractin	3	3	156.36	0.000152	SEC	2.71
FLOT2_HUMAN	Flotillin-2	9	9	568.21	2.87E-05	SEC	2.70
QSPP_HUMAN	Queuosine salvage protein	1	1	57.68	0.12417	SEC	2.69
IMPA3_HUMAN	Golgi-resident adenosine 3',5'-bisphosphate 3'-phosphatase	1	1	57.48	0.229443	SEC	2.69
5NTD_HUMAN	5'-nucleotidase	2	2	103.48	0.057404	SEC	2.66
S4A7_HUMAN	Sodium bicarbonate cotransporter 3	14	11	978.07	2.52E-05	SEC	2.65
S39AE_HUMAN	Metal cation symporter ZIP14	1	1	32.99	0.001787	SEC	2.63
BROX_HUMAN	BRO1 domain-containing protein BROX	6	6	329.55	0.000104	SEC	2.61
UFC1_HUMAN	Ubiquitin-fold modifier-conjugating enzyme 1	1	1	42.73	0.151834	SEC	2.61

T cell 18 h ACdEV proteomes when isolated by SEC versus UC

Accession	Description	Peptide count	Unique peptides	Confidence score	Anova (p)	Highest mean condition	Max fold change
ELP3_HUMAN	Elongator complex protein 3	1	1	41.12	0.163605	UC	2.61
M4K3_HUMAN	Mitogen-activated protein kinase kinase kinase kinase 3	1	1	31.36	0.112288	SEC	2.60
NDRG1_HUMAN	Protein NDRG1	2	2	148.49	1.54E-05	SEC	2.60
CPZIP_HUMAN	CapZ-interacting protein	1	1	57.33	6.47E-06	SEC	2.60
S19A1_HUMAN	Reduced folate transporter	2	2	153.8	0.000462	SEC	2.59
ALBU_HUMAN	Albumin	4	4	391.27	0.000478	UC	2.58
DEFI6_HUMAN	Differentially expressed in FDCP 6 homolog	1	1	55.35	0.014023	UC	2.58
AIMP2_HUMAN	Aminoacyl tRNA synthase complex-interacting multifunctional protein 2	2	2	152.66	0.001714	UC	2.58
M4K4_HUMAN	Mitogen-activated protein kinase kinase kinase kinase 4	2	1	92.76	0.006915	SEC	2.58
AP2A2_HUMAN	AP-2 complex subunit alpha-2	4	2	253.68	9.70E-05	SEC	2.58
ROA3_HUMAN	Heterogeneous nuclear ribonucleoprotein A3	2	1	73.5	0.050475	UC	2.58
UBE2N_HUMAN	Ubiquitin-conjugating enzyme E2 N	2	1	111.14	0.015235	SEC	2.57
ARP10_HUMAN	Actin-related protein 10	1	1	63.4	7.03E-05	SEC	2.57
SCRN1_HUMAN	Secernin-1	2	2	116.28	0.000905	SEC	2.56
CD1D_HUMAN	Antigen-presenting glycoprotein CD1d	1	1	33.4	3.82E-05	SEC	2.55
GNAI3_HUMAN	Guanine nucleotide-binding protein G(i) subunit alpha-3	10	4	742.52	2.70E-06	SEC	2.55
GNAO_HUMAN	Guanine nucleotide-binding protein G(o) subunit alpha	9	6	702.39	1.17E-05	SEC	2.55
PTBP1_HUMAN	Polypyrimidine tract-binding protein 1	6	5	432.4	0.002515	UC	2.54
SNF8_HUMAN	Vacuolar-sorting protein SNF8	3	3	220.17	0.005498	SEC	2.54
TBCA_HUMAN	Tubulin-specific chaperone A	2	2	79.18	0.000484	SEC	2.54
HYOU1_HUMAN	Hypoxia up-regulated protein 1	1	1	63.87	0.043505	UC	2.54
DEST_HUMAN	Destrin	2	1	78.1	0.017642	SEC	2.53
SPS1_HUMAN	Selenide, water dikinase 1	2	2	132.46	0.022604	UC	2.52
WDR82_HUMAN	WD repeat-containing protein 82	2	1	77.76	0.004371	UC	2.52
S12A2_HUMAN	Solute carrier family 12 member 2	6	4	351.22	3.23E-05	SEC	2.52
MBLC2_HUMAN	Metallo-beta-lactamase domain-containing protein 2	2	2	93.91	0.000333	SEC	2.51
MRGX2_HUMAN	Mas-related G-protein coupled receptor member X2	1	1	34.95	0.051893	SEC	2.51
WDR12_HUMAN	Ribosome biogenesis protein WDR12	1	1	84.47	0.000527	UC	2.51
SRSF6_HUMAN	Serine/arginine-rich splicing factor 6	5	4	249.5	1.60E-05	UC	2.51
CSK22_HUMAN	Casein kinase II subunit alpha'	2	1	95.4	0.049397	SEC	2.50
UB2V2_HUMAN	Ubiquitin-conjugating enzyme E2 variant 2	7	3	392.73	0.001727	SEC	2.48
PPIB_HUMAN	Peptidyl-prolyl cis-trans isomerase B	1	1	100.86	0.034934	UC	2.47
CFAH_HUMAN	Complement factor H	1	1	33.46	0.005396	UC	2.47
RAB8B_HUMAN	Ras-related protein Rab-8B	9	3	655.31	0.001003	SEC	2.46
CNOT1_HUMAN	CCR4-NOT transcription complex subunit 1	1	1	32.48	0.001019	UC	2.45
TP4A1_HUMAN	Protein tyrosine phosphatase type IVA 1	1	1	73.16	0.018159	SEC	2.45
SYHM_HUMAN	Histidine--tRNA ligase, mitochondrial	2	1	141.35	0.017098	UC	2.43
C1GLT_HUMAN	Glycoprotein-N-acetylgalactosamine 3-beta-galactosyltransferase 1	1	1	31.08	0.001179	UC	2.43
IF4E_HUMAN	Eukaryotic translation initiation factor 4E	3	3	132.08	0.077327	SEC	2.43
GLYM_HUMAN	Serine hydroxymethyltransferase, mitochondrial	2	2	98.83	0.002812	UC	2.42
PSME3_HUMAN	Proteasome activator complex subunit 3	3	3	190.47	0.00076	UC	2.41
THOC6_HUMAN	THO complex subunit 6 homolog	4	3	274.89	0.001042	UC	2.40

T cell 18 h ACdEV proteomes when isolated by SEC versus UC

Accession	Description	Peptide count	Unique peptides	Confidence score	Anova (p)	Highest mean condition	Max fold change
SPRE_HUMAN	Sepiapterin reductase	1	1	67.64	0.012953	SEC	2.40
H90B4_HUMAN	Putative heat shock protein HSP 90-beta 4	8	1	525.25	0.000311	UC	2.39
MCM7_HUMAN	DNA replication licensing factor MCM7	6	5	366.97	0.000493	UC	2.38
CD9_HUMAN	CD9 antigen	1	1	51.88	0.000456	SEC	2.37
PEF1_HUMAN	Peflin	2	2	89.04	0.000571	UC	2.36
BDH2_HUMAN	3-hydroxybutyrate dehydrogenase type 2	1	1	44.8	0.020019	SEC	2.35
SNR40_HUMAN	U5 small nuclear ribonucleoprotein 40 kDa protein	3	2	128.76	0.001068	UC	2.34
VAMP5_HUMAN	Vesicle-associated membrane protein 5	1	1	79.77	0.065389	SEC	2.34
STAU1_HUMAN	Double-stranded RNA-binding protein Staufen homolog 1	1	1	64.22	0.056184	UC	2.33
8ODP_HUMAN	7,8-dihydro-8-oxoguanine triphosphatase	2	2	126.13	0.004253	SEC	2.32
DDX1_HUMAN	ATP-dependent RNA helicase DDX1	2	2	117.69	0.101916	UC	2.29
ACL6A_HUMAN	Actin-like protein 6A	2	1	117.25	0.268614	SEC	2.29
MOT4_HUMAN	Monocarboxylate transporter 4	2	2	109.92	0.00408	SEC	2.29
RB11A_HUMAN	Ras-related protein Rab-11A	10	2	702.03	0.921302	UC	2.29
PI42A_HUMAN	Phosphatidylinositol 5-phosphate 4-kinase type-2 alpha	8	5	430.75	0.000717	SEC	2.29
ECH1_HUMAN	Delta(3,5)-Delta(2,4)-dienoyl-CoA isomerase, mitochondrial	3	3	206.94	0.063742	UC	2.28
CLDN1_HUMAN	Claudin domain-containing protein 1	3	3	217.46	0.000148	SEC	2.28
UBTD2_HUMAN	Ubiquitin domain-containing protein 2	1	1	42.01	0.001514	SEC	2.28
RADI_HUMAN	Radixin	21	6	1380.81	0.000119	SEC	2.28
CC113_HUMAN	Coiled-coil domain-containing protein 113	1	1	32.83	0.682382	SEC	2.27
AMPD2_HUMAN	AMP deaminase 2	3	2	118.65	0.002577	UC	2.26
MCM3_HUMAN	DNA replication licensing factor MCM3	5	4	291.57	0.000413	UC	2.26
PTPRC_HUMAN	Receptor-type tyrosine-protein phosphatase C	32	28	2626.69	2.31E-06	SEC	2.26
CUL2_HUMAN	Cullin-2	3	2	140.74	0.00014	UC	2.26
UMPS_HUMAN	Uridine 5'-monophosphate synthase	1	1	57.16	0.035071	UC	2.25
CHMP6_HUMAN	Charged multivesicular body protein 6	4	3	368.15	0.006383	SEC	2.25
HNRPF_HUMAN	Heterogeneous nuclear ribonucleoprotein F	2	2	115.97	0.000169	UC	2.25
RL36A_HUMAN	60S ribosomal protein L36a	1	1	33.62	0.111179	SEC	2.24
SUMO2_HUMAN	Small ubiquitin-related modifier 2	1	1	101.58	0.01561	SEC	2.24
IF4A1_HUMAN	Eukaryotic initiation factor 4A-I	19	11	1435.99	0.000121	UC	2.23
GSTO1_HUMAN	Glutathione S-transferase omega-1	6	6	339.31	0.000107	SEC	2.23
EPB41_HUMAN	Protein 4.1	10	8	485.52	2.67E-05	SEC	2.23
PNMA2_HUMAN	Paraneoplastic antigen Ma2	4	3	311.93	0.000612	SEC	2.21
MYO19_HUMAN	Unconventional myosin-XIX	1	1	37.7	0.00039	SEC	2.20
PRAF3_HUMAN	PRA1 family protein 3	1	1	99.44	0.026935	SEC	2.20
THOC3_HUMAN	THO complex subunit 3	1	1	56.41	0.831492	SEC	2.20
IF6_HUMAN	Eukaryotic translation initiation factor 6	1	1	48.37	0.286895	SEC	2.19
DYLT1_HUMAN	Dynein light chain Tctex-type 1	1	1	40.32	0.124538	SEC	2.19
CSK21_HUMAN	Casein kinase II subunit alpha	7	1	426.82	0.107378	SEC	2.19
ICAM3_HUMAN	Intercellular adhesion molecule 3	3	2	211.05	0.000749	SEC	2.19
RIR1_HUMAN	Ribonucleoside-diphosphate reductase large subunit	5	4	303.4	8.14E-05	UC	2.18
BTK_HUMAN	Tyrosine-protein kinase BTK	1	1	33.98	0.000311	SEC	2.18

T cell 18 h ACdEV proteomes when isolated by SEC versus UC

Accession	Description	Peptide count	Unique peptides	Confidence score	Anova (p)	Highest mean condition	Max fold change
PRS10_HUMAN	26S proteasome regulatory subunit 10B	2	2	120.23	0.011643	UC	2.18
CTL1_HUMAN	Choline transporter-like protein 1	4	4	221.81	0.000136	SEC	2.18
ARF4_HUMAN	ADP-ribosylation factor 4	8	1	566.73	0.013137	SEC	2.18
RNH2A_HUMAN	Ribonuclease H2 subunit A	1	1	44.87	0.014454	UC	2.16
RL7A_HUMAN	60S ribosomal protein L7a	9	7	646.43	0.000412	SEC	2.15
TPD54_HUMAN	Tumor protein D54	1	1	72.81	0.003232	SEC	2.15
RAB8A_HUMAN	Ras-related protein Rab-8A	10	4	679.87	0.001499	SEC	2.15
SH3L3_HUMAN	SH3 domain-binding glutamic acid-rich-like protein 3	1	1	74.36	0.086449	SEC	2.14
VP13C_HUMAN	Vacuolar protein sorting-associated protein 13C	1	1	89.42	0.085157	SEC	2.14
PLXA1_HUMAN	Plexin-A1	3	2	135.25	0.002266	SEC	2.13
SLIT1_HUMAN	Slit homolog 1 protein	1	1	47.2	0.001008	UC	2.13
TPM3_HUMAN	Tropomyosin alpha-3 chain	9	4	688.5	0.014711	SEC	2.13
PVR_HUMAN	Poliovirus receptor	1	1	45.63	1.73E-05	SEC	2.13
SPTN1_HUMAN	Spectrin alpha chain, non-erythrocytic 1	122	113	10949.99	2.32E-07	SEC	2.13
KAP2_HUMAN	cAMP-dependent protein kinase type II-alpha regulatory subunit	6	6	395.18	0.006291	SEC	2.12
PSMG2_HUMAN	Proteasome assembly chaperone 2	4	4	222	0.002069	SEC	2.11
CD38_HUMAN	ADP-ribosyl cyclase/cyclic ADP-ribose hydrolase 1	4	4	255.32	6.21E-05	SEC	2.11
DKC1_HUMAN	H/ACA ribonucleoprotein complex subunit DKC1 O	2	1	93.77	0.00047	SEC	2.11
NSF1C_HUMAN	NSFL1 cofactor p47	2	1	131.86	0.000135	UC	2.09
KNL1_HUMAN	Kinetochore scaffold 1	1	1	33.43	0.010655	UC	2.09
SPTB2_HUMAN	Spectrin beta chain, non-erythrocytic 1	95	78	8442.33	1.35E-06	SEC	2.09
LEUK_HUMAN	Leukosialin	5	5	360.9	0.034537	SEC	2.08
CHM2B_HUMAN	Charged multivesicular body protein 2b	2	2	113.94	0.000361	SEC	2.08
PSA7_HUMAN	Proteasome subunit alpha type-7	9	8	612.88	0.002777	UC	2.07
STX4_HUMAN	Syntaxin-4	8	8	573.38	0.00801	SEC	2.07
FUBP2_HUMAN	Far upstream element-binding protein 2	2	1	118.72	0.001572	UC	2.07
SYAC_HUMAN	Alanine--tRNA ligase, cytoplasmic	12	12	840.43	4.00E-05	UC	2.07
TAFA5_HUMAN	Chemokine-like protein TAFA-5	1	1	35.59	0.294492	UC	2.07
AP2S1_HUMAN	AP-2 complex subunit sigma	1	1	65.47	0.001543	SEC	2.06
TRBC1_HUMAN	T cell receptor beta constant 1	4	3	375.88	1.22E-05	SEC	2.06
SATT_HUMAN	Neutral amino acid transporter A	6	6	414.98	0.000179	SEC	2.06
TKT_HUMAN	Transketolase	14	12	1070.1	5.40E-06	UC	2.06
HNRPD_HUMAN	Heterogeneous nuclear ribonucleoprotein D0	4	3	403.19	0.004615	UC	2.06
PPCE_HUMAN	Prolyl endopeptidase	1	1	96.49	0.00324	SEC	2.06
HNRPU_HUMAN	Heterogeneous nuclear ribonucleoprotein U	1	1	84.57	0.073175	UC	2.06
PCBP2_HUMAN	Poly(rC)-binding protein 2	3	2	188.4	0.003984	UC	2.06
DDX5_HUMAN	Probable ATP-dependent RNA helicase DDX5	5	2	315.51	1.08E-05	UC	2.05
H2B1C_HUMAN	Histone H2B type 1-C/E/F/G/I	10	2	1185.95	0.005647	SEC	2.05
HS904_HUMAN	Putative heat shock protein HSP 90-alpha A4	4	1	350.14	0.004289	UC	2.05
S43A3_HUMAN	Solute carrier family 43 member 3	4	4	318.55	3.14E-05	SEC	2.04
HCDH_HUMAN	Hydroxyacyl-coenzyme A dehydrogenase, mitochondrial	2	1	73.71	0.145642	UC	2.04
FYB1_HUMAN	FYN-binding protein 1	2	2	144	0.009687	SEC	2.04

T cell 18 h ACdEV proteomes when isolated by SEC versus UC

Accession	Description	Peptide count	Unique peptides	Confidence score	Anova (p)	Highest mean condition	Max fold change
MPRD_HUMAN	Cation-dependent mannose-6-phosphate receptor	1	1	183.7	0.000442	SEC	2.04
AGRE5_HUMAN	Adhesion G protein-coupled receptor E5	4	3	266.61	0.000481	SEC	2.04
PSB4_HUMAN	Proteasome subunit beta type-4	7	7	700.41	0.004681	UC	2.03
TCPG_HUMAN	T-complex protein 1 subunit gamma	26	25	2129.86	2.03E-07	UC	2.03
HNRPL_HUMAN	Heterogeneous nuclear ribonucleoprotein L	2	2	104.41	2.08E-06	UC	2.03
RALA_HUMAN	Ras-related protein Ral-A	7	4	530.93	0.007036	SEC	2.03
ESYT1_HUMAN	Extended synaptotagmin-1	1	1	110.2	0.058672	SEC	2.02
CYTB_HUMAN	Cystatin-B	1	1	56.43	0.007794	SEC	2.02
XPO1_HUMAN	Exportin-1	12	12	697.34	0.000433	UC	2.01
ERF1_HUMAN	Eukaryotic peptide chain release factor subunit 1	4	4	297.12	0.004154	SEC	2.01
ITB1_HUMAN	Integrin beta-1	14	14	1266.85	0.000163	SEC	2.01
PDCL3_HUMAN	Phosducin-like protein 3	2	2	137.71	0.000459	UC	2.00
ACTN1_HUMAN	Alpha-actinin-1	23	10	1907.04	5.50E-06	SEC	2.00
MGRN1_HUMAN	E3 ubiquitin-protein ligase MGRN1	1	1	58.41	0.076649	SEC	1.99
DLG1_HUMAN	Disks large homolog 1	1	1	95	0.001106	SEC	1.99
GFPT1_HUMAN	Glutamine--fructose-6-phosphate aminotransferase [isomerizing] 1 O	5	3	295.91	0.000377	UC	1.99
PSME2_HUMAN	Proteasome activator complex subunit 2	5	4	362.45	0.011364	SEC	1.99
IF4H_HUMAN	Eukaryotic translation initiation factor 4H	2	2	87.4	0.115801	SEC	1.98
AT1B3_HUMAN	Sodium/potassium-transporting ATPase subunit beta-3	9	9	782.4	0.0002	SEC	1.98
BAG6_HUMAN	Large proline-rich protein BAG6	3	2	169.86	0.007864	UC	1.98
PUR1_HUMAN	Amidophosphoribosyltransferase	6	6	383.74	0.005194	UC	1.98
CDK2_HUMAN	Cyclin-dependent kinase 2	4	2	269.51	8.03E-06	UC	1.97
RS19_HUMAN	40S ribosomal protein S19	1	1	61.29	0.189063	SEC	1.97
CIB1_HUMAN	Calcium and integrin-binding protein 1	1	1	155.17	0.009315	SEC	1.97
DNJC5_HUMAN	DnaJ homolog subfamily C member 5	1	1	98.33	0.001301	SEC	1.97
CTNA1_HUMAN	Catenin alpha-1	6	4	460.29	0.002283	SEC	1.97
PFD2_HUMAN	Prefoldin subunit 2	2	2	148.15	0.006605	SEC	1.97
SERB_HUMAN	Phosphoserine phosphatase	2	2	94.95	0.000745	SEC	1.96
6PGL_HUMAN	6-phosphogluconolactonase	5	5	279.99	0.000406	SEC	1.96
GNAI2_HUMAN	Guanine nucleotide-binding protein G(i) subunit alpha-2	16	9	1471.27	1.26E-05	SEC	1.96
ACTN4_HUMAN	Alpha-actinin-4	30	17	2777.18	2.32E-05	SEC	1.96
HBB_HUMAN	Hemoglobin subunit beta	2	1	80.69	0.000974	UC	1.95
CD48_HUMAN	CD48 antigen	3	3	206.75	0.000659	SEC	1.95
GRAN_HUMAN	Grancalcin	1	1	44.98	0.067744	SEC	1.94
FPPS_HUMAN	Farnesyl pyrophosphate synthase	4	4	284.18	0.000132	SEC	1.94
TIAR_HUMAN	Nucleolysin TIAR	1	1	40.56	0.024433	UC	1.94
RAB2A_HUMAN	Ras-related protein Rab-2A	4	3	293.11	0.01478	SEC	1.94
1433T_HUMAN	14-3-3 protein theta	12	5	965.63	0.000722	SEC	1.93
KAD2_HUMAN	Adenylate kinase 2, mitochondrial	2	1	107.84	0.004833	UC	1.93
IF4G2_HUMAN	Eukaryotic translation initiation factor 4 gamma 2	5	4	272.2	0.002266	SEC	1.93
LIN7A_HUMAN	Protein lin-7 homolog A	2	1	109.23	0.571604	UC	1.92
PLSI_HUMAN	Plastin-1	5	3	411.41	0.004906	SEC	1.92

T cell 18 h ACdEV proteomes when isolated by SEC versus UC

Accession	Description	Peptide count	Unique peptides	Confidence score	Anova (p)	Highest mean condition	Max fold change
JAM1_HUMAN	Junctional adhesion molecule A	4	4	223.71	0.002541	SEC	1.92
ROAA_HUMAN	Heterogeneous nuclear ribonucleoprotein A/B	1	1	63.94	0.009339	UC	1.91
XPO2_HUMAN	Exportin-2	12	12	910.06	0.002456	UC	1.91
IMA1_HUMAN	Importin subunit alpha-1	4	4	239.49	0.000669	UC	1.91
ARPC3_HUMAN	Actin-related protein 2/3 complex subunit 3	8	8	499.72	0.008702	SEC	1.90
RAB21_HUMAN	Ras-related protein Rab-21	2	1	161.71	0.026898	SEC	1.90
MOT1_HUMAN	Monocarboxylate transporter 1	10	10	784.28	1.19E-05	SEC	1.90
DYH9_HUMAN	Dynein axonemal heavy chain 9	1	1	38.6	0.681657	SEC	1.90
BAP31_HUMAN	B-cell receptor-associated protein 31	1	1	37.46	0.169291	SEC	1.89
HLAA_HUMAN	HLA class I histocompatibility antigen, A alpha chain	11	5	931.39	0.000164	SEC	1.89
TSN7_HUMAN	Tetraspanin-7	5	5	478.95	0.000127	SEC	1.89
RACK1_HUMAN	Receptor of activated protein C kinase 1	10	10	672.13	0.000329	UC	1.89
RL6_HUMAN	60S ribosomal protein L6	9	8	835.88	0.003424	SEC	1.89
UBP7_HUMAN	Ubiquitin carboxyl-terminal hydrolase 7	7	7	417.08	0.000328	UC	1.89
PSN1_HUMAN	Presenilin-1	2	1	103.9	0.006873	SEC	1.88
CLH1_HUMAN	Clathrin heavy chain 1	63	43	5507.94	1.29E-05	SEC	1.88
SF3A2_HUMAN	Splicing factor 3A subunit 2	2	2	85.77	0.05222	UC	1.88
PUR2_HUMAN	Trifunctional purine biosynthetic protein adenosine-3	3	3	200.68	0.002776	UC	1.88
RTN1_HUMAN	Reticulon-1	1	1	53.53	0.009552	SEC	1.87
THEGL_HUMAN	Testicular haploid expressed gene protein-like	1	1	44.7	0.000221	UC	1.87
TCPZ_HUMAN	T-complex protein 1 subunit zeta	23	15	2172.69	3.71E-06	UC	1.87
MB12A_HUMAN	Multivesicular body subunit 12A	1	1	70.29	0.08059	SEC	1.87
RL5_HUMAN	60S ribosomal protein L5	7	7	404.8	0.007332	SEC	1.87
2A5G_HUMAN	Serine/threonine-protein phosphatase 2A 56 kDa regulatory subunit gamma isoform	1	1	35.47	0.080727	UC	1.87
RFA2_HUMAN	Replication protein A 32 kDa subunit	1	1	78.49	5.54E-05	UC	1.86
PRS6B_HUMAN	26S proteasome regulatory subunit 6B	4	4	307.16	0.003449	UC	1.86
GTR14_HUMAN	Solute carrier family 2, facilitated glucose transporter member 14	3	2	178.03	0.444473	SEC	1.86
NPM_HUMAN	Nucleophosmin	6	5	495.17	0.006831	UC	1.86
CTBL1_HUMAN	Beta-catenin-like protein 1	1	1	32.79	0.023616	SEC	1.86
FAM3C_HUMAN	Protein FAM3C	1	1	49.52	0.049405	SEC	1.85
GLO2_HUMAN	Hydroxyacylglutathione hydrolase, mitochondrial	2	2	99.95	0.160904	SEC	1.85
NIBA2_HUMAN	Protein Niban 2	5	5	269.68	0.001492	SEC	1.85
SGTA_HUMAN	Small glutamine-rich tetratricopeptide repeat-containing protein alpha	2	2	156.48	0.000543	UC	1.85
TPD52_HUMAN	Tumor protein D52	1	1	58.8	0.844146	SEC	1.84
ARP5L_HUMAN	Actin-related protein 2/3 complex subunit 5-like protein	3	2	151.72	0.006511	SEC	1.84
RCC2_HUMAN	Protein RCC2	5	5	272.32	0.011988	UC	1.83
GNAS1_HUMAN	Guanine nucleotide-binding protein G(s) subunit alpha isoforms XLas	10	8	736.29	5.77E-06	SEC	1.83
LCAP_HUMAN	Leucyl-cystinyl aminopeptidase	1	1	95.34	0.001278	SEC	1.82
CHM4A_HUMAN	Charged multivesicular body protein 4a	1	1	112.78	0.074367	SEC	1.82
NNRE_HUMAN	NAD(P)H-hydrate epimerase	3	3	213.65	0.017606	SEC	1.82
BPNT1_HUMAN	3'(2'),5'-bisphosphate nucleotidase 1	1	1	62.17	0.111623	SEC	1.82
JAM3_HUMAN	Junctional adhesion molecule C	4	4	206.83	1.05E-05	SEC	1.82

T cell 18 h ACdEV proteomes when isolated by SEC versus UC

Accession	Description	Peptide count	Unique peptides	Confidence score	Anova (p)	Highest mean condition	Max fold change
MOES_HUMAN	Moesin	61	44	5587.52	3.03E-06	SEC	1.82
CD3Z_HUMAN	T-cell surface glycoprotein CD3 zeta chain	4	4	426.47	0.022764	SEC	1.82
PIPNB_HUMAN	Phosphatidylinositol transfer protein beta isoform	5	4	259.5	0.005273	SEC	1.82
ZN626_HUMAN	Zinc finger protein 626	1	1	37.94	0.0009	SEC	1.81
RS5_HUMAN	40S ribosomal protein S5	4	4	231.26	0.00016	SEC	1.81
AMPL_HUMAN	Cytosol aminopeptidase	4	4	265.67	5.11E-05	UC	1.81
TNPO1_HUMAN	Transportin-1	2	1	147.51	0.00038	UC	1.80
TIF1B_HUMAN	Transcription intermediary factor 1-beta	1	1	35.4	0.034094	UC	1.80
FERM2_HUMAN	Fermitin family homolog 2	4	3	269.75	0.001291	SEC	1.80
DDX21_HUMAN	Nucleolar RNA helicase 2	1	1	39.48	0.024491	UC	1.80
PECA1_HUMAN	Platelet endothelial cell adhesion molecule	5	5	352.05	0.00044	SEC	1.79
PRP19_HUMAN	Pre-mRNA-processing factor 19	9	8	434.84	2.16E-05	UC	1.79
RFTN1_HUMAN	Raftlin	2	1	96.82	0.109216	SEC	1.79
BRDT_HUMAN	Bromodomain testis-specific protein	1	1	35.4	0.005419	UC	1.79
BASI_HUMAN	Basigin	8	8	785.24	7.56E-06	SEC	1.79
P85A_HUMAN	Phosphatidylinositol 3-kinase regulatory subunit alpha	1	1	40.3	0.346004	UC	1.78
PSB7_HUMAN	Proteasome subunit beta type-7	8	8	496.69	0.008482	UC	1.78
CHIP_HUMAN	E3 ubiquitin-protein ligase CHIP	1	1	35.45	0.037874	SEC	1.78
PIPNA_HUMAN	Phosphatidylinositol transfer protein alpha isoform	2	1	74.02	0.006359	SEC	1.78
DIAP1_HUMAN	Protein diaphanous homolog 1	2	2	190.34	0.072396	SEC	1.78
TBCE_HUMAN	Tubulin-specific chaperone E	1	1	54.92	0.014672	UC	1.78
NAMPT_HUMAN	Nicotinamide phosphoribosyltransferase	2	2	124.15	0.002071	UC	1.78
RHOG_HUMAN	Rho-related GTP-binding protein RhoG	4	4	304.43	0.049433	SEC	1.78
PSB1_HUMAN	Proteasome subunit beta type-1	7	7	611.15	0.00643	UC	1.78
PARVG_HUMAN	Gamma-parvin	1	1	42.58	0.016072	UC	1.77
H15_HUMAN	Histone H1.5	1	1	84.9	0.006727	UC	1.77
CHM1A_HUMAN	Charged multivesicular body protein 1a	3	3	137.46	6.25E-05	SEC	1.77
HGS_HUMAN	Hepatocyte growth factor-regulated tyrosine kinase substrate	1	1	67.49	0.194433	SEC	1.77
RO60_HUMAN	60 kDa SS-A/Ro ribonucleoprotein	1	1	62.02	0.17342	UC	1.77
WDR61_HUMAN	WD repeat-containing protein 61	1	1	77.7	0.033501	UC	1.77
HNRPK_HUMAN	Heterogeneous nuclear ribonucleoprotein K	10	9	677.24	0.000192	UC	1.77
SNP23_HUMAN	Synaptosomal-associated protein 23	7	6	535.99	0.004877	SEC	1.77
GNAQ_HUMAN	Guanine nucleotide-binding protein G(q) subunit alpha	12	8	915.12	0.000776	SEC	1.76
MYL6_HUMAN	Myosin light polypeptide 6	5	3	477.57	4.62E-05	SEC	1.76
NIBA1_HUMAN	Protein Niban 1	1	1	115.21	0.00169	SEC	1.76
SCAM3_HUMAN	Secretory carrier-associated membrane protein 3	1	1	149.04	0.002183	SEC	1.75
HLAB_HUMAN	HLA class I histocompatibility antigen, B alpha chain	6	2	402.51	0.000277	SEC	1.75
CD1C_HUMAN	T-cell surface glycoprotein CD1c	2	1	94.52	0.484343	SEC	1.75
AIMP1_HUMAN	Aminoacyl tRNA synthase complex-interacting multifunctional protein 1	1	1	71.97	0.002253	SEC	1.75
GBB1_HUMAN	Guanine nucleotide-binding protein G(I)/G(S)/G(T) subunit beta-1	6	2	363.8	0.048001	SEC	1.75
PEBP1_HUMAN	Phosphatidylethanolamine-binding protein 1	3	3	341.77	0.030853	SEC	1.75
ITA4_HUMAN	Integrin alpha-4	20	19	1231.61	0.000124	SEC	1.75

T cell 18 h ACdEV proteomes when isolated by SEC versus UC

Accession	Description	Peptide count	Unique peptides	Confidence score	Anova (p)	Highest mean condition	Max fold change
RL31_HUMAN	60S ribosomal protein L31	3	2	178.46	0.053192	SEC	1.75
SOX30_HUMAN	Transcription factor SOX-30	1	1	35.28	0.043728	UC	1.75
DCTN3_HUMAN	Dynactin subunit 3	2	2	106.43	0.02458	SEC	1.74
CD3E_HUMAN	T-cell surface glycoprotein CD3 epsilon chain	3	3	161.93	0.128058	SEC	1.74
FAAA_HUMAN	Fumarylacetoacetase	3	3	208.68	4.27E-05	SEC	1.74
CD53_HUMAN	Leukocyte surface antigen CD53	2	2	107.48	0.000414	SEC	1.74
CATD_HUMAN	Cathepsin D	3	2	177.21	0.011053	SEC	1.73
S29A1_HUMAN	Equilibrative nucleoside transporter 1	9	8	628.46	7.84E-06	SEC	1.73
CTNB1_HUMAN	Catenin beta-1	11	8	635.95	9.36E-05	SEC	1.73
PIBF1_HUMAN	Progesterone-induced-blocking factor 1	1	1	33.27	0.000751	SEC	1.73
KPRA_HUMAN	Phosphoribosyl pyrophosphate synthase-associated protein 1	2	1	121.69	0.023357	SEC	1.73
ANM5_HUMAN	Protein arginine N-methyltransferase 5	10	9	709.55	1.58E-05	UC	1.73
EFHD2_HUMAN	EF-hand domain-containing protein D2	1	1	84.06	0.000775	SEC	1.73
NRX1A_HUMAN	Neurexin-1	1	1	33.15	0.000504	UC	1.72
FEN1_HUMAN	Flap endonuclease 1	1	1	33.13	0.010786	UC	1.72
GDE_HUMAN	Glycogen debranching enzyme	3	3	153.3	0.003898	UC	1.72
ROA1_HUMAN	Heterogeneous nuclear ribonucleoprotein A1	4	3	399.16	0.002043	UC	1.72
FUMH_HUMAN	Fumarate hydratase, mitochondrial	4	4	285.91	0.000212	UC	1.72
RAB10_HUMAN	Ras-related protein Rab-10	7	4	480.34	0.00444	SEC	1.72
GDIB_HUMAN	Rab GDP dissociation inhibitor beta	26	18	2228.4	0.000133	SEC	1.72
MYH10_HUMAN	Myosin-10	47	29	3245.07	4.26E-05	SEC	1.72
PSB2_HUMAN	Proteasome subunit beta type-2	6	5	410.55	0.021489	UC	1.71
CAPR1_HUMAN	Caprin-1	2	2	133.32	4.79E-05	SEC	1.71
METK2_HUMAN	S-adenosylmethionine synthase isoform type-2	3	2	197.51	0.001666	UC	1.71
IDHP_HUMAN	Isocitrate dehydrogenase [NADP], mitochondrial	1	1	71.75	0.002261	UC	1.71
CD166_HUMAN	CD166 antigen	2	2	105.95	0.012981	SEC	1.71
RASA2_HUMAN	Ras GTPase-activating protein 2 OS	1	1	50.99	0.029133	UC	1.71
ICAM1_HUMAN	Intercellular adhesion molecule 1	6	6	393.88	0.002048	SEC	1.71
HDHD1_HUMAN	Pseudouridine-5'-phosphatase	2	2	104.91	0.290382	UC	1.71
CAN1_HUMAN	Calpain-1 catalytic subunit	2	2	84.56	0.038016	SEC	1.71
KIF23_HUMAN	Kinesin-like protein KIF23	1	1	59.16	0.128743	UC	1.71
TCPE_HUMAN	T-complex protein 1 subunit epsilon	36	33	3455.54	7.89E-06	UC	1.71
ILF2_HUMAN	Interleukin enhancer-binding factor 2	6	6	400.69	1.69E-05	UC	1.71
FLNB_HUMAN	Filamin-B	63	56	4821.04	4.47E-08	SEC	1.70
ICAM2_HUMAN	Intercellular adhesion molecule 2	4	3	237.12	9.96E-05	SEC	1.70
TOP2A_HUMAN	DNA topoisomerase 2-alpha OS	1	1	66.44	0.169335	UC	1.70
CD2_HUMAN	T-cell surface antigen CD2	5	5	278.66	0.000662	SEC	1.70
SMD2_HUMAN	Small nuclear ribonucleoprotein Sm D2	3	2	155.22	0.043288	SEC	1.70
PPIA_HUMAN	Peptidyl-prolyl cis-trans isomerase A	10	8	754.31	0.015586	SEC	1.70
PTCA_HUMAN	Protein tyrosine phosphatase receptor type C-associated protein	6	6	424.86	0.000556	SEC	1.70
PSB3_HUMAN	Proteasome subunit beta type-3	4	4	416.75	0.010962	UC	1.70
KHDR1_HUMAN	KH domain-containing, RNA-binding, signal transduction-associated protein 1	1	1	43.83	0.004174	UC	1.69

T cell 18 h ACdEV proteomes when isolated by SEC versus UC

Accession	Description	Peptide count	Unique peptides	Confidence score	Anova (p)	Highest mean condition	Max fold change
AT5F1_HUMAN	ATP synthase F(0) complex subunit B1, mitochondrial	1	1	39.16	0.022764	SEC	1.69
EIF3I_HUMAN	Eukaryotic translation initiation factor 3 subunit I	6	6	320.99	0.001608	SEC	1.69
PSA5_HUMAN	Proteasome subunit alpha type-5	8	7	659.5	0.001164	UC	1.69
TTYH3_HUMAN	Protein tweety homolog 3	2	2	164.03	0.000155	SEC	1.68
SYMC_HUMAN	Methionine--tRNA ligase, cytoplasmic	5	5	265.53	0.001072	UC	1.68
UBC12_HUMAN	NEDD8-conjugating enzyme Ubc12	2	2	66.53	0.002079	SEC	1.68
ADA10_HUMAN	Disintegrin and metalloproteinase domain-containing protein 10	6	6	349.42	2.02E-05	SEC	1.68
RFA1_HUMAN	Replication protein A 70 kDa DNA-binding subunit	3	3	144.28	0.005142	UC	1.68
PRDX6_HUMAN	Peroxiredoxin-6	3	2	155.26	0.01273	SEC	1.68
IQGA1_HUMAN	Ras GTPase-activating-like protein IQGAP1	62	53	5106.03	8.06E-06	SEC	1.68
FLII_HUMAN	Protein flightless-1 homolog	1	1	72.03	0.096016	UC	1.67
PSMD6_HUMAN	26S proteasome non-ATPase regulatory subunit 6	10	9	661.24	0.035301	SEC	1.67
PSB6_HUMAN	Proteasome subunit beta type-6	4	4	311.47	0.013194	UC	1.67
APT_HUMAN	Adenine phosphoribosyltransferase	2	2	90.28	0.096864	UC	1.67
EFC12_HUMAN	EF-hand calcium-binding domain-containing protein 12	1	1	40.37	0.13436	SEC	1.67
IGSF8_HUMAN	Immunoglobulin superfamily member 8	13	12	1133.32	2.22E-05	SEC	1.67
VATH_HUMAN	V-type proton ATPase subunit H	1	1	58.46	0.060304	UC	1.67
DDX17_HUMAN	Probable ATP-dependent RNA helicase DDX17	4	1	248.7	0.009572	UC	1.67
TJA3_HUMAN	T cell receptor alpha joining 3	1	1	57.79	0.000695	SEC	1.67
ADHX_HUMAN	Alcohol dehydrogenase class-3	3	3	187.44	5.70E-05	UC	1.67
ARF1_HUMAN	ADP-ribosylation factor 1	10	6	841.55	0.00979	SEC	1.66
PROF1_HUMAN	Profilin-1	8	8	741.24	0.03456	SEC	1.66
PA1B3_HUMAN	Platelet-activating factor acetylhydrolase IB subunit alpha1	3	3	137.34	0.118774	UC	1.66
C2CD5_HUMAN	C2 domain-containing protein 5	6	5	403.36	0.004647	SEC	1.66
CD47_HUMAN	Leukocyte surface antigen CD47	7	7	437.35	4.79E-05	SEC	1.66
PHB2_HUMAN	Prohibitin-2	1	1	82.18	0.005131	UC	1.66
RS10_HUMAN	40S ribosomal protein S10	2	2	134.91	0.133377	SEC	1.65
PNPH_HUMAN	Purine nucleoside phosphorylase	11	11	920.85	0.006782	SEC	1.65
HPCA_HUMAN	Neuron-specific calcium-binding protein hippocalcin	1	1	54.24	0.744668	UC	1.65
TCPD_HUMAN	T-complex protein 1 subunit delta	24	23	2357.85	3.47E-06	UC	1.65
STOM_HUMAN	Stomatin	11	9	1003.49	0.000172	SEC	1.65
DIP2B_HUMAN	Disco-interacting protein 2 homolog B	26	22	1927.27	0.000313	SEC	1.64
DC1L1_HUMAN	Cytoplasmic dynein 1 light intermediate chain 1	1	1	33.62	0.357661	UC	1.64
NUCB2_HUMAN	Nucleobindin-2	1	1	58.25	0.361713	UC	1.64
ALDOC_HUMAN	Fructose-bisphosphate aldolase C	17	14	1464.97	0.000235	SEC	1.64
HNRPR_HUMAN	Heterogeneous nuclear ribonucleoprotein R	5	1	335.46	9.45E-05	UC	1.64
PLSL_HUMAN	Plastin-2	37	32	3955.55	0.000299	SEC	1.64
CAB45_HUMAN	45 kDa calcium-binding protein	1	1	38.6	0.002546	UC	1.64
TCPH_HUMAN	T-complex protein 1 subunit eta	25	25	2274.08	4.09E-05	UC	1.64
NIT1_HUMAN	Deaminated glutathione amidase	1	1	48.17	0.001163	UC	1.64
MCM4_HUMAN	DNA replication licensing factor MCM4	9	8	570.74	0.001139	UC	1.63
MYO1G_HUMAN	Unconventional myosin-Ig	9	8	567.79	0.006549	UC	1.63

T cell 18 h ACdEV proteomes when isolated by SEC versus UC

Accession	Description	Peptide count	Unique peptides	Confidence score	Anova (p)	Highest mean condition	Max fold change
EF1A1_HUMAN	Elongation factor 1-alpha 1	18	8	1316.91	7.80E-05	UC	1.63
FAS_HUMAN	Fatty acid synthase	29	27	1984.62	0.000379	UC	1.63
UBR4_HUMAN	E3 ubiquitin-protein ligase UBR4	7	6	479.64	0.003495	UC	1.63
SRRT_HUMAN	Serrate RNA effector molecule homolog	2	2	122.34	0.004071	UC	1.63
1433F_HUMAN	14-3-3 protein eta	14	6	867.41	0.001782	SEC	1.63
UB2L3_HUMAN	Ubiquitin-conjugating enzyme E2 L3	2	2	128.02	0.001113	SEC	1.63
IMPA1_HUMAN	Inositol monophosphatase 1	5	4	298.48	0.003492	SEC	1.63
SMCE1_HUMAN	SWI/SNF-related matrix-associated actin-dependent regulator of chromatin subfamily E member 1	1	1	49.9	0.146719	UC	1.63
GPA33_HUMAN	Cell surface A33 antigen	2	2	63.2	0.08119	SEC	1.62
NUDT5_HUMAN	ADP-sugar pyrophosphatase	6	6	468.39	0.004393	SEC	1.62
CLCA_HUMAN	Clathrin light chain A	3	2	156.67	0.011796	SEC	1.62
1433Z_HUMAN	14-3-3 protein zeta/delta	17	11	1697.74	0.000156	SEC	1.61
EMB_HUMAN	Embigin	2	2	100.53	0.000717	SEC	1.61
KT3K_HUMAN	Ketosamine-3-kinase	2	2	66.35	0.008798	UC	1.61
CYFP1_HUMAN	Cytoplasmic FMR1-interacting protein 1	11	1	773.94	0.315199	UC	1.61
HEM3_HUMAN	Porphobilinogen deaminase	1	1	113.24	0.023388	SEC	1.61
LZIC_HUMAN	Protein LZIC	1	1	71.22	0.014268	UC	1.61
RD23A_HUMAN	UV excision repair protein RAD23 homolog A	2	1	203.52	0.182572	SEC	1.61
WASF2_HUMAN	Wiskott-Aldrich syndrome protein family member 2	3	3	170.61	0.016154	UC	1.60
TCPB_HUMAN	T-complex protein 1 subunit beta	37	35	3898.51	2.48E-06	UC	1.60
NHRF1_HUMAN	Na(+)/H(+) exchange regulatory cofactor NHE-RF1	10	10	659.99	0.000231	SEC	1.60
NRDC_HUMAN	Nardilysin	3	3	208.26	0.011789	SEC	1.60
6PGD_HUMAN	6-phosphogluconate dehydrogenase, decarboxylating	15	15	1202.81	5.11E-05	SEC	1.60
ROS1_HUMAN	Proto-oncogene tyrosine-protein kinase ROS	1	1	41.29	0.070466	UC	1.60
PAIRB_HUMAN	Plasminogen activator inhibitor 1 RNA-binding protein	3	2	115.38	0.001602	UC	1.60
RL24_HUMAN	60S ribosomal protein L24	1	1	33.23	0.123251	SEC	1.60
ABRX2_HUMAN	BRISC complex subunit Abraxas 2	3	3	158.42	0.003963	SEC	1.60
GSHR_HUMAN	Glutathione reductase, mitochondrial	2	2	119.84	0.003444	SEC	1.60
PRKDC_HUMAN	DNA-dependent protein kinase catalytic subunit	4	4	241.56	0.002543	UC	1.59
PP1B_HUMAN	Serine/threonine-protein phosphatase PP1-beta catalytic subunit	3	2	294.36	0.026778	UC	1.59
LCK_HUMAN	Tyrosine-protein kinase Lck	12	10	1241.91	0.000869	UC	1.59
SND1_HUMAN	Staphylococcal nuclease domain-containing protein 1	6	6	306.37	0.021914	UC	1.59
FA5_HUMAN	Coagulation factor V	12	11	801.61	0.000705	SEC	1.59
PSA2_HUMAN	Proteasome subunit alpha type-2	7	7	525.24	0.012348	UC	1.59
TCPA_HUMAN	T-complex protein 1 subunit alpha	26	26	2912.64	9.64E-06	UC	1.59
RL10_HUMAN	60S ribosomal protein L10	5	2	391.68	0.001646	SEC	1.59
MFGM_HUMAN	Lactadherin	11	11	812.38	0.011302	SEC	1.59
IPO11_HUMAN	Importin-11	2	2	147.52	0.11311	UC	1.59
PSD12_HUMAN	26S proteasome non-ATPase regulatory subunit 12	10	10	695.9	0.000299	UC	1.58
RS24_HUMAN	40S ribosomal protein S24	1	1	104.49	0.047707	SEC	1.58
VATC1_HUMAN	V-type proton ATPase subunit C 1	3	3	165.25	0.011312	SEC	1.58
CHRD1_HUMAN	Cysteine and histidine-rich domain-containing protein 1	2	1	82.57	0.075163	UC	1.58

T cell 18 h ACdEV proteomes when isolated by SEC versus UC

Accession	Description	Peptide count	Unique peptides	Confidence score	Anova (p)	Highest mean condition	Max fold change
TPC10_HUMAN	Trafficking protein particle complex subunit 10	1	1	39.48	0.021043	SEC	1.58
PRS7_HUMAN	26S proteasome regulatory subunit 7	10	10	695.57	2.49E-05	UC	1.58
PARP1_HUMAN	Poly [ADP-ribose] polymerase 1	1	1	37.81	0.201409	UC	1.58
XRCC6_HUMAN	X-ray repair cross-complementing protein 6	14	13	1031.52	1.05E-05	UC	1.57
CLU_HUMAN	Clustered mitochondria protein homolog	1	1	75.29	0.023929	SEC	1.57
EP15R_HUMAN	Epidermal growth factor receptor substrate 15-like 1	2	2	128.39	0.052185	SEC	1.57
SYFB_HUMAN	Phenylalanine--tRNA ligase beta subunit	9	8	522.41	0.000251	UC	1.57
RL18_HUMAN	60S ribosomal protein L18	4	4	417.29	0.005801	SEC	1.57
SF3A3_HUMAN	Splicing factor 3A subunit 3	1	1	51.6	0.197178	SEC	1.57
TPM4_HUMAN	Tropomyosin alpha-4 chain	14	7	934.03	0.003852	SEC	1.56
ANXA5_HUMAN	Annexin A5	10	10	1069.62	0.006281	UC	1.56
EZRI_HUMAN	Ezrin	32	18	2488.11	0.001962	SEC	1.56
RS15_HUMAN	40S ribosomal protein S15	7	7	566.96	0.080551	SEC	1.56
MOT10_HUMAN	Monocarboxylate transporter 10	2	2	120.04	0.002513	SEC	1.56
PRS6A_HUMAN	26S proteasome regulatory subunit 6A	8	8	713.69	0.00088	UC	1.56
TYSY_HUMAN	Thymidylate synthase	3	3	341.27	0.011801	UC	1.56
SYLC_HUMAN	Leucine--tRNA ligase, cytoplasmic	6	6	371.44	0.008628	UC	1.56
XPO7_HUMAN	Exportin-7	6	5	362.48	0.001263	UC	1.56
SMD3_HUMAN	Small nuclear ribonucleoprotein Sm D3	1	1	55.06	0.161419	SEC	1.56
ESYT2_HUMAN	Extended synaptotagmin-2	1	1	37.09	0.033026	UC	1.55
DDX6_HUMAN	Probable ATP-dependent RNA helicase DDX6	2	1	81.35	0.000152	UC	1.55
GMFG_HUMAN	Glia maturation factor gamma	1	1	69.77	0.161177	SEC	1.55
SERC_HUMAN	Phosphoserine aminotransferase	13	11	873.62	5.64E-05	SEC	1.55
SF3B1_HUMAN	Splicing factor 3B subunit 1	8	6	527.85	0.000132	UC	1.55
PAK2_HUMAN	Serine/threonine-protein kinase PAK 2	11	7	714.65	0.000453	SEC	1.55
CUL4A_HUMAN	Cullin-4A	1	1	61.79	0.052983	UC	1.55
CTL2_HUMAN	Choline transporter-like protein 2	1	1	50.73	0.000406	SEC	1.55
CHMP3_HUMAN	Charged multivesicular body protein 3	1	1	59.06	0.035666	SEC	1.55
RS26L_HUMAN	Putative 40S ribosomal protein S26-like 1	1	1	67.24	0.000308	SEC	1.55
VINC_HUMAN	Vinculin	5	5	290.17	0.000807	SEC	1.55
CAB39_HUMAN	Calcium-binding protein 39	11	8	560.81	0.001773	SEC	1.55
RL12_HUMAN	60S ribosomal protein L12	3	3	258.58	0.010783	SEC	1.54
VAT1_HUMAN	Synaptic vesicle membrane protein VAT-1 homolog	12	11	1105.21	1.68E-05	SEC	1.54
RRAS2_HUMAN	Ras-related protein R-Ras2	3	2	196.95	0.10756	UC	1.54
LAMP2_HUMAN	Lysosome-associated membrane glycoprotein 2	1	1	42.85	0.179371	UC	1.54
MTAP2_HUMAN	Microtubule-associated protein 2	1	1	31.63	0.001955	SEC	1.53
ISOC1_HUMAN	Isochorismatase domain-containing protein 1	4	4	241.78	0.020017	SEC	1.53
COPA_HUMAN	Coatomer subunit alpha	13	11	751.31	0.009231	SEC	1.53
ATPA_HUMAN	ATP synthase subunit alpha, mitochondrial	9	8	626.29	0.000456	UC	1.53
TBB4B_HUMAN	Tubulin beta-4B chain	28	1	2708.9	2.34E-05	UC	1.53
AATC_HUMAN	Aspartate aminotransferase, cytoplasmic	12	12	854.66	0.001583	SEC	1.53
PRS4_HUMAN	26S proteasome regulatory subunit 4	6	5	361.63	0.000726	UC	1.53

T cell 18 h ACdEV proteomes when isolated by SEC versus UC

Accession	Description	Peptide count	Unique peptides	Confidence score	Anova (p)	Highest mean condition	Max fold change
RS14_HUMAN	40S ribosomal protein S14	5	5	371.46	0.076001	SEC	1.52
RBP56_HUMAN	TATA-binding protein-associated factor 2N	2	1	182.79	0.026479	UC	1.52
SIT1_HUMAN	Signaling threshold-regulating transmembrane adapter 1	4	4	335.05	6.73E-05	SEC	1.52
TSYL5_HUMAN	Testis-specific Y-encoded-like protein 5	1	1	52.97	0.35422	UC	1.52
TCPQ_HUMAN	T-complex protein 1 subunit theta	34	34	3277.63	7.48E-06	UC	1.52
DENR_HUMAN	Density-regulated protein	1	1	76.14	3.00E-06	SEC	1.52
TMOD3_HUMAN	Tropomodulin-3	8	7	609.47	0.001444	SEC	1.52
ECHD1_HUMAN	Ethylmalonyl-CoA decarboxylase	4	3	230.7	0.002385	UC	1.52
DNJA1_HUMAN	DnaJ homolog subfamily A member 1	5	4	253.09	0.00538	UC	1.52
FMNL2_HUMAN	Formin-like protein 2	3	1	154.11	0.070645	SEC	1.52
CD82_HUMAN	CD82 antigen	6	6	597.41	0.000446	SEC	1.52
PIPSL_HUMAN	Putative PIP5K1A and PSMD4-like protein	2	2	124.2	0.00595	SEC	1.51
CLIC6_HUMAN	Chloride intracellular channel protein 6	1	1	54.76	0.011829	SEC	1.51
RL27_HUMAN	60S ribosomal protein L27	1	1	71.12	0.027621	SEC	1.51
RL15_HUMAN	60S ribosomal protein L15	4	4	282.53	0.038678	SEC	1.51
R13P3_HUMAN	Putative 60S ribosomal protein L13a protein RPL13AP3	3	1	134.97	0.197907	SEC	1.51
MERL_HUMAN	Merlin	1	1	55.35	0.021854	SEC	1.51
IF2B_HUMAN	Eukaryotic translation initiation factor 2 subunit 2	2	2	128.56	0.001822	UC	1.51
FRIL_HUMAN	Ferritin light chain	1	1	92.54	0.011051	UC	1.51
DHX9_HUMAN	ATP-dependent RNA helicase A	13	13	830.81	0.001059	UC	1.51
RL29_HUMAN	60S ribosomal protein L29	1	1	113.1	0.011218	SEC	1.51
PDC10_HUMAN	Programmed cell death protein 10	5	5	323.56	0.000202	SEC	1.51
NUDC_HUMAN	Nuclear migration protein nudC	11	9	703.89	0.000962	SEC	1.50
MPRI_HUMAN	Cation-independent mannose-6-phosphate receptor	7	6	446.35	0.000727	SEC	1.50
SERC5_HUMAN	Serine incorporator 5	1	1	35.19	0.047249	UC	1.50
SQOR_HUMAN	Sulfide:quinone oxidoreductase, mitochondrial	1	1	44.83	0.011037	SEC	1.50
EVL_HUMAN	Ena/VASP-like protein	1	1	93.98	0.068714	UC	1.50
RIR2_HUMAN	Ribonucleoside-diphosphate reductase subunit M2	5	4	365.36	0.005966	SEC	1.50
PCBP1_HUMAN	Poly(rC)-binding protein 1	2	1	118.74	0.000718	UC	1.50
U5S1_HUMAN	116 kDa U5 small nuclear ribonucleoprotein component	4	3	255.26	0.010674	UC	1.50
FNBP1_HUMAN	Formin-binding protein 1	4	3	206.09	0.00107	SEC	1.49
CYFP2_HUMAN	Cytoplasmic FMR1-interacting protein 2	11	2	762.03	0.000321	SEC	1.49
BIEA_HUMAN	Biliverdin reductase A	2	2	130.87	2.60E-05	SEC	1.49
KTN1_HUMAN	Kinectin	5	4	225.02	0.000204	SEC	1.49
ALDOA_HUMAN	Fructose-bisphosphate aldolase A	21	20	2022.78	9.20E-05	SEC	1.49
CHM1B_HUMAN	Charged multivesicular body protein 1b	1	1	76.13	0.006649	SEC	1.49
LR75A_HUMAN	Leucine-rich repeat-containing protein 75A	1	1	33.6	0.013096	SEC	1.49
TBB5_HUMAN	Tubulin beta chain	29	6	3217.41	2.74E-05	UC	1.48
EIF3M_HUMAN	Eukaryotic translation initiation factor 3 subunit M	3	3	295.41	0.020078	SEC	1.48
A2MG_HUMAN	Alpha-2-macroglobulin	6	4	379.84	0.002231	UC	1.48
1433E_HUMAN	14-3-3 protein epsilon	28	26	2338.89	0.000293	SEC	1.48
IF5_HUMAN	Eukaryotic translation initiation factor 5	2	2	172.01	0.0579	UC	1.48

T cell 18 h ACdEV proteomes when isolated by SEC versus UC

Accession	Description	Peptide count	Unique peptides	Confidence score	Anova (p)	Highest mean condition	Max fold change
LASP1_HUMAN	LIM and SH3 domain protein 1	1	1	61.84	0.236585	SEC	1.48
HBA_HUMAN	Hemoglobin subunit alpha	1	1	62.41	0.495675	UC	1.48
PICAL_HUMAN	Phosphatidylinositol-binding clathrin assembly protein	1	1	38.98	0.169045	SEC	1.48
AAKG1_HUMAN	5'-AMP-activated protein kinase subunit gamma-1	6	4	545.34	0.004753	SEC	1.48
ABCE1_HUMAN	ATP-binding cassette sub-family E member 1	8	8	473.54	0.000387	UC	1.48
DX39A_HUMAN	ATP-dependent RNA helicase DDX39A	1	1	72.72	0.002939	UC	1.48
DPP3_HUMAN	Dipeptidyl peptidase 3	9	9	611.26	0.000106	SEC	1.48
H2AY_HUMAN	Core histone macro-H2A.1	1	1	45.57	0.213342	SEC	1.48
MYL9_HUMAN	Myosin regulatory light polypeptide 9	4	1	321.14	0.007694	UC	1.48
GLGB_HUMAN	1,4-alpha-glucan-branching enzyme	1	1	47.43	0.361861	SEC	1.48
XRCC5_HUMAN	X-ray repair cross-complementing protein 5	20	18	1370.13	0.000123	UC	1.48
RAP1A_HUMAN	Ras-related protein Rap-1A	7	1	529.21	0.000242	UC	1.47
CAPZB_HUMAN	F-actin-capping protein subunit beta	7	7	533.89	0.002278	SEC	1.47
DEOC_HUMAN	Deoxyribose-phosphate aldolase	1	1	31.7	0.088182	UC	1.47
EIF3D_HUMAN	Eukaryotic translation initiation factor 3 subunit D	4	3	291.5	0.021292	UC	1.47
CXAR_HUMAN	Coxsackievirus and adenovirus receptor	2	2	122.04	0.011617	SEC	1.47
ESTD_HUMAN	S-formylglutathione hydrolase	5	5	304.8	0.003469	SEC	1.47
STMN1_HUMAN	Stathmin	5	3	476.08	0.0163	SEC	1.47
SYIC_HUMAN	Isoleucine--tRNA ligase, cytoplasmic	16	13	858.8	0.000614	UC	1.47
TATD1_HUMAN	Putative deoxyribonuclease TATDN1	3	3	169.34	0.000931	SEC	1.47
ASPD_HUMAN	Putative L-aspartate dehydrogenase	1	1	37.53	0.076057	UC	1.46
RIDA_HUMAN	2-iminobutanoate/2-iminopropanoate deaminase	1	1	63.9	0.791517	UC	1.46
DRG1_HUMAN	Developmentally-regulated GTP-binding protein 1	2	2	141.28	0.013562	SEC	1.46
FIBP_HUMAN	Acidic fibroblast growth factor intracellular-binding protein	4	4	262.81	0.007529	SEC	1.46
PSA1_HUMAN	Proteasome subunit alpha type-1	12	12	880.14	0.002917	UC	1.46
ARF5_HUMAN	ADP-ribosylation factor 5	7	1	512.86	0.03256	SEC	1.45
MYH9_HUMAN	Myosin-9	98	76	8818.92	0.000255	SEC	1.45
HIF1N_HUMAN	Hypoxia-inducible factor 1-alpha inhibitor	1	1	57.6	0.961343	SEC	1.45
PLS3_HUMAN	Phospholipid scramblase 3	2	2	183.72	0.038616	SEC	1.45
CLIC4_HUMAN	Chloride intracellular channel protein 4	4	3	207.94	0.000677	SEC	1.45
ADA_HUMAN	Adenosine deaminase	18	18	1387.82	0.000672	SEC	1.45
ANXA1_HUMAN	Annexin A1	11	11	1090.66	0.00326	UC	1.44
HEM2_HUMAN	Delta-aminolevulinic acid dehydratase	1	1	45.77	0.036555	UC	1.44
HDAC1_HUMAN	Histone deacetylase 1	5	3	311.69	0.000492	UC	1.44
DCUP_HUMAN	Uroporphyrinogen decarboxylase	1	1	37.25	0.004334	SEC	1.44
FUS_HUMAN	RNA-binding protein FUS	5	4	328.79	0.008607	UC	1.44
PDIA3_HUMAN	Protein disulfide-isomerase A3	3	2	142.11	0.072622	UC	1.44
MOB1A_HUMAN	MOB kinase activator 1A	4	4	202.93	0.003452	SEC	1.44
PACN2_HUMAN	Protein kinase C and casein kinase substrate in neurons protein 2	6	5	394.28	0.012811	SEC	1.44
1433G_HUMAN	14-3-3 protein gamma	18	8	1194.68	0.0002	SEC	1.44
RAC1_HUMAN	Ras-related C3 botulinum toxin substrate 1	3	3	221.17	0.011964	SEC	1.44
ILF3_HUMAN	Interleukin enhancer-binding factor 3	3	2	152.25	0.015499	UC	1.44

T cell 18 h ACdEV proteomes when isolated by SEC versus UC

Accession	Description	Peptide count	Unique peptides	Confidence score	Anova (p)	Highest mean condition	Max fold change
COPZ1_HUMAN	Coatomer subunit zeta-1	1	1	78.06	0.150401	SEC	1.44
CKLF6_HUMAN	CKLF-like MARVEL transmembrane domain-containing protein 6	1	1	83.87	0.031741	SEC	1.43
BTF3_HUMAN	Transcription factor BTF3	2	2	142.56	0.015499	SEC	1.43
ML12A_HUMAN	Myosin regulatory light chain 12A	6	2	482.84	0.184657	SEC	1.43
HDDC2_HUMAN	5'-deoxynucleotidase HDDC2	2	2	152.05	0.091921	SEC	1.43
MTA2_HUMAN	Metastasis-associated protein MTA2	3	2	128.94	0.004793	SEC	1.43
RASH_HUMAN	GTPase HRas	3	1	274.68	0.032847	UC	1.43
CGL_HUMAN	Cystathionine gamma-lyase	4	4	270.79	0.013159	SEC	1.43
PTMA_HUMAN	Prothymosin alpha	3	3	331.24	0.18424	SEC	1.43
VP26A_HUMAN	Vacuolar protein sorting-associated protein 26A	1	1	39.89	0.186283	SEC	1.43
MITD1_HUMAN	MIT domain-containing protein 1	1	1	51.58	0.175373	UC	1.43
GDIR2_HUMAN	Rho GDP-dissociation inhibitor 2	9	8	549.77	0.024844	SEC	1.43
GRB2_HUMAN	Growth factor receptor-bound protein 2	2	2	132.33	0.05916	SEC	1.43
GBG5_HUMAN	Guanine nucleotide-binding protein G(I)/G(S)/G(O) subunit gamma-5	1	1	45.82	0.551986	UC	1.43
ARPC2_HUMAN	Actin-related protein 2/3 complex subunit 2	11	10	767.27	0.059322	SEC	1.43
LIS1_HUMAN	Platelet-activating factor acetylhydrolase IB subunit beta	8	7	457.41	0.005605	UC	1.43
PXDNL_HUMAN	Peroxidasin-like protein	1	1	32.46	0.09314	UC	1.43
KPRB_HUMAN	Phosphoribosyl pyrophosphate synthase-associated protein 2	5	4	333.25	0.002304	SEC	1.42
DOC10_HUMAN	Dedicator of cytokinesis protein 10	5	5	290.74	0.017329	SEC	1.42
H2B1B_HUMAN	Histone H2B type 1-B	9	1	1152.79	0.079697	UC	1.42
UBQL2_HUMAN	Ubiquilin-2	3	1	160.16	0.106163	SEC	1.42
MPZL1_HUMAN	Myelin protein zero-like protein 1	5	5	235.99	0.000421	SEC	1.42
BZW2_HUMAN	Basic leucine zipper and W2 domain-containing protein 2	5	4	277.55	0.02596	SEC	1.42
IST1_HUMAN	IST1 homolog	5	5	298.91	0.010239	SEC	1.42
SCRB1_HUMAN	Scavenger receptor class B member 1	2	2	145.75	0.010423	SEC	1.42
PGK1_HUMAN	Phosphoglycerate kinase 1	32	24	2427.04	0.000348	SEC	1.42
RL10L_HUMAN	60S ribosomal protein L10-like	3	1	198.43	0.07755	UC	1.42
ITAL_HUMAN	Integrin alpha-L	3	2	165.86	0.003504	SEC	1.42
NC2A_HUMAN	Dr1-associated corepressor	1	1	40.96	0.103605	SEC	1.41
ASNS_HUMAN	Asparagine synthetase [glutamine-hydrolyzing]	6	6	397.09	0.002556	UC	1.41
LDHA_HUMAN	L-lactate dehydrogenase A chain	21	18	1711.13	0.002458	SEC	1.41
SKP1_HUMAN	S-phase kinase-associated protein 1	1	1	42.91	0.328469	UC	1.41
CD63_HUMAN	CD63 antigen	1	1	65.86	0.02128	SEC	1.41
RS18_HUMAN	40S ribosomal protein S18	8	6	596.63	0.076697	SEC	1.41
SNX1_HUMAN	Sorting nexin-1	2	2	98.75	0.170469	UC	1.41
TAGL2_HUMAN	Transgelin-2	16	12	1433.63	0.045913	SEC	1.41
PSA6_HUMAN	Proteasome subunit alpha type-6	7	7	511.68	0.024086	UC	1.41
GDIA_HUMAN	Rab GDP dissociation inhibitor alpha	16	8	1170.34	0.000363	SEC	1.41
DCD_HUMAN	Dermcidin	1	1	65.68	0.400251	UC	1.41
FYN_HUMAN	Tyrosine-protein kinase Fyn	2	1	123.1	0.023344	UC	1.41
GGCT_HUMAN	Gamma-glutamylcyclotransferase	3	3	185.27	0.076025	SEC	1.41
E41L2_HUMAN	Band 4.1-like protein 2	20	18	1278.07	3.48E-06	SEC	1.40

T cell 18 h ACdEV proteomes when isolated by SEC versus UC

Accession	Description	Peptide count	Unique peptides	Confidence score	Anova (p)	Highest mean condition	Max fold change
DCTN5_HUMAN	Dynactin subunit 5	1	1	34.46	0.949773	UC	1.40
LA_HUMAN	Lupus La protein	1	1	42.85	0.014591	SEC	1.40
ABHEB_HUMAN	Protein ABHD14B	1	1	68.56	0.100785	SEC	1.40
GLOD4_HUMAN	Glyoxalase domain-containing protein 4	7	7	460.39	0.007136	SEC	1.40
RS27A_HUMAN	Ubiquitin-40S ribosomal protein S27a	5	5	394.46	0.003283	SEC	1.40
CUL5_HUMAN	Cullin-5	2	2	77.15	0.105296	UC	1.40
PLCG1_HUMAN	1-phosphatidylinositol 4,5-bisphosphate phosphodiesterase gamma-1	8	6	410.67	0.013137	SEC	1.40
SYFA_HUMAN	Phenylalanine--tRNA ligase alpha subunit	4	4	239.31	0.012556	UC	1.40
TXD17_HUMAN	Thioredoxin domain-containing protein 17	1	1	45.67	0.261257	SEC	1.40
TFIP8_HUMAN	Tumor necrosis factor alpha-induced protein 8	2	2	240.68	0.058917	SEC	1.40
RAB35_HUMAN	Ras-related protein Rab-35	4	2	273.53	0.201591	SEC	1.39
IF4A3_HUMAN	Eukaryotic initiation factor 4A-III	6	5	352.07	0.039731	UC	1.39
RS20_HUMAN	40S ribosomal protein S20	2	2	125.51	0.001857	SEC	1.39
LANC1_HUMAN	Glutathione S-transferase LANCL1	2	2	132.45	0.038225	SEC	1.39
PP2BA_HUMAN	Serine/threonine-protein phosphatase 2B catalytic subunit alpha isoform	1	1	56.79	0.05286	SEC	1.39
CNOT9_HUMAN	CCR4-NOT transcription complex subunit 9	1	1	54.81	0.23749	SEC	1.39
VATE1_HUMAN	V-type proton ATPase subunit E 1	3	3	243.95	0.084262	SEC	1.39
GDIR1_HUMAN	Rho GDP-dissociation inhibitor 1	5	3	268.81	0.159984	UC	1.39
TPIS_HUMAN	Triosephosphate isomerase	8	8	722.26	0.047856	SEC	1.39
SNAA_HUMAN	Alpha-soluble NSF attachment protein	6	4	482.12	0.021233	SEC	1.38
PCNA_HUMAN	Proliferating cell nuclear antigen	9	9	578.26	0.007455	UC	1.38
CAPG_HUMAN	Macrophage-capping protein	9	9	794.59	0.000137	SEC	1.38
TRIB1_HUMAN	Tribbles homolog 1	1	1	35.7	0.181909	SEC	1.38
GSTP1_HUMAN	Glutathione S-transferase P	8	8	1065.42	0.048896	SEC	1.38
SFPQ_HUMAN	Splicing factor, proline- and glutamine-rich	4	3	273	0.00118	UC	1.38
FBLN2_HUMAN	Fibulin-2	1	1	61.12	0.024454	UC	1.38
MAGA4_HUMAN	Melanoma-associated antigen 4	4	1	206.13	0.355715	UC	1.38
PAAF1_HUMAN	Proteasomal ATPase-associated factor 1	1	1	72.33	0.177302	SEC	1.38
RAB5B_HUMAN	Ras-related protein Rab-5B	3	2	177.65	0.175018	SEC	1.38
PPRC1_HUMAN	Peroxisome proliferator-activated receptor gamma coactivator-related protein 1	1	1	37.61	0.168845	UC	1.38
CALM1_HUMAN	Calmodulin-1	3	2	168.48	0.391722	SEC	1.38
TAOK3_HUMAN	Serine/threonine-protein kinase TAO3	2	1	92.8	0.395124	UC	1.38
CPNE3_HUMAN	Copine-3	1	1	71.52	0.069216	UC	1.38
STK10_HUMAN	Serine/threonine-protein kinase 10	1	1	61.02	0.054575	SEC	1.37
TF3C4_HUMAN	General transcription factor 3C polypeptide 4	1	1	98.85	0.076844	UC	1.37
FRIH_HUMAN	Ferritin heavy chain	2	2	111	0.00554	UC	1.37
GNA13_HUMAN	Guanine nucleotide-binding protein subunit alpha-13	6	4	329.12	0.000266	SEC	1.37
DREB_HUMAN	Drebrin	5	4	316.37	0.006849	SEC	1.37
RL19_HUMAN	60S ribosomal protein L19	4	4	283.59	0.099334	SEC	1.36
ATX10_HUMAN	Ataxin-10	5	5	336.38	0.024283	UC	1.36
CDC42_HUMAN	Cell division control protein 42 homolog	3	3	254.15	0.141493	SEC	1.36
ACTZ_HUMAN	Alpha-centractin	7	3	633.7	0.004289	UC	1.36

T cell 18 h ACdEV proteomes when isolated by SEC versus UC

Accession	Description	Peptide count	Unique peptides	Confidence score	Anova (p)	Highest mean condition	Max fold change
RL21_HUMAN	60S ribosomal protein L21	4	3	220.28	0.006986	UC	1.35
LMNB1_HUMAN	Lamin-B1	1	1	64.41	0.064227	UC	1.35
MRCKA_HUMAN	Serine/threonine-protein kinase MRCK alpha	1	1	62.74	0.013182	UC	1.35
PGAM1_HUMAN	Phosphoglycerate mutase 1	10	5	837.3	0.133878	SEC	1.35
SET_HUMAN	Protein SET	3	1	166.24	0.143955	UC	1.35
THIO_HUMAN	Thioredoxin	1	1	55.05	0.744907	UC	1.35
HMCS1_HUMAN	Hydroxymethylglutaryl-CoA synthase, cytoplasmic	1	1	36.42	0.053556	SEC	1.35
MEF2D_HUMAN	Myocyte-specific enhancer factor 2D	1	1	35.13	0.000292	UC	1.35
HS71A_HUMAN	Heat shock 70 kDa protein 1A	17	8	1069.76	0.000222	SEC	1.35
SNP29_HUMAN	Synaptosomal-associated protein 29	4	4	322.47	0.002294	SEC	1.35
NCKPL_HUMAN	Nck-associated protein 1-like	4	4	235.99	0.078317	SEC	1.35
RS13_HUMAN	40S ribosomal protein S13	5	5	339.78	0.025693	SEC	1.35
VDAC1_HUMAN	Voltage-dependent anion-selective channel protein 1	1	1	47.26	0.113954	UC	1.35
ARGL1_HUMAN	Arginine and glutamate-rich protein 1	1	1	47.97	0.124537	UC	1.35
TBB2A_HUMAN	Tubulin beta-2A chain	25	1	2235.27	0.189356	UC	1.35
WDR1_HUMAN	WD repeat-containing protein 1	13	13	1008.95	0.00076	SEC	1.35
ENOA_HUMAN	Alpha-enolase	44	36	4403.63	0.001618	SEC	1.35
RLA0_HUMAN	60S acidic ribosomal protein P0	12	4	1023.86	0.05902	SEC	1.35
UN45A_HUMAN	Protein unc-45 homolog A	1	1	58.54	0.777998	UC	1.35
IF2A_HUMAN	Eukaryotic translation initiation factor 2 subunit 1	8	8	642.08	0.05146	SEC	1.35
FMNL1_HUMAN	Formin-like protein 1	13	11	888.13	0.000195	SEC	1.35
DHX15_HUMAN	Pre-mRNA-splicing factor ATP-dependent RNA helicase DHX15	5	4	402.43	0.009384	UC	1.34
CSN1_HUMAN	COP9 signalosome complex subunit 1	6	6	316.85	0.036928	UC	1.34
YTHD1_HUMAN	YTH domain-containing family protein 1	1	1	41.38	0.031628	UC	1.34
RL8_HUMAN	60S ribosomal protein L8	4	4	257.43	0.000122	SEC	1.34
CPPED_HUMAN	Serine/threonine-protein phosphatase CPPED1	2	2	133.44	0.035672	SEC	1.34
ENOG_HUMAN	Gamma-enolase	13	10	1169.36	0.002102	SEC	1.34
COPD_HUMAN	Coatomer subunit delta	4	4	283.2	0.018536	SEC	1.34
DDAH2_HUMAN	N(G),N(G)-dimethylarginine dimethylaminohydrolase 2	5	5	547.16	0.000677	SEC	1.34
MCM2_HUMAN	DNA replication licensing factor MCM2	10	8	734.41	0.00561	UC	1.34
RS4X_HUMAN	40S ribosomal protein S4, X isoform	10	5	625.11	8.05E-05	SEC	1.34
IF2G_HUMAN	Eukaryotic translation initiation factor 2 subunit 3	8	1	493.06	0.00028	SEC	1.34
STXB3_HUMAN	Syntaxin-binding protein 3	11	10	682.89	0.001592	SEC	1.34
NP1L4_HUMAN	Nucleosome assembly protein 1-like 4	5	4	562.08	0.003463	SEC	1.33
GSHB_HUMAN	Glutathione synthetase	3	3	137.01	0.000411	SEC	1.33
SDCB1_HUMAN	Syntenin-1	9	9	696.23	0.017407	SEC	1.33
1433B_HUMAN	14-3-3 protein beta/alpha	20	7	1300.88	0.005023	SEC	1.33
XRP2_HUMAN	Protein XRP2	5	5	323	0.042147	SEC	1.33
MYH6_HUMAN	Myosin-6	1	1	33.04	0.089003	SEC	1.33
SELPL_HUMAN	P-selectin glycoprotein ligand 1	2	2	111.5	0.086562	SEC	1.33
RAB5A_HUMAN	Ras-related protein Rab-5A	3	1	198.69	0.001378	SEC	1.33
SLAF6_HUMAN	SLAM family member 6	4	3	228.65	0.000745	SEC	1.33

T cell 18 h ACdEV proteomes when isolated by SEC versus UC

Accession	Description	Peptide count	Unique peptides	Confidence score	Anova (p)	Highest mean condition	Max fold change
FLNA_HUMAN	Filamin-A	28	25	1795.42	0.000151	SEC	1.33
RL22_HUMAN	60S ribosomal protein L22	3	3	237.51	0.107219	SEC	1.33
MERB1_HUMAN	bMERB domain-containing protein 1	1	1	32.98	0.062254	SEC	1.33
RS7_HUMAN	40S ribosomal protein S7	6	5	334.88	0.029047	UC	1.32
NMT1_HUMAN	Glycylpeptide N-tetradecanoyltransferase 1	1	1	54.78	0.083163	SEC	1.32
PGM1_HUMAN	Phosphoglucomutase-1	11	9	801.8	0.000131	SEC	1.32
ANM1_HUMAN	Protein arginine N-methyltransferase 1	6	5	392.68	0.00296	UC	1.32
HNRPM_HUMAN	Heterogeneous nuclear ribonucleoprotein M	3	3	110.57	0.057145	UC	1.32
VTA1_HUMAN	Vacuolar protein sorting-associated protein VTA1 homolog	4	4	223.01	0.00058	SEC	1.32
DUT_HUMAN	Deoxyuridine 5'-triphosphate nucleotidohydrolase, mitochondrial	3	3	158.92	0.202799	UC	1.32
MDHC_HUMAN	Malate dehydrogenase, cytoplasmic	5	5	366.52	0.013182	SEC	1.32
HS74L_HUMAN	Heat shock 70 kDa protein 4L	4	1	186.52	0.011285	UC	1.32
IPO5_HUMAN	Importin-5	8	7	516.23	0.001584	SEC	1.32
H2B1A_HUMAN	Histone H2B type 1-A	4	1	221.01	0.037075	SEC	1.32
DC1I2_HUMAN	Cytoplasmic dynein 1 intermediate chain 2	3	3	106.14	0.000689	SEC	1.31
FLOT1_HUMAN	Flotillin-1	8	7	583.55	0.000109	SEC	1.31
SMAGP_HUMAN	Small cell adhesion glycoprotein	2	2	98.4	0.061094	SEC	1.31
LRRF1_HUMAN	Leucine-rich repeat flightless-interacting protein 1	1	1	66.12	0.107236	SEC	1.31
PFD3_HUMAN	Prefoldin subunit 3	2	2	95.25	0.190789	UC	1.31
PPAC_HUMAN	Low molecular weight phosphotyrosine protein phosphatase	1	1	74.17	0.282855	SEC	1.31
GLU2B_HUMAN	Glucosidase 2 subunit beta	1	1	56.58	0.374937	UC	1.31
IDI1_HUMAN	Isopentenyl-diphosphate Delta-isomerase 1	3	2	164.27	0.097692	SEC	1.31
SCAM2_HUMAN	Secretory carrier-associated membrane protein 2	1	1	44.63	0.372348	SEC	1.31
PSA4_HUMAN	Proteasome subunit alpha type-4	9	9	544.56	0.009288	UC	1.31
MARE1_HUMAN	Microtubule-associated protein RP/EB family member 1	4	3	194.23	0.024282	SEC	1.31
XPP1_HUMAN	Xaa-Pro aminopeptidase 1	5	5	370.52	0.008867	SEC	1.31
AP2B1_HUMAN	AP-2 complex subunit beta	14	8	892.94	0.004474	SEC	1.30
SYEP_HUMAN	Bifunctional glutamate/proline--tRNA ligase	18	16	1161.45	0.010545	UC	1.30
PSMD8_HUMAN	26S proteasome non-ATPase regulatory subunit 8	5	4	209.15	0.011843	SEC	1.30
NCBP1_HUMAN	Nuclear cap-binding protein subunit 1	3	3	222.14	0.03662	UC	1.30
PTER_HUMAN	Phosphotriesterase-related protein	1	1	66.62	0.372543	SEC	1.30
ACLY_HUMAN	ATP-citrate synthase	33	32	2606.09	3.72E-05	UC	1.30
PRPK_HUMAN	EKC/KEOPS complex subunit TP53RK	1	1	32.86	0.019978	UC	1.30
EIF3K_HUMAN	Eukaryotic translation initiation factor 3 subunit K	3	3	187.88	0.046652	UC	1.30
MIF_HUMAN	Macrophage migration inhibitory factor	1	1	91	0.08761	UC	1.30
PYRG1_HUMAN	CTP synthase 1	8	6	585.24	0.008255	UC	1.30
AK1A1_HUMAN	Aldo-keto reductase family 1 member A1	5	3	275.61	0.05339	SEC	1.30
RAB7A_HUMAN	Ras-related protein Rab-7a	11	9	958.64	0.015357	SEC	1.30
TCTP_HUMAN	Translationally-controlled tumor protein	1	1	70.57	0.292277	SEC	1.30
ANXA3_HUMAN	Annexin A3	4	4	267.78	0.020978	UC	1.29
OSTF1_HUMAN	Osteoclast-stimulating factor 1	1	1	99.71	0.117323	UC	1.29
LRIQ1_HUMAN	Leucine-rich repeat and IQ domain-containing protein 1	1	1	33.39	0.409292	UC	1.29

T cell 18 h ACdEV proteomes when isolated by SEC versus UC

Accession	Description	Peptide count	Unique peptides	Confidence score	Anova (p)	Highest mean condition	Max fold change
PURA2_HUMAN	Adenylosuccinate synthetase isozyme 2	6	5	395	0.000152	SEC	1.29
RSU1_HUMAN	Ras suppressor protein 1	8	8	632.16	0.003587	SEC	1.29
TSN_HUMAN	Translin	4	3	272.32	0.097677	SEC	1.29
C1QBP_HUMAN	Complement component 1 Q subcomponent-binding protein, mitochondrial	1	1	63.21	0.044351	UC	1.28
PFD5_HUMAN	Prefoldin subunit 5	3	3	174.4	0.285454	SEC	1.28
ARC1B_HUMAN	Actin-related protein 2/3 complex subunit 1B	5	4	240.76	0.052523	UC	1.28
LZTL1_HUMAN	Leucine zipper transcription factor-like protein 1	1	1	38.68	0.029762	SEC	1.28
AT2B1_HUMAN	Plasma membrane calcium-transporting ATPase 1	13	2	948.28	0.385136	SEC	1.28
RAB14_HUMAN	Ras-related protein Rab-14	2	1	145.08	0.093863	UC	1.28
EXOS2_HUMAN	Exosome complex component RRP4	1	1	66.21	0.05134	UC	1.28
IPO4_HUMAN	Importin-4	2	2	138.12	0.115833	UC	1.28
LFA3_HUMAN	Lymphocyte function-associated antigen 3	1	1	72.98	0.035352	SEC	1.28
RTCB_HUMAN	RNA-splicing ligase RtcB homolog	6	6	375.49	0.090655	UC	1.28
FKBP3_HUMAN	Peptidyl-prolyl cis-trans isomerase FKBP3	2	2	121.21	0.064286	UC	1.27
THOC2_HUMAN	THO complex subunit 2	4	3	197.7	0.009737	UC	1.27
MCM6_HUMAN	DNA replication licensing factor MCM6	8	7	516.9	0.168947	UC	1.27
CPNE1_HUMAN	Copine-1	2	2	146.09	0.187399	UC	1.27
GNPI1_HUMAN	Glucosamine-6-phosphate isomerase 1	3	2	166.15	0.012725	SEC	1.27
MDHM_HUMAN	Malate dehydrogenase, mitochondrial	5	5	425.24	0.101516	UC	1.27
VATB1_HUMAN	V-type proton ATPase subunit B, kidney isoform	3	1	194.22	0.212568	SEC	1.27
PLPP_HUMAN	Chronophin	1	1	100.2	0.097009	SEC	1.27
COPE_HUMAN	Coatomer subunit epsilon	4	4	316.09	0.120755	UC	1.27
SSRP1_HUMAN	FACT complex subunit SSRP1	7	7	329.74	0.006989	UC	1.27
HNRPC_HUMAN	Heterogeneous nuclear ribonucleoproteins C1/C2	5	5	286.32	0.032744	UC	1.27
HPBP1_HUMAN	Hsp70-binding protein 1	2	2	98.8	0.378487	SEC	1.27
OLA1_HUMAN	Obg-like ATPase 1	4	3	320.41	0.005836	SEC	1.27
RS9_HUMAN	40S ribosomal protein S9	6	6	369.23	0.052123	SEC	1.27
RL17_HUMAN	60S ribosomal protein L17	2	2	111.9	0.169269	SEC	1.27
SRSF4_HUMAN	Serine/arginine-rich splicing factor 4	3	1	132.92	0.104492	UC	1.26
MYH14_HUMAN	Myosin-14	7	1	581.12	0.006962	UC	1.26
DDB1_HUMAN	DNA damage-binding protein 1	18	18	1079.58	0.012543	UC	1.26
SERA_HUMAN	D-3-phosphoglycerate dehydrogenase	12	10	915.05	0.000698	UC	1.26
RL11_HUMAN	60S ribosomal protein L11	2	1	154.69	0.106568	SEC	1.26
AP1G1_HUMAN	AP-1 complex subunit gamma-1	5	4	227.57	0.014718	SEC	1.26
CATG_HUMAN	Cathepsin G	3	2	155.42	0.324247	SEC	1.26
CSN3_HUMAN	COP9 signalosome complex subunit 3	1	1	41.88	0.011049	SEC	1.26
GARS_HUMAN	Glycine--tRNA ligase	19	18	1322.19	0.001011	UC	1.26
IHO1_HUMAN	Interactor of HORMAD1 protein 1	1	1	39.4	0.039549	SEC	1.26
G6PI_HUMAN	Glucose-6-phosphate isomerase	21	20	1982.46	0.031556	SEC	1.26
KCAB2_HUMAN	Voltage-gated potassium channel subunit beta-2	4	3	288.93	0.142574	SEC	1.26
COPB2_HUMAN	Coatomer subunit beta'	8	7	468.24	0.006582	SEC	1.26
ANXA7_HUMAN	Annexin A7	6	6	361.66	0.009946	UC	1.26

T cell 18 h ACdEV proteomes when isolated by SEC versus UC

Accession	Description	Peptide count	Unique peptides	Confidence score	Anova (p)	Highest mean condition	Max fold change
GLPC_HUMAN	Glycophorin-C	1	1	94.08	0.344399	SEC	1.25
RBM3_HUMAN	RNA-binding protein 3	1	1	68.12	0.795692	UC	1.25
RS3A_HUMAN	40S ribosomal protein S3a	15	15	902.66	0.003845	SEC	1.25
CHM2A_HUMAN	Charged multivesicular body protein 2a	3	2	145.39	0.077223	SEC	1.25
HSP7C_HUMAN	Heat shock cognate 71 kDa protein	41	26	3799.49	0.000123	SEC	1.25
DNJA2_HUMAN	DnaJ homolog subfamily A member 2	6	6	268.26	0.016764	SEC	1.25
CN37_HUMAN	2',3'-cyclic-nucleotide 3'-phosphodiesterase	14	14	801.83	0.001793	UC	1.25
PSMD7_HUMAN	26S proteasome non-ATPase regulatory subunit 7	5	5	398	0.430283	SEC	1.25
STX3_HUMAN	Syntaxin-3	2	2	134.24	0.254904	SEC	1.24
ITB2_HUMAN	Integrin beta-2	2	1	106.74	0.998606	SEC	1.24
SF3A1_HUMAN	Splicing factor 3A subunit 1	1	1	54.68	0.065726	UC	1.24
H31T_HUMAN	Histone H3.1t	3	2	155.31	0.113965	UC	1.24
PLIN3_HUMAN	Perilipin-3	2	2	165.35	0.130886	SEC	1.24
NB5R3_HUMAN	NADH-cytochrome b5 reductase 3	1	1	64.4	0.298753	SEC	1.24
CHM4B_HUMAN	Charged multivesicular body protein 4b	2	2	226.15	0.48729	SEC	1.24
RHG01_HUMAN	Rho GTPase-activating protein 1	1	1	61.54	0.054098	SEC	1.24
PABP4_HUMAN	Polyadenylate-binding protein 4	4	1	251.15	0.08478	SEC	1.24
EIF3J_HUMAN	Eukaryotic translation initiation factor 3 subunit J	1	1	33.79	0.342642	SEC	1.24
RL27A_HUMAN	60S ribosomal protein L27a	1	1	88.25	0.018481	SEC	1.24
PLCB3_HUMAN	1-phosphatidylinositol 4,5-bisphosphate phosphodiesterase beta-3	1	1	76.09	0.298618	SEC	1.24
UBQL1_HUMAN	Ubiquilin-1	3	1	142.06	0.751975	SEC	1.24
PPP6_HUMAN	Serine/threonine-protein phosphatase 6 catalytic subunit	2	1	104.88	0.102508	UC	1.24
HS90B_HUMAN	Heat shock protein HSP 90-beta	59	13	4952.09	0.000242	UC	1.24
DCTN6_HUMAN	Dynactin subunit 6	1	1	89.96	0.340208	UC	1.24
SC24C_HUMAN	Protein transport protein Sec24C	2	2	126.16	0.074827	UC	1.23
BACH_HUMAN	Cytosolic acyl coenzyme A thioester hydrolase	9	9	725.65	0.074809	SEC	1.23
SYPL1_HUMAN	Synaptophysin-like protein 1	1	1	74.69	0.024743	SEC	1.23
IPO7_HUMAN	Importin-7	4	4	271.21	0.245995	UC	1.23
MYO1D_HUMAN	Unconventional myosin-Id	2	2	79.82	0.485713	UC	1.23
SYWC_HUMAN	Tryptophan--tRNA ligase, cytoplasmic	6	6	403.27	0.013314	SEC	1.23
EIF3L_HUMAN	Eukaryotic translation initiation factor 3 subunit L	17	16	1285.33	0.008404	SEC	1.23
NASP_HUMAN	Nuclear autoantigenic sperm protein	3	3	160.22	0.015218	SEC	1.23
CLIC1_HUMAN	Chloride intracellular channel protein 1	7	6	623.02	0.010782	SEC	1.23
TFG_HUMAN	Protein TFG	2	2	67.4	0.073401	SEC	1.23
XPOT_HUMAN	Exportin-T	2	2	151.16	0.012852	UC	1.23
FKBP4_HUMAN	Peptidyl-prolyl cis-trans isomerase FKBP4	20	18	1399.35	0.00352	SEC	1.23
DYN2_HUMAN	Dynamin-2	6	3	277.44	0.260333	UC	1.23
IPO9_HUMAN	Importin-9	3	3	259.27	0.213936	SEC	1.23
IF4A2_HUMAN	Eukaryotic initiation factor 4A-II	10	2	719.15	0.059178	UC	1.23
PGAM5_HUMAN	Serine/threonine-protein phosphatase PGAM5, mitochondrial	3	1	132.47	0.28536	UC	1.22
UBP14_HUMAN	Ubiquitin carboxyl-terminal hydrolase 14	5	5	284.9	0.050862	UC	1.22
SRPK1_HUMAN	SRSF protein kinase 1	1	1	39.03	0.141667	UC	1.22

T cell 18 h ACdEV proteomes when isolated by SEC versus UC

Accession	Description	Peptide count	Unique peptides	Confidence score	Anova (p)	Highest mean condition	Max fold change
ARP3_HUMAN	Actin-related protein 3	13	9	883.32	0.01061	SEC	1.22
TLN1_HUMAN	Talin-1	50	43	4780.16	0.002532	SEC	1.22
ATPB_HUMAN	ATP synthase subunit beta, mitochondrial	13	12	1021.55	0.165416	UC	1.22
CD81_HUMAN	CD81 antigen	2	2	279.28	0.065996	SEC	1.22
LDHB_HUMAN	L-lactate dehydrogenase B chain	21	19	2024.63	0.041541	SEC	1.22
HS90A_HUMAN	Heat shock protein HSP 90-alpha	49	19	4020.44	0.000236	SEC	1.22
RAC2_HUMAN	Ras-related C3 botulinum toxin substrate 2	2	1	127.6	0.321976	SEC	1.22
PDC6I_HUMAN	Programmed cell death 6-interacting protein	25	25	2121.26	0.00843	SEC	1.22
CHST1_HUMAN	Carbohydrate sulfotransferase 1	1	1	42.12	0.795555	SEC	1.21
MCTS1_HUMAN	Malignant T-cell-amplified sequence 1	3	3	296.45	0.088638	UC	1.21
SORCN_HUMAN	Sorcin	3	3	184.43	0.001732	SEC	1.21
RHOA_HUMAN	Transforming protein RhoA	5	2	294.48	0.128505	SEC	1.21
PSA_HUMAN	Puromycin-sensitive aminopeptidase	8	5	483.09	0.123434	SEC	1.21
IF4G1_HUMAN	Eukaryotic translation initiation factor 4 gamma 1	4	3	223.7	0.121489	SEC	1.21
RSSA_HUMAN	40S ribosomal protein SA	4	4	629.95	0.021482	UC	1.21
CCAR2_HUMAN	Cell cycle and apoptosis regulator protein 2	2	2	122.47	0.058482	SEC	1.21
ENPL_HUMAN	Endoplasmin	9	5	674.84	0.230209	UC	1.21
SYSC_HUMAN	Serine--tRNA ligase, cytoplasmic	9	9	505.47	0.014428	SEC	1.21
RL32_HUMAN	60S ribosomal protein L32	1	1	74.28	0.406184	SEC	1.21
ACPH_HUMAN	Acylamino-acid-releasing enzyme	10	9	722.26	0.000763	UC	1.21
STRAP_HUMAN	Serine-threonine kinase receptor-associated protein	8	7	401.6	0.015753	UC	1.20
PSMD1_HUMAN	26S proteasome non-ATPase regulatory subunit 1	13	13	871.04	0.000357	SEC	1.20
ASSY_HUMAN	Argininosuccinate synthase	6	6	286.82	0.008406	UC	1.20
CSN8_HUMAN	COP9 signalosome complex subunit 8	2	2	79.58	0.276904	UC	1.20
SYRC_HUMAN	Arginine--tRNA ligase, cytoplasmic	6	6	355.62	0.043181	SEC	1.20
CAZA1_HUMAN	F-actin-capping protein subunit alpha-1	6	6	697.93	0.156178	SEC	1.20
COR1C_HUMAN	Coronin-1C	7	5	313.64	0.024247	SEC	1.20
RBBP4_HUMAN	Histone-binding protein RBBP4	4	3	277.64	0.012849	UC	1.20
RANG_HUMAN	Ran-specific GTPase-activating protein	4	3	235.44	0.013587	UC	1.20
GBB4_HUMAN	Guanine nucleotide-binding protein subunit beta-4	5	1	314.27	0.169614	SEC	1.20
ANX11_HUMAN	Annexin A11	9	8	554.35	0.020141	SEC	1.20
IPYR_HUMAN	Inorganic pyrophosphatase	4	4	304.55	0.107085	UC	1.20
ARC1A_HUMAN	Actin-related protein 2/3 complex subunit 1A	1	1	84.11	0.099073	SEC	1.20
MCM5_HUMAN	DNA replication licensing factor MCM5	11	11	680.68	0.276077	UC	1.20
AL9A1_HUMAN	4-trimethylaminobutyraldehyde dehydrogenase	4	4	251.11	0.010691	SEC	1.20
HUWE1_HUMAN	E3 ubiquitin-protein ligase HUWE1	6	6	456.44	0.095913	UC	1.19
RS8_HUMAN	40S ribosomal protein S8	7	7	511.2	0.016462	SEC	1.19
EIF3E_HUMAN	Eukaryotic translation initiation factor 3 subunit E	18	18	1390.18	0.003032	SEC	1.19
RL4_HUMAN	60S ribosomal protein L4	8	7	384.68	0.00583	SEC	1.19
DACT1_HUMAN	Dapper homolog 1	1	1	43.3	0.139555	SEC	1.19
RAP2B_HUMAN	Ras-related protein Rap-2b	5	2	448.9	0.422639	UC	1.19
EIF3F_HUMAN	Eukaryotic translation initiation factor 3 subunit F	9	8	844.61	0.052231	UC	1.19

T cell 18 h ACdEV proteomes when isolated by SEC versus UC

Accession	Description	Peptide count	Unique peptides	Confidence score	Anova (p)	Highest mean condition	Max fold change
COR1A_HUMAN	Coronin-1A	15	14	1224.34	0.001439	SEC	1.19
MCA3_HUMAN	Eukaryotic translation elongation factor 1 epsilon-1	4	4	240.3	0.31341	SEC	1.19
ACTB_HUMAN	Actin, cytoplasmic 1	36	8	4214.42	0.014797	SEC	1.19
NGBR_HUMAN	Dehydrodolichyl diphosphate synthase complex subunit NUS1	1	1	37.7	0.002946	SEC	1.19
SMC3_HUMAN	Structural maintenance of chromosomes protein 3	2	2	152.01	0.490767	UC	1.18
STXB2_HUMAN	Syntaxin-binding protein 2	7	6	415.02	0.002626	SEC	1.18
YKT6_HUMAN	Synaptobrevin homolog YKT6	4	4	250.13	0.08762	SEC	1.18
ACOC_HUMAN	Cytoplasmic aconitate hydratase	12	10	720.96	0.000847	SEC	1.18
TALDO_HUMAN	Transaldolase	12	11	781.8	0.003565	SEC	1.18
UFD1_HUMAN	Ubiquitin recognition factor in ER-associated degradation protein 1	2	2	98.1	0.021997	SEC	1.18
SMC1A_HUMAN	Structural maintenance of chromosomes protein 1A	4	3	247.38	0.01573	UC	1.18
VIME_HUMAN	Vimentin	13	8	882.36	0.01167	SEC	1.18
SEPT7_HUMAN	Septin-7	8	7	555.23	0.009108	UC	1.17
SEPT2_HUMAN	Septin-2	9	9	819.03	0.100214	SEC	1.17
IMDH2_HUMAN	Inosine-5'-monophosphate dehydrogenase 2	8	8	453.84	0.001493	UC	1.17
RGS19_HUMAN	Regulator of G-protein signaling 19	1	1	32.15	0.37769	SEC	1.17
SYNC_HUMAN	Asparagine--tRNA ligase, cytoplasmic	10	10	629.24	0.014855	SEC	1.17
THY1_HUMAN	Thy-1 membrane glycoprotein	1	1	59.53	0.530782	SEC	1.17
PLCG2_HUMAN	1-phosphatidylinositol 4,5-bisphosphate phosphodiesterase gamma-2	1	1	72.22	0.491398	UC	1.17
RTRAF_HUMAN	RNA transcription, translation and transport factor protein	1	1	50.57	0.742429	UC	1.17
PUR6_HUMAN	Multifunctional protein ADE2	19	19	1513.61	0.005807	UC	1.17
KAP0_HUMAN	cAMP-dependent protein kinase type I-alpha regulatory subunit	2	1	80.64	0.433124	SEC	1.17
HYES_HUMAN	Bifunctional epoxide hydrolase 2	2	2	69.16	0.377831	UC	1.17
VTNC_HUMAN	Vitronectin	1	1	59.15	0.003207	SEC	1.17
NEP1_HUMAN	Ribosomal RNA small subunit methyltransferase NEP1	1	1	50.86	0.366301	SEC	1.17
HSP74_HUMAN	Heat shock 70 kDa protein 4	21	20	1613.96	0.008418	UC	1.17
KPYM_HUMAN	Pyruvate kinase PKM	32	28	3167.65	6.82E-05	UC	1.17
EF2_HUMAN	Elongation factor 2	39	36	3138.7	0.000855	UC	1.17
PDIA4_HUMAN	Protein disulfide-isomerase A4	2	2	152.76	0.024864	UC	1.16
VPS29_HUMAN	Vacuolar protein sorting-associated protein 29	3	3	193.42	0.531373	UC	1.16
VP26B_HUMAN	Vacuolar protein sorting-associated protein 26B	1	1	63.27	0.015373	SEC	1.16
HEBP2_HUMAN	Heme-binding protein 2	4	4	254.62	0.107066	SEC	1.16
CAZA2_HUMAN	F-actin-capping protein subunit alpha-2	4	3	310.28	0.251318	SEC	1.16
RPAC1_HUMAN	DNA-directed RNA polymerases I and III subunit RPAC1	2	1	93.39	0.054203	SEC	1.16
UAP1_HUMAN	UDP-N-acetylhexosamine pyrophosphorylase	1	1	52.94	0.360198	UC	1.16
RBGP1_HUMAN	Rab GTPase-activating protein 1	1	1	59.84	0.959195	UC	1.16
EF1G_HUMAN	Elongation factor 1-gamma	14	14	1065.99	0.002319	SEC	1.16
FKBP5_HUMAN	Peptidyl-prolyl cis-trans isomerase FKBP5	1	1	34.57	0.851599	SEC	1.16
IMA3_HUMAN	Importin subunit alpha-3	1	1	98.17	0.174217	SEC	1.16
TERA_HUMAN	Transitional endoplasmic reticulum ATPase	27	26	2690.45	0.003312	UC	1.16
DHSO_HUMAN	Sorbitol dehydrogenase	7	7	437.46	0.050322	UC	1.15
G6PD_HUMAN	Glucose-6-phosphate 1-dehydrogenase	5	5	188.83	0.002198	UC	1.15

T cell 18 h ACdEV proteomes when isolated by SEC versus UC

Accession	Description	Peptide count	Unique peptides	Confidence score	Anova (p)	Highest mean condition	Max fold change
PPIH_HUMAN	Peptidyl-prolyl cis-trans isomerase H	2	2	91.13	0.287782	SEC	1.15
MACF1_HUMAN	Microtubule-actin cross-linking factor 1, isoforms 1/2/3/5	3	2	123.01	0.026178	SEC	1.15
RHOC_HUMAN	Rho-related GTP-binding protein RhoC	4	1	191.02	0.558126	SEC	1.15
EHD1_HUMAN	EH domain-containing protein 1	16	12	1062.16	0.013159	SEC	1.15
RL34_HUMAN	60S ribosomal protein L34	1	1	61.51	0.073405	SEC	1.15
COF1_HUMAN	Cofilin-1	8	4	719.48	0.21664	SEC	1.15
PSA3_HUMAN	Proteasome subunit alpha type-3	8	8	602.96	0.119447	UC	1.15
DHYS_HUMAN	Deoxyhypusine synthase	8	8	486.3	0.030299	UC	1.15
RAB1A_HUMAN	Ras-related protein Rab-1A	10	2	906.61	0.414556	SEC	1.15
NAA15_HUMAN	N-alpha-acetyltransferase 15, NatA auxiliary subunit	4	3	215.77	0.2442	SEC	1.14
ARK72_HUMAN	Aflatoxin B1 aldehyde reductase member 2	4	2	225.39	0.19609	SEC	1.14
DNJC8_HUMAN	DnaJ homolog subfamily C member 8 OS=Homo sapiens OX=9606 GN=DNAJC8 PE=1 SV=2	1	1	63.1	0.490897	UC	1.14
PRPS1_HUMAN	Ribose-phosphate pyrophosphokinase 1	7	3	434.72	0.350232	UC	1.14
GYS1_HUMAN	Glycogen [starch] synthase, muscle	1	1	57.13	0.496734	SEC	1.14
CD3G_HUMAN	T-cell surface glycoprotein CD3 gamma chain	2	2	85.98	0.386047	SEC	1.14
SRSF1_HUMAN	Serine/arginine-rich splicing factor 1	7	7	465.23	0.070145	UC	1.14
FCL_HUMAN	GDP-L-fucose synthase	5	5	257.84	0.097688	UC	1.14
TBA1A_HUMAN	Tubulin alpha-1A chain	16	1	1784.31	0.551232	SEC	1.14
CDC37_HUMAN	Hsp90 co-chaperone Cdc37	6	6	354.99	3.85E-05	UC	1.14
ANXA4_HUMAN	Annexin A4 OS	1	1	57.39	0.18086	SEC	1.14
EIF3G_HUMAN	Eukaryotic translation initiation factor 3 subunit G	1	1	74.82	0.38969	UC	1.14
ARPC4_HUMAN	Actin-related protein 2/3 complex subunit 4	3	3	161.1	0.435001	SEC	1.14
RPAB3_HUMAN	DNA-directed RNA polymerases I, II, and III subunit RPABC3	1	1	96.12	0.493711	UC	1.14
VASP_HUMAN	Vasodilator-stimulated phosphoprotein	1	1	70.25	0.391795	SEC	1.14
ANXA2_HUMAN	Annexin A2	15	5	1288.68	0.086561	UC	1.14
PUR8_HUMAN	Adenylosuccinate lyase	8	7	652.05	0.001496	UC	1.14
HS105_HUMAN	Heat shock protein 105 kDa	3	2	177.2	0.137523	UC	1.14
COPB_HUMAN	Coatomer subunit beta	7	7	375.65	0.072749	UC	1.14
RS2_HUMAN	40S ribosomal protein S2	6	6	388.61	0.017376	UC	1.14
CMC4_HUMAN	Cx9C motif-containing protein 4	1	1	42.02	0.892779	UC	1.14
SYCC_HUMAN	Cysteine--tRNA ligase, cytoplasmic	6	6	293.84	0.10612	SEC	1.13
URP2_HUMAN	Fermitin family homolog 3	3	2	153.88	0.050233	SEC	1.13
EF1B_HUMAN	Elongation factor 1-beta	3	3	281.82	0.050979	SEC	1.13
HORN_HUMAN	Hornerin	2	2	85.94	0.873102	SEC	1.13
SAHH2_HUMAN	S-adenosylhomocysteine hydrolase-like protein 1	4	1	192.04	0.082705	SEC	1.13
UGPA_HUMAN	UTP--glucose-1-phosphate uridylyltransferase	1	1	60.73	0.568596	UC	1.13
ALDR_HUMAN	Aldo-keto reductase family 1 member B1	7	5	422.59	0.077191	SEC	1.13
SORT_HUMAN	Sortilin	1	1	77.81	0.150294	SEC	1.13
UBA1_HUMAN	Ubiquitin-like modifier-activating enzyme 1	27	26	2719.04	0.002831	UC	1.13
RL23A_HUMAN	60S ribosomal protein L23a	3	3	189.61	0.143434	UC	1.13
CHMP5_HUMAN	Charged multivesicular body protein 5	5	5	305.76	0.188731	UC	1.12
COPG1_HUMAN	Coatomer subunit gamma-1	2	1	151.66	0.531697	UC	1.12

T cell 18 h ACdEV proteomes when isolated by SEC versus UC

Accession	Description	Peptide count	Unique peptides	Confidence score	Anova (p)	Highest mean condition	Max fold change
VATB2_HUMAN	V-type proton ATPase subunit B, brain isoform	9	5	586.24	0.04574	UC	1.12
KCY_HUMAN	UMP-CMP kinase	2	2	149.71	0.314213	SEC	1.12
RL14_HUMAN	60S ribosomal protein L14	3	3	122.17	0.46449	SEC	1.12
SGT1_HUMAN	Protein SGT1 homolog	3	2	174.19	0.07242	UC	1.12
PUR4_HUMAN	Phosphoribosylformylglycinamidine synthase	10	9	727.58	0.046128	UC	1.12
2AAA_HUMAN	Serine/threonine-protein phosphatase 2A 65 kDa regulatory subunit A alpha isoform	11	10	977	0.009774	UC	1.12
BST2_HUMAN	Bone marrow stromal antigen 2	1	1	63.65	0.397853	UC	1.12
CSN7A_HUMAN	COP9 signalosome complex subunit 7a	1	1	53.01	0.226448	UC	1.12
CNDP2_HUMAN	Cytosolic non-specific dipeptidase	13	12	959.31	0.015587	SEC	1.12
PTPA_HUMAN	Serine/threonine-protein phosphatase 2A activator	5	5	379.25	0.20904	SEC	1.12
DOCK2_HUMAN	Dedicator of cytokinesis protein 2	2	2	143.41	0.284133	UC	1.12
NICA_HUMAN	Nicastrin	6	5	371.24	0.149699	SEC	1.12
AP1B1_HUMAN	AP-1 complex subunit beta-1	8	2	434.7	0.08774	UC	1.12
PDCD6_HUMAN	Programmed cell death protein 6	1	1	97.83	0.43108	SEC	1.12
TEBP_HUMAN	Prostaglandin E synthase 3	1	1	54.1	0.294809	SEC	1.12
MRCKB_HUMAN	Serine/threonine-protein kinase MRCK beta	1	1	64.09	0.194861	UC	1.12
CAP1_HUMAN	Adenylyl cyclase-associated protein 1	21	20	1380.86	0.009773	SEC	1.12
G3P_HUMAN	Glyceraldehyde-3-phosphate dehydrogenase	30	28	2712.92	0.043804	UC	1.12
TSNAX_HUMAN	Translin-associated protein X	5	5	392.91	0.371286	UC	1.12
MK01_HUMAN	Mitogen-activated protein kinase 1	2	1	101.09	0.63984	UC	1.12
RUVB2_HUMAN	RuvB-like 2	13	13	1040.99	0.066075	SEC	1.11
SYDC_HUMAN	Aspartate--tRNA ligase, cytoplasmic	16	16	1017.69	0.039022	UC	1.11
SC23A_HUMAN	Protein transport protein Sec23A	1	1	83.42	0.499085	SEC	1.11
CRKL_HUMAN	Crk-like protein	1	1	35.46	0.277642	UC	1.11
RL18A_HUMAN	60S ribosomal protein L18a	2	2	93.35	0.138014	SEC	1.11
TOP2B_HUMAN	DNA topoisomerase 2-beta	1	1	58.59	0.568851	UC	1.11
BZW1_HUMAN	Basic leucine zipper and W2 domain-containing protein 1	1	1	54.58	0.415295	SEC	1.11
RUXE_HUMAN	Small nuclear ribonucleoprotein E	1	1	72.71	0.637598	SEC	1.11
SEPT9_HUMAN	Septin-9	9	9	537.94	0.041804	UC	1.11
VPS28_HUMAN	Vacuolar protein sorting-associated protein 28 homolog	2	1	144.88	0.988997	UC	1.11
ARP2_HUMAN	Actin-related protein 2	6	6	410.01	0.066008	SEC	1.11
RS3_HUMAN	40S ribosomal protein S3	14	14	900.86	0.107936	UC	1.11
CKAP5_HUMAN	Cytoskeleton-associated protein 5	1	1	78.12	0.761573	UC	1.10
DPYL2_HUMAN	Dihydropyrimidinase-related protein 2	12	9	931.52	0.18986	UC	1.10
RAB5C_HUMAN	Ras-related protein Rab-5C	9	6	741.81	0.403952	SEC	1.10
PSB9_HUMAN	Proteasome subunit beta type-9	2	1	170.9	0.490673	UC	1.10
VPS35_HUMAN	Vacuolar protein sorting-associated protein 35	7	7	519.61	0.071268	SEC	1.10
PFKAP_HUMAN	ATP-dependent 6-phosphofructokinase, platelet type	11	9	645.46	0.535518	UC	1.10
SF3B3_HUMAN	Splicing factor 3B subunit 3	18	18	1321.47	0.028047	SEC	1.10
CRTC2_HUMAN	CREB-regulated transcription coactivator 2	1	1	36.29	0.777289	SEC	1.10
AHSA1_HUMAN	Activator of 90 kDa heat shock protein ATPase homolog 1	8	8	475.83	0.122795	UC	1.10
BCAT1_HUMAN	Branched-chain-amino-acid aminotransferase, cytosolic	4	4	252.17	0.467024	SEC	1.10

T cell 18 h ACdEV proteomes when isolated by SEC versus UC

Accession	Description	Peptide count	Unique peptides	Confidence score	Anova (p)	Highest mean condition	Max fold change
YBOX1_HUMAN	Y-box-binding protein 1	10	7	842.71	0.262828	UC	1.10
PRP8_HUMAN	Pre-mRNA-processing-splicing factor 8 OS	4	4	264.04	0.211991	UC	1.10
IGBP1_HUMAN	Immunoglobulin-binding protein 1	1	1	58.21	0.185817	SEC	1.10
ADPRS_HUMAN	ADP-ribose glycohydrolase ARH3	1	1	73.36	0.162658	UC	1.10
BIP_HUMAN	Endoplasmic reticulum chaperone BiP	13	12	943.48	0.042965	SEC	1.09
RAN_HUMAN	GTP-binding nuclear protein Ran	5	5	480.78	0.344544	UC	1.09
SEPT6_HUMAN	Septin-6	9	6	578.1	0.051069	UC	1.09
G3BP2_HUMAN	Ras GTPase-activating protein-binding protein 2	1	1	76	0.041443	SEC	1.09
T185A_HUMAN	Transmembrane protein 185A	1	1	55.51	0.726358	SEC	1.09
TFR1_HUMAN	Transferrin receptor protein 1	19	19	1631.83	0.074153	UC	1.09
GLYC_HUMAN	Serine hydroxymethyltransferase, cytosolic	2	2	119.97	0.477553	SEC	1.09
TS101_HUMAN	Tumor susceptibility gene 101 protein	5	5	281.75	0.332469	UC	1.09
PSMD5_HUMAN	26S proteasome non-ATPase regulatory subunit 5	6	5	372.24	0.318887	SEC	1.09
TIPRL_HUMAN	TIP41-like protein	5	4	231.62	0.368288	SEC	1.09
C1TC_HUMAN	C-1-tetrahydrofolate synthase, cytoplasmic	17	17	1207.09	0.004524	UC	1.09
PP1A_HUMAN	Serine/threonine-protein phosphatase PP1-alpha catalytic subunit	3	3	269.77	0.365645	SEC	1.09
PP2AA_HUMAN	Serine/threonine-protein phosphatase 2A catalytic subunit alpha isoform	3	2	246.03	0.418	UC	1.09
VP37B_HUMAN	Vacuolar protein sorting-associated protein 37B	5	4	310.98	0.423365	UC	1.09
PRDX2_HUMAN	Peroxiredoxin-2	12	10	977.69	0.128199	SEC	1.09
EIF3B_HUMAN	Eukaryotic translation initiation factor 3 subunit B	9	8	586.32	0.358297	SEC	1.09
IMB1_HUMAN	Importin subunit beta-1	20	20	1806.5	0.044611	SEC	1.09
ELMO1_HUMAN	Engulfment and cell motility protein 1	3	3	171.48	0.222327	UC	1.09
NIT2_HUMAN	Omega-amidase NIT2	2	2	223.09	0.500779	SEC	1.09
PSD11_HUMAN	26S proteasome non-ATPase regulatory subunit 11	8	8	685.09	0.03457	UC	1.09
VATD_HUMAN	V-type proton ATPase subunit D	1	1	38.36	0.669721	SEC	1.08
NDKA_HUMAN	Nucleoside diphosphate kinase A	6	2	444.9	0.046026	UC	1.08
PEPD_HUMAN	Xaa-Pro dipeptidase	2	1	117.56	0.568756	SEC	1.08
BAG2_HUMAN	BAG family molecular chaperone regulator 2	7	5	429.01	0.451876	SEC	1.08
RS12_HUMAN	40S ribosomal protein S12	1	1	54.25	0.323863	UC	1.08
RB11B_HUMAN	Ras-related protein Rab-11B	10	1	748.23	0.627747	UC	1.08
FNTA_HUMAN	Protein farnesyltransferase/geranylgeranyltransferase type-1 subunit alpha	2	2	156.75	0.127431	SEC	1.08
SAHH_HUMAN	Adenosylhomocysteinase	15	10	1073.2	0.000586	UC	1.08
FSD1_HUMAN	Fibronectin type III and SPRY domain-containing protein 1	1	1	38.5	0.779152	UC	1.08
PSMD3_HUMAN	26S proteasome non-ATPase regulatory subunit 3	13	11	828.36	0.055898	SEC	1.08
PSD13_HUMAN	26S proteasome non-ATPase regulatory subunit 13	11	11	777.81	0.138482	SEC	1.08
HNRPQ_HUMAN	Heterogeneous nuclear ribonucleoprotein Q	5	2	344.8	0.195095	SEC	1.08
AN32B_HUMAN	Acidic leucine-rich nuclear phosphoprotein 32 family member B	4	1	220.53	0.489909	SEC	1.08
MD2L1_HUMAN	Mitotic spindle assembly checkpoint protein MAD2A	3	2	164.38	0.547412	UC	1.08
U520_HUMAN	U5 small nuclear ribonucleoprotein 200 kDa helicase	2	2	218.95	0.073027	UC	1.08
RL3_HUMAN	60S ribosomal protein L3	6	5	342.28	0.475892	SEC	1.08
CALR_HUMAN	Calreticulin	5	5	429.2	0.45977	SEC	1.08
RWDD1_HUMAN	RWD domain-containing protein 1	1	1	45.75	0.522659	UC	1.08

T cell 18 h ACdEV proteomes when isolated by SEC versus UC

Accession	Description	Peptide count	Unique peptides	Confidence score	Anova (p)	Highest mean condition	Max fold change
PKHO1_HUMAN	Pleckstrin homology domain-containing family O member 1	1	1	54.4	0.992694	UC	1.08
ERBIN_HUMAN	Erbin	2	2	145.99	0.448641	SEC	1.07
DCTN2_HUMAN	Dynactin subunit 2	13	12	794.84	0.437456	UC	1.07
PTK7_HUMAN	Inactive tyrosine-protein kinase 7	5	3	227.98	0.505867	UC	1.07
PSDE_HUMAN	26S proteasome non-ATPase regulatory subunit 14	6	6	469.38	0.37316	SEC	1.07
LKHA4_HUMAN	Leukotriene A-4 hydrolase	3	3	170.22	0.244191	UC	1.07
PUR9_HUMAN	Bifunctional purine biosynthesis protein ATIC	18	17	1210.87	0.003036	UC	1.07
DYHC1_HUMAN	Cytoplasmic dynein 1 heavy chain 1	6	6	361.78	0.595467	UC	1.07
PSB5_HUMAN	Proteasome subunit beta type-5	9	7	710.88	0.848051	UC	1.07
PP1G_HUMAN	Serine/threonine-protein phosphatase PP1-gamma catalytic subunit	2	1	219.69	0.594543	SEC	1.07
ELP1_HUMAN	Elongator complex protein 1	1	1	31.53	0.43496	SEC	1.07
RLA1_HUMAN	60S acidic ribosomal protein P1	2	1	233.61	0.606333	SEC	1.07
F10A1_HUMAN	Hsc70-interacting protein	8	4	539.31	0.420837	SEC	1.07
DCTN1_HUMAN	Dynactin subunit 1	14	11	993.41	0.025171	SEC	1.07
RS26_HUMAN	40S ribosomal protein S26	2	1	237.11	0.613138	SEC	1.07
FIGL1_HUMAN	Fidgetin-like protein 1	1	1	66.49	0.635041	UC	1.07
SYK_HUMAN	Lysine--tRNA ligase	8	6	519.92	0.404822	SEC	1.06
COMD1_HUMAN	COMM domain-containing protein 1	1	1	62.94	0.455776	SEC	1.06
MYO1B_HUMAN	Unconventional myosin-Ib	11	10	849.69	0.414876	UC	1.06
TRA2B_HUMAN	Transformer-2 protein homolog beta	1	1	34.46	0.661775	SEC	1.06
CAND1_HUMAN	Cullin-associated NEDD8-dissociated protein 1	19	17	1600.35	0.038414	SEC	1.06
DNJB1_HUMAN	DnaJ homolog subfamily B member 1	2	1	106.59	0.324888	UC	1.06
NACAM_HUMAN	Nascent polypeptide-associated complex subunit alpha, muscle-specific form	3	3	372.9	0.354993	SEC	1.06
ACTA_HUMAN	Actin, aortic smooth muscle	27	2	2287.22	0.52987	UC	1.06
RL13_HUMAN	60S ribosomal protein L13	7	7	447.48	0.257408	UC	1.06
RAP2A_HUMAN	Ras-related protein Rap-2a	3	2	294.97	0.504343	UC	1.06
SPEE_HUMAN	Spermidine synthase	6	6	406.94	0.541529	UC	1.06
AP1M1_HUMAN	AP-1 complex subunit mu-1	1	1	65.46	0.636988	UC	1.06
RHEB_HUMAN	GTP-binding protein Rheb	5	3	216.37	0.908403	UC	1.06
SSRA_HUMAN	Translocon-associated protein subunit alpha	1	1	48.98	0.542276	UC	1.06
CSN6_HUMAN	COP9 signalosome complex subunit 6	2	2	96.3	0.704616	SEC	1.06
PARK7_HUMAN	Parkinson disease protein 7	7	7	517.82	0.548135	UC	1.06
IDHC_HUMAN	Isocitrate dehydrogenase [NADP] cytoplasmic	3	3	266.43	0.29608	UC	1.06
RS11_HUMAN	40S ribosomal protein S11	2	2	94.47	0.559175	UC	1.05
GMPR2_HUMAN	GMP reductase 2	1	1	33.72	0.809409	SEC	1.05
PRDX1_HUMAN	Peroxiredoxin-1	16	11	1193.44	0.126369	UC	1.05
PLPHP_HUMAN	Pyridoxal phosphate homeostasis protein	4	4	256.37	0.369294	SEC	1.05
RD23B_HUMAN	UV excision repair protein RAD23 homolog B	4	3	235.98	0.451329	SEC	1.05
TRXR1_HUMAN	Thioredoxin reductase 1, cytoplasmic	8	8	484.68	0.718874	SEC	1.05
RS6_HUMAN	40S ribosomal protein S6	7	7	481.55	0.324599	SEC	1.05
STK24_HUMAN	Serine/threonine-protein kinase 24	1	1	54.37	0.70224	UC	1.05
PALS2_HUMAN	Protein PALS2	3	3	179.32	0.836267	SEC	1.05

T cell 18 h ACdEV proteomes when isolated by SEC versus UC

Accession	Description	Peptide count	Unique peptides	Confidence score	Anova (p)	Highest mean condition	Max fold change
THIC_HUMAN	Acetyl-CoA acetyltransferase, cytosolic	5	4	305.15	0.325999	UC	1.05
EIF3A_HUMAN	Eukaryotic translation initiation factor 3 subunit A	19	19	1369.56	0.083921	UC	1.05
RL9_HUMAN	60S ribosomal protein L9	3	3	316.15	0.607366	SEC	1.05
FILA2_HUMAN	Filaggrin-2	2	2	111.08	0.760744	UC	1.05
RAB6A_HUMAN	Ras-related protein Rab-6A	5	1	331.38	0.622059	SEC	1.05
RLA0L_HUMAN	60S acidic ribosomal protein P0-like	8	2	567.46	0.848335	SEC	1.04
PTN11_HUMAN	Tyrosine-protein phosphatase non-receptor type 11	1	1	40.58	0.894625	UC	1.04
CDK1_HUMAN	Cyclin-dependent kinase 1	6	2	368.98	0.709459	SEC	1.04
SYTC_HUMAN	Threonine--tRNA ligase 1, cytoplasmic	14	12	860.39	0.365736	SEC	1.04
ROCK1_HUMAN	Rho-associated protein kinase 1	4	2	190.67	0.739013	UC	1.04
PA2G4_HUMAN	Proliferation-associated protein 2G4	10	10	649.8	0.328497	UC	1.04
EIFCL_HUMAN	Eukaryotic translation initiation factor 3 subunit C-like protein	13	12	838.22	0.325621	UC	1.04
CSN4_HUMAN	COP9 signalosome complex subunit 4	8	8	799.91	0.305281	UC	1.04
PSMD2_HUMAN	26S proteasome non-ATPase regulatory subunit 2	18	16	1506.16	0.196527	SEC	1.04
ARF6_HUMAN	ADP-ribosylation factor 6	3	2	205.3	0.942457	UC	1.04
RASK_HUMAN	GTPase KRas	4	3	248.64	0.942351	UC	1.04
KINH_HUMAN	Kinesin-1 heavy chain	4	3	386.61	0.859895	SEC	1.04
ITPA_HUMAN	Inosine triphosphate pyrophosphatase	1	1	80.47	0.859492	UC	1.04
IF5A1_HUMAN	Eukaryotic translation initiation factor 5A-1	3	2	215.92	0.830154	SEC	1.04
GLYG_HUMAN	Glycogenin-1	1	1	53.66	0.722084	UC	1.04
SYYC_HUMAN	Tyrosine--tRNA ligase, cytoplasmic	8	8	465.93	0.384919	SEC	1.04
SNAG_HUMAN	Gamma-soluble NSF attachment protein	3	3	171.22	0.706252	SEC	1.03
APEX1_HUMAN	DNA-(apurinic or apyrimidinic site) endonuclease	1	1	138.36	0.943183	SEC	1.03
LIPA1_HUMAN	Liprin-alpha-1	1	1	33.96	0.712142	SEC	1.03
PRS8_HUMAN	26S proteasome regulatory subunit 8	5	3	362.01	0.737263	UC	1.03
MRP_HUMAN	MARCKS-related protein	6	6	591.46	0.795086	SEC	1.03
EF1D_HUMAN	Elongation factor 1-delta	10	9	860.1	0.570578	SEC	1.03
RS16_HUMAN	40S ribosomal protein S16	8	8	515.46	0.720357	SEC	1.03
RS15A_HUMAN	40S ribosomal protein S15a	5	5	239.8	0.782057	SEC	1.03
AP2A1_HUMAN	AP-2 complex subunit alpha-1	6	3	356.09	0.425458	UC	1.03
GUAA_HUMAN	GMP synthase [glutamine-hydrolyzing]	2	2	82.41	0.733559	UC	1.03
BLMH_HUMAN	Bleomycin hydrolase	5	4	295.83	0.81268	SEC	1.03
RS25_HUMAN	40S ribosomal protein S25	3	2	186.8	0.659163	UC	1.03
SYVC_HUMAN	Valine--tRNA ligase	5	5	422.15	0.576732	UC	1.03
SWI5_HUMAN	DNA repair protein SWI5 homolog	1	1	32.53	0.980549	SEC	1.02
BABA2_HUMAN	BRISC and BRCA1-A complex member 2	1	1	70.65	0.680342	UC	1.02
NONO_HUMAN	Non-POU domain-containing octamer-binding protein	4	3	256.7	0.752881	SEC	1.02
DCTN4_HUMAN	Dynactin subunit 4	1	1	42.11	0.845196	SEC	1.02
EIF3H_HUMAN	Eukaryotic translation initiation factor 3 subunit H	7	7	408.86	0.601519	UC	1.02
NP1L1_HUMAN	Nucleosome assembly protein 1-like 1	5	3	514.16	0.656696	SEC	1.02
TXNL1_HUMAN	Thioredoxin-like protein 1	4	4	223.47	0.540374	SEC	1.02
QOR_HUMAN	Quinone oxidoreductase	7	7	438.08	0.757725	UC	1.02

T cell 18 h ACdEV proteomes when isolated by SEC versus UC

Accession	Description	Peptide count	Unique peptides	Confidence score	Anova (p)	Highest mean condition	Max fold change
ANXA6_HUMAN	Annexin A6	48	47	4051.99	0.692741	SEC	1.02
EHD4_HUMAN	EH domain-containing protein 4	3	1	166.36	0.807464	UC	1.02
SYQ_HUMAN	Glutamine--tRNA ligase	7	5	355.91	0.767329	UC	1.02
CSN7B_HUMAN	COP9 signalosome complex subunit 7b	1	1	62.25	0.804457	SEC	1.02
GOGA7_HUMAN	Golgin subfamily A member 7	1	1	56.41	0.816632	SEC	1.02
RU17_HUMAN	U1 small nuclear ribonucleoprotein 70 kDa	2	2	100.69	0.725472	UC	1.02
AN32A_HUMAN	Acidic leucine-rich nuclear phosphoprotein 32 family member A	5	2	256.11	0.780017	UC	1.02
NUCL_HUMAN	Nucleolin	24	24	2069.69	0.655995	UC	1.02
TSN14_HUMAN	Tetraspanin-14	1	1	42.33	0.937192	UC	1.01
RS17_HUMAN	40S ribosomal protein S17	3	3	200.36	0.934024	UC	1.01
PPCS_HUMAN	Phosphopantothenate--cysteine ligase	2	2	111.22	0.966204	SEC	1.01
PSMG1_HUMAN	Proteasome assembly chaperone 1	3	3	225.21	0.937453	UC	1.01
CSN5_HUMAN	COP9 signalosome complex subunit 5	2	2	148.32	0.887827	UC	1.01
PP1R7_HUMAN	Protein phosphatase 1 regulatory subunit 7	5	5	508.01	0.883673	UC	1.01
HAP28_HUMAN	28 kDa heat- and acid-stable phosphoprotein	1	1	31.16	0.939056	SEC	1.01
SP16H_HUMAN	FACT complex subunit SPT16	4	3	256.82	0.956432	UC	1.01
PSME1_HUMAN	Proteasome activator complex subunit 1	4	4	232.96	0.940695	SEC	1.01
IRF3_HUMAN	Interferon regulatory factor 3	1	1	55.43	0.964908	SEC	1.01
DNJC9_HUMAN	DnaJ homolog subfamily C member 9	1	1	63.51	0.854776	SEC	1.01
PABP1_HUMAN	Polyadenylate-binding protein 1	8	1	526.37	0.86219	UC	1.01
RB_HUMAN	Retinoblastoma-associated protein	1	1	44.26	0.736954	SEC	1.01
RUVB1_HUMAN	RuvB-like 1	11	11	912.68	0.793492	UC	1.01
ELAV1_HUMAN	ELAV-like protein 1	1	1	41.43	0.81619	SEC	1.01
SNX5_HUMAN	Sorting nexin-5	2	1	99.4	0.983372	SEC	1.01
HPRT_HUMAN	Hypoxanthine-guanine phosphoribosyltransferase	6	6	405.29	0.892776	SEC	1.01
RPIA_HUMAN	Ribose-5-phosphate isomerase	3	3	192.9	0.892783	SEC	1.01
RL28_HUMAN	60S ribosomal protein L28	3	3	172.73	0.946295	UC	1.01
VATA_HUMAN	V-type proton ATPase catalytic subunit A	13	12	837.28	0.809428	UC	1.01
STIP1_HUMAN	Stress-induced-phosphoprotein 1	21	21	1490.87	0.906273	UC	1.01
2ABA_HUMAN	Serine/threonine-protein phosphatase 2A 55 kDa regulatory subunit B alpha isoform	2	1	195.6	0.933938	SEC	1.01
CNN2_HUMAN	Calponin-2	4	3	218.94	0.88532	SEC	1.01
TPP2_HUMAN	Tripeptidyl-peptidase 2	29	27	1832.54	0.89731	SEC	1.01
CYBP_HUMAN	Calcyclin-binding protein	9	8	633.46	0.91016	UC	1.00
TBCB_HUMAN	Tubulin-folding cofactor B	3	3	179.37	0.920335	SEC	1.00
H1X_HUMAN	Histone H1.10	1	1	37.81	0.462505	UC	1.00
SRC_HUMAN	Proto-oncogene tyrosine-protein kinase Src	2	1	120.43	0.949035	SEC	1.00
RL35A_HUMAN	60S ribosomal protein L35a	2	2	99.42	0.873467	SEC	1.00
PGTB2_HUMAN	Geranylgeranyl transferase type-2 subunit beta	1	1	69.3	0.996355	UC	1.00